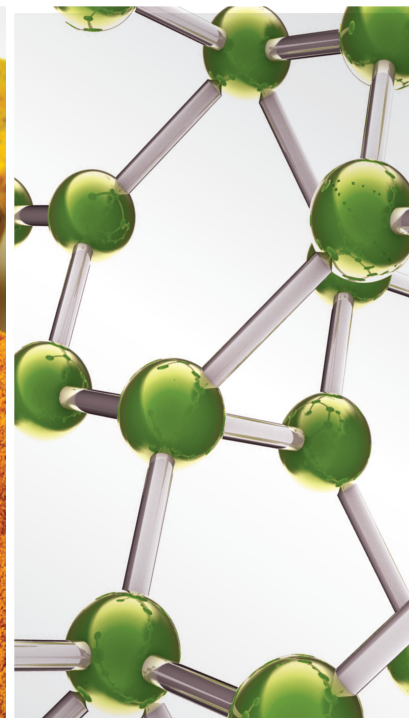
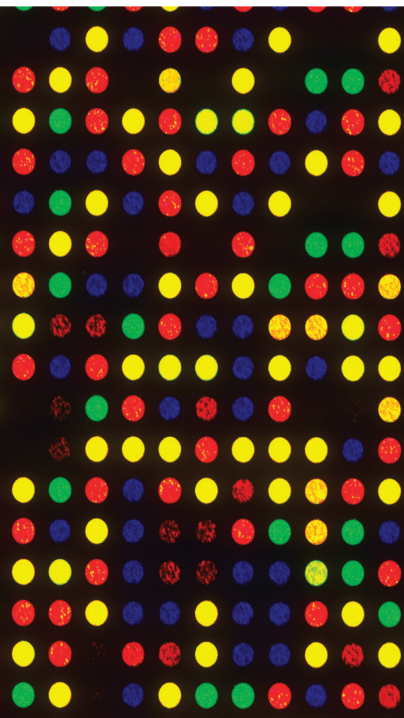


Complementary and Alternative Medicine for Ameliorating Bone and Joint Disorders

Lead Guest Editor: Arham Shabbir

Guest Editors: Muhammad Shahzad and Yang Xudong





Complementary and Alternative Medicine for Ameliorating Bone and Joint Disorders

**Complementary and Alternative
Medicine for Ameliorating Bone and
Joint Disorders**

Lead Guest Editor: Arham Shabbir

Guest Editors: Muhammad Shahzad and Yang
Xudong



Copyright © 2021 Hindawi Limited. All rights reserved.

This is a special issue published in "Evidence-Based Complementary and Alternative Medicine." All articles are open access articles distributed under the Creative Commons Attribution License, which permits unrestricted use, distribution, and reproduction in any medium, provided the original work is properly cited.

Chief Editor

Jian-Li Gao , China








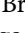
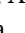
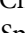
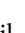
Associate Editors

Hyunsu Bae , Republic of Korea
Raffaele Capasso , Italy
Jae Youl Cho , Republic of Korea
Caigan Du , Canada
Yuewen Gong , Canada
Hai-dong Guo , China
Kuzhuvelil B. Harikumar , India
Ching-Liang Hsieh , Taiwan
Cheorl-Ho Kim , Republic of Korea
Victor Kuete , Cameroon
Hajime Nakae , Japan
Yoshiji Ohta , Japan
Olumayokun A. Olajide , United Kingdom
Chang G. Son , Republic of Korea
Shan-Yu Su , Taiwan
Michał Tomczyk , Poland
Jenny M. Wilkinson , Australia

Academic Editors

Eman A. Mahmoud , Egypt
Ammar AL-Farga , Saudi Arabia
Smail Aazza , Morocco
Nahla S. Abdel-Azim, Egypt
Ana Lúcia Abreu-Silva , Brazil
Gustavo J. Acevedo-Hernández , Mexico
Mohd Adnan , Saudi Arabia
Jose C Adsuar , Spain
Sayeed Ahmad, India
Touqeer Ahmed , Pakistan
Basiru Ajiboye , Nigeria
Bushra Akhtar , Pakistan
Fahmida Alam , Malaysia
Mohammad Jahoor Alam, Saudi Arabia
Clara Albani, Argentina
Ulysses Paulino Albuquerque , Brazil
Mohammed S. Ali-Shtayeh , Palestinian Authority
Ekram Alias, Malaysia
Terje Alraek , Norway
Adolfo Andrade-Cetto , Mexico
Letizia Angiolella , Italy
Makoto Arai , Japan

Daniel Dias Rufino Arcanjo , Brazil
Duygu AĞAGÜNDÜZ , Turkey
Neda Baghban , Iran
Samra Bashir , Pakistan
Rusliza Basir , Malaysia
Jairo Kenupp Bastos , Brazil
Arpita Basu , USA
Mateus R. Beguelini , Brazil
Juana Benedí, Spain
Samira Boulbaroud, Morocco
Mohammed Bourhia , Morocco
Abdelhakim Bouyahya, Morocco
Nunzio Antonio Cacciola , Italy
Francesco Cardini , Italy
María C. Carpinella , Argentina
Harish Chandra , India
Guang Chen, China
Jianping Chen , China
Kevin Chen, USA
Mei-Chih Chen, Taiwan
Xiaojia Chen , Macau
Evan P. Cherniack , USA
Giuseppina Chianese , Italy
Kok-Yong Chin , Malaysia
Lin China, China
Salvatore Chirumbolo , Italy
Hwi-Young Cho , Republic of Korea
Jeong June Choi , Republic of Korea
Jun-Yong Choi, Republic of Korea
Kathrine Bisgaard Christensen , Denmark
Shuang-En Chuang, Taiwan
Ying-Chien Chung , Taiwan
Francisco José Cidral-Filho, Brazil
Daniel Collado-Mateo , Spain
Lisa A. Conboy , USA
Kieran Cooley , Canada
Edwin L. Cooper , USA
José Otávio do Amaral Corrêa , Brazil
Maria T. Cruz , Portugal
Huantian Cui , China
Giuseppe D'Antona , Italy
Ademar A. Da Silva Filho , Brazil
Chongshan Dai, China
Laura De Martino , Italy
Josué De Moraes , Brazil

Arthur De Sá Ferreira , Brazil
Nunziatina De Tommasi , Italy
Marinella De leo , Italy
Gourav Dey , India
Dinesh Dhamecha, USA
Claudia Di Giacomo , Italy
Antonella Di Sotto , Italy
Mario Dioguardi, Italy
Jeng-Ren Duann , USA
Thomas Effërth , Germany
Abir El-Alfy, USA
Mohamed Ahmed El-Esawi , Egypt
Mohd Ramli Elvy Suhana, Malaysia
Talha Bin Emran, Japan
Roger Engel , Australia
Karim Ennouri , Tunisia
Giuseppe Esposito , Italy
Tahereh Eteraf-Oskouei, Iran
Robson Xavier Faria , Brazil
Mohammad Fattahi , Iran
Keturah R. Faurot , USA
Piergiorgio Fedeli , Italy
Laura Ferraro , Italy
Antonella Fioravanti , Italy
Carmen Formisano , Italy
Hua-Lin Fu , China
Liz G Müller , Brazil
Gabino Garrido , Chile
Safoora Gharibzadeh, Iran
Muhammad N. Ghayur , USA
Angelica Gomes , Brazil
Elena González-Burgos, Spain
Susana Gorzalczany , Argentina
Jiangyong Gu , China
Maruti Ram Gudavalli , USA
Jian-You Guo , China
Shanshan Guo, China
Narcís Gusi , Spain
Svein Haavik, Norway
Fernando Hallwass, Brazil
Gajin Han , Republic of Korea
Ihsan Ul Haq, Pakistan
Hicham Harhar , Morocco
Mohammad Hashem Hashempur , Iran
Muhammad Ali Hashmi , Pakistan

Waseem Hassan , Pakistan
Sandrina A. Heleno , Portugal
Pablo Herrero , Spain
Soon S. Hong , Republic of Korea
Md. Akil Hossain , Republic of Korea
Muhammad Jahangir Hossen , Bangladesh
Shih-Min Hsia , Taiwan
Changmin Hu , China
Tao Hu , China
Weicheng Hu , China
Wen-Long Hu, Taiwan
Xiao-Yang (Mio) Hu, United Kingdom
Sheng-Teng Huang , Taiwan
Ciara Hughes , Ireland
Attila Hunyadi , Hungary
Liaqat Hussain , Pakistan
Maria-Carmen Iglesias-Osma , Spain
Amjad Iqbal , Pakistan
Chie Ishikawa , Japan
Angelo A. Izzo, Italy
Satveer Jagwani , USA
Rana Jamous , Palestinian Authority
Muhammad Saeed Jan , Pakistan
G. K. Jayaprakasha, USA
Kyu Shik Jeong, Republic of Korea
Leopold Jirovetz , Austria
Jeeyoun Jung , Republic of Korea
Nurkhalida Kamal , Saint Vincent and the
Grenadines
Atsushi Kameyama , Japan
Kyungsu Kang, Republic of Korea
Wenyi Kang , China
Shao-Hsuan Kao , Taiwan
Nasiara Karim , Pakistan
Morimasa Kato , Japan
Kumar Katragunta , USA
Deborah A. Kennedy , Canada
Washim Khan, USA
Bonglee Kim , Republic of Korea
Dong Hyun Kim , Republic of Korea
Junghyun Kim , Republic of Korea
Kyungho Kim, Republic of Korea
Yun Jin Kim , Malaysia
Yoshiyuki Kimura , Japan

Nebojša Kladar , Serbia
Mi Mi Ko , Republic of Korea
Toshiaki Kogure , Japan
Malcolm Koo , Taiwan
Yu-Hsiang Kuan , Taiwan
Robert Kubina , Poland
Chan-Yen Kuo , Taiwan
Kuang C. Lai , Taiwan
King Hei Stanley Lam, Hong Kong
Fanuel Lampiao, Malawi
Ilaria Lampronti , Italy
Mario Ledda , Italy
Harry Lee , China
Jeong-Sang Lee , Republic of Korea
Ju Ah Lee , Republic of Korea
Kyu Pil Lee , Republic of Korea
Namhun Lee , Republic of Korea
Sang Yeoup Lee , Republic of Korea
Ankita Leekha , USA
Christian Lehmann , Canada
George B. Lenon , Australia
Marco Leonti, Italy
Hua Li , China
Min Li , China
Xing Li , China
Xuqi Li , China
Yi-Rong Li , Taiwan
Vuanghao Lim , Malaysia
Bi-Fong Lin, Taiwan
Ho Lin , Taiwan
Shuibin Lin, China
Kuo-Tong Liou , Taiwan
I-Min Liu, Taiwan
Suhuan Liu , China
Xiaosong Liu , Australia
Yujun Liu , China
Emilio Lizarraga , Argentina
Monica Loizzo , Italy
Nguyen Phuoc Long, Republic of Korea
Zaira López, Mexico
Chunhua Lu , China
Ângelo Luís , Portugal
Anderson Luiz-Ferreira , Brazil
Ivan Luzardo Luzardo-Ocampo, Mexico

Michel Mansur Machado , Brazil
Filippo Maggi , Italy
Juraj Majtan , Slovakia
Toshiaki Makino , Japan
Nicola Malafrente, Italy
Giuseppe Malfa , Italy
Francesca Mancianti , Italy
Carmen Mannucci , Italy
Juan M. Manzanque , Spain
Fatima Martel , Portugal
Carlos H. G. Martins , Brazil
Maulidiani Maulidiani, Malaysia
Andrea Maxia , Italy
Avijit Mazumder , India
Isac Medeiros , Brazil
Ahmed Mediani , Malaysia
Lewis Mehl-Madrona, USA
Ayikoé Guy Mensah-Nyagan , France
Oliver Micke , Germany
Maria G. Miguel , Portugal
Luigi Milella , Italy
Roberto Miniero , Italy
Letteria Minutoli, Italy
Prashant Modi , India
Daniel Kam-Wah Mok, Hong Kong
Changjong Moon , Republic of Korea
Albert Moraska, USA
Mark Moss , United Kingdom
Yoshiharu Motoo , Japan
Yoshiki Mukudai , Japan
Sakthivel Muniyan , USA
Saima Muzammil , Pakistan
Benoit Banga N'guessan , Ghana
Massimo Nabissi , Italy
Siddavaram Nagini, India
Takao Namiki , Japan
Srinivas Nammi , Australia
Krishnadas Nandakumar , India
Vitaly Napadow , USA
Edoardo Napoli , Italy
Jorddy Neves Cruz , Brazil
Marcello Nicoletti , Italy
Eliud Nyaga Mwaniki Njagi , Kenya
Cristina Nogueira , Brazil

Sakineh Kazemi Noureini , Iran
Rômulo Dias Novaes, Brazil
Martin Offenbaecher , Germany
Oluwafemi Adeleke Ojo , Nigeria
Olufunmiso Olusola Olajuyigbe , Nigeria
Luís Flávio Oliveira, Brazil
Mozaniel Oliveira , Brazil
Atolani Olubunmi , Nigeria
Abimbola Peter Oluyori , Nigeria
Timothy Omara, Austria
Chiagoziem Anariochi Otuechere , Nigeria
Sokcheon Pak , Australia
Antônio Palumbo Jr, Brazil
Zongfu Pan , China
Siyaram Pandey , Canada
Niranjan Parajuli , Nepal
Gunhyuk Park , Republic of Korea
Wansu Park , Republic of Korea
Rodolfo Parreira , Brazil
Mohammad Mahdi Parvizi , Iran
Luiz Felipe Passero , Brazil
Mitesh Patel, India
Claudia Helena Pellizzon , Brazil
Cheng Peng, Australia
Weijun Peng , China
Sonia Piacente, Italy
Andrea Pieroni , Italy
Haifa Qiao , USA
Cláudia Quintino Rocha , Brazil
DANIELA RUSSO , Italy
Muralidharan Arumugam Ramachandran,
Singapore
Manzoor Rather , India
Miguel Rebollo-Hernanz , Spain
Gauhar Rehman, Pakistan
Daniela Rigano , Italy
José L. Rios, Spain
Francisca Rius Diaz, Spain
Eliana Rodrigues , Brazil
Maan Bahadur Rokaya , Czech Republic
Mariangela Rondanelli , Italy
Antonietta Rossi , Italy
Mi Heon Ryu , Republic of Korea
Bashar Saad , Palestinian Authority
Sabi Saheed, South Africa















Mohamed Z.M. Salem , Egypt
Avni Sali, Australia
Andreas Sandner-Kiesling, Austria
Manel Santafe , Spain
José Roberto Santin , Brazil
Tadaaki Satou , Japan
Roland Schoop, Switzerland
Sindy Seara-Paz, Spain
Veronique Seidel , United Kingdom
Vijayakumar Sekar , China
Terry Selfe , USA
Arham Shabbir , Pakistan
Suzana Shahar, Malaysia
Wen-Bin Shang , China
Xiaofei Shang , China
Ali Sharif , Pakistan
Karen J. Sherman , USA
San-Jun Shi , China
Insop Shim , Republic of Korea
Maria Im Hee Shin, China
Yukihiro Shoyama, Japan
Morry Silberstein , Australia
Samuel Martins Silvestre , Portugal
Preet Amol Singh, India
Rajeev K Singla , China
Kuttulebbai N. S. Sirajudeen , Malaysia
Slim Smaoui , Tunisia
Eun Jung Sohn , Republic of Korea
Maxim A. Solovchuk , Taiwan
Young-Jin Son , Republic of Korea
Chengwu Song , China
Vanessa Steenkamp , South Africa
Annarita Stringaro , Italy
Keiichiro Sugimoto , Japan
Valeria Sulsen , Argentina
Zewei Sun , China
Sharifah S. Syed Alwi , United Kingdom
Orazio Tagliatalata-Scafati , Italy
Takashi Takeda , Japan
Gianluca Tamagno , Ireland
Hongxun Tao, China
Jun-Yan Tao , China
Lay Kek Teh , Malaysia
Norman Temple , Canada

Kamani H. Tennekoon , Sri Lanka
Seong Lin Teoh, Malaysia
Menaka Thounaojam , USA
Jinhui Tian, China
Zipora Tietel, Israel
Loren Toussaint , USA
Riaz Ullah , Saudi Arabia
Philip F. Uzor , Nigeria
Luca Vanella , Italy
Antonio Vassallo , Italy
Cristian Vergallo, Italy
Miguel Vilas-Boas , Portugal
Aristo Vojdani , USA
Yun WANG , China
QIBIAO WU , Macau
Abraham Wall-Medrano , Mexico
Chong-Zhi Wang , USA
Guang-Jun Wang , China
Jinan Wang , China
Qi-Rui Wang , China
Ru-Feng Wang , China
Shu-Ming Wang , USA
Ting-Yu Wang , China
Xue-Rui Wang , China
Youhua Wang , China
Kenji Watanabe , Japan
Jintanaporn Wattanathorn , Thailand
Silvia Wein , Germany
Katarzyna Winska , Poland
Sok Kuan Wong , Malaysia
Christopher Worsnop, Australia
Jih-Huah Wu , Taiwan
Sijin Wu , China
Xian Wu, USA
Zuoqi Xiao , China
Rafael M. Ximenes , Brazil
Guoqiang Xing , USA
JiaTuo Xu , China
Mei Xue , China
Yong-Bo Xue , China
Haruki Yamada , Japan
Nobuo Yamaguchi, Japan
Junqing Yang, China
Longfei Yang , China

Mingxiao Yang , Hong Kong
Qin Yang , China
Wei-Hsiung Yang, USA
Swee Keong Yeap , Malaysia
Albert S. Yeung , USA
Ebrahim M. Yimer , Ethiopia
Yoke Keong Yong , Malaysia
Fadia S. Youssef , Egypt
Zhilong Yu, Canada
RONGJIE ZHAO , China
Sultan Zahiruddin , USA
Armando Zarrelli , Italy
Xiaobin Zeng , China
Y Zeng , China
Fangbo Zhang , China
Jianliang Zhang , China
Jiu-Liang Zhang , China
Mingbo Zhang , China
Jing Zhao , China
Zhangfeng Zhong , Macau
Guoqi Zhu , China
Yan Zhu , USA
Suzanna M. Zick , USA
Stephane Zingue , Cameroon




Contents

Acupotomy Contributes to Suppressing Subchondral Bone Resorption in KOA Rabbits by Regulating the OPG/RANKL Signaling Pathway

Tong Wang , Yan Guo , Xiao-Wei Shi , Yang Gao , Jia-Yi Zhang , Chun-Jiu Wang , Xue Yang , Qi Shu , Xi-Lin Chen , Xin-Yi Fu , Wen-Shan Xie , Yi Zhang , Bin Li , and Chang-Qing Guo 





Research Article (17 pages), Article ID 8168657, Volume 2021 (2021)

Effect of Naringin Treatment on Postmenopausal Osteoporosis in Ovariectomized Rats: A Meta-Analysis and Systematic Review

Zhu Zhu , Wenjing Xie , Yanyan Li , Zaiou Zhu , and Wei Zhang 

Research Article (8 pages), Article ID 6016874, Volume 2021 (2021)

Effects of Various Preextraction Treatments of *Crinum asiaticum* Leaf on Its Anti-Inflammatory Activity and Chemical Properties

Chonthicha Kongkwamcharoen , Arunporn Itharat , Weerachai Pipatrattanaseree , and Buncha Ooraikul 







Research Article (11 pages), Article ID 8850744, Volume 2021 (2021)

Platelet-Rich Plasma Ameliorates Monosodium Iodoacetate-Induced Ankle Osteoarthritis in the Rat Model via Suppression of Inflammation and Oxidative Stress

G. H. Ragab , F. M. Halfaya , O. M. Ahmed , W. Abou El-Kheir , E. A. Mahdi , T. M. Ali , M. M. Almehmadi , and U. Hagag 


Research Article (13 pages), Article ID 6692432, Volume 2021 (2021)

Combinatory Effects of Bone Marrow-Derived Mesenchymal Stem Cells and Indomethacin on Adjuvant-Induced Arthritis in Wistar Rats: Roles of IL-1 β , IL-4, Nrf-2, and Oxidative Stress

Eman A. Ahmed , Osama M. Ahmed , Hanaa I. Fahim , Emad A. Mahdi, Tarek M. Ali , Basem H. Elesawy , and Mohamed B. Ashour 



Research Article (15 pages), Article ID 8899143, Volume 2021 (2021)

Evaluation of Immunomodulatory and Antiarthritic Potential of *Trigonella gharuensis* Extracts

Aisha Mobashar, Arham Shabbir , Muhammad Shahzad, and Saeed-ul-Hassan




Research Article (7 pages), Article ID 8836080, Volume 2020 (2020)

Clinical Efficacy and Safety of Thai Herbal Formulation-6 in the Treatment of Symptomatic Osteoarthritis of the Knee: A Randomized-Controlled Trial

Nut Koonrungsesomboon , Saowaros Nopnithipat, Supanimit Teekachunhatean, Natthakarn Chiranthanut, Chaichan Sangdee, Sunee Chansakaow, Pramote Tipduangta, and Nutthiya Hanprasertpong 




Research Article (9 pages), Article ID 8817374, Volume 2020 (2020)

Meta-Analysis of Randomized Controlled Trials of Xueshuantong Injection in Prevention of Deep Venous Thrombosis of Lower Extremity after Orthopedic Surgery

Shu-ting Yan , Feng Gao, Tai-wei Dong, Hao Fan, Miao-miao Xi, Feng Miao , and Pei-feng Wei 





Review Article (9 pages), Article ID 8877791, Volume 2020 (2020)

Jisuikang Promotes the Repair of Spinal Cord Injury in Rats by Regulating Ngr/RhoA/ROCK Signal Pathway

Chengjie Wu , Yuxin Zhou, Pengcheng Tu, Guanglu Yang, Suyang Zheng, Yalan Pan, Jie Sun, Yang Guo , and Yong Ma 


Research Article (13 pages), Article ID 9542359, Volume 2020 (2020)

The Protective Effects of the Ethyl Acetate Part of Er MiaoSan on Adjuvant Arthritis Rats by Regulating the Function of Bone Marrow-Derived Dendritic Cells

Jiemin Ding , Min Liu, Zihua Xuan, Meng li Liu , Ning Wang , and Xiaoyi Jia 


Research Article (10 pages), Article ID 8791657, Volume 2020 (2020)

Amelioration of Rheumatoid Arthritis by *Anacardium occidentale* via Inhibition of Collagenase and Lysosomal Enzymes

Rabiya Naz, Zaheer Ahmed , Muhammad Shahzad, Arham Shabbir , and Faiza Kamal

Research Article (11 pages), Article ID 8869484, Volume 2020 (2020)

Effects and Mechanism of Berberine on the Dexamethasone-Induced Injury of Human Tendon Cells

Shangjun Fu, Zongyun He, Yongfeng Tang, and Bo Lan 






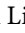

Research Article (8 pages), Article ID 8832218, Volume 2020 (2020)

Integrated Network and Experimental Pharmacology for Deciphering the Medicinal Substances and Multiple Mechanisms of Duhuo Jisheng Decoction in Osteoarthritis Therapy

Wenyu Xiao , Weibing Sun , Hui Lian , and Juexin Shen 









Research Article (13 pages), Article ID 7275057, Volume 2020 (2020)

Integrating Network Pharmacology with Molecular Docking to Unravel the Active Compounds and Potential Mechanism of Simiao Pill Treating Rheumatoid Arthritis

Mengshi Tang , Xi Xie , Pengji Yi , Jin Kang , Jiafen Liao , Wenqun Li , and Fen Li 


Research Article (16 pages), Article ID 5786053, Volume 2020 (2020)

Acupotomy Therapy for Knee Osteoarthritis Pain: Systematic Review and Meta-Analysis

Jigao Sun , Yan Zhao , Ruizheng Zhu , Qianglong Chen , Mengge Song , Zhipeng Xue , Rongtian Wang , and Weiheng Chen 


Review Article (17 pages), Article ID 2168283, Volume 2020 (2020)

***In Vitro* Antiosteoporosis Activity and Hepatotoxicity Evaluation in Zebrafish Larvae of Bark Extracts of *Prunus jamasakura* Medicinal Plant**

Richard Komakech, Ki-Shuk Shim, Nam-Hui Yim, Jun Ho Song, Sun Kyu Yang, Goya Choi, Jun Lee, Yong-goo Kim, Francis Omujal, Moses Agwaya, Grace Kyeyune Nambatya, Hyemin Kan, Kyu-Seok Hwang, Gilbert Matsabisa Motlalepula, and Youngmin Kang 

Research Article (9 pages), Article ID 8582318, Volume 2020 (2020)



Efficacy of Acupoints Dual-Frequency Low-Level Laser Therapy on Knee Osteoarthritis

Fang-Yin Liao, Chien-Lin Lin, Sui-Foon Lo, Chun-Ching Chang, Wen-Yen Liao, and Li-Wei Chou 

Research Article (7 pages), Article ID 6979105, Volume 2020 (2020)

Contents

Effect of Qing's Decoction on Leptin/Leptin Receptor and Bone Metabolism in Naturally Aging Rats

Pan Sun , Yuanyuan Zhang, Zhenpu Wei, Zhiqiang Wang, Shiming Guo, and Yanping Lin 

Research Article (12 pages), Article ID 2532081, Volume 2020 (2020)

Antiarthritic and Antihyperalgesic Properties of Ethanolic Extract from *Gomphrena celosioides* Mart. (Amaranthaceae) Aerial Parts

Luis Fernando Benitez Macorini, Joyce Alencar Santos Radai, Rafael Souza Maris , Saulo Euclides Silva-Filho, Maicon Matos Leitao, Sérgio Faloni de Andrade, Dayanna Isabel Araque Gelves, Marcos Jose Salvador, Arielle Cristina Arena, and Cândida Aparecida Leite Kassuya 






Research Article (11 pages), Article ID 4170589, Volume 2020 (2020)

Jingui Shenqi Pills Regulate Bone-Fat Balance in Murine Ovariectomy-Induced Osteoporosis with Kidney Yang Deficiency

Qi Shang , Wenhua Zhao, Gengyang Shen, Xiang Yu, Zhida Zhang, Xuan Huang, Weicheng Qin, Guifeng Chen, Fuyong Yu, Kai Tang, Honglin Chen, Juanmin Li, De Liang, Jingjing Tang , Xiaobing Jiang , and Hui Ren 

Research Article (9 pages), Article ID 1517596, Volume 2020 (2020)

Deciphering the Molecular Targets and Mechanisms of HGWD in the Treatment of Rheumatoid Arthritis via Network Pharmacology and Molecular Docking

Wei Liu , Yihua Fan , Chunying Tian , Yue Jin , Shaopeng Du , Ping Zeng, and Aihua Wang












Research Article (13 pages), Article ID 7151634, Volume 2020 (2020)

The Effect of Kinesitherapy on Bone Mineral Density in Primary Osteoporosis: A Systematic Review and Meta-Analysis of Randomized Controlled Trial

Shanxi Wang, Shuzhen Li , Xing Xie, and Juying Xie

Review Article (10 pages), Article ID 5074824, Volume 2020 (2020)

***Zingiber officinale* Roscoe Prevents DNA Damage and Improves Muscle Performance and Bone Integrity in Old Sprague Dawley Rats**

Suzana Makpol , Nur Fathiah Abdul Sani , Nur Haleeda Hakimi , Nazirah Ab Rani , Siti Nor Asyikin Zakaria , Ahmad Fais Abd Rasid , Geetha Gunasekaran , Nur Fatin Nabilah Mohd Sahardi , Jen Kit Tan , Norzana Abd Ghafar , and Mariam Firdhaus Mad Nordin 

Research Article (18 pages), Article ID 3823780, Volume 2020 (2020)

Research Article

Acupotomy Contributes to Suppressing Subchondral Bone Resorption in KOA Rabbits by Regulating the OPG/RANKL Signaling Pathway

Tong Wang ¹, Yan Guo ², Xiao-Wei Shi ³, Yang Gao ¹, Jia-Yi Zhang ⁴,
Chun-Jiu Wang ¹, Xue Yang ¹, Qi Shu ¹, Xi-Lin Chen ¹, Xin-Yi Fu ¹,
Wen-Shan Xie ¹, Yi Zhang ¹, Bin Li ² and Chang-Qing Guo ¹

¹School of Acupuncture-Moxibustion and Tuina, Beijing University of Chinese Medicine, Beijing 100029, China

²Acupuncture and Moxibustion Department, Beijing Hospital of Traditional Chinese Medicine affiliated with Capital Medical University, Beijing 100010, China

³Massage Department, The Third Affiliated Hospital of Beijing University of Chinese Medicine, Beijing 100029, China

⁴Traditional Chinese Medicine Department, Beijing Nankou Hospital, Beijing 102200, China

Correspondence should be addressed to Chang-Qing Guo; guochangqing0066@163.com

Received 17 July 2020; Revised 11 October 2020; Accepted 11 April 2021; Published 26 April 2021

Academic Editor: Arham Shabbir

Copyright © 2021 Tong Wang et al. This is an open access article distributed under the Creative Commons Attribution License, which permits unrestricted use, distribution, and reproduction in any medium, provided the original work is properly cited.

Subchondral bone lesions, as the crucial inducement for accelerating cartilage degeneration, have been considered as the initiating factor and the potential therapeutic target of knee osteoarthritis (KOA). Acupotomy, the biomechanical therapy guided by traditional Chinese meridians theory, alleviates cartilage deterioration by correcting abnormal mechanics. Whether this mechanical effect of acupotomy inhibits KOA subchondral bone lesions is indistinct. This study aimed to investigate the effects of acupotomy on inhibiting subchondral bone resorption and to define the possible mechanism in immobilization-induced KOA rabbits. After KOA modeling, 8 groups of rabbits (4w/6w acupotomy, 4w/6w electroacupuncture, 4w/6w model, and 4w/6w control groups) received the indicated intervention for 3 weeks. Histological and bone histomorphometry analyses revealed that acupotomy prevented both cartilage surface erosion and subchondral bone loss. Further, acupotomy suppressed osteoclast activity and enhanced osteoblast activity in KOA subchondral bone, showing a significantly decreased expression of tartrate-resistant acid phosphatase (TRAP), matrix metalloproteinases-9 (MMP-9), and cathepsin K (Ctsk) and a significantly increased expression of osteocalcin (OCN); this regulation may be mediated by blocking the decrease in osteoprotegerin (OPG) and the increase in NF- κ B receptor activated protein ligand (RANKL). These findings indicated that acupotomy inhibited osteoclast activity and promoted osteoblast activity to ameliorate hyperactive subchondral bone resorption and cartilage degeneration in immobilization-induced KOA rabbits, which may be mediated by the OPG/RANKL signaling pathway. Taken together, our results indicate that acupotomy may have therapeutic potential in KOA by restoring the balance between bone formation and bone resorption to attenuate subchondral bone lesions.

1. Introduction

Although cartilage degeneration is the most typical pathological feature of knee osteoarthritis (KOA) [1]; the critical role of subchondral bone lesions in KOA has gradually become an area of focus in recent years [2, 3]. Increasing evidence implies that subchondral bone lesions may be the initiating factor in KOA [4, 5]. Subchondral

bone lesions were accompanied by a reduced ability of cushioning mechanical stress, which induced and accelerated the overlying cartilage degeneration under abnormal mechanical stress [6, 7]. Clinical studies have confirmed that inhibiting subchondral bone lesions can effectively relieve cartilage erosion [8, 9], which implied that subchondral bone was a potential therapeutic target for protecting cartilage and treating KOA.

During the course of KOA, persistent abnormal load within the joint leads to subchondral bone microfractures, which initiate bone remodeling [10]. Bone remodeling is the result of disrupting the balance between bone formation and bone resorption. In the early-stage KOA, due to the abnormal activation of osteoclasts [11] in the subchondral bone, bone remodeling is mainly characterized by hyperactive bone resorption [12]. Osteoprotegerin (OPG)/NF- κ B receptor activated protein ligand (RANKL) is the critical pathway to regulate bone remodeling [13, 14], which is mainly realized by regulating osteoclast activity. RANKL binds to RANK to accelerate osteoclast precursor differentiation and promote osteoclast maturation [15]. OPG can inhibit osteoclast activity by blocking the binding of RANK and RANKL [16]. Studies confirmed that bone resorption can be effectively alleviated by regulating OPG/RANKL pathway [17, 18].

Inhibition of subchondral bone resorption as a therapeutic target for KOA has been carried out extensively. Bone loss inhibitors, such as bisphosphonates, are potentially effective modalities for KOA treatment by inhibiting subchondral bone resorption [19]. However, the latest meta-analysis showed that the clinical efficacy of bisphosphonates remains to be verified [20]. Thus, nonpharmacological therapies to inhibit subchondral bone resorption deserve extensive investigation.

Acupotomy is a biomechanical therapy under the guidance of traditional Chinese meridians theory. Acupotomy, also referred to as miniscalpel-needle acupuncture, is a fairly recent development in the practice of acupuncture. Acupotomy combines the characteristics of acupuncture needle insertion and surgical incision and has a definite clinical effect on KOA. The biomechanical effect of acupotomy is the unique superiority that distinguishes it from other KOA therapies. Preliminary studies [21–24] have confirmed that acupotomy can prevent cartilage degeneration and delay KOA pathological progression by correcting the abnormal mechanical stress in KOA joints. Is the chondroprotective effect of acupotomy related to the inhibition of KOA subchondral bone resorption? Is it mediated by the OPG/RANKL signaling pathway to regulate osteoclast activity in subchondral bone?

Based on this hypothesis, we established the KOA model rabbits with Videman's extended immobilization method to explore whether acupotomy intervention could alleviate KOA subchondral bone lesions by inhibiting bone resorption, to observe the changes in activity biomarkers of osteoclasts and to evaluate the effect of the OPG/RANKL signaling pathway in subchondral bone.

2. Methods

2.1. Ethics Statement. Animal experiments were strictly handled in conformity to the recommendations in the Guidance Suggestions for the Care and Use of Laboratory Animals of Beijing University of Traditional Chinese Medicine (Beijing, China). The protocol was approved by the Committee on the Ethics of Animal Experiments of Beijing University of Traditional Chinese Medicine. All operations

are carried out under pentobarbital anesthesia to ensure that pain was minimized.

2.2. Reagents and Materials. Disposable acupuncture needles (specification: 0.25 × 25 mm) were purchased from Beijing Research Taihe Pharmaceutical Co., Ltd. (Beijing, China). The HZ series disposable acupotomy (specification: 0.4 × 40 mm) was purchased from Beijing Outstanding Huayou Medical Instrument Co., Ltd. (Beijing, China). Resin bandages (5#: 150 mm × 1800 mm) were purchased from Hengshui Kangjie Medical Instrument Co., Ltd. (Hebei, China). Orthopedic casting tapes (160 series tape: 5.0 cm × 360 cm) were purchased from Suzhou Connect Medical Technology Co., Ltd. (Jiangsu, China). The HANS acupoint nerve stimulator (LH202H) was purchased from Beijing Huawei Industry Development Co., Ltd. (Beijing, China).

Anti-OCN, anti-MMP-9, and anti-GAPDH antibodies were purchased from Abcam Biotechnology Co. Ltd. (USA). Anti-OPG and anti-RANKL antibodies were purchased from Bioss Biotechnology Co. Ltd. (USA). Horseradish peroxidase- (HRP-) conjugated secondary antibodies were provided by Beijing Zhongshan Golden Bridge Biotechnology Co. Ltd. (Beijing, China). Bicinchoninic acid (BCA) protein assay kit and Chemiluminescence ECL reagent were provided by Beyotime Biotechnology Co. Ltd. (Shanghai, China). The mouse polymer method detection kit was purchased from Beijing Zhongshan Golden Bridge Biotechnology Co. Ltd. (Beijing, China). TRIzol Reagent and Reverse Transcription kit were provided by Thermo Fisher Biotechnology Co. Ltd. (USA). PCR SYBR Green Master Mix was provided by Promega Biotechnology Co. Ltd. (USA). The commercial TRAP kit was provided by Sigma Biotechnology Co. Ltd. (Missouri, USA).

2.3. Animals and Study Design. Fifty-six male New Zealand white rabbits (6 months old) weighing approximately 2.5 kg were provided by the Laboratory Animal Center of Beijing Keyu Technology Co., Ltd. (Beijing, China). Rabbits were acclimatized for one week before the experiment began and were given unlimited food and water. Animals were raised in separate cages, with the temperature and humidity maintained at (22 ± 2)°C and 50%–60%, respectively. The rabbits were randomly divided into 8 groups as follows: KOA induced by immobilization for 4 or 6 weeks with vehicle treatment (4w model group, $n = 7$; 6w model group, $n = 7$), blank control group compared with the 4w or 6w Model group with vehicle treatment (4w control group, $n = 7$; 6w control group, $n = 7$), KOA induced by immobilization for 4 weeks or 6 weeks with acupotomy treatment (4w acupotomy group, $n = 7$; 6w acupotomy group, $n = 7$), and KOA induced by immobilization for 4 weeks or 6 weeks with electroacupuncture treatment (4w electroacupuncture group, $n = 7$; 6w electroacupuncture group, $n = 7$).

2.4. Induction of KOA Rabbits. The modified Videman method was performed to induce the KOA model. Before the

operation, each rabbit was fasted and deprived of water for 10 to 16 hours; then, the rabbits were anesthetized by intravenous injection of 3% sodium pentobarbital (30 mg/kg) into the ear marginal vein. After anesthesia was completed, each rabbit was posited supinely on the operating table with the left hind leg exposed. The left hind leg was fixed with the resin bandage from the groin to the toe to maintain the extended position of the knee joint, and additional double layers of orthopedic casting tapes were wrapped to reinforce the fixation; the antibiting bandage was then applied at the outermost layer. During the immobilization period, extremity swelling and mold shedding were observed at all times, adjusting and refixing as necessary. The KOA model was established after effective immobilization for 4 weeks in the 4w model group, the 4w acupotomy group, and the 4w electroacupuncture group, and for 6 weeks in the 6w model group, the 6w acupotomy group, and the 6w electroacupuncture group. Rabbits in the 4w/6w control group did not undergo any operation.

2.5. Acupotomy and Electroacupuncture Interventions. After removing the bandages in the 4w/6w acupotomy groups, acupotomy intervention was performed once a week for 3 weeks. We selected four points as the fixed intervention points, located at the tendons of vastus medialis, vastus lateralis, rectus femoris, and biceps femoris. In addition, 1-2 knot nodes of muscle fibers in the extensor and flexor groups around the knee joint were selected according to individual conditions. After routine disinfection, the acupotome was pierced to release these points. The specific operations on each point were as follows. (1) The acupotome was inserted into the tendons by vertical insertion into the skin, and the blade of the acupotome was parallel to the longitudinal axis of the tendons. The local adhesion to the direction of tendons and bone connection was released by longitudinal dredging and transverse stripping, with 1-2 strikes per point; then, pressing the points for several minutes after the acupotome was withdrawn. (2) The acupotome was inserted into the knot nodes of muscle fibers by searching and locating the knot nodes of muscle fibers around the knee joint by palpation. The acupotome was inserted into the skin vertically, and the blade of the acupotome was parallel to the longitudinal axis of the muscle fibers. The local adhesion was released by longitudinal dredging and transverse stripping, with 1-2 strikes per point; then, pressing the points for several minutes after the acupotome was withdrawn.

After removing the bandages in the 4w/6w electroacupuncture groups, electroacupuncture intervention was performed every other day for 3 weeks. We selected four acupoints as the needle insertion points, namely, Xuehai (SP10), Liangqiu (ST34), Neixiyan (EX-LE4), and Waixiyan (EX-LE5). After routine disinfection, the needles were inserted into the four acupoints. Electroacupuncture intervention was performed with Han's acupoint nerve stimulator, which connected SP10 and ST34, EX-LE4 and EX-LE5, respectively. Waveforms with dense and dense waves: frequency 2/100 Hz, intensity 3 mA, 15 min each. In the 4w/6w control groups and 4w/6w model groups, only

grabbing and fixing were administered. Animals were humanely sacrificed after the indicated intervention.

2.6. Cartilage Histology and Mankin Score. The cartilage-subchondral bone complex samples of the central weight-bearing area of the femur were fixed in 4% paraformaldehyde (Boster, Wuhan, China) for 24 hours at 4°C. All the samples were decalcified in neutral 10% EDTA (Boster, Wuhan, China) for 4 weeks. All samples were embedded in paraffin after dehydration with gradient alcohol and submersion in xylene and paraffin. The paraffin-embedded samples were sectioned from the sagittal position into 5 μ m thick sections. For histological analysis of cartilage, the sections were stained with safranin O and fast green (Solarbio, Beijing, China). The sections were evaluated for pathology of cartilage degeneration with a modified Mankin scoring system [25] by a double-blinded, independent pathologists.

2.7. Subchondral Bone Morphometric Parameter Calculation. To analyze the morphometric parameters of subchondral bone, the sections were stained with hematoxylin and eosin (HE) (Solarbio, Beijing, China) using standard protocols. Five fields were taken from each section and photographed under an optical microscope. Bone tissue static parameters including tissue area (T.Ar), trabecular area (Tb.Ar), and trabeculae perimeter (Tb.Pm) were performed using Image pro plus 6.0 (IPP) software. According to the T.Ar, Tb.Ar, and Tb.Pm data, the following parameters were quantified to represent the bone structure: percent of trabecular area (BV/TV), trabecular number (Tb.N), and trabecular separation (Tb.Sp) using bone histomorphometry [26].

2.8. Tartrate-Resistant Acid Phosphatase (TRAP) Staining. The osteoclast biomarker TRAP was applied to visualize the activity of osteoclasts. The sections were stained with a commercial TRAP kit according to the standard protocols. In general, after dewaxing with xylene and reconstituting with gradient ethanol, the sections were fixed with TRAP fixative solution at 4°C for 90 seconds and then incubated with an AS-BI Buffer, GBC staining solution, and TRAP Buffer mixture at 37°C for 60 min. Nuclei were counterstained for 2 min in hematoxylin solution. Three continuous sections from one sample were stained, and five fields were randomly selected from each section. TRAP-positive stained cells were quantified in subchondral bone regions.

2.9. Western Blot Analysis of OPG and RANKL. All soft tissues were stripped from the tibia. In the central weight-bearing area of the tibia, the cylindrical cartilage-subchondral bone complex tissues ($\varnothing = 8$ mm, Height = 10 mm) were intercepted with the circular drill. The cartilage was quickly separated from the subchondral bone at low temperature with a bone rongeur, and then the samples were quickly placed in liquid nitrogen. Total proteins were extracted from the subchondral bone using ultrasonication

in RIPA lysis buffer containing 1% protease inhibitor cocktails (Beyotime Biotechnology, Shanghai, China), and then the protein concentrations were calculated with a bicinchoninic acid (BCA) protein assay kit (Beyotime Biotechnology, Shanghai, China). Equal quantities (50 μ g) of proteins were separated by electrophoresis using 12% sodium dodecyl sulfate-polyacrylamide electrophoresis (SDS-PAGE) (Solarbio, Beijing, China) gels and then transferred to 0.45 μ m PVDF membranes (Millipore, USA). Subsequently, the membranes were blocked with 5% nonfat milk for 2 hours at room temperature (RT) and then incubated with primary antibodies against OPG (1:500), RANKL (1:500), and GAPDH (1:1000) on a shaker at 4°C overnight. After washing in TBST, the membranes were incubated with horseradish peroxidase- (HRP-) conjugated secondary antibodies for 1 hour at RT. Finally, the bands were emerged with chemiluminescence ECL reagent. The grayscale value of the protein bands was analyzed using Image J software (Rockville, USA).

2.10. Real-Time PCR Analysis of OPG, RANKL, and Ctsk. The method of obtaining subchondral bone samples was the same as described above. Total RNA was extracted from the subchondral bone using TRIzol Reagent. RNA was reverse-transcribed into cDNA using the reverse transcription kit. For real-time PCR, cDNA amplification was handled using qPCR SYBR Green Master Mix. Based on the published sequences, specific PCR primers for OPG, RANKL, and Cathepsin K (Ctsk) were constructed. The relative expression of the target genes was calculated by the $2^{-\Delta\Delta C_t}$ method and normalized to the mRNA expression of GAPDH. Primer pairs were 5'-ATCATTGAATGGACAACCCAGG-3' and 5'-TGCCTGGCTTCTCTGTTTCC-3' for OPG, 5'-GGTTCCCATAAAGTGAGTCTGT-3' and 5'-TTAAAAGCCCCAAAGTATG-3' for RANKL, and 5'-CTTCCAATACGTGCAGCAGA-3' and 5'-TCTTCAGGGCTTTCTCGTTC-3' for Ctsk, and 5'-CCACTTTGTGAAGCTCATTTCC-3' and 5'-TCGTCCTCCTCTGGTGCTCT-3' for GAPDH, respectively.

2.11. Immunohistochemistry Analysis of OPG, RANKL, OCN, and MMP-9. Paraffin-embedded samples were prepared to detect the distribution of OPG, RANKL, osteocalcin (OCN) and matrix metalloproteinases-9 (MMP-9) in subchondral bone. Immunohistochemical staining was carried out using standard protocols. Briefly, the sections sustained the heat-induced antigen retrieval in citrate buffer (Solarbio, Beijing, China) for 15 min, incubated with anti-OPG, anti-RANKL, anti-OCN, or anti-MMP-9 primary antibodies overnight, incubated with HRP-conjugated secondary antibody for 20 min, and developed using the chromogenic reaction (brown) with DAB (Solarbio, Beijing, China) in the dark for 5–8 min. Five fields were randomly selected for each section. The sections stained with OPG and RANKL were counted to determine the number of positively stained cells, and the average optical densities of OCN and MMP-9 were calculated.

2.12. Statistical Analysis. Statistical analysis was performed with SPSS software (version 20.0, SPSS, Inc., Chicago, IL, USA) and was presented as the mean \pm SD. Multiple comparisons of differences between groups were achieved by the least significant difference (LSD) test, and those among multiple groups were assessed by performing one-way ANOVA. Differences were regarded as statistically significant at $P < 0.05$ and $P < 0.01$.

3. Results

3.1. Acupotomy Intervention Alleviated KOA Cartilage Damage. Safranin O-Fast Green staining detected no pathological erosion in the superficial cartilage in the 4w/6w control group (Figures 1(A1) and 1(B1)). In the 4w model group, the content of proteoglycan decreased in the cartilage, which was manifested by the partial deletion of Safranin O staining. Obvious cracks, fibrosis, and a disordered arrangement of chondrocytes were detected in the superficial cartilage (Figure 1(A2)). In the 6w model group with extensive exfoliation, prominent reduction of chondrocytes, continuous extension of fractures, and marked atrophy and necrosis of chondrocytes, large-scale deletion of Safranin O staining was detected in the superficial cartilage (Figure 1(B2)). The reduced deletion of Safranin O staining, relief of the disordered chondrocyte arrangement, and few cracks and fibrosis in the superficial cartilage were observed in the 4w/6w acupotomy compared with the corresponding 4w/6w model group (Figures 1(A3) and 1(B3)). No significant changes in the deletion of Safranin O staining, relief of disordered chondrocyte arrangement, reduction of chondrocyte loss, atrophic chondrocytes and cracks in the superficial cartilage were observed in the 4w/6w electroacupuncture compared with the corresponding 4w/6w model group (Figures 1(A4) and 1(B4)). However, deletion of Safranin O staining was significantly reduced in the 4w/6w acupotomy groups compared with the corresponding 4w/6w electroacupuncture groups. Moreover, the Mankin score results revealed that it was significantly increased in the 4w/6w model group ($P < 0.01$) compared with the corresponding 4w/6w control group, while it was significantly decreased ($P < 0.01$) in the 4w/6w acupotomy and electroacupuncture compared with the corresponding 4w/6w model groups (Figure 1(c)). Furthermore, it was significantly decreased ($P < 0.01$) in the 4w/6w acupotomy compared with the 4w/6w electroacupuncture groups (Figure 1(c)). These results suggested that both acupotomy and electroacupuncture interventions alleviated the cartilage damage in the KOA rabbits. The earlier the intervention, the better the effect. Moreover, the protective effect of acupotomy on KOA cartilage was better than that of electroacupuncture.

3.2. Acupotomy Intervention Inhibited Subchondral Bone Loss in KOA Rabbits. The subchondral bone morphometric parameters calculated by HE stained sections are presented in Figures 2(a) and 2(b). Tb.Ar, Tb.Pm, Tb.N, and BV/TV were markedly decreased, and Tb.Sp was markedly increased in the 4w/6w model group ($P < 0.01$) compared with the

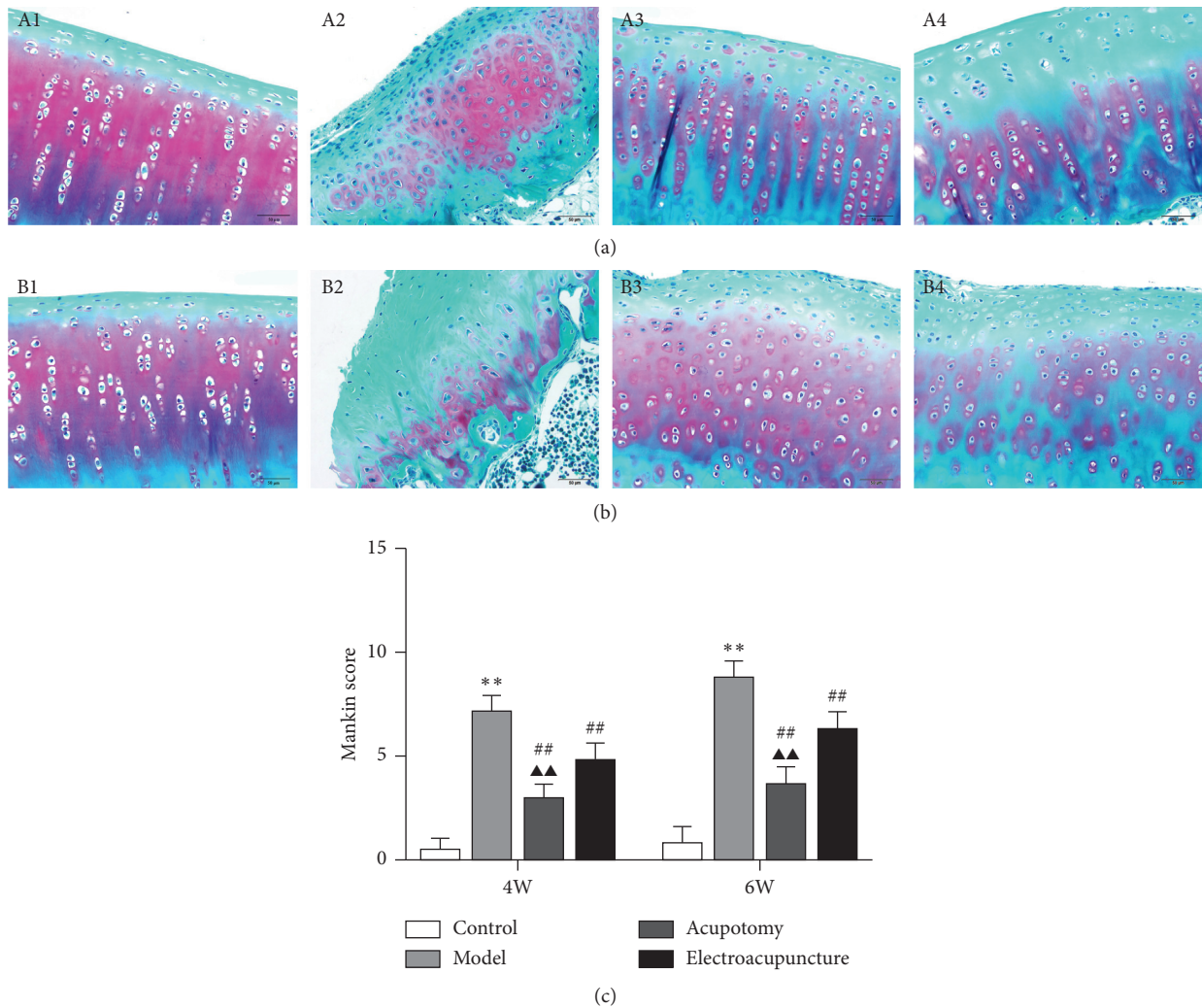
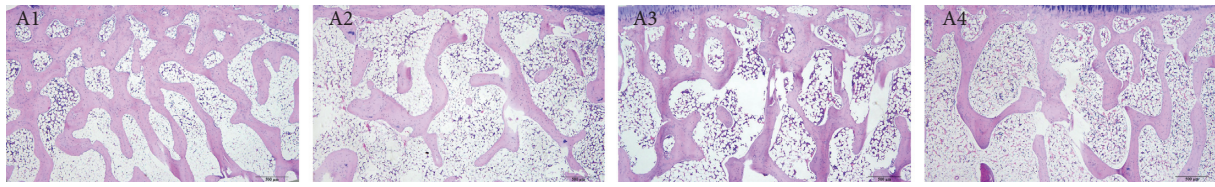


FIGURE 1: Acupotomy intervention alleviated KOA cartilage damage. (a) (b) Staining of cartilage with Safranin O-Fast green (magnification $\times 400$). A1: 4w control group, A2: 4w model group, A3: 4w acupotomy group, A4: 4w electroacupuncture group; B1: 6w control group, B2: 6w model group, B3: 6w acupotomy group, B4: 6w electroacupuncture group. (c) Analysis of the Mankin score. Values are means \pm SEMs. $n = 6$ per group. Compared with the corresponding control group: * $P < 0.05$ and ** $P < 0.01$; compared with the corresponding model group: # $P < 0.05$ and ## $P < 0.01$; compared with the corresponding electroacupuncture group: $\blacktriangle P < 0.05$ and $\blacktriangle\blacktriangle P < 0.01$.

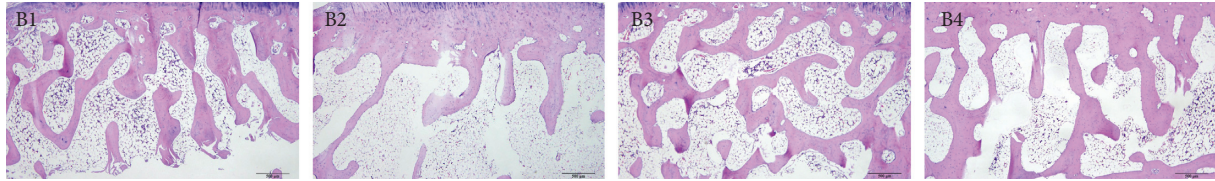
corresponding 4w/6w control group, while Tb.Ar, Tb.Pm, Tb.N, and BV/TV were significantly increased ($P < 0.01$) and Tb.Sp significantly decreased in the 4w/6w acupotomy and electroacupuncture compared with the corresponding 4w/6w model groups. Moreover, except for Tb.Ar in the 6w acupotomy group, Tb.Ar, Tb.Pm, Tb.N, and BV/TV were markedly increased and Tb.Sp markedly decreased in the 4w/6w acupotomy group ($P < 0.01$) compared with the corresponding 4w/6w electroacupuncture group (Figures 2(c), 2(d), and 2(f)–2(h)). These data indicated that in KOA rabbits induced by immobilization for 4 weeks, lesions began to appear in the microstructure of subchondral bone, mainly manifested as trabecular destruction and bone mass reduction, which were gradually aggravated until model establishment for 6 weeks. After acupotomy or electroacupuncture intervention, the relevant parameters of subchondral bone structure were significantly altered, indicating that both interventions could effectively inhibit the

subchondral bone resorption of KOA rabbits. Apparently, acupotomy can better inhibit the hyperactive bone resorption in KOA subchondral bone.

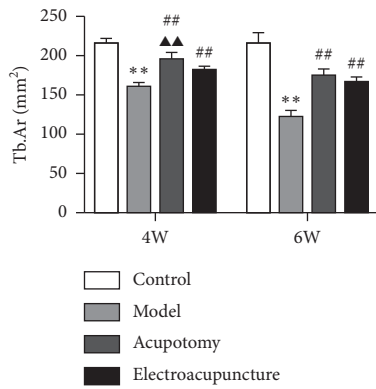
3.3. Acupotomy Intervention Enhanced Osteoblast Activity in KOA Subchondral Bone. Immunohistochemical analysis detected low expression of OCN in subchondral bone in the 4w/6w control group (Figures 3(A1) and 3(B1)). Both 4w and 6w model groups showed higher expression of OCN ($P < 0.01$) compared with the 4w and 6w control group (Figures 3(A2) and 3(B2)). As expected, the expression of OCN in the 4w/6w acupotomy and electroacupuncture groups was markedly higher ($P < 0.01$) than in the corresponding 4w/6w model group, while it was significantly increased ($P < 0.01$, $P < 0.05$) in the 4w/6w acupotomy group compared with the 4w/6w electroacupuncture group (Figures 3(A3)–3(A4) and 3(B3)–3(B4)). These results



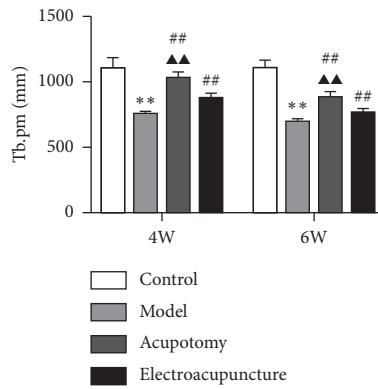
(a)



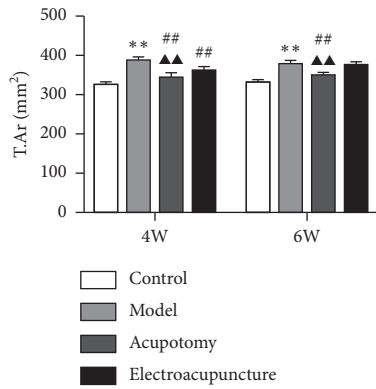
(b)



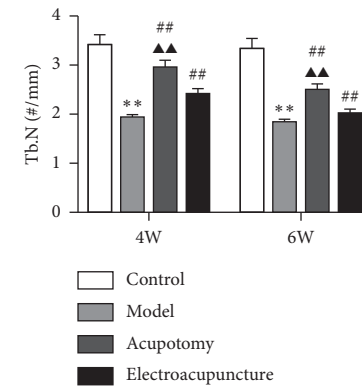
(c)



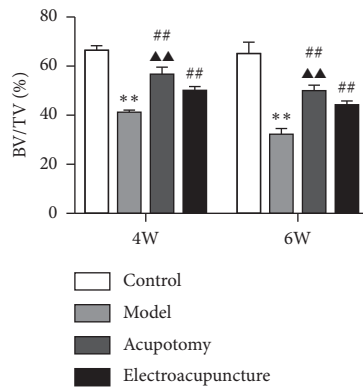
(d)



(e)



(f)



(g)

FIGURE 2: Continued.

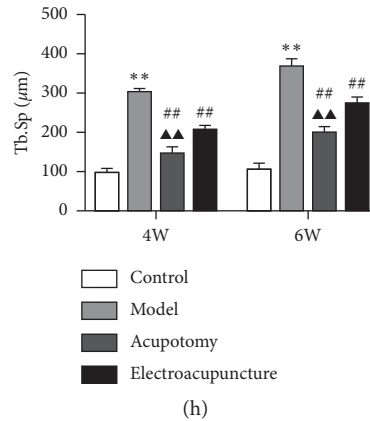


FIGURE 2: Acupotomy intervention inhibited subchondral bone loss in KOA rabbits. (a) (b) HE staining of subchondral bone (magnification $\times 40$). A1: 4w control group, A2: 4w model group, A3: 4w acupotomy group, A4: 4w electroacupuncture group; B1: 6w control group, B2: 6w model group, B3: 6w acupotomy group, B4: 6w electroacupuncture group. (c) Analysis of Tb.Ar in subchondral bone. (d) Analysis of Tb.pm in subchondral bone. (e) Analysis of T.Ar in subchondral bone. (f) Analysis of Tb.N in subchondral bone. (g) Analysis of BV/TV in subchondral bone. (h) Analysis of Tb.Sp in subchondral bone. Values are means \pm SEMs. $n = 6$ per group. Compared with the corresponding control group: * $P < 0.05$ and ** $P < 0.01$; compared with the corresponding model group: # $P < 0.05$ and ## $P < 0.01$; compared with the corresponding electroacupuncture group: ▲ $P < 0.05$ and ▲▲ $P < 0.01$.

indicated that OCN was compensatorily activated in the KOA damaged subchondral bone. The upregulation of OCN after the acupotomy or electroacupuncture intervention indicated that both delayed bone resorption by enhancing osteoblast activity of KOA subchondral bone. Acupotomy intervention could clearly better enhance osteoblast activity by upregulating OCN expression in KOA subchondral bone.

3.4. Acupotomy Intervention Suppressed the Activity of Osteoclasts in KOA Subchondral Bone. The MMP-9 immunohistochemical staining results were consistent with the TRAP staining results. TRAP-positive and MMP-9-positive cells were occasionally observed in the subchondral bone in the 4w/6w control group (Figures 4(A1)–4(D1)). The number of TRAP-positive cells and MMP-9-positive cells in subchondral bone was significantly increased in the 4w/6w model group ($P < 0.01$) compared with the corresponding 4w/6w control group. It was apparent from the results that the number of TRAP-positive and MMP-9-positive cells increased in a more pronounced manner in the 6w model group, indicating the occurrence of more robust subchondral bone resorption (Figures 4(A2)–4(D2)). Both the 4w/6w acupotomy and electroacupuncture groups showed significantly lower ($P < 0.01$) expression of TRAP and MMP-9 compared with the corresponding 4w/6w model groups. Moreover, the expression of TRAP and MMP-9 in the 4w/6w acupotomy group was markedly lower ($P < 0.01$) than in the corresponding 4w/6w electroacupuncture group (Figures 4(A3)–4(D3) and 4(A4)–4(D4)). The expression of Ctsk mRNA further confirmed the results. However, there was no difference ($P > 0.05$) in the expression of Ctsk mRNA between the 4w/6w acupotomy and electroacupuncture groups (Figure 4(g)). These results indicated that TRAP, MMP-9, and Ctsk were overexpressed in the subchondral bone of immobilization-induced KOA rabbits, which

signified that the osteoclasts were highly active and that bone remodeling had occurred mainly with bone resorption. By downregulating the expression of TRAP, MMP-9, and Ctsk, acupotomy or electroacupuncture intervention inhibited the activity of osteoclasts to suppress subchondral bone resorption.

3.5. Acupotomy Intervention Regulated the OPG/RANKL Pathway in KOA Subchondral Bone. Changes in the expression of OPG and RANKL were quantified using real-time PCR, Western blot and immunohistochemistry. The results of the real-time PCR assay demonstrated that mRNA expression of OPG was significantly decreased ($P < 0.01$, $P < 0.05$) in the 4w/6w model group compared with the corresponding 4w/6w control group, while it was significantly increased ($P < 0.01$) in the 4w/6w acupotomy and electroacupuncture groups compared with the 4w/6w model group. However, acupotomy intervention further effectively promoted the mRNA expression of OPG ($P < 0.01$) compared with electroacupuncture intervention (Figure 5(a)). As expected, mRNA expression of RANKL in the 4w/6w model group was significantly increased ($P < 0.01$) compared with the corresponding 4w/6w control group, while it was significantly decreased ($P < 0.01$) in the 4w/6w acupotomy and electroacupuncture groups compared with the 4w/6w model group. Acupotomy intervention further effectively suppressed the mRNA expression of RANKL ($P < 0.01$, $P < 0.05$) compared with electroacupuncture intervention (Figure 5(b)). The immunohistochemical staining of OPG and RANKL further confirmed the results (Figure 6). The expression levels of OPG and RANKL proteins were consistent with those of mRNA results between the 4w/6w model and control groups. Only OPG protein expression was significantly upregulated ($P < 0.05$) between the 4w acupotomy and 4w model group, while there was no difference ($P > 0.05$) between the 6w acupotomy group and 6w

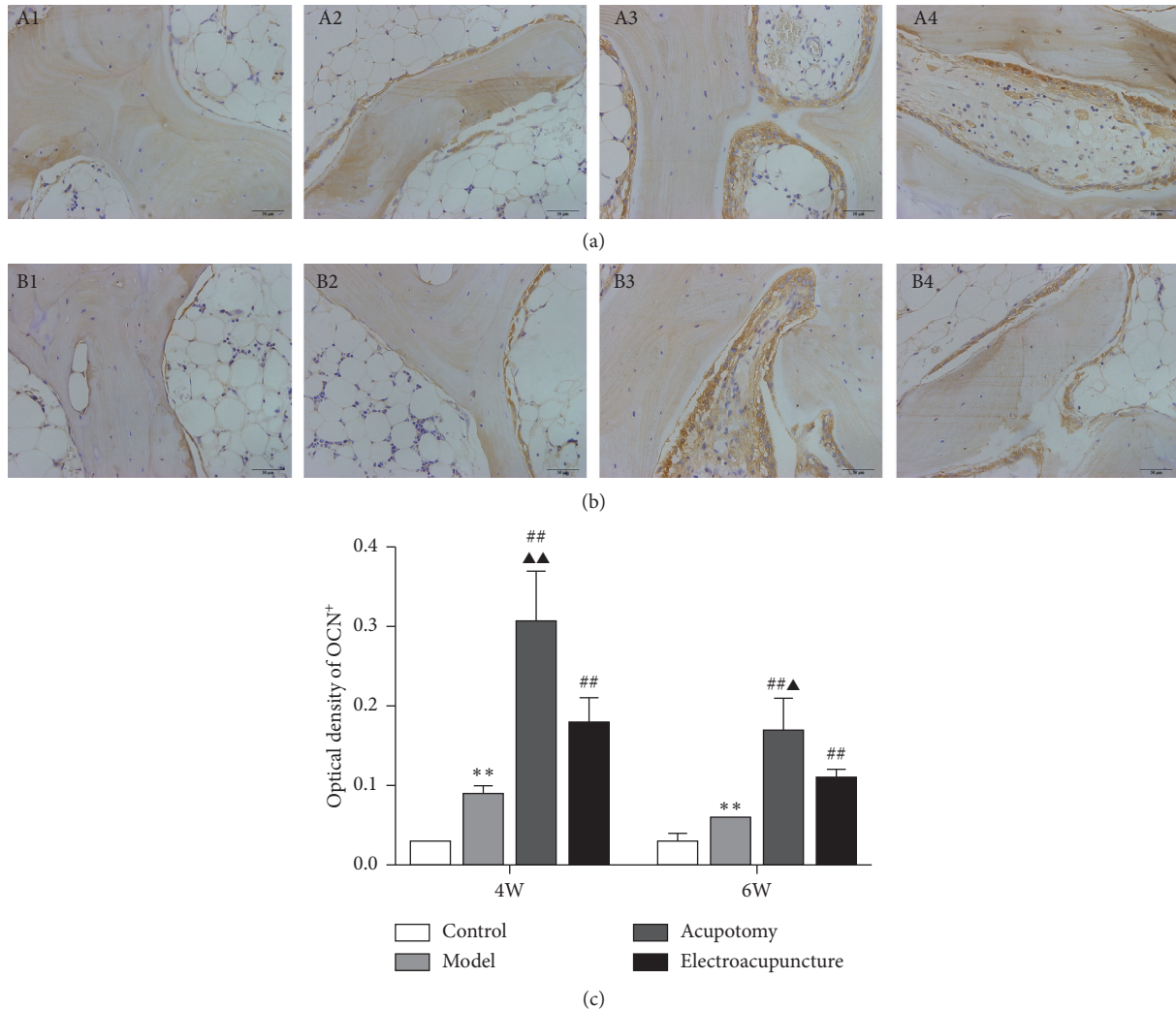


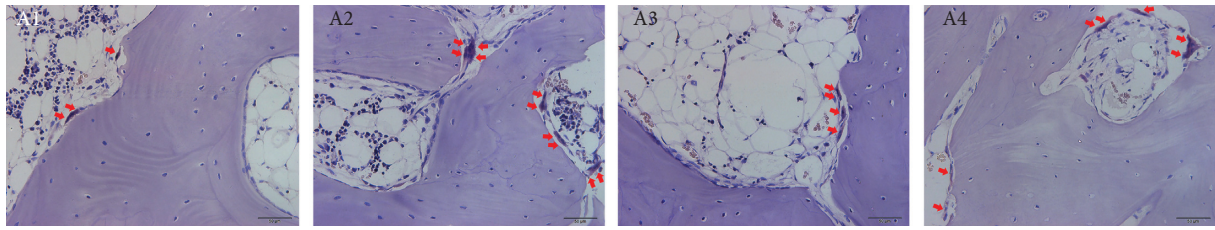
FIGURE 3: Acupotomy intervention enhanced the expression of OCN in KOA subchondral bone. (a, b) Immunohistochemical staining of OCN (magnification $\times 400$). A1: 4w control group, A2: 4w model group, A3: 4w acupotomy group, A4: 4w electroacupuncture group; B1: 6w control group, B2: 6w model group, B3: 6w acupotomy group, B4: 6w electroacupuncture group. (c) Optical density values of OCN. Values are means \pm SEMs. $n = 6$ per group. Compared with the corresponding control group: * $P < 0.05$ and ** $P < 0.01$; compared with the corresponding model group: # $P < 0.05$ and ## $P < 0.01$; compared with the corresponding electroacupuncture group: ▲ $P < 0.05$ and ▲▲ $P < 0.01$.

model group. There was no difference ($P > 0.05$) in OPG protein expression between the 4w/6w electroacupuncture group and the 4w/6w model group. OPG protein expression also did not significantly differ ($P > 0.05$) in the 4w/6w acupotomy and electroacupuncture groups (Figures 5(c)–5(e)). RANKL protein expression was significantly decreased ($P < 0.01$) in the 4w/6w acupotomy and 6w electroacupuncture groups compared with the 4w/6w model group. Only RANKL protein expression was significantly decreased ($P < 0.05$) in the 6w acupotomy group compared with the 6w electroacupuncture group (Figures 5(c), 5(d), and 5(f)). The immunohistochemistry and Western blot results also showed that the ratio of OPG/RANKL significantly decreased in the 4w/6w model group compared with the 4w/6w control group (Figures 5(g) and 6(g)), indicating highly active osteoclasts in KOA subchondral bone and strong bone resorption. The ratio of OPG/RANKL was also significantly

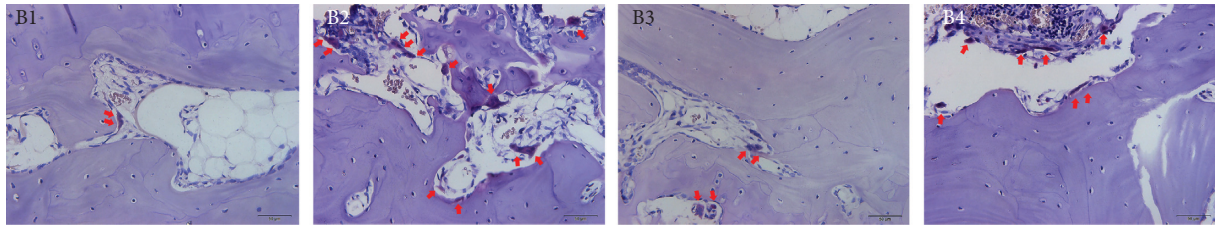
increased in the 4w/6w acupotomy compared with the 4w/6w model group. These results suggested that acupotomy inhibition of subchondral bone resorption might be exerted by reducing the activity of osteoclasts via the OPG/RANKL pathway in KOA rabbits.

4. Discussion

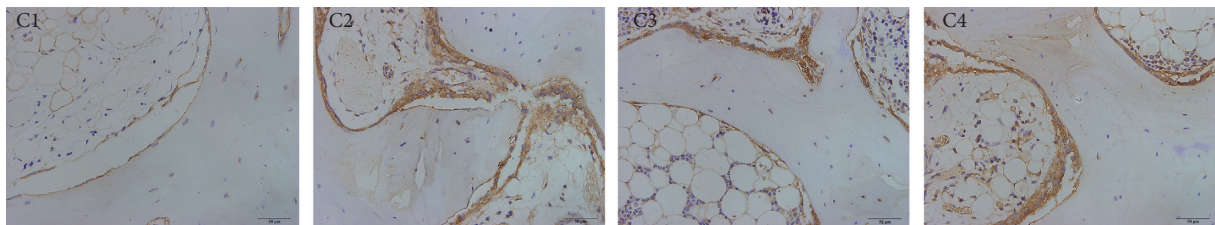
Subchondral bone lesions play an indispensable effect in the KOA process, which is thought to be crucial for accelerating cartilage degeneration. Under physiological conditions, the subchondral bone serves as a mechanical support for articular cartilage, which can buffer and disperse mechanical stress from the joint to prevent cartilage injury by localized stress concentration [27]. Continuously abnormal mechanical load induced by KOA in the knee joint is the most common initiator of subchondral bone lesions [10]. When



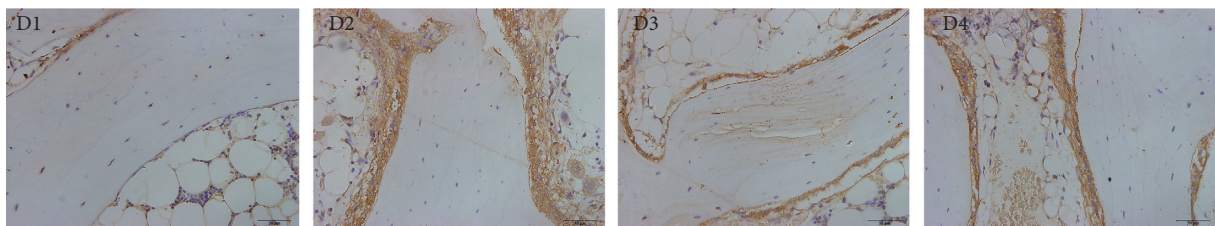
(a)



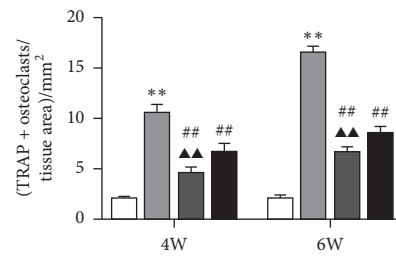
(b)



(c)



(d)



(e)

FIGURE 4: Continued.

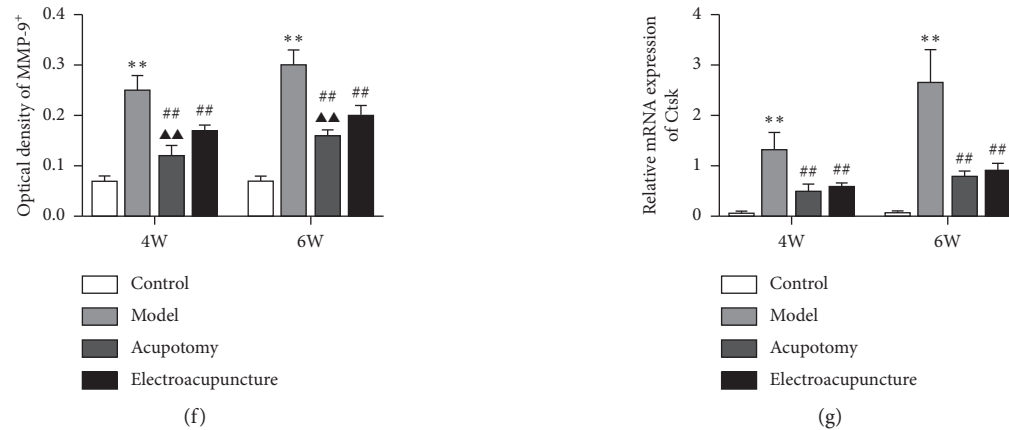


FIGURE 4: Acupotomy intervention suppressed the expression of TRAP, MMP-9, and Ctsk in KOA subchondral bone. (a, b) TRAP staining (magnification $\times 400$). A1: 4w control group, A2: 4w model group, A3: 4w acupotomy group, A4: 4w electroacupuncture group; B1: 6w control group, B2: 6w model group, B3: 6w acupotomy group, B4: 6w electroacupuncture group. (c, d) Immunohistochemical staining of MMP-9 (magnification $\times 400$). C1: 4w control group, C2: 4w model group, C3: 4w acupotomy group, C4: 4w electroacupuncture group; D1: 6w control group, D2: 6w model group, D3: 6w acupotomy group, D4: 6w electroacupuncture group. (e) The analysis of TRAP-positive cells in subchondral bone. (f) Optical density values of MMP-9. (g) Real-time PCR analysis of Ctsk. Values are means \pm SEMs. $n = 6$ per group. Compared with the corresponding control group: * $P < 0.05$ and ** $P < 0.01$; compared with the corresponding model group: # $P < 0.05$ and ## $P < 0.01$; compared with the corresponding electroacupuncture group: $\blacktriangle P < 0.05$ and $\blacktriangle\blacktriangle P < 0.01$.

this abnormal mechanical load exceeds the physiological endurance of the subchondral bone, it will eventually lead to subchondral bone microfracture and initiate bone remodeling [28]. Subchondral bone lesions will weaken its mechanical strength and the ability to buffer mechanical stress accordingly [29], which increases the risk of cartilage injury and accelerates the KOA process. Previous studies have found that the increased subchondral bone loss was positively correlated with the level of cartilage erosion in KOA [30, 31].

Promoting the repair of damaged cartilage remains the core of KOA therapy. Strategies were proposed to alleviate KOA cartilage degeneration by inhibiting subchondral bone remodeling, including estrogens, bisphosphonates, strontium ranelate, and cathepsin K inhibitors. However, the present clinical efficacy of bone metabolism therapy still has certain limitations. The currently available anti-osteoporotic drugs can improve the radiographic structure of subchondral bone by inhibiting bone resorption to a certain extent, but none of them can retard the progress of KOA in clinical practice [12]. The role of mechanical load in subchondral bone remodeling and injury repair has been of gradual concern. Studies have shown that a suitable mechanical load can effectively inhibit KOA-induced subchondral bone osteoporosis and decrease bone mass [32–34], thereby retarding KOA procession. Based on evidence showing that mechanical loads were involved in the pathogenesis in bones and regulated bone remodeling [35, 36], biomechanical therapy has become an emerging method for KOA treatment by affecting subchondral bone. However, whether acupotomy as biomechanical therapy is sufficient to prevent or reverse KOA-induced subchondral bone lesions has not been directly investigated. The biomechanical effects of acupotomy have been confirmed in our preliminary studies [21–24]. It is well known that muscle

dysfunction, characterized by weakened muscle strength and reduced coordination of muscle groups, is a crucial cause of KOA knee mechanical imbalance [37]. We chose tendons around the knee as the acupotomy intervention points to correct the abnormal mechanical environment in the knee joint by regulating the mechanical function of muscle-tendons, followed by effectively activating integrin $\beta 1$ [22], the crucial mechanical receptor of chondrocytes, and the downstream FAK-PI3K mechanical signaling pathway [21], which inhibited the degradation of the chondrocyte extracellular matrix and promoted chondrocyte proliferation in KOA rabbits [24]. Can this intra-articular benign mechanical load ameliorate KOA subchondral bone lesions through the OPG/RANKL mechanical signaling pathway after acupotomy intervention? Does the inhibition of benign mechanical loading on subchondral bone remodeling contribute to chondroprotective effects of acupotomy?

Immobilization of the knee joint is a widely used method for KOA model induction [38], which has been applied in research on acupuncture treatment of KOA. In previous studies, we found that immobilization of the knee joints of rabbits induced joint rigidity, as measured by passive range of motion (PROM), and the cartilage eroded integrally with extensive bone marrow edema in subchondral bone as observed by MRI [24], accompanied by reduced expression of COL-II and Aggrecan in cartilage [21]. Further, cartilage oligomeric matrix protein (COMP), the biomarker of KOA cartilage degradation, markedly increased in the serum of rabbits [24], which was consistent with the changes in serum COMP observed in KOA patients [39]. In this study, obvious cartilage erosion, significant deletion of Safranin O staining, and subchondral bone destruction were observed after 4 or 6 weeks of immobilization. These indicators suggested that OA-like cartilage lesions and subchondral bone destruction could be duplicated in rabbits with immobilized knee joints

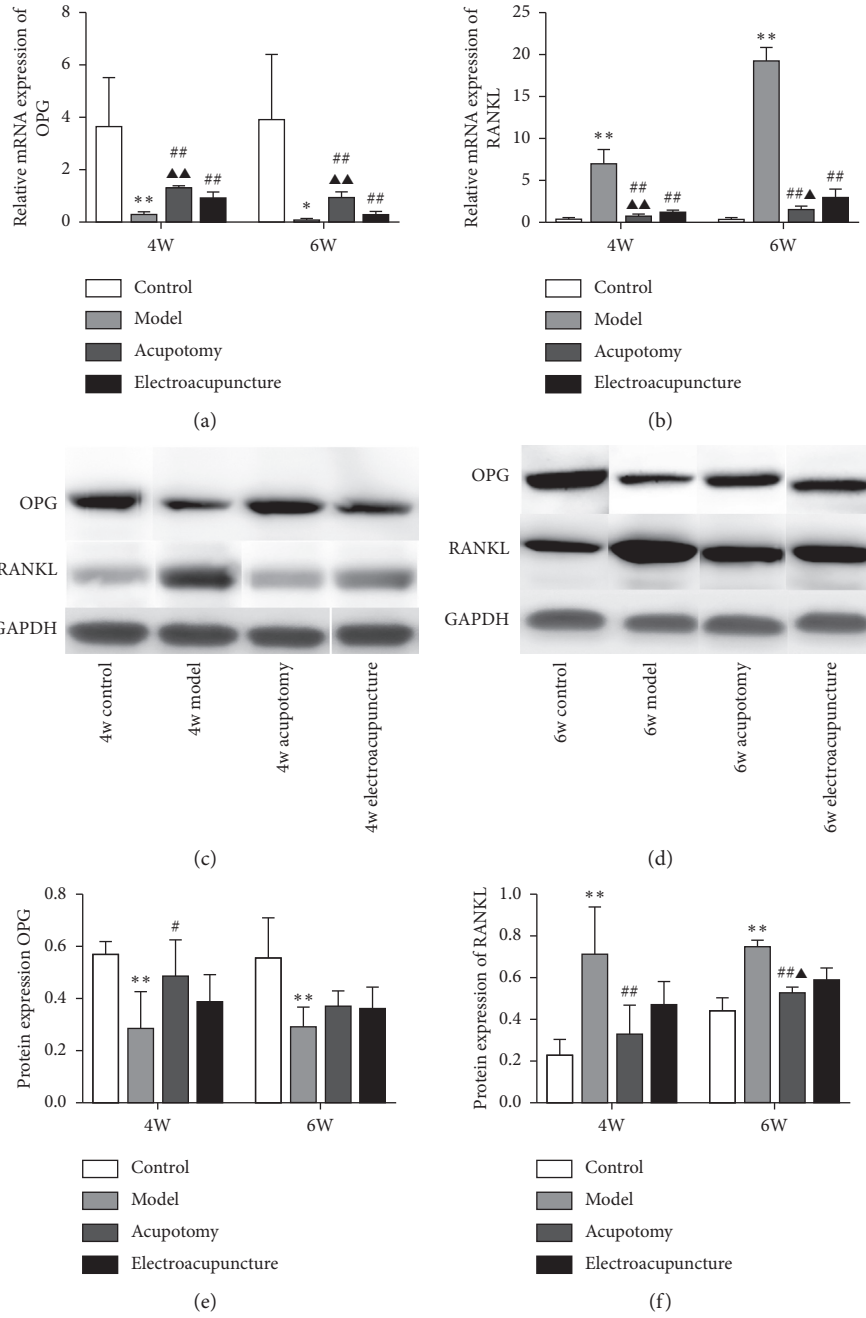


FIGURE 5: Continued.

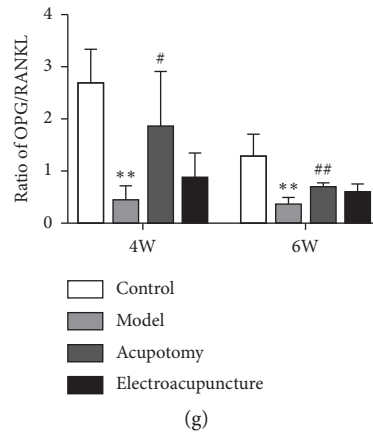


FIGURE 5: Acupotomy intervention upregulated the expression of OPG and downregulated the expression of RANKL in KOA subchondral bone measured by real-time PCR and Western blot. (a, b) Real-time PCR analysis of OPG and RANKL. (c–f) Western blot assay of OPG and RANKL. (g) Ratio of OPG/RANKL measured by Western blotting. Values are means \pm SEMs. $n=6$ per group. Compared with the corresponding control group: * $P < 0.05$ and ** $P < 0.01$; compared with the corresponding model group: # $P < 0.05$ and ## $P < 0.01$; compared with the corresponding electroacupuncture group: $\blacktriangle P < 0.05$ and $\blacktriangle\blacktriangle P < 0.01$.

similar to the phenomena observed in human clinical cases (Figure 1).

Evidence shows that cartilage surface defects, deletion of Safranin O staining, and disorder of the chondrocyte arrangement, as determined by morphological observation, gradually worsened in KOA cartilage induced by immobilization for 4 and 6 weeks; these symptoms were accompanied by a continuous increase in the Mankin score, indicating the rapid development of KOA. We found that both the acupotomy and electroacupuncture intervention successfully protected against cartilage degeneration and effectively decreased the Mankin score. However, the enhancement of correction of the abnormal mechanics by acupotomy seemed to be more effective in slowing cartilage erosion, and neither intervention could fully reverse the pathological changes in cartilage. These data further support the direct effect of acupotomy and electroacupuncture on promoting KOA cartilage repair (Figure 1).

As reported previously in numerous studies, enhanced bone resorption was the most typical pathological characteristic of KOA subchondral bone [40], which was manifested by a marked decrease in Tb.N and BV/TV and a marked increase in Tb.Sp [34, 41]. The studies clarified that ameliorating the subchondral bone structure of KOA by inhibiting the decrease in Tb.N and BV/TV and the increase in Tb.Sp was an effective approach to relieve KOA cartilage degeneration [42, 43]. HE staining was used to probe into the effects of acupotomy intervention on bone structure [43]. The obvious subchondral bone destruction in the Model group showed that Tb.Ar, Tb.Pm, Tb.N, and BV/TV were significantly decreased and Tb.Sp was significantly increased. Moreover, by observing the subchondral bone changes in the KOA model induced by 4 or 6 weeks of immobilization, bone destruction gradually increased. Further research of bone structural properties proved that acupotomy or electroacupuncture-treated rabbits had observably increased BV/TV and Tb.N and decreased Tb.Sp compared with the rabbits in the Model group. However,

whether in the 4- or the 6-week group, the effect of acupotomy on subchondral bone destruction inhibition was superior. To our knowledge, this is the first study to show that acupotomy intervention in immobilization-induced KOA rabbits improves the morphometric parameters of subchondral bone, suggesting that acupotomy can inhibit KOA subchondral bone loss. According to the pathological Mankin score of cartilage in each group, the reduction of subchondral bone loss was accompanied by the improvement of cartilage damage, suggesting that acupotomy intervention alleviated KOA cartilage degeneration by inhibiting subchondral bone lesion. Compared with electroacupuncture, acupotomy shows a superior effect in suppressing KOA subchondral bone remodeling by correcting the abnormal mechanical load in the joint (Figure 2).

What are the underlying mechanisms of acupotomy intervention in suppressing subchondral bone lesions? The initiation of KOA subchondral bone remodeling is coupled with disruption of the balance between bone resorption and bone formation [44]. Osteoclasts are first activated to enhance bone resorption in the damaged bone area [3, 45]. Subchondral bone loss, characterized by decreased Tb.N and BV/TV and increased Tb.Sp, is the secondary result of hyperactive bone resorption by osteoclasts in early-stage KOA [46]. Activating osteoclasts is a central event and driving force in the pathogenesis of subchondral bone lesion, while inhibiting osteoclast activity contributes to preventing bone resorption and KOA procession [40, 47]. By combining with RANK, RANKL promotes osteoclast maturation and differentiation, and it activates signaling pathways related to osteoclastogenesis, thus promoting the expression of osteoclast-specific genes including TRAP, MMP-9, and Ctsk [48]. Studies have shown that, by downregulating the expression of MMP9, TRAP [49], and Ctsk [50], osteoclastogenesis can be inhibited and osteoclast activity can be confined to reduce KOA subchondral bone resorption. In our study, osteoclasts were typically activated, showing that the expression of TRAP and MMP-9-positive cells and Ctsk

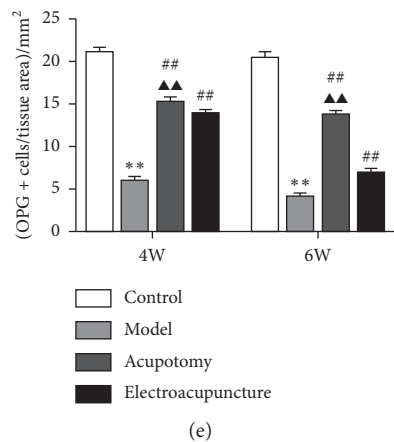
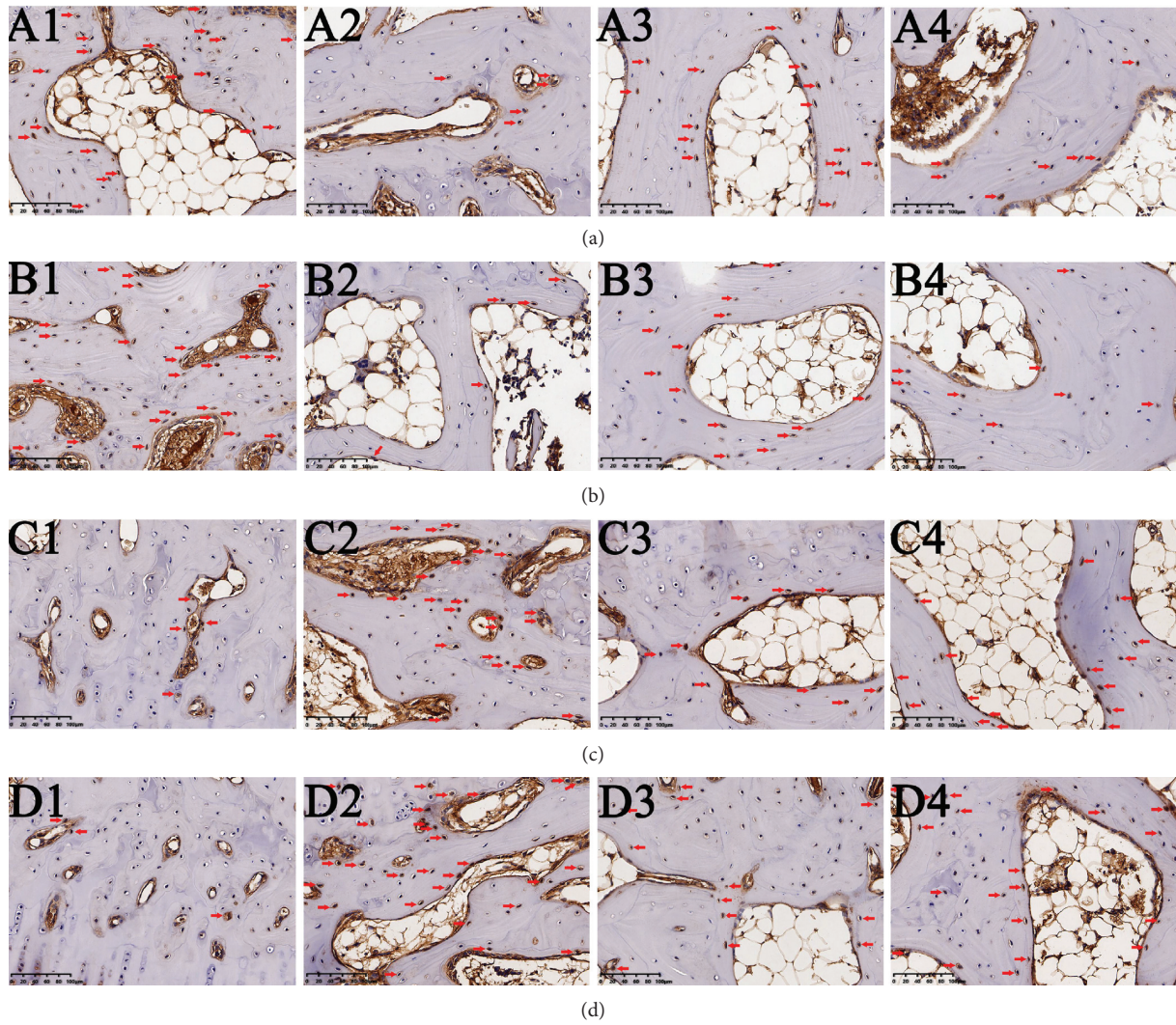


FIGURE 6: Continued.

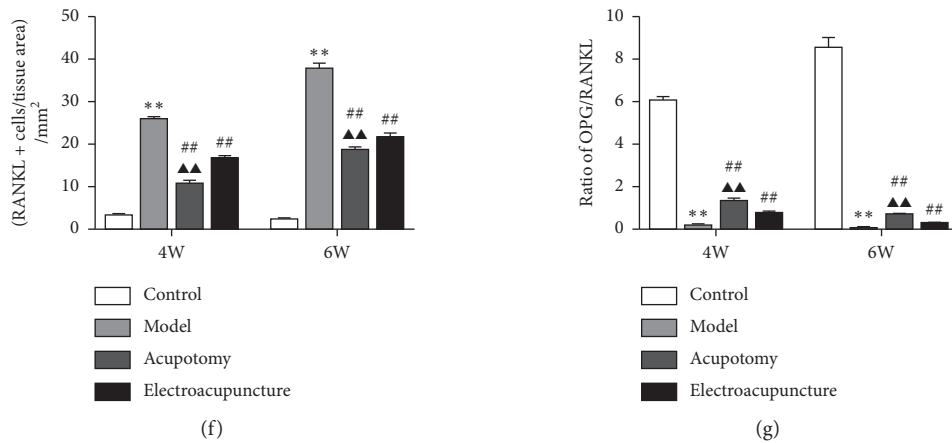


FIGURE 6: Acupotomy intervention upregulated the expression of OPG and downregulated the expression of RANKL in KOA subchondral bone measured by immunohistochemistry. (a) (b) Immunohistochemical staining of OPG (magnification $\times 200$). A1: 4w control group, A2: 4w model group, A3: 4w acupotomy group, A4: 4w electroacupuncture group; B1: 6w control group, B2: 6w model group, B3: 6w acupotomy group, B4: 6w electroacupuncture group. (c, d) Immunohistochemical staining of RANKL (magnification $\times 200$). C1: 4w control group, C2: 4w model group, C3: 4w acupotomy group, C4: 4w electroacupuncture group; D1: 6w control group, D2: 6w model group, D3: 6w acupotomy group, D4: 6w electroacupuncture group. (e) Expression of OPG-positive cells in subchondral bone. (f) Expression of RANKL-positive cells in subchondral bone. (g) Ratio of OPG/RANKL measured by immunohistochemistry. Values are means \pm SEMs. $n = 6$ per group. Compared with the corresponding control group: * $P < 0.05$ and ** $P < 0.01$; compared with the corresponding model group: # $P < 0.05$ and ## $P < 0.01$; compared with the corresponding electroacupuncture group: ▲ $P < 0.05$ and ▲▲ $P < 0.01$.

mRNA were significantly increased in subchondral bone of KOA rabbits. In addition, osteoclast activity continued to increase with extension of the immobilization, which was consistent with the variation in morphometric parameters of subchondral bone. Further analysis of the osteoclast activity indicated that acupotomy or electroacupuncture-treated rabbits had a significant reduction of TRAP and MMP-9-positive cells and Ctsk mRNA expression. In both the 4-week and 6-week immobilization-induced KOA rabbits, acupotomy was more advantageous in confining osteoclast activity than electroacupuncture. Our results further corroborated the finding that acupotomy intervention was sufficient to inhibit KOA subchondral bone lesions by downregulating the expression of MMP9, TRAP, and Ctsk to suppress osteoclast activity (Figure 4).

To further confirm that acupotomy suppressed bone resorption, expression of the osteoblast-specific gene OCN was examined. Osteoblasts are essential for bone formation, and OCN is indispensable for osteoblast differentiation [51]. The content of OCN is a direct response to osteoblast activity and the bone formation rate. Although osteoblasts were compensatorily activated in KOA subchondral bone, it was completely insufficient to reverse the continuous increase in hyperactive osteoclasts. Furthermore, with an extension of immobilization, osteoblast activity continued to decrease, as reflected by the reduction of OCN expression, suggesting that the balance between bone resorption of osteoclasts and bone formation of osteoblasts was broken in immobilization-induced KOA rabbits. A previous study has indicated that low expression of OCN is observed in KOA subchondral bone with severe bone loss, resulting in a reduction of bone formation [52], while increasing the content of OCN can effectively promote osteoblast activity in damaged bone [53]. Our study demonstrated that acupotomy and

electroacupuncture effectively promoted bone formation by activating OCN expression. In both 4-week and 6-week immobilization-induced KOA rabbits, acupotomy was more advantageous in promoting osteoblast activity than electroacupuncture. Our results further corroborate the finding that acupotomy intervention was superior for restoring the dynamic balance of osteoclastic bone absorption and osteoblastic bone formation in KOA subchondral bone (Figure 3).

How acupotomy intervention regulates osteoclast activity remains to be determined. The maturation, differentiation, and osteoclast activity were mediated by the OPG/RANKL pathway. The actions of OPG and RANKL in damaged subchondral bone have been closely investigated since elevated expression of RANKL and declining expression of OPG have been observed in KOA [54]. Studies have revealed that blockade of the increase in RANKL and decrease in OPG protects against hyperactive osteoclasts and inhibits bone resorption [55, 56]. In addition, the OPG/RANKL ratio is one of the best characterized biomarkers associated with the bone destruction pathology [57]. As reported previously in numerous studies, OPG/RANKL is a mechanically sensitive signaling pathway [58, 59]. Benign mechanical stimulation can increase the OPG/RANKL ratio in KOA subchondral bone, which effectively inhibits osteoclast activity and bone resorption [60]. Our previous studies [21] have confirmed that acupotomy intervention activates the FAK-PI3K mechanical pathway to relieve KOA cartilage degeneration by correcting abnormal mechanical stress. However, whether this benign mechanical stimulation can promote subchondral bone recovery from KOA-induced bone resorption by the OPG/RANKL pathway remains to be explored. In our study, increased expression of RANKL mRNA and protein and decreased expression of

OPG mRNA and protein were measured in KOA subchondral bone. Immobilization for 6 weeks revealed higher RANKL and lower OPG expression, suggesting an enhancement of osteoclast activity and stronger bone resorption. The results obtained with real-time PCR and immunohistochemical staining showed that acupotomy or electroacupuncture-treated rabbits had significantly decreased expression of RANKL and markedly increased expression of OPG. However, the Western blot results showed that acupotomy intervention upregulated the decrease in OPG protein and downregulated the increase in RANKL protein, while electroacupuncture intervention had a poor effect. As expected, the OPG/RANKL ratio determined by Western blotting and immunohistochemistry was roughly consistent with the expression of the osteoclast-specific genes TRAP, MMP-9, and Ctsk. These data confirmed that the benign mechanical stress after acupotomy intervention effectively inhibited the increase in RANKL and the decrease in OPG of KOA subchondral bone. Acupotomy, a biomechanical therapy, can extensively confine hyperactive osteoclasts via the OPG/RANKL mechanical signaling pathway to inhibit bone resorption in KOA subchondral bone (Figures 5 and 6).

The present study has the following limitations. First, a positive drug group was not set as the control group for acupotomy, but rather the electroacupuncture group. Based on many reports [12, 20], bone metabolism regulators represented by bisphosphonates can only inhibit subchondral bone resorption in the KOA animal model, and the efficacy in the clinic has been disappointing. Considering the use of KOA subchondral bone as the entry point to explore the mechanism of acupotomy treatment of KOA from the biomechanical perspective and to comprehensively evaluate the operability in this study, electroacupuncture may be the most appropriate control group at present. Electroacupuncture, as a usual and effective therapy, is also a nonsurgical and nonpharmacological intervention to treat KOA. Moreover, the position of the intervention points of the electroacupuncture and acupotomy is close. If there is a more feasible biomechanical therapy that can be used as a control group in the future, we will continue to conduct in-depth research. Second, we successfully established the KOA model by 6-week immobilization in the previous study, which was consistent with early and mid-stage KOA lesions. In the current study, in view of the dynamic pathological changes of subchondral bone in the development of KOA, we established immobilization-induced KOA models for 4 and 6 weeks to evaluate the therapeutic effects of acupotomy on subchondral bone lesions from the onset of KOA to early and mid-stage KOA. In subsequent studies, we should continue to extend the duration of knee immobilization to 8 or even 12 weeks to dynamically observe the regulatory effect of acupotomy on subchondral bone remodeling during the entire pathogenesis of KOA.

5. Conclusion

In summary, we found that acupotomy inhibited osteoclast activity and promoted osteoblast activity to ameliorate

hyperactive subchondral bone resorption and relieve cartilage degeneration in immobilization-induced KOA rabbits, which may be mediated by the OPG/RANKL signaling pathway. The mechanical effect of acupotomy exerts chondroprotective effects by mitigating KOA subchondral bone lesions, which might supply original insights into the treatment of KOA with acupotomy and a novel therapeutic approach in the biomechanical treatment of KOA.

Data Availability

The data supporting the conclusions of this study are available from the corresponding author upon reasonable request.

Conflicts of Interest

The authors declare no conflicts of interest.

Authors' Contributions

Tong Wang and Yan Guo contributed equally to this work.

Acknowledgments

This work was supported by research grants from the National Natural Science Foundation of China (Grant no. 81874504) and Beijing Natural Science Foundation (Grant no. 7192110).

References

- [1] R. F. Loeser, J. A. Collins, B. O. Diekmann et al., "Ageing and the pathogenesis of osteoarthritis," *Nature Reviews Rheumatology*, vol. 12, no. 7, pp. 412–420, 2016.
- [2] D. Muratovic, D. M. Findlay, F. M. Cicuttini et al., "Bone marrow lesions in knee osteoarthritis: regional differences in tibial subchondral bone microstructure and their association with cartilage degeneration," *Osteoarthritis and Cartilage*, vol. 27, no. 11, pp. 1653–1662, 2019.
- [3] K. Aso, S. M. Shahtaheri, R. Hill, D. Wilson, D. F. McWilliams, and D. A. Walsh, "Associations of symptomatic knee osteoarthritis with histopathologic features in subchondral bone," *Arthritis & Rheumatology*, vol. 71, no. 6, pp. 916–924, 2019.
- [4] J.-P. Pelletier, C. Roubille, J.-P. Raynaud et al., "Disease-modifying effect of strontium ranelate in a subset of patients from the Phase III knee osteoarthritis study SEKOIA using quantitative MRI: reduction in bone marrow lesions protects against cartilage loss," *Annals of the Rheumatic Diseases*, vol. 74, no. 2, pp. 422–429, 2015.
- [5] G. J. Kazakia, D. Kuo, J. Schooler et al., "Bone and cartilage demonstrate changes localized to bone marrow edema-like lesions within osteoarthritic knees," *Osteoarthritis and Cartilage*, vol. 21, no. 1, pp. 94–101, 2013.
- [6] H. Iijima, T. Aoyama, J. Tajino et al., "Subchondral plate porosity colocalizes with the point of mechanical load during ambulation in a rat knee model of post-traumatic osteoarthritis," *Osteoarthritis and Cartilage*, vol. 24, no. 2, pp. 354–363, 2016.
- [7] T. Neogi, M. Nevitt, J. Niu et al., "Subchondral bone attrition may be a reflection of compartment-specific mechanical load:

- the MOST Study,” *Annals of the Rheumatic Diseases*, vol. 69, no. 5, pp. 841–844, 2010.
- [8] M. Moreau, P. Rialland, J. Pelletier et al., “Tiludronate treatment improves structural changes and symptoms of osteoarthritis in the canine anterior cruciate ligament model,” *Arthritis Research & Therapy*, vol. 13, no. 3, pp. 1–13, 2011.
 - [9] T. Hayami, Y. Zhuo, G. A. Wesolowski, M. Pickarski, and L. T. Duong, “Inhibition of cathepsin K reduces cartilage degeneration in the anterior cruciate ligament transection rabbit and murine models of osteoarthritis,” *Bone*, vol. 50, no. 6, pp. 1250–1259, 2012.
 - [10] S. Donell, “Subchondral bone remodelling in osteoarthritis,” *EFORT Open Reviews*, vol. 4, no. 6, 2019.
 - [11] F. Xu and S. L. Teitelbaum, “Osteoclasts: new insights,” *Bone Research*, vol. 1, no. 1, pp. 11–26, 2013.
 - [12] E. Vaysbrot, M. C. Osani, M. Musetti et al., “Are bisphosphonates efficacious in knee osteoarthritis? a meta-analysis of randomized controlled trials,” *Osteoarthritis and Cartilage*, vol. 26, no. 2, pp. 154–164, 2017.
 - [13] X. Chen, Z. Wang, N. Duan, G. Zhu, E. M. Schwarz, and C. Xie, “Osteoblast-osteoclast interactions,” *Connective Tissue Research*, vol. 59, no. 2, pp. 99–107, 2018.
 - [14] L. C. Hofbauer and M. Schoppet, “Clinical implications of the osteoprotegerin/RANKL/RANK system for bone and vascular diseases,” *JAMA*, vol. 292, no. 4, pp. 490–495, 2004.
 - [15] C. Menale, E. Campodoni, E. Palagano et al., “Mesenchymal stromal cell-seeded biomimetic scaffolds as a factory of soluble RANKL in rankl-deficient osteopetrosis,” *Stem Cells Translational Medicine*, vol. 8, no. 1, pp. 22–34, 2019.
 - [16] S. Khosla, “Minireview: the OPG/RANKL/RANK system,” *Endocrinology*, vol. 142, no. 12, pp. 5050–5055, 2001.
 - [17] C. C. Wei, D. Q. Ping, F. T. You et al., “Icariin prevents cartilage and bone degradation in experimental models of arthritis,” *Mediators of Inflammation*, vol. 2016, Article ID 9529630, 2016.
 - [18] Y. Chen, H. Li, X. Luo et al., “Moxibustion of Zusanli (ST36) and Shenshu (BL23) alleviates cartilage degradation through RANKL/OPG signaling in a rabbit model of rheumatoid arthritis,” *Evidence-Based Complementary and Alternative Medicine*, vol. 2019, p. 8, 2019.
 - [19] E. F. Eriksen, M. Shabestari, A. Ghouri, and P. G. Conaghan, “Bisphosphonates as a treatment modality in osteoarthritis,” *Bone*, vol. 2020, Article ID 115352, 2020.
 - [20] X. Zhang, G. Cai, G. Jones, and L. Laslett, “Intravenous bisphosphonates for knee pain and bone marrow lesions in people with knee osteoarthritis: a meta-analysis,” *Osteoarthritis and Cartilage*, vol. 28, no. 28, p. S366, 2020.
 - [21] S. Ma, Z. Xie, Y. Guo et al., “Effect of acupotomy on FAK-PI3K signaling pathways in KOA rabbit articular cartilages,” *Evidence-Based Complementary and Alternative Medicine*, vol. 2017, Article ID 4535326, 2017.
 - [22] L. Chu-Xi, G. Yan, T. Lin et al., “Effects of acupotomy intervention on regional pathological changes and expression of cartilage-mechanics related proteins in rabbits with knee osteoarthritis,” *Acupuncture Research*, vol. 40, no. 2, pp. 119–124, 2015.
 - [23] Z. Wei, G. Yang, G. Changqing et al., “Effect of acupotomy versus electroacupuncture on ethology and morphology in a rabbit model of knee osteoarthritis,” *Journal of Traditional Chinese Medicine*, vol. 39, no. 2, pp. 81–88, 2019.
 - [24] X. An, T. Wang, W. Zhang et al., “Chondroprotective effects of combination therapy of acupotomy and human adipose mesenchymal stem cells in knee osteoarthritis rabbits via the gsk3 β -cyclin D1-CDK4/CDK6 signaling pathway,” *Aging and Disease*, vol. 11, no. 5, p. 1116, 2020.
 - [25] G. Tiraloche, C. Girard, L. Chouinard et al., “Effect of oral glucosamine on cartilage degradation in a rabbit model of osteoarthritis,” *Arthritis & Rheumatism*, vol. 52, no. 4, pp. 1118–1128, 2005.
 - [26] C. R. Slyfield, E. V. Tkachenko, D. L. Wilson, and C. J. Hernandez, “Three-dimensional dynamic bone histomorphometry,” *Journal of Bone and Mineral Research*, vol. 27, no. 2, pp. 486–495, 2012.
 - [27] D. B. Burr and M. A. Gallant, “Bone remodelling in osteoarthritis,” *Nature Reviews Rheumatology*, vol. 8, no. 11, pp. 665–673, 2012.
 - [28] J. Zhu, Y. Zhu, W. Xiao, Y. Hu, and Y. Li, “Instability and excessive mechanical loading mediate subchondral bone changes to induce osteoarthritis,” *Annals of Translational Medicine*, vol. 8, no. 6, p. 350, 2020.
 - [29] Z. He, L. Chu, X. Liu et al., “Differences in subchondral trabecular bone microstructure and finite element analysis-based biomechanical properties between osteoporosis and osteoarthritis,” *Journal of Orthopaedic Translation*, vol. 24, pp. 39–45, 2020.
 - [30] R. J. Lories and F. P. Luyten, “The bone-cartilage unit in osteoarthritis,” *Nature Reviews Rheumatology*, vol. 7, no. 1, pp. 43–49, 2011.
 - [31] F. T. Heegde, A. P. Luiz, S. Santanavarela et al., “Osteoarthritis-related nociceptive behaviour following mechanical joint loading correlates with cartilage damage,” *Osteoarthritis and Cartilage*, vol. 28, no. 3, pp. 383–395, 2020.
 - [32] W. Zheng, B. Ding, X. Li, D. Liu, H. Yokota, and P. Zhang, “Knee loading repairs osteoporotic osteoarthritis by relieving abnormal remodeling of subchondral bone via Wnt/ β -catenin signaling,” *The FASEB Journal*, vol. 34, no. 2, pp. 3399–3412, 2020.
 - [33] F. M. Conesa-Buendía, A. Mediero-Muñoz, R. Fujikawa et al., “AB0088 mechanical stimulus induced by chiropractic manipulation reduces cartilage, subchondral bone damage and synovial inflammation in an experimental model of osteoarthritis,” *Annals of the Rheumatic Diseases*, vol. 78, p. 1507, 2019.
 - [34] A. Liphardt, S. H. Windahl, E. Sehic et al., “Changes in mechanical loading affect arthritis-induced bone loss in mice,” *Bone*, vol. 131, 2020.
 - [35] D. M. Findlay and G. J. Atkins, “Osteoblast-chondrocyte interactions in osteoarthritis,” *Current Osteoporosis Reports*, vol. 12, no. 1, pp. 127–134, 2014.
 - [36] B. Poulet, R. De Souza, A. V. Kent et al., “Intermittent applied mechanical loading induces subchondral bone thickening that may be intensified locally by contiguous articular cartilage lesions,” *Osteoarthritis and Cartilage*, vol. 23, no. 6, pp. 940–948, 2015.
 - [37] S. Farrokhi, C. A. Voycheck, J. A. Gustafson, G. K. Fitzgerald, and S. Tashman, “Knee joint contact mechanics during downhill gait and its relationship with varus/valgus motion and muscle strength in patients with knee osteoarthritis,” *The Knee*, vol. 23, no. 1, pp. 49–56, 2016.
 - [38] M. M. Smith and C. B. Little, “Animal models of osteoarthritis,” *Current Rheumatology Reviews*, vol. 4, no. 3, pp. 175–182, 2008.
 - [39] E. M. Bartels, R. Christensen, P. Christensen et al., “Effect of a 16 weeks weight loss program on osteoarthritis biomarkers in obese patients with knee osteoarthritis: a prospective cohort study,” *Osteoarthritis and Cartilage*, vol. 22, no. 11, pp. 1817–1825, 2014.
 - [40] M. Siebelt, J. H. Waarsing, H. C. Groen et al., “Inhibited osteoclastic bone resorption through alendronate treatment in rats reduces severe osteoarthritis progression,” *Bone*, vol. 66, pp. 163–170, 2014.

- [41] Z. Zhao, Q. Tan, A. Jiang et al., "Evidence of subchondral bone's effects on articular cartilage damage in OVX-OA rat," *Engineering Fracture Mechanics*, vol. 233, p. 107081, 2020.
- [42] Z.-M. Zhang, Z.-C. Li, L.-S. Jiang, S.-D. Jiang, and L.-Y. Dai, "Micro-CT and mechanical evaluation of subchondral trabecular bone structure between postmenopausal women with osteoarthritis and osteoporosis," *Osteoporosis International*, vol. 21, no. 8, pp. 1383–1390, 2010.
- [43] G. Dai, H. Xiao, J. Liao et al., "Osteocyte TGF β 1-Smad2/3 is positively associated with bone turnover parameters in subchondral bone of advanced osteoarthritis," *International Journal of Molecular Medicine*, vol. 46, no. 1, 2020.
- [44] A. Bertuglia, M. Lacourt, C. Girard, G. Beauchamp, H. Richard, and S. Laverty, "Osteoclasts are recruited to the subchondral bone in naturally occurring post-traumatic equine carpal osteoarthritis and may contribute to cartilage degradation," *Osteoarthritis and Cartilage*, vol. 24, no. 3, pp. 555–566, 2016.
- [45] M. D. Ryser and K. A. Murgas, "Bone remodeling as a spatial evolutionary game," *Journal of Theoretical Biology*, vol. 418, no. 7, pp. 16–26, 2017.
- [46] H. Lofvall, H. Newbould, M. A. Karsdal et al., "Osteoclasts degrade bone and cartilage knee joint compartments through different resorption processes," *Arthritis Research and Therapy*, vol. 20, no. 1, p. 67, 2018.
- [47] C. M. Bagi, E. Berryman, D. E. Zakur et al., "Effect of anti-resorptive and anabolic bone therapy on development of osteoarthritis in a posttraumatic rat model of OA," *Arthritis Research and Therapy*, vol. 17, no. 1, p. 315, 2015.
- [48] Y. Ikebuchi, S. Aoki, M. Honma et al., "Coupling of bone resorption and formation by RANKL reverse signalling," *Nature*, vol. 561, no. 7722, pp. 195–200, 2018.
- [49] J. Zhang, B. Fu, X. Chen et al., "Protocatechuic acid attenuates anterior cruciate ligament transection-induced osteoarthritis by suppressing osteoclastogenesis," *Experimental and Therapeutic Medicine*, vol. 19, no. 1, pp. 232–240, 2019.
- [50] W. Shen, Y. Guan, R. Wu et al., "Protective effects of Wang-Bi tablet on bone destruction in collagen-induced arthritis by regulating osteoclast-osteoblast functions," *Journal of Ethnopharmacology*, vol. 238, Article ID 111861, 2019.
- [51] S. Posritong, J. M. Hong, P. P. Eleniste et al., "Pyk2 deficiency potentiates osteoblast differentiation and mineralizing activity in response to estrogen or raloxifene," *Molecular and Cellular Endocrinology*, vol. 474, pp. 35–47, 2018.
- [52] Y. Chen, Y. Huang, C. H. Yan et al., "Abnormal subchondral bone remodeling and its association with articular cartilage degradation in knees of type 2 diabetes patients," *Bone Research*, vol. 5, no. 1, pp. 17–34, 2017.
- [53] X. Guo, S. Wei, F. Xu et al., "MicroRNA-532-5p is implicated in the regulation of osteoporosis by forkhead box O1 and osteoblast differentiation," *BMC Musculoskeletal Disord*, vol. 21, no. 296, 2020.
- [54] A. R. Upton, C. A. Holding, A. A. S. S. K. Dharmapatni, and D. R. Haynes, "The expression of RANKL and OPG in the various grades of osteoarthritic cartilage," *Rheumatology International*, vol. 32, no. 2, pp. 535–540, 2012.
- [55] Y. Chen, H. Li, X. Luo et al., "Moxibustion of Zusanli (ST36) and Shenshu (BL23) alleviates cartilage degradation through RANKL/OPG signaling in a rabbit model of rheumatoid arthritis," *Evidence-Based Complementary and Alternative Medicine*, vol. 2019, 2019.
- [56] C. Zhang, Q. Liao, J.-H. Ming et al., "The effects of chitosan oligosaccharides on OPG and RANKL expression in a rat osteoarthritis model," *Acta Cirurgica Brasileira*, vol. 32, no. 6, pp. 418–428, 2017.
- [57] J. E. Fonseca, N. Cortezdias, A. Francisco et al., "Inflammatory cell infiltrate and RANKL/OPG expression in rheumatoid synovium: comparison with other inflammatory arthropathies and correlation with outcome," *Clinical and Experimental Rheumatology*, vol. 23, no. 2, pp. 185–192, 2005.
- [58] Y. Zhang, E. M. Paul, V. Sathyendra et al., "Enhanced osteoclastic resorption and responsiveness to mechanical load in gap junction deficient bone," *PLoS One*, vol. 6, no. 8, Article ID e23516, 2011.
- [59] W. R. Thompson, C. T. Rubin, J. Rubin et al., "Mechanical regulation of signaling pathways in bone," *Gene*, vol. 503, no. 2, pp. 179–193, 2012.
- [60] D. Fu, K. Qin, S. Yang et al., "Proper mechanical stress promotes femoral head recovery from steroid-induced osteonecrosis in rats through the OPG/RANK/RANKL system," *BMC Musculoskeletal Disorders*, vol. 21, no. 1, 2020.

Research Article

Effect of Naringin Treatment on Postmenopausal Osteoporosis in Ovariectomized Rats: A Meta-Analysis and Systematic Review

Zhu Zhu ^{1,2}, Wenjing Xie ², Yanyan Li ², Zaiou Zhu ^{1,3} and Wei Zhang ¹

¹Jiangsu Key Laboratory of Oral Diseases, Nanjing Medical University, Nanjing, Jiangsu, China

²Department of Oral Special Consultation, Affiliated Stomatological Hospital of Nanjing Medical University, Nanjing, Jiangsu, China

³Department of Oral and Maxillofacial Surgery, Affiliated Stomatological Hospital of Nanjing Medical University, Nanjing, Jiangsu, China

Correspondence should be addressed to Wei Zhang; sxm813121@163.com

Received 5 August 2020; Revised 30 September 2020; Accepted 28 January 2021; Published 10 February 2021

Academic Editor: Arham Shabbir

Copyright © 2021 Zhu Zhu et al. This is an open access article distributed under the Creative Commons Attribution License, which permits unrestricted use, distribution, and reproduction in any medium, provided the original work is properly cited.

Background. Osteoporosis is a major disease that affects the quality of life of middle-aged and old people, so it is very important to find efficient and safe drugs to treat osteoporosis. The purpose of this study was to investigate the therapeutic effect of naringin on postmenopausal osteoporosis in ovariectomized (OVX) rats. **Methods.** Chinese biomedical databases, CNKI, PubMed, EMBASE, and Wan Fang were searched for articles from inception to March 2020. Two independent researchers screened articles according to inclusion criteria. RevMan 5.3 was used for data analysis. **Results.** Ten studies were included in the systematic review. The bone mineral density (BMD) significantly increased after naringin treatment (weighted mean difference, 0.06; 95% CI, 0.03–0.09; $P < 0.01$). There was no significant increase in BMD after estrogen treatment compared with naringin (weighted mean difference, 0.00; 95% CI, –0.00 to 0.01; $P = 0.06$). The trabecular bone volume (BV/TV) (weighted mean difference, 2.09; 95% CI, 1.85–2.34; $P < 0.01$) and trabecular thickness (Tb.Th) (weighted mean difference, 6.65; 95% CI, 6.55–6.74; $P < 0.01$) significantly increased after using naringin. **Conclusions.** Naringin had been shown to promote bone formation in OVX rats. However, the mechanism of naringin needs more research to confirm.

1. Background

Osteoporosis is a global public health problem, which primarily threatens postmenopausal women and senior citizens [1]. The pathological characteristics of osteoporosis include bone mineral density (BMD) reduction, bone microstructure deterioration, and matrix protein degradation, resulting in an increased bone fragility and risk of fracture [2]. It not only reduces the quality of life of the elderly, but also causes huge financial burden to patients' families and society. Postmenopausal osteoporosis is the most common type of osteoporosis [3]. At menopause, estrogen withdrawal accelerates bone remodeling with a net increase in bone resorption, which leads to bone loss and even osteoporosis [4, 5]. The ovariectomized (OVX) rats are the most commonly used animal models to study postmenopausal

osteoporosis. In fact, so far, a fully curative treatment for osteoporosis has yet to be developed. In an effort to discover new drugs that treat osteoporosis effectively, much focus has been put on the pursuit of natural-based products because of their availability, cost-effectiveness, and biological activity.

Naringin, a polymethoxylated flavonoid glycoside, is the main bioactive flavonoid extracted from citrus fruits [6, 7] and has a positive effect on osteoporosis caused by postmenopause, glucocorticoid, orchidectomy, and aging [8]. Studies have shown that naringin can promote the differentiation and proliferation of various types of cells [9–12] and improve the bone mass in an osteoporotic rat model [9]. Naringin also promotes osteoclast apoptosis through the mitochondrial-mediated apoptotic pathway, so as to inhibit bone loss in OVX rat models and exhibit antiosteoporotic pharmacological activity [13, 14].

The main purpose of this systematic review was to collect and analyze all the data available to investigate the therapeutic effect of naringin on postmenopausal osteoporosis in OVX rats.

2. Methods

2.1. Selection of Studies. All articles published in Chinese and English databases from their inception to March 2020 were searched, including Chinese Biomedical databases, CNKI, PubMed, EMBASE, and Wan Fang. Search keywords were as follows: ovariectomized, ovariectomy, ovariectomies, bone diseases, osteoporosis, bone loss, bone mineral density, naringin (And or OR). Meanwhile, the references of selected articles were used as a supplement. There were no language restrictions. This review followed the Preferred Reporting Items for Systematic Reviews and Meta-Analyses (PRISMA) reporting criteria [15]. The Stroke Therapy Academic Industry Roundtable (STAIR) list was used for methodological quality assessment in our study [16].

2.2. Inclusion and Exclusion Criteria. Studies were included if they met all of the following criteria: studies with (1) experimental and control groups; (2) OVX-induced bone loss and osteoporosis; (3) evaluation of therapeutic effects of naringin. Exclusion criteria were as follows: (1) duplicate articles; (2) studies without control groups; (3) studies without the use of BMD; (4) all clinical case reports and only in vitro studies.

2.3. Data Extraction. According to inclusion criteria, two investigators (Z. Z. and W. X.) independently scrutinized all articles and the reference list of all relevant articles was also screened to identify other potential data sources. Data were also extracted from these studies independently by two investigators (Z. Z. and W. X.) using a spreadsheet, including column names of the first author, publication date, the age and species of animal studies, experimental designs, naringin treatment dosage, administration time, and intervention protocols. If two authors disagreed on the choice of research and data interpretation, inconsistencies were settled by discussion with another independent investigator (Y. L.). The final results needed to be discussed with all the investigators to reach a consensus.

2.4. Statistical Analysis. Statistical analyses were performed using RevMan 5.3 (Cochrane Collaboration, Oxford, United Kingdom). Heterogeneity among studies was assessed using the I^2 statistic [17]. $I^2 < 50\%$ meant that the homogeneity of the study was high and there was no significant heterogeneity, so the fixed effect model should be used. Otherwise, the random effect model was used. $P < 0.05$ indicated significant differences between groups. Continuous variable data were analyzed with the relative risk or weighted mean difference and its 95% confidence interval (CI).

3. Results

3.1. Selection of Studies. A total of 241 related studies were selected by searching the databases and the literature references of the articles retrieved. After deleting duplicates, 47 studies remained by reading their titles and abstracts. A thorough review of the remaining 47 articles was carried out, of which 37 articles were excluded. The reason for exclusion was the absence of BMD measurements, being clinic reports, or studies only in vitro. Ultimately, 10 studies (three studies were published in Chinese and seven studies were published in English) were selected [8, 9, 18–25] for this systematic review. The flow diagram of the study selection process is shown in Figure 1.

3.2. Characteristics of the Included Studies. Characteristics of the studies are shown in Table 1. Eight studies used Sprague-Dawley (80%) female rats, one study [18] used C57/BL6j (10%) female rats, and another study [21] did not specify which animal model to use. The age range of OVX in rats was 1–6 weeks, except for one study which did not report the age of the rats. In a total of 10 studies, the animal sample size ranged from 20 to 75, and the median sample size was 48 rats. All the studies were administered by oral gavage. The daily dosage range of naringin was 1–1500 mg/kg. The duration of naringin administration varied from 2 to 13 weeks. In all studies, BMD was used to evaluate the results. 3 studies provided data on trabecular bone volume (BV/TV) and trabecular thickness (Tb.Th).

3.3. Risk of Bias. In general, the methodological quality of the studies was not high. None of the studies included any description of sample size calculation or inclusion and exclusion criteria. All studies had reported randomization; however, none of them described allocation concealment. Further, none of the studies reported on their sources of funding or support or any potential conflicts of interest. Table 2 shows the risk of bias reported for each publication included in this meta-analysis.

3.4. BMD BV/TV Tb.Th Changes after Using Naringin. Due to the high heterogeneity of the study, we adopted the random effect model. Compared with the blank control group, the BMD significantly increased after naringin treatment (ten studies, $n = 101$; weighted mean difference, 0.06; 95% CI, 0.03–0.09; $P < 0.01$) (Figure 2). Besides, in studies where estrogen treatment served as the positive control group, we found that there was no significant increase in BMD after estrogen treatment compared with naringin (three studies, $n = 32$; weighted mean difference, 0.00; 95% CI, -0.00 to 0.01; $P = 0.06$) (Figure 3).

Only three studies [8, 21, 22] used BV/TV, Tb.Th as outcome measures. The BV/TV (%) values significantly increased after using naringin (three studies, $n = 31$; weighted mean difference, 2.09; 95% CI, 1.85–2.34; $P < 0.01$) (Figure 4). There was a statistically significant difference in Tb.Th (um) values between the two groups. The weighted

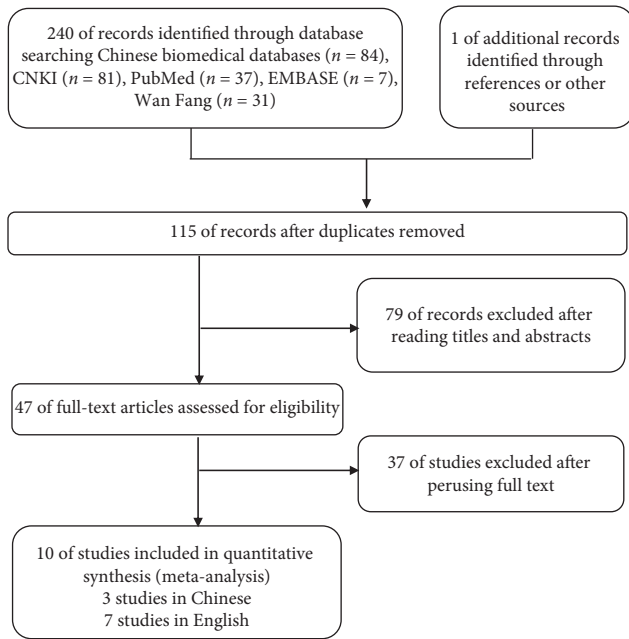


FIGURE 1: Flow diagram of the article selection process for review of Chinese biomedical databases, CNKI, PubMed, EMBASE, and Wan Fang.

mean difference was found to be 6.65, with 95% CI = 6.55–6.74 and $P < 0.01$ (Figure 5).

4. Discussion

Osteoporosis is an age-related disease that affects millions of people. Although the application of traditional Chinese medicine in the treatment of osteoporosis has a long history, its specific mechanism is not known yet [26]. The research on the monomer of traditional Chinese medicine still remains in basic research. For this, we focus our attention on animal models.

OVX is mainly used to establish animal models of osteoporosis [27]. OVX reduces the level of estrogen and induces bone loss in animals, which is similar to postmenopausal bone loss [28], including rapid bone loss and bone resorption, as well as similar bone reactions to therapy with estrogen, bisphosphonates, tamoxifen, and calcitonin. These wide-ranging similarities make OVX animal models widely used as clinically relevant models of postmenopausal bone loss in women [29]. The OVX rat model was approved by the US Food and Drug Administration (FDA) as a preclinical model [30]. Systematic reviews of animal experiments can improve the accuracy of clinical trial effectiveness prediction, reduce the risk of negative results, and also determine when clinical results of animal experiments can be accepted and terminate unnecessary clinical trials.

As far as we know, this is the first meta-analysis to report the effect of naringin on bone mass in OVX rats. We used random effect models to study. The results showed that the BMD value of the experimental group increased significantly, indicating that naringin could promote bone formation in OVX rats and improve osteoporosis caused by

estrogen deficiency. In addition, the effect of naringin in OVX rats was not significantly different from that of estrogen, suggesting that the mechanism of naringin may be the same as that of estrogen, giving us a new direction of research. Compared with the control group, the BV/TV and Tb.Th values of naringin treated group were significantly higher, which also proved the effect of naringin on bone formation.

BMD is an important sign of bone quality, which is of great significance in medicine [31]. It is of great significance in the occurrence, diagnosis, treatment, prognosis, and follow-up observation of osteoporosis, osteomalacia, fibrosis, and other diseases that affect calcium and phosphorus metabolism [32]. BMD was calculated by x-ray absorption of bone. In all ten studies, most of the studies were conducted with dual energy x-ray absorptiometry (DEXA).

With the help of image processing software, regions of interest (ROI) can be selected on the scanning image of micro-CT for threshold segmentation, so that cortical bone and cancellous bone can be segmented and extracted into different tissue regions, respectively [33]. Finally, various morphological characteristics of cortical bone and cancellous bone (trabecular bone) can be studied and analyzed. In general, when the bone tissue in the ROI is the same, the BV/TV value can reflect the bone mass, which is a common index for evaluating the bone mass of cortical bone and cancellous bone [34]. For the cancellous bone in the medullary cavity, the BV/TV value can reflect the trabecular bone mass of different samples. The increased value indicates that bone metabolism is greater than catabolism and bone mass increases, thereby indirectly reflecting bone metabolism. It has the same value in evaluating bone mass and bone metabolism in the middle part of long bone.

The porous trabecular structure connected with trabecular bone is regularly arranged in accordance with the stress curve and has nonuniform anisotropy. This arrangement can increase the bone strength [35]. It can be said that the bone mass of the bone trabeculae is closely related to its microstructure. Therefore, the microstructural analysis of trabecular bone is very important in bone analysis. Micro-CT can perform nondestructive 3D imaging of trabecular bone microstructure and display the microstructure of trabecular bone, making it possible to analyze the topology of trabecular bone microstructure [36]. Tb.Th is one of the main indexes to evaluate the spatial structure of trabeculae [37]. When bone catabolism is greater than bone anabolism, such as in the case of osteoporosis, the Tb.Th value decreases, whereas it increases when bone anabolism is greater than bone catabolism.

Functions of naringin in bone development are largely unknown. Many studies have reported the potential mechanism of naringin promoting osteogenesis. Wang et al. observed that coadministration of AMPK and Akt inhibitors partly reversed naringin effects in vivo, suggesting that the osteogenic activity of this flavonoid is in part via its stimulation of the Wnt/b-catenin signaling upon interaction with AMPK and Akt [20]. Studies found that naringin inhibits osteoclast formation and bone resorption by the suppression of RANKL-induced activation of NF- κ B and

TABLE 1: Characteristics of the included studies.

| Study | Animals | Age, mo | Sample size | Experimental group | Control group | Duration, wk |
|-----------------------|---------------------------------------|---------|-----------------------|--|--|--------------|
| Pang et al 2010 | C57/BL6J mice | 1 | 10/10/10/ 10/10 | A : OVX + naringin (200 mg/kg daily); B : OVX + naringin (400 mg/kg daily) | A: sham vehicle (2% ethanol); B : OVX + vehicle; C : OVX + 17 β -estradiol (E2, 2 ug/g daily) | 6 |
| Shangguan et al. 2017 | SD rats (body weight, 220 \pm 8 g) | 6 | 12/12/12/ 12 | A : OVX + naringin (200 mg/kg daily); B : OVX + naringin (100 mg/kg daily) | A: sham group (physiological saline solution, 6 ml/kg daily); B : OVX group (physiological saline solution, 6 ml/kg daily) | 12 |
| Li et al. 2014 | SD rats (body weight, 230 \pm 10 g) | 6 | 10/10/10/ 10/10/10 | A : OVX + naringin (40 mg/kg daily); B : OVX + naringin (100 mg/kg daily); C : OVX + naringin (200 mg/kg daily) | A: sham group (H2O); B : OVX group (H2O); C : OVX + E2 (22.5 ug/kg daily) | 12 |
| Song et al. 2016 | SD rats (body weight, 240 \pm 12 g) | 3 | 18/18/18/ 18 | A : OVX + naringin (40 mg/kg daily); B : OVX + naringin (100 mg/kg daily); C : OVX + naringin (300 mg/kg daily) | B : OVX group (normal saline) | 8 |
| Wang et al. 2015 | Unclear | 1 | 5/5/5/5 | A : OVX naringin (5 nM); B : OVX naringin with PTH | A: sham vehicle; B : OVX vehicle (PBS) | 6 |
| Sun et al. 2015 | SD rats (body weight, 230 \pm 10 g) | 3 | 15/15/15/ 15/15 | A : OVX naringin (300 mg/kg daily); B : OVX naringin plus treadmill exercise (300 mg/kg daily + EX) | A: sham group (H2O); B : OVX vehicle; C : OVX exercise | 12 |
| Li et al. 2013 | SD rats (body weight, 220g) | 3 | 6/6/6/6 | A : OVX + naringin (60 mg/kg daily); B : OVX + naringin (300 mg/kg daily); C : OVX + naringin (1500 mg/kg daily) | A : OVX vehicle (PBS) | 8 |
| Li et al. 2012 | SD rats (body weight, 280g) | 4 | 12/12/12/ 12/12 | A : OVX + naringin (4 mg/kg daily); B : OVX + naringin (2 mg/kg daily) | A: sham group (H2O); B : OVX vehicle (H2O); C : OVX + E2 | 13 |
| Wang et al. 2016 | SD rats (body weight, 230 \pm 25 g) | 6 | 10/10/10/ 10/10 | A : OVX + naringin (1 mg/kg daily); B : OVX + naringin (10 mg/kg daily); C : OVX + naringin (100 mg/kg daily) | A: sham group; B : OVX + N | 4 |
| Zhao et al. 2016 | SD rats (body weight, 230 \pm 20 g) | Unclear | 15/15 | A : OVX + naringin (300 mg/kg daily) | A : OVX vehicle (normal saline) | 2 |

TABLE 2: Risk of bias.

| Study | Sample size calculation | Inclusion and exclusion criteria | Randomization | Allocation concealment | Reporting of animals excluded from analysis | Blinded assessment of outcome | Reporting potential conflicts of interest |
|-----------------------|-------------------------|----------------------------------|---------------|------------------------|---|-------------------------------|---|
| Pang et al 2010 | Unclear | Unclear | Yes | Unclear | Unclear | Yes | No |
| Shangguan et al. 2017 | Unclear | Unclear | Yes | Unclear | Unclear | Yes | No |
| Li et al. 2014 | Unclear | Unclear | Yes | Unclear | Unclear | Yes | No |
| Song et al. 2016 | Unclear | Unclear | Yes | Unclear | Unclear | Yes | No |
| Wang et al. 2015 | Unclear | Unclear | Yes | Unclear | Unclear | Yes | No |
| Sun et al. 2015 | Unclear | Unclear | Yes | Unclear | Unclear | Yes | No |
| Li et al. 2013 | Unclear | Unclear | Yes | Unclear | Unclear | Yes | No |
| Li et al. 2012 | Unclear | Unclear | Yes | Unclear | Unclear | Yes | No |
| Wang et al. 2016 | Unclear | Unclear | Yes | Unclear | Unclear | Yes | No |
| Zhao et al. 2016 | Unclear | Unclear | Yes | Unclear | Unclear | Yes | No |

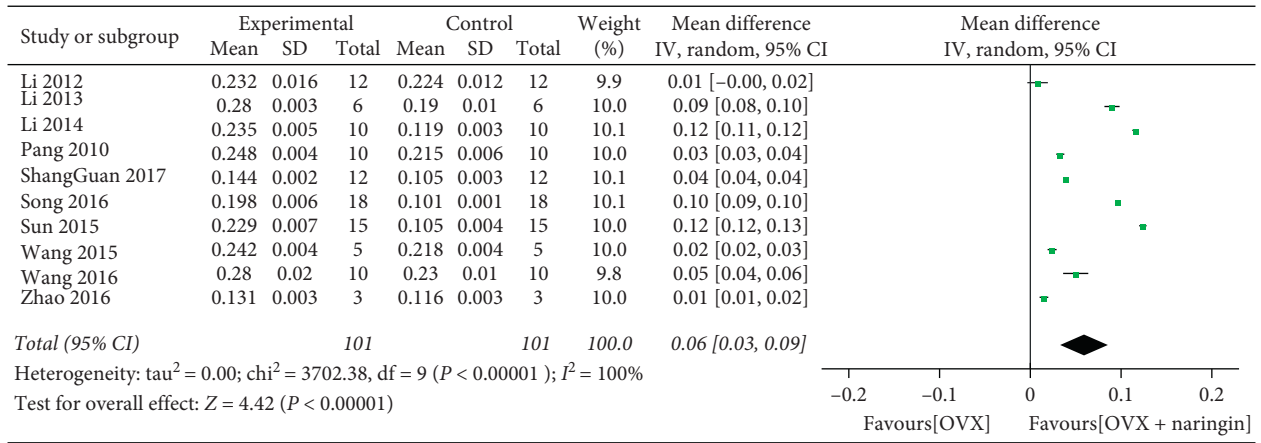


FIGURE 2: BMD changes after naringin treatment.

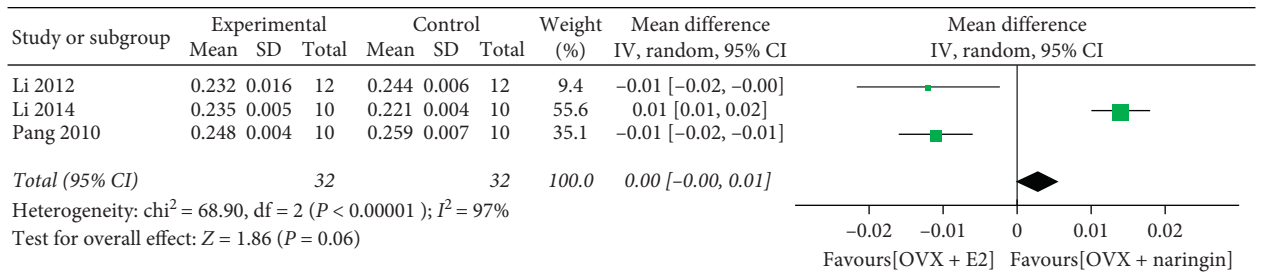


FIGURE 3: Comparison of the effects of naringin and estrogen on BMD.

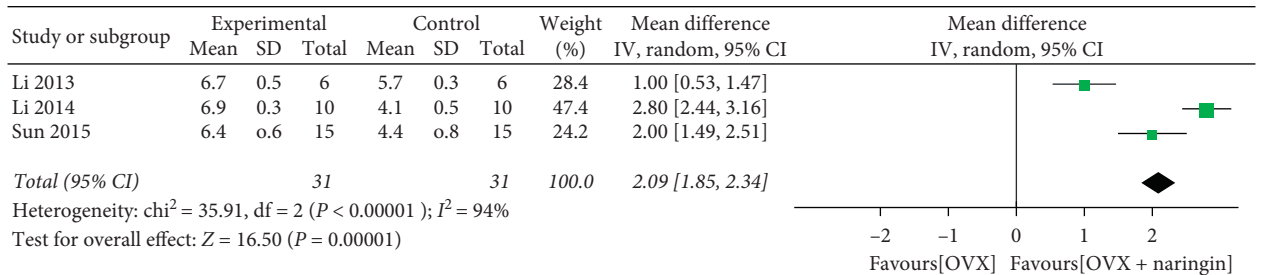


FIGURE 4: BV/TV changes after naringin treatment.

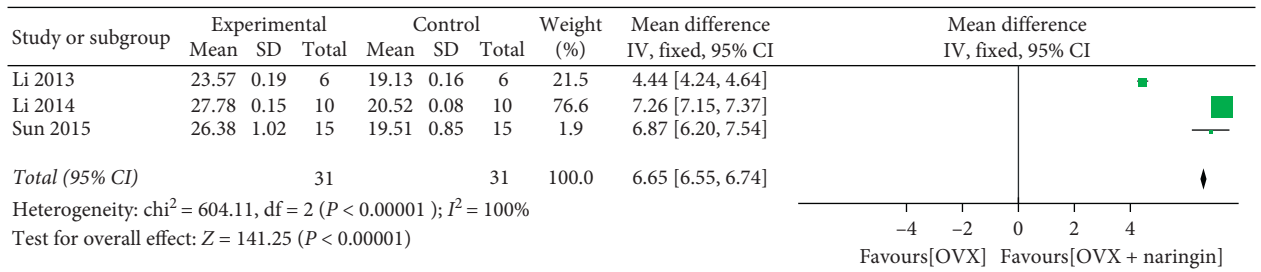


FIGURE 5: Tb.Th changes after naringin treatment.

ERK [38]. Fan et al. revealed that naringin is able to promote BMSC differentiation into osteoblasts, via the upregulation of miR-20a, and the downregulation of PPAR γ [39]. Wu

et al. demonstrated that naringin increased BMP-2 expression via PI3K, Akt, c-Fos/c-Jun, and AP-1-dependent pathways, which can induce osteoblast proliferation,

differentiation, and maturation in cultured osteoblasts [40]. In this study, we hypothesized that the mechanism of naringin should be similar to estrogen. Naringin exerted antiosteoporotic effects by binding to estrogen receptors (ERs), which may replace the estrogen replacement therapy (ERT) in clinical use [41], but more experiments were needed to confirm this hypothesis [42].

The STAIR list was used in this systematic review, which was concise and contained the basic criteria that focus on high quality, such as sample size calculation, randomization, allocation concealment, and blinded outcome assessment.

This meta-analysis also had many limitations. First, despite the best efforts we had made, there was no way to ensure that all relevant studies were found. Second, the quality evaluation of this research is low. There was a lack of calculation of sample size, explanation of random allocation method, and reports of animals excluded from analysis. At the same time, there were biases caused by publication bias. In particular, systematic reviews of animal studies were more susceptible to publication bias than clinical studies [43]. Third, all results (BMD, BV/TV, and Tb. Th) were highly heterogeneous in this study, indicating that the results may not be convincing. For BV/TV and Tb.Th index, it was difficult to establish a unified ROI, which resulted in a large heterogeneity between the studies. The different time of OVX and the different dosage and durations of naringin treatment in rats may lead to higher heterogeneity. However, due to the small number of studies, there was limited ability to consider subgroup analyses. Fourth, this study did not accurately infer the optimal concentration of naringin in OVX rats and could not provide guidance for future animal experiments, so more research and analysis are needed.

5. Conclusions

In OVX rats model, the BMD, BV/TV, and Tb. Th values of naringin treatment group were significantly increased, which proved that naringin promoted bone formation. At the same time, we speculated that the mechanism of naringin was the same as estrogen, which needs more research to confirm.

Abbreviations

| | |
|---------|--|
| OVX: | Ovariectomized |
| BMD: | Mineral density |
| BV/TV: | Trabecular bone volume |
| Tb.Th: | Trabecular thickness |
| PRISMA: | Preferred Reporting Items for Systematic Reviews and Meta-Analyses |
| STAIR: | Stroke Therapy Academic Industry Roundtable |
| CI: | Confidence interval |
| FDA: | US Food and Drug Administration |
| DEXA: | Dual energy x-ray absorptiometry |
| ROI: | Regions of interest |
| ERs: | Estrogen receptors |
| ERT: | Estrogen replacement therapy |
| E2: | 17- β -Estradiol |
| PTH: | Parathyroid hormone |

| | |
|------|---------------------------|
| EX: | Exercise |
| PBS: | Phosphate-buffered saline |
| N: | Nothing. |

Data Availability

The data used to support the findings of this study are available from the corresponding author upon request.

Conflicts of Interest

The authors declare that they have no conflicts of interest.

Authors' Contributions

ZZ designed the study and prepared the first draft of the paper. ZZ, WJX, and YYL contributed to the experimental work. ZO and WZ were responsible for statistical analysis of the data. WZ is guarantor. All authors revised the paper critically for intellectual content and approved the final version. All authors agree to be accountable for the work and to ensure that any questions relating to the accuracy and integrity of the paper are investigated and properly resolved.

Acknowledgments

This research was supported by Natural Science Foundation of Jiangsu Province (CN) (SBK2017043261). Funding was provided in the design of the study and collection, analysis, and interpretation of data and in writing the manuscript.

References

- [1] C.-H. Chen, S.-J. Lim, J.-K. Oh et al., "Teriparatide in East Asian postmenopausal women with osteoporosis in a real-world setting: a baseline analysis of the Asia and Latin America fracture observational study (ALAFOS)," *Clinical Interventions in Aging*, vol. 15, pp. 111–121, 2020.
- [2] S. Shetty, B. John, S. Mohan, and T. V. Paul, "Vertebral fracture assessment by dual-energy X-ray absorptiometry along with bone mineral density in the evaluation of postmenopausal osteoporosis," *Archives of Osteoporosis*, vol. 15, no. 1, p. 25, 2020.
- [3] R. Recker, D. Dempster, B. Langdahl et al., "Effects of odanacatib on bone structure and quality in postmenopausal women with osteoporosis: 5-year data from the phase 3 long-term odanacatib fracture trial (LOFT) and its Extension," *Journal of Bone and Mineral Research*, vol. 35, no. 7, p. 1289, 2020.
- [4] J. Li, X. Chen, L. Lu, and X. Yu, "The relationship between bone marrow adipose tissue and bone metabolism in postmenopausal osteoporosis," *Cytokine & Growth Factor Reviews*, vol. 52, pp. 88–98, 2020.
- [5] J. I. Francisco, Y. Yu, R. A. Oliver, and W. R. Walsh, "Relationship between age, skeletal site, and time post-ovariectomy on bone mineral and trabecular microarchitecture in rats," *Journal of Orthopaedic Research*, vol. 29, no. 2, pp. 189–196, 2011.
- [6] S. Bharti, N. Rani, B. Krishnamurthy, and D. Arya, "Pre-clinical evidence for the pharmacological actions of naringin: a review," *Planta Medica*, vol. 80, no. 6, pp. 437–451, 2014.

- [7] H. Awasthi, D. Mani, D. Singh, and A. Gupta, "The underlying pathophysiology and therapeutic approaches for osteoporosis," *Medicinal Research Reviews*, vol. 38, no. 6, pp. 2024–2057, 2018.
- [8] F. Li, X. Sun, J. Ma et al., "Naringin prevents ovariectomy-induced osteoporosis and promotes osteoclasts apoptosis through the mitochondria-mediated apoptosis pathway," *Biochemical and Biophysical Research Communications*, vol. 452, no. 3, pp. 629–635, 2014.
- [9] W. Gengqi, W. Liming, X. Lin, S. Daoxi, T. Tian, and X. Wenqiang, "Effect of naringin on osteoporotic fracture healing in ovariectomized rats," *Acta Universitatis Traditionis Medicae Sinensis Pharmacologiae Shanghai*, vol. 30, no. 4, pp. 73–79, 2016.
- [10] Z. Zhao, X. Ma, J. Ma, X. Sun, F. Li, and J. Lv, "Naringin enhances endothelial progenitor cell (EPC) proliferation and tube formation capacity through the CXCL12/CXCR4/PI3K/Akt signaling pathway," *Chemico-biological Interactions*, vol. 286, pp. 45–51, 2018.
- [11] J.-y. Long, J.-m. Chen, Y.-j. Liao, Y.-j. Zhou, B.-y. Liang, and Y. Zhou, "Naringin provides neuroprotection in CCL2-induced cognition impairment by attenuating neuronal apoptosis in the hippocampus," *Behavioral and Brain Functions*, vol. 16, no. 1, p. 4, 2020.
- [12] H. Zhao, M. Liu, H. Liu, R. Suo, and C. Lu, "Naringin protects endothelial cells from apoptosis and inflammation by regulating the Hippo-YAP Pathway," *Bioscience Reports*, vol. 40, no. 3, 2020.
- [13] R. Chen, Q.-L. Qi, M.-T. Wang, and Q.-Y. Li, "Therapeutic potential of naringin: an overview," *Pharmaceutical Biology*, vol. 54, no. 12, pp. 3203–3210, 2016.
- [14] K. Shirani, B. S. Yousefsani, M. Shirani, and G. Karimi, "Protective effects of naringin against drugs and chemical toxins induced hepatotoxicity: a review," *Phytotherapy Research*, vol. 34, no. 8, p. 1734, 2020.
- [15] W. M. Bernardo, "PRISMA statement and PROSPERO," *International Braz J Urol*, vol. 43, no. 3, pp. 383–384, 2017.
- [16] A. Thomas, J. Detilleux, P. Flecknell, and C. Sandersen, "Impact of stroke therapy academic industry roundtable (STAIR) guidelines on peri-Anesthesia care for rat models of stroke: a meta-analysis comparing the years 2005 and 2015," *PLoS One*, vol. 12, no. 1, p. e0170243, 2017.
- [17] J. P. T. Higgins, S. G. Thompson, J. J. Deeks, and D. G. Altman, "Measuring inconsistency in meta-analyses," *BMJ*, vol. 327, no. 7414, pp. 557–560, 2003.
- [18] W.-Y. Pang, X.-L. Wang, S.-K. Mok et al., "Naringin improves bone properties in ovariectomized mice and exerts oestrogen-like activities in rat osteoblast-like (UMR-106) cells," *British Journal of Pharmacology*, vol. 159, no. 8, pp. 1693–1703, 2010.
- [19] W. J. Shangguan, Y. H. Zhang, Z. C. Li, L. M. Tang, J. Shao, and H. Li, "Naringin inhibits vascular endothelial cell apoptosis via endoplasmic reticulum stress- and mitochondrial-mediated pathways and promotes intraosseous angiogenesis in ovariectomized rats," *International Journal of Molecular Medicine*, vol. 40, no. 6, pp. 1741–1749, 2017.
- [20] N. Song, Z. Zhao, X. Ma et al., "Naringin promotes fracture healing through stimulation of angiogenesis by regulating the VEGF/VEGFR-2 signaling pathway in osteoporotic rats," *Chemico-biological Interactions*, vol. 261, pp. 11–17, 2017.
- [21] D. Wang, W. Ma, F. Wang et al., "Stimulation of wnt/ β -catenin signaling to improve bone development by naringin via interacting with AMPK and Akt," *Cellular Physiology and Biochemistry*, vol. 36, no. 4, pp. 1563–1576, 2015.
- [22] X. Sun, L. Fengbo, M. Xinlong et al., "The effects of combined treatment with naringin and treadmill Exercise on osteoporosis in ovariectomized rats," *Scientific Reports*, vol. 5, no. 1, p. 13009, 2015.
- [23] N. Li, Y. Jiang, P. H. Wooley, Z. Xu, and S. Y. Yang, "Naringin promotes osteoblast differentiation and effectively reverses ovariectomy-associated osteoporosis," *Journal of Orthopaedic Science: Official Journal of the Japanese Orthopaedic Association*, vol. 18, no. 3, pp. 478–485, 2013.
- [24] L. Jinping, L. Xin, M. Xinmin, L. Shijie, and G. Guoxin, "Effects of naringin on bone biomechanics and bone mineral density in postmenopausal osteoporosis rats," *Journal of Modern Medicine and Health*, vol. 28, no. 5, pp. 683–684.
- [25] Z. Zhihu, M. Xinming, S. Xiaolei et al., "Effect and mechanism of naringin on vascular development of fracture callus in ovariectomized rats," *Chinese Journal of Orthopaedics*, vol. 36, no. 3, pp. 177–183, 2016.
- [26] M. Y. George, E. T. Menze, A. Esmat, M. G. Tadros, and E. El-Demerdash, "Potential therapeutic antipsychotic effects of Naringin against ketamine-induced deficits in rats: involvement of Akt/GSK-3 β and Wnt/ β -catenin signaling pathways," *Life Sciences*, vol. 249, p. 117535, 2020.
- [27] N. Mathavan, M. J. Turunen, M. Tägil, and H. Isaksson, "Characterising bone material composition and structure in the ovariectomized (OVX) rat model of osteoporosis," *Calcified Tissue International*, vol. 97, no. 2, pp. 134–144, 2015.
- [28] D. N. Kalu, "The ovariectomized rat model of postmenopausal bone loss," *Bone and Mineral*, vol. 15, no. 3, pp. 175–191, 1991.
- [29] I. Meyer, S. L. Morgan, A. D. Markland, J. M. Szychowski, and H. E. Richter, "Pelvic floor disorder symptoms and bone strength in postmenopausal women," *International Urogynecology Journal*, vol. 31, no. 9, p. 1777, 2020.
- [30] B. D. Johnston and W. E. Ward, "The ovariectomized rat as a model for studying alveolar bone loss in postmenopausal women," *BioMed Research International*, vol. 2015, Article ID 635023, 1 page, 2015.
- [31] T. Ikeda, H. Kaji, Y. Tamura, and M. Akagi, "Once-weekly teriparatide reduces serum sclerostin levels in postmenopausal women with osteoporosis," *Journal of Orthopaedic Science*, vol. 24, no. 3, pp. 532–538, 2019.
- [32] M. Fotouk-Kiai, S. R. Hoseini, N. Meftah et al., "Relationship between *Helicobacter pylori* infection (HP) and bone mineral density (BMD) in elderly people," *Caspian Journal of Internal Medicine*, vol. 6, no. 2, pp. 62–66, 2015.
- [33] T. J. Ziemlewicz, A. Maciejewski, N. Binkley, A. D. Brett, J. K. Brown, and P. J. Pickhardt, "Opportunistic quantitative CT bone mineral density measurement at the proximal femur using routine contrast-Enhanced scans: direct comparison with DXA in 355 Adults," *Journal of Bone and Mineral Research*, vol. 31, no. 10, pp. 1835–1840, 2016.
- [34] Y. Jin, T. Zhang, J. P. Y. Cheung et al., "A novel mechanical parameter to quantify the microarchitecture effect on apparent modulus of trabecular bone: a computational analysis of ineffective bone mass," *Bone*, vol. 135, p. 115314, 2020.
- [35] R. Inai, R. Nakahara, Y. Morimitsu et al., "Bone microarchitectural analysis using ultra-high-resolution CT in tiger vertebra and human tibia," *European Radiology Experimental*, vol. 4, no. 1, p. 4, 2020.
- [36] N. M. Jandl, T. Rolvien, T. Schmidt et al., "Impaired bone microarchitecture in patients with hereditary hemochromatosis and skeletal complications," *Calcified Tissue International*, vol. 106, no. 5, p. 465, 2020.
- [37] X. Y. Qiao, Y. Xiao, B. W. Xia et al., "High-resolution peripheral quantitative computed tomography for the

- assessment of bone strength and structure in obstructive sleep Apnea patients,” *Zhongguo Yi Xue Ke Xue Yuan Xue Bao Acta Academiae Medicinae Sinicae*, vol. 41, no. 6, pp. 761–771, 2019.
- [38] E. S. M. Ang, X. Yang, H. Chen, Q. Liu, M. H. Zheng, and J. Xu, “Naringin abrogates osteoclastogenesis and bone resorption via the inhibition of RANKL-induced NF- κ B and ERK activation,” *FEBS Letters*, vol. 585, no. 17, pp. 2755–2762, 2011.
- [39] J. Fan, J. Li, and Q. Fan, “Naringin promotes differentiation of bone marrow stem cells into osteoblasts by upregulating the expression levels of microRNA-20a and downregulating the expression levels of PPAR γ ,” *Molecular Medicine Reports*, vol. 12, no. 3, pp. 4759–4765, 2015.
- [40] J.-B. Wu, Y.-C. Fong, H.-Y. Tsai, Y.-F. Chen, M. Tsuzuki, and C.-H. Tang, “Naringin-induced bone morphogenetic protein-2 expression via PI3K, Akt, c-Fos/c-Jun and AP-1 pathway in osteoblasts,” *European Journal of Pharmacology*, vol. 588, no. 2-3, pp. 333–341, 2008.
- [41] K. Wiren, A. Chapman Evans, and X. Zhang, “Osteoblast differentiation influences androgen and estrogen receptor-alpha and -beta expression,” *Journal of Endocrinology*, vol. 175, no. 3, pp. 683–694, 2002.
- [42] R. O. C. Oreffo, V. Kusec, A. S. Viridi et al., “Expression of estrogen receptor-alpha in cells of the osteoclastic lineage,” *Histochemistry and Cell Biology*, vol. 111, no. 2, pp. 125–133, 1999.
- [43] N. V. Puranik, P. Srivastava, G. Bhatt, D. J. S. John Mary, A. M. Limaye, and J. Sivaraman, “Determination and analysis of agonist and antagonist potential of naturally occurring flavonoids for estrogen receptor (ER α) by various parameters and molecular modelling approach,” *Scientific Reports*, vol. 9, no. 1, p. 7450, 2019.

Research Article

Effects of Various Preextraction Treatments of *Crinum asiaticum* Leaf on Its Anti-Inflammatory Activity and Chemical Properties

Chonthicha Kongkwamcharoen ¹, Arunporn Itharat ^{2,3},
Weerachai Pipatrattanaseree ⁴, and Buncha Ooraikul ⁵

¹Graduate School on Applied Thai Traditional Medicine Program, Faculty of Medicine, Thammasat University, Pathum Thani 12120, Thailand

²Department of Applied Thai Traditional Medicine, Faculty of Medicine, Thammasat University, Pathum Thani 12120, Thailand

³Center of Excellence on Applied Thai Traditional Medicine Research (CEATMR), Faculty of Medicine, Thammasat University, Pathum Thani 12120, Thailand

⁴Regional Medical Science Center 12 Songkhla, Department of Medical Sciences, Songkhla 90100, Thailand

⁵Department of Agricultural Food and Nutritional Science, Faculty of Agricultural Life and Environmental Sciences, University of Alberta, Edmonton, AB T6G 2P5, Canada

Correspondence should be addressed to Arunporn Itharat; iarunporn@yahoo.com

Received 25 September 2020; Revised 20 December 2020; Accepted 4 January 2021; Published 28 January 2021

Academic Editor: Arham Shabbir

Copyright © 2021 Chonthicha Kongkwamcharoen et al. This is an open access article distributed under the Creative Commons Attribution License, which permits unrestricted use, distribution, and reproduction in any medium, provided the original work is properly cited.

Crinum asiaticum Linn. has been used in Thai traditional medicine to relieve inflammatory symptoms and treat osteoarthritis. There have been reports on its potent anti-inflammatory property but nothing on the effects of different pretreatments on its chemical properties and anti-inflammatory activity. Pretreatment of herbal raw materials is an important step which affects the overall quality of Thai traditional medicine. The objectives of this study were to investigate different treatments of *C. asiaticum* leaves prior to ethanolic extraction and to compare the extracts for their anti-inflammatory activity and chemical properties. The treatments included hot air drying in an oven, microwave drying, traditional grilling on a charcoal stove before drying in an oven, and temperature shock in hot and cold water before hot air drying. The anti-inflammatory activity and chemical properties of the extracts were analyzed using the established methods. Results showed that 95% ethanolic extract of hot air oven-dried leaves had the highest anti-inflammatory activity and total phenolic and lycorine contents. We recommend hot air drying as a preextraction treatment for *C. asiaticum* leaves for its simplicity, best retention of the herbal quality, and suitability for scaling up to an industrial process.

1. Introduction

Inflammation is a primary physiologic response of tissue to pathogens, cell injury, and damaged tissues. Proinflammatory cytokines, inflammatory mediators such as nitric oxide (NO), prostaglandin E₂ (PGE₂), and tumor necrosis factor-alpha (TNF- α) produced during the inflammatory process cause damage of cell, tissue, and organ [1, 2]. Regarding the pathophysiology of inflammatory diseases, osteoarthritis (OA) is the most common chronic degenerative disease among elderly people. The inflammatory mediators such as nitric oxide, IL-1, TNF- α , and COX-2

contribute to cartilage and joint degeneration [3]. Nonsteroidal anti-inflammatory drugs (NSAIDs) are the common treatment for OA pain and inflammation. However, adverse effects have been observed in elderly patients [4].

Crinum asiaticum L. (Amaryllidaceae family) has long been used in Southeast Asian and Thai traditional medicine to relieve pain and as a treatment for inflammatory diseases. According to ethnopharmacology, Southeast Asian countries use *C. asiaticum* for treatments of wounds, swellings, pain injuries, and inflamed joints, and as an antidote for poisons or toxins [5–7]. In Thai traditional medicine, *C. asiaticum* leaf is a plant component in Phra-aung-kob-phra-sean remedy commonly used to treat

injurious, inflamed joints [8], and ankle pain and for postpartum care [9].

Local practitioners grill *C. asiaticum* leaves on a charcoal stove until they are softened and hot before covering the localized pain areas. However, the effects of this traditional heating treatment on the inflammatory activity of the leaves have not been elucidated.

Previous researches have reported on the bioactivity of *C. asiaticum* leaves including antioxidation [10] and anti-inflammation by inhibiting nitric oxide production [11]. An *in vivo* study on leaf extract also showed a significant anti-inflammatory effect [12]. Among the phytochemical components in *C. asiaticum*, lycorine is the most common of *Crinum* alkaloids that exerts potent immunological, anti-tumor, and anti-inflammatory activities [13–15] and decreases autophagy in osteoclasts *in vivo* [16]. These studies have reported on the potent anti-inflammatory effect of *C. asiaticum* but so far no study has been done on the effects of different preextraction treatments on its chemical properties and anti-inflammatory activity. Our study was designed to fill this gap in knowledge.

Traditional Thai doctors usually have their own methods of preparation before they apply the herbs. These may involve heating, grilling, or pounding the fresh herb for topical applications, or boiling it in water or alcohol, if it is to be taken internally. These pretreatment techniques are applied for several reasons, for example, for long-term storage, quality control, increasing efficacy, and reducing the toxicity of the herbs [8].

Preextraction treatments are physical preparations of the herb which include cleaning, size reduction, and drying prior to solvent extraction. Ethanolic extraction with 95% ethanol is usually an extraction method of choice for most herbal materials for the purpose of scientific studies on their bioactive components and efficacy against target diseases. However, the quality of herbal extracts is usually influenced by the treatment of the herbs before extraction, especially the drying process. Drying temperature and time and how the drying process is applied to the fresh herb can have a profound effect on the chemical composition of the extracts and hence medicinal efficacy [17, 18].

In this research, we applied four methods of pretreatments to get *C. asiaticum* leaves ready for ethanolic extraction and to evaluate what effects each of them has on the chemical and anti-inflammation properties of the herb. The first method was grilling on a charcoal stove, a common practice in the Thai traditional medicine. The second method was hot air drying in an oven in which the temperature and time could be conveniently controlled in order to minimize damage to the leaves. The third method was microwave drying which employs direct electromagnetic heating to the material enabling ease of temperature control and faster drying to better retain herbal qualities. The fourth method was temperature shock in water which might help preserve color and some important substances in the leaves. We then compared the effects of the four preextraction treatments of *C. asiaticum* leaf on its anti-inflammatory activity, as determined by the inhibition of NO, PGE₂, and TNF- α production, and its chemical properties such as total phenolic

compound and lycorine content. From the results, we recommended the most suitable treatment that would best preserve the quality of *C. asiaticum* leaves for the development of an anti-inflammation product for pain relief in OA patients.

2. Material and Methods

2.1. Plant Materials and Preextraction Treatment Methods. *C. asiaticum* leaves were collected from the Faculty of Medicine, Thammasat University, Pathum Thani, Thailand. The specimen voucher (SKP-008 03 01 01) was deposited at the herbarium of Southern Center of Thai Medicinal Plants, Faculty of Pharmaceutical Sciences, Prince of Songkla University, Thailand. The concept diagram of the steps in the experiments is shown in Figure 1.

Fresh leaves were cleaned with water and sliced into medium-size pieces before being subjected to the following four different preextraction treatments:

- (1) Hot air drying in an oven (CAA) with the oven set at 40°C for 10 hours.
- (2) Microwave drying (CAM) with a microwave power of 80°MhZ for 20 minutes.
- (3) Traditional grilling on a charcoal stove before drying in an oven (CAG): the leaves were placed on the grid of a charcoal stove and grilled lightly for 15 minutes before drying in a hot air oven at 40°C for 8 hours.
- (4) Temperature shock in hot and cold water before hot air drying (CAC): the leaves were dipped in a water bath at 100°C for 5 seconds and then immediately plunged into an ice-cold water bath (0°C) for 15 seconds before drying in a hot air oven at 40°C for 8 hours.

2.2. Maceration and Extraction Method. The dried leaves from each preextraction treatment (40 g) were macerated with 95% ethanol for three days and filtered through a Whatman No. 1 filter paper. The maceration was repeated twice and the extracts were combined. The crude extract was dried in a rotary evaporator.

2.3. Reagents and Chemicals. Standard lycorine (purity > 98%) was purchased from Chem Faces (Wuhan, China). Dimethyl sulfoxide (DMSO), phosphoric acid, triethylamine, and purified water were prepared by Milli Q® system from Millipore (Bedford, MA, USA). Acetonitrile HPLC grade was purchased from RCI Lab Scan (Bangkok, Thailand). Murine macrophage leukemia cell line (RAW 264.7: ATCC® TIB-71™) was purchased from American Type Culture Collection (ATCC®, VA, USA). Fetal bovine serum (FBS) was purchased from Gibco® (OK, USA). Dulbecco's Modified Eagle's Medium (DMEM), phosphate buffer saline (PBS), and penicillin-streptomycin (P/S) were purchased from Biochrom (MA, Germany). 3-(4, 5-Dimethyl-2-thiazolyl)-2, 5-diphenyl-2H-tetrazolium bromide (MTT) was purchased from Sigma (MO, USA).

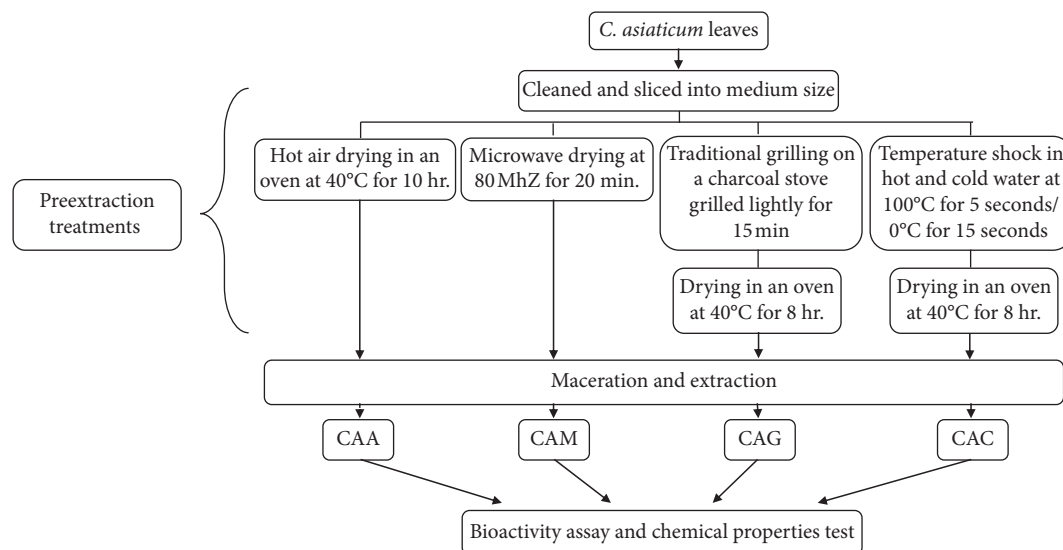


FIGURE 1: Concept diagram of the steps in the experiments; CAA means *C. asiaticum* extract of hot air drying in oven method, CAM means *C. asiaticum* extract of microwave drying method, CAG means *C. asiaticum* extract of traditional grilling on a charcoal stove method, and CAC means *C. asiaticum* extract of temperature shock method.

2.4. Instruments. The HPLC system (Agilent® 1200; Agilent Technologies, USA) consisted of a solvent degasser (G1322A), an autosampler (G1329A), a quaternary solvent pump (G1311A), a photodiode array detector (G1315D), and a column oven (G1316A). The chromatographic data were processed by the Chemstation® software version B.04.01 SP1.

2.5. Anti-Inflammatory Activity by Inhibition of Nitric Oxide Production from RAW 264.7 Cells and Cytotoxicity by MTT Assay. Anti-inflammatory activity by inhibition of nitric oxide production in RAW264.7 cells was determined according to the method of Tewtrakul and Itharat, with slight modifications [19]. Briefly, RAW264.7 cells were cultured in DMEM medium with 10% fetal bovine serum (FBS), penicillin (100 units/mL), and streptomycin (100 µg/mL) and incubated at 37°C under 5% CO₂. The cells were seeded into 96-well plate and incubated for 24 hours. The cells were treated with LPS (lipopolysaccharide) at the final concentration of 5 ng/mL. A sample solution was added and incubated for 24 hours. The supernatant was transferred to a new 96-well plate and Griess reagent was added. The plate optical density (OD) was measured with a microplate reader at a wavelength of 570 nm. The viability of the treated cells was determined by MTT solution. The OD was measured at 570 nm. The %inhibition and %toxicity were calculated. The half inhibitory concentration (IC₅₀) was determined by regression analysis using GraphPad Prism software (CA, USA).

2.6. Anti-Inflammatory Activity by Inhibition of TNF-α Production from RAW 264.7 Cells. Inhibitory effects on the TNF-α production from RAW 264.7 cells were evaluated by using Quantikine® mouse TNF-α ELISA test kit (Darmstadt, Germany) according to the method of Makchuchit et al. [20]

with slight modifications. In brief, the cells were seeded in 96-well plates at a density of 1×10^5 cells/well and incubated for 24 hours. After that, the medium was replaced with fresh medium containing 5 ng/mL of LPS and test samples at various concentrations and incubated for 24 hours. The supernatant was transferred into 96-well ELISA. The OD was measured at 450 nm. Inhibition percentage of TNF-α production was calculated and the Prism program used for calculating IC₅₀ values.

2.7. Anti-Inflammatory Activity by Inhibition of Prostaglandins E2 (PGE2) from RAW 264.7 Cells Line. RAW264.7 macrophage cells were seeded in 96-well plates with 1×10^5 cells/well and incubated for 18–20 hours. Afterward, the medium was replaced by a fresh medium containing 0.08 µg/mL of LPS with various concentrations of sample and incubated for 24 hours. The supernatant was transferred into 96-well PGE₂ ELISA plate (Cayman Chemical Company). The absorbance was measured at 420 nm. Inhibition percentage of PGE₂ production was calculated and the Prism program used to calculate IC₅₀ values.

2.8. Determination of Total Phenolic Content. The total phenolic content of the extracts was determined by the modified Folin–Ciocalteu method [21]. A 20 µL aliquot of the extracts was mixed with 100 µL of Folin–Ciocalteu's reagent and 80 µL of sodium carbonate. The plate was mixed well and allowed to stand at room temperature to develop color for 30 minutes. The absorbance was measured at 765 nm. Total phenolic content was expressed as mg gallic acid equivalents (GAE)/g. It was calculated from a calibration curve of gallic acid standard solutions (ranging from 2.5 to 100 µg/mL). All tests were performed in triplicate.

2.9. Determination of Lycorine Content by HPLC

2.9.1. Preparation of Standard and Sample Solution. A stock standard solution of lycorine was prepared at a concentration of 0.5 mg/mL in DMSO. A calibration curve was constructed by using the serially diluted standard solution at the concentrations of 50, 100, 150, 200, 300, and 500 $\mu\text{g/mL}$. For sample solutions, each *C. asiaticum* extract obtained from various preextraction treatments was dissolved in DMSO to produce a sample solution containing 10 mg/mL of the extract.

2.9.2. Chromatographic Conditions. Chemical constituents of the crude extract were separated along a C18 reverse-phase column (Zorbax® C18, 4.6 \times 250 mm, 5 microns). The mobile phase consisted of 0.1%v/v triethylamine in water adjusting pH to 3.0 with phosphoric acid (A) and acetonitrile (B). Gradient elution was programmed as follows: 0–5 min, 5%B; 25 min, 30%B; 25.1–30 min, 80%B; 30.1–35 min, 5%B. The flow rate was set at 1 mL/min. Samples (10 μL) were injected into the HPLC system and detected by using a diode array detector at the wavelength of 290 nm.

2.9.3. Validation of the HPLC Method. Validation of the HPLC method was conducted according to the guideline of the International Conference on Harmonization (ICH 2005) [22]. The validation parameters included selectivity, linearity, accuracy, precision, limit of detection (LOD), and limit of quantitation (LOQ).

2.10. Statistical Analysis. The evaluations of anti-inflammatory activities were conducted in triplicate and the results were expressed as mean \pm SEM. The IC_{50} values were calculated by using the Prism program. The data were analyzed using one-way ANOVA and Tukey's multiple comparison tests. The results of the HPLC analysis were expressed as mean \pm SD. The level of statistical significance was taken at $P < 0.05$.

3. Results

3.1. Extraction of the Dried Leaves of *C. asiaticum*. Yields (%) of the ethanolic extracts of *C. asiaticum* leaves obtained from different preextraction treatments are shown in Table 1. The highest yield was obtained from the grilling method (CAG; 25.75%). Other methods, CAM, CAA, and CAC, yielded 24.23%, 22.88%, and 21.53%, respectively.

3.2. Anti-Inflammatory Activity by Inhibition of Nitric Oxide Production from RAW 264.7 Cells. As shown in Table 2, CAA showed the highest inhibitory activity with IC_{50} value of $16.66 \pm 1.42 \mu\text{g/mL}$. CAM, CAG, and CAC exerted anti-inflammatory activity with IC_{50} values of 20.42 ± 0.57 , 21.35 ± 0.56 , and $22.48 \pm 1.09 \mu\text{g/mL}$, respectively. All of them exhibited anti-inflammatory activity significantly less than the positive control, prednisolone ($\text{IC}_{50} = 1.05 \pm 0.13 \mu\text{g/mL}$). Lycorine, a major component of

C. asiaticum, exerted potent activity with IC_{50} value of $0.40 \pm 0.01 \mu\text{g/mL}$. On the contrary, diclofenac was not active in this pathway. The results demonstrated that CAA could affect significantly lower levels of NO production compared with CAG and CAC (Table 1).

3.3. Anti-Inflammatory Activity by Inhibition of TNF- α Production from RAW 264.7 Cells. The results in Table 1 showed that CAA exerted the highest activity with IC_{50} value of $25.21 \pm 1.11 \mu\text{g/mL}$. CAM, CAG, and CAC showed anti-inflammatory activity with IC_{50} values of 37.60 ± 0.58 , 46.36 ± 0.48 , and $45.63 \pm 1.54 \mu\text{g/mL}$, respectively. However, all of them have significantly less ($p < 0.05$) anti-inflammatory activity than prednisolone ($\text{IC}_{50} = 0.07 \pm 0.00 \mu\text{g/mL}$). Lycorine showed inhibition of 14.0% at the concentration of 0.8 $\mu\text{g/mL}$. Higher lycorine concentrations showed >30% cytotoxicity to RAW 264.7 cell. On the contrary, diclofenac was not active in this pathway. The results showed that CAA could significantly lower the level of TNF- α production when compared with CAM, CAG, and CAC ($p < 0.05$).

3.4. Anti-Inflammatory Activity by Inhibition of PGE2 Production from RAW 264.7 Cells. As shown in Table 1, all extracts of *C. asiaticum* were not active in this pathway. However, prednisolone, the positive control, showed strong anti-inflammatory activity with IC_{50} value of $0.07 \pm 0.00 \mu\text{g/mL}$. All extracts were significantly different from prednisolone ($p < 0.05$) in this respect. Diclofenac showed potent inhibition with IC_{50} value of $0.004 \pm 0.001 \mu\text{g/mL}$ while lycorine was not active in this pathway.

3.5. Cytotoxicity of Extracts on RAW 264.7 Cells by MTT Assay. Cytotoxicity on RAW 264.7 cells of the ethanolic extracts from different preextraction treatments of *C. asiaticum* leaf was determined by MTT assay. As shown in Table 2, all extracts were not toxic at all concentrations. Lycorine showed cytotoxicity at a concentration greater than 1 $\mu\text{g/mL}$.

3.6. Total Phenolic Content. As shown in Table 1, CAA had the highest total phenolic content with the value of $23.20 \pm 1.36 \text{ mg GAE/g}$. CAM, CAG, and CAC showed total phenolic content of 14.53 ± 0.63 , 13.10 ± 1.02 , and $12.01 \pm 0.84 \text{ mg GAE/g}$, respectively.

3.7. High-Performance Liquid Chromatography (HPLC) Analysis and Method Validation. The HPLC system showed good separation of lycorine from other substances in the extract, the peak of lycorine matched that of the standard peak at $\text{RT} = 5.8$, and the blank (DMSO) showed no peak at the same RT in the standard (Figure 2). The chromatograms of the crude extracts and standard solutions paralleled those of the UV spectrum of the lycorine peaks. Peak purity of lycorine in the sample chromatograms was assessed by comparing the UV spectra at the start, apex, and end of the peak of lycorine standard. The results showed that the UV spectrum of each sample (CAA, CAM, CAG, and CAC) was similar to that of the lycorine standard (Figure 3).

TABLE 1: Yields (%w/w), anti-inflammatory activity by the inhibitory effect on three pathways in RAW 264.7 cells, and %total phenolic content of the ethanolic extracts from different preextraction treatments of *C. asiaticum*.

| Sample | %yields | Anti-inflammatory activity by inhibitory effect on three pathways in RAW 264.7 cells (IC ₅₀ ± SEM) (μg/mL) | | | %Total phenolic content (mg GAE/g) |
|--------------|---------|---|---------------|---------------------|------------------------------------|
| | | NO | TNF-α | PGE ₂ | |
| CAA | 22.88 | 16.66 ± 1.42 | 25.21 ± 1.11 | >100 | 23.20 ± 1.36 |
| CAM | 24.23 | 20.42 ± 0.57 | 37.60 ± 0.58* | >100 | 14.53 ± 0.63* |
| CAG | 25.75 | 21.35 ± 0.56* | 46.36 ± 0.48* | >100 | 13.10 ± 1.02* |
| CAC | 21.53 | 22.48 ± 1.09* | 45.63 ± 1.54* | >100 | 12.01 ± 0.84* |
| Prednisolone | — | 1.05 ± 0.13 | 0.07 ± 0.00 | 0.07 ± 0.00 | — |
| Diclofenac | — | >100 | >100 | 0.004 ± 0.001 | — |
| Lycorine | — | 0.40 ± 0.00 | >0.8 | >0.8 ^(t) | — |

*Significant difference ($p < 0.05$) compared with CAA analyzed by Tukey's multiple comparison test. ^(t)Cytotoxicity was observed at a higher concentration.

The HPLC system for lycorine analysis showed excellent linearity via the coefficient of determination ($r^2 = 1$) within the range of 50–500 μg/mL (Table 3). LOD and LOQ of lycorine were 1 and 3.25 μg/mL, respectively (Table 3). The accuracy of the method was presented as % recovery intraday and interday within 99.76–101.96% and 99.07–100.62%, respectively (Table 4). The precision RSD % values were lower than 2%, exhibiting a great precision of the method (Table 4). The good linearity, accuracy, and precision of the HPLC method signify its suitability for the determination of lycorine in the ethanolic extracts of *C. asiaticum* leaves after different preextraction treatments. The comparative values of lycorine content of *C. asiaticum* leaf extracts after different preextraction treatments are shown in Figure 4. CAA, CAM, CAG, and CAC show the contents to be 34.40 ± 0.41, 21.05 ± 0.28, 17.71 ± 0.13, and 17.48 ± 0.24 mg/g, respectively.

4. Discussion

Osteoarthritis is a common ailment among the elderly in Thailand and elsewhere. The overproduction of NO, TNF-α, and PGE₂ are found in inflamed articular tissues and human chondrocytes in OA patients [23, 24]. In addition, oxidation can lead to tissue injury, cartilage, and joints degeneration [25].

C. asiaticum, a medicinal plant in Phra-aung-kob-phra-sean remedy, has long been used to treat injuries and joint inflammation. Thai traditional/folk medicine uses grilled leaves of the herb for this purpose. The guidelines for certification of folk medicine describe that fresh leaves are grilled lightly by fire from a charcoal stove then pressed and wrapped around the pain area [26].

Previous phytochemical studies on *C. asiaticum* reported that alkaloids, coumarins, glycosides, triterpenes, phenolics, and flavonoids are constituents of *C. asiaticum* leaf [27, 28]. Lycorine is one of the major *Crinum* alkaloids [14, 28]. A previous study reported that ethanolic extract of the leaves exerted *in vitro* anti-inflammatory activity by the inhibition of nitric oxide production [11]. Leaf extract also showed a significant anti-inflammatory effect *in vivo* [12, 29]. Another study reported that methanol and chloroform extracts of hot air-dried leaf of *C. asiaticum* exerted antinociceptive effect [27].

To date, there has been no report on the effects of different preextraction treatments on its chemical properties and anti-inflammatory activity. Our research addressed this gap of knowledge by comparing the effects of four preextraction treatments of the leaf on its anti-inflammatory activity and chemical properties.

All extracts prepared by different preextraction treatments showed inhibition of NO production. The extract obtained from hot air oven-dried leaves (CAA) exerted the highest activity with IC₅₀ value of 16.66 ± 1.42 μg/mL. This compares well with the result from a previous study showing IC₅₀ value of 9.99 ± 0.00 μg/mL [11]. All extracts showed less inhibitory activity than the positive control, prednisolone. Extract from CAA also exerted the highest activity on TNF-α production with IC₅₀ value of 25.21 ± 1.11 μg/mL. Extracts from other preextraction treatments exerted less activity with IC₅₀ higher than 35 μg/mL. All extracts exerted less inhibition of TNF-α production than prednisolone. Diclofenac was not active in TNF-α pathway. None of the extracts inhibited PGE₂ production. Our study showed that lycorine exerted strong anti-inflammatory activity by inhibiting NO production, but it only slightly inhibited TNF-α and PGE₂ production in RAW264.7 cells. A previous study reported that lycorine from ethanolic extract of *Crinum yemense* inhibited LPS-induced iNOS but not COX-2 gene expression [30]. From another previous research [31], lycorine inhibited NO production in RAW 264 cells with IC₅₀ value of 1.2 ± 0.4 μM as compared with our result of 0.4 μg/mL or 1.43 μM. The difference in the results may be caused by the different assay procedures such as the concentrations of seeded cells in 96-well plates and the concentrations of LPS for inducing the nitric oxide production in RAW264.7 cells.

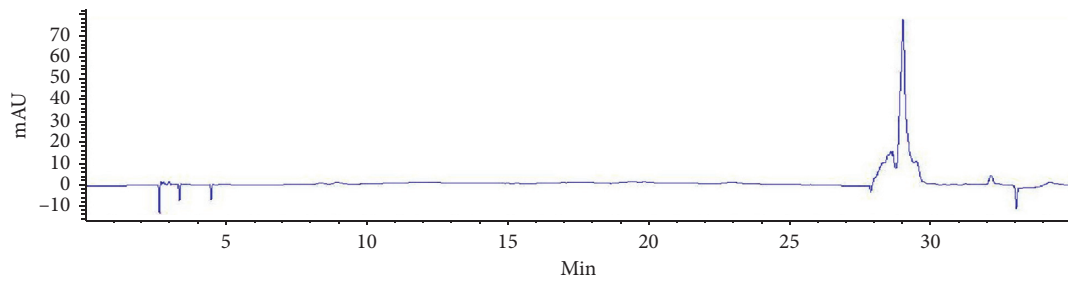
For the phytochemical study, we investigated the effect of various preextraction treatments of *C. asiaticum* leaf on total phenolic and lycorine contents. The CAA extract showed the highest total phenolic content (23.20 ± 1.36 mg GAE/g), as compared to the result in a previous research of 60.28 ± 0.38 TAE/g [10]. The difference may be due to factors such as season, temperature, and soil composition for plant growth as well as processing methods.

Phenolic compounds contribute to antioxidant activity [32, 33]. Oxidative stress activates inflammatory mediators linked to the overproduction of ROS involved in several chronic

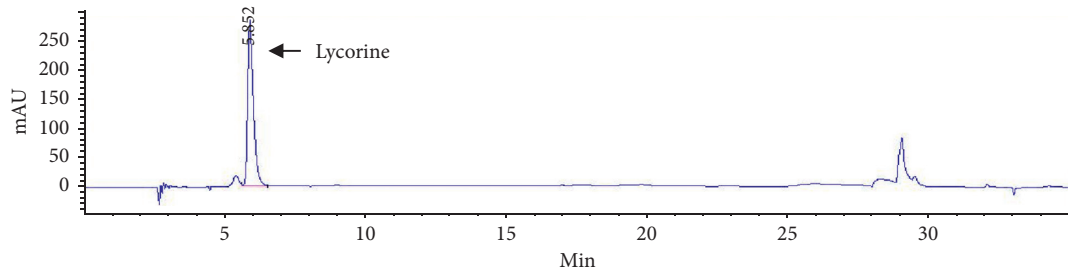
TABLE 2: Inhibitory effect of the ethanolic extracts from different preextraction treatments of *C. asiaticum* on LPS-induced NO production from RAW 264.7 cells (mean \pm SEM, $n = 3$).

| Sample | % inhibition of NO production from RAW 264.7 cells at various concentrations ($\mu\text{g/mL}$) (% cytotoxicity) | | | | | | | | | | IC50 \pm SEM ($\mu\text{g/mL}$) |
|--------------|--|--------------------------------------|--|--|---|---|---|---|---|---|-------------------------------------|
| | 0.1 | 0.2 | 0.4 | 0.8 | 1 | 10 | 30 | 50 | 100 | 100 | |
| CAA | — | — | — | — | -2.58 \pm 2.36 (-6.08 \pm 12.47) | 23.49 \pm 5.96 (-10.10 \pm 9.18) | 96.48 \pm 1.82 (2.95 \pm 0.82) | 97.49 \pm 1.23 (-15.27 \pm 9.52) | 98.26 \pm 0.50 (23.91 \pm 0.85) | 98.26 \pm 0.50 (23.91 \pm 0.85) | 16.66 \pm 1.42 |
| CAM | — | — | — | — | -10.80 \pm 8.07 (-0.63 \pm 8.29) | 11.03 \pm 2.75 (-3.40 \pm 2.59) | 83.44 \pm 4.58 (8.07 \pm 1.05) | 102.39 \pm 5.33 (9.45 \pm 0.52) | 96.12 \pm 0.56 (12.00 \pm 5.64) | 96.12 \pm 0.56 (12.00 \pm 5.64) | 20.42 \pm 0.57 |
| CAG | — | — | — | — | -4.63 \pm 1.18 (-1.94 \pm 6.54) | 6.78 \pm 2.44 (2.62 \pm 6.01) | 83.37 \pm 1.62 (-5.60 \pm 12.94) | 96.09 \pm 0.37 (3.72 \pm 7.17) | 101.55 \pm 3.49 (10.41 \pm 8.68) | 101.55 \pm 3.49 (10.41 \pm 8.68) | 21.35 \pm 0.56 |
| CAC | — | — | — | — | -6.33 \pm 1.28 (2.33 \pm 6.41) | -1.25 \pm 7.92 (0.92 \pm 2.94) | 81.21 \pm 2.68 (7.23 \pm 2.52) | 96.61 \pm 2.71 (11.66 \pm 5.08) | 96.59 \pm 0.99 (17.07 \pm 4.07) | 96.59 \pm 0.99 (17.07 \pm 4.07) | 22.48 \pm 1.09 |
| Prednisolone | 32.85 \pm 7.64 (2.02 \pm 3.15) | — | — | — | 48.04 \pm 2.07 (5.35 \pm 3.43) | 64.11 \pm 7.46 (3.88 \pm 4.68) | — | 79.16 \pm 3.18 (9.64 \pm 4.74) | — | — | 1.05 \pm 0.13 |
| Diclofenac | — | — | — | — | — | — | — | -8.57 \pm 0.86 (-20.36 \pm 0.68) | 1.16 \pm 0.90 (11.88 \pm 1.49) | 1.16 \pm 0.90 (11.88 \pm 1.49) | >100 |
| Lycorine | -10.93 \pm 2.34 (5.46 \pm 4.37) | 7.46 \pm 0.44 (9.98 \pm 8.20) | 50.72 \pm 0.37 (15.29 \pm 4.92) | 82.63 \pm 3.90 (27.35 \pm 1.30) | 86.86 \pm 3.66 ⁽¹⁾ (36.96 \pm 4.15) | — | — | — | — | — | 0.40 \pm 0.00 |

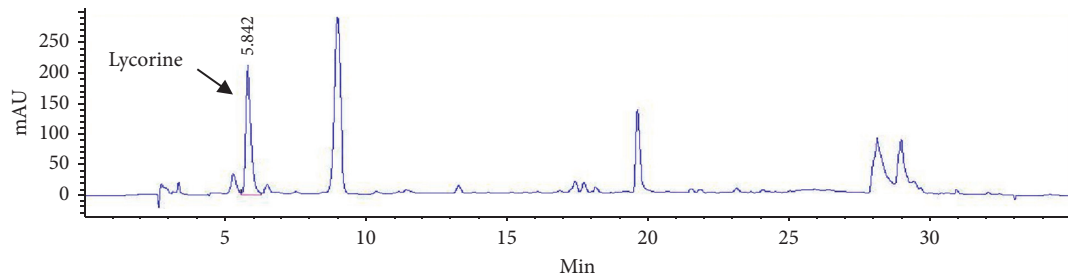
(—) means not tested. ⁽¹⁾ cytotoxicity greater than 30%.



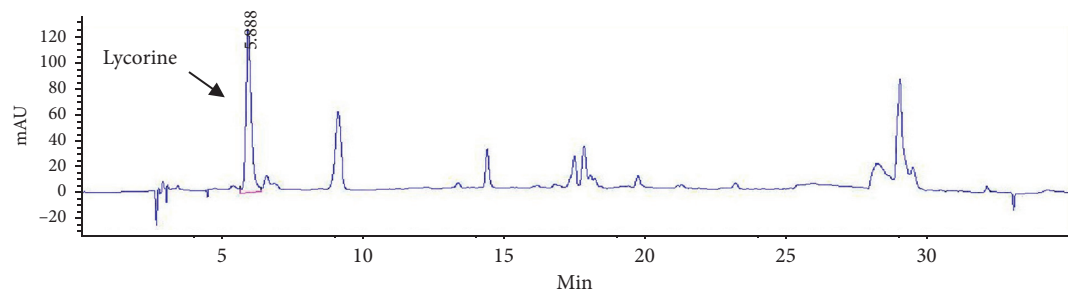
(a)



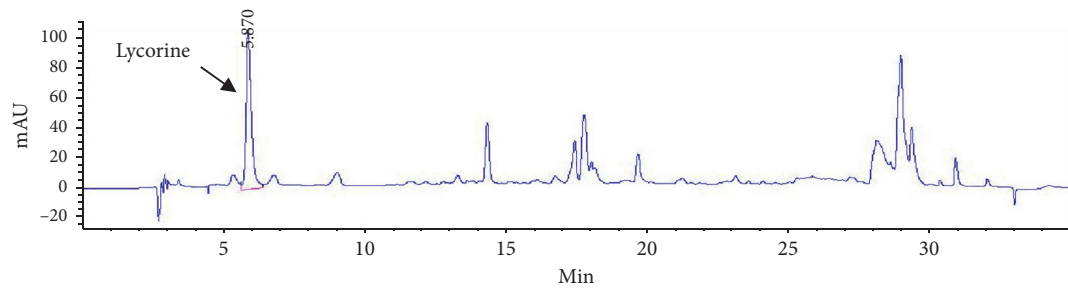
(b)



(c)



(d)



(e)

FIGURE 2: Continued.

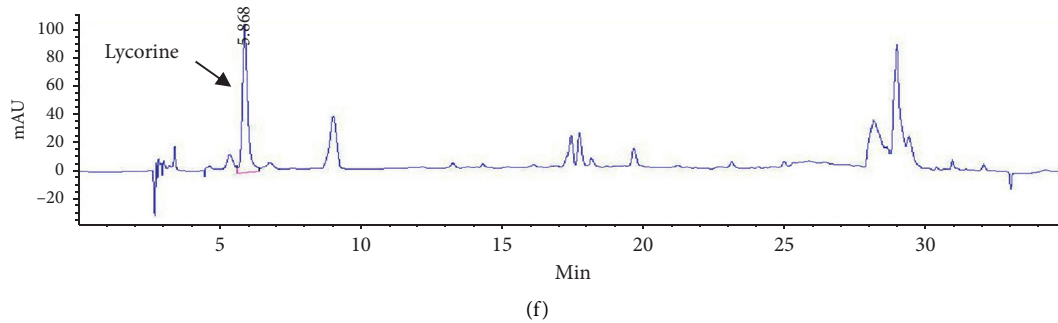


FIGURE 2: HPLC chromatograms of blank (DMSO) (a), standard lycorine solution (0.5 mg/mL) (b), CAA extract at 10 mg/mL (c), CAM extract at 10 mg/mL (d), CAG extract at 10 mg/mL (e) and CAC extract at 10 mg/mL (f) by using HPLC analysis with mobile phase consisting of 0.1%v/v triethylamine in water adjusting pH to 3.0 with phosphoric acid (A) and acetonitrile (B). Gradient elution was programmed as follows: 0–5 min, 5%B; 25 min, 30%B; 25.1–30 min, 80%B; 30.1–35 min, 5%B and detected at the wavelength of 290 nm. The chromatograms of standard lycorine solution (b) and crude extracts solutions (c), (d), (e), and (f) show similar peaks at RT = 5.8.

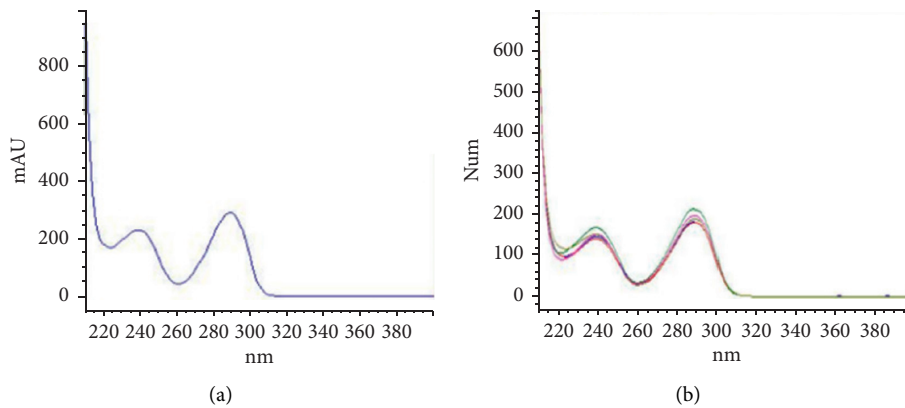


FIGURE 3: Comparing the UV absorption spectra of peak start, peak apex, and peak end at RT = 5.8 of lycorine standard (a), overlaying UV spectrum of each sample solution (CAA, CAM, CAG, and CAC) (b) by using HPLC analysis.

TABLE 3: Linearity, range, LOD, and LOQ of lycorine.

| Validation parameters | Lycorine |
|----------------------------------|-----------------------|
| Linear equation ($y = ax + b$) | $y = 8.2971x + 46.55$ |
| Linearity (r^2) | 1 |
| Range ($\mu\text{g/mL}$) | 50–500 |
| LOD ($\mu\text{g/mL}$) | 1 |
| LOQ ($\mu\text{g/mL}$) | 3.25 |

inflammatory diseases [34]. Therefore, phenolic compounds may contribute to the anti-inflammatory activity via their antioxidant effect. A recent study reported the antioxidant activity of ethanolic extracts of *C. asiaticum* leaf and bulk [35].

Lycorine content in ethanolic extracts of *C. asiaticum* leaves obtained from various preextraction treatments was determined using a validated HPLC method. The method showed good specificity, accuracy, and precision. CAA extract showed the highest lycorine content (34.40 ± 0.41 mg/g) which was significantly higher than that of CAM, CAG, and CAC extracts (p value < 0.05). Our results showed CAA extract exerted the highest inhibitory activity on NO production from LPS-induced RAW 264.7

cells. Lycorine has been shown to have a potent inhibitory activity on NO production. This suggested that lycorine may be the responsible marker of *C. asiaticum* leaves for inhibitory activity on NO production. NO, one of the inflammatory mediators important in the inflammation process which have a destructive effect on articular cartilage, helps bring about osteoarthritis which is the most common chronic degenerative disease. Additionally, lycorine has potent immunological, antitumor, and anti-inflammatory activities [14, 15] and has been shown to decrease autophagy in osteoclasts in vivo [16]. Therefore, lycorine is most likely the responsible active compound in *C. asiaticum* extract thus supporting the traditional use of *C. asiaticum* in the mitigation of joint pain.

Due to lycorine cytotoxicity to RAW264.7, its inhibitory activity on TNF- α and PGE₂ production could not be demonstrated, though it exerted inhibition at a concentration higher than 0.8 $\mu\text{g/mL}$. However, lycorine is not the only active compound in *C. asiaticum*; there are other compounds [36, 37] but they have not been investigated, which should be a subject for future research.

Results of this study confirmed our hypothesis that different preextraction treatments affected the anti-

TABLE 4: Accuracy and precision validation of the analytical method for lycorine.

| Lycorine | Spiked concentration ($\mu\text{g/mL}$) | Measured concentration ($\mu\text{g/mL}$; mean \pm SD) | % RSD | % accuracy |
|----------------------|---|--|-------|------------|
| Intraday ($n = 3$) | 100 | 99.82 \pm 1.20 | 1.21 | 99.82 |
| | 150 | 152.93 \pm 1.83 | 1.19 | 101.96 |
| | 300 | 299.29 \pm 1.38 | 0.46 | 99.76 |
| Interday ($n = 9$) | 100 | 99.07 \pm 1.03 | 0.89 | 99.07 |
| | 150 | 150.93 \pm 2.42 | 1.44 | 100.62 |
| | 300 | 300.08 \pm 1.16 | 0.38 | 100.03 |

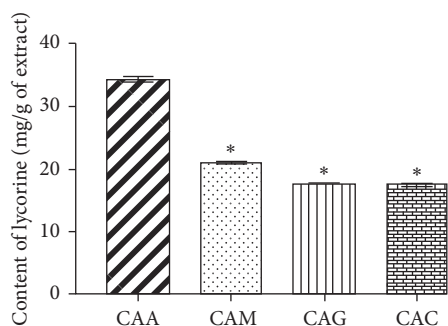


FIGURE 4: Comparison of lycorine contents (mg/g of extract) of the ethanolic extracts of *C. asiaticum* leaves after different preextraction treatments by using HPLC analysis. *Significant difference ($p < 0.05$) compared with CAA analyzed by Tukey's multiple comparisons test.

inflammatory activities and chemical properties of *C. asiaticum* leaves. The extract obtained after hot air (40°C) oven drying (CAA) showed the highest inhibitory activity on NO and TNF- α production, and total phenolic and lycorine contents. Extracts from other preextraction treatments were significantly lower, especially the traditional grilling on a charcoal stove (CAG) and temperature shock in hot and cold water before hot air drying (CAC). It appears that in the case of charcoal stove, factors such as high temperature, smoke, and ashes formed on the leaf surface may cause the degradation of the active compounds. Charcoal on the grilled leaf may adsorb the chemical constituents causing a decrease in total phenolic content and other bioactive components [38]. For the CAC method, the leaves were directly dipped into boiling water (approx. 100°C) and then ice water (approx. 0°C). This process may cause the degradation and leaching of some bioactive compounds. The extract from the CAC method showed the lowest lycorine content. The microwave drying method (CAM) is the technique that transforms electromagnetic energy into thermal energy. The electromagnetic energy may affect some compounds at the molecular level and the rapid heating of the material may cause thermal degradation of heat-sensitive components. A previous report showed that total phenolic content was decreased by microwave heating [39, 40]. Moreover, another study revealed that lycorine was unstable to light, oxygen, and heat. Since ring C of this alkaloid contains a double bond and at least one hydroxyl group, amino function and aromatization of this ring do occur under a variety of reaction conditions [41]. Hence, the results of our study suggested

that different preextraction treatments affect the anti-inflammatory activity and chemical properties of *C. asiaticum* leaves differently, some of which are quite detrimental.

Results of this study support the use of *C. asiaticum* in Thai traditional medicine for pain relief in osteoarthritis. Hot air drying in an oven at 40°C for 10 hours should be recommended as a preextraction treatment for *C. asiaticum* leaves for its simplicity and best retention of the herbal quality. It can also be easily scaled up to industrial level for further development of *C. asiaticum* as a drug to treat joint pain in osteoarthritis. However, more study may be needed to investigate other bioactive compounds in the extract and the mechanisms through which they mitigate the pain.

5. Conclusion

Our study showed that air drying at 40°C is the best preextraction treatment for *C. asiaticum* leaves prior to 95% ethanolic extraction. It produced the extract with the highest anti-inflammatory activity as shown by its ability to inhibit nitric oxide and TNF- α production in RAW264.7 cells and was not toxic to the cells. The extract also had the highest total phenolic and lycorine contents which are antioxidants that influence its anti-inflammatory activity. Therefore, this study supports the traditional use of *C. asiaticum* to mitigate joint pain and hot air drying should be used as the preextraction treatment.

Data Availability

The data used to support the findings of this study are included within the article.

Conflicts of Interest

The authors declare that they have no conflicts of interest.

Acknowledgments

The authors would like to thank Thailand Research Fund through the Royal Golden Jubilee Ph.D. Program (Grant no. PHD/0078/2558) for the support of this work. They also wish to thank the Center of Excellence in Applied Thai Traditional Medicine Research (CEATMR) and Bualuang ASEAN Chair Professorship, Faculty of Medicine, Thammasat University, for financial support and the use of laboratory facilities.

References

- [1] R. Zamora, Y. Vodovotz, and T. R. Billiar, "Inducible nitric oxide synthase and inflammatory diseases," *Molecular Medicine*, vol. 6, no. 5, pp. 347–373, 2000.
- [2] H. L. Wright, R. J. Moots, R. C. Bucknall, and S. W. Edwards, "Neutrophil function in inflammation and inflammatory diseases," *Rheumatology*, vol. 49, no. 9, pp. 1618–1631, 2010.
- [3] M. Kapoor, J. Martel-Pelletier, D. Lajeunesse, J.-P. Pelletier, and H. Fahmi, "Role of proinflammatory cytokines in the pathophysiology of osteoarthritis," *Nature Reviews Rheumatology*, vol. 7, no. 1, pp. 33–42, 2011.
- [4] I. Ozguney, "An alternative topical treatment of osteoarthritis of the knee with cutaneous diclofenac solution," *Expert Opinion on Pharmacotherapy*, vol. 9, no. 10, pp. 1805–1816, 2008.
- [5] C. W. Fennell and J. van Staden, "Crinum species in traditional and modern medicine," *Journal of Ethnopharmacology*, vol. 78, no. 1, pp. 15–26, 2001.
- [6] I. H. Burkill, W. Birtwistle, F. W. Foxworthy et al., *A Dictionary of the Economic Products of the Malay Peninsula*, Published on behalf of the governments of Malaysia and Singapore by the Ministry of Agriculture and Cooperative, Kuala Lumpur, Malaysia, 1996.
- [7] P. W. Grosvenor, P. K. Gothard, N. C. McWilliam, A. Supriono, and D. O. Gray, "Medicinal plants from riau province, sumatra, Indonesia. Part 1: uses," *Journal of Ethnopharmacology*, vol. 45, no. 2, pp. 75–95, 1995.
- [8] C. Pichiansunthorn, M. Chawalit, and V. Jeerawong, "The Describe of Osod Phra Narai Textbook, pp. 221–227, Amarin Publishing, Bangkok, Thailand, 2001.
- [9] R. Pholhiamhan, S. Saensouk, and P. Saensouk, "Ethnobotany of phu Thai ethnic group in nakhon phanom province, Thailand," *Walailak Journal of Science and Technology*, vol. 15, no. 10, pp. 679–699, 2018.
- [10] S. G. Ghane, U. A. Attar, P. B. Yadav, and M. M. Lekhak, "Antioxidant, anti-diabetic, acetylcholinesterase inhibitory potential and estimation of alkaloids (lycorine and galanthamine) from Crinum species: an important source of anti-cancer and anti-Alzheimer drug," *Industrial Crops and Products*, vol. 125, pp. 168–177, 2018.
- [11] A. Anuthakoengkun and A. Itharat, "Inhibitory effect on nitric oxide production and free radical scavenging activity of Thai medicinal plants in osteoarthritic knee treatment," *Journal of the Medical Association of Thailand*, vol. 97, no. 8, pp. 116–124, 2014.
- [12] A. M. Samud, M. Z. Asmawi, J. N. Sharma, and A. P. M. Yusof, "Anti-inflammatory activity of Crinum asiaticum plant and its effect on bradykinin-induced contractions on isolated uterus," *Immunopharmacology*, vol. 43, no. 2-3, pp. 311–316, 1999.
- [13] Y. B. Ji, P. Tian, Q. C. Dai, S. T. Wang, and N. Chen, "The present research situation of Crinum asiaticum alkaloids active ingredient," *Applied Mechanics and Materials*, vol. 411-414, pp. 3181–3186, 2013.
- [14] M. Khalifa, E. Attia, J. Fahim, and M. Kamel, "An overview on the chemical and biological aspects of lycorine alkaloid," *Journal of Advanced Biomedical and Pharmaceutical Sciences*, vol. 1, no. 2, pp. 41–49, 2018.
- [15] Y. Li, J. Liu, L. J. Tang, Y. W. Shi, W. Ren, and W. X. Hu, "Apoptosis induced by lycorine in KM3 cells is associated with the G0/G1 cell cycle arrest," *Oncology Reports*, vol. 17, no. 2, pp. 377–384, 2007.
- [16] H. J. Park, M. G. Zadeh, J. H. Suh, and H. S. Choi, "Lycorine attenuates autophagy in osteoclasts via an Axis of mROS/TRPML1/TFEB to reduce LPS-induced bone loss," *Oxidative Medicine and Cellular Longevity*, vol. 2019, Article ID 8982147, 11 pages, 2019.
- [17] G. O. Sinir, A. O. Karabacak, C. E. Tamer, and O. U. Copur, "The effect of hot air, vacuum and microwave drying on drying characteristics, rehydration capacity, color, total phenolic content and antioxidant capacity of Kumquat (Citrus japonica)," *Food Science and Technology*, vol. 39, no. 2, pp. 475–484, 2019.
- [18] L. Zou, F. Lu, B. Lin et al., "Stability of alkaloids during drying process and their effect on anticoagulating activity of uncariaie ramulus cum uncis," *Journal of Analytical Methods in Chemistry*, vol. 2019, Article ID 7895152, 7 pages, 2019.
- [19] S. Tewtrakul and A. Itharat, "Nitric oxide inhibitory substances from the rhizomes of Dioscorea membranacea," *Journal of Ethnopharmacology*, vol. 109, no. 3, pp. 412–416, 2007.
- [20] S. Makchuchit, R. Rattarom, and A. Itharat, "The anti-allergic and anti-inflammatory effects of Benjakul extract (a Thai traditional medicine), its constituent plants and its some pure constituents using in vitro experiments," *Biomedicine and Pharmacotherapy*, vol. 89, pp. 1018–1026, 2017.
- [21] O. Folin and V. Ciocalteu, "On tyrosine and tryptophan determination in proteins," *Journal of Biological Chemistry*, vol. 73, pp. 627–650, 1927.
- [22] ICH Harmonised Tripartite Guideline, "Validation of analytical procedures: text and methodology Q2(R1)," in *Proceedings of the International Conference on Harmonisation of Technical Requirements for Registration of Pharmaceuticals for Human Use*, pp. 6–13, Geneva, Switzerland, November 2005.
- [23] S. Krasnokutsky, M. Attur, G. Palmer, J. Samuels, and S. B. Abramson, "Current concepts in the pathogenesis of osteoarthritis," *Osteoarthritis and Cartilage*, vol. 16, no. 3, pp. 1–3, 2008.
- [24] P. Wojdasiewicz, L. A. Poniatowski, and D. Szukiewicz, "The role of inflammatory and anti-inflammatory cytokines in the pathogenesis of osteoarthritis," *Mediators of Inflammation*, vol. 2014, Article ID 561459, 19 pages, 2014.
- [25] R. Rainbow, W. Ren, and L. Zeng, "Inflammation and joint tissue interactions in oa: implications for potential therapeutic approaches," *Arthritis*, vol. 2012, Article ID 741582, 8 pages, 2012.
- [26] Ministry Publishing, *Department of Thai Traditional and Alternative Medicine, Guidelines for Certification of Folk Medicine*, Ministry Publishing, Bangkok, Thailand, 2019.
- [27] M. Z. Asmawi, O. M. Arafat, S. Amirin, and I. M. Eldeen, "In vivo antinociceptive activity of leaf extract of Crinum asiaticum and phytochemical analysis of the bioactive fractions," *International Journal of Pharmacology*, vol. 7, no. 1, pp. 125–129, 2011.
- [28] C. K. Chen, F. H. Lin, L. H. Tseng, C. L. Jiang, and S. S. Lee, "Comprehensive study of alkaloids from Crinum asiaticum var. sinicum Assisted by HPLC-DAD-SPE-NMR," *Journal of Natural Products*, vol. 74, no. 3, pp. 411–419, 2011.
- [29] M. A. Rahman, H. S. M. A. Hossain, N. U. Ahmed, and M. S. Islam, "Analgesic and anti-inflammatory effects of Crinum asiaticum leaf alcoholic extract in animal models," *African Journal of Biotechnology*, vol. 12, no. 2, pp. 212–218, 2013.
- [30] J. Kang, Y. Zhang, X. Cao et al., "Lycorine inhibits lipopolysaccharide-induced iNOS and COX-2 up-regulation in RAW264.7 cells through suppressing P38 and STATs activation and increases the survival rate of mice after LPS challenge," *International Immunopharmacology*, vol. 12, no. 1, pp. 249–256, 2012.

- [31] Y. Yamazaki and Y. Kawano, "Inhibitory effects of herbal alkaloids on the tumor necrosis factor- α and nitric oxide production in lipopolysaccharide-stimulated RAW264 macrophages," *Chemical & Pharmaceutical Bulletin*, vol. 59, no. 3, pp. 388–391, 2011.
- [32] G. Piluzza and S. Bullitta, "Correlations between phenolic content and antioxidant properties in twenty-four plant species of traditional ethnoveterinary use in the Mediterranean area," *Pharmaceutical Biology*, vol. 49, no. 3, pp. 240–247, 2011.
- [33] S. Goswami, R. Das, P. Ghosh et al., "Comparative antioxidant and antimicrobial potentials of leaf successive extract fractions of poison bulb, *Crinum asiaticum* L.," *Industrial Crops and Products*, vol. 154, Article ID 112667, 2020.
- [34] A. P. Wagner, S. Mitran, S. Sivanesan, E. Chang, and A. M. Buga, "ROS and brain diseases: the good, the bad, and the ugly," *Oxidative Medicine and Cellular Longevity*, vol. 2013, Article ID 963520, 14 pages, 2013.
- [35] I. D. Riris, M. Simorangkir, and A. Silalahi, "Antioxidant, toxicity and antibacterial properties of ompu-ompu (*Crinum asiaticum*-L) ethanol extract," *RASAYAN Journal of Chemistry*, vol. 11, no. 3, pp. 1229–1235, 2018.
- [36] M. A. Arai, R. Akamine, S. K. Sadhu, F. Ahmed, and M. Ishibashi, "Hedgehog/GLI-mediated transcriptional activity inhibitors from *Crinum asiaticum*," *Journal of Natural Medicines*, vol. 69, no. 4, pp. 538–542, 2015.
- [37] M. F. Mahomoodally, N. B. Sadeer, S. Suroowanc et al., "Ethnomedicinal, phytochemistry, toxicity and pharmacological benefits of poison bulb *Crinum asiaticum* L.," *South African Journal of Botany*, pp. 1–14, 2020, In press.
- [38] C. Xiao, L. Zheng, G. Su, and M. Zhao, "Effect of solution pH and activated carbon dosage on the decolorization ability, nitrogen components and antioxidant activity of peanut meal hydrolysate," *International Journal of Food Science and Technology*, vol. 49, no. 12, 2014.
- [39] P. Sharma and H. S. Gujral, "Effect of sand roasting and microwave cooking on antioxidant activity of barley," *Food Research International*, vol. 44, no. 1, pp. 235–240, 2011.
- [40] M. Zhang, H. Chen, J. Li, Y. Pei, and Y. Liang, "Antioxidant properties of tartary buckwheat extracts as affected by different thermal processing methods," *LWT - Food Science and Technology*, vol. 43, no. 1, pp. 181–185, 2010.
- [41] W. C. Wildman, "Chapter 9 alkaloids of the amaryllidaceae," *The Alkaloids: Chemistry and Physiology*, vol. 6, pp. 289–413, 1960.

Research Article

Platelet-Rich Plasma Ameliorates Monosodium Iodoacetate-Induced Ankle Osteoarthritis in the Rat Model via Suppression of Inflammation and Oxidative Stress

G. H. Ragab ¹, F. M. Halfaya ¹, O. M. Ahmed ², W. Abou El-Kheir ³, E. A. Mahdi ⁴,
T. M. Ali ^{5,6}, M. M. Almeahmadi ⁷, and U. Hagag ¹

¹Anesthesiology and Radiology Department, Faculty of Veterinary Medicine, Beni-Suef University, Beni-Suef, Egypt

²Physiology Division, Zoology Department, Faculty of Science, Beni-Suef University, P.O. Box 62521, Beni-Suef, Egypt

³Department of Immunology, Military Medical Academy, Cairo, Egypt

⁴Pathology Department, Faculty of Veterinary Medicine, Beni-Suef University, Beni-Suef, Egypt

⁵Physiology Department, College of Medicine, Taif University, Taif, Saudi Arabia

⁶Physiology Department, Faculty of Medicine, Beni-Suef University, Beni-Suef, Egypt

⁷Department of Clinical Laboratory Sciences, College of Applied Medical Sciences, Taif University, P.O. Box 11099, Taif 21944, Saudi Arabia

Correspondence should be addressed to F. M. Halfaya; fma_vet2010@yahoo.com

Received 3 October 2020; Revised 19 December 2020; Accepted 7 January 2021; Published 19 January 2021

Academic Editor: Arham Shabbir

Copyright © 2021 G. H. Ragab et al. This is an open access article distributed under the Creative Commons Attribution License, which permits unrestricted use, distribution, and reproduction in any medium, provided the original work is properly cited.

Until now, there is no treatment that cause complete cure of the chronic inflammatory and degenerative disease, osteoarthritis (OA). Moreover, the underlying mechanisms of OA development and progress are not fully elucidated, and the present pharmacological treatment alternatives are restricted and associated with adverse side effects. Thus, the present study was conducted to evaluate the role of platelet-rich plasma (PRP) in the remedy of OA in the rat model in terms of inflammation, ankle histopathological alterations, and oxidative stress. OA was induced in male Wistar rats by injection of MIA (2 mg)/50 μ L isotonic saline in the right ankle joint for two successive days in each rat. After the 2nd MIA injection, the osteoarthritic rats were allocated into two groups such as the MIA group (group 2) and MIA + PRP group (group 3). The MIA + PRP group was treated with PRP (50 μ L) by injection into the ankle joint of the right hind limb of each rat at days 14, 21, and 28 after the 2nd injection of MIA. The same equivalent volume of saline, as a substitute of PRP, was injected into the ankle joint of each rat of the normal control group (group 1) and MIA group (group 2) at the same tested periods. Swelling of joint, bodyweight, total leucocytes count (TLC), and morphological as well as histological changes of ankle joints were evaluated. Serum lipid peroxides (LPO), glutathione (GSH), and glutathione S-transferase (GST) levels were examined as biomarkers of oxidative stress. Serum tumor necrosis factor- α (TNF- α), interleukin-17 (IL-17), and interleukin-4 (IL-4) were investigated by ELISA as biomarkers of inflammation. In addition, magnetic resonance imaging (MRI) was carried out to investigate the soft tissues in joints. The obtained results revealed that PRP reduced LPO and increased GSH and GST levels in osteoarthritic rats. Also, PRP significantly diminished serum TNF- α and IL-17 levels, while it increased IL-4 serum levels in rats with MIA-induced OA. Morphological observations, histological analysis, and MRI revealed a gradual diminishing in joint inflammation and destruction of cartilage in PRP-injected osteoarthritic rats. Based on these results, it can be suggested that PRP has antiarthritic potential in MIA-induced OA, which may be mediated via suppression of inflammation and oxidative stress.

1. Introduction

Osteoarthritis (OA), the main pervasive and destructive joint maladies, is a chronic inflammatory joint disease, which is characterized by alterations in synovial membrane, loss of joint cartilage, thickening of the joint capsule, and finally leading to pain, lameness due to stiffness of joints [1].

OA is a main reason of lameness and a popular trouble in all types of animal especially equine and pet animals. It can influence various joints. In performance and racing equines, it frequently influences the high mobility joints such as fetlock and carpal joints; although in equines utilized for less hard activities, it is more popular in the low motion joints, for example, the distal tarsal and pastern joints [2].

OA is initiated by several causes, and though elderly, it is the utmost common cause related to the OA progress; other etiological factors such as mechanical and hereditary factors also lead to OA progress. Moreover, OA is distinguished by the gradual damage of articular cartilage and osteophytes formation and is related to cartilage deterioration and subchondral bone alterations, which produce long-lasting pain and functional restrictions in the joint [3].

Although now accessible, clinical treatments for OA that incorporates usual analgesics and calming nonsteroidal anti-inflammatory drugs (NSAIDs) are unavailing in decelerating disease development, and they slightly improve signs by diminishing pain and increasing joint motion. Furthermore, their long-lasting usage has been restricted by their harmful aspect effects, and surgical interferences are ultimately needed [4].

Platelets-rich plasma (PRP) acts like a biologic incentive to affect cartilage restoration. Despite the verity that the mixture of growth factors essential to the PRP regenerative properties is ambiguous, the transforming growth factor- β 1 (TCF- β 1) has been proposed to promote stem cells, proliferation of chondrocyte, and restrict catabolic action [5].

PRP has achieved publicity as a clinical treatment in soft and hard tissues in all surgical fields, most prominently in acute surgical conditions and in the lasting wound management. Surgeons are utilizing PRP to take benefit of fibrin clot that help in hemostasis accompanied by growth factors supplying in this form to enhance wound healing [6].

The accomplishment of this curative sits is not only restricted to the characteristic of PRP but also to its reliable treatment. Improper use of PRP can promote an ineffectual biological reply and inappropriate clinical outcomes. Thus, intraarticular injection that extends to the cartilage and the synovial membrane successfully improves the joint environment, slows joint pain progression, and adjusts the clinical symptoms [7].

Therefore, the purpose of the existing work was to assess the efficacy of intraarticular ankle injection of PRP in ameliorating inflammation, joint damage, and oxidative stress induced by monosodium iodoacetate- (MIA-) induced ankle OA in the rat model.

2. Materials and Methods

2.1. Animals. Thirty male Wistar rats were used in the current investigation. Their weights ranged from 100 g to

120 g, being 7–9 weeks of age. The animals were obtained from the Laboratory Animal Unit of Helwan Farm, Holding Company for Biological Products and Vaccines (VAC-SERA), Egypt. Animals were retained under observance for about 10 days prior to the beginning of the research to eradicate any infections. The animals were kept in cages made from polypropylene with ventilated covers of stainless steel in the Animal House of Department of Zoology, Faculty of Science, Beni-Suef University, Egypt, at standard temperature (20–25°C) and ordinary daily lighting cycle (10–12 h/day) and were supplemented balanced standard diet and water ad libitum.

2.2. Induction of Osteoarthritis. Under anesthesia using ketamine (70 mg/kg) and xylazine (7 mg/kg), OA was induced by injecting 50 μ L physiological saline containing 2 mg MIA (2 mg/50 μ L) (Sigma-Aldrich, St. Louis, MO) with a 21-gauge needle into the ankle joint of the right hind leg on 2 succeeding days, as formerly illustrated [8].

2.3. PRP Preparation. PRP was prepared using the double spin method in accordance with the manner of Pacheco et al. [9] and Asjid et al. [10] with some modifications. Blood was collected by puncture of the heart of 5 healthy rats and kept in tubes with anticoagulant (3.8% sodium citrate). The technique was performed under sterile condition, in a Biobase vertical laminar flow cabinet (Biobase model: BBS V1300; NO-51, South Gongye Road, Jinan, Shandong Province, China). Lysing platelets were averted to preclude their ability loss to excrete growth factors. Samples of blood were centrifuged at 1000 round per minute (rpm) for ten minutes to separate RBCs, WBCs, and platelet cells. The upper part of the supernatant, up to the fog zone edge, which corresponds to plasma and platelets, was collected into new tubes. PRP was obtained by centrifugation of these tubes at 2000 rpm for 10 minutes and disposal of the supernatant, merely the lower 20% of the plasma was reaped (PRP or plasma rich in platelets). Around, the upper 80% of the plasma was taken away and kept into another tube considered as PPP (plasma poor in platelets). The residual material including the platelet pellet was resuspended, producing the PRP that was deemed appropriate for the study's aim. PRP prepared in this experiment was utilized within 6 hours. PRP was activated by adding 50 μ L 10% calcium chloride (LABiTec GmbH, Germany) (0.025 mol/L) to 3 ml blood. PRP was administrated by intraarticular injection immediately after activation.

2.4. Animal Grouping. After the accommodation period, the Wistar rats were randomly allocated into three groups (10 rats/each group).

2.4.1. Normal Control Group. It is composed of normal rats that were injected with 50 μ L isotonic sterile saline in the ankle joint of the right hind limb of each rat at 14, 21, and 28 days.

2.4.2. MIA Group. Rats in this osteoarthritic group were injected with MIA in the ankle joint of the right hind limb in two consecutive days. The rats within this group were also injected with 50 μ L isotonic sterile saline in the ankle joint of the right hind limb at 14, 21, and 28 days after MIA injection.

2.4.3. MIA-PRP Group. This osteoarthritic group were injected with MIA in the ankle joint of the right hind limb in two consecutive days and also injected with PRP (50 μ L) into the ankle joint of the right hind limb at 14, 21, and 28 days after injection of MIA.

The bodyweight was measured once a week. At the end of experimental periods, under diethyl ether anesthesia, we collected blood samples from jugular vein. A portion of blood from every rat was collected in tubes having ethylenediamine tetra acetic acid (EDTA) solution (50 ml of 15% EDTA/2.5 ml blood) for leukocytes count. Another portion of blood was collected in tubes having no anticoagulant and allowed to coagulate and then centrifuged at 3000 rpm for 15 min. The clear nonhaemolysed supernatant sera were quickly aspirated and preserved at -20°C until utilized.

2.5. Ankle Measurement. The alterations in the transverse and anteroposterior diameters of the osteoarthritic and normal ankles were observed. Ankle diameters were measured using a micrometer [11]. The measurements were recorded every week (on the day zero till the end of experiment) after MIA injection. Also, the right legs were photographed by a camera.

2.6. Magnetic Resonance Imaging (MRI). The right hind legs of normal, MIA, and MIA-PRP Wistar rats were subjected to random scan by MRI before and after treatment. Rats were chosen from every group and scanned after anesthesia by ketamine and xylazine (70 mg/kg ketamine and 7 mg/kg xylazine). The rats were examined on a 1.5 Tesla whole body MR scanner (Philip Medical System, Intera) with an extremity coil. The rats were located sited in prone situation with the hind legs expanded caudolaterally through using tape to fix the rat, so that the right ankle joint was placed in the middle of the scanning coil. MR images were obtained with a sequence of T1 weighted in coronal slice orientation by the succeeding series parameters (TR = 3000 ms, TE = 15 ms, and slice thickness = 2 mm).

2.7. Detection of Total Leukocytes Count. TLC was assessed by using Turk's solution that composed of a stain (gentian violet) and 1% acetic acid [12].

2.8. Detection of Serum Cytokines. TNF- α , IL-17, and IL-4 levels were assayed by utilizing special ELISA (enzyme-linked immunosorbent assay) kits obtained from R and A systems, USA.

2.9. Detection of Serum Oxidative Stress and Antioxidant Defense Markers. Serum lipid peroxides (LPO) and

glutathione (GSH) levels were detected based on the procedures of Preuss et al. [13] and Beutler et al. [14], respectively, with some minor alterations. The activity of serum glutathione S-transferase (GST) was determined in accordance with Mannervik et al. [15].

2.10. Histopathological Examination. After sacrifice (42 days after MIA injection), the right ankles were removed and placed in 10% buffered formalin for 48 hours. Decalcification was performed with 10% formic acid which was replaced twice weekly for two weeks. The end point of decalcification was assessed physically with a surgical blade. After complete decalcification, the samples were washed with phosphate buffer solution (PBS), dehydrated in a graded ethanol series, and embedded in paraffin wax. Sagittal sections measuring 5 μ m in thickness were prepared and stained with hematoxylin and eosin (H&E) [16]. Histopathological examination of synovial inflammation, cartilage, and bone damages were performed by a pathologist blindly.

2.11. Statistical Analysis. Statistical analysis was achieved by using SPSS v.25. Results were expressed as mean \pm standard error (SE), and all statistical comparisons were performed by Duncan's test post hoc. Values of $p < 0.05$ were deemed significant; however, those of $p > 0.05$ were deemed nonsignificant.

3. Results

3.1. Morphological Feature. The morphological alterations in the right ankles of the normal control, osteoarthritic group (MIA group), and osteoarthritic-treated group (MIA + PRP group) are shown in Figures 1–4. The right legs showed noticeable swelling and redness at the 1st week (Figure 2) and 6th week (Figure 3) after injection of MIA when compared with those of normal control groups (Figure 1). These worsened signs were more distinct at the 1st week (acute inflammation). The remedy of osteoarthritic rats with PRP resulted in a significant improvement of these morphological symptoms as shown in Figure 4 (at the 6st week).

3.2. Effect on Bodyweight. The changes of bodyweight in the normal control, MIA-administered group, and MIA + PRP-administered group through six weeks after MIA administration are shown in Figure 5. The MIA-administered group exhibited a significant decrease ($p < 0.05$) in the bodyweight at periods 4, 5, and 6 weeks; the recorded percentage decreases were -6.8% , -16.5% , and -19.8% , respectively, as compared to the normal control group.

The remedy of the osteoarthritic rats with PRP produced a significant increase ($p < 0.05$) in bodyweight at the 5th and 6th weeks; the recording percentage changes were 6.9% and 15.9% in comparison with the MIA group.

3.3. Alterations in Ankle Swelling Indices. As compared with normal control animals, MIA rats exhibited a significant



FIGURE 1: Ankle joint of normal control rat.



FIGURE 4: Ankle joint of osteoarthritic rat treated on PRP 6th week.



FIGURE 2: Ankle joint of osteoarthritic rat on 1st week.



FIGURE 3: Ankle joint of osteoarthritic rat on 6th week.

increase in the right ankle anteroposterior and transverse diameters at all check periods except at zero time (Figures 6(a) and 6(b)). On the other hand, the MIA + PRP group exhibited a marked decrease in the right ankle anteroposterior and transverse diameters at all check timepoints after MIA injection. The effect PRP on anteroposterior diameter was significant at the 4th, 5th, and 6th weeks after MIA injection, while the effect on transverse diameter at the 3rd, 4th, 5th, and 6th weeks in comparison with MIA control. The ameliorating effects were more pronounced at the period extended to 6 weeks. Hence, PRP treatment yielded obvious influences on the swelling rate of ankle.

3.4. MRI Evaluation of OA. MRI of the normal ankle joint demonstrating normal anatomy of the joint and foot is shown in Figure 7(a). On the other hand, MRI of an osteoarthritic ankle joint after MIA injection reflects the increased diameter of the joint and displays extensive soft tissue edema in acute osteoarthritis (Figure 7(b)) and soft tissue edema decreased in chronic osteoarthritis (Figure 7(c)). In contrast, the treatment with PRP exhibited mostly low signals and diminished diameter of the joint (Figure 7(d)), showing an effective suppression of inflammation and curative outcome.

3.5. Effect on TLC. TLC was significantly raised ($p < 0.05$) in the MIA-induced osteoarthritic group when compared with the normal control group. Osteoarthritic rat's treatment with PRP resulted in a marked improvement ($p < 0.05$) in TLC (Figure 8).

3.6. Effect on Serum TNF- α (Th1 Cytokine), IL-17 (Th17 Cytokine), and IL-4 (Th2 Cytokine) Levels. The serum TNF- α and IL-17 levels were significantly ($p < 0.05$) increased in MIA-induced osteoarthritic rats when compared to normal control rats. The remedy of MIA-induced osteoarthritic rats with PRP resulted in a significant ($p < 0.05$) reduction of the

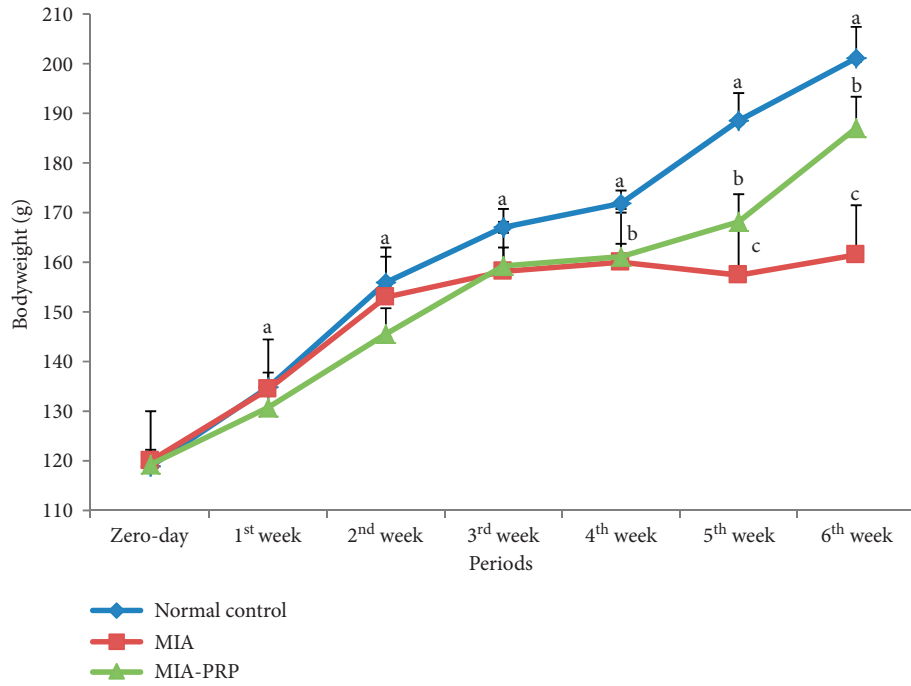
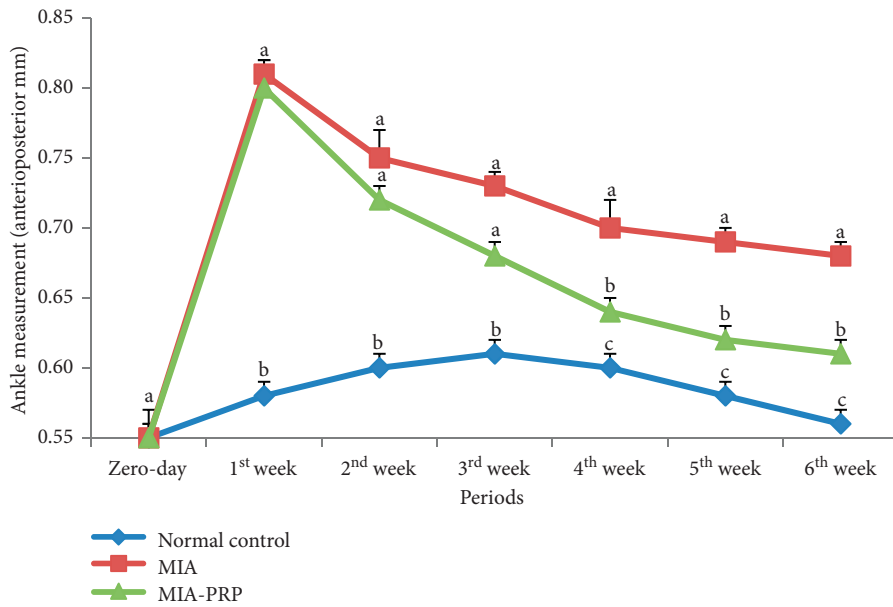
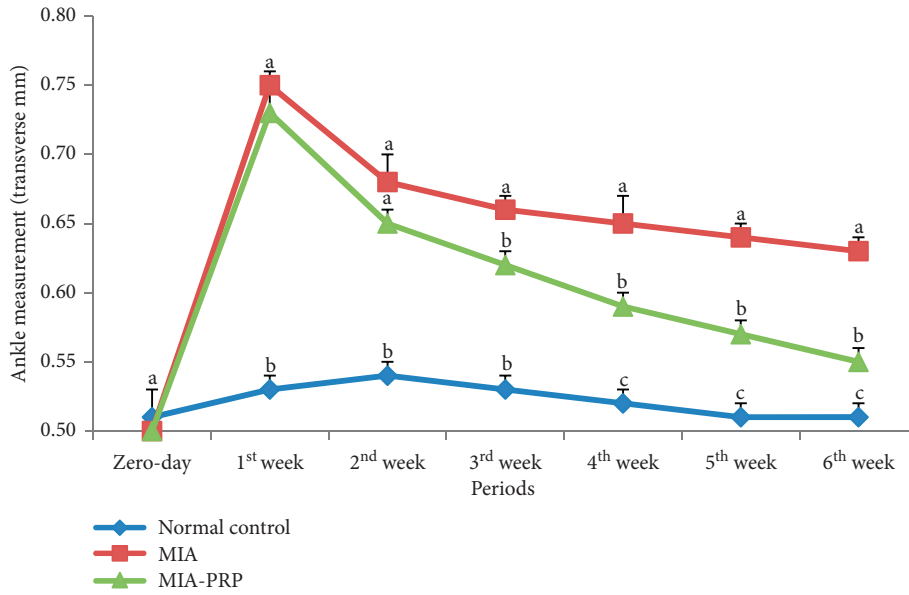


FIGURE 5: Bodyweight changes in normal control, MIA, and MIA-PRP groups. At each period, the means, which have different symbols (letters), are significantly different at $p < 0.05$.



(a)

FIGURE 6: Continued.



(b)

FIGURE 6: (a) Ankle measurements (anteroposterior) in normal control, MIA, and MIA-PRP groups. At each period, the means, which have different symbols (letters), are significantly different at $p < 0.05$. (b) Ankle measurements (transverse) in normal control, MIA, and MIA-PRP groups. At each period, the means, which have different symbols (letters), are significantly different at $p < 0.05$.

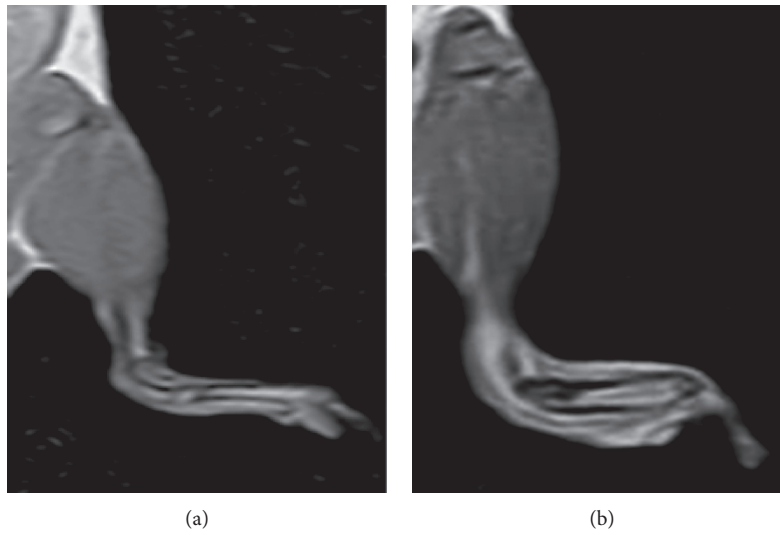


FIGURE 7: Continued.

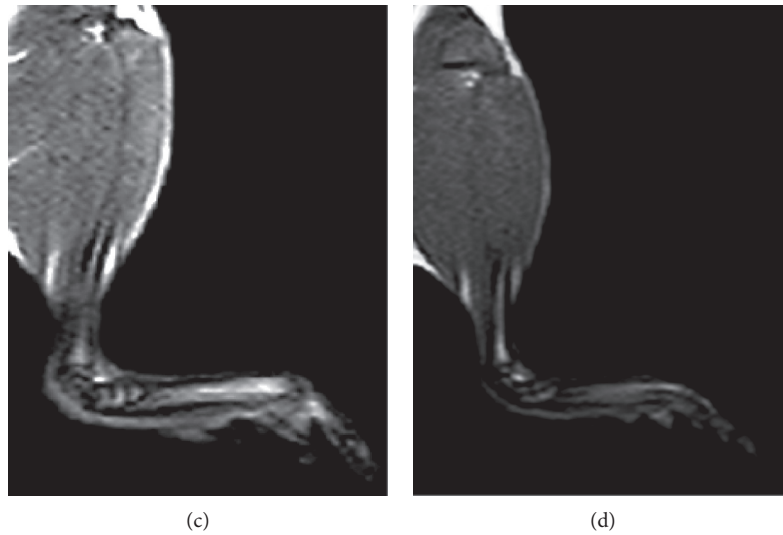


FIGURE 7: T1-weighted MR images of the right ankle joints of normal control, MIA, and MIA + PRP groups showing normal joint and foot anatomy (Figure 7(a)), enlarged diameter of the joint with extensive soft-tissue edema in acute osteoarthritic rats (Figure 7(b)), and reduced soft tissue edema in chronic osteoarthritic rats and still enlarged joint diameter as compared to the normal control (Figure 7(c)). In contrast, PRP treatment revealed a diminished diameter of the joint resembling that of normal control (Figure 7(d)). (a) Normal control. (b) Acute OA (MIA group). (c) Chronic OA (MIA group). (d) MIA-PRP group.

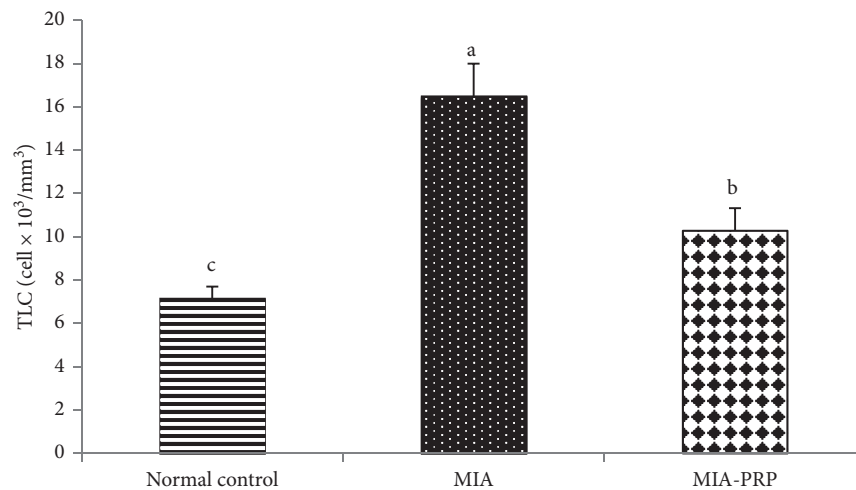


FIGURE 8: TLC in normal control, MIA, and MIA-PRP groups. The means, which have different symbols (letters), are significantly different at $p < 0.05$.

raised $\text{TNF-}\alpha$ and IL-17 levels (Figures 9 and 10). In contrast to $\text{TNF-}\alpha$ and IL-17, the IL-4 level in serum was extensively lessened ($p < 0.05$) in MIA-induced osteoarthritic rats. The remedy of osteoarthritic rats with PRP markedly boosted ($p < 0.05$) the lessened IL-4 level (Figure 11).

3.7. Effect on Antioxidant Defense and Oxidative Stress. Administration of MIA significantly elevated serum oxidative stress as evidenced by the significant increase ($p < 0.05$) in the serum LPO level and obvious lessening ($p < 0.05$) in the serum GSH level and GST activity when compared to normal control rats. Treatment with PRP hindered oxidative stress induced by MIA as recognized by marked decrease ($p < 0.05$) in the serum LPO level and raises

($p < 0.05$) of the diminished serum GSH level and GST activity when compared to the MIA group; hence, PRP diminished oxidative stress and enhanced antioxidant defense mechanism (Table 1).

Data are expressed as mean \pm standard error. Number of noticed samples in every group is 6. Means, which have the similar superscript symbol (s), are not significantly different. Percentage changes were estimated by the MIA group with the normal control group and the PRP group with the MIA group.

3.8. Histopathological Changes. Hematoxylin and eosin-stained sections of ankle joint tissues from normal control rats revealed no inflammation and normal histological

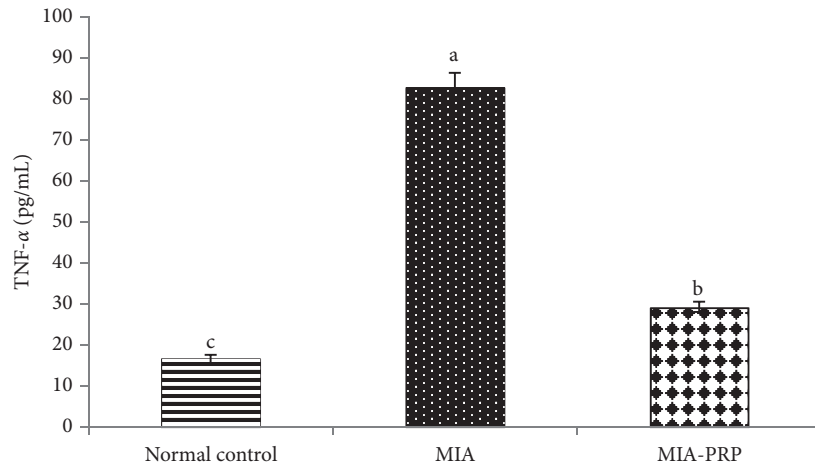


FIGURE 9: Serum TNF- α level in normal control, MIA, and MIA-PRP groups. The means, which have different symbols (letters), are significantly different at $p < 0.05$.

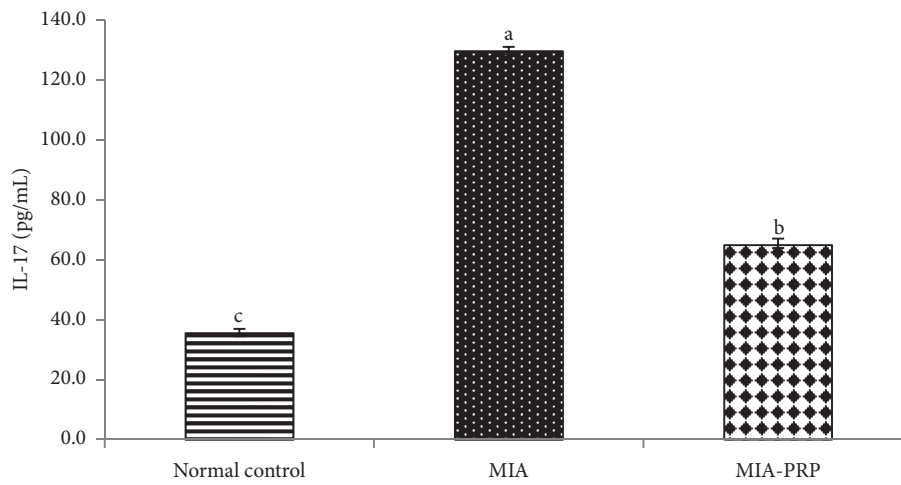


FIGURE 10: Serum IL-17 level in normal control, MIA, and MIA-PRP groups. The means, which have different symbols (letters), are significantly different at $p < 0.05$.

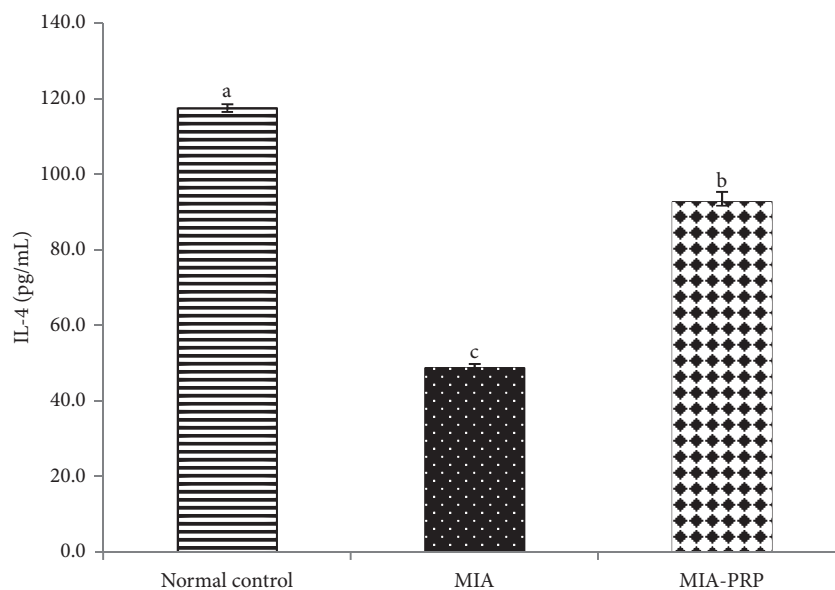


FIGURE 11: Serum IL-4 level in normal control, MIA, and MIA-PRP groups. The means, which have different symbols (letters), are significantly different at $p < 0.05$.

TABLE 1: Serum LPO, GSH level and GST activity in normal control, MIA, and MIA-PRP groups.

| Groups | LPO (nmol/100 mL/hr) | % | GSH ($\times 10^2$) (nmol/100 mL) | % | GST (nmol/L) | % |
|-----------|----------------------|-----|-------------------------------------|------|----------------|-----|
| Normal | 0.12 ± 0.02^c | - | 78 ± 8^a | - | 303 ± 40^a | - |
| MIA | 0.79 ± 0.05^a | 543 | 27 ± 6^b | -100 | 130 ± 16^b | -57 |
| MIA + PRP | 0.33 ± 0.06^b | -64 | 93 ± 7^a | 250 | 298 ± 25^a | 130 |

structure of the joint (bone, cartilage, and fibrous joint capsule) (Figure 12(a)). However, stained sections of osteoarthritic control rats (MIA) revealed marked histopathological changes in the form of synovial hyperplasia with infiltration of a large number of inflammatory cells (lymphocytes, macrophages, and sometimes plasma cells), extensive pannus formation, and severe cartilage and bone destruction (Figure 12(b)). On the other hand, osteoarthritic rats treated with PRP showed mild to moderate degree of osteoarthritis (Figures 12(c) and 12(d)). Microscopically, MIA rats showed synovitis characterized by proliferating synovial lining cells, in 2-3 layers, as well as proliferation of the underlying blood vessels, which was associated with perivascular edema and diffused cellular infiltration composed of mononuclear cells. In many tissue specimens, the inflammatory cellular exudate extended to involve the whole periarticular soft tissues such as connective tissue and muscles. There was synovial sloughing in some areas of synovial membrane and mild proliferative lesions of fibroblast-like cells. Pannus formation was in the form of single or multiple proliferating granulation tissue containing hyperplastic synoviocytes and inflammatory cells at the articular cartilage margin and at the cartilage-bone level. The articular cartilages of some arthritic rats had uneven articular surface and demonstrated superficial fibrillation accompanied by cell death or proliferation and in some cases extended to the midzone portion of the articular cartilage. Moreover, the articular bone destruction was visualized by osteoclast activity and fibroplasia. However, osteoarthritic rats treated with PRP showed the previously mentioned histopathological lesions of arthritis but with mild to moderate degree.

4. Discussion

OA is a lasting progressive joint disease. Its origin is multifactorial and characterized by gradual articular cartilage damage, subchondral bone sclerosis, and synovitis [17]. Existing therapy alternatives involve analgesics, intra-articular hyaluronic acid, corticosteroid, NSAIDs, and PRP injection as well as physical treatment and surgical interferences [18].

Therefore, in the current investigation, the influence of intraarticular PRP administration on MIA-induced osteoarthritic rats was evaluated, and the roles of oxidative stress, antioxidant defense mechanism, and the inflammatory status were scrutinized.

MIA-induced osteoarthritis is a usually used experimental model for preclinical investigations. Because the duration of testing is short, its application is simple, and it is similar to animal and human OA, and this model is used commonly to assess curative agents [19]. In our study, the

bodyweight loss is used as the clinical outcome associated with OA. The osteoarthritic rats showed a significant decrease in the bodyweight at the 4th, 5th, and 6th weeks when compared to the normal control rats. These results are in accordance with the previous study, which reported that progressive lessening of bodyweight has been achieved between arthritic animals throughout the progress of arthritis [20]. Also, it was reported that the injection of MIA caused a marked reduction in bodyweight when compared with normal animals [21]. No obvious variations were noticed in bodyweight between the MIA-induced OA and normal control at the first 3 weeks, while the PRP-treated group exhibited a significantly ($p < 0.05$) higher bodyweight than the MIA group at the 5th and 6th weeks. The bodyweight rate elevated in this period, proposing that the rats were under fewer stress and/or in fewer pain.

In the present study, significant increases in both the right ankle anteroposterior and transverse diameters in the MIA group were noticed at all periods after MIA administration relative to the normal control group. These results are in accordance with previous publications that revealed that MIA injection increased the ankle anteroposterior and transverse diameters [22]. In the current study, PRP produced a significant decrease in the elevated values of the right ankle anteroposterior and transverse diameters when compared to MIA animals after the 4th and 3rd weeks, respectively. In parallel with this study, Aniss et al. (2020) stated that the treatment of rats with PRP for six weeks in CFA-induced arthritis results in the decline of paw swelling [23].

Over the previous years, the diagnostic use of MRI in the osteoarthritis study has advanced from a technique to one of the applications for imaging of soft tissue and changes of the bone in arthritic joints [24]. The synovial membrane of arthritic rats with early OA is characterized with hyperplasia and increased vascularization. MRI also depicts hyperemia of the synovial membrane prior to damaging lesions of the cartilage and bone. However, the usual usage of MRI is restricted due to it is expensive and time consuming [25]. In this work, magnets with low field strength 1.5 Tesla lead to poor anatomic resolution. Extra shortage involved an incapability to illustrate the underlying pathology relating to alterations in hydrogen content in osteoarthritic joints. The final aim of this investigation was to assess the data of MRI in the perspective of a collection of physiologic (bodyweight and ankle measurement), biochemical (oxidative stress and cytokines), cellular (TLC), and parameters of histology. This assessment was not aimed at defining if MRI could replace for any one indicator of disease development but to define if alterations in MRI images could be related with any other systemic actions. In our study, boosts intensity of MRI signal in the right hind paw strongly reflected rises in ankle

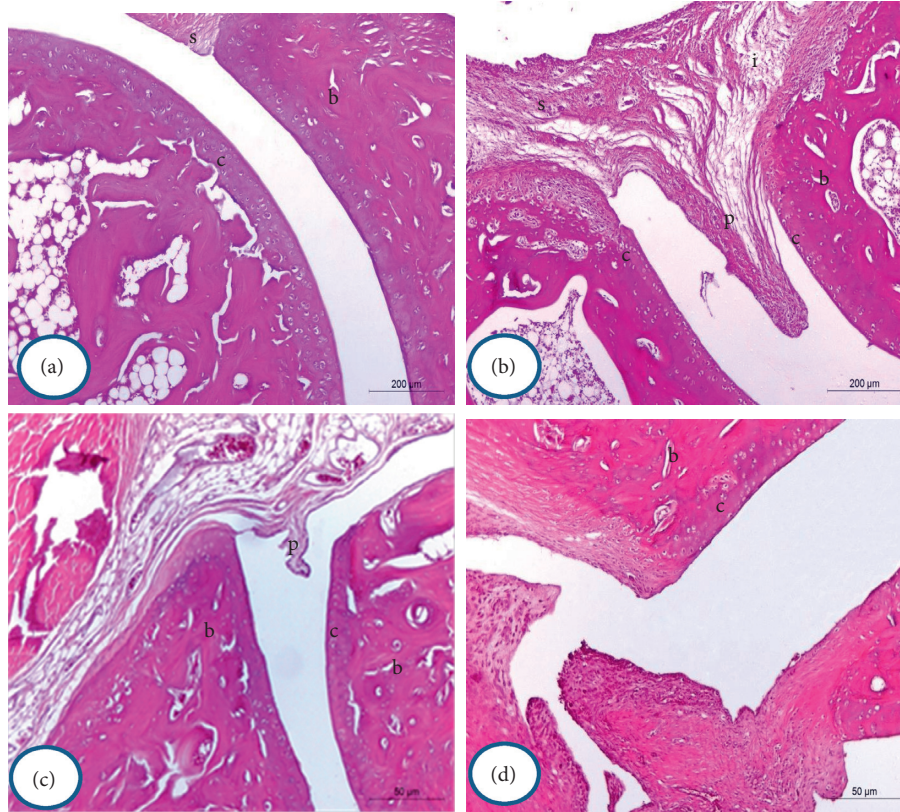


FIGURE 12: Photomicrographs of H&E-stained sections of the hind right leg ankle of normal control (a), MIA rats (b), and MIA + PRP rats (c and d) (H&E X100). The normal histological image (a) showed the normal histological structure of the synovial membrane (s), articular cartilage (c), and bone (b). Photomicrographs of ankle joint of MIA rats illustrated hyperplasia of synovial membrane (s), infiltration of inflammatory cells (i), marked pannus formation (p), damage of cartilage (c), and bone erosion (b). The photomicrographs of hind ankle joints of PRP-treated rats (c and d) revealed mild to moderate arthritis pathology, respectively.

measurement and leucocytic counts. These last inflammatory replies peaked among days 3 and 14 after administration of MIA. After treatment of osteoarthritic rats with PRP, the intensity of the signals of MRI subside at 4–6th week, similar to the reduction detected in ankle measurements and morphological changes, demonstrating that the inflammatory response was in diminution in osteoarthritic rats treated with PRP. The TLC data showed a profound leukocytosis in the MIA-induced osteoarthritic animals. This leukocytosis is attributed to inflammation induced by MIA [26]. In the existing study, it was found that in the PRP-treated osteoarthritic group, the elevated TLC declined markedly near to their normal levels. PRP has an anti-inflammatory effect which is mostly related to reduction in TLC [27]. New experiments have suggested a role of oxidative stress in the pathogenesis of OA.

Oxidative stress is always created, influencing cells and the extracellular matrix. Excessive ROS levels, in combination with the antioxidant reduction, take part in the development of disease (Figure 12) [28, 29]. In the current investigation, the induction of OA using MIA was produced via various mechanisms. One of these mechanisms was the beginning of oxidative stress as illustrated by marked increase in the serum LPO level in association with marked decrease in the serum GSH level and GST activity. This is in line with the observation of previous

report, which found that MIA or its metabolites yield free radicals which attack lipid components, resulting in formation of LPO [30]. Amplified free radical production from inflammatory site leads to reinforced osteoarthritis and the decreased level of cellular antioxidant [31]. In the current study, the GSH level and GST activity in the MIA-induced osteoarthritic rats was significantly decreased as compared to the normal control rats. Similar effects on GSH and GST levels were revealed in plasma of MIA-induced osteoarthritic rats [32]. In the current investigation, intraarticular injection of PRP to MIA-induced osteoarthritic rats markedly diminished the serum LPO level, while it noticeably elevated the GSH and GST levels. These attained data confirmed the antioxidant characteristic of PRP. This effect has been studied in previous publications [33, 34] that stated that PRP might forbid oxidative stress via the incitation of the transcription nuclear erythroid 2-related factor (Nrf-2) antioxidant response element signaling. Furthermore, several growth factors released from PRP can stimulate T cell which can reduce ROS production and raise the resistance level to oxidation [35]. The increase in the oxidative stress stimulates DNA damage and expression of proapoptotic protein (p53); thus, it activates the intrinsic pathway of apoptosis [36] in addition to necrosis leading to cartilage erosion and bone damage (Figure 13).

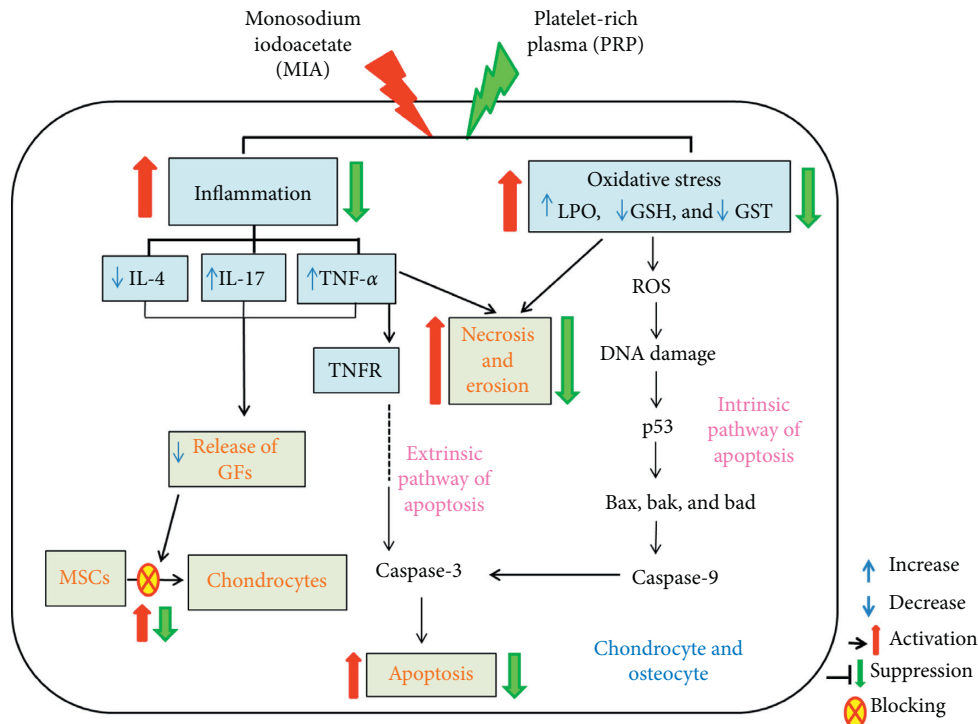


FIGURE 13: The roles of inflammation and oxidative stress in MIA-induced osteoarthritis and effects of treatment with PRP. GFs, growth factors; MSCs, mesenchymal stem cells; TNFR, tumor necrosis factor receptor.

Other suggested mechanism for MIA-induced osteoarthritis is the motivation of inflammatory cytokines. Inflammation and inflammatory response are considered as crucial factors that begin and hasten the OA development (Figure 13). It is extensively believed that inflammatory cytokines are essential mediators in the troubled metabolism and boosted tissue catabolism in OA joint [37]. The long-lasting inflammatory process is mediated via a complicated cytokine network [38]. In the OA pathogenesis, there is an important reason that inflammatory mechanisms play a vital role in OA [39]. In the current study, the concentrations of TNF- α and IL-17 (proinflammatory cytokines) in addition to IL-4 (anti-inflammatory cytokine) were detected in the serum of all rat groups to check the inflammatory status. Current data demonstrated that the MIA group exhibited an obvious increment in levels of TNF- α and IL-17 in rat serum and a significant decrease in the serum IL-4 level when compared to the normal control rats evidencing the inflammation induction in the joints of rats (Figure 13). Like to the existing results, former data proved that MIA significantly increased levels of IL-17 and TNF- α in serum of rats [40], whereas the serum IL-4 level was notably diminished after MIA injection as compared with normal control rats [41]. These increments in the concentrations of proinflammatory cytokines may mirror their critical role in the arthritis progress pathophysiology in animal models [42]. The MIA injection to the rats provokes the increase in the inflammatory cytokines, while it suppresses the anti-inflammatory cytokines, thereby developing the inflammation process. In addition to the necrotic effects of TNF- α , it activates the tumor necrosis factor receptor or death

receptors, thereby activating the extrinsic pathway of apoptosis (Figure 13) [43, 44]. Furthermore, the inflammatory environment and the increased levels of TNF- α and IL-17 could result in a decrease in the formation and release of growth factors (GFs) such as transforming growth factor (TGF) leading to reduced chondrogenesis and formation of chondrocytes from mesenchymal stem cells (Figure 13) [45]. The osteoarthritic rats treated with PRP showed a significant decline in serum TNF- α and IL-17 levels when compared to the elevated level of the osteoarthritic control animals, while they exhibited a significant elevation of the lowered serum IL-4 level. Thus, PRP may counteract cartilage erosion by inhibiting the TNF- α (proinflammatory cytokine) and increasing the anti-inflammatory cytokine IL-4 level (Figure 13) [46, 47].

The pannus formation, degeneration of cartilage, synovial hyperplasia, and inflammation exhibited that the MIA-induced osteoarthritis model is closely similar to human OA [22]. Therefore, in the current work, a rat model of MIA-induced osteoarthritis was established and utilized by ankle intraarticular injection of MIA. MRI and histological examinations performed in this study exhibited that the OA rats exposed obvious deterioration of joint structure and reduced ankle joint space. Furthermore, according to analysis of histopathology results of the ankle joint, synovial hyperplasia, cartilage destruction, erosion of bone, and inflammatory cells were observed in the MIA rats. These phenomena were also illustrated in former studies [48, 49]. In the current study, the treatment with PRP obviously declined swelling of paw and osteoarthritis induced by MIA as compared with MIA control rats. This investigation

further verified its curative effect by histopathological evaluation. It was evidenced effective in diminishing hyperplasia of synovial membrane, cartilage destruction, and bone erosion degree. These results are in agreement with the previous study [23].

5. Conclusion

Intraarticular injection of PRP offers trust for osteoarthritis improvement. Intraarticular PRP treatment diminishes manifestations of OA due to its anti-inflammatory effects and antioxidant effects. Though, additional studies are necessitated to evaluate PRP effectiveness in human beings.

Data Availability

The data used to support the findings of this study are available from the corresponding author upon request.

Additional Points

A main limitation is that the PRP utilized in this investigation was not characterized by its composition and physical characteristics. Besides variations between donors, consequently, the composition of the PRP isolated will differ from one individual to another in composition.

Ethical Approval

All animal procedures are in accordance with the guidelines of Experimental Animal Ethics Committee, Faculty of Science, Beni-Suef University, Beni-Suef, Egypt (ethical approval number: 020107).

Conflicts of Interest

The authors declare that there are no conflicts of interest.

Acknowledgments

The authors like to thank Taif University, Taif, Saudi Arabia, for their support (Taif University Researchers Supporting Project number: TURSP-2020/80), Taif University, Taif, Saudi Arabia. The work was funded by Faculty of Veterinary Medicine, Beni-Suef University, Egypt, and Taif University, Taif, Saudi Arabia.







References

- [1] R. James, "Metabolomic and proteomic stratification of equine osteoarthritis," 2020.
- [2] Y. J. Jeong and J. Cho, "Anti-osteoarthritic effects of the litsea japonica fruit in a rat model of osteoarthritis induced by monosodium iodoacetate," *PLoS ONE*, vol. 10, 2015.
- [3] S. D. Preston, "Epidemiology of lameness and athletic performance in thoroughbred pinhooked horses," Ph D. thesis, University of Florida, Florida, FL, USA, 2011.
- [4] X. Chevalier, "Intraarticular treatments for osteoarthritis: new perspectives," *Current Drug Targets*, vol. 11, no. 5, pp. 546–560, 2010.
- [5] L. A. Boakye, K. A. Ross, J. M. Pinski et al., "Platelet-rich plasma increases transforming growth factor-beta1 expression at graft-host interface following autologous osteochondral transplantation in a rabbit model," *World Journal of Orthopedics*, vol. 6, no. 11, p. 961, 2015.
- [6] M. J. Kim, J. A. Lee, M. R. Shin, H. J. Park, and S. S. Roh, "Improvement effect of corni fructus 30% ethanol extract by MIA-induced osteoarthritis animal model," *The Korea Journal of Herbology*, vol. 35, no. 1, pp. 35–44, 2020.
- [7] M. Sánchez, E. Anitua, D. Delgado et al., "A new strategy to tackle severe knee osteoarthritis: combination of intra-articular and intraosseous injections of platelet rich plasma," *Expert Opinion on Biological Therapy*, vol. 16, no. 5, pp. 627–643, 2016.
- [8] K. Å Möller, S. Klein, F. Seeliger, A. Finn, C. Stenfors, and C. I. Svensson, "Monosodium iodoacetate-induced monoarthritis develops differently in knee versus ankle joint in rats," *Neurobiology of Pain*, vol. 6, p. 100036, 2019.
- [9] C. M. Pacheco and R. Borges, "Use of platelet-rich plasma in an experimental rheumatoid arthritis mode," 2016.
- [10] R. Asjid, T. Faisal, K. Qamar, S. Malik, F. Umbreen, and M. Fatima, "Effect of platelet-rich plasma on mankin scoring in chemically-induced animal model of osteoarthritis," *Journal of the College of Physicians and Surgeons Pakistan*, vol. 29, no. 11, pp. 1067–1071, 2019.
- [11] S. Jimbo, Y. Terashima, A. Teramoto et al., "Antinociceptive effects of hyaluronic acid on monoiodoacetate-induced ankle osteoarthritis in rats," *Journal of Pain Research*, vol. 12, 2019.
- [12] J. B. Miale, "Laboratory medicine: haematology," 1972.
- [13] H. G. Preuss, S. T. Jarrell, R. Scheckenbach, S. Lieberman, and R. A. Anderson, "Comparative effects of chromium, vanadium and gymnema sylvestre on sugar-induced blood pressure elevations in SHR," *Journal of the American College of Nutrition*, vol. 17, no. 2, pp. 116–123, 1998.
- [14] E. Beutler, O. Duron, and B. M. Kelly, "Improved method for the determination of blood glutathione," *The Journal of Laboratory and Clinical Medicine*, vol. 61, pp. 882–888, 1963.
- [15] B. Mannervik and C. Guthenberg, "Glutathione transferase (human placenta)," in *Methods in Enzymology*, Academic Press, London, UK, 1981.
- [16] K. S. Suvarna, C. Layton, and J. D. Bancroft, *Bancroft's Theory and Practice of Histological Techniques E-Book*, Elsevier Health Sciences, London, UK, 2017.
- [17] Y. Smit, H. J. Marais, P. N. Thompson, A. T. Mahne, and A. Goddard, "Clinical findings, synovial fluid cytology and growth factor concentrations after intra-articular use of a platelet-rich product in horses with osteoarthritis," *Journal of the South African Veterinary Association*, vol. 90, no. 1, pp. 1–9, 2019.
- [18] O. Bruyère, C. Cooper, J. P. Pelletier et al., "An algorithm recommendation for the management of knee osteoarthritis in Europe and internationally: a report from a task force of the European Society for Clinical and Economic Aspects of Osteoporosis and Osteoarthritis (ESCEO)," *Seminars in Arthritis and Rheumatism*, vol. 44, 2014.
- [19] S. South, K. Crabtree, P. Vijayagopal, D. Averitt, and S. Juma, "Dose dependent effects of whole blueberry on cartilage health and pain in a monosodium iodoacetate (MIA) induced rat model of osteoarthritis," *Current Developments in Nutrition*, vol. 4, no. 2, p. 477, 2020.
- [20] Y. Jasemian, P. Svendsen, B. Deleuran, and F. Dagnaes-Hansen, "Refinement of the collagen induced arthritis model in rats by infrared thermography," *British Journal of Medicine and Medical Research*, vol. 1, no. 4, pp. 469–477, 2011.

- [21] H. Lee, H.-S. Choi, Y. Park et al., "Effects of deer bone extract on the expression of pro-inflammatory cytokine and cartilage-related genes in monosodium iodoacetate-induced osteoarthritic rats," *Bioscience, Biotechnology, and Biochemistry*, vol. 78, no. 10, pp. 1703–1709, 2014.
- [22] S. Jimbo, Y. Terashima, T. Takebayashi, A. Teramoto, and I. Ogon, "A novel rat model of ankle osteoarthritis induced by the application of monoiodoacetate," *British Journal of Medicine and Medical Research*, vol. 6, no. 260, p. 2, 2017.
- [23] N. N. D. Aniss, A. M. Zaaza, and M. R. A. Saleh, "Anti-arthritis effects of platelets rich plasma and hyaluronic acid on adjuvant-induced arthritis in rats," *Pharmacology*, vol. 16, no. 1, pp. 33–46, 2020.
- [24] P. B. Jacobson, S. J. Morgan, D. M. Wilcox et al., "A new spin on an old model: in vivo evaluation of disease progression by magnetic resonance imaging with respect to standard inflammatory parameters and histopathology in the adjuvant arthritic rat," *Arthritis & Rheumatism*, vol. 42, no. 10, pp. 2060–2073, 1999.
- [25] I. Gemeinhardt, D. Puls, O. Gemeinhardt et al., "Near-infrared fluorescence imaging of experimentally collagen-induced arthritis in rats using the nonspecific dye tetrasulfocyanine in comparison with gadolinium-based contrast-enhanced magnetic resonance imaging, histology, and clinical score," *Journal of Biomedical Optics*, vol. 17, no. 10, p. 106008, 2012.
- [26] A. Bahtiar, M. Nurazizah, T. Roselina, A. P. Tambunan, and A. Arsianti, "Ethanol extracts of babandotan leaves (*Ageratum conyzoides* L.) prevents inflammation and proteoglycan degradation by inhibiting TNF- α and MMP-9 on osteoarthritis rats induced by monosodium iodoacetate," *Asian Pacific Journal of Tropical Medicine*, vol. 10, no. 3, pp. 270–277, 2017.
- [27] I. Andia and N. Maffulli, "Platelet-rich plasma for managing pain and inflammation in osteoarthritis," *Nature Reviews Rheumatology*, vol. 9, no. 12, pp. 721–730, 2013.
- [28] E. F. Yamada, A. F. Salgueiro, A. D. S. Goulart et al., "Evaluation of monosodium iodoacetate dosage to induce knee osteoarthritis: relation with oxidative stress and pain," *International Journal of Rheumatic Diseases*, vol. 22, no. 3, pp. 399–410, 2019.
- [29] F. M. Halfaya, G. H. Ragab, U. Hagag, O. M. Ahmed, and W. A. Elkheir, "Efficacy of hyaluronic acid in the treatment of MIA-induced ankle osteoarthritis in rats and its effect on antioxidant response element," *Journal of Veterinary Medical Research*, vol. 27, no. 2, 2020.
- [30] O. M. Zahan, O. Serban, C. Gherman, and D. Fodor, "The evaluation of oxidative stress in osteoarthritis," *Medicine and Pharmacy Reports*, vol. 93, no. 1, p. 12, 2020.
- [31] F. Vaillancourt, H. Fahmi, Q. Shi et al., "4-Hydroxynonenal induces apoptosis in human osteoarthritic chondrocytes: the protective role of glutathione-S-transferase," *Arthritis Research & Therapy*, vol. 10, no. 5, p. R107, 2008.
- [32] D. Kumar, A. K. Sharma, and S. K. Tandan, "Effect of atorvastatin, a HMG-coa reductase inhibitor in monosodium 4 iodoacetate-induced osteoarthritic pain: implication for osteoarthritis 5 therapy," 2014.
- [33] M. Tohidnezhad, C.-J. Wruck, A. Slowik et al., "Role of platelet-released growth factors in detoxification of reactive oxygen species in osteoblasts," *Bone*, vol. 65, pp. 9–17, 2014.
- [34] R. P. Martins, D. D. Hartmann, J. P. de Moraes, F. A. A. Soares, and G. O. Puntel, "Platelet-rich plasma reduces the oxidative damage determined by a skeletal muscle contusion in rats," *Platelets*, vol. 27, no. 8, pp. 784–790, 2016.
- [35] F. M. Halfaya, G. H. Ragab, U. Hagag, O. M. Ahmed, and W. A. Elkheir, "Effect of platelet-rich plasma on MMP-13, ARE and TGF- β 1 in MIA-induced osteoarthritis in rats," *Journal of Veterinary Medical Research*, vol. 27, no. 2, 2020.
- [36] P.-R. Chiu, C. Hu, T.-C. Huang et al., "Vitamin C protects chondrocytes against monosodium iodoacetate-induced osteoarthritis by multiple pathways," *Journal of Veterinary Medical Research*, vol. 18, p. 38, 2017.
- [37] C. Chen, C. Zhang, L. Cai et al., "Baicalin suppresses IL-1 β -induced expression of inflammatory cytokines via blocking NF- κ B in human osteoarthritis chondrocytes and shows protective effect in mice osteoarthritis models," *International Immunopharmacology*, vol. 52, pp. 218–226, 2017.
- [38] P. Jin and E. Wang, "Polymorphism in clinical immunology—from HLA typing to immunogenetic profiling," *Journal of Translational Medicine*, vol. 1, no. 1, p. 8, 2003.
- [39] G. Gundogdu and K. Gundogdu, "A novel biomarker in patients with knee osteoarthritis: adropin," *Clinical Rheumatology*, vol. 37, no. 8, pp. 2179–2186, 2018.
- [40] H. Li, S. Xie, Y. Qi, H. Li, R. Zhang, and Y. Lian, "TNF- α increases the expression of inflammatory factors in synovial fibroblasts by inhibiting the PI3K/AKT pathway in a rat model of monosodium iodoacetate-induced osteoarthritis," *Experimental and Therapeutic Medicine*, vol. 16, no. 6, pp. 4737–4744, 2018.
- [41] X. Zhang, Y. Yang, X. Li, H. Zhang, Y. Gang, and L. Bai, "Alterations of autophagy in knee cartilage by treatment with treadmill exercise in a rat osteoarthritis model," *International Journal of Molecular Medicine*, vol. 43, no. 1, pp. 336–344, 2019.
- [42] Y.-L. Liu, H.-M. Lin, R. Zou et al., "Suppression of complete Freund's adjuvant-induced adjuvant arthritis by cobra toxin," *Acta Pharmacologica Sinica*, vol. 30, no. 2, pp. 219–227, 2009.
- [43] O. M. Ahmed, H. I. Fahim, H. Y. Ahmed et al., "The preventive effects and the mechanisms of action of navel orange peel hydroethanolic extract, naringin, and naringenin in N-Acetyl-p-aminophenol-Induced liver injury in wistar rats," *Oxidative Medicine and Cellular Longevity*, vol. 2019, 2019.
- [44] O. M. Ahmed, H. Ebaid, E.-S. El-Nahass, M. Ragab, and I. M. Alhazza, "Nephroprotective effect of pleurotus ostreatus and agaricus bisporus extracts and carvedilol on ethylene glycol-induced urolithiasis: roles of NF- κ B, p53, bcl-2, bax and bak," *Biomolecules*, vol. 10, no. 9, p. 1317, 2020.
- [45] Y. Tanaka, "Acquiring chondrocyte phenotype from human mesenchymal stem cells under inflammatory conditions," *Current Reviews in Musculoskeletal Medicine*, vol. 15, pp. 21270–21285, 2014.
- [46] M. I. Kennedy, K. Whitney, T. Evans, and R. F. LaPrade, "Platelet-rich plasma and cartilage repair," *Current Reviews in Musculoskeletal Medicine*, vol. 11, no. 4, pp. 573–582, 2018.
- [47] H. J. Braun, H. J. Kim, C. R. Chu, and J. L. Dragoo, "The effect of platelet-rich plasma formulations and blood Products on human synoviocytes," *The American Journal of Sports Medicine*, vol. 42, no. 5, pp. 1204–1210, 2014.
- [48] H.-J. Park, C.-K. Lee, S.-H. Song, J.-H. Yun, A. Lee, and H.-J. Park, "Highly bioavailable curcumin powder suppresses articular cartilage damage in rats with mono-iodoacetate (MIA)-induced osteoarthritis," *Food Science and Biotechnology*, vol. 29, no. 2, pp. 251–263, 2020.
- [49] S. G. Kim, C. H. Chung, Y. K. Kim, J. C. Park, and S. C. Lim, "Use of particulate dentin-plaster of paris combination with/without platelet-rich plasma in the treatment of bone defects around implants," *International Journal of Oral & Maxillo-facial Implants*, vol. 17, no. 1, 2002.

Research Article

Combinatory Effects of Bone Marrow-Derived Mesenchymal Stem Cells and Indomethacin on Adjuvant-Induced Arthritis in Wistar Rats: Roles of IL-1 β , IL-4, Nrf-2, and Oxidative Stress

Eman A. Ahmed ¹, Osama M. Ahmed ¹, Hanaa I. Fahim ¹, Emad A. Mahdi,²
Tarek M. Ali ^{3,4}, Basem H. Elesawy ^{5,6} and Mohamed B. Ashour ¹

¹Physiology Division, Zoology Department, Faculty of Science, Beni-Suef University, P.O. Box 62521, Beni-Suef, Egypt

²Pathology Department, Faculty of Veterinary Medicine, Beni-Suef University, Beni-Suef, Egypt

³Department of Physiology, College of Medicine, Taif University, P.O. Box 11099, Taif 21944, Saudi Arabia

⁴Department of Physiology, Faculty of Medicine, Beni-Suef University, Beni-Suef, Egypt

⁵Department of Clinical Laboratory Sciences, College of Applied Medical Sciences, Taif University, P.O. Box 11099, Taif 21944, Saudi Arabia

⁶Department of Pathology, Faculty of Medicine, Mansoura University, Mansoura, Egypt

Correspondence should be addressed to Osama M. Ahmed; osama.ahmed@science.bsu.edu.eg

Received 1 October 2020; Revised 25 November 2020; Accepted 19 December 2020; Published 5 January 2021

Academic Editor: Arham Shabbir

Copyright © 2021 Eman A. Ahmed et al. This is an open access article distributed under the Creative Commons Attribution License, which permits unrestricted use, distribution, and reproduction in any medium, provided the original work is properly cited.

Rheumatoid arthritis (RA) is a disorder triggered by autoimmune reactions and related with chronic inflammation and severe disability. Bone Marrow-derived Mesenchymal Stem Cells (BM-MSCs) have shown a hopeful immunomodulatory effect towards repairing cartilage and restoring joint function. Additionally, indomethacin (IMC), a nonsteroidal compound, has been considered as a potent therapeutic agent that exhibits significant antipyretic properties and analgesic effects. The target of the current research is to assess the antiarthritic efficacy of BM-MSCs (10^6 cells/rat at 1, 6, 12 and 18 days) and IMC (2 mg/kg body weight/day for 3 weeks) either alone or concurrently administered against complete Freund's adjuvant-induced arthritic rats. Changes in paw volume, body weight, gross lesions, and antioxidant defense system, as well as oxidative stress, were assessed. The Th1 cytokine (IL-1 β) serum level and Th2 cytokine (IL-4) and Nrf-2 ankle joint expression were detected. In comparison to normal rats, it was found that the CFA-induced arthritic rats exhibited significant leukocytosis and increase in paw volume, LPO level, RF, and IL-1 β serum levels. In parallel, arthritic rats that received BM-MSCs and/or IMC efficiently exhibited decrease in paw edema, leukocytosis, and enhancement in the antioxidant enzymatic levels of SOD, GPx, GST, and GSH in serum besides upregulation of Nrf-2 and anti-inflammatory IL-4 expression levels in the ankle articular joint. Likewise, these analyses were more evidenced by the histopathological sections and histological score. The data also revealed that the combined administration of BM-MSC and IMC was more potent in suppressing inflammation and enhancing the anti-inflammatory pathway than each agent alone. Thus, it can be concluded that the combined therapy with BM-MSC and IMC may be used as a promising therapeutic choice after assessing their efficacy and safety in human beings with RA, and the antiarthritic effects may be mediated via modulatory effects on Th1/Th2 cytokines, oxidative stress, and Nrf-2.

1. Introduction

Rheumatoid arthritis (RA) is a predominant inflammatory disorder that is accompanied by a relapsing and remitting course of joint inflammation and synovitis, swelling,

autoantibody production, bone dysfunction, and cartilage degradation [1]. RA is accompanied with systemic and additional extraarticular complications of some organs including the lungs and heart. Such systemic manifestations reduce the quality of life and are responsible for disability,

early mortality, and socioeconomic costs [2]. The prevalence of RA is more common in the aged people; around 1.3 million adults are suffering from RA as reported by the National Health Institutes [3]. Probably, more than 1% around the world has been established with RA [4]. Up till now, the pathogenesis of RA is unknown; several etiological causes have been involved such as genetic, as well as environmental, factors, infectious agents, heat shock proteins, and sex hormones. Nonetheless, such causes, by themselves, are insufficient to explain the etiology [5]. Among other models, arthritis induced in rodents via injection with Complete Freund's adjuvant (CFA), shares the majority of disease similarities with that of human; thus, this makes it the most appropriate model for inducing arthritis, and it is recommended for studying and testing various therapeutic agents against RA [6–8]. Currently, there is no optimal therapy for RA except for systemic immune suppressants. The most widely used medications such as nonsteroidal anti-inflammatory drugs (NSAIDs) besides the biological agents (e.g., antitumor necrosis- α antibody) are helpful in relieving the symptoms, but serious adverse reactions are associated with extended use of these medications. Furthermore, these drugs are costly, and not all patients are reacting well to them [9].

Because of these restrictions, the need for other treatment modalities has emerged in an attempt to develop a treating agent that is as effective as those conventional drugs but devoid of their serious side effects. One of these recently tried approaches is the use of mesenchymal stem cells (MSCs). Bone marrow-derived MSCs (BM-MSCs) are nonhematopoietic multipotential progenitor cells that have positive effects on the reconstruction and integration of the host tissue. They are capable of differentiating into various mesenchymal tissues, including osteocytes, chondrocytes, and adipocytes, thus repairing the cartilage and bone simultaneously [10]. Also, BM-MSCs modulate immune cell responses such as natural killers (NK), antigen presenting cells, T lymphocytes, and B lymphocytes [11, 12]. BM-MSCs, thus, were of considerable importance for both the diagnosis and recognition of the inflammatory autoimmune diseases as well. In osteoarthritis, for example, normal BM-MSCs can help restore damaged cartilage and minimize the low-grade-related synovial inflammation recently verified by a human clinical trial [13]. Such advantages introduced them as a novel therapeutic choice and a promising tool for the prolonged RA treatment.

Moreover, indomethacin (IMC), 1-(p-chlorobenzoyl)-5-methoxy-2-methylindol-3-acetic acid, is one of the NSAIDs that were extensively used in both inflammation and pain management. It was introduced in 1963 as a potent agent in treatment of many inflammatory disorders including osteoarthritis, ankylosing spondylitis, gout, acute musculoskeletal disorders, degenerative joint diseases, and RA. IMC has prominent analgesic, anti-inflammatory, and antipyretic properties via inhibiting the activity of cyclooxygenase and, thereby, inhibiting the synthesis of inflammatory mediators [14]. However, therapeutic effects of IMC in reducing inflammation and edema are brilliant, whereas the extended use of these NSAIDs may result in serious side effects,

including gastrointestinal harms and cardiovascular toxicity. Thus, configuring new dosing approaches and reducing the side effects of NSAIDs became of growing importance [15]. Therefore, in our study, we administered IMC at a lower dose (0.2 mg/kg body weight (b.w.)) day after day to adjust and control this limitation.

In conductance with the previous literature, the present study aimed to assess the combinatory antiarthritic efficacy of BM-MSCs and IMC, in comparison with the supplementation of each alone in CFA-induced arthritis in Wistar rats. The study also tried to scrutinize the roles of IL-1 β (Th1 cytokine), IL-4 (Th2 cytokine), oxidative stress, antioxidant defense system, and Nrf-2 in the antiarthritic effects.

2. Materials and Methods

2.1. Animals. The recent experiment was conducted in the period of October 2018 to October 2019 in Egypt, in the Faculty of Science at Beni-Suef University. It included 50 Wistar rats of male gender (120–150 g in weight; 10–12 weeks old). Rats were bought from Egyptian Organization for Biological Products and Vaccines (VACSERA), Helwan Station, Cairo, Egypt. The animals were overseen for two weeks before the starting of the experiment to exclude any intercurrent infection. Rats were accommodated in calibrated cages of polypropylene and kept in controlled circumstances with a humidity around (55 \pm 5%); also, room temperature of (22 \pm 2°C), and 12-hour lighting and 12-hour darkness cycle. Animals were given drinking water and fed rat chow diet ad libitum. The experimental animals used in the current research were treated in accordance with the Canadian Council's Principals and Guidelines of Animal Care and Experimental Animal Ethics Regional Committee, Faculty of Science, University of Beni-Suef, Egypt, which approved the experimental work. All attempts were made to minimize the number of struggling animals during the study as possible.

2.2. Induction of Arthritis. For arthritis induction, animals were inoculated by a subcutaneous injection of 0.1 mL/rat CFA solution (Sigma Chemical Co., St Louis, Mo., USA) into the footpad of the right hind paw as described by Snehalatha et al. [16] at dose of 1 mg/kg-b.w. For more extensive severity of arthritis, a booster dose (0.1 mL) of emulsion was administered in the second day.

2.3. Animal Grouping. The experimental design contained five groups, each consisting of ten rats and described as follow:

Group 1 (normal): it consists of healthy rats that were given the equivalent volumes carboxy methylcellulose (CMC) daily and orally for 3 weeks and Dulbecco's Modified Eagles Medium (DMEM) intravenously at the 1st, 6th, 12th, and 18th days.

Group 2 (CFA): it is composed of CFA-induced arthritic rats and was orally given the equivalent volumes

CMC daily and orally for 3 weeks and DMEM intravenously at the 1st, 6th, 12th, and 18th days.

Group 3 (CFA + BM-MSCs): this group consists of CFA-induced arthritic rats that received four doses of BM-MSCs (1×10^6 cells/rat/dose) by intravenous injection through lateral tail vein per rat [17]. Each dose suspended in 0.2 ml DMEM (Dulbecco's modified Eagles medium). Doses were given at the 1st, 6th, 12th, and 18th days after CFA injection.

Group 4 (CFA + IMC): this group is composed of CFA-induced arthritic rats supplemented orally with IMC daily in a dose of 2 mg/kg body weight (b.w.). IMC was freshly prepared immediately before administration by dissolving in 5 mL of 1% CMC for three weeks. IMC was acquired from Sigma Chemical Company (Sigma Chemical Co., St Louis, Mo., USA).

Group 5 (AIA + BM-MSCs + IMC): this group consists of CFA-induced arthritic rats that were concurrently supplemented with BM-MSCs and IMC as described in groups 3 and 4.

2.4. Isolation and Culture of BM-MSCs. In the current study, our method of isolation, as well culture of BM-MSCs, is based on the procedure of Chaudhary and Rath [18] and our previous publication in 2020 [19].

2.5. Assessment of Arthritis Severity (Represented by Paw Edema). For monitoring of arthritis development, paw volume is measured as a pointer of paw edema and swelling rate. Measurements were taken at various times at day 7, 14, and 21 following arthritis induction by CFA, and day 0 was the first of CFA injection. Hind paw volume was calculated depending on the water replacement method by subtracting the difference in water volume before and after applying the paw in a calibrated cylinder containing specific volume of isotonic saline. Edema or swelling for the CFA rats was compared to the nonarthritic normal group, while the arthritic-treated rats were compared to the CFA group. The rats were anesthetized by ether inhalation before measurement.

2.6. Histopathological Investigation. At the end of the study, at day 21 after induction of arthritis, rats were sacrificed and right hind leg ankle joints of 4 rats from each group were detached and placed for 48 hours in formalin 10% buffered. Decalcification of bone was performed using 10% formic acid. This solution was changed two times per week and for two weeks, and the end of the decalcification process was physically considered using a surgical blade. When decalcification completed, the specimens washed away with PBS, then dehydrated with a graded ethanol series, and embedded in wax cubes made of paraffin. Finally, 5 μ m thicknesses sagittal sections were prepared and then stained with haematoxylin and eosin (H & E).

Histological checkups were blindly performed by a pathologist including synovial inflammation, cartilage, and

bone damages. Sections were graded in accordance with the system described by Sancho et al. [20] for inflammation (mononuclear cell infiltration), synovial hypertrophy (pannus formation), and erosion of bone, as well as destruction of cartilage. A scale of 0–3-point was used for each parameter (0 grade was considered normal, grade 1 was considered mild inflammation, grade 2 was moderate inflammation, and grade 3 for severe inflammation), and 12 was the maximum possible score.

2.7. Detection of IL-4 by RT-PCR. The mRNA expression level of IL-4 in relation to the housekeeping gene β -actin (β -actin) was determined using semiquantitative Reverse transcription-polymerase chain reaction (RT-PCR).

2.7.1. Ribonucleic Acid (RNA) Isolation. RNA was extracted totally from 3 ankle joints of three different rats in each group using the Thermo Scientific GeneJET RNA extraction kit purchased from Thermo Fisher Scientific Inc., Rochester, New York, USA, according to the manufacturer's instructions. In liquid nitrogen, samples were homogenized and then lysed in lysis buffer solution that contains guanidine thiocyanate, a chaotropic salt which protects RNA from endogenous RNases. The obtained lysate was then mixed with ethyl alcohol and loaded on a purification column. Both the chaotropic salt and the ethyl alcohol made RNA bind to the silica membrane as the lysate is spun through the column. Impurities were subsequently removed away from the membrane by washing the column with washing buffer solution. Then, pure RNA was eluted under low ionic strength conditions with nuclease-free water. Also, the amount of purified RNA was quantified by using a UV Spectrophotometer according to the following formula: $\text{RNA } \mu\text{g}/\mu\text{l} = \text{O.D. } 260 \text{ nm} \times (40 \mu\text{g RNA/ml}) \times \text{dilution factor}/1000$. To ensure the high purity of the isolated RNA, we checked the purity of RNA and should be ranged between 1.8 and 2.0. By the end, 0.5 μ g of purified RNA was used for production of complementary deoxyribonucleic acid (cDNA) kept at -20°C , for further assay of the mRNA.

2.7.2. Reverse Transcription-Polymerase Chain Reaction (RT-PCR) Analysis. cDNA was prepared by reverse transcription and amplified by using the Thermo Scientific Verso 1-Step RT-PCR Reddy Mix kit obtained from Thermo Scientific Inc., Rochester, New York, USA. The final reaction volume was 50 μ l. The mixture of reaction consisted of 2X 1-Step PCR Reddy Mix (25 μ l), Verso Enzyme Mix (1 μ l), RT Enhancer (2.5 μ l), sense primer (10 μ M) (1 μ l), anti-sense primer (10 μ M) (1 μ l), nuclease-free water (17.5 μ l), and template RNA (2 μ l). The PCR tubes of the reaction were located in a double-heated led thermal cycler, and a sequence of reactions occurred including verso inactivation at 95°C for 2 min followed by 35 cycles initial denaturation at 95°C for 20 sec, then at $50\text{--}60^\circ\text{C}$ for 30 sec, and at 72°C for 1 min, finally, followed by 1 cycle at 72°C for 5 min. After that, we separated the PCR products by electrophoresis on agarose gel (1.5%), and the cDNA bands were observed using a UV

transilluminator in a dark chamber. Gel images were investigated and analyzed by scanning densitometry (Gel Doc. Advanced ver 3.0). The primer sequences for IL-4 mRNA are as follows: forward: 5'GGAACACCACGGAGAACG3' and reverse: 5'GCACGGAGGTACATCACG3'. The primer sequences for β -actin mRNA are as follows: forward: 5'TCACCTGAAGTACCCCATGGAG3' and reverse: 5'TTGGCCTTGGGGTTCAGGGGG3'. All the primers used in this experiment were synthesized by Sangon Biotech (Shanghai, China) [21].

2.8. Hematological Parameters and Cytokine Analysis in Blood. By the end of experiment (after 21 days), the rats were anesthetized under mild diethyl ether and blood was obtained from the jugular vein. Part of the blood was collected in tubes containing ethylenediamine tetraacetic acid solution (EDTA) (50 μ L of 15% EDTA 2.5 mL blood) for total and differential leukocyte counting. Total count of leukocyte (TLC) was calculated through a gentian solution diluted sample loaded on a Neubauer hemaocytometer slide for counting, while differential count of leukocyte (DLC) was prepared using Giemsa stain [9].

Although, the other remaining amount of blood was collected directly in pipes without anticoagulant and centrifuged for 15 minutes at 3000 rpm. The clear non-hemolyzed supernatant or sera of different samples were quickly removed and maintained at -30°C . Determination of serum RF and 1L-1 β levels was performed in normal and arthritic control, as well as the arthritic-treated rats, using specific enzyme-linked immunosorbent assay (ELISA). The kits were purchased from R & D Systems (R & D Systems, Inc., Minneapolis, MN, USA) in accordance with standard procedures.

2.9. Oxidative Stress and Antioxidant System. The malondialdehyde (MDA) level was used as an indicator of the lipid peroxides (LPO) level in tissues [22]. Also, the glutathione (GSH) content in serum was determined according to the method of Beutler et al. [23]. Moreover, the antioxidant enzymes including glutathione peroxidase (GPx), superoxide dismutase (SOD), and glutathione-S-transferase (GST) activities in sera were assessed based on the methods reported by previous publications [24–26].

2.10. Western Blot Analysis. The western blot technique was used to determine the amount of Nrf-2 protein. In short, proteins were extracted from 3 ankle joints of the right hind leg of three rats in each group using ice-cold radio-immunoprecipitation assay (RIPA) buffer (Beyotime Biotechnology, China) containing 0.1 percent phenylmethylsulfonyl fluoride. Equivalent protein amounts (30 μ g) were divided using 10% sodium dodecyl sulfate polyacrylamide (SDS-PAGE) gel electrophoresis. Next, the proteins loaded on the gel were shifted onto membranes of polyvinylidene fluoride (PVDF). Then, overnight, the membrane was probed at 4°C with the Nrf-2-specific primary antibody (cat. no. 68817; Thermo Fisher Scientific).

After washing with tris-buffered saline with Tween 20 (TBST) for three times, the blots were prepared for incubation with horseradish peroxidase-conjugated secondary antibodies (1:5000, Santa Cruz Biotechnology, CA) at room temperature 25°C for 30 minutes. The blots were washed again, and then, the signal of the chemiluminescence was visualized with an X-ray film [27].

2.11. Statistical Analysis. Statistical research was carried out with the package of statistics for social science version 22 (SPSS, Chicago, IL) statistical program. Comparisons among the mean of different groups were carried out according to one-way analysis of variance (ANOVA) followed by Tukey's postmultiple comparison test. Values are expressed as the mean \pm standard error of mean (mean \pm SE). $P < 0.05$ was regarded a statistically significant result.

3. Results

3.1. Treatments Effect on Paw Volume. Rats of all arthritic groups developed arthritis after CFA induction. The CFA-induced arthritic rats exhibited significant ($P < 0.05$) increase in paw volume (edema) maintained for 21 days when compared with the normal group (Figure 1). In contrary, by the end of the experiment, the BM-MSCs- and/or IMC-treated arthritic rats distinctly reduced the paw edema with inhibition percentages of 36.97, 40.20, and 57.98 %, respectively, in comparison with the CFA-induced arthritic group (Figure 1).

3.2. Effect of Treatments on Gross Lesions of the Paw and Ankle Joint. Edema and redness of the right hind paw and ankle joint acted as external measures for determining the severity of the arthritic inflammatory model. The CFA-induced arthritic control group displayed gradual decrease in both of them following BM-MSCs and/or IMC treatments (Figure 2).

3.3. Histopathological Changes and Arthritic Score

3.3.1. Histopathological Changes. Hematoxylin and eosin (H & E) stained sections of the right hind leg ankle joint from normal control rats showed no inflammation. In contrast, the CFA-induced arthritic rats exhibited striking histopathological alterations in the form of hyperplasia of the synovium with infiltration of a large number of inflammatory cells, severe formation of pannus, and widespread cartilage destruction. On the other side, the CFA-induced arthritic rats treated with IMC showed less severe pathological arthritis with moderate inflammation, while both rats treated with BM-MSCs and those in concurrently administered group (BM-MSCs plus IMC) showed mild degrees of arthritis (Figure 3).

Microscopically, CFA-induced arthritic rats revealed synovitis characterized by proliferation of the synovial membrane, arranged in 2 to 3 cell lining layers besides proliferation of the underneath vessels of blood that linked with perivascular edema and diffused infiltration of

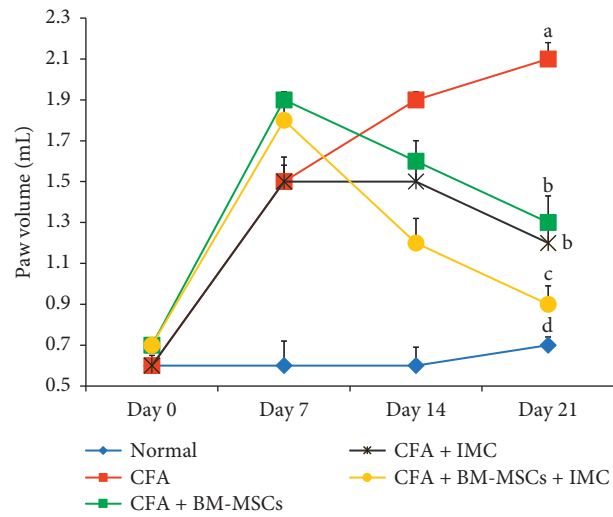


FIGURE 1: Effect of BM-MSCs and/or IMC on right hind paw volume in CFA-induced arthritic rats. Means, which have different symbols, are significantly different at $P < 0.05$.

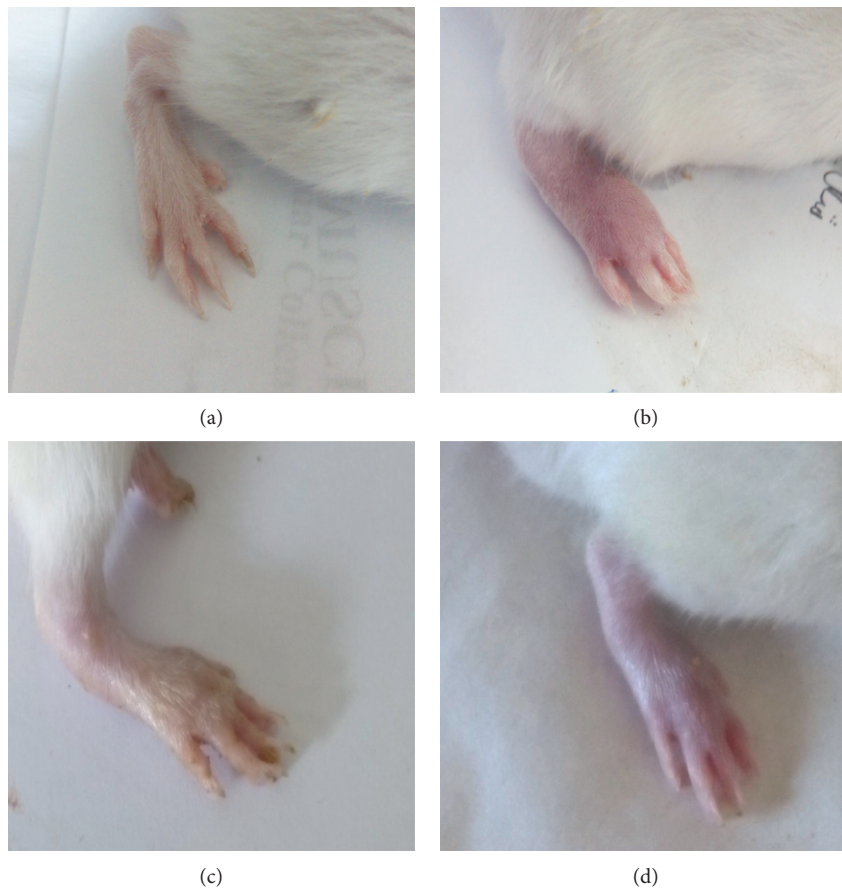


FIGURE 2: Continued.



(e)

FIGURE 2: Effect of BM-MSCs and/or IMC on gross lesions in CFA-induced rats showing (a) normal rat, (b) CFA-induced arthritic rat, (c) CFA + BM-MSCs-treated rat, (d) CFA + IMC-treated rat, and (e) CFA + BM-MSCs + IMC-treated rat.

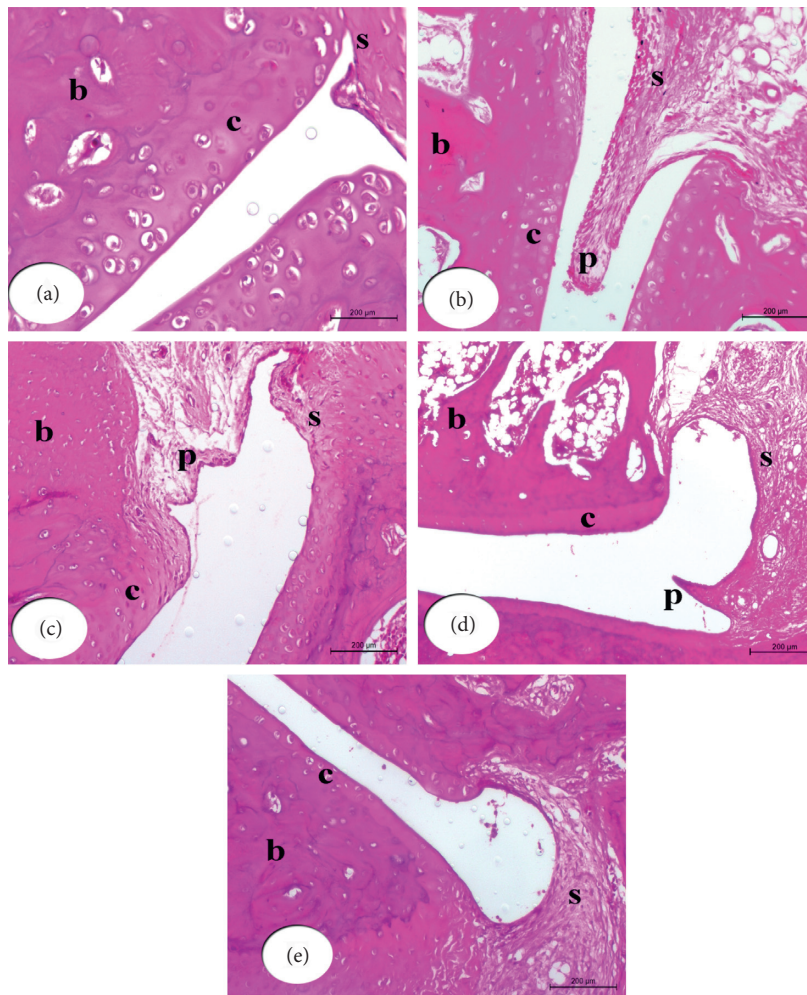


FIGURE 3: Photomicrographs of (H & E 200 \times) stained sections of right hind leg ankle joints show histopathological effects of BM-MSCs and/or IMC treatments on CFA-induced arthritic rats. Ankle joint section from normal rat (a) shows normal structure of the synovial membrane (s), cartilage (c), and bone (b). Ankle joint section from CFA-induced arthritic rat (b) shows the substantially expanding synovial membrane with severe pannus formation (p). Ankle joint section from CFA + BM-MSCs rat (c) shows the synovial membrane with mild infiltration and pannus formation (p). Ankle joint section from CFA + IMC rat (d) shows moderate infiltration and pannus formation. Ankle joint section from CFA + BM-MSCs plus IMC rat (e) shows nearly normal histological structure of the hind ankle joint with a normal synovial membrane and mild cellular infiltration.

mononuclear cells. In many samples, the exudates of the inflammatory cells spread to involve entire periarticular soft tissues of the connective tissue and muscles. There was detachment in some regions of the synovial membrane and mild proliferative lesions of fibroblast-like cells. Also, the pannus development was in the form of one or more proliferating granulation tissues containing inflammatory cells and hyperplastic synovitis at the joint-cartilage boundary and at the cartilage-bone level. Many arthritic rats' articular cartilage had an irregular articular surface and displayed superficial fibrillation followed by cell death or proliferation, which, in some cases, spread to the articular cartilage's mildly formed part. In addition, osteoclast activity and fibroplasia visualized the joint bone injury. In contrast, arthritic rats treated with BM-MSCs, as well as the concurrently administered group BM-MSCs plus IMC, showed the aforementioned histopathological arthritis lesions but with mild degrees, while arthritic rats treated with IMC showed moderate degrees of those lesions (Figure 3).

3.3.2. Histopathologic Score of Arthritis. Histopathologic analysis comprising synovitis (synovial hyperplasia), pannus formation, cartilage destruction, and bone erosion were scored by a blinded observer on a 0–3 scale in H & E-stained sections. The present data revealed that the arthritic-treated rats significantly exhibited decrease in the total histopathological score as compared to those in arthritic control; the treatment with BM-MSCs + IMC was the most potent (Figure 4). In detail, all cures obviously lessened the synovitis, decreased pannus formation, and reduced cartilage degradation compared to CFA rats. However, bone erosion in treated rats displayed a nonsignificant change ($P > 0.05$) compared with the CFA animal group (Figure 4).

For each score, means, which have different symbols, are significantly different at $P < 0.05$.

3.4. Assessment of Total and Differential Leukocyte (TLC and DLC) Count. TLC was significantly ($P < 0.05$) increased in the CFA-induced arthritic group with a change percentage of 212.07% when compared to those of the normal control group. However, the CFA-induced arthritic rats supplemented with BM-MSCs and/or IMC showed a marked decline of leukocytosis to close normal levels, and the BM-MSCs + IMC-treated group was the most potent to overcome the elevation of leukocyte total count (Figure 5). Furthermore, differentiation of leukocytes showed a noticeable rise in lymphocyte, as well as neutrophil, count in the CFA-rats two times more than normal rats. However, the BM-MSCs either alone or BM-MSCs plus IMC to arthritic rats significantly improved all leukocytes' counts (lymphocyte, as well as neutrophil and others) near to normal ranges, while IMC supplementation alone declined lymphocyte, neutrophil, and eosinophil count clearly and did not significantly affect monocyte and basophile counts in comparison with the CFA-induced arthritic group (Table 1). The treatment with BM-MSCs + IMC was the most effective in decreasing the elevated lymphocyte and neutrophil counts.

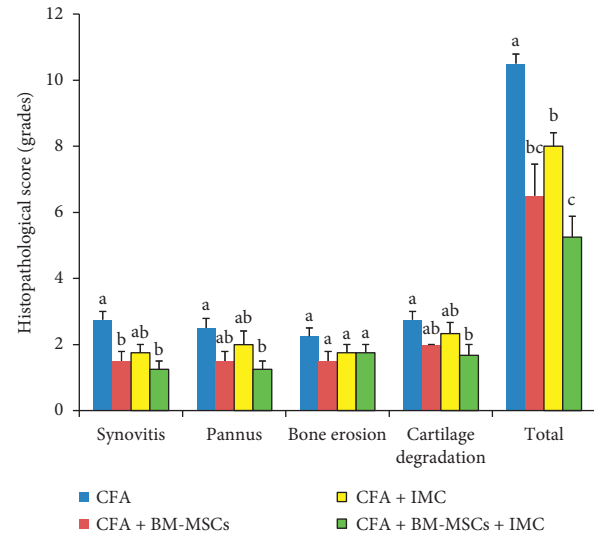


FIGURE 4: Effect of BM-MSCs and/or IMC on the arthritic score in CFA-induced rats.

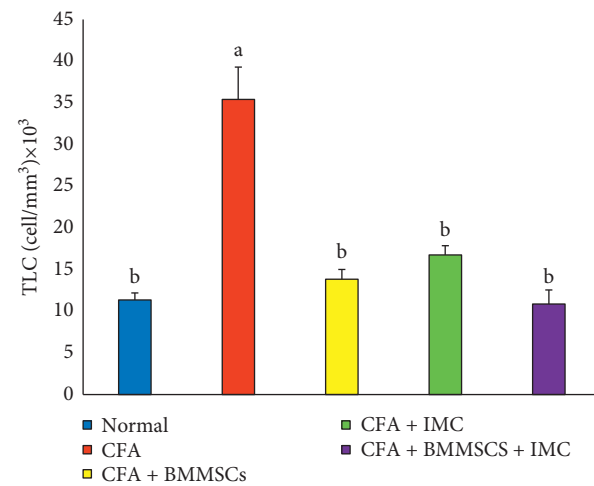


FIGURE 5: Effect of BM-MSCs and/or IMC on TLC count in CFA-induced rats.

Means, which have different symbols, are significantly different at $P < 0.05$.

3.5. Effect on LPO and Antioxidant Status. Table 2 shows the effect of BM-MSCs and/or IMC treatments on oxidative stress and antioxidant defense system markers in serum samples of CFA-induced arthritic rats.

The MDA level showed a ten-fold increase (989.52%) in CFA-induced rats as compared with the normal rats. On the other hand, the treatment of arthritic rats with BM-MSCs and/or IMC treatments decreased ($P < 0.05$) the elevated LPO level significantly in all treated groups with change percentages of -72.99% , -61.06% , and -46.37% for BM-MSCs plus IMC-, BM-MSCs alone-, and IMC alone-treated groups, respectively. Hence, BM-MSCs plus IMC followed by BM-MSCs seemed to be more efficient in improving the LPO level in arthritic animals.

TABLE 1: Effect BM-MSCs and/or IMC on DLC count of CFA-induced arthritic rats.

| Leukocyte | | | | | | | | | | |
|---------------------|-------------------------|------------|-----------------------|------------|------------------------|------------|------------------------|------------|-----------------------|------------|
| Groups | Lymphocyte | (%) change | Neutrophil | (%) change | Monocyte | (%) change | Eosinophil | (%) change | Basophile | (%) change |
| Normal | 613 ± 46 ^{bc} | – | 325 ± 14 ^b | – | 114 ± 29 ^{ab} | – | 68 ± 23 ^a | – | 15 ± 8 ^b | – |
| CFA | 1913 ± 204 ^a | 2.12 | 980 ± 97 ^a | 2.0 | 153 ± 31 ^a | 0.35 | 425 ± 124 ^b | 5.24 | 71 ± 20 ^a | 3.68 |
| CFA + BM-MSCs | 761 ± 40 ^{bc} | –0.60 | 434 ± 51 ^b | –0.56 | 74 ± 5 ^b | –0.52 | 92 ± 18 ^a | –0.78 | 23 ± 12 ^b | –0.67 |
| CFA + IMC | 838 ± 0.0 ^b | –0.56 | 480 ± 30 ^b | –0.51 | 156 ± 11 ^a | 0.02 | 156 ± 30 ^a | –0.63 | 45 ± 11 ^{ab} | –0.37 |
| CFA + BM-MSCs + IMC | 445 ± 44 ^c | –0.77 | 431 ± 40 ^b | –0.56 | 83 ± 10 ^b | –0.46 | 98 ± 17 ^a | –0.77 | 29 ± 7 ^b | –0.59 |

(i) Data are expressed as mean ± standard error. Number of samples in each group is eight. (ii) For each type of leucocytes, means, which have different superscript symbols, are significantly different at $P < 0.05$. (iii) Percentage (%) changes were calculated by comparing the arthritic group with normal and arthritic-treated groups with the arthritic group.

TABLE 2: Effect of BM-MSCs and/or IMC on lipid peroxides and antioxidant status of CFA-induced arthritic rats.

| Parameters | | | | | | | | | | |
|---------------------|-------------------------|----------|---------------------------------|----------|--------------------------|----------|----------------------------|----------|-----------------------------|----------|
| Groups | MDA (nmole/L) × 10 | % change | GSH (nmole/L) × 10 ² | % change | SOD (U/L) × 10 | % change | GPx (U/L) | % change | GST (U/L) × 10 ² | % change |
| Normal | 1.8 ± 0.6 ^d | — | 43.74 ± 0.94 ^a | — | 15.5 ± 1.6 ^a | — | 87.00 ± 3.06 ^a | — | 9.35 ± 1.19 ^a | — |
| CFA | 19.1 ± 3.6 ^a | 961.11 | 35.1 ± 1.97 ^b | –19.75 | 7.1 ± 0.9 ^b | –54.19 | 36.17 ± 7.39 ^c | –58 | 6.11 ± 0.42 ^b | –34.71 |
| CFA + BM-MSCs | 7.4 ± 0.5 ^{bc} | –61.26 | 42.07 ± 1.17 ^a | 19.86 | 10.6 ± 0.7 ^{ab} | 49.30 | 61.00 ± 3.87 ^b | 69 | 7.97 ± 0.15 ^{ab} | 30.45 |
| CFA + IMC | 10.2 ± 1.9 ^b | –46.60 | 37.27 ± 0.96 ^b | 6.18 | 11.7 ± 1.2 ^{ab} | 64.79 | 60.00 ± 5.29 ^b | 66 | 7.64 ± 0.82 ^{ab} | 25.11 |
| CFA + BM-MSCs + IMC | 5.2 ± 0.6 ^{cd} | –72.77 | 43.22 ± 1.75 ^a | 23.13 | 15.1 ± 2.5 ^a | 112.68 | 80.00 ± 5.51 ^{ab} | 121 | 10.18 ± 1.15 ^a | 66.74 |

(i) Data are described as mean ± standard error. Number of samples in each group is eight. (ii) For each parameter, means, which have different superscript symbols, are significantly different at $P < 0.05$. (iii) Percentage (%) changes were calculated by comparing the CFA-arthritic control group with normal and comparing the arthritic-treated groups with the CFA-arthritic group.

The administration of CFA to Wistar rats significantly ($P < 0.01$) decreased the serum GSH content (–19.75%). While the treatment of CFA-induced arthritic rats with IMC did not significantly ($P > 0.05$) affect the GSH level (6.18%), the treatment with BM-MSCs alone or in combination with IMC produced a significant ($P < 0.05$) increase in the lowered GSH level. The combinatory effect of BM-MSCs was the most potent in increasing the GSH level.

The activities of antioxidant enzymes including SOD, GPx, and GST activities exhibited significant decreases in CFA-induced arthritic rats; the recorded percentage changes were –54.19%, –58%, and –34.71%, respectively, as compared to normal animals.

SOD activity significantly increased ($P < 0.01$) in CFA-induced arthritic rats treated with BM-MSCs + IMC (112.68%), while it was not significantly ($P > 0.05$) decreased as a result of treatments with either BM-MSCs (49.30%) or IMC (64.79%).

GPx activity exhibited significant increase ($P < 0.01$) in CFA-induced arthritic rats treated with BM-MSCs, IMC, and BM-MSCs + IMC recording percentage decreases of 69.00, 66.00, and 121.00%, respectively, as compared with CFA-induced arthritic control.

The lowered GST activity in serum of CFA-induced arthritic rats showed an increase as a result of treatment with BM-MSCs, IMC, and BM-MSCs + IMC. But, the effect was significant only due to treatment with the combination of BM-MSCs and IMC.

Overall, the BM-MSCs + IMC was the most potent in suppressing the LPO level and enhancing the antioxidant defense system.

3.6. Effect of Treatments on IL-1 β and RF Expression Levels. IL-1 β and RF concentrations in serum were estimated using a standard ELISA and represented as in Figures 6 and 7. CFA-induced arthritic rats had significantly ($P < 0.05$) elevated IL-1 β and RF level recording percentage changes of 289.67% and 419.74%, respectively, as compared with those in the normal control group. On the other hand, administrations of MSCs and/or IMC lead to significant reductions in IL-1 β and RF levels. The concurrent administration was the most efficient than BM-MSC than IMC drug in both IL-1 β and RF concentration levels.

3.7. Evaluation of the IL-4 mRNA Expression Level and Protein Level of Nrf-2 in Ankle Joints. IL-4 mRNA expression determined in the articular ankle joint by PCR is represented in Figure 8. Data exhibited significant downregulation ($P < 0.05$) of the IL-4 level in CFA animals (–33%) as compared with the normal. Otherwise, IL-4 levels in arthritic rats administered with BM-MSCs plus IMC, BM-MSCs alone, and IMC alone were significantly upregulated recording percentage changes of 58, 100, and 108%, respectively, in comparison with arthritic control rats.

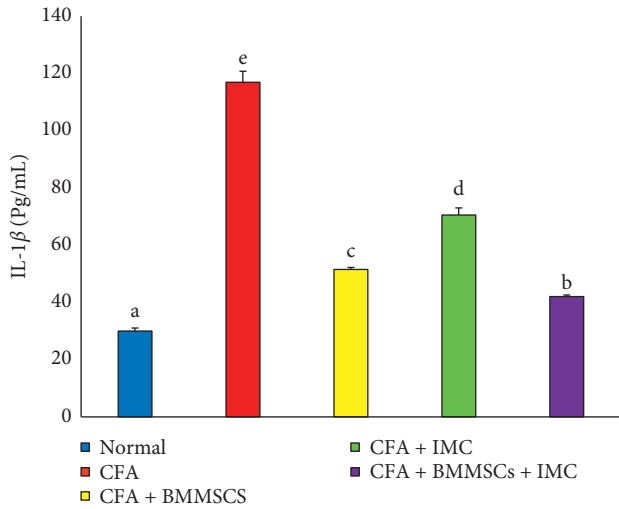


FIGURE 6: Effect of BM-MSCs and/or IMC on the IL-1 β level in CFA-induced animals. Means, which have different symbols, are significantly different at $P < 0.05$.

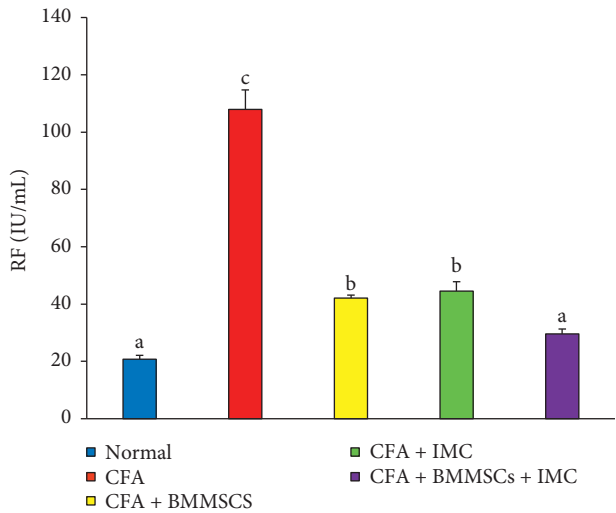


FIGURE 7: Effect of BM-MSCs and/or IMC on the RF level (mIU/mL) in CFA-induced animals. Means, which have different symbols, are significantly different at $P < 0.05$.

The Nrf-2 protein level in the ankle joint was measured by the western blotting technique that showed marked decline (-63%) in the CFA-induced arthritic rats compared to the normal rats, whereas the supplementation with BM-MSCs plus IMC, BM-MSCs alone, and IMC alone markedly alleviated the Nrf-2 level of these groups with a percentage of increase 249, 127, and 149%, respectively, in comparison with arthritic control rats (Figure 9).

4. Discussion

RA is considered an autoimmune inflammatory syndrome causing synovial proliferation, progressive erosion of bone, and destruction of the articular cartilage. The disease affects the quality of life and has a striking impact on societal and economic cost and is considered as an important cause of premature death [28, 29]. Nowadays, treatment with stem

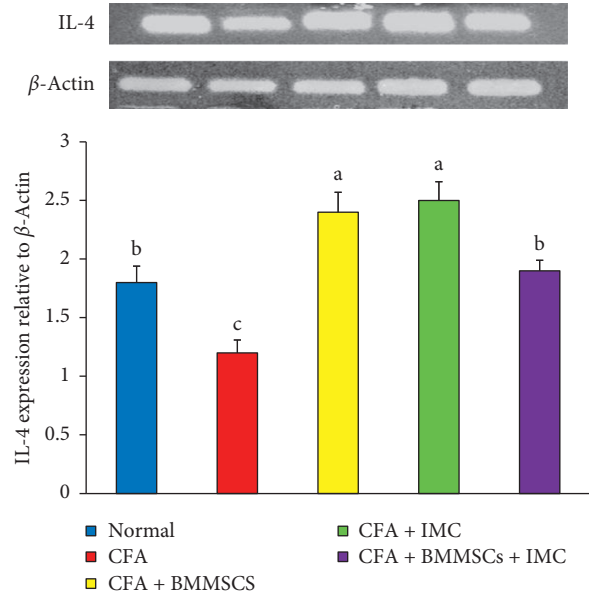


FIGURE 8: Effect of BM-MSCs and/or IMC on the IL-4 expression level in arthritic rats. Means, which have different symbols, are significantly different at $P < 0.05$.

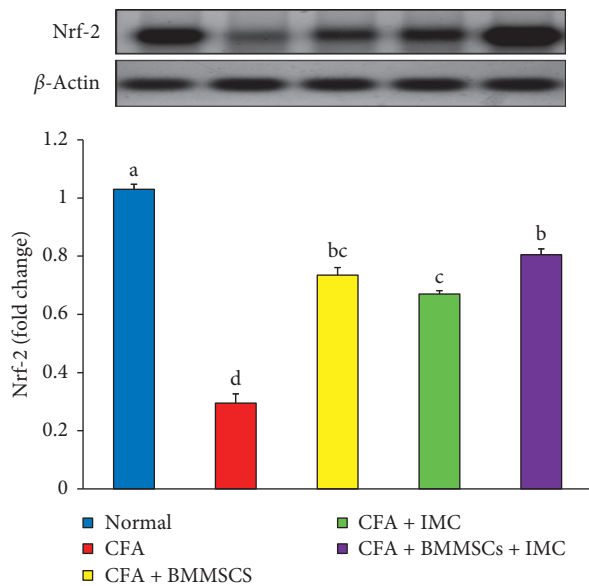


FIGURE 9: Effect of BM-MSCs and/or IMC on the Nrf-2 expression level in arthritic rats. Means, which have different symbols, are significantly different at $P < 0.05$.

cells is considered as one of the most promising signs for the proximate future. This form of therapy could boost or even reverse certain degenerative diseases and probably have applications in alternative and regenerative medicine [19, 30]. MSCs are a remarkable and effective tool in bone and cartilage tissue repair, as they can differentiate into several connective tissues including fat, cartilage, and bone. In addition, they have immunomodulatory and anti-inflammatory effects, self-renewal ability, stemming maintenance, and plasticity for allo- and xenotransplant applications [31]. Also, the use of IMC in the treatment of

RA has attracted many researchers because of their analgesic, anti-inflammatory, and antirheumatic influences on the inflammatory disorders. This directed us to evaluate the usefulness of the combination of BM-MSCs plus IMC agents on CFA-induced arthritis as a convenient, easy, and replicable model with short duration of the experiment.

Severe paw swelling (edema), synovial proliferation, accumulation of neutrophils, and bone, as well as cartilage, damage are a marked features of the CFA-induced arthritis model [32]. Here, the right hind paw volume was estimated weekly, and CFA-induced arthritic rats exhibited increased paw volume and swelling in comparison with normal animals. The current data showed that the supplementation of the arthritic rats with BM-MSCs and/or IMC either alone or combined successfully reduced the hind paw volume by the end of the experiment in relation to arthritic rats; thus, the tested agents efficiently suppressed the inflammation inside tissues. Similarly, the research of a previous publication [33] revealed that treatment with IMC decreased the injected paw and contralateral paw edema by 35% and 30%, respectively. Such macroscopic investigation was more elucidated via further microscopic examination of paw sections and their histological score. Histopathologically, rats in the CFA-arthritic control group exhibited severe stage of inflammation described as invasion of leukocytes, synovial hyperplasia, cartilage degradation, and bone resorption. Conversely, animals supplemented by IMC greatly alleviated the joint damage and displayed moderate stage of these lesions. Furthermore, the BM-MSCs-treated arthritic group and BM-MSCs + IMC-treated arthritic group afforded a significant protection against those alterations and exhibited mild stage of such lesions where normal joint space, less infiltration of leukocytes, and an intact appearance of the cartilage were detected. Such observations were more elucidated by the histological score that exhibited a significant reduction in the total score by treatments in this order: BM-MSCs plus IMC > BM-MSCs > IMC as compared to CFA-induced arthritic control rats. Particularly, BM-MSCs plus IMC treatment markedly declined the synovitis, suppressed pannus formation, and reduced degradation of the cartilage as compared to arthritis control rats, while bone resorption was not significantly changed. Hence, such findings obviously evidenced the potency of the tested agents in suppressing the inflammatory reactions inside tissues and illustrated the suppressed inflammatory reactions and paw swelling induced by arthritis.

Likewise, changes in body weight are a valuable index for evaluating disease course and response to an anti-inflammatory drug under research. In the present study, after two weeks of adjuvant injection, the CFA-induced arthritic rats showed observable loss of weight in comparison to normal animals. This finding is in agreement with Da Silva et al. [33] who reported that the adjuvant administered rats developed a significant body weight loss 8 days after injection compared with the healthy control group. This could be attributed to loss of appetite and loss of weight as a result of CFA injection and expansion of arthritis as the study of Da Silva et al. [33] illustrated. On the other hand, supplementation of rats with BM-MSCs and/or IMC treatments

either alone or concurrently resulted in remarkable reduction of weight loss in regard with the arthritic group. The BM-MSCs plus IMC was more efficient (44.53%) than IMC (36.97%) and BM-MSCs (34.45%). Our results were entirely consistent with the study of Moases Ghaffary and Abtahi [34] who reported a significant reduction in the average body weight of RA rats when compared with the normal control rats but the extent of weight loss was significantly restricted in RA rats received both caffeine pulsed MSCs and unpulsed MSCs therapies, compared to the vehicle-treated RA animals. Also, Da Silva et al. [33] stated that the weight gain of IMC-treated arthritic rats was higher than untreated arthritic rats but still lower than normal rats. Overall, the macroscopic examinations such as inhibited paw volume and alleviated body weight, as well as the microscopic results, suggested the first indication of the protective and anti-inflammatory action of BM-MSC and/or IMC treatments as therapeutic targets for RA.

In the same line, leukocytes pass to inflammatory sites in response to chemotactic stimuli, causing tissue swelling and oedema, thereby playing a critical role in pathogenesis of both acute and chronic inflammatory disorders [35]. In relation to TLC, as well as DLC, our data revealed that the AIA animals exhibited severe leukocytosis with concomitant increase of lymphocytes, as well as neutrophils comparing to normal animals. These results are in accordance with Pinal et al. [36] who established marked leukocytosis in rats on day 21 after arthritis induction and the study of Franch et al. [37] who explored leukocytosis with higher number and percentage of both neutrophils and lymphocytes in adjuvant-induced rats regarding to normal. Side by side, Pinal et al. [36] informed that leukocytosis and neutrophilia were detected as a result of CFA injection. Such fluctuations in leukocytes are likely due to the inflammatory process present in arthritis involving the fenestration of the microvasculature, element leakage into the interstitial space, and the transfer of white blood cells into inflamed tissues [38]. In this study, our data revealed that these changes were returned near to normal levels in animals treated with test drugs in comparison to the arthritic rats. The BM-MSCs plus IMC and BM-MSCs rats efficiently reversed their alleviated counts to normal ranges whereas the IMC significantly improved neutrophils, lymphocytes, and eosinophils but decreased monocytes, as well as basophils, slightly when compared to the normal group. These results recommended the potential anti-inflammatory and anti-arthritic effectiveness against the disease development and progression.

Another factor of RA pathogenesis which cannot be ignored is oxidative stress. Former studies of Holley and Cheeseman [39] and Ali et al. [40] illustrated that accumulation of macrophages and granulocytes in the inflamed region facilitates the formation of reactive oxygen species (ROS) and free radical species (FR), such as superoxide (O_2^-) and hydrogen peroxide radicals (H_2O_2). Reactive oxidants are formed in many compartments inside the cell, either normally from internal metabolism or due to external exposure to toxic or pathological insults [41, 42]. In normal conditions, ROS are produced in a restricted way, and some have useful purposes such as acting as essential regulators of

both physiological and pathophysiological outcomes [43]. They are developed in response to physiological indications to control processes such as division of the cell, autophagy, stress, immune function response, and inflammation as essential signaling molecules [42]. Inversely, uncontrolled oxidant production results in oxidative stress which also impairs cellular functions and causes cancer, chronic disease, and toxicity development [44, 45]. It is not surprising that the role of oxidative stress or ROS in arthritis serves as a mediator in the pathogenesis of cartilage destruction and tissue damage. A common feature which defines the oxidative stress present in rats is lipid peroxidation or LPO production. MDA is regarded a prooxidant component and used to determine LPO. Generating ROS/RNS is normally stabilized by endogenous antioxidants involving SOD, GSH, GPx, and GST. The first line of antioxidants, GSH and SOD, catalytically scavenge the free radicals (O_2^- and H_2O_2). SOD converts the O_2^- to H_2O_2 and is widely used during the toxic effects of O_2^- to protect cell damage. Endogenous antioxidant GPx reduced the H_2O_2 to form oxidized glutathione and water in the presence of GSH [39]. Imbalance in this process during an exacerbated cell response results in cellular dysfunction and excessive pathological circumstances including bone and cartilage degradation [46, 47]. Furthermore, injection of CFA into rats induces substantial release of ROS and FR at the site of inflammation [48]. Our findings offer good support to these studies because we observed a significant increase in the level of MDA in parallel with marked reduction of antioxidant levels of GSH, GPx, GST, and SOD in serum samples of arthritic control animals in comparison with normal animals. Elevation in MDA levels may be due to extreme accumulation of leukocytes in the blood and inflamed regions that raise LPO production rates and suppress the antioxidant protection system. These observations were also in accordance with our histological analysis showing damage of tissue and intense infiltration of immune cells.

Regarding to the treated groups, the supplementation with BM-MSCs and/or IMC decreased the oxidative damage significantly via suppressing the LPO level in all treated animals. This is in full agreement with the case study of Nejad-Moghaddam et al. [49] who treated the lungs of a subject previously exposed to sulfur mustard gas utilizing MSCs and reported that favorable results were attributed to the antioxidant properties of MSCs, and this was evidenced by reduced LPO levels in the sputum. Moreover, the antioxidant defense mechanism of BM-MSCs and/or IMC therapeutic agents against oxidative stress was achieved mainly via activation of GPx enzyme that played a crucial role in reducing oxidative stress by the elimination of H_2O_2 used as a cell death inducing oxidative stimulus. This finding is in consistent with the study of Chang et al. [50] who showed that MSC treatment upregulated the GPx expression in small bowel ischemia/reperfusion (I/R) injury, septic lung injury, sever acute pancreatitis, and Friedreich's ataxia.

Also, Stavely and Nurgali [51] and Kim et al. [52] revealed that MSC can also promote activity of GPx in fibroblasts during oxidative stimuli. Besides, Huang et al. [53] proved that IMC drug was highly effective in enhancing the

GPx activity in the AIA animal model. However, the SOD, as well as GST, activities were increased slightly but were not significant in improving the antioxidant processes GPx enzyme. In the current research, it was concluded that BM-MSCs plus IMC was the most potent than either BM-MSCs or IMC in enhancing the antioxidant defense system on the expense of the oxidative stress in tissues and, thereby, inhibiting the subsequent inflammatory processes.

Furthermore, another indicator of the oxidative damage in the body is nuclear erythroid 2-related factor (Nrf-2) protein that was detected in the current study in ankle joint articular tissue. The former data clearly illustrated the pronounced amelioration of the oxidative stress biomarkers, as well as the ability of the tested drugs in scavenging FR and neutralizing ROS. Nrf-2 is a principal regulator of cellular replies against environmental disorders, and it is probable that Nrf-2 activation can protect against factors triggering autoimmune pathogenesis. Activating this signaling pathway, which contributes to detoxification and protective manners, has prompted a wealth of studies on the potential health benefits and therapeutic application of Nrf-2 [54].

Nrf-2 is a key transcription factor that regulates intracellular redox balance. The latter acts as a sensor of oxidative stress mainly present in the cytoplasm; when the level of ROS is elevated, the transcription of antioxidative stress proteins, including SOD^{-1} , NQO^{-1} , and HO^{-1} , is enhanced. These genes play a vital role in prevention of oxidative stress and tissue damage [38, 55]. Nrf-2-targeted genes include genes involved in the synthesis and conjugation of GSH, metabolism of heme and iron, and metabolism and transport of drugs, as well as antioxidant proteins, enzymes, and transcription factors.

Our current research detected a marked downregulation of the Nrf-2 expression level in ankle joint articular tissues of CFA-induced arthritic rats as compared with the normal rats, thus elevating the oxidative damage in this group. On the contrary, the administration of BM-MSCs and IMC either alone or combined together to the arthritic rats produced apparently upregulated expression levels of Nrf-2 in ankle joint tissues as compared to the arthritic control. This finding supports our supposing of the antioxidant effect of the current investigated therapies. In another way, Yoshinaga et al. [56] stated that IMC may be an appropriate therapeutic strategy for choroidal neovascularization (CNV) because of its antiangiogenic effect and that the Nrf-2 signaling is a contributing underlying mechanism. In addition, Wang et al. [57] found that BM-MSCs transplantation in Spinal Cord Injury (SCI) in rats significantly increased the expression of Nrf-2 protein, thereby inhibiting oxidative stress triggered by SCI and promoting spinal cord repair. Overall, these results validate our choice of using BM-MSCs or IMC either alone or combined in inflammatory conditions as reference drugs via their ability of upregulating the Nrf-2 pathway and, therefore, suppressing the oxidative stresses occurred as a result of the disease development (Figure 10).

Furthermore, RA is an autoimmune illness that is well known with formation autoantibodies in serum, as well synovial fluid (SF), samples in 50–80% of RA patients. RF

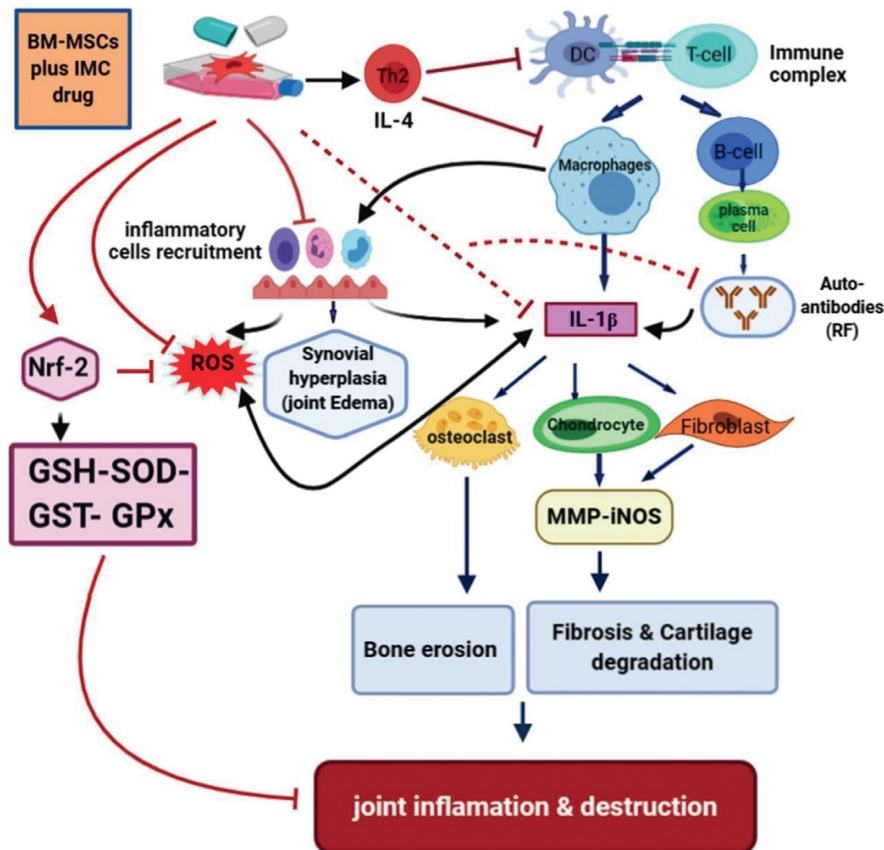


FIGURE 10: Schematic diagram showing the immunodulatory effect of BM-MSCs plus IMC administered concurrently in CFA-induced arthritis.

was the first described autoantibody system in RA and focused on Fc portion of human IgG. Despite its suboptimal specificity, the RF occurrence was considered so representative for RA and included in the criteria of the ACR classification in 1987 [58]. Then, it has been included in the 2010 American College for Rheumatology European League Against Rheumatism (ACREULA) classification criteria. However, the RF has been studied for decades, and its role in the pathogenesis of RA remains incompletely known. RF is likely to exert its pathogenic properties via the creation of immune complexes. Then, proinflammatory cytokines, such as $\text{TNF-}\alpha$ and $\text{IL-1}\beta$, are stimulated and contributing in chronic inflammation and bone destruction [59].

Additionally, cytokines play a crucial role in the pathogenesis of the disease. RA is well known for the ongoing influx of immune cell (monocytes and lymphocytes) into the joints [60]. The process of inflammation is tightly controlled frequently, utilizing both mediators that induce and sustain inflammation which called inflammatory cytokines ($\text{TNF-}\alpha$, $\text{IL-1}\beta$, and IL-6) and mediators that shut down the process and called anti-inflammatory cytokines (IL-10 and IL-4). In chronic states of inflammation, an inequality between the two mediators resulting in cellular damage, cartilage and bone destruction, and inflammation [61].

$\text{IL-1}\beta$, the most significant cytokine in pathogenic arthritis progression, has been reported to be correlated with disease behavior such as morning stiffness period [62]. This

Th1 cytokine is mainly secreted by macrophages and plays a dominant role in infiltration of inflammatory cells, as well as destruction of bones and cartilage. It also stimulates nuclear factor-B ligand receptor activator on macrophages to differentiate into osteoclasts which resorb and damage the bone. In addition, $\text{IL-1}\beta$ prompts the production of inducible nitric oxide (iNOS), prostaglandins (PGE-2), and matrix metalloproteinase (MMP), thus inducing the degradation of the cartilage (Figure 10) [63, 64]. In comparison, IL-4 is an anti-inflammatory cytokine produced by Th2 helper and reduces IL-1 and $\text{TNF-}\alpha$ production and inhibits cartilage damage. Similarly, the data reported by Chomarat et al. [65] suggested that IL-4 inhibited the development of IL-1 and increased the expression of its receptor antagonism, and both actions would decrease inflammation in synovial culture samples from patients with RA. Hence, IL-4 could be considered as a potential tool for treating autoimmune diseases as evidenced by its protective effect in murine models of RA [66, 67].

In harmony with all our preceding results, data of the arthritic control group showed a significant elevation in the RF level detected in serum in parallel with a remarkable upregulation of $\text{IL-1}\beta$ and downregulation of the IL-4 protein level expressed in joint articular tissues as compared to the normal one. These findings are a strong indicator of prominence of the inflammatory pathway on the expense of the anti-inflammatory one as a result of CFA administration.

However, the rats supplemented with BM-MSC and IMC either alone or concurrently exhibited a noticeable shift toward the anti-inflammatory pathway and predominance of Th2 on Th1 as evidenced by the apparent upregulated IL-4 and downregulated IL-1 β expression level in joints accompanied with a significant decline of the RF level in sera of the treated rats compared to the CFA arthritic rats. In accordance with our study, Hoogduijn et al. [68] added that MSCs can alter the cytokine secretion profile of immune cells such as raising the secretion of suppressive cytokines (IL-4 and IL-10) and decreasing the secretion of TNF- α and interferon- γ (IFN- γ) secretion. Besides, it was reported by Selleri et al. [69] and Zhang et al. [70] that the coculture of macrophages with MSCs induces production of M2 macrophages, which upregulates the phagocytic activity and secretion of Th2 cytokines and downregulates levels of Th1 cytokines, such as IL-1 β , IFN- γ , TNF- α , and IL-12. Such modulation of the immune response suggests their enhancement of Th2 signaling which directly inhibits the Th1 cascade reaction via suppressing the inflammation propagation (Figure 10). Nrf-2, which has enhanced suppression by the effect of BM-MSCs and IMC, is able to suppress oxidative stress and inflammation and activate the antioxidant defense system (Figure 10). These results represented and introduced a clear interpretation of the efficiency of BM-MSC and/or IMC as antiarthritic and anti-inflammatory agents in overcoming the course of RA.

5. Conclusions

Taken together, the present study evidenced that the concomitant treatment with BM-MSCs and IMC administration is more effective in producing anti-inflammatory and antiarthritic effects other than use of each alone during the course of RA in CFA-induced arthritic Wistar rats. This suggestion was supported through the obvious inhibition of the inflammatory signs such as hind paw swelling, weight loss, oxidative stress (LPO), and inflammatory cytokines (RF and IL-1 β). Moreover, this tested combination succeeds to monitor the disease progression through alleviation of the antioxidant enzyme levels (GPx, SOD, GSH, and GST) and upregulation of Th2 anti-inflammatory cytokine (IL4) and Nrf-2 in joint articular tissues as well. Likewise, the combined treatment alleviated the synovitis, pannus formation, and cartilage destruction occurred as a result of the disease. Eventually, BM-MSCs concurrently administered with IMC could provide an additional promising therapeutic strategy for RA. However, further research should be performed to clarify the mechanisms of the antirheumatic activity of BM-MSCs plus IMC specifically to overcome RA.

Data Availability

The data used to support the findings of this study are available from the corresponding author upon reasonable request.

Conflicts of Interest

The authors declare that they have no conflicts of interest.

Acknowledgments

The authors acknowledge Taif University, Taif, Saudi Arabia, for supporting this study (Taif University Researchers Supporting Project number: TURSP-2020/127).

References

- [1] E. Silvagni, A. Giollo, G. Sakellariou et al., "One year in review 2020: novelties in the treatment of rheumatoid arthritis," *Clinical and Experimental Rheumatology*, vol. 38, no. 2, pp. 181–194, 2020.
- [2] S.-Y. Gwon, K.-J. Rhee, and H. J. Sung, "Gene and protein expression profiles in a mouse model of collagen-induced arthritis," *International Journal of Medical Sciences*, vol. 15, no. 1, pp. 77–85, 2018.
- [3] C. G. Helmick, D. T. Felson, R. C. Lawrence et al., "Estimates of the prevalence of arthritis and other rheumatic conditions in the United States: Part I," *Arthritis & Rheumatism*, vol. 58, no. 1, pp. 15–25, 2008.
- [4] P. E. Lipsky, Kasper, "Rheumatoid arthritis," in *Harrison's Principles of Internal Medicine*, A. Fauci and E. Braunwald, Eds., pp. 2083–2092, McGraw Hill, New York, NY, USA, 17th edition, 2008.
- [5] N. Gözel, M. Çakirer, A. Karataş et al., "Sorafenib reveals antiarthritic potentials in collagen induced experimental arthritis model," *Archives of Rheumatology*, vol. 33, no. 3, pp. 309–315, 2018.
- [6] O. M. Ahmed, S. F. EL-Abd, E. A. El Mahdi et al., "Curcumin ameliorative efficacy on type 1 diabetes mellitus coexisted with rheumatoid arthritis in Wistar rats," *Merit Research Journal of Medicine and Medical Sciences*, vol. 3, no. 7, pp. 256–270, 2015.
- [7] O. M. Ahmed, H. A. Soliman, B. Mahmoud, and R. R. Gheryany, "Ulva lactuca hydroethanolic extract suppresses experimental arthritis via its anti-inflammatory and antioxidant activities," *Beni-Suef University Journal of Basic and Applied Sciences*, vol. 6, no. 4, pp. 394–408, 2017.
- [8] M. Luisa Corvo, J. C. S. Jorge, R. Van't Hof, M. E. M. Cruz, D. J. A. Crommelin, and G. Storm, "Superoxide dismutase entrapped in long-circulating liposomes: formulation design and therapeutic activity in rat adjuvant arthritis," *Biochimica et Biophysica Acta (BBA)-Biomembranes*, vol. 1564, no. 1, pp. 227–236, 2002.
- [9] O. Ahmed, H. Fahim, A. Mahmoud, and E. Ahmed, "Bee venom and hesperidin effectively mitigate complete Freund's adjuvant-induced arthritis via immunomodulation and enhancement of antioxidant defense system," *Archives of Rheumatology*, vol. 33, no. 2, pp. 198–212, 2018.
- [10] J. M. Berthelot, B. Le Goff, and Y. Maugars, "Bone marrow mesenchymal stem cells in rheumatoid arthritis, spondyloarthritis, and ankylosing spondylitis: problems rather than solutions?" *Arthritis Research and Therapy*, vol. 21, no. 1, p. 239, 2019.
- [11] R. A. Contreras, F. E. Figueroa, F. Djouad, and P. Luz-Crawford, "Mesenchymal stem cells regulate the innate and

- adaptive immune responses dampening arthritis progression,” *Stem Cells International*, vol. 2016, Article ID 3162743, 2016.
- [12] J. Cagliani, D. Grande, E. P. Molmenti, E. J. Miller, and H. L. R. Rilo, “Immunomodulation by mesenchymal stromal cells and their clinical applications,” *Journal of Stem Cell and Regenerative Biology*, vol. 3, no. 1, pp. 126–139, 2017.
- [13] J. Chahal, A. Gómez-Aristizábal, K. Shestopaloff et al., “Bone marrow mesenchymal stromal cell treatment in patients with osteoarthritis results in overall improvement in pain and symptoms and reduces synovial inflammation,” *Stem Cells Translational Medicine*, vol. 8, no. 8, pp. 746–757, 2019.
- [14] N. Yin, X. Guo, R. Sun et al., “Intra-articular injection of indomethacin-methotrexate in situ hydrogel for the synergistic treatment of rheumatoid arthritis,” *Journal of Materials Chemistry B*, vol. 8, no. 5, pp. 993–1007, 2020.
- [15] J. Tan, Z. Deng, G. Liu, J. Hu, and S. Liu, “Anti-inflammatory polymersomes of redox-responsive polyprodrug amphiphiles with inflammation-triggered indomethacin release characteristics,” *Biomaterials*, vol. 178, pp. 608–619, 2018.
- [16] U. Snehalatha, M. Anburajan, B. Venkatraman, and M. Menaka, “Evaluation of complete Freund’s adjuvant-induced arthritis in a Wistar rat model,” *Zeitschrift für Rheumatologie*, vol. 72, no. 4, pp. 375–382, 2013.
- [17] T. A. Mohamed and M. F. Abouel-Nour, “Therapeutic effects of bone marrow stem cells in diabetic rats,” *Journal of Computer Science & Systems Biology*, vol. 9, no. 2, 2016.
- [18] J. K. Chaudhary and P. C. Rath, “A simple method for isolation, propagation, characterization, and differentiation of adult mouse bone marrow-derived multipotent mesenchymal stem cells,” *Journal of Cell Science & Therapy*, vol. 8, no. 1, 2017.
- [19] O. M. Ahmed, M. A. Hassan, and A. S. Saleh, “Combinatory effect of hesperetin and mesenchymal stem cells on the deteriorated lipid profile, heart and kidney functions and antioxidant activity in STZ-induced diabetic rats,” *Biocell*, vol. 44, no. 1, pp. 27–29, 2020.
- [20] D. Sancho, M. Gómez, F. Viedma et al., “CD69 downregulates autoimmune reactivity through active transforming growth factor- β production in collagen-induced arthritis,” *Journal of Clinical Investigation*, vol. 112, no. 6, pp. 872–882, 2003.
- [21] O. Ahmed, M. Ashour, H. Fahim, and N. Ahmed, “Citrus limon and paradisi fruit peel hydroethanolic extracts prevent the progress of complete Freund’s adjuvant-induced arthritis in male Wistar rats,” *Advances in Animal and Veterinary Sciences*, vol. 6, no. 10, pp. 443–455, 2018.
- [22] H. G. Preuss, S. T. Jarrell, R. Scheckenbach, S. Lieberman, and R. A. Anderson, “Comparative effects of chromium, vanadium and gymnema sylvestre on sugar-induced blood pressure elevations in SHR,” *Journal of the American College of Nutrition*, vol. 17, no. 2, pp. 116–123, 1998.
- [23] E. Beutler, O. Duron, and B. M. Kelly, “Improved method for the determination of blood glutathione,” *Journal of Laboratory and Clinical Medicine*, vol. 61, pp. 882–888, 1963.
- [24] B. Mannervik and C. Guthenberg, “Glutathione transferase (human placenta),” *Methods in Enzymology*, vol. 77, pp. 231–235, 1981.
- [25] S. Marklund and G. Marklund, “Involvement of the superoxide anion radical in the autoxidation of pyrogallol and a convenient assay for superoxide dismutase,” *European Journal of Biochemistry*, vol. 47, no. 3, pp. 469–474, 1974.
- [26] B. Matkovic, M. Kotorman, I. S. Varga, D. Q. Hai, and C. Varga, “Oxidative stress in experimental diabetes induced by streptozotocin,” *Acta Physiologica Hungarica*, vol. 85, no. 1, pp. 29–38, 1998.
- [27] J. Chu, X. Wang, H. Bi, L. Li, M. Ren, and J. Wang, “Dihydromyricetin relieves rheumatoid arthritis symptoms and suppresses expression of pro-inflammatory cytokines via the activation of Nrf-2 pathway in rheumatoid arthritis model,” *International Immunopharmacology*, vol. 59, pp. 174–180, 2018.
- [28] M. Abbasi, M. J. Mousavi, S. Jamalzahi et al., “Strategies toward rheumatoid arthritis therapy; the old and the new,” *Journal of Cellular Physiology*, vol. 234, no. 7, pp. 10018–10031, 2019.
- [29] M. A. El-Ghazaly, N. A. Fadel, D. H. Abdel-Naby, H. A. Abd El-Rehim, H. F. Zaki, and S. A. Kenawy, “Potential anti-inflammatory action of resveratrol and piperine in adjuvant-induced arthritis: effect on pro-inflammatory cytokines and oxidative stress biomarkers,” *The Egyptian Rheumatologist*, vol. 42, no. 1, pp. 71–77, 2020.
- [30] O. M. Ahmed, M. B. Ashour, H. I. Fahim, and N. A. Ahmed, “The role of Th1/Th2/Th17 cytokines and antioxidant defense system in mediating the effects of lemon and grapefruit peel hydroethanolic extracts on adjuvant-induced arthritis in rats,” *Journal of Applied Pharmaceutical Science*, vol. 8, no. 10, pp. 69–81, 2018.
- [31] D. Mehrabani, F. Mojtahed Jaber, M. Zakerinia et al., “The healing effect of bone marrow-derived stem cells in knee osteoarthritis: a case report,” *World Journal of Plastic Surgery*, vol. 5, no. 2, pp. 168–174, 2016.
- [32] L. Bevaart, M. J. Vervoordeldonk, and P. P. Tak, “Evaluation of therapeutic targets in animal models of arthritis: how does it relate to rheumatoid arthritis?” *Arthritis and Rheumatism*, vol. 62, no. 8, pp. 2192–2205, 2010.
- [33] M. A. R. C. P. Da Silva, C. A. Bersani-Amado, E. L. Ishii-Iwamoto, L. Bracht, and S. M. Caparroz-Assef, “Protective effects of indomethacin and cyclophosphamide but not of infliximab on liver metabolic changes caused by adjuvant-induced arthritis,” *Inflammation*, vol. 34, no. 6, pp. 519–530, 2011.
- [34] E. Moases Ghaffary and S. M. Abtahi Froushani, “Immunomodulatory benefits of mesenchymal stem cells treated with Caffeine in adjuvant-induced arthritis,” *Life Sciences*, vol. 246, Article ID 117420, 2020.
- [35] A. U. Tatiya and A. K. Saluja, “Further studies on membrane stabilizing, anti-inflammatory and FCA induced arthritic activity of various fractions of bark of machilus macrantha in rats,” *Revista Brasileira de Farmacognosia*, vol. 21, no. 6, pp. 1052–1064, 2011.
- [36] P. Pinal, P. Dharmik, and P. Natvarlal, “Experimental investigation of anti-rheumatoid activity of *Pleurotus sajorcaju* in adjuvant-induced arthritic rats,” *Chinese Journal of Natural Medicines*, vol. 10, no. 4, pp. 269–274, 2012.
- [37] A. Franch, C. Castellote, and M. Castell, “Blood lymphocyte subsets in rats with adjuvant arthritis,” *Annals of the Rheumatic Diseases*, vol. 53, no. 7, pp. 461–466, 1994.
- [38] H. Abd El-fatah, M. Ezz, H. El-kabany, and S. M. ElSonbaty, “Reduction of some extra-articular complications associated with arthritis development in rats by low dose γ -irradiation,” *Arab Journal of Nuclear Sciences and Applications*, vol. 53, no. 1, pp. 172–181, 2019.
- [39] A. E. Holley and K. H. Cheeseman, “Measuring free radical reactions in vivo,” *British Medical Bulletin*, vol. 49, no. 3, pp. 494–505, 1993.
- [40] E. A. I. Ali, B. M. Barakat, and R. Hassan, “Antioxidant and angiostatic effect of spirulina platensis suspension in complete

- Freund's adjuvant-Induced arthritis in rats," *PLoS One*, vol. 10, no. 4, 2015.
- [41] Q. Ma, "Transcriptional responses to oxidative stress: pathological and toxicological implications," *Pharmacology and Therapeutics*, vol. 125, no. 3, pp. 376–393, 2010.
- [42] T. Finkel, "Signal transduction by mitochondrial oxidants," *Journal of Biological Chemistry*, vol. 287, no. 7, pp. 4434–4440, 2012.
- [43] Q. Ma, "Role of Nrf-2 in oxidative stress and toxicity," *Annual Review of Pharmacology and Toxicology*, vol. 53, no. 1, pp. 401–426, 2013.
- [44] E. Bossy-Wetze, R. Schwarzenbacher, and S. A. Lipton, "Molecular pathways to neurodegeneration," *Nature Medicine*, vol. 10, 2004.
- [45] R. S. Balaban, S. Nemoto, and T. Finkel, "Mitochondria, oxidants, and aging," *Cell*, vol. 120, no. 4, pp. 483–495, 2005.
- [46] M. Grootveld, E. B. Henderson, A. Farrell, D. R. Blake, H. G. Parkes, and P. Haycock, "Oxidative damage to hyaluronate and glucose in synovial fluid during exercise of the inflamed rheumatoid joint. Detection of abnormal low-molecular-mass metabolites by proton-n.m.r. spectroscopy," *Biochemical Journal*, vol. 273, no. 2, pp. 459–467, 1991.
- [47] V. Kumar, P. C. Bhatt, M. Rahman et al., "*Melastoma malabathricum* Linn attenuates complete Freund's adjuvant-induced chronic inflammation in Wistar rats via inflammation response," *BMC Complementary Alternative Medicine*, vol. 16, no. 1, pp. 1–16, 2016.
- [48] R. Cascão, B. Vidal, H. Raquel et al., "Potent anti-inflammatory and antiproliferative effects of gambogic acid in a rat model of antigen-induced arthritis," *Mediators of Inflammation*, vol. 2014, Article ID 195327, 2014.
- [49] A. Nejad-Moghaddam, S. Ajdari, E. Tahmasbpour et al., "Adipose-derived mesenchymal stem cells for treatment of airway injuries in a patient after long-term exposure to sulfur mustard," *Cell Journal*, vol. 19, no. 1, p. 117, 2017.
- [50] C.-L. Chang, P.-H. Sung, C.-K. Sun et al., "Protective effect of melatonin-supported adipose-derived mesenchymal stem cells against small bowel ischemia-reperfusion injury in rat," *Journal of Pineal Research*, vol. 59, no. 2, pp. 206–220, 2015.
- [51] R. Stavely and K. Nurgali, "The emerging antioxidant paradigm of mesenchymal stem cell therapy," *Stem Cells Translational Medicine*, vol. 9, no. 9, 2020.
- [52] W.-S. Kim, B.-S. Park, H.-K. Kim et al., "Evidence supporting antioxidant action of adipose-derived stem cells: protection of human dermal fibroblasts from oxidative stress," *Journal of Dermatological Science*, vol. 49, no. 2, pp. 133–142, 2008.
- [53] G. Huang, T. Guan, P. Wang, and S. Qin, "Anti-arthritis effect of baicalin exert on complete Freund's adjuvant-induced arthritis in rats by reducing the inflammatory reaction," *International Journal of Pharmacology*, vol. 15, no. 7, pp. 880–890, 2019.
- [54] T. Suzuki and M. Yamamoto, "Stress-sensing mechanisms and the physiological roles of the Keap1–Nrf-2 system during cellular stress," *Journal of Biological Chemistry*, vol. 292, no. 41, pp. 16817–16824, 2017.
- [55] Z. Chen, H. Zhong, J. Wei et al., "Inhibition of Nrf-2/HO-1 signaling leads to increased activation of the NLRP3 inflammasome in osteoarthritis," *Arthritis Research & Therapy*, vol. 21, no. 1, pp. 1–13, 2019.
- [56] N. Yoshinaga, N. Arimura, H. Otsuka et al., "NSAIDs inhibit neovascularization of choroid through HO-1-dependent pathway," *Laboratory Investigation*, vol. 91, no. 9, pp. 1277–1290, 2011.
- [57] X. Wang, L. Ye, K. Zhang, L. Gao, J. Xiao, and Y. Zhang, "Upregulation of microRNA-200a in bone marrow mesenchymal stem cells enhances the repair of spinal cord injury in rats by reducing oxidative stress and regulating Keap1/Nrf-2 pathway," *Artificial Organs*, vol. 44, no. 7, pp. 744–752, 2020.
- [58] L. A. Trouw, T. Rispens, and R. E. M. Toes, "Beyond citrullination: other post-translational protein modifications in rheumatoid arthritis," *Nature Reviews Rheumatology*, vol. 13, no. 6, pp. 331–339, 2017.
- [59] M. A. M. Van Delft and T. W. J. Huizinga, "An overview of autoantibodies in rheumatoid arthritis," *Journal of Autoimmunity*, vol. 110, Article ID 102392, 2020.
- [60] Z. Chen, A. Bozec, A. Ramming, and G. Schett, "Anti-inflammatory and immune-regulatory cytokines in rheumatoid arthritis," *Nature Reviews Rheumatology*, vol. 15, no. 1, pp. 9–17, 2019.
- [61] E. H. S. Choy and G. S. Panayi, "Cytokine pathways and joint inflammation in rheumatoid arthritis," *New England Journal of Medicine*, vol. 344, no. 12, pp. 907–916, 2001.
- [62] S. Mateen, S. Moin, S. Shahzad, and A. Q. Khan, "Level of inflammatory cytokines in rheumatoid arthritis patients: correlation with 25-hydroxy vitamin D and reactive oxygen species," *PLoS One*, vol. 12, no. 6, 2017.
- [63] H. Sakaki, T. Matsumiya, A. Kusumi et al., "Interleukin-1 β induces matrix metalloproteinase-1 expression in cultured human gingival fibroblasts: role of cyclooxygenase-2 and prostaglandin E $_2$," *Oral Diseases*, vol. 10, no. 2, pp. 87–93, 2004.
- [64] S. Mateen, A. Zafar, S. Moin, A. Q. Khan, and S. Zubair, "Understanding the role of cytokines in the pathogenesis of rheumatoid arthritis," *Clinica Chimica Acta*, vol. 455, pp. 161–171, 2016.
- [65] P. Chomarat, E. Vannier, J. Dechanet et al., "Balance of IL-1 receptor antagonist/IL-1 beta in rheumatoid synovium and its regulation by IL-4 and IL-10," *Journal of Immunology (Baltimore, Md: 1950)*, vol. 154, no. 3, pp. 1432–1439, 1995.
- [66] J. M. Woods, K. J. Katschke, M. V. Volin et al., "IL-4 adenoviral gene therapy reduces inflammation, proinflammatory cytokines, vascularization, and bony destruction in rat adjuvant-induced arthritis," *The Journal of Immunology*, vol. 166, no. 2, pp. 1214–1222, 2001.
- [67] A. Finnegan, M. J. Grusby, C. D. Kaplan et al., "IL-4 and IL-12 regulate proteoglycan-induced arthritis through stat-dependent mechanisms," *The Journal of Immunology*, vol. 169, no. 6, pp. 3345–3352, 2002.
- [68] M. J. Hoogduijn, F. Popp, R. Verbeek et al., "The immunomodulatory properties of mesenchymal stem cells and their use for immunotherapy," *International Immunopharmacology*, vol. 10, no. 12, pp. 1496–1500, 2010.
- [69] S. Selleri, P. Bifsha, S. Civini et al., "Human mesenchymal stromal cell-secreted lactate induces M2-macrophage differentiation by metabolic reprogramming," *Oncotarget*, vol. 7, no. 21, pp. 30193–30210, 2016.
- [70] Q.-Z. Zhang, W.-R. Su, S.-H. Shi et al., "Human gingiva-derived mesenchymal stem cells elicit polarization of M2 macrophages and enhance cutaneous wound healing," *Stem Cells*, vol. 28, no. 10, pp. 1856–1868, 2010.

Research Article

Evaluation of Immunomodulatory and Antiarthritic Potential of *Trigonella gharuensis* Extracts

Aisha Mobashar,¹ Arham Shabbir ,² Muhammad Shahzad,³ and Saeed-ul-Hassan⁴

¹Faculty of Pharmacy, The University of Lahore, Lahore, Pakistan

²Institute of Pharmacy, Faculty of Pharmaceutical and Allied Health Sciences, Lahore College for Women University, Jail Road, Lahore, Pakistan

³Department of Pharmacology, University of Health Sciences, Lahore, Punjab, Pakistan

⁴Imran Idrees College of Pharmacy, 3 km Daska Road, Sialkot, Pakistan

Correspondence should be addressed to Arham Shabbir; charham007@hotmail.com

Received 17 August 2020; Revised 8 November 2020; Accepted 3 December 2020; Published 12 December 2020

Academic Editor: Shao-Hsuan Kao

Copyright © 2020 Aisha Mobashar et al. This is an open access article distributed under the Creative Commons Attribution License, which permits unrestricted use, distribution, and reproduction in any medium, provided the original work is properly cited.

The genus of *Trigonella* has long been used for the treatment of arthritis and inflammatory disorders. This study was aimed to investigate the immunomodulatory activities of ethanol and *n*-hexane extracts of *T. gharuensis* in the rat model of rheumatoid arthritis. Freund's complete adjuvant (FCA) model was used to induce arthritis in rats. Arthritis was induced on day 0, while treatment which was started on day 8 continued for twenty days. Arthritic development and paw edema were determined using an arthritic scoring index and plethysmometer, respectively. Histopathology was evaluated using H&E staining. RNA extraction, reverse transcription, and polymerase chain reaction (RT-PCR) were performed to determine expression levels of proinflammatory markers such as TNF- α , NF- κ B, IL-6, IL-1 β , COX2, and anti-inflammatory cytokine IL-4. Prostaglandin E2 level (PGE2) was evaluated using ELISA. Blood analysis and biochemical parameters were also determined. The significance level was set as $P < 0.05$. Treatment with extracts reduced paw edema, arthritic progression, and histopathological parameters. Expression levels of abovementioned proinflammatory cytokines and COX2 were downregulated, while IL-4 was upregulated. PGE2 levels were found reduced with extract treatment. Blood parameters were nearly normalized in treatment groups. Extract treatment did not alter biochemical parameters. Both extracts had effects comparable with piroxicam. In conclusion, extracts of *T. gharuensis* ameliorated experimentally induced arthritis that may be ascribed to its immunomodulatory effects.

1. Introduction

Rheumatoid arthritis (RA) is a chronic inflammatory and autoimmune disorder that presents with bone erosion, cartilage damage, and inflammation. Major symptoms include varying degrees of joint stiffness, pain, and swelling, while systemic symptoms include fever, fatigue, and weight loss [1].

Various cytokines and proinflammatory mediators are involved in the pathogenesis of RA. These cytokines are released by activated macrophages and fibroblasts. Tumor necrosis factor (TNF- α) stimulates IL-6 which is responsible for activation of chondrocytes and fibroblasts in articular cartilage. This leads to erosion of collagen and proteoglycans

resulting in joint destruction. IL-1 β in diseased synovial membrane is considered responsible for pannus formation and bone erosion. IL-6 stimulates production of nuclear factor kappaB (NF- κ B) which, in turn, activates osteoclasts, abnormal apoptosis, and proliferation of synovial cells [2]. Likewise, augmented levels of COX2 activate PGE2 production which leads to angiogenesis and articular cartilage destruction along with pain and inflammation [3].

Nonsteroidal anti-inflammatory drugs (NSAID) and opiates have been extensively used for the symptomatic treatment of arthritis [4]. Adverse effects of NSAIDs include gastric perforation and bleeding due to reduced prostaglandin production [5]. Continued use of opiates poses a serious risk of respiratory depression, dependence, and

tolerance [6]. Corticosteroids are associated with peptic ulcer, osteoporosis, precipitation of diabetes, and higher susceptibility to infections due to immunosuppressive properties [7]. Other drugs used to treat autoimmune disorders, such as DMARDs and cytokines antagonist, have been associated with increased susceptibility to infections seen in the patients [8].

Due to many adverse effects of synthetic drugs, modern research focuses on the use of medicinal plants for treatment of inflammation and arthritis due to their easy availability and lower cost value [9]. *Trigonella gharuensis* is an herb of worldwide distribution [10]. It belongs to the second largest family of flowering plants, i.e., fabaceae [11]. Our previous study has established anti-inflammatory properties of *T. gharuensis* using different paw edema models of acute inflammation such as carrageenan, histamine, serotonin-induced paw edema models, and xylene-induced ear edema model. Moreover, GCMS analysis in our study showed that both extracts possessed considerable constituents responsible for anti-inflammatory and antioxidant properties [12]. Our current study focuses on antiarthritic potential of *T. gharuensis* using FCA-induced chronic model of inflammation in arthritic rats.

2. Methodology

2.1. Plant Collection and Identification. *T. gharuensis* was collected from Quetta district of Balochistan. It was identified by Department of Botany, University of Balochistan (UOB), Quetta, Pakistan. The voucher specimen (TG-RBT-05) was kept in the herbarium of university [12].

2.2. Preparation of Extracts. Herb was dried under shade. It was then chopped followed by grinding. Maceration was done by soaking powder into ethanol and *n*-hexane, respectively. The mixtures were kept at 25°C. The mixtures were filtered and then concentrated at 37°C in a rotary evaporator (IKA Germany) under reduced pressure. After that, extracts were dried in an incubator at 40°C. The EETG (ethanolic extract of *T. gharuensis*) and NHTG (*n*-hexane extract of *T. gharuensis*) were dissolved in 1% Tween 80 before administration.

2.3. Test Animals. Sprague Dawley rats (6–8 weeks old) were placed in animal house of The University of Lahore, Lahore. They were acclimatized with environment for one week under controlled humidity conditions (60–70%) and temperature 25°C ± 2, respectively. Food and water access was freely provided. Light and dark cycles were maintained. Approval from the Institutional Research Ethics Committee, The University of Lahore (IREC-2017-23), was taken for the experiment.

2.4. Evaluation of Antiarthritic Activities. Thirty rats were distributed into 5 groups. Vehicle control (group 1) and arthritic control (group 2) were given vehicle, i.e., 1% Tween 80 in water [13]. EETG (group 3) and NHTG (group 4) were

given extracts (400 mg/kg b.w., p.o., each) [14]. Piroxicam was given (10 mg/kg b.w., i.p.,) to group 5. FCA (0.15 ml) was injected into left paws of all the animals (subplantar region) except vehicle control group at 0 day. Animals were treated with extracts, and piroxicam was started from day 8 till day 28. Treatment with EETG, NHTG, and piroxicam was commenced at day 8 and ended on day 28 [15].

2.5. Arthritic Score Measurement. Different parameters such as inflammation, redness, and erythema were observed on different day intervals of 8, 15, 22, and 28 using macroscopic criteria. Score 0 was given to normal, score 1 to minimal, score 2 to mild, score 3 to moderate, and score 4 to severe changes [16].

2.6. Paw Volume Assessment. Digital water displacement plethysmometer was used to measure paw edema of all groups at days 0, 8, 15, 22, and 28.

2.7. Histopathological Evaluation. On day 28, all rats were sacrificed. Ankle joints were cut longitudinally and placed in formalin (10%) for fixation. Formic acid was used for decalcification of samples. Tissues were cut into thin slices, and paraffin wax was used for embedding the tissues. H&E (hematoxylin and eosin) staining was used. The slides were examined by a blinded histopathologist for presence of pannus formation, bone erosion, and inflammation. Scoring criteria were followed as mentioned previously [15].

2.8. Determination of mRNA Expression Levels of TNF- α , NF- κ B, IL-6, IL-1 β , COX2, and IL-4. Conventional PCR was used to assess mRNA expression levels of cytokines involved in pathogenesis of RA. First, blood samples were taken for RNA extraction, and it was achieved using TRizol reagent according to protocol. The extracted RNA samples were quantified through a nanodrop spectrophotometer. cDNA was synthesized using kit manufacturer's protocol (Thermo Scientific, America). GAPDH was used as reference. Primers of TNF- α and GAPDH were designed manually. Sequence of primers such as IL-6, IL-1 β , NF- κ B, IL-4, and COX2 was selected from previously published studies [17–19], as mentioned in Table 1. cDNA (2 μ l) was mixed with forward-reverse primer mix (1 μ l), nuclease-free water (3 μ l), and PCR Master Mix (6 μ l). Thermal cycle was programmed for denaturation (95°C for 10 s), annealing (58°C and 60°C for 20 s), and extension (72°C for 30 s) cycles.

2.9. Determination PGE2 Levels. PGE2 levels were measured from serum using ELISA kit (Elab Science E-EL-0034 96T). Optical density was measured using ELISA reader (BioTek, ELx-800) 450 nm length.

2.10. Evaluation of Hematological Parameters. Blood samples were collected through intracardiac puncture. Automated hematology analyzer (Sysmex XT-1800i) was used to

TABLE 1: Primer sequences.

| Genes | Forward primer | Reverse primer | Product size | Reference |
|----------------|----------------------------|-----------------------------|--------------|-------------|
| IL-4 | 5'-CACCTTGCTGTACCCTGTT-3' | 5'-TCACCGAGAACCCAGACTT-3' | 231 | [18] |
| IL-6 | 5'-CCCACCAAGAACGATAGTCA-3' | 5'-CTCCGACTTGTGAAAGTGGTA-3' | 247 | [26] |
| TNF- α | 5'-AGTCCGGGCAGGTCTACTTT-3' | 5'-GGAAATCTGAGCCCGGAGT-3' | 202 | NM_012675.3 |
| NF- κ B | 5'-TGAGATCCATGCCATTGGCC-3' | 5'-AGCTGAGCATGAAGGTGGATG-3' | 207 | [18] |
| COX2 | 5'-CCAGATGGCCAGAGGACTCA-3' | 5'-TGTGAGTCCCAGGGGAATAGA-3' | 237 | [18] |
| IL-1 β | 5'-GCTGTCCAGATGAGAGCATC-3' | 5'-GTCAGACAGCACGAGGCATT-3' | 293 | [19] |
| GAPDH | 5'-GTCATCAACGGGAAACCCAT-3' | 5'-ATCACAACATGGGGGCATC-3' | 197 | NM_017008.4 |

evaluate hemoglobin content and levels of RBCs, WBCs, and platelets.

2.11. Biochemical Parameters. Serum was separated from blood. Different biochemical parameters such as urea, creatinine, aspartate aminotransferase (AST), alanine transaminase (ALT), and alkaline phosphatase (ALP) were analyzed by an automated chemistry analyzer (Humalyzer 3500) by following kit manufacturer's protocols (Analyticon Biotechnologies AG, Germany).

2.12. Statistical Analysis. All values were expressed as mean \pm SEM. Data were analyzed using Graph Pad Prism (v 6.0). One-way ANOVA followed by Tukey's post hoc test was used for comparison. Significance level was observed as $P < 0.05$.

3. Results

3.1. *T. gharuensis* Inhibited Arthritic Development. The arthritic progression was induced by using FCA, and it was measured through macroscopic criteria. The increased trend of arthritic development was continued in the diseased control group because no treatment was provided to this group. Table 2 shows that ($P < 0.001$) arthritic score was reduced at days 15, 22, and 28, respectively, with extract treatment as compared to the positive control group. The piroxicam also significantly reduced ($P < 0.001$) arthritic score at different day intervals which is comparable to EETG and NHTG groups.

3.2. *T. gharuensis* Prevented Paw Edema. Remarkable edema was observed in the FCA-induced model, and it was measured through digital water plethysmometer on different day intervals such as 15, 22, and 28. The values of vehicle control group were considered zero because there was no induction of disease in this group. Table 3 shows increased trend in inflammation, and score was continued until the 28th day of this experimental study in the positive control group. EETG, NHTG, and piroxicam treatment significantly ($P < 0.001$) reduced paw edema when compared with the arthritic control group. The results of extracts treatment were comparable to the piroxicam group.

3.3. *T. gharuensis* Significantly Reduced Histopathological Parameters. EETG, NHTG, and piroxicam showed significant inhibition of inflammation, bone erosion, and pannus

formation in comparison to the arthritic control group (Table 4). H&E staining picture revealed that aggregates of inflammatory cells presented in the arthritic control group were markedly reduced in piroxicam- and extract-treated groups.

3.4. *T. gharuensis* Downregulated Proinflammatory and Upregulated Anti-Inflammatory Cytokines. The collected blood sample on the 28th day was processed for mRNA expression levels. Table 5 shows that significant levels of proinflammatory markers such as TNF- α , IL-6, IL-1 β , NF- κ B, and COX2 were increased in the positive control group. The augmented levels of these cytokines were markedly reduced ($P < 0.001$) in EETG and NHTG extract- and piroxicam-treated groups in comparison to the positive control group. Levels of anti-inflammatory cytokines such as IL-4 decreased in the positive control group. IL-4 levels were increased in extract- and piroxicam-treated group in contrast to the positive control group.

3.5. *T. gharuensis* Significantly Reduced PGE2 Levels. Increased ($P < 0.001$) serum PGE2 levels were noticed in the arthritic control group as compared to the vehicle control group. Significant reduction ($P < 0.001$) in PGE2 levels was observed in piroxicam-, EETG-, and NHTG-treated groups, as presented in Figure 1.

3.6. *T. gharuensis* Modulated Hematological Parameters. The reduction in hematological parameters, such as RBC and Hb levels, were seen in the positive control group. These parameters were nearly normalized in treatment groups as compared to the positive control group. Similarly, elevated WBC and platelets levels were observed in the arthritic control groups which were nearly normalized after treatment with extracts and the reference drug in contrast to the positive control group (Table 6).

3.7. *T. gharuensis* Nearly Normalized Biochemical Parameters. The serum was separated from the blood sample, and different hepatic markers such as ALT and AST along with renal parameters such as urea and creatinine were measured through commercially available kits. Table 7 shows that *T. gharuensis* extracts and piroxicam did not alter liver and renal parameters. Statistically nonsignificant differences were found in AST, ALT, urea, and creatinine levels when groups were compared with each other.

TABLE 2: *T. gharuensis* extracts attenuated arthritic development.

| Days | Vehicle control | Arthritic control | Piroxicam | EETG | NHTG |
|--------|-----------------|-------------------|------------------|------------------|------------------|
| Day 8 | 0.000 ± 0.000 | 2.999 ± 0.073 | 3.003 ± 0.073 | 3.083 ± 0.083 | 3.083 ± 0.083 |
| Day 15 | 0.000 ± 0.000 | 3.389 ± 0.073 | 2.245 ± 0.110*** | 2.833 ± 0.105*** | 2.833 ± 0.106** |
| Day 22 | 0.000 ± 0.000 | 3.499 ± 0.122 | 2.495 ± 0.172*** | 2.667 ± 0.105** | 2.917 ± 0.153* |
| Day 28 | 0.000 ± 0.000 | 3.489 ± 0.149 | 2.093 ± 0.073*** | 2.533 ± 0.105*** | 2.500 ± 0.129*** |

EETG, ethanolic extract of *T. gharuensis* (400 mg/kg); NHTG, *n*-hexane extract of *T. gharuensis* (400 mg/kg); piroxicam (10 mg/kg). Values were denoted as mean ± SEM. * $P < 0.05$, ** $P < 0.01$ and *** $P < 0.001$ when compared with the arthritic group.

TABLE 3: *T. gharuensis* extracts significantly reduced paw edema in arthritic rats.

| Days | Vehicle control | Arthritic control (ml) | Piroxicam (ml) | EETG (ml) | NHTG (ml) |
|--------|-----------------|------------------------|------------------|------------------|------------------|
| Day 8 | 0.000 ± 0.000 | 0.938 ± 0.012 | 0.953 ± 0.012 | 0.937 ± 0.008 | 0.932 ± 0.014 |
| Day 15 | 0.000 ± 0.000 | 1.138 ± 0.015 | 0.773 ± 0.007*** | 0.770 ± 0.013*** | 0.863 ± 0.006*** |
| Day 22 | 0.000 ± 0.000 | 1.232 ± 0.010 | 0.699 ± 0.006*** | 0.737 ± 0.009*** | 0.727 ± 0.010*** |
| Day 28 | 0.000 ± 0.000 | 1.372 ± 0.008 | 0.622 ± 0.007*** | 0.630 ± 0.007*** | 0.670 ± 0.017*** |

Value of normal paw is considered as zero. EETG, ethanolic extract of *T. gharuensis*; NHTG, *n*-hexane extract of *T. gharuensis* (400 mg/kg); piroxicam (10 mg/kg). Values were denoted as mean ± SEM. *** $P < 0.001$ when compared with the arthritic control group.

TABLE 4: *T. gharuensis* attenuated histopathological parameters.

| Parameters | Vehicle control | Arthritic control | Piroxicam | EETG | NHTG |
|------------------------------------|-----------------|-------------------|------------------|------------------|------------------|
| Infiltration of inflammatory cells | 0.000 ± 0.000 | 2.573 ± 0.073 | 1.566 ± 0.073*** | 1.917 ± 0.154*** | 2.083 ± 0.083* |
| Pannus formation | 0.000 ± 0.000 | 3.405 ± 0.073 | 2.522 ± 0.103*** | 2.583 ± 0.083*** | 2.583 ± 0.083*** |
| Bone erosion | 0.000 ± 0.000 | 2.543 ± 0.073 | 2.073 ± 0.073** | 2.083 ± 0.083** | 2.167 ± 0.105* |

Value of normal paw is considered as zero. EETG, ethanolic extract of *T. gharuensis* (400 mg/kg); NHTG, *n*-hexane extract of *T. gharuensis* (400 mg/kg); piroxicam (10 mg/kg). Values were denoted as mean ± SEM. ** $P < 0.01$ and *** $P < 0.001$ when compared with the arthritic control group.

TABLE 5: *T. gharuensis* downregulated proinflammatory and upregulated anti-inflammatory cytokines.

| Markers | Vehicle control | Arthritic control | Piroxicam | EETG | NHTG |
|----------------|-----------------|-------------------|------------------|------------------|------------------|
| TNF- α | 32.40 ± 1.777 | 49.97 ± 1.967### | 33.72 ± 1.033*** | 34.29 ± 1.538*** | 35.38 ± 0.571*** |
| NF- κ B | 33.01 ± 1.538 | 52.59 ± 0.679### | 34.82 ± 1.226*** | 39.08 ± 1.365*** | 41.25 ± 0.690*** |
| IL-6 | 32.65 ± 1.741 | 39.61 ± 1.178## | 31.99 ± 1.033** | 33.86 ± 0.850** | 33.61 ± 1.195** |
| IL-1 β | 33.09 ± 1.462 | 51.79 ± 1.439### | 31.99 ± 1.226** | 34.46 ± 1.239** | 35.83 ± 0.649*** |
| COX2 | 33.89 ± 1.699 | 55.96 ± 1.300### | 34.07 ± 0.878*** | 31.06 ± 0.791*** | 34.73 ± 0.499*** |
| IL-4 | 33.95 ± 1.001 | 22.49 ± 0.505### | 29.72 ± 0.724*** | 31.82 ± 0.551*** | 33.16 ± 0.427*** |

EETG, ethanolic extract of *T. gharuensis* (400 mg/kg); NHTG, *n*-hexane extract of *T. gharuensis* (400 mg/kg); piroxicam (10 mg/kg). Values were denoted as mean ± SEM. * $P < 0.05$, ** $P < 0.01$ and *** $P < 0.001$ when compared with the arthritic control group. ## $P < 0.01$ and ### $P < 0.001$.

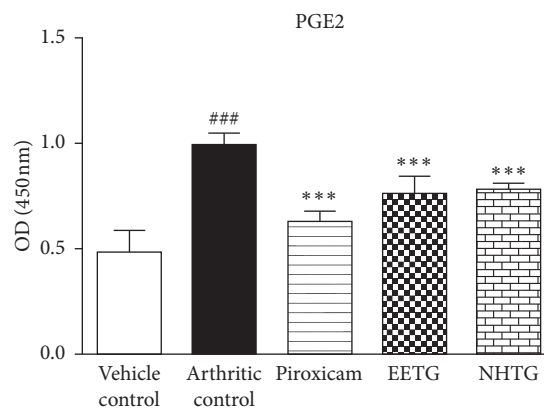


FIGURE 1: EETG, NHTG (400 mg/kg, each), and piroxicam (10 mg/kg) significantly reduced PGE2 levels as compared to the control group. *** P indicates < 0.001 as compared to the arthritic group while ### presents comparison between control and arthritic groups.

TABLE 6: *T. gharuensis* nearly normalized hematological parameters.

| Parameters | Control | Arthritic control | Piroxicam | EETG | NHTG |
|--------------------|----------------|-------------------|------------------|------------------|-----------------|
| RBC (106/Ul) | 8.293 ± 0.310 | 5.650 ± 0.365### | 8.399 ± 0.332** | 7.360 ± 0.365** | 7.337 ± 0.304** |
| Hb (g/dl) | 13.999 ± 0.129 | 11.93 ± 0.241### | 12.58 ± 0.207** | 14.02 ± 0.425*** | 13.67 ± 0.353** |
| WBC (103/Ul) | 10.13 ± 0.325 | 15.19 ± 0.246### | 11.99 ± 0.225*** | 12.88 ± 0.209*** | 13.25 ± 0.324** |
| Platelets (103/Ul) | 782.7 ± 26.82 | 1434 ± 17.24### | 1018 ± 31.31*** | 910.8 ± 15.84*** | 1099 ± 34.13*** |

EETG, ethanolic extract of *T. gharuensis* (400 mg/kg); NHTG, *n*-hexane extract of *T. gharuensis* (400 mg/kg); piroxicam (10 mg/kg). Values were denoted as mean ± SEM. ** $P < 0.01$ and *** $P < 0.001$ when compared with the arthritic control group. ###Difference between vehicle control group and positive control group.

TABLE 7: Evaluation of biochemical parameters.

| Biochemical parameters | Vehicle control | Arthritic control | Piroxicam | EETG | NHTG |
|------------------------|-----------------|-------------------|---------------|---------------|---------------|
| Urea (mg/dl) | 27.01 ± 0.609 | 27.10 ± 0.846 | 25.98 ± 0.391 | 27.67 ± 0.421 | 26.17 ± 0.477 |
| Creatinine (mg/dl) | 0.829 ± 0.200 | 0.835 ± 0.014 | 0.839 ± 0.030 | 0.866 ± 0.021 | 0.858 ± 0.020 |
| AST (IU/L) | 95.99 ± 1.712 | 97.88 ± 1.510 | 93.99 ± 1.182 | 98 ± 0.617 | 96.71 ± 1.34 |
| ALT (IU/L) | 30.29 ± 0.549 | 31.63 ± 0.470 | 33.69 ± 0.321 | 33.17 ± 0.654 | 33.17 ± 0.792 |

Value of normal paw is considered as zero. EETG, ethanolic extract of *T. gharuensis* (400 mg/kg); NHTG, *n*-hexane extract of *T. gharuensis* (400 mg/kg); piroxicam (10 mg/kg). Values were denoted as mean ± SEM.

4. Discussion

Medicinal plants have proved to be safer and cheaper in comparison to synthetic medicines for the treatment of arthritis. Rheumatoid arthritis is characterized by bone damage, deformity, hyperplasia, pannus formation, and inflammation in the joints [20, 21]. The preferred model used for this study is FCA-induced model due to its similarities with arthritic disorder seen in human. Ethanolic and *n*-hexane extracts of *T. gharuensis* extracts are shown to reduce paw edema and arthritic progression. These results are further supported by the histopathological investigations which showed clear amelioration of hallmarks of RA.

After FCA immunization, different cytokines are released by activated macrophages and monocytes which, in turn, release various cytokines such as TNF- α , IL-6, and IL-1 β . These cytokines aggravate inflammation, bone erosion, and cartilage destruction in joint tissues [22]. These cytokines also stimulate NF- κ B, a transcriptional factor, which promotes bone resorption by activating osteoclasts and proliferation of synovial cells in joints. This factor also worsens the symptoms of RA by favoring Th1 response [17]. Hence, NF- κ B inhibitors might be useful therapeutically and efficacious in ameliorating symptoms of RA. Our study shows marked decreased in the levels of TNF- α , IL-6, NF- κ B, and IL-1 β in extract-treated groups in comparison to the arthritic group.

The COX2 and prostaglandins are crucial mediators which are involved in pain and swelling. TNF- α and IL-1 β increase levels of COX2 and PGE2 in activated synovial cells. COX2 also activates process of bone erosion in juxta-articular cartilage. The extracts in current study reduced the levels of COX2 and PGE2 which might be responsible for the amelioration of inflammation and cartilage damage found in the study.

Immunomodulatory potential of *T. gharuensis* is further validated by augmented levels of IL-4 in EETG-,

NHTG-, and piroxicam-treated groups in contrast to the arthritic group. One of the reasons for the development of RA is imbalance between the levels of proinflammatory and anti-inflammatory cytokines. Elevation in the levels of proinflammatory cytokines or reduction in the levels of anti-inflammatory cytokines might lead to imbalance and result in development of RA. IL-4 mediates an anti-inflammatory response in RA. IL-4 inhibits Th1 response and favors Th2 immunomodulatory cells. Therapy with recombinant IL-4 has proved to inhibit cytokine production [17, 23]. This study showed significant elevation in the expression levels of IL-4 in extract-treated groups, probably in an attempt to ameliorate Th1 response.

Arthritic patients were found to have altered hematological picture with increased levels of WBCs and platelets, while reduced RBC count and Hb levels. The anemia may be attributed to inadequate erythropoiesis by the bone marrow and disorganized deposition of iron in synovial tissue and reticuloendothelial system [24, 25]. Increased WBC and platelet counts may be ascribed to overactive immune response. Treatment with *T. gharuensis* extracts led to normalisation of these values in the blood picture. In order to determine the safety of the plant extracts, biochemical parameters such as AST, ALT, urea, and creatinine were measured. The increased levels of these markers are indicative of liver injury and kidney dysfunction, respectively. The results showed no significant differences among all the groups which deemed that extracts were safe to use. The inferences of current study are in line with the study of Shabbir et al. [18].

Previously, we published the identification of phytochemical constituents in both plant extracts using GCMS analysis. The data showed the presence of different anti-inflammatory compounds in the extracts, e.g., ethylpalmitate, phytol, *n*-hexadecanoic acid, ethyl linoleate, nanocosane, and coumarin. Presence of these constituents might be responsible for anti-inflammatory activities of both the extracts [12].

5. Conclusion

Amelioration of joint inflammation confirmed that *T. gharuensis* extracts possessed significant immunomodulatory and antiarthritic potential in the FCA-induced arthritic rat model. *T. gharuensis* extracts significantly reduced paw edema, arthritic progression, and histopathological parameters. The attenuation of RA might be ascribed to downregulation of proinflammatory markers such as TNF- α , IL-1 β , IL-6, NF- κ B, and COX2 and upregulation of anti-inflammatory IL-4. Moreover, PGE2 levels were also found reduced after treatment with plant extracts.

Data Availability

Data used to support the findings of this study are available on request.

Conflicts of Interest

The authors declare that there are no conflicts of interest.

Acknowledgments

The authors wish to thank Department of Pharmacology and Department of Immunology, University of Health Sciences, Lahore, for providing necessary facilities to conduct experiments. The research was partially supported by Higher Education Commission of Pakistan under international research support initiative program awarded to Ms. Aisha Mobashar.

References

- [1] G. Akhtar and A. Shabbir, "Urginea indica attenuated rheumatoid arthritis and inflammatory paw edema in diverse animal models of acute and chronic inflammation," *Journal of Ethnopharmacology*, vol. 238, Article ID 111864, 2019.
- [2] E. Brzustewicz and E. Bryl, "The role of cytokines in the pathogenesis of rheumatoid arthritis—practical and potential application of cytokines as biomarkers and targets of personalized therapy," *Cytokine*, vol. 76, no. 2, pp. 527–536, 2015.
- [3] A. Saleem, M. Saleem, M. F. Akhtar, M. Shahzad, and S. Jahan, "Polystichum braunii extracts inhibit Complete Freund's adjuvant-induced arthritis via upregulation of I- κ B, IL-4, and IL-10, downregulation of COX-2, PGE2, IL-1 β , IL-6, NF- κ B, and TNF- α , and subsiding oxidative stress," *Inflammopharmacology*, vol. 28, no. 6, pp. 1633–1648, 2020.
- [4] C. Sostres, C. J. Gargallo, M. T. Arroyo, and A. Lanás, "Adverse effects of non-steroidal anti-inflammatory drugs (NSAIDs, aspirin and coxibs) on upper gastrointestinal tract," *Best Practice & Research Clinical Gastroenterology*, vol. 24, no. 2, pp. 121–132, 2010.
- [5] J. M. Scheiman, "NSAID-induced gastrointestinal injury," *Journal of Clinical Gastroenterology*, vol. 50, no. 1, pp. 5–10, 2016.
- [6] R. Costello, T. David, and M. Jani, "Impact of adverse events associated with medications in the treatment and prevention of rheumatoid arthritis," *Clinical Therapeutics*, vol. 41, no. 7, pp. 1376–1396, 2019.
- [7] M. Oray, K. Abu Samra, N. Ebrahimiadib, H. Meese, and C. S. Foster, "Long-term side effects of glucocorticoids," *Expert Opinion on Drug Safety*, vol. 15, no. 4, pp. 457–465, 2016.
- [8] O. Benjamin, P. Bansal, A. Goyal, and S. L. Lappin, *Disease Modifying Anti-rheumatic Drugs (DMARD)*, StatPearls [Internet]: StatPearls Publishing, Treasure Island, FL, USA, 2020.
- [9] F. Jamshidi-Kia, Z. Lorigooini, and H. Amini-Khoei, "Medicinal plants: past history and future perspective," *Journal of Hermed Pharmacology*, vol. 7, no. 1, 2018.
- [10] E. Martin, H. Akan, M. Ekici, and Z. Aytac, "New chromosome numbers in the genus *Trigonella* L. (Fabaceae) from Turkey," *African Journal of Biotechnology*, vol. 10, no. 2, pp. 116–125, 2011.
- [11] M. Ranjbar, Z. Hajmoradi, and R. Karamian, "Cytogenetic study and pollen viability of four populations of *Trigonella spruneriana* Boiss. (Fabaceae) in Iran," *Journal of Cell and Molecular Research*, vol. 3, no. 1, pp. 19–24, 2011.
- [12] A. Mobashar, A. Shabbir, and S. Hassan, "Anti-inflammatory effects of *Trigonella gharuensis*: comparative analysis in BALB/C mouse model," *Pakistan Journal of Pharmaceutical Sciences*, vol. 32, no. 5 (Supplementary), pp. 2287–2293, 2019.
- [13] N. Sridhar, D. Lakshmi, and P. Goverdhan, "Effect of ethanolic extracts of *Justicia neesii* Ramam. against experimental models of pain and pyrexia," *Indian Journal of Pharmacology*, vol. 47, no. 2, pp. 177–180, 2015.
- [14] P. Suresh, C. N. Kavitha, S. M. Babu, V. P. Reddy, and A. K. Latha, "Effect of ethanol extract of *Trigonella foenum graecum* (fenugreek) seeds on Freund's adjuvant-induced arthritis in albino rats," *Inflammation*, vol. 35, no. 4, pp. 1314–1321, 2012.
- [15] A. Shabbir, S. A. Batool, M. I. Basheer et al., "Ziziphora clinopodioides ameliorated rheumatoid arthritis and inflammatory paw edema in different models of acute and chronic inflammation," *Biomedicine & Pharmacotherapy*, vol. 97, pp. 1710–1721, 2018.
- [16] M. Uroos, Z. Abbas, S. Sattar, N. Umer, A. Shabbir, and A. Sharif, "Nyctanthes arbor-tristis ameliorated FCA-induced experimental arthritis: a comparative study among different extracts," *Evidence-Based Complementary and Alternative Medicine*, vol. 2017, Article ID 4634853, 2017.
- [17] A. Shabbir, M. Shahzad, A. Ali, and M. Zia-ur-Rehman, "Anti-arthritis activity of N'-[(2,4-dihydroxyphenyl)methylidene]-2-(3,4-dimethyl-5,5-dioxidopyrazolo [4,3-c][1,2]benzothiazin-1(4H)-yl)acetohydrazide," *European Journal of Pharmacology*, vol. 738, pp. 263–272, 2014.
- [18] A. Shabbir, M. Shahzad, A. Ali, and M. Zia-ur-Rehman, "Discovery of new benzothiazine derivative as modulator of pro- and anti-inflammatory cytokines in rheumatoid arthritis," *Inflammation*, vol. 39, no. 6, pp. 1918–1929, 2016.
- [19] A. M. Uttra, M. Alamgeer, M. Shahzad, A. Shabbir, and S. Jahan, "Ephedra gerardiana aqueous ethanolic extract and fractions attenuate Freund complete adjuvant induced arthritis in sprague dawley rats by downregulating PGE2, COX2, IL-1 β , IL-6, TNF- α , NF- κ B and upregulating IL-4 and IL-10," *Journal of Ethnopharmacology*, vol. 224, pp. 482–496, 2018.
- [20] Y.-Y. Xing, J.-Y. Wang, K. Wang et al., "Inhibition of rheumatoid arthritis using bark, leaf, and male flower extracts of *eucommia ulmoides*," *Evidence-Based Complementary and Alternative Medicine*, vol. 2020, Article ID 3260278, 2020.
- [21] M. Ghoryani, Z. Shariati-Sarabi, J. Tavakkol-Afshari, A. Ghasemi, J. Poursamimi, and M. Mohammadi, "Amelioration of clinical symptoms of patients with refractory rheumatoid arthritis following treatment with autologous bone marrow-derived mesenchymal stem cells: a successful

- clinical trial in Iran,” *Biomedicine & Pharmacotherapy*, vol. 109, pp. 1834–1840, 2019.
- [22] C. Das, A. Bose, and D. Das, “Ayurvedic Balarista ameliorate anti-arthritic activity in adjuvant induced arthritic rats by inhibiting pro-inflammatory cytokines and oxidative stress,” *Journal of Traditional and Complementary Medicine*, 2020.
- [23] H. Aslam, M. Shahzad, A. Shabbir, and S. Irshad, “Immunomodulatory effect of thymoquinone on atopic dermatitis,” *Molecular Immunology*, vol. 101, pp. 276–283, 2018.
- [24] A. Avau, T. Mitera, S. Put et al., “Systemic juvenile idiopathic arthritis-like syndrome in mice following stimulation of the immune system with freund’s complete adjuvant: regulation by interferon- γ ,” *Arthritis & Rheumatology*, vol. 66, no. 5, pp. 1340–1351, 2014.
- [25] S.-N. J. Song, M. Iwahashi, N. Tomosugi et al., “Comparative evaluation of the effects of treatment with tocilizumab and TNF- α inhibitors on serum hepcidin, anemia response and disease activity in rheumatoid arthritis patients,” *Arthritis Research & Therapy*, vol. 15, no. 5, p. R141, 2013.
- [26] R. S. Aziz, A. Siddiqua, M. Shahzad, A. Shabbir, and N. Naseem, “Oxyresveratrol ameliorates ethanol-induced gastric ulcer via downregulation of IL-6, TNF- α , NF- κ B, and COX-2 levels, and upregulation of TFF-2 levels,” *Biomedicine & Pharmacotherapy*, vol. 110, pp. 554–560, 2019.

Research Article

Clinical Efficacy and Safety of Thai Herbal Formulation-6 in the Treatment of Symptomatic Osteoarthritis of the Knee: A Randomized-Controlled Trial

Nut Koonrungsesomboon ^{1,2}, Saowaros Nopnithipat,¹ Supanimit Teekachunhatean,^{1,3} Natthakarn Chiranthanut,^{1,3} Chaichan Sangdee,¹ Sunee Chansakaow,⁴ Pramote Tipduangta,⁴ and Nutthiya Hanprasertpong ¹

¹Department of Pharmacology, Faculty of Medicine, Chiang Mai University, Chiang Mai 50200, Thailand

²Musculoskeletal Science and Translational Research Center, Chiang Mai University, Chiang Mai 50200, Thailand

³Center of Thai Traditional and Complementary Medicine, Faculty of Medicine, Chiang Mai University, Chiang Mai 50200, Thailand

⁴Department of Pharmaceutical Sciences and Medicinal Plant Innovation Center, Faculty of Pharmacy, Chiang Mai University, Chiang Mai 50200, Thailand

Correspondence should be addressed to Nutthiya Hanprasertpong; nutthiya.h@cmu.ac.th

Received 3 September 2020; Revised 24 October 2020; Accepted 3 November 2020; Published 9 December 2020

Academic Editor: Arham Shabbir

Copyright © 2020 Nut Koonrungsesomboon et al. This is an open access article distributed under the Creative Commons Attribution License, which permits unrestricted use, distribution, and reproduction in any medium, provided the original work is properly cited.

Background. Osteoarthritis of the knee is the most common form of arthritis. Identifying effective and safe herbal formulations that are locally available is viewed as a priority for sustainable development in a region. This study aimed to evaluate the efficacy and safety of Thai herbal formulation-6 (THF-6) in comparison with oral diclofenac in patients with moderate-to-severe osteoarthritis of the knee. **Methods.** This randomized, double-blind, active-controlled, noninferiority trial randomly assigned patients with osteoarthritis of the knee to receive either THF-6 or diclofenac for four weeks. The primary outcome measure was the change from baseline in knee pain as measured by a 100 mm visual analog scale (VAS). Secondary outcome measures included knee stiffness, a stair climb test, the Knee Injury and Osteoarthritis Outcome Score, and safety parameters. Outcomes were assessed on a biweekly basis. Modified intention-to-treat (MITT) and perprotocol (PP) analyses were applied. **Results.** A total of 200 patients were enrolled of whom 175 (87.5%) were included in the MITT analysis and 153 (76.5%) in the PP analysis. The mean change in VAS pain did not differ between the two groups, and the upper limit of the two-sided 95% confidence interval (CI) for comparison between the two groups was within the prespecified margin of 10 mm for noninferiority (MITT analysis: mean difference = 0.86, 95% CI = -4.39 to 6.10, $p = 0.748$; PP analysis: mean difference = 1.98, 95% CI = -3.61 to 7.56, $p = 0.486$). Significant improvement was observed in all the efficacy parameters in both groups. Dyspepsia was the most common adverse event: 23 patients in the THF-6 group and 28 in the diclofenac group ($p = 0.417$). **Conclusions.** THF-6 offers an alternative to oral diclofenac for the short-term treatment of osteoarthritis of the knee. It was shown to be noninferior to oral diclofenac in relieving knee pain. This trial is registered with ChiCTR-IPR-15007213.

1. Introduction

Osteoarthritis is the most common form of arthritis, commonly affecting knee joints and causing pain, functional disability, and reduced quality of life [1, 2]. Osteoarthritis of the knee is one of the leading causes of global disability

among older adults [3]. The burden of disease on the healthcare system, in addition to its impacts on individual patients, has been increasing worldwide over the past three decades [4, 5]. Nearly half of the population may develop symptomatic osteoarthritis of the knee by age 85, and the lifetime risk is doubled among obese individuals [6]. With

increasing life expectancy, osteoarthritis of the knee is anticipated to cause even more economic challenges in the future that every country and international community needs to grapple with [7].

Nonsteroidal anti-inflammatory drugs (NSAIDs) are one of the most widely used medications for the management of knee pain in patients with osteoarthritis of the knee [8]. The efficacy of oral NSAIDs, diclofenac in particular, for symptomatic relief of knee osteoarthritis has been well established in the literature [9]. Thanks to their good analgesic and antiphlogistic effects, NSAIDs are recommended by several international and national guidelines as the initial oral medication of choice in the treatment of symptomatic osteoarthritis of the knee with moderate-to-severe pain intensity [10, 11]. Several NSAIDs, including oral diclofenac, are available as over-the-counter medications in many countries, so the use of this drug is particularly widespread [12, 13].

Given the large number of people affected with osteoarthritis of the knee and societal trends in population aging and obesity [14], identifying effective and safe therapeutic options that are available in a region is viewed as a priority for sustainable development in a country [15]. In this regard, herbal medicine could be a promising approach to be employed in developing such therapeutic options [16]. Several herbal extracts and formulations have been discovered and proven that they can bring about therapeutic benefits in terms of pain and mobility in patients with osteoarthritis of the knee [17–19]. In Thailand, the Thai herbal formulation-6 (THF-6) comprising six herbal materials, all of which are locally available in Thailand, has traditionally been used to augment longevity as well as for the treatment of muscle and joint pain [20–22]. Although anecdotal evidence exists supporting the efficacy and tolerability of THF-6 in the treatment of osteoarthritis of the knee [22], scientific proof of its benefits is required to verify its therapeutic potential.

The present study was designed to clinically assess the efficacy and safety of THF-6 in comparison with the standard drug, oral diclofenac, for the treatment of moderate-to-severe osteoarthritis of the knee.

2. Methods

2.1. Trial Design and Setting. This prospective, randomized, double-blind, double-dummy, and active-controlled trial was conducted at the Faculty of Medicine, Chiang Mai University, Thailand. The trial followed the OARSI Clinical Trials recommendations for the design, conduct, and reporting of clinical trials for osteoarthritis of the knee [23]. It was prospectively registered with the Chinese Clinical Trials Registry (ChiCTR-IPR-15007213). The clinical trial protocol and related documents were approved by the Research Ethics Committee of the Faculty of Medicine, Chiang Mai University (EC273/2015). The full-trial protocol (in Thai) is available from the corresponding author upon reasonable request. Written informed consent was obtained from all patients prior to their participation in the trial.

2.2. Trial Participants. Eligible patients were 45 years of age or older with osteoarthritis in one or both knees for more than three months. The disease was diagnosed according to the American College of Rheumatology criteria [24] with radiographic confirmation (Kellgren–Lawrence grade 2 or higher). Patients were eligible for inclusion if they had osteoarthritic knee pain of at least moderate intensity (defined as a pain score of ≥ 35 mm at baseline on a 100 mm visual analog scale (VAS)) [25]. Patients were excluded if they also had any other underlying arthritis (e.g., rheumatoid arthritis or gouty arthritis), signs or symptoms of active inflammation at the knee, a condition requiring knee surgery in the next few months, or a recent knee injury; had used intra-articular corticosteroid injections in the previous six weeks; had used symptomatic slow-acting drugs for osteoarthritis (e.g., glucosamine sulfate or chondroitin sulfate) within the previous four months or had discontinued those drugs for less than six months; had a history of an allergic reaction to oral NSAIDs or herbal ingredients in THF-6; or had a history of gastrointestinal ulcer, perforation, or hemorrhage. Other exclusion criteria were pregnancy or lactation and any clinically significant abnormalities of blood chemistry (including serum uric acid of >9 mg/dL) or other hematological parameters.

2.3. Sample Size Determination. With 69 patients per group, the trial was estimated to have 90% power at a two-sided alpha level of 0.05 based on a noninferiority margin of 10 [26, 27] and assuming a mean difference (MD) of 0 and a standard deviation (SD) of 20 [28]. Anticipating a 30% premature discontinuation or poor compliance, a total of 200 patients (100 per group) were planned to be enrolled in this trial.

2.4. Trial Interventions. The THF-6 (given at the dose of 1,500 mg/day) consisted of six herbs: fruit of *Streblus asper* Lour, stems of *Tinospora cordifolia* (Willd.) Miers, corms of *Cyperus rotundus*, bark of *Albizia procera* (Roxb.) Benth, bark of *Diospyros rhodocalyx* Kurz, and fruit of *Piper nigrum* Linn [21]. The components and preparation of THF-6 are summarized in Table S1. The THF-6 capsules (250 mg/capsule) were manufactured by the Department of Pharmaceutical Sciences and Medicinal Plant Innovation Center, Faculty of Pharmacy, Chiang Mai University, in compliance with the Thai Pharmacopoeia standards and requirements. High-performance liquid chromatography and thin-layer chromatography were used for quality control of THF-6.

Diclofenac (Voltaren[®]) (25 mg/tablet) was purchased from Olic Thailand limited and used as an active control in this trial. Placebo tablets of THF-6 and diclofenac were manufactured by the Department of Pharmaceutical Sciences and Medicinal Plant Innovation Center, Faculty of Pharmacy, Chiang Mai University.

2.5. Trial Procedures and Outcome Assessments. The trial consisted of a one-week run-in phase followed by a four-week treatment phase (Figure 1). During the one-week run-

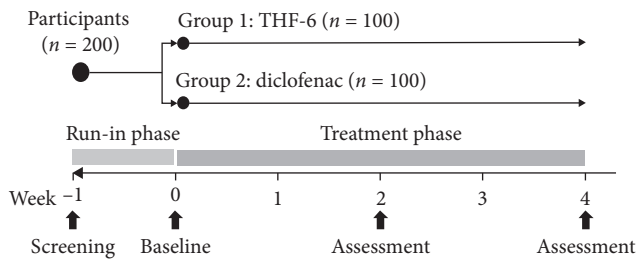


FIGURE 1: Study design.

in period, eligible patients were instructed to discontinue all pain relief medications (including NSAIDs and other analgesics). At the beginning of the treatment phase, eligible patients with at least moderate pain intensity were randomly assigned in a 1:1 ratio to receive either THF-6 (1,500 mg/day) or diclofenac (75 mg/day) (Figure 1). The treatment group assignment was based on a randomization list prepared in advance by independent research staff with the use of a computer-based random number generator. Sequentially numbered, opaque envelopes containing the list were employed to safeguard allocation concealment. The envelopes were opened only after each patient had met the eligibility criteria at the end of the run-in phase. Both patients and outcome assessors were blinded to the treatment allocation.

In the THF-6 group, patients took two capsules of THF-6 (250 mg/capsule) and one placebo diclofenac tablet three times a day after meals. In the diclofenac group, patients took two placebo THF-6 capsules and one diclofenac tablet (25 mg/tablet) three times a day after meals. Enrolled patients were instructed to avoid other analgesics, anti-inflammatory drugs (including other NSAIDs), and other treatment modalities (e.g., acupuncture) while participating in the trial. Omeprazole tablets (20 mg/tablet) were prepared as rescue therapy in case of adverse gastrointestinal consequences following the administration of the study drugs. Patients were prematurely withdrawn from the trial if they developed intolerable knee pain necessitating other medications or treatment modalities, used other analgesics or anti-inflammatory drugs, had severe adverse drug reactions or allergic reactions to the study drugs, or were lost to follow-up.

This trial assessed efficacy outcomes for pain, function, and global assessment according to the recommendations of a core domain set for outcome measurement in clinical trials of knee osteoarthritis [29, 30]. Outcome assessment was performed on a biweekly basis, that is, at the end of the one-week run-in phase (baseline) and at the end of Week 2 and Week 4 (Figure 1).

The primary efficacy metric was the change from baseline in knee pain as measured by a horizontal 100 mm VAS (rated on a scale of 0 to 100, with higher scores indicating worse knee pain) [31]. The secondary efficacy outcomes included VAS stiffness (rated on a scale of 0 to 100, with higher scores indicating more severe stiffness), a 10-step stair climb test (SCT) (time in seconds to ascend and descend a flight of 10 steps) [32], the Knee Injury and

Osteoarthritis Outcome Score (KOOS) (which included 42 items across five domains; each item was rated on a 5-point Likert scale and transformed to a scale of 0 to 100, with higher scores indicating fewer knee problems) [33, 34], and the patient's and the physician's opinions of overall improvement on a 100 mm VAS (rated on a scale of 0 to 100, with higher scores indicating better improvement). In patients with bilateral osteoarthritis of the knee, efficacy outcomes were assessed only for the knee with worse symptoms at baseline.

Adverse events observed by the investigators or reported by the patients following a nondirective question were recorded. Drug compliance was assessed by counting returned unused medications at each visit. Any patient taking less than 70% of the allocated dose of study drugs was regarded as noncompliant.

2.6. Statistical Analysis. Analyses of efficacy outcomes were conducted using the perprotocol (PP) and the modified intention-to-treat (MITT) approaches, with the last observation carried forward method. For the safety evaluation, all patients who had received at least one dose of study drugs were analyzed. Statistical analysis was performed using SPSS version 22.0. A p value of <0.05 was considered to indicate statistical significance.

Continuous variables are presented as mean \pm SD. Within-group comparisons were conducted to determine any differences in the mean values of each variable between baseline and the two consecutive follow-up visits; a repeated measures ANOVA, with the least significant difference (LSD) test, was applied. For between-group comparisons, mean changes from baseline were compared using Student's t -test. Patients were classified as having had a response if their VAS pain scores decreased by 50% or more from baseline [35]. Dichotomous variables are reported as frequencies; the chi-squared test or Fisher's exact test, as appropriate, was used to compare the distribution of dichotomous variables between the two groups.

For assessment of noninferiority, a comparison between the THF-6 group and the diclofenac group on VAS pain was conducted, with a prespecified noninferiority margin of 10 mm [26, 27]. Noninferiority was declared if the upper limit of the two-sided 95% confidence interval (CI) for the MD of VAS pain did not exceed a margin of 10 mm.

3. Results

From February 2016 to July 2016, a total of 349 patients were screened for eligibility and 200 underwent randomization, 100 of whom were allocated to each arm (Figure 2). Predominant reasons for screening failure were that the patient did not meet the inclusion criteria (115 patients, 77.2%) and that the patient had abnormal laboratory results (31 patients, 20.8%). The mean age of the enrolled patients was 61.1 ± 6.1 years; 85.5% were women and 86% had osteoarthritis in both knees. Baseline demographic and clinical characteristics of the patients were comparable between the two groups (Table 1). Of the 200 patients randomized, 175

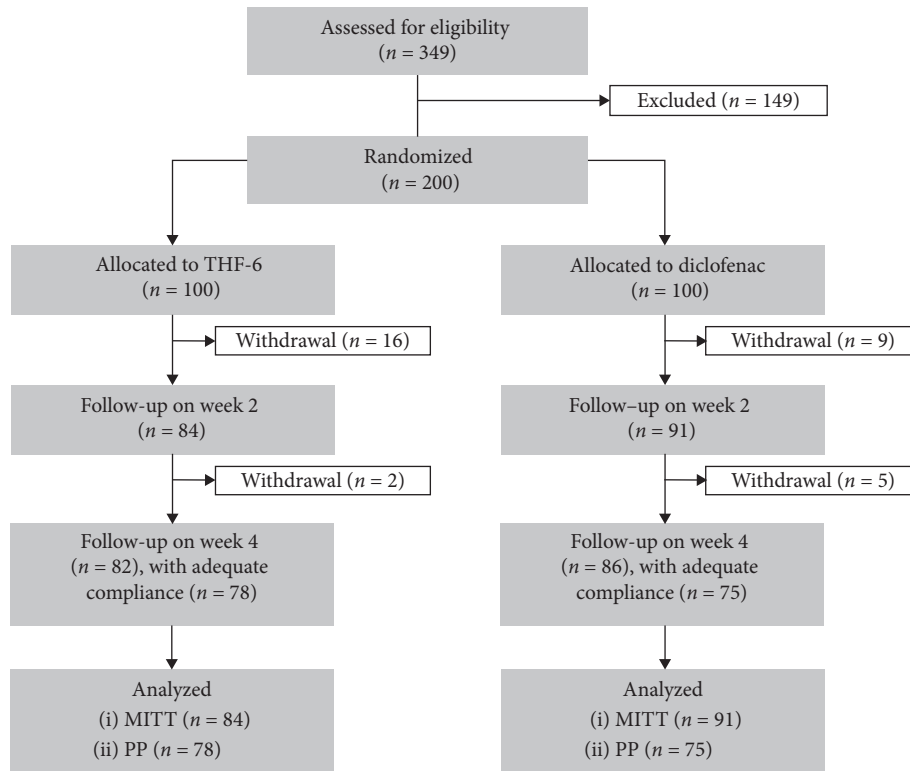


FIGURE 2: Flow diagram of the progress through all phases of this two-arm, randomized-controlled study (enrollment, intervention allocation, follow-up, and data analysis).

TABLE 1: Demographic and clinical characteristics of the enrolled patients.

| | THF-6 (n = 100) | Diclofenac (n = 100) |
|--|-----------------|-------------------------|
| Age (years) | 62.0 ± 6.1 | 60.3 ± 6.1 |
| Female sex (%) | 87 | 84 |
| BMI (kg/m ²) | 26.0 ± 4.7 | 25.7 ± 6.3 ^a |
| Location of osteoarthritis (n) | | |
| Right knee | 9 | 7 |
| Left knee | 5 | 7 |
| Both knees | 86 | 86 |
| Kellgren–Lawrence grade (n) | | |
| Grade 2 | 62 | 68 |
| Grade 3 | 68 | 73 |
| Grade 4 | 56 | 45 |
| Duration of osteoarthritis of the knee (years) | 4.9 ± 4.7 | 4.7 ± 4.3 |
| Underlying disease (n) | | |
| Hypertension | 43 | 50 |
| Dyslipidemia | 27 | 30 |
| Diabetes mellitus | 13 | 12 |
| Miscellaneous | 7 | 12 |
| None | 49 | 37 |
| Baseline measures | | |
| VAS pain (mm) | 60.0 ± 14.8 | 61.9 ± 15.7 |
| VAS stiffness (mm) | 54.9 ± 20.2 | 56.9 ± 22.3 |
| KOOS | | |
| Pain | 49.5 ± 14.3 | 51.4 ± 17.1 |
| Other knee symptoms | 55.2 ± 15.3 | 53.7 ± 18.3 |
| Activities of daily living | 51.3 ± 16.7 | 53.3 ± 18.3 |
| Sport and recreation function | 24.4 ± 19.4 | 26.8 ± 20.4 |
| Knee-related quality of life | 32.1 ± 15.8 | 32.0 ± 17.6 |
| SCT (sec) | 12.1 ± 5.9 | 11.5 ± 5.6 |

^an = 99. KOOS, Knee Injury and Osteoarthritis Outcome Score; SCT, 10-step stair climb test; VAS, visual analog scale.

(87.5%) were included in the MITT analysis and 153 (76.5%) in the PP analysis (Figure 2).

With regard to the primary endpoint, the mean change in VAS pain was not statistically significantly different between the two groups, and THF-6 (1,500 mg/day) was found to be noninferior to diclofenac (75 mg/day) in both the MITT and PP analyses. The upper limit of the two-sided 95% CI for the comparison between the THF-6 group and the diclofenac group was within the prespecified margin of 10 mm for noninferiority (Figure 3).

None of the mean changes in any of the efficacy outcome measures differed statistically significantly between the two groups (Table 2). Significant improvements in all efficacy parameters among patients receiving THF-6 as well as those receiving oral diclofenac were observed by the end of Week 2, and significant improvements continued to be seen at the end of Week 4 (Figures S1 and S2). There were 42 responders (50%) at the end of the four-week treatment with THF-6 compared to 40 (44%) with oral diclofenac (MITT analysis: 42/84 vs. 40/91, $p = 0.423$; PP analysis: 39/78 vs. 36/75, $p = 0.805$). Overall improvement self-assessed by the patients was similar in both groups: no statistically significant difference between the two groups was observed at the end of the treatment phase (MITT analysis: 63.57 ± 22.46 vs. 64.20 ± 22.92 , $p = 0.859$; PP analysis: 63.65 ± 21.86 vs. 63.00 ± 23.71 , $p = 0.859$). Upon completion of this trial, the physician's assessment of overall improvement did not differ between the two groups (Figure S3).

Dyspepsia was the most common adverse event reported in both groups: 23 patients (23%) in the THF-6 group and 28 (28%) in the diclofenac group (relative risk = 0.821, 95% CI = 0.510 to 1.323, $p = 0.417$). Overall, the proportion of patients reporting any adverse events in the safety population was fairly similar between the two groups (Table 3). All the adverse events reported were mild to moderate in intensity. Adverse events led to the premature discontinuation of 14 patients in the THF-6 group and 12 patients in the diclofenac group (χ^2 (1, $n = 200$) = 0.177, $p = 0.674$). Gastrointestinal intolerance was the major reason for discontinuation of therapy (9 in the THF-6 group vs. 6 in the diclofenac group, χ^2 (1, $n = 200$) = 0.649, $p = 0.421$). During the trial, there was only one serious adverse event, hospitalization due to pesticide exposure, which was judged as definitely unrelated to the study drug.

4. Discussion

In this randomized-controlled trial, THF-6 offered the potential to achieve analgesic efficacy with acceptable safety profiles in patients with moderate-to-severe osteoarthritis of the knee. In both the MITT and PP analyses, the upper limit of 95% CIs of MD in VAS pain was within the predefined noninferiority margin of 10 mm. This allowed us to conclude that THF-6 was noninferior to oral diclofenac (75 mg/day) in terms of knee pain relief. Oral administration of THF-6 also resulted in significant improvement, comparable to oral diclofenac, across several outcome measures. As THF-6 and oral diclofenac displayed comparable efficacy and safety, it

seems appropriate to consider THF-6 an alternative for the treatment of moderate-to-severe osteoarthritis of the knee.

The present clinical trial was designed to evaluate the efficacy and safety of THF-6 versus oral diclofenac for the short-term treatment of symptomatic osteoarthritis of the knee. In clinical practice, pain relief medications, including oral NSAIDs, are typically prescribed on an as-needed basis for a short duration due to safety concerns [36]. Most randomized-controlled trials evaluating the effects of pharmacological interventions, especially oral NSAIDs, often last only a few weeks with only a small number of trials going beyond four weeks of treatment [26]. Therefore, the present trial design, with a treatment duration of four weeks, can be considered appropriate for determining the effects of THF-6 in symptomatic osteoarthritis of the knee.

With respect to osteoarthritic knee pain of moderate-to-severe intensity, this trial demonstrated that THF-6 was comparable to oral diclofenac in relieving pain symptoms. An average reduction of around 26 mm on a 100 mm VAS pain scale with THF-6 treatment can be considered a clinically important improvement [37]. A 50% decrease in pain score, which represents a reasonable cut-off value for indicating a clinically meaningful pain reduction from the patient's perspective, was observed in approximately half of the patients in the THF-6 group [35]. These findings support the efficacy of THF-6 in osteoarthritic knee pain relief.

Even though the precise mechanism of THF-6's action has not yet been elucidated, the herbal constituents in the formulation have been shown individually to possess several pharmacological activities, perceptibly contributing to the beneficial effects of THF-6 in the treatment of symptomatic osteoarthritis of the knee. Previous comprehensive literature reviews of *C. rotundus* have found that the plant extracts have a broad range of pharmacological activities, including anti-inflammatory, antinociceptive, antiarthritic, and antioxidant activities [38–40]. *P. nigrum* also exhibits various pharmacological activities, for example, anti-inflammatory, antinociceptive, antiarthritic, and antioxidant activities, in both *in vitro* and animal experiments [41–43]. *S. asper* contains a number of bioactive compounds which possess anti-inflammatory and antioxidant properties [44, 45]. The crude extracts and isolated compounds of *T. cordifolia* have a wide range of pharmacological effects, including anti-inflammatory, antioxidant, antiarthritic, and analgesic properties [46, 47] as does *A. procera* [48–50]. As a result, it is reasonable to assume that the favorable outcomes following THF-6 administration in this trial might be attributable to the combined and possibly synergistic pharmacological activities of the several herbal ingredients in the formulation. Further research is warranted to ascertain the mechanisms of THF-6's action as well as understanding the molecular basis of its effects in symptomatic relief of osteoarthritic knee pain.

In this trial, the overall safety profiles of both pharmacological interventions were more or less the same. Around one-fourth of the patients in each group experienced gastrointestinal adverse events following drug administration. Dyspepsia was the most common adverse event in both groups and its frequency did not differ between

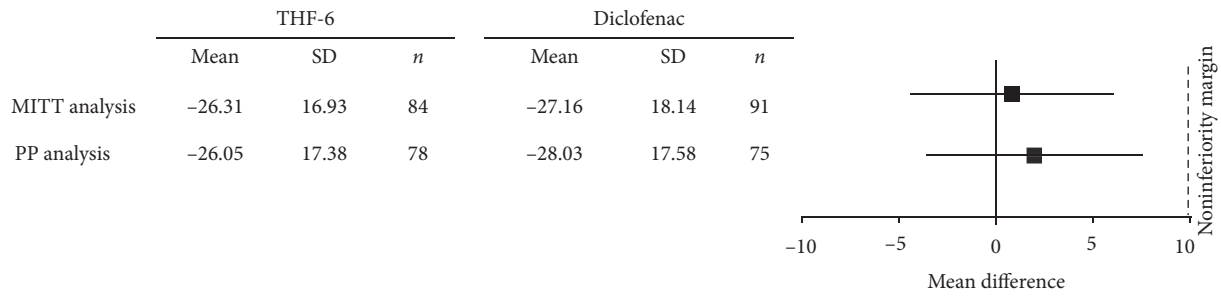


FIGURE 3: Noninferiority analysis of VAS pain.

TABLE 2: Efficacy outcome assessments.

| | THF-6 | Diclofenac | Mean difference | (95% CI) | <i>p</i> value ^a |
|---|----------------|----------------|-----------------|------------------|-----------------------------|
| Mean change of VAS pain (mm) | | | | | |
| MITT analysis | -26.31 ± 16.93 | -27.16 ± 18.14 | 0.86 | (-4.39 to 6.10) | 0.748 |
| PP analysis | -26.05 ± 17.38 | -28.03 ± 17.58 | 1.98 | (-3.61 to 7.56) | 0.486 |
| Mean change of VAS stiffness (mm) | | | | | |
| MITT analysis | -22.52 ± 17.70 | -23.26 ± 19.12 | 0.74 | (-4.77 to 6.25) | 0.791 |
| PP analysis | -22.53 ± 17.82 | -23.28 ± 18.10 | 0.75 | (-4.98 to 6.49) | 0.795 |
| Mean change of SCT (sec) | | | | | |
| MITT analysis | -3.35 ± 3.55 | -3.42 ± 4.33 | 0.07 | (-1.12 to 1.26) | 0.148 |
| PP analysis | -3.44 ± 3.61 | -3.27 ± 4.09 | -0.17 | (-1.40 to 1.06) | 0.786 |
| Mean change of KOOS pain | | | | | |
| MITT analysis | 14.88 ± 14.98 | 15.77 ± 15.89 | -0.89 | (-5.50 to 3.73) | 0.705 |
| PP analysis | 15.24 ± 15.29 | 15.77 ± 14.54 | -0.53 | (-5.30 to 4.24) | 0.827 |
| Mean change of KOOS other symptoms | | | | | |
| MITT analysis | 12.29 ± 14.92 | 15.29 ± 16.90 | -3.00 | (-7.77 to 1.77) | 0.216 |
| PP analysis | 12.49 ± 15.17 | 16.01 ± 16.22 | -3.53 | (-8.54 to 1.49) | 0.167 |
| Mean change of KOOS activities of daily living | | | | | |
| MITT analysis | 13.25 ± 15.22 | 14.46 ± 17.78 | -1.21 | (-6.17 to 3.75) | 0.640 |
| PP analysis | 13.62 ± 15.23 | 14.05 ± 16.76 | -0.44 | (-5.55 to 4.67) | 0.866 |
| Mean change of KOOS sport and recreation function | | | | | |
| MITT analysis | 15.18 ± 17.28 | 18.57 ± 21.23 | -3.39 | (-9.20 to 2.41) | 0.250 |
| PP analysis | 15.64 ± 17.48 | 19.27 ± 21.79 | -3.63 | (-9.91 to 2.66) | 0.256 |
| Mean change of KOOS knee-related quality of life | | | | | |
| MITT analysis | 8.42 ± 16.23 | 13.71 ± 19.65 | -5.30 | (-10.70 to 0.10) | 0.054 |
| PP analysis | 9.38 ± 16.30 | 13.95 ± 18.01 | -4.56 | (-10.05 to 0.92) | 0.102 |

^aStudent's *t*-test. KOOS, Knee Injury and Osteoarthritis Outcome Score; SCT, 10-step stair climb test; VAS, visual analog scale.

the groups. Nine patients in the THF-6 group discontinued treatment early due to gastrointestinal adverse consequences, as did six patients in the diclofenac group. These findings are not surprising given that similar gastrointestinal tolerability problems with oral diclofenac, particularly dyspepsia, have been regularly observed in other clinical trials assessing the safety and tolerability of oral NSAIDs [51, 52]. Based on its safety profile as described above, THF-6 should be used with caution, especially in patients at high risk of upper gastrointestinal complications.

There were limitations to this trial. First and foremost, there was no placebo comparison in the trial where a subjective outcome measure was used as a primary endpoint. In the context where standard therapy is widely used to treat a condition, a placebo comparison might not be possible due primarily to ethical reasons [53]. In such a context, noninferiority design could be applied to compare the intervention under investigation with another active treatment

provided that the reference treatment's efficacy is well established [54], as is the case for oral diclofenac [9]. This is of particular relevance in the present trial where the target groups had baseline knee pain of moderate-to-severe intensity. To minimize the risk of bias in the assessment of subjective outcomes, this trial assessed knee symptoms using several different measures to help ensure a comprehensive evaluation and also included a 10-step SCT measure which is less subject to contextual effects [55]. It should also be acknowledged that the MITT approach may be prone to attrition bias associated with the exclusion of some patients from the analysis [56, 57]. Notwithstanding, it does not necessarily bias trial results [58]. In noninferiority trials, a PP analysis typically yields a more conservative estimate of treatment effects; therefore, the MITT approach is less likely to have a significant impact on estimated treatment benefits especially when both PP and MITT analyses consistently support noninferiority, as is the case of the present study

TABLE 3: Safety outcome assessments.

| Adverse events | THF-6 (<i>n</i> = 100) | Diclofenac (<i>n</i> = 100) | <i>p</i> value ^a |
|--|-------------------------|------------------------------|-----------------------------|
| Gastrointestinal system | | | |
| Dyspepsia | 23 | 28 | 0.417 |
| Nausea and vomiting | 3 | 4 | 1.000 |
| Gastroesophageal reflux disease | 2 | 2 | 1.000 |
| Loss of appetite | 4 | 1 | 0.369 |
| Diarrhea | 3 | 1 | 0.621 |
| Constipation | 5 | 5 | 1.000 |
| Hematochezia | 1 | 0 | 1.000 |
| Other systems | | | |
| Peripheral edema | 4 | 5 | 1.000 |
| Peripheral neuropathy | 2 | 1 | 1.000 |
| Dizziness | 1 | 2 | 1.000 |
| Headache | 1 | 0 | 1.000 |
| Drowsiness | 1 | 0 | 1.000 |
| Insomnia | 0 | 1 | 1.000 |
| Dry mouth | 0 | 1 | 1.000 |
| Blurred vision | 1 | 0 | 1.000 |
| Low back pain | 2 | 2 | 1.000 |
| Myalgia | 2 | 0 | 0.497 |
| Cramp | 1 | 1 | 1.000 |
| Rashes | 2 | 0 | 0.497 |
| Itching | 2 | 0 | 0.497 |
| AST elevation (>2.5–3.0 times from baseline) | 2 | 1 | 1.000 |
| Creatinine rising (>1.5–2.0 times from baseline) | 0 | 3 | 0.246 |

^aChi-square test or Fisher's exact test. AST: aspartate aminotransferase.

[59]. Lastly, it is notable that the trial length of four weeks may not be long enough to determine long-term adverse outcomes of THF-6, including cardiovascular complications [60]. On the basis of the evidence currently available, this trial does not guarantee the safety of long-term use of THF-6.

5. Conclusions

THF-6 offers an alternative to oral diclofenac for the short-term treatment of moderate-to-severe osteoarthritis of the knee. Administration of THF-6 was shown to be noninferior to oral diclofenac in relieving knee pain. None of the outcome measures assessed in this trial favored either THF-6 or oral diclofenac with respect to symptomatic osteoarthritis of the knee.

Data Availability

All data used to support the findings of this study are available from the corresponding author upon reasonable request.

Conflicts of Interest

The authors declare no conflicts of interest regarding the publication of this article.

Authors' Contributions

NK, SN, ST, NC, CS, SC, and NH contributed to study conception and design. SN and NH developed the study

protocol and related documents. SC supervised a manufacturing process of herbal preparations and placebo. PT contributed to the HPLC method development. SN and NH conducted the study and collected data. NK analyzed the data. NK and NH interpreted the results. NK drafted and finalized the manuscript with support and comments from ST, SN, NC, CS, SC, and NH. All authors read and approved the final manuscript.

Acknowledgments

The authors are grateful for the editorial assistance of Dr. G. Lamar Robert, English language consultant to the Department of Pharmacology, Faculty of Medicine, Chiang Mai University. The authors would also like to extend their thanks to Ms. Sujitra Techatoei for her secretarial assistance. This work was supported by the Department of Thai Traditional and Alternative Medicine, Ministry of Public Health.

Supplementary Materials

Table S1: components of Thai herbal recipe-6 (THF-6). Figure S1: VAS pain, VAS stiffness, and SCT at baseline, Week 2, and Week 4. Figure S2: KOOS at baseline, Week 2, and Week 4. Figure S3: Patient's and physician's opinion of overall improvement. (*Supplementary Materials*)

References



- [1] D. J. Hunter and S. Bierma-Zeinstra, "Osteoarthritis," *The Lancet*, vol. 393, no. 10182, pp. 1745–1759, 2019.

- [2] M. Kloppenburg and F. Berenbaum, "Osteoarthritis year in review 2019: epidemiology and therapy," *Osteoarthritis and Cartilage*, vol. 28, no. 3, pp. 242–248, 2020.
- [3] M. Cross, E. Smith, D. Hoy et al., "The global burden of hip and knee osteoarthritis: estimates from the Global Burden of Disease 2010 study," *Annals of the Rheumatic Diseases*, vol. 73, no. 7, pp. 1323–1330, 2014.
- [4] GBD 2015 DALYs and HALE Collaborators, "Global, regional, and national disability-adjusted life-years (DALYs) for 315 diseases and injuries and healthy life expectancy (HALE), 1990–2015: a systematic analysis for the Global burden of disease study 2015," *Lancet*, vol. 388, no. 10053, pp. 1603–1658, 2016.
- [5] GBD 2017 DALYs and HALE Collaborators, "Global, regional, and national disability-adjusted life-years (DALYs) for 359 diseases and injuries and healthy life expectancy (HALE) for 195 countries and territories, 1990–2017: a systematic analysis for the Global burden of disease study 2017," *Lancet*, vol. 392, no. 10159, pp. 1859–1922, 2018.
- [6] L. Murphy, T. A. Schwartz, C. G. Helmick et al., "Lifetime risk of symptomatic knee osteoarthritis," *Arthritis & Rheumatism*, vol. 59, no. 9, pp. 1207–1213, 2008.
- [7] D. J. Hunter, D. Schofield, and E. Callander, "The individual and socioeconomic impact of osteoarthritis," *Nature Reviews Rheumatology*, vol. 10, no. 7, pp. 437–441, 2014.
- [8] S. R. Kingsbury, E. M. Hensor, C. A. Walsh, M. C. Hochberg, and P. G. Conaghan, "How do people with knee osteoarthritis use osteoarthritis pain medications and does this change over time? data from the osteoarthritis Initiative," *Arthritis Research & Therapy*, vol. 15, no. 5, p. R106, 2013.
- [9] B. R. da Costa, S. Reichenbach, N. Keller et al., "Effectiveness of non-steroidal anti-inflammatory drugs for the treatment of pain in knee and hip osteoarthritis: a network meta-analysis," *The Lancet*, vol. 390, no. 10090, pp. e21–e33, 2017.
- [10] R. R. Bannuru, M. C. Osani, E. E. Vaysbrot et al., "OARSI guidelines for the non-surgical management of knee, hip, and polyarticular osteoarthritis," *Osteoarthritis and Cartilage*, vol. 27, no. 11, pp. 1578–1589, 2019.
- [11] S. L. Kolasinski, T. Neogi, M. C. Hochberg et al., "2019 American college of rheumatology/arthritis foundation guideline for the management of osteoarthritis of the hand, hip, and knee," *Arthritis Care & Research*, vol. 72, no. 2, pp. 149–162, 2020.
- [12] J. Hasford, N. Moore, and K. Hoyer, "Safety and usage pattern of low-dose diclofenac when used as an over-the-counter medication: results of an observational cohort study in a community-based pharmacy setting," *International Journal of Clinical Pharmacology and Therapeutics*, vol. 42, no. 08, pp. 415–422, 2004.
- [13] N. Moore and J. M. Scheiman, "Gastrointestinal safety and tolerability of oral non-aspirin over-the-counter analgesics," *Postgraduate Medicine*, vol. 130, no. 2, pp. 188–199, 2018.
- [14] K. J. Foreman, N. Marquez, A. Dolgert et al., "Forecasting life expectancy, years of life lost, and all-cause and cause-specific mortality for 250 causes of death: reference and alternative scenarios for 2016–40 for 195 countries and territories," *The Lancet*, vol. 392, no. 10159, pp. 2052–2090, 2018.
- [15] N. Koonrungsomboon, S. Teekachunhatean, S. Chansakaow, and N. Hanprasertpong, "Clinical efficacy and safety of yellow oil formulations 3 and 4 versus indomethacin solution in patients with symptomatic osteoarthritis of the knee: a randomized controlled trial," *Evidence-Based Complementary and Alternative Medicine*, vol. 2020, Article ID 5782178, , 2020.
- [16] D. Dragos, M. Gilca, L. Gaman et al., "Phytomedicine in joint disorders," *Nutrients*, vol. 9, no. 1, p. 70, 2017.
- [17] M. Cameron and S. Chrusasik, "Oral herbal therapies for treating osteoarthritis," *Cochrane Database Syst Rev*, vol. 5, no. 5, Article ID CD002947, 2014.
- [18] B. Chen, H. Zhan, J. Marszalek et al., "Traditional Chinese medications for knee osteoarthritis pain: a meta-analysis of randomized controlled trials," *The American Journal of Chinese Medicine*, vol. 44, no. 04, pp. 677–703, 2016.
- [19] F. Wang, L. Shi, Y. Zhang et al., "A traditional herbal formula Xianlinggubao for pain control and function improvement in patients with knee and hand osteoarthritis: a multicenter, randomized, open-label, controlled trial," *Evidence-Based Complementary and Alternative Medicine*, vol. 2018, Article ID 1827528, 2018.
- [20] C. Chailom, *Pramuan Tamrap Ya Thai*, Sripanya, Nonthaburi, Thailand, in Thai, 2011.
- [21] P. W. Rattananangri, *Petnamnueng Khong Borannachan*, Odeon Store, Bangkok, Thailand, in Thai, 1991.
- [22] S. Pitiphon, "Samunphrai Abhaibhubejhr Suebsab Phum Phanya Thaid," Pauramutha Karnpim Co., Ltd., Bangkok, Thailand, in Thai, 2004.
- [23] T. E. McAlindon, J. B. Driban, Y. Henrotin et al., "OARSI clinical trials recommendations: design, conduct, and reporting of clinical trials for knee osteoarthritis," *Osteoarthritis and Cartilage*, vol. 23, no. 5, pp. 747–760, 2015.
- [24] R. Altman, E. Asch, D. Bloch et al., "Development of criteria for the classification and reporting of osteoarthritis: classification of osteoarthritis of the knee," *Arthritis & Rheumatism*, vol. 29, no. 8, pp. 1039–1049, 1986.
- [25] A. M. Boonstra, H. R. Schiphorst Preuper, G. A. Balk, and R. E. Stewart, "Cut-off points for mild, moderate, and severe pain on the visual analogue scale for pain in patients with chronic musculoskeletal pain," *Pain*, vol. 155, no. 12, pp. 2545–2550, 2014.
- [26] J. M. Bjordal, A. Klovning, A. E. Ljunggren, and L. Slordal, "Short-term efficacy of pharmacotherapeutic interventions in osteoarthritic knee pain: a meta-analysis of randomised placebo-controlled trials," *European Journal of Pain*, vol. 11, no. 12, pp. 125–138, 2007.
- [27] A. van Walsem, S. Pandhi, R. M. Nixon et al., "Relative benefit-risk comparing diclofenac to other traditional non-steroidal anti-inflammatory drugs and cyclooxygenase-2 inhibitors in patients with osteoarthritis or rheumatoid arthritis: a network meta-analysis," *Arthritis Research & Therapy*, vol. 17, no. 1, p. 66, 2015.
- [28] S. A. Julious, "Sample sizes for clinical trials with normal data," *Statistics in Medicine*, vol. 23, no. 12, pp. 1921–1986, 2004.
- [29] S. R. Kingsbury, N. Corp, F. E. Watt et al., "Harmonising data collection from osteoarthritis studies to enable stratification: recommendations on core data collection from an arthritis research UK clinical studies group," *Rheumatology*, vol. 55, no. 8, pp. 1394–1402, 2016.
- [30] T. O. Smith, G. A. Hawker, D. J. Hunter et al., "The OMERACT-OARSI core domain set for measurement in clinical trials of hip and/or knee osteoarthritis," *The Journal of Rheumatology*, vol. 46, no. 8, pp. 981–989, 2019.
- [31] G. A. Hawker, S. Mian, T. Kendzerska, and M. French, "Measures of adult pain: visual analog scale for pain (VAS pain), numeric rating scale for pain (NRS pain), McGill pain questionnaire (MPQ), short-form McGill pain questionnaire (SF-MPQ), chronic pain grade scale (CPGS), short form-36

- bodily pain scale (SF),” *Arthritis Care & Research*, vol. 63, no. S11, pp. S240–S252, 2011.
- [32] K. Bennell, F. Dobson, and R. Hinman, “Measures of physical performance assessments: self-paced walk test (SPWT), stair climb test (SCT), six-minute walk test (6MWT), chair stand test (CST), timed up & go (TUG), sock test, lift and carry test (LCT), and car task,” *Arthritis Care & Research*, vol. 63, no. S11, pp. S350–S370, 2011.
- [33] N. J. Collins, D. Misra, D. T. Felson, K. M. Crossley, and E. M. Roos, “Measures of knee function: international knee documentation committee (IKDC) subjective knee evaluation form, knee injury and osteoarthritis outcome score (KOOS), knee injury and osteoarthritis outcome score physical function short form (KOOS-PS), knee ou,” *Arthritis Care & Research*, vol. 63, no. S11, pp. S208–S228, 2011.
- [34] K. Chaipinyo, “Test-retest reliability and construct validity of Thai version of knee osteoarthritis outcome score (KOOS),” *Thai Journal of Physical Therapy Science*, vol. 31, pp. 67–76, 2009.
- [35] T. Pham, D. van der Heijde, R. D. Altman et al., “OMERACT-OARSI Initiative: osteoarthritis Research Society International set of responder criteria for osteoarthritis clinical trials revisited,” *Osteoarthritis and Cartilage*, vol. 12, no. 5, pp. 389–399, 2004.
- [36] C. Cooper, R. Chapurlat, N. Al-Daghri et al., “Safety of oral non-selective non-steroidal anti-inflammatory drugs in osteoarthritis: what does the literature say?” *Drugs Aging*, vol. 36, no. 1, pp. 15–24, 2019.
- [37] F. Tubach, P. Ravaud, G. Baron et al., “Evaluation of clinically relevant changes in patient reported outcomes in knee and hip osteoarthritis: the minimal clinically important improvement,” *Annals of the Rheumatic Diseases*, vol. 64, no. 1, pp. 29–33, 2005.
- [38] A. E. Al-Snafi, “A review on *Cyperus rotundus* A potential medicinal plant,” *IOSR Journal of Pharmacy (IOSRPHR)*, vol. 6, no. 7, pp. 32–48, 2016.
- [39] N. Singh, B. R. Pandey, P. Verma et al., “Phyto-pharmacotherapeutics of *Cyperus rotundus* Linn. (Motha): an overview,” *Indian Journal of Natural Products and Resources*, vol. 3, no. 4, pp. 467–476, 2012.
- [40] S. R. Sivapalan, “Medicinal uses and pharmacological activities of *Cyperus rotundus* Linn—a review,” *International Journal of Science and Research*, vol. 3, no. 5, pp. 1–8, 2013.
- [41] J. S. Bang, D. H. Oh, H. M. Choi et al., “Anti-inflammatory and antiarthritic effects of piperine in human interleukin 1 β -stimulated fibroblast-like synoviocytes and in rat arthritis models,” *Arthritis Research & Therapy*, vol. 11, no. 2, p. R49, 2009.
- [42] M. Meghwal and T. K. Goswami, “*Piper nigrum* and piperine: an update,” *Phytotherapy Research*, vol. 27, no. 8, pp. 1121–1130, 2013.
- [43] F. Tasleem, I. Azhar, S. N. Ali et al., “Analgesic and anti-inflammatory activities of *Piper nigrum* L,” *Asian Pacific Journal of Tropical Medicine*, vol. 7, no. Suppl 1, pp. S461–S468, 2014.
- [44] N. Ibrahim, I. Mat, V. Lim, and R. Ahmad, “Antioxidant activity and phenolic content of *Streblus asper* leaves from various drying methods,” *Antioxidants*, vol. 2, no. 3, pp. 156–166, 2013.
- [45] B. Sripanidkulchai, J. Junlatat, N. Wara-aswapati, and D. Hormdee, “Anti-inflammatory effect of *Streblus asper* leaf extract in rats and its modulation on inflammation-associated genes expression in RAW 264.7 macrophage cells,” *Journal of Ethnopharmacology*, vol. 124, no. 3, pp. 566–570, 2009.
- [46] S. Saha and S. Ghosh, “*Tinospora cordifolia*: one plant, many roles,” *Ancient Science of Life*, vol. 31, no. 4, pp. 151–159, 2012.
- [47] S. Upadhayay, M. Bora, L. Kawlani et al., “Comprehensive pharmacology review of *guduchi* [*Tinospora cordifolia* (wild.) Miers],” *Journal of Drug Research in Ayurvedic Sciences*, vol. 3, no. 1, pp. 48–52, 2018.
- [48] M. M. Khatoun, M. H. Khatun, M. E. Islam, and M. S. Parvin, “Analgesic, antibacterial and central nervous system depressant activities of *Albizia procera* leaves,” *Asian Pacific Journal of Tropical Biomedicine*, vol. 4, no. 4, pp. 279–284, 2014.
- [49] K. Kokila, S. D. Priyadharshini, and V. Sujatha, “Phyto-pharmacological properties of *Albizia* species: a review,” *International Journal of Pharmacy and Pharmaceutical Sciences*, vol. 5, no. 3, pp. 70–73, 2013.
- [50] S. Sivakrishnan and A. Kottai Muthu, “In vivo antioxidant activity of ethanolic extract of aerial parts of *Albizia procera* roxb (benth.) against paracetamol induced liver toxicity on Wistar rats,” *Journal of Pharmaceutical Sciences and Research*, vol. 5, no. 9, pp. 174–177, 2013.
- [51] Coxib and traditional NSAID Trialists’ (CNT) Collaboration, N. Bhal, J. Emberson et al., “Vascular and upper gastrointestinal effects of non-steroidal anti-inflammatory drugs: meta-analyses of individual participant data from randomised trials,” *Lancet*, vol. 382, no. 9894, pp. 769–779, 2013.
- [52] S. R. Mallen, M. N. Essex, and R. Zhang, “Gastrointestinal tolerability of NSAIDs in elderly patients: a pooled analysis of 21 randomized clinical trials with celecoxib and nonselective NSAIDs,” *Current Medical Research and Opinion*, vol. 27, no. 7, pp. 1359–1366, 2011.
- [53] A. S. Skierka and K. B. Michels, “Ethical principles and placebo-controlled trials—interpretation and implementation of the declaration of Helsinki’s placebo paragraph in medical research,” *BMC Med Ethics*, vol. 19, no. 1, p. 24, 2018.
- [54] L. Mauri and R. B. D’Agostino, “Challenges in the design and interpretation of noninferiority trials,” *New England Journal of Medicine*, vol. 377, no. 14, pp. 1357–1367, 2017.
- [55] F. Dobson, R. S. Hinman, E. M. Roos et al., “OARSI recommended performance-based tests to assess physical function in people diagnosed with hip or knee osteoarthritis,” *Osteoarthritis and Cartilage*, vol. 21, no. 8, pp. 1042–1052, 2013.
- [56] I. Abraha and A. Montedori, “Modified intention to treat reporting in randomised controlled trials: systematic review,” *BMJ*, vol. 340, p. c2697, 2010.
- [57] E. Nuesch, S. Trelle, S. Reichenbach et al., “The effects of excluding patients from the analysis in randomised controlled trials: meta-epidemiological study,” *BMJ*, vol. 339, p. b3244, 2009.
- [58] A. Dossing, S. Tarp, D. E. Furst et al., “Modified intention-to-treat analysis did not bias trial results,” *Journal of Clinical Epidemiology*, vol. 72, pp. 66–74, 2016.
- [59] S. J. Oczkowski, “A clinician’s guide to the assessment and interpretation of noninferiority trials for novel therapies,” *Open Medicine: A Peer-Reviewed, Independent, Open-Access Journal*, vol. 8, no. 2, pp. e67–72, 2014.
- [60] C. A. Barcella, M. Lamberts, P. McGettigan et al., “Differences in cardiovascular safety with non-steroidal anti-inflammatory drug therapy—a nationwide study in patients with osteoarthritis,” *Basic & Clinical Pharmacology & Toxicology*, vol. 124, no. 5, pp. 629–641, 2019.

Review Article

Meta-Analysis of Randomized Controlled Trials of Xueshuantong Injection in Prevention of Deep Venous Thrombosis of Lower Extremity after Orthopedic Surgery

Shu-ting Yan ^{1,2}, Feng Gao,² Tai-wei Dong,^{1,2} Hao Fan,² Miao-miao Xi,¹ Feng Miao ¹,
and Pei-feng Wei ^{1,2}

¹The Second Affiliated Hospital of Shaanxi University of Traditional Chinese Medicine, Weiyang West Road, Qindu District, Xianyang, Shaanxi 712046, China

²College of Pharmacy, Shaanxi University of Chinese Medicine, Shiji Road, Qindu District, Xianyang, Shaanxi 712046, China

Correspondence should be addressed to Feng Miao; 2936185913@qq.com and Pei-feng Wei; peifeng_ad@163.com

Received 7 September 2020; Revised 20 October 2020; Accepted 28 October 2020; Published 29 November 2020

Academic Editor: Arham Shabbir

Copyright © 2020 Shu-ting Yan et al. This is an open access article distributed under the Creative Commons Attribution License, which permits unrestricted use, distribution, and reproduction in any medium, provided the original work is properly cited.

Objective. To systematically evaluate the clinical efficacy of Xueshuantong injection (*Panax notoginseng* saponins) in preventing deep venous thrombosis (DVT) of lower extremity after orthopedic surgery. **Methods.** The randomized controlled trials (RCTs) of Xueshuantong injection in prevention of lower extremity DVT after orthopedic surgery were retrieved from CNKI, Wanfang database, VIP, PubMed, and Cochrane Library by August 2020. Revman5.2 was used to analyze the results. **Results.** A total of 20 articles including 2336 patients were included. The results of meta-analysis showed that the incidence of DVT in the experimental group was lower than that in the control group; after operation, the D-dimer (Ddimer), thrombin time (APTT), and prothrombin time (PT) in the experimental group were significantly improved compared with those in the control group, and the difference between the two groups was statistically significant. **Conclusion.** Xueshuantong injection can effectively prevent the formation of lower extremity DVT after orthopedic surgery and antagonize the postoperative hypercoagulable state of blood, which has high clinical value.

1. Background

DVT is a common perioperative complication of fractures, with a potential disability rate and fatality rate of 40%~70% for patients with traumatic fractures [1–4]. If venous thrombosis is not treated in time, it may cause swelling, pain, and dysfunction of affected limbs in mild cases, and in severe cases, pulmonary embolism will occur and even life-threatening when thrombus enters the pulmonary circulation [5–9]. According to current research reports, the incidence of DVT after fracture surgery is as high as 9%~62%. The Guidelines of the American College of Chest Physicians (ACCP) and the American College of Orthopedic Surgeons (AAOS) all suggest that if there are no contraindications, the drugs or physical methods should be used to prevent venous thromboembolism after fracture surgery [10, 11]. Xueshuantong injection (*Panax notoginseng* saponins) has

antiplatelet aggregation effect and is widely used in orthopedic surgery for thromboprophylaxis [12, 13]. At present, the clinical studies on Xueshuantong injection to prevent venous thrombosis of lower extremity after fracture surgery are mainly concentrated in China. In contrast, there is a lack of meta-analysis on the prevention of DVT after fracture with Xueshuantong injection. Therefore, the purpose of this meta-analysis is to examine the efficacy of Xueshuantong injection in the prevention of DVT by summarizing the existing clinical studies.

2. Data and Methods

2.1. Retrieval Strategy. According to the PRISMA, two researchers independently searched PubMed, Cochrane Library, CNKI, Wanfang, and VIP. To conduct a comprehensive search, studies published prior to August 15,

2020, were investigated without language limitations. The search terms used were as follows: “Xueshuantong” and “fracture” and “deep venous thrombosis of lower” or “DVT.” All corresponding articles were downloaded into Note-Express (version 3.0, Beijing, China) for further investigation.

2.2. Inclusion Criteria. According to the guidelines for the prevention of venous thromboembolism in Chinese orthopedic surgery, color Doppler ultrasound examination has gradually superseded venography as the primary diagnostic procedure, which is a preferred method for the diagnosis of DVT with high sensitivity and accuracy. DVT screening was required for all patients before and after treatment. (1) Study type: randomized controlled trial, blinded or not, complete data, and language limited to Chinese/English. (2) Subjects: patients with fractures confirmed by imaging examination and requiring surgical treatment. (3) Intervention measures: Xueshuantong injection or Xueshuantong injection combined with other drugs was used in the experimental group, while low molecular weight heparin sodium (LMWH), other anticoagulants, or blank control were used in the control group. (4) The following indices in the articles must contain at least one of the following: incidence of DVT, D-D, PT, and APTT.

2.3. Exclusion Criteria. (1) Non-RCT study. (2) Repetitive articles. (3) Nonoriginal research. (4) Patients with DVT before the surgery, included patients with conditions that may easily cause DVT. (5) Studies such as reviews, animal experiments, and case reports that were considered to be irrelevant to the theme.

2.4. Data Extraction. Two researchers (Shu-ting Yan and Feng Gao) independently searched and extracted the data. When the opinions were different, they discussed together or asked another author for advice (Tai-wei Dong). This information is provided and arranged in Table 1.

2.5. Literature Quality Evaluation. Two researchers independently evaluated each of the included articles according to the bias risk assessment tool in the Cochrane Handbook. Evaluation contents: (1) whether the random sequence is generated properly. (2) Whether the random distribution is hidden. (3) Whether the blind method is used. (4) Whether the result data are reported completely. (5) Whether there is selective report. (6) Whether there is other bias.

2.6. Statistical Analysis. The analysis was performed by RevMan5.2 software. I^2 test ($p = 0.1$) was used for heterogeneity analysis between included study results. $I^2 < 50\%$ indicated no statistical significance for heterogeneity among studies, and the fixed effect model was used for heterogeneity analysis; $I^2 \geq 50\%$ showed that the heterogeneity among the studies was statistically significant, and random effect model analysis was used. In the continuous variable study, the

weighted average difference (WMD) was used as the effect indicator, and the risk ratio (RR) was used as the effect indicator of the dichotomous variable. For each study, we calculated the risk ratios (RRs) with their 95% confidence interval (CI), and $p < 0.05$ indicated a statistically significant difference. Begg’s test was used to assess publication bias using STATA 13.0 statistical software (Stata Corp, College Station, TX, USA), and $p < 0.1$ indicated a statistically significant difference.

GRADE profiler software was used to input and quantify the quality of evidence for the included outcome indicators.

3. Result

3.1. Results of Study Retrieval. Studies took place between 2006 and 2019 (Table 1). A total of 270 potentially corresponding studies were identified by our primary search, and 223 articles were exempted for repeat. Then, a full-text review was conducted on the remaining 47 articles. A total of 27 studies were exempted for the following reasons: 18 articles had vague diagnoses, 6 articles are not RCTs, and the results of the 3 articles are inconsistent. Twenty studies had adequate index data to permit the calculation of effect sizes for inclusion in this meta-analysis (Figure 1). Of the 20 included studies, 2336 patients with fractures underwent fracture surgery (1175 cases in the experimental group and 1161 cases in the control group) and used in this meta-analysis.

3.2. Literature Quality Evaluation. All trials were RCTs of participants according to Cochrane risk of bias estimation. Particular information on distribution was absent from most articles. All studies did not use blinding of participants and consequence assessment. All articles had integral outcome data with a low risk of attrition bias and low risk of reporting bias as detailed results are given (Figure 2).

3.3. Meta-Analysis Results

3.3.1. Comparison of DVT Incidence. A total of 17 articles reported the incidence of DVT. The fixed effect model was used for analysis. The results showed that the incidence of DVT after fracture surgery could be significantly reduced by using Xueshuantong injection (RR = 0.42, [95% CI (0.32, 0.55)], $p < 0.00001$; Figure 3). There was no statistically significant heterogeneity among the individual trials ($I^2 = 36\%$, $p = 0.07$).

3.3.2. D-D. 10 studies measured D-D levels in patients after fracture surgery. There was a statistically significant degree of heterogeneity among individual studies ($I^2 = 99\%$, $p < 0.00001$); therefore, a random effect model was performed for a meta-analysis, which showed that Xueshuantong injection or it combined with other treatment can reduce patients’ D-D level (MD = -0.51 [95% CI ($-0.67, 88, -0.35$)]; Figure 4).

TABLE 1: Principal characteristics of the studies included in the meta-analysis.

| No. | Included study | Sample size (T/C) | Experimental group | | Control group | | Treatment course (days) | Evaluation indicators |
|-----|-----------------------|-------------------|--|---------------|------------------------|---------------|-------------------------|-----------------------|
| | | | Treatment | Age (years) | Treatment | Age (years) | | |
| 1 | Cai [14] | 58/54 | Xueshuantong injection | 56.6 | LMWH | 56.6 | 14 | ①④⑤ |
| 2 | Deng [15] | 31/29 | Xueshuantong injection | 44 ± 1.6 | | 45 ± 1.5 | 7 | ① |
| 3 | He and Cao [16] | 40/40 | Xueshuantong injection + LMHC | 62.87 ± 1.65 | LMHC | 62.45 ± 1.28 | 14 | ①④⑤ |
| 4 | Huang[17] | 104/104 | Xueshuantong injection + Tongmaidan | 67 | LMHC | 68 | 7 | ①② |
| 5 | Jia and Tang [18] | 80/80 | Xueshuantong injection | 84.30 ± 1.61 | Conventional treatment | 84.21 ± 1.58 | 7 | ①②④⑤⑥ |
| 6 | Li [19] | 31/31 | Xueshuantong injection | 52.2 ± 8.9 | Conventional treatment | 50.5 ± 10.6 | 6 | ①②④ |
| 7 | Li et al. (2014) [20] | 60/60 | Xueshuantong injection | 57.93 ± 2.68 | LMWH | 58.79 ± 2.97 | 14 | ①④⑤ |
| 8 | Li [21] | 62/63 | Xueshuantong injection + rivaroxaban | 35.1 ± 9.1 | Xueshuantong injection | 34.7 ± 8.9 | 14 | ①②⑥ |
| 9 | Huang [22] | 40/40 | Xueshuantong injection + LMHC | 59.3 ± 3.3 | LMHC | 60.0 ± 2.9 | 7 | ① |
| 10 | Liu [23] | 40/40 | Xueshuantong injection | | LMHC | | 14 | ⑦ |
| 11 | Liu [24] | 160/160 | Xueshuantong injection | 76.5 ± 5.3 | Conventional treatment | 76.5 ± 5.3 | 7 | ①②④⑤⑥ |
| 12 | Liu [25] | 62/62 | Xueshuantong injection | 65.91 ± 12.25 | Rivaroxaban | 65.89 ± 12.22 | 14 | ①②⑥ |
| 13 | Pan and Tang[26] | 43/36 | Xueshuantong injection | 52.6 ± 1.1 | LMHC | 51.8 ± 1.5 | 14 | ①⑥ |
| 14 | Wang [27] | 62/62 | Xueshuantong injection | 71.69 ± 5.02 | Rivaroxaban | 72.16 ± 6.21 | 14 | ①②⑥ |
| 15 | Wang [28] | 130/130 | Xueshuantong injection | 46.62 ± 12.15 | Conventional treatment | 46.15 ± 12.12 | 3 | ①③ |
| 16 | Wu [29] | 40/40 | Xueshuantong injection | 73.45 | LMHC | 70.58 | 14 | ③ |
| 17 | Yang [30] | 36/36 | Xueshuantong injection + low-frequency physiotherapy | 46.5 ± 5.3 | Conventional treatment | 45.4 ± 4.1 | 14 | ②④⑤ |
| 18 | Ye et al. ([31]) | 38/38 | Xueshuantong injection + electric acupuncture | 68 ± 5 | LMHC | 66 ± 3.4 | 14 | ①②③ |
| 19 | Zeng et al. ([32]) | 30/30 | Xueshuantong injection | 61.23 ± 4.82 | LMHC | 61.34 ± 4.34 | 14 | ①②④⑤⑥ |
| 20 | Zhao ([33]) | 28/26 | Xueshuantong injection + LMHC | 45.62 ± 18.89 | LMHC | 45.20 ± 15.48 | 10 | ①②③⑥ |

Note. ①: DVT; ②: D-D; ③: therapeutic effect; ④: PT; ⑤: APTT; ⑥: hemorheology; ⑦: curative effect.

3.3.3. *PT*. Nine studies observed PT levels in patients after fracture surgery. There was a statistically significant degree of heterogeneity among individual studies ($I^2 = 99%$, $p < 0.00001$); therefore, a random effect model was performed for a meta-analysis, which showed that Xueshuantong injection or it combined with other treatment can improve patients' PT level (MD = 2.40 [95% CI (1.35, 3.44)]; Figure 5).

3.3.4. *APTT*. A total of 9 articles measured APTT. There was a statistically significant degree of heterogeneity among individual studies ($I^2 = 98%$, $p < 0.00001$); therefore, a random effect model was performed for a meta-analysis, which showed that Xueshuantong injection or it combined with other treatment can improve patients' APTT level (MD = 2.67 [95% CI (0.53, 4.81)]; Figure 6).

3.3.5. *Publication Bias Was Assessed Based on the Incidence of DVT*. The incidence of DVT included in the literature was

evaluated (Figure 7). Funnel plot results indicate that there is a certain publication bias in the study of Xueshuantong injection in the prevention of lower extremity deep vein thrombosis after orthopedic surgery. In order to further evaluate whether there is publication bias, STATA 13.0 software was used for the Begg test, and the results showed that $Z = 0.87$, $p = 0.387$, in which $p < 0.05$, had statistical difference, indicating no publication bias (Figure 8).

3.3.6. *Sensitivity Analysis*. The sensitivity analysis was carried out for the studies with $I^2 > 50%$. After each study was excluded one by one, the systematic evaluation was conducted. The change of I^2 was not significant, and the results did not change, indicating that the systematic evaluation was stable, and the results were reliable.

3.3.7. *Grading Evaluation of Evidence Quality*. GRADE was used to grade the evidence quality of the included literature.

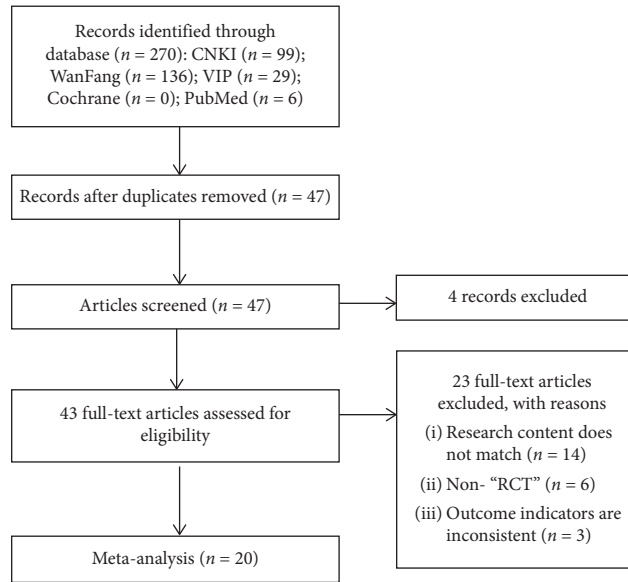


FIGURE 1: Document screening flowchart.

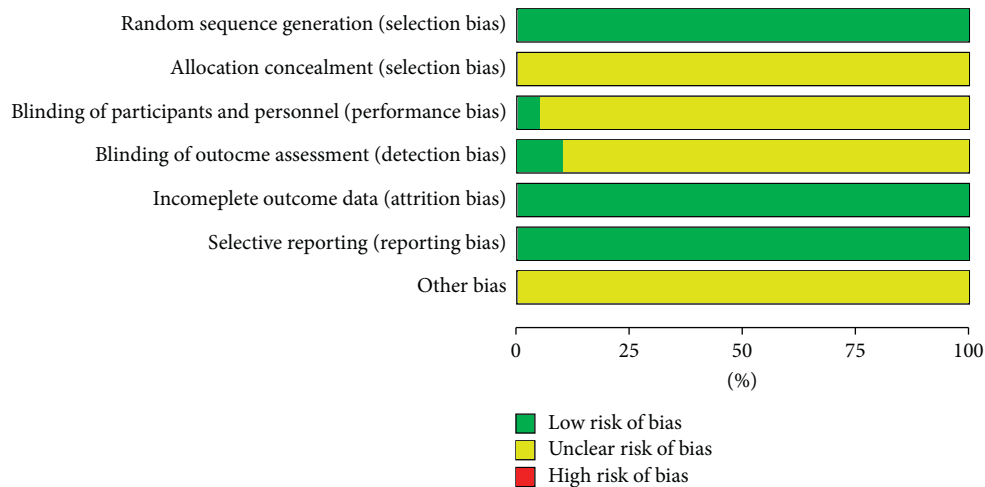


FIGURE 2: Document quality evaluation chart.

The incidence of DVT was the key outcome indicator, while D-D, PT, and APTT were the important outcome indicators. The results showed that the incidence of DVT was of moderate quality, and the other three indexes were all of low quality (Figure 9).

4. Discussion

The results of meta-analysis showed that the incidence of DVT and the level of D-D, PT, and APTT in the experimental group were better than those in the control group. The difference between the two groups was statistically significant, suggesting that Xueshuantong injection has played a great advantage in the prevention of deep venous thrombosis of lower limbs.

The incidence rate of DVT is caused by congenital factors in the postoperative stage of fracture, such as surgical correction, infection, and activity level [34, 35], especially in

large department of orthopedics operations, such as total hip replacement and total knee replacement, the risk of hip fracture is the largest [36, 37]. For patients with traumatic fracture, huge external energy such as falling injury or traffic injury may lead to vascular damage. In addition, immobility combined with long-term bed rest will slow down venous return, making patients prone to DVT, which may lead to lower limb paralysis or even death [38, 39]. Although low molecular weight heparin calcium, rivaroxaban, and other anticoagulants are widely used in patients with traumatic fracture, the incidence of perioperative DVT is still very high, so there are great challenges in exploring the prevention of postoperative DVT in fracture patients [40–42]. Traditional Chinese medicine (TCM) classifies DVT into the categories of “blood stasis syndrome,” “femoral swelling,” “pulse obstruction,” and “edema.” The main pathological factors are blood stasis. Due to surgical trauma and bed rest, the blood is damaged, the vein is damaged, the blood does

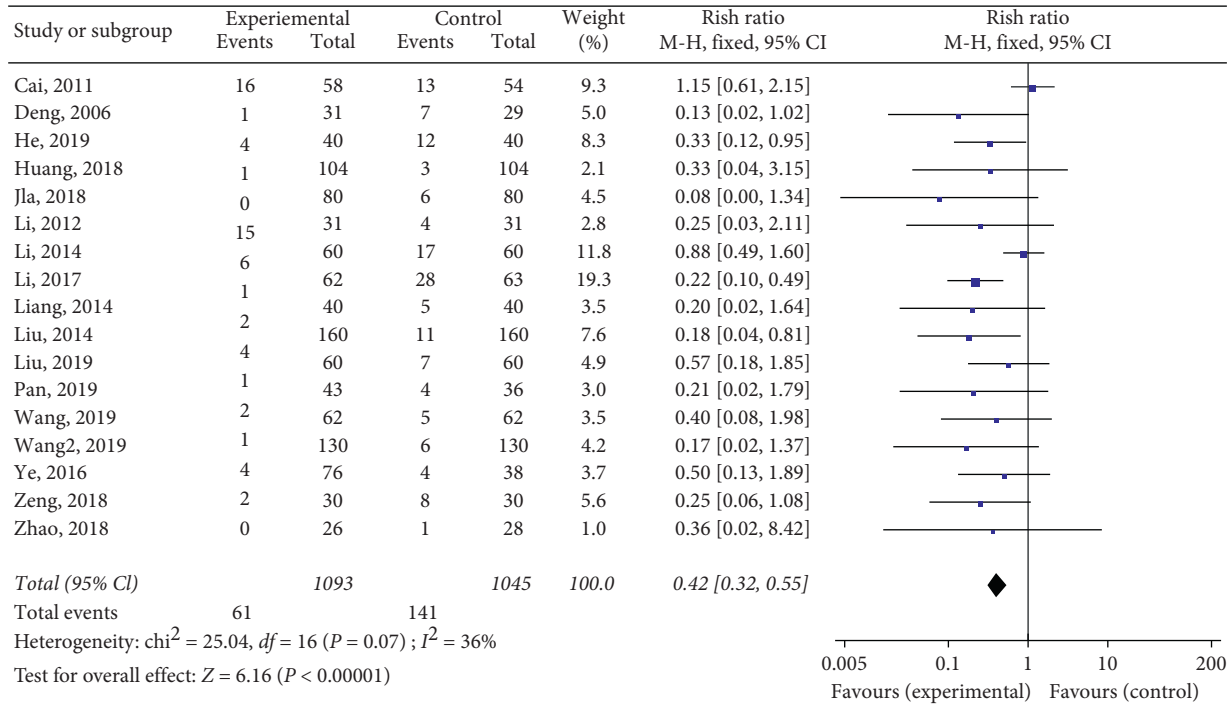


FIGURE 3: Forest map of incidence rate of DVT after Xueshuantong injection for preventing fracture.

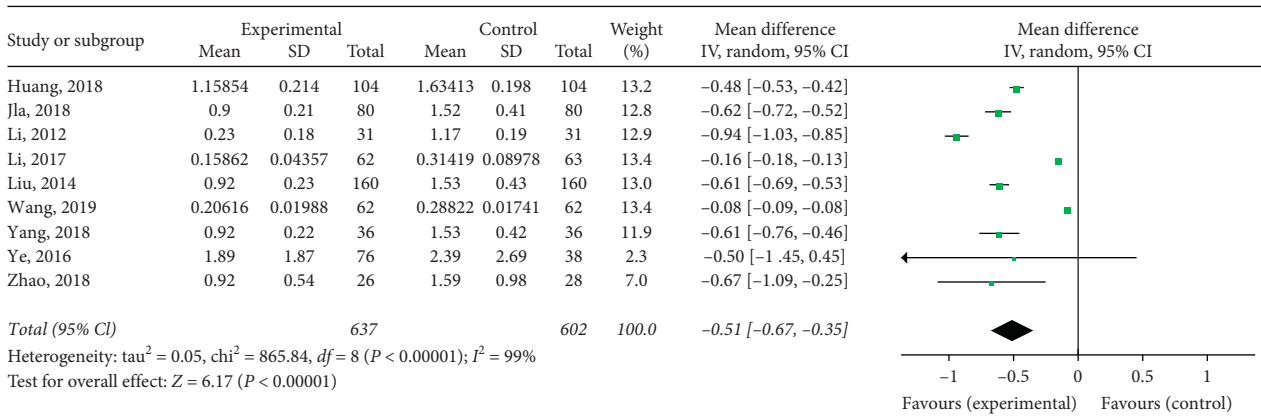


FIGURE 4: Forest map of D-D level in patients with Xueshuantong injection after fracture prevention.

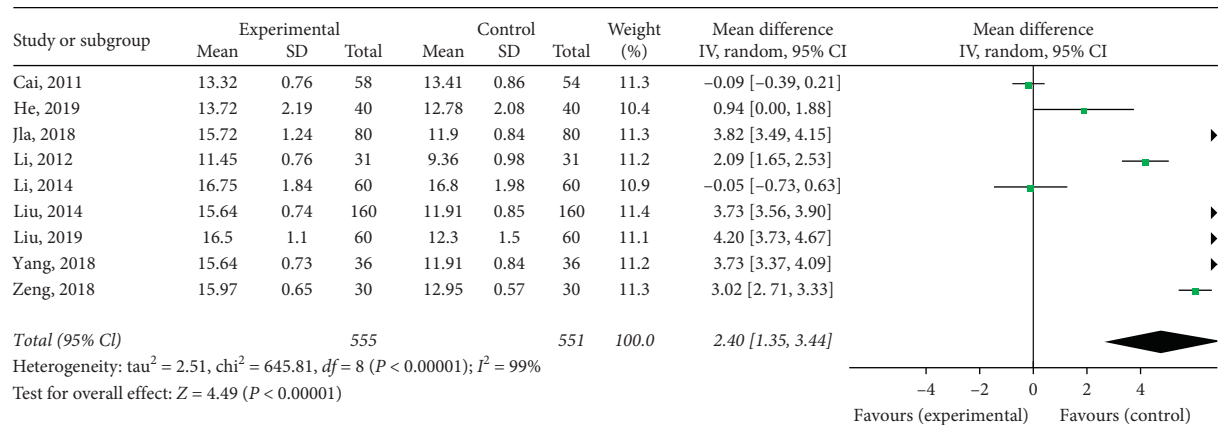


FIGURE 5: Forest map of PT level in patients with Xueshuantong injection after fracture prevention.

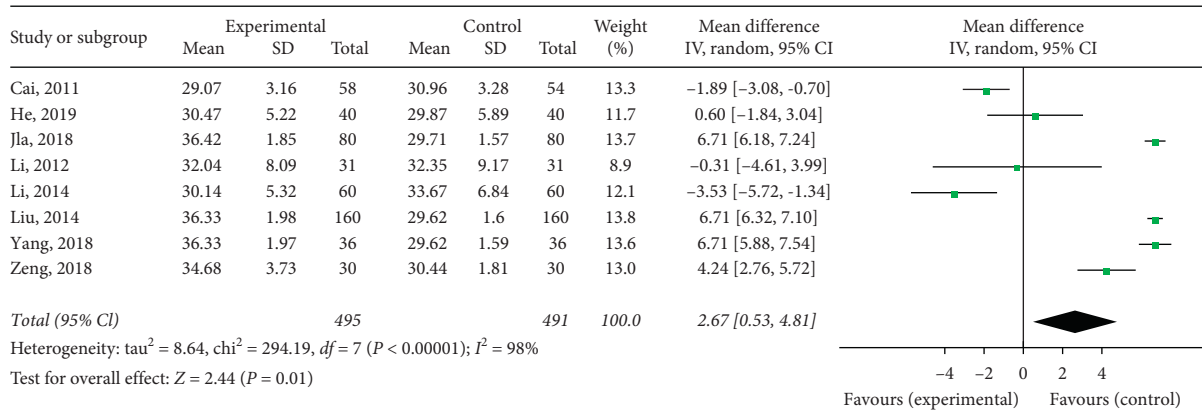


FIGURE 6: Forest map of APTT level in patients with Xueshuantong injection after fracture prevention.

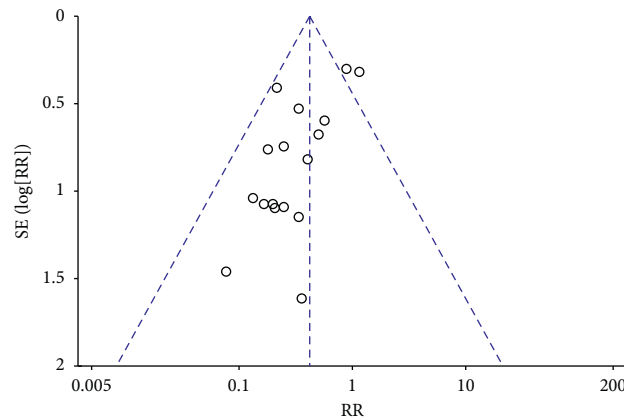


FIGURE 7: Funnel plot of incidence rate of DVT after Xueshuantong injection for preventing fracture.

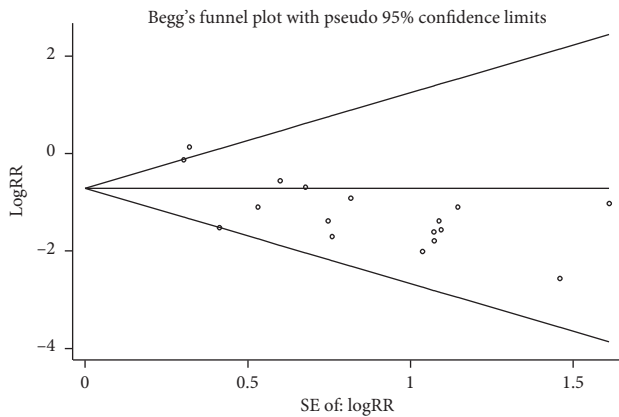


FIGURE 8: Begg's regression diagram with incidence of DVT.

not pass through, the blood away from the pulse is blocked, and the reflux is not smooth, which leads to thrombosis. Blood stasis can cause skin temperature to rise and become painful for a long time. According to the patient's constitution, kidney tonifying, heat clearing, dampness removing, and other methods are used. Xueshuantong injection is a traditional Chinese medicine injection made of total saponins extracted from *Panax notoginseng*, which belongs to a

modern dosage form of Chinese patent medicine [43]. Modern research shows that the main effective component of Xueshuantong injection is *Panax notoginseng* saponins, which can be widely used to treat various diseases, such as atherosclerosis, acute lung injury, cancer, and cardiovascular diseases [44–46]. In the related basic research and clinical application, its exact curative effect has been confirmed.

From the results of this study, the use of Xueshuantong injection in the prevention of lower limb venous thrombosis after fracture surgery was significantly lower than that of the control group, worthy of further study. In this meta-analysis, we mainly studied the efficacy of Xueshuantong injection to prevent the incidence of DVT in patients after fracture surgery in China and made a systematic analysis. On the basis of comparing the incidence of DVT, we also included the commonly used clinical observation indexes such as D-D, PT, and APTT, so as to observe the effect of Xueshuantong injection more comprehensively. However, there are still some deficiencies in this meta-analysis: (1) Although all the included literatures mentioned the method of randomized grouping, some of them lacked a detailed description of the concealment of the randomized scheme; (2) the number of included literatures was small, all of them were Chinese literatures, and there were some problems such as large sample size gap between literatures, insufficient detailed basic data, and incomplete

| Xueshuantong injection for DVT | | | | | | |
|--|--|---|---------------------------|------------------------------|---------------------------------|----------|
| Patient of population: patients with DVT | | | | | | |
| Settings: | | | | | | |
| Intervention: Xueshuantong injection | | | | | | |
| Outcomes | Illustrative comparative risks* (95% CI) | | Relative effect (95% CI) | No of participants (studies) | Quality of the evidence (GRADE) | Comments |
| | Assumed risk Control | Corresponding risk Xueshuantong injection | | | | |
| DVT Follow-up: 7-14 days | Study population 135 per 1000 | | RR 0.42 (0.32 to 0.55) | 2138 (17 studies) | ⊕⊕⊕⊕ moderate ¹ | |
| | Moderate 117 per 1000 | | | | | |
| D-D | The mean d-d in the intervention groups was 0.51 lower (0.67 to 0.35 lower) | | | 1239 (9 studies) | ⊕⊕⊕⊕ low ^{1,2} | |
| PT | The mean pt in the intervention groups was 2.40 higher (1.35 to 6.44 lower) | | | 1106 (9 studies) | ⊕⊕⊕⊕ low ¹ | |
| APTT | The mean aptt in the intervention groups was 2.67 higher (0.53 to 4.81 lower) | | | 986 (8 studies) | ⊕⊕⊕⊕ low ² | |

*The basis for the assumed risk (e.g. the median control group risk across studies) is provided in footnotes. The corresponding risk (and its 95% confidence interval) is based on the assumed risk in the comparison group and the relative effect of the intervention (and its 95% CI)

CI: Confidence interval; RR: Risk ratio;
GRADE Working Group grades of evidence
High quality: Further research is very unlikely to change out confidence in the estimate of effect.
Moderate quality: Further research is likely to have an important impact on out confidence in the estimate of effect and may change the estimate.
Low quality: Further research is very likely to have an important impact on out confidence in the estimate of effect and is likely to change the estimate.
Very low quality: We are very uncertain about the estimate

¹ Random methods are not described in detail
² No explanation was provided

FIGURE 9: Grading evaluation chart of evidence quality.

unification of treatment cycle; (3) all the included literatures were published articles. If there are no unpublished results, studies with negative results may be missed, and there is a risk of reducing the strength of the argument. Therefore, the evidence strength of the conclusion of this study needs to be further improved, and more high-quality RCTs are needed to verify, so as to obtain a more accurate conclusion on the effect of Xueshuantong injection in preventing lower extremity deep vein thrombosis after fracture surgery, so as to provide good clinical guidance for the prevention of lower extremity deep vein thrombosis after fracture surgery.

Data Availability

The data used to support the findings of this study are included within the article.

Conflicts of Interest

The authors declare no conflicts of interest.

Authors' Contributions

Shu-ting Yan, Feng Gao, and Tai-Wei Dong contributed equally to this work.

Acknowledgments

This work was financially supported by grants from the innovative team plan of the Second Affiliated Hospital of Shaanxi University of Chinese Medicine (2020XKTD-A04).

References

- [1] K. Song, Z. Rong, Y. Shen, M. Zheng, and Q. Jiang, "pre-operative incidence of deep vein thrombosis (DVT) and its correlation with postoperative DVT in patients undergoing elective surgery for femoral neck fractures," *Archives of Orthopaedic and Trauma Surgery*, vol. 136, no. 10, pp. 1459–1464, 2016.
- [2] S. M. Yao, H. Murakami, and M. Nakane, "Deep vein thrombosis in the lower extremities in comatose elderly patients with acute neurological diseases," *Yonsei Medical Journal*, vol. 57, no. 2, pp. 388–392, 2016.
- [3] J. D. F. Tomita, E. Domeij-Arverud, C. N. van Dijk, and P. W. Ackermann, "Meta-analysis and suggested guidelines for prevention of venous thromboembolism (VTE) in foot and ankle surgery," *Knee Surgery, Sports Traumatology, Arthroscopy*, vol. 24, no. 4, pp. 1409–1420, 2016.
- [4] S. Freeman, "Management of deep vein thrombosis (DVT) prophylaxis in trauma patients," *Bull Emerg Trauma*, vol. 1, no. 4, pp. 1–7, 2016.
- [5] S. Decker and M. J. Weaver, "Deep venous thrombosis following different isolated lower extremity fractures: what is known about prevalences, locations, risk factors and prophylaxis?" *European Journal of Trauma and Emergency Surgery*, vol. 39, no. 6, pp. 591–598, 2013.
- [6] M. McCullough and R. T. Zamanian, "Prevention of deep vein thrombosis and pulmonary embolism in high-risk medical patients," *Clinics in Chest Medicine*, vol. 39, no. 3, pp. 483–492, 2018.
- [7] S. Y. Kholdani, C. Y. Chung, K. M. Lee, S.-S. Kwon, K. H. Sung, and M. S. Park, "Incidence of f deep vein thrombosis after major lower limb orthopedic surgery: analysis of a nationwide claim registry," *Yonsei Medical Journal*, vol. 56, no. 1, pp. 139–145, 2015.

- [8] Y.-H. Ro, J.-W. Park, and J.-S. Kim, "Prevalence of deep vein thrombosis and pulmonary embolism treated with mechanical compression device after total knee arthroplasty in asian patients," *The Journal of Arthroplasty*, vol. 30, no. 9, pp. 1633–1637, 2015.
- [9] C. J. Kulkarni, "Atrial fibrillation increases the risk of peripheral arterial disease with relative complications and mortality: a population-based cohort study," *Medicine (Baltimore)*, vol. 9, no. 95, e3002 pages, 2016.
- [10] American College of Clinical Pharmacy, *Accp/Scm Critical Care Pharmacy Preparatory Review and Recertification Course*, American College of Clinical Pharmacy, Lenexa, KS, USA, 2016.
- [11] American Academy of Orthopaedic Surgeons, *Aaos Comprehensive Orthopaedic Review*, American Academy of Orthopaedic Surgeons, Rosemont, IL, USA, 2nd edition, 2014.
- [12] Y. Huang, B. Shi, Q. Gao, and Q. Zhou, "Chinese herbal medicine xueshuantong enhances cerebral blood flow and improves neural functions in alzheimer's disease mice," *Journal of Alzheimer's Disease*, vol. 63, no. 3, pp. 1089–1107, 2018.
- [13] R. L. Guo, "Xueshuantong for injection (lyophilized,) alleviates streptozotocin-induced diabetic retinopathy in rats," *Chinese Journal of Integrative Medicine*, vol. 5, no. 15, pp. 32–34, 2020.
- [14] H. Cai, "A comparative study of Chinese herbal medicine and western medicine for prophylaxis Against deep venous thrombosis," *Orthopedic Journal of China*, vol. 19, no. 19, pp. 1585–1588, 2011.
- [15] S. L. Deng, "Cutative effect observation of panax notoginsenosidum in preventing DVT in lower limb fracture," *Journal of Military Surgeon in Southwest China*, vol. 6, no. 8, pp. 19–20, 2006.
- [16] Y. L. He and D. Cao, "Effect of xueshuantong injection and low-molecular-weight heparin for anticoagulation of senile hip fracture patients received operation," *Contemporary Medical Symposium*, vol. 2, no. 17, pp. 9–11, 2019.
- [17] X. J. Huang, "Effect of xueshuantong combined with tongmaidan on dimer in elderly patients with hip fracture during perioperative period," *Journal of SNAKE (Science & Nature)*, vol. 4, no. 30, pp. 600–603, 2018.
- [18] S. L. Jia and H. Tang, "Study on the effect of thrombolysis therapy on the prevention of lower extremity deep venous thrombosis in elderly patients," *Biped and Health*, vol. 14, no. 07, pp. 113–114, 2018.
- [19] J. Li, "Xueshuotong injection improved hypercoagulability after orthopedic surgery in 31 cases," *Herald of Medicine*, vol. 8, no. 31, pp. 1032–1034, 2012.
- [20] Z. Y. Li, "Effect study of Chinese and western medicine used in prevention of deep vein thrombosis after artificial hip joint surgery," *China Modern Medicine*, vol. 13, no. 21, pp. 61–63, 2014.
- [21] W. H. Li, C. E. Chiang, C. P. Lau et al., "Efficacy and safety of dabigatran, rivaroxaban, and warfarin for stroke prevention in Chinese patients with atrial fibrillation: the Hong Kong Atrial fibrillation Project," *Clinical Cardiology*, vol. 40, no. 4, pp. 222–229, 2017.
- [22] J. Y. Huang, "Xueshuantong combined with low molecular heparin for deep vein thrombosis after hip fracture surgery in elderly patients," *International Medicine and Health Guidance News*, vol. 24, no. 20, pp. 3796–3798, 2014.
- [23] S. W. Liu, "The prevention and treatment of deep vein thrombosis of lower extremity after fracture operation," *China Practical Medicine*, vol. 18, no. 7, pp. 62–63, 2012.
- [24] J. P. Liu, "Analysis of the effect of xueshuantong injection on the prevention of lower extremity deep venous thrombosis in elderly patients after operation," *Chinese and Foreign Medical Research*, vol. 7, no. 12, pp. 28–30, 2014.
- [25] F. S. Liu, "Preventive effect of xueshuantong combined with low molecular weight heparin on deep vein thrombosis after hip fracture surgery," *Chinese Journal of Thrombosis and Hemostasis*, vol. 6, no. 26, pp. 923–924, 2019.
- [26] X. M. Pan and L. Teng, "Analysis of the effect of xueshuantong injection combined with low molecular weight heparin calcium on the prevention of deep venous thrombosis after hip fracture," *Journal of Frontiers of Medicine*, vol. 33, no. 9, pp. 87–88, 2019.
- [27] Q. Wang, "Analysis of the curative effect of xueshuantong injection in treating traumatic fracture," *Chinese Journal of Modern Drug Application*, vol. 24, no. 13, pp. 195–197, 2019.
- [28] S. G. Wang, "Effect of xueshuantong on blood hyper-coagulability, bone metabolism, and rehabilitation process in osteoporotic patients with replacement therapy after femoral neck fractures," *Chinese Journal of Osteoporosis*, vol. 9, no. 25, pp. 1312–1317, 2019.
- [29] H. Wu, "After the thrombus passes the prevention old age hip department bone fracture technique, lower limb deep vein thrombus curative effect observation," *Chinese Manipulation and Rehabilitation Medicine*, vol. 6, no. 2, pp. 64–65, 2012.
- [30] X. H. Yang, "Prevention of venous thrombosis in patients undergoing orthopedic lower extremity surgery by xueshuantong injection combined with low frequency physiotherapy," *Heilongjiang Journal of Traditional Chinese Medicine*, vol. 05, no. 47, pp. 133–144, 2018.
- [31] L. J. Ye, "The clinical research into deep vein thrombosis of lower extremity after senior hip fractures operation treated with electro-acupuncture in combination with xueshuantong," *Henan Traditional Chinese Medicine*, vol. 6, no. 36, pp. 1048–1050, 2016.
- [32] X. B. Zeng, "Effect of xueshuantong combined with low molecular weight heparin calcium in the prevention of deep vein thrombosis of lower limbs after hip fracture surgery," *Clinical Medicine & Engineering*, vol. 11, no. 25, pp. 1461–1462, 2018.
- [33] X. F. Zhao, "Clinical observation on prevention of DVT with xueshuantong Injection after operation of tibial plateau fracture," Shaanxi University of Traditional Chinese Medicine, Xi'an, China, 2017.
- [34] M. Choi and M. Hector, "Management of venous thromboembolism for older adults in long-term care facilities," *Journal of the American Academy of Nurse Practitioners*, vol. 24, no. 6, pp. 335–344, 2012.
- [35] F. J. I. Fowkes and F. G. R. Fowkes, "Incidence of diagnosed deep vein thrombosis in the general population: systematic review," *European Journal of Vascular and Endovascular Surgery*, vol. 25, no. 1, pp. 1–5, 2003.
- [36] F. Price, "Venous thromboembolism prophylaxis in major orthopaedic surgery: a multicenter, prospective, observational study," *Acta Orthopaedica et Traumatologica Turcica*, vol. 5, no. 42, pp. 322–327, 2008.
- [37] S. B. Deitelzweig, A. N. Amin, D. J. Brotman, A. K. Jaffer, and A. C. Spyropoulos, "Prevention of venous thromboembolism in the orthopedic surgery patient," *Cleveland Clinic Journal of Medicine*, vol. 75, no. Suppl_3, S27 pages, 2008.
- [38] F. Y. McKean, "Endovascular embolization of pulmonary arteriovenous malformations," *Chinese Medical Journal* (, vol. 1, no. 123, pp. 23–28, 2010.

- [39] R. Goldfisher, "Lower-extremity venous ultrasound - past, present and future," *Pediatric Radiology*, vol. 47, no. 9, pp. 1209–1213, 2017.
- [40] C. Kearon, J. Ornelas, A. Blaivas et al., "Antithrombotic Therapy for VTE Disease," *Chest*, vol. 149, no. 2, pp. 315–352, 2016.
- [41] V. Akl, S. Patel, C. Gibbons, and M. Vizcaychipi, "Efficacy and safety of rivaroxaban thromboprophylaxis after arthroplasty of the hip or knee: retrospective cohort study," *The Annals of The Royal College of Surgeons of England*, vol. 98, no. 7, pp. 507–515, 2016.
- [42] W. M. Hua, J. P. Johnson, and A. H. Daniels, "Assessment of 30-day mortality and complication rates associated with extended deep vein thrombosis prophylaxis following hip fracture surgery," *Injury*, vol. 49, no. 6, pp. 1141–1148, 2018.
- [43] T. Goodman, R. Guo, G. Zhou et al., "Traditional uses, botany, phytochemistry, pharmacology and toxicology of panax notoginseng (burk.) F.H. Chen: a review," *Journal of Ethnopharmacology*, vol. 188, pp. 234–258, 2016.
- [44] K. Kitamura, T. Iwamoto, M. Nomura et al., "Dammarane-type triterpene extracts of panax notoginseng root ameliorates hyperglycemia and insulin sensitivity by enhancing glucose uptake in skeletal muscle," *Bioscience, Biotechnology, and Biochemistry*, vol. 81, no. 2, pp. 335–342, 2017.
- [45] B. Takamura and W.-H. Chan, "Oxidative stresses-mediated apoptotic effects of ginsenoside Rb1 on pre- and post-implantation mouse embryos in vitro and in vivo," *Environmental Toxicology*, vol. 32, no. 8, pp. 1990–2003, 2017.
- [46] C. Xu, W. Wang, B. Wang et al., "Analytical methods and biological activities of panax notoginseng saponins: recent trends," *Journal of Ethnopharmacology*, vol. 236, pp. 443–465, 2019.

Research Article

Jisuikang Promotes the Repair of Spinal Cord Injury in Rats by Regulating NgR/RhoA/ROCK Signal Pathway

Chengjie Wu ^{1,2}, Yuxin Zhou,² Pengcheng Tu,^{1,2} Guanglu Yang,^{1,2} Suyang Zheng,^{1,2} Yalan Pan,³ Jie Sun,^{1,2} Yang Guo ^{1,2}, and Yong Ma ^{1,2}

¹Department of Traumatology and Orthopedics, Affiliated Hospital of Nanjing University of Chinese Medicine, Nanjing, China

²Laboratory of New Techniques of Restoration & Reconstruction, Institute of Traumatology & Orthopedics, Nanjing University of Chinese Medicine, Nanjing, China

³Laboratory of Chinese Medicine Nursing Intervention for Chronic Diseases, Nanjing University of Chinese Medicine, Nanjing, China

Correspondence should be addressed to Yang Guo; drguoyang@126.com and Yong Ma; mayong@njucm.edu.cn

Received 10 June 2020; Revised 14 September 2020; Accepted 17 October 2020; Published 28 November 2020

Academic Editor: Arham Shabbir

Copyright © 2020 Chengjie Wu et al. This is an open access article distributed under the Creative Commons Attribution License, which permits unrestricted use, distribution, and reproduction in any medium, provided the original work is properly cited.

Jisuikang (JSK) is an herbal formula composed of many kinds of traditional Chinese medicine, which has been proved to be effective in promoting the rehabilitation of patients with spinal cord injury (SCI) after more than ten years of clinical application. However, the mechanisms of JSK promoting nerve regeneration are yet to be clarified. The aim of this study was to investigate the effects of JSK protecting neurons, specifically the regulation of NgR/RhoA/ROCK signal pathway. The motor function of rats was evaluated by the BBB score and inclined plate test, Golgi staining and transmission electron microscope were used to observe the microstructure of nerve tissue, and fluorescence double-labeling method was used to detect neuronal apoptosis. In this study, we found that JSK could improve the motor function of rats with SCI, protect the microstructure (mitochondria, endoplasmic reticulum, and dendritic spine) of neurons, and reduce the apoptosis rate of neurons in rats with SCI. In addition, JSK could inhibit the expression of Nogo receptor (NgR) in neurons and the NgR/RhoA/ROCK signal pathway in rats with SCI. These results indicated JSK could improve the motor function of rats with SCI by inhibiting the NgR/RhoA/ROCK signal pathway, which suggests the potential applicability of JSK as a nerve regeneration agent.

1. Introduction

Spinal cord injury (SCI) is a disease with severe damage to the central nervous system, which has a complex pathological process and is difficult to recover in the later stage. The incidence of SCI is increasing year by year, so it is urgent to find a treatment to reduce the disability rate [1, 2]. However, traditional Chinese medicine has been concerned by more and more clinicians and scholars because of its advantages of multitargets and low side effects. The pathogenesis core of SCI is “deficiency of kidney governor, stasis of governor pulse, and dereliction of duty of cardinal command.” JSK is a compound prescription of traditional Chinese medicine established under the guidance of this theory, which is very effective in the clinical treatment of SCI [3, 4].

In China, Buyang Huanwu decoction, as an important representative herbal formula for the treatment of SCI, has the function of restoring nerve and has a history of hundreds of years [5, 6]. However, the mechanism of Buyang Huanwu decoction is not clear, mainly related to thioredoxin system [7], glutamate [8], cAMP/CREB/RhoA signal pathway [9], apoptosis-related proteins [10], etc. JSK is formed by the addition and subtraction of Buyang Huanwu decoction, which is in line with the current clinical characteristics of SCI. After a large number of clinical tests, JSK has achieved satisfactory clinical efficacy, and part of its mechanism has been explained by animal and cell experiments [3, 4, 11–14]. *Astragalus membranaceus*, *Salvia miltiorrhiza*, and Ligustrazine are the main pharmacological components of JSK and have important therapeutic effects. *Astragalus membranaceus* has antioxidant and neuroprotective effects in

vivo, which provides the possibility for improving the symptoms of SCI [15–17]. *Salvia miltiorrhiza* has the effects of promoting blood circulation [18], antioxidation, and anti-inflammation [19], neuroprotection [20], etc. Ligustrazine can protect SCI by inhibiting inflammatory cytokines [21], inhibiting apoptosis [22, 23], and scavenging oxygen free radicals [24].

SCI is generally considered to be a devastating injury, and the growth of axons in the central nervous system is limited, so it could not be recovered. However, Aguayo et al. transplanted part of the peripheral nerve tissue into the transected spinal cord and found that the axons of the central nervous system could grow into the transplanted tissue, suggesting that neurons could grow after the adult central nervous system was damaged, but it was limited by the environment [25, 26]. Other studies have shown that the white matter homogenate of the central nervous system limits the growth of nerve axons [27], and oligodendrocytes and myelin sheath of the central nervous system can induce the collapse of the growth cone [28]. These proteins that inhibit axon growth are called myelin-associated inhibitors (MAIs), which mainly include neurite outgrowth inhibitor (Nogo), myelin-associated glycoprotein (MAG), and oligodendrocyte myelin glycoprotein (OMgp) [29]. Nogo receptor (NgR) can specifically bind to the above three kinds of MAIs and inhibit axonal regeneration [30], and the expression of NgR is directly related to the ability of central nervous cell regeneration [31], so NgR is considered to be one of the important targets for promoting axonal regeneration. In addition, the NgR/RhoA/ROCK signal pathway is an important way to inhibit neuronal axonal regeneration. Therefore, in this study, the development of NgR/RhoA/ROCK signal pathway in rats with SCI in different time periods and the intervention effect of JSK were studied to explore part of the mechanism of improving SCI.

2. Methods and Materials

2.1. Chemicals. Prednisone (Tianjin Chemical Company, Tianjin, China) was dissolved and diluted in salt solution (final concentration is 0.3%), pentobarbital sodium (China Pharmaceutical Group Shanghai Chemical Reagents Co. LTD), and paraformaldehyde (Nanjing Fumace Biotechnology Co. LTD); JSK was composed of milkvetch root (30 g), Chinese angelica (12 g), red peony root (12 g), earthworm (10 g), *Cistanche deserticola* (10 g), *Salvia miltiorrhiza* (10 g), Szechwan lovage rhizome (10 g), peach seed (10 g), safflower (10 g), etc. (Pharmacy, Affiliated Hospital of Nanjing University of Chinese Medicine). JSK (crude drug 1.25 g/mL) was prepared by boiling, steam boiling, and concentration.

2.2. Animals. The animals used in this study were from the Animal Experimental Center of Nanjing University of Chinese Medicine, and the research scheme was approved by the Animal Ethics Committee of the affiliated Hospital of Nanjing University of Chinese Medicine. The experimental procedure follows the National Institutes of Health Guide

for the Care and Use of Laboratory Animals (Institute of Laboratory Animal Resources 1996). Eighty female SD rats with weight of 180–200 g were purchased from Qinglongshan Animal Breeding Farm in Nanjing, and the experimental animal license number was SYXK (SU) 2018-0049. Rats were kept in captivity at the Animal Experimental Institute of Nanjing University of Chinese Medicine (Nanjing, China) to eat and drink freely under controlled temperature and humidity.

2.3. SCI Rat Model. The acute SCI model based on the improved Allen method was used [32]. In short, all rats were anesthetized intraperitoneally with 1% pentobarbital sodium (50 mg/kg). The segment T9–11 of spinal cord was exposed surgically, and the segment T10 of spinal cord was hit with spinal cord percussion device (RWD Company). The weight and diameter of the falling object were 10 g and 2.5 mm, respectively, and the falling height and depth were 10 cm and 2 mm, respectively. The tension of the rat hind limbs was eliminated immediately, indicating that the model was established successfully. In the sham group, the spinal cord was exposed but not injured. The rats were randomly divided into four groups: sham group (intra-gastric infusion with normal saline, 20 mL/kg/d), model group (intra-gastric infusion with normal saline, 20 mL/kg/d), prednisone (PED) group (intra-gastric infusion with prednisone, 60 mg/kg/d), and JSK group (intra-gastric infusion with JSK, 25 g/kg/d). The rats were killed after the last intervention, and the samples were taken on the 7th, 14th, 21st, and 28th days after injury.

2.4. Basso, Beattie, and Bresnahan (BBB) Score. According to the observation of hindlimb movement, especially gait and coordination, the BBB test was carried out in the open field. Through double-blind and double-independent observation, all groups were evaluated on the 7th, 14th, 21st, and 28th days after operation [33].

2.5. Oblique Board Test. The oblique board test was carried out on all rats before operation and on the 1st, 7th, 14th, 21st, and 28th day after operation. The rats were placed on a rectangular oblique board perpendicular to the longitudinal axis of the oblique board. The oblique board was lifted, and the maximum angle was recorded at which the rats stayed on the board for more than 5 seconds. Each rat was tested for 3 times, and the average value was taken as the final result.

2.6. Golgi Staining. The spinal cord was fixed in 4% polyformaldehyde solution and cut into 2–3 mm thick tissue blocks after rinsing. The brain tissue blocks were completely immersed in Golgi staining solution and treated without light for 14 days. After being removed, it was dehydrated at 4°C in 15% sucrose solution and dehydrated for 1 day under the condition of avoiding light and dehydrated in 30% sucrose solution for 2 days. It was immersed in concentrated ammonia water for 45 minutes, distilled water for 1 minute, fixing solution treatment for 45 minutes, and distilled water

washing for 1 minute. It was dehydrated in 30% sucrose solution for 2-3 days and cut into 100 μm frozen section, sealed by glycerin gelatin. Microscopic examination and image acquisition were carried out.

2.7. Observation by Using Transmission Electron Microscope.

After the spinal cord was removed, it was fixed with electron microscope fixation solution at 4°C for 2–4 hours and rinsed with 1% osmic acid at 20°C for 2 hours. The organization in turn enters 50%-70%-80%-90%-95%-100%-100% alcohol-100% acetone-100% acetone, each time by 15 minutes. Acetone: 812 embedding agent = 1 : 1 was permeated for 2–4 hours; acetone: 812 embedding agent = 2 : 1 was permeated overnight, and pure 812 embedding agent was permeated for 5–8 hours, and then it was in 37°C oven overnight and polymerized at 60°C for 48 hours. It was cut into the ultrathin slices of 60–80 nm and double stained by uranium and lead, and the slices were dried at room temperature overnight. The images were collected and analyzed under the transmission electron microscope.

2.8. Fluorescent Double-Labeling Method of TUNEL and NeuN.

Frozen sections of the spinal cord were fixed with 4% paraformaldehyde for 15 minutes and washed twice by PBS. 0.5% TritonX-100 was added to incubate for 5 minutes at room temperature. 5% fetal bovine serum was added at room temperature for 2 hours; NeuN first antibody of 1 : 1000 was added and incubated overnight at 4°C and washed 3 times. Fluorescent secondary antibody Alexa fluor 594 was added and incubated at room temperature and hidden from light for 1 hour. According to the instructions of the TUNEL kit, proper amount of detection solution was added sequentially and washed 3 times after incubation at 37°C for 1 hour. The plates were sealed with antifluorescence quenching solution and observed under the fluorescence inverted microscope.

2.9. Fluorescent Double-Labeling Method of NeuN and NgR.

Frozen sections of spinal cord were fixed with 4% paraformaldehyde for 15 minutes, permeated with 0.5% Triton-100 for 10 minutes, and washed with PBS for 3 times. 5% goat serum was added at room temperature for 60 minutes. The first antibody NeuN (1 : 300) and NGR (1 : 300) was added and incubated overnight at 4°C. The second antibody Alexa fluor 594 and Alexa fluor 488 was added and incubated for 1 hour. After Dapi restaining, the plates were observed under fluorescence inverted microscope.

2.10. *Immunohistochemistry.* After the paraffin sections were dewaxed to water, the slides were immersed in citric acid antigen repair buffer, boiled water for antigen repair. They were transferred to 3% hydrogen peroxide solution and incubated in room temperature for 25 minutes. 3% BSA was dripped to cover the tissue evenly at room temperature for 30 minutes. The first antibody was dripped and incubated overnight at 4°C. HRP-labeled secondary antibody was dripped and incubated at room temperature for 60 minutes.

After drying, the slices were dripped with DAB chromogenic solution, then hematoxylin restaining was done, followed by hydrochloric acid alcohol differentiation, ammonia water returning to blue, and rinsed with running water. The slices were dehydrated and transparent in gradient alcohol and xylene, and the plates were observed under the microscope.

2.11. *Western Blot Assay.* The protein from the spinal cord was extracted and quantified by the BCA method. After adding buffer, the protein was boiled for 10 minutes and stored at –20°C to be tested. After preparing the glue, electrophoresis was carried out by 100 V constant voltage for 90 minutes, and PVDF membrane was used by 100 V for 60 minutes. 5% skimmed milk powder was added at room temperature for 2 hours, GAPDH and NgR, RhoA, and ROCK antibodies were prepared according to the ratio of 1 : 1000 and incubated overnight at 4°C. On the next day, the second antibody was prepared according to the proportion of 1 : 10000 and incubated at room temperature for 2 hours. An ECL developer was added, a gel imaging system was developed, and the ImageJ image analysis system was used to analyze the bands.

2.12. *qRT-PCR.* The RNA in the spinal cord was extracted with RNAiso for RNA (Takara, Japan) and then reverse transcribed with TaKaRa reverse transcription kit and frozen at –20°C. The sequence was found on Genbank, and primers were designed and synthesized in Shanghai Shenggong. GAPDH and NgR were detected by qPCR using TaKaRa TB Green TM Premix Ex Taq TM II PCR kit (Takara, Japan).

2.13. *Statistic Analysis.* SPSS 20.0 software was used for statistical analysis. The data were shown as mean \pm SD. One-way ANOVA and SNK-q test were used to analyze the differences among groups. The figures were edited by GraphPad Prism 8.0.2 software. A value of $P < 0.05$ was considered statistically significant.

3. Results

3.1. *JSK Promotes the Recovery of Motor Function in Rats with SCI.* The BBB score and oblique board test were carried out before operation and on the 1st, 7th, 14th, 21st, and 28th days after operation. The rats with SCI showed a gradual recovery of motor function, while JSK could gradually accelerate the process, and the effect was similar to the PED (Figure 1). The above results show that JSK has the potential to treat SCI.

3.2. *JSK Can Improve the Microstructure of Neurons in Rats with SCI.* The results of the transmission electron microscope showed that the microstructure of spinal myelin sheath and neurons were destroyed after SCI. JSK could alleviate the injury of myelin sheath and neurons after SCI, and at 7 d–28 d, it gradually improved (Figure 2). Golgi staining results showed that, after SCI, the dendrites were destroyed, the length became shorter, and the number of dendritic spines decreased. JSK could alleviate the injury of

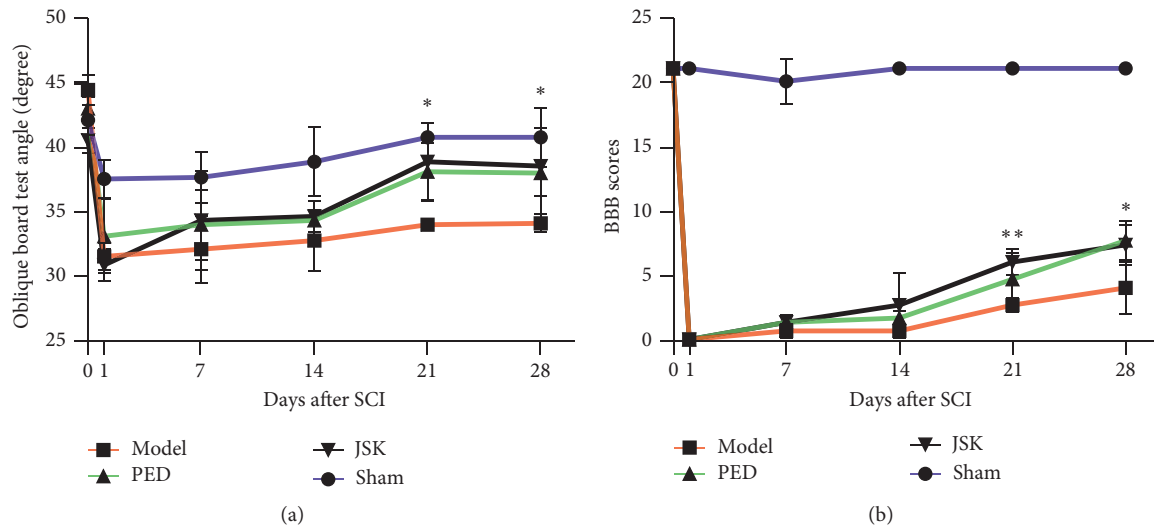


FIGURE 1: JSK and PED promoted the recovery of motor function in rats with SCI. (a) The oblique board test showed that the motor ability of rats decreased after SCI, and the recovery of motor function could be accelerated after using JSK and PED. At the third week, the promoting effect of JSK was significantly different from the model group. (b) BBB score showed that the motor ability of rats decreased after SCI, and the recovery of motor function could be accelerated after using JSK and PED. At the third and fourth weeks, the promoting effect of JSK was significantly different from that of the model group. The data were presented as mean \pm SD; $n = 3/\text{group}$, * $P < 0.05$, and ** $P < 0.01$.

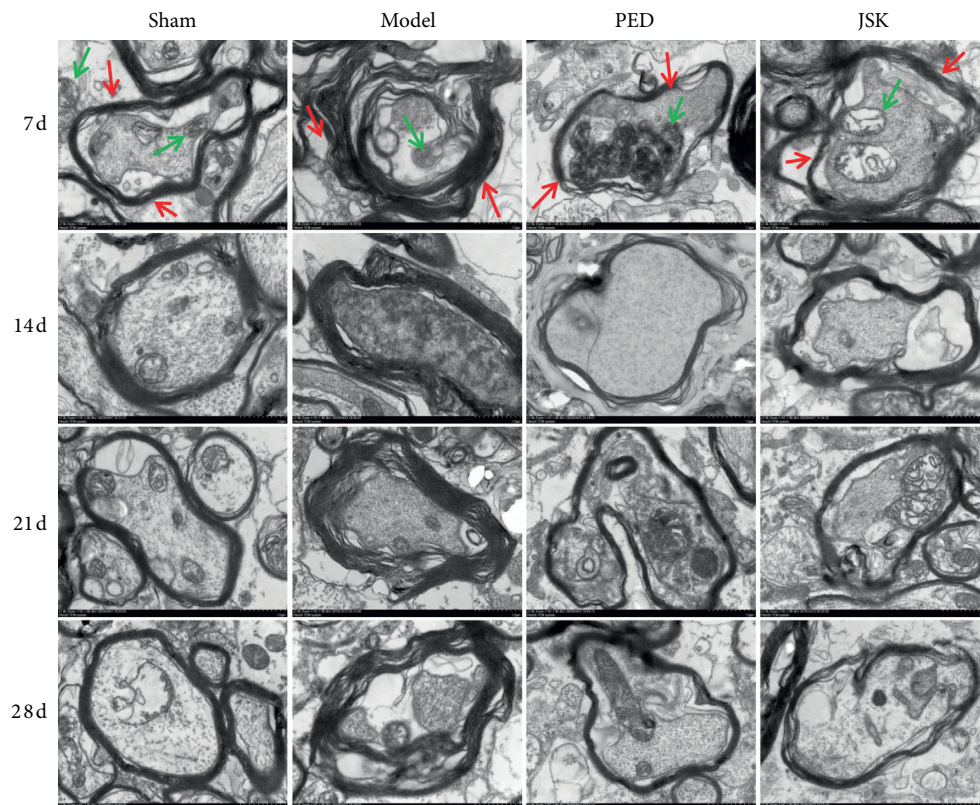
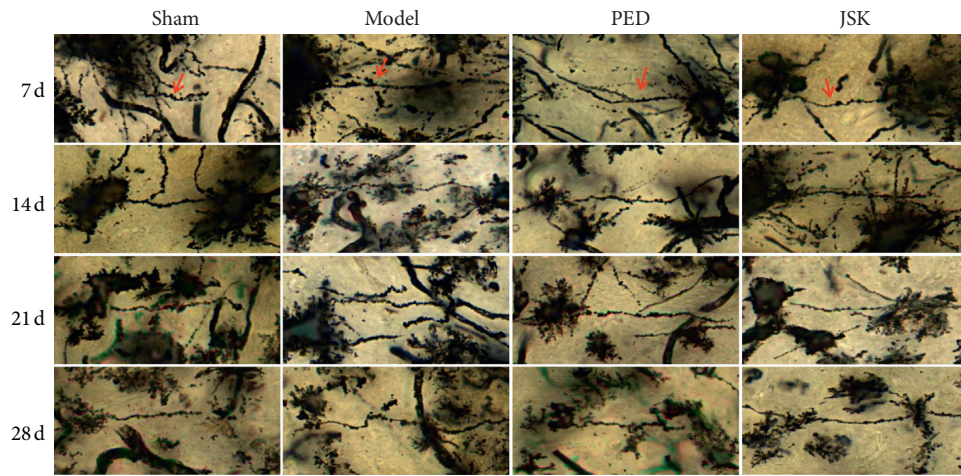
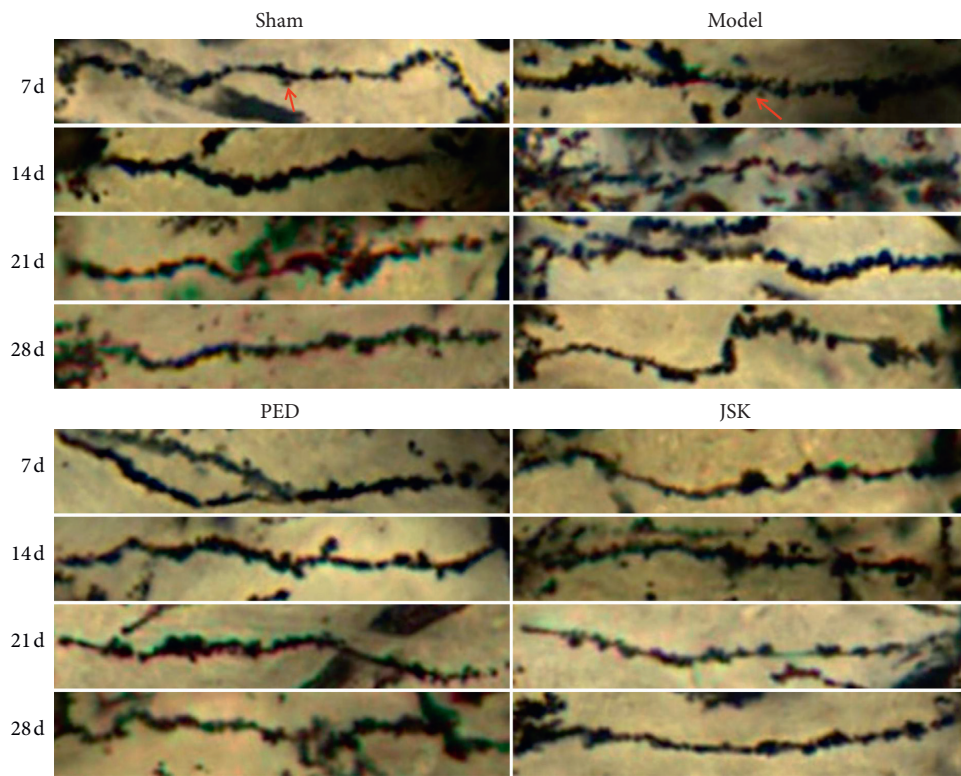


FIGURE 2: JSK improved the microstructure of neurons in rats with SCI. In the sham group, the shape of spinal myelin sheath was regular, like concentric circular arrangement, and it had a complete structure. The neurons were oval and had complete cell membrane structure, abundant organelles, more mitochondria and rough endoplasmic reticulum, no obvious rupture, or deletion of mitochondrial crest, and the morphology at 7 d–28 d was basically the same. In the model group, the shape of spinal myelin sheath was irregular, and the structure was disordered and incomplete, with partial breakage or deletion, local curl, and wrinkle. The number of neurons and mitochondria decreased, and there were dissolution of part of mitochondria, rupture and deletion of mitochondrial crest, and little change in morphology on 7 d–28 d. The myelin sheath shape of the spinal cord in the JSK group and the prednisone group was improved, the shape was more regular, the structure was more complete, the number of neurons and mitochondria was more, and the morphology of 7 d–28 d was greatly improved compared with the model group. *Note.* The red arrow indicates the myelin sheath and the green arrow indicates the mitochondria.



(a)



(b)

FIGURE 3: Continued.

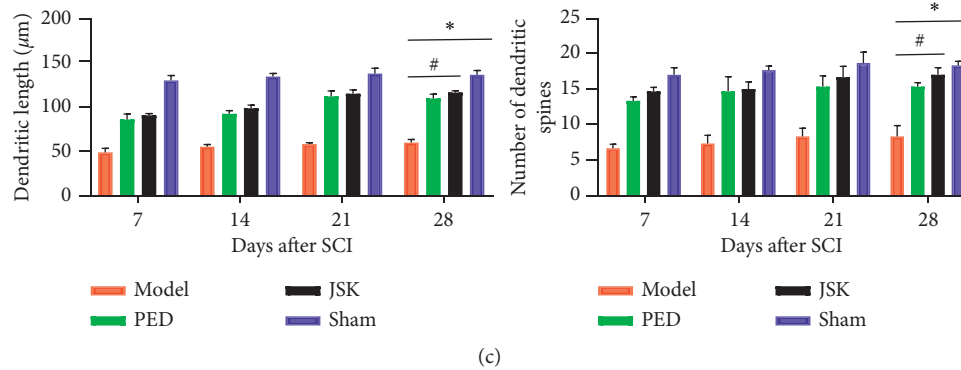


FIGURE 3: JSK improved the dendritic morphology of neurons in rats with SCI. (a) In the sham group, the morphology of spinal cord dendrites was regular, complete, and long, the dendritic spines arranged neatly, compact, and numerous, and the morphology at 7 d–28 d was basically the same. In the model group, the morphology of spinal cord dendrites was irregular, partially missing, and short, and the arrangement of dendritic spines was disordered and sparse, the number was less, and the morphological changes of 7 d–28 d were not much. In prednisone group and JSK group, the morphology of the spinal cord dendrites was improved, the shape was more regular, the structure was more complete, the length was longer, the dendritic spines were arranged neatly, the density was more uniform, the number was more, and the morphology of 7 d–28 d gradually improved. ((b), (c)) The length of dendrites and the number of dendritic spines in each group were statistically analyzed. The length of dendrites in the sham group was the longest and the number of dendritic spines was the most, while that in the model group was the shortest and the number of dendritic spines was the fewest. Compared with the sham group, the dendritic length and the number of dendritic spines in the model group were significantly decreased, and the dendritic length and the number of dendritic spines in the JSK group were significantly increased compared with the model group. Note. The red arrow indicates the dendritic spine, and the data were presented as mean \pm SD; $n = 3/\text{group}$, $*P < 0.05$, and $\#P < 0.05$.

dendrites and dendritic spines after SCI, and the morphology of 7 d–28 d was gradually improved (Figure 3). The above results suggested that JSK could improve the microstructure of neurons (mitochondria, endoplasmic reticulum, dendritic spines, etc.) in rats with SCI.

3.3. JSK Can Reduce the Apoptosis Rate of Neurons in Rats with SCI. The double-labeling results of TUNEL and NeuN showed that the apoptosis rate of neurons increased after SCI, while JSK could reduce the apoptosis rate of neurons after SCI, and gradually improved between 7 d–28 d (Figure 4).

3.4. JSK Can Inhibit the Expression of NgR in Neurons of Rats with SCI. The double-labeling results of NeuN and NgR showed that the expression of NgR in neurons increased after SCI, but JSK could reduce the expression of NgR in neurons after SCI. On the 28th day, JSK significantly inhibited the expression of NgR in neurons (Figure 5).

3.5. JSK Can Inhibit the Expression of NgR/RhoA/ROCK in the Injured Area of Rats with SCI. Immunohistochemistry showed that the expression of NgR in the injured area of rats increased after SCI, but JSK could reduce the expression of NgR in the injured area of rats with SCI. Western blot and qRT-PCR showed that the expression of NgR/RhoA/ROCK in the injured area of rats increased after SCI, but JSK could reduce the expression of NgR/RhoA/ROCK in the injured area of rats with SCI. On the 28th day, JSK significantly inhibited the expression of NgR/RhoA/ROCK in the injured area of the spinal cord (Figure 6).

4. Discussion

It was estimated that the incidence of SCI in the United States was about 54 new cases per million people per year. Although the average life expectancy of patients with SCI has increased greatly in the past few decades, due to the aging of the population, the number of cases may continue to increase, and its serious complications can lead to higher economic burden [34]. However, there are few effective treatments for SCI, and the main treatment is still methylprednisolone, which only slightly improves the clinical results. Therefore, there is an urgent need to find a more effective method for the treatment of SCI. SCI belongs to central nervous system injury, and its self-repair ability is very poor, but it maintains the ability of nerve tissue remodeling and axonal plasticity. Its endogenous repair mechanism is mainly related to the properties of the neurons and glial cells, in particular, the local extracellular environment, and the specific inflammatory process caused by the lesion [34]. The current research direction of SCI mainly includes neutralization of myelin-derived inhibitors (e.g., anti-Nogo-antibodies [35]), downstream inhibition of related intracellular signaling pathways (Rho-GTPase signaling [36]), degradation of glial scar inhibitors (CSPG degradation by enzyme [37–39]), neuronal signal pathway (mTOR/PTEN [40]), and transplantation of neural progenitor cells and stem cells [41].

NgR is a GPI-anchored protein expressed in the neurons and axons of the central nervous system [31, 42]. It mediates the inhibitory effect of three kinds of MAIs by forming a receptor complex with p75 and MAIs [43]. When NgR specifically binds to MAIs, it is transmitted to RhoA by p75 and then acts on the effector ROCK to complete the signal

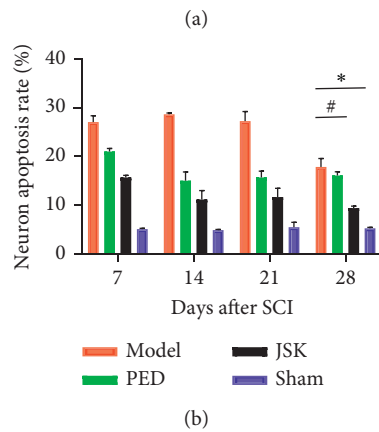
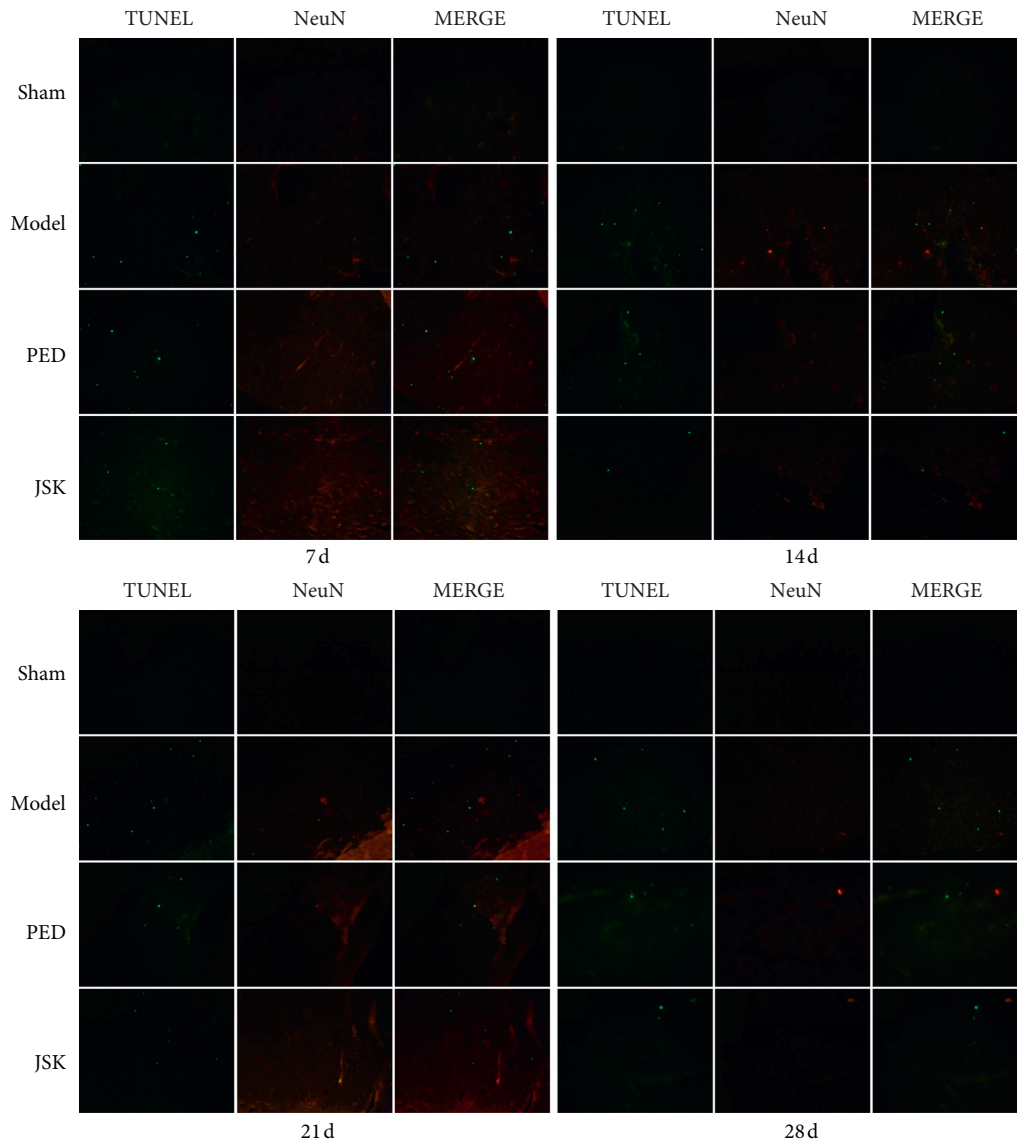


FIGURE 4: JSK could reduce the apoptosis rate of neurons in rats with SCI. (a) Representative images of TUNEL and NeuN double-labeling results. (b) The results of statistical analysis showed that the apoptosis rate of neurons increased after SCI in rats but decreased after intervention of JSK. Compared with the sham group, the apoptosis rate of neurons in the model group increased significantly. Compared with the model group, JSK could significantly reduce the apoptosis rate of neurons. The data were presented as mean \pm SD; $n = 3$ /group, $*P < 0.05$, and $\#P < 0.05$.

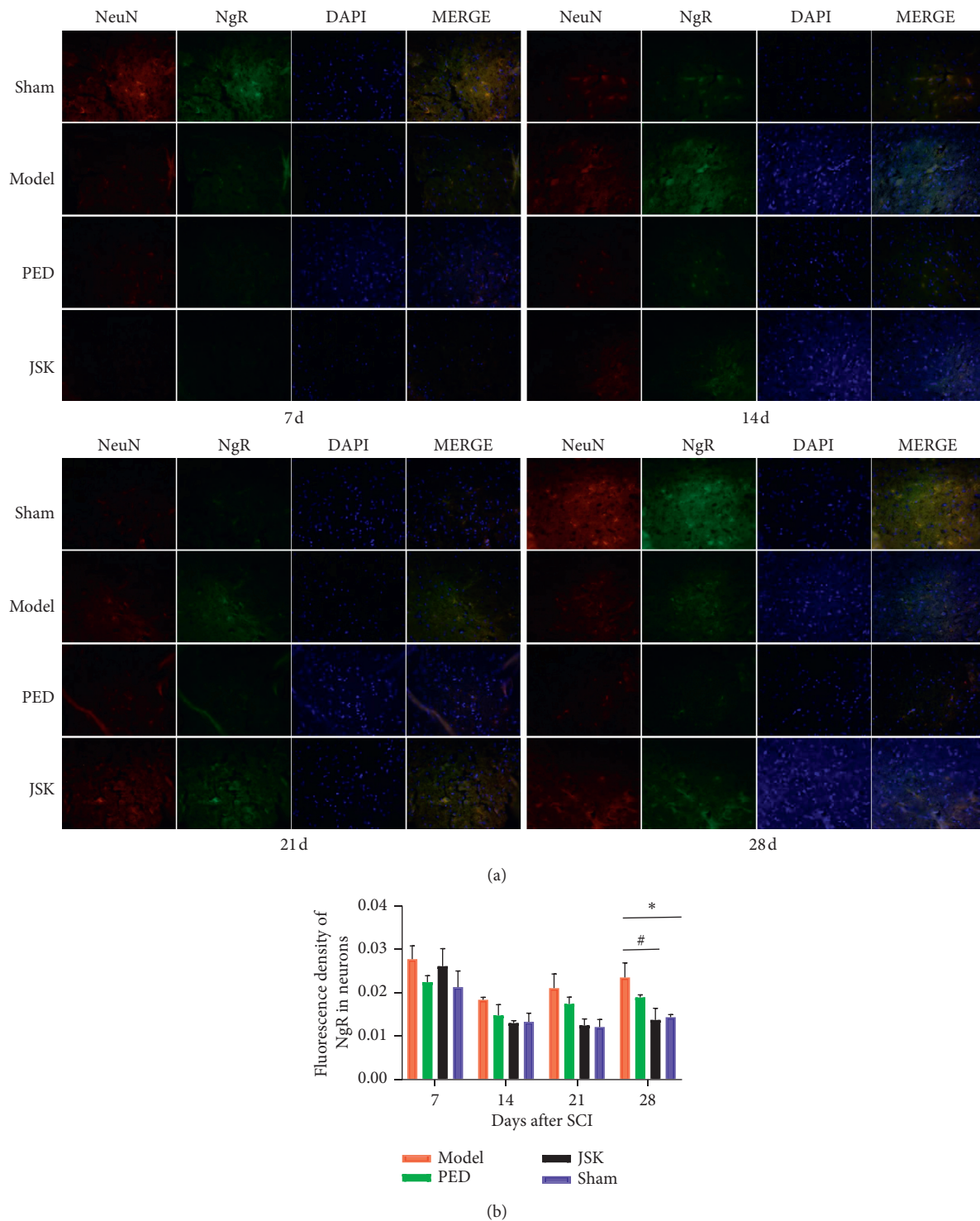


FIGURE 5: JSK could reduce the expression of NgR in neurons of rats with SCI. (a) Representative images of double-labeling results of NeuN and NgR. (b) The results of statistical analysis showed that the expression of NgR in neurons increased after SCI in rats but decreased after intervention of JSK. Compared with the sham group, the expression of NgR in the model group was significantly increased, and compared with the model group, JSK could significantly reduce the expression of NgR in neurons. The data were presented as mean \pm SD; $n = 3$ /group, * $P < 0.05$, and # $P < 0.05$.

transmission in the cell body, resulting in the collapse of the growth cone and inhibiting axonal regeneration [44–46]. The activation of RhoA is considered to be a key step for

MAIs to exert its inhibitory effect on axonal regeneration. Intervention of RhoA inactivating agent C3 transferase in vivo weakened the inhibitory effect of MAIs on axonal

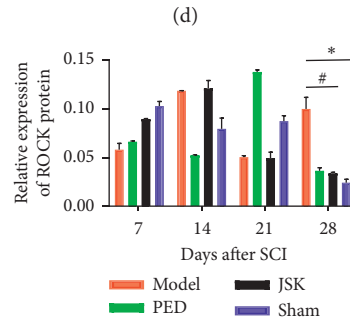
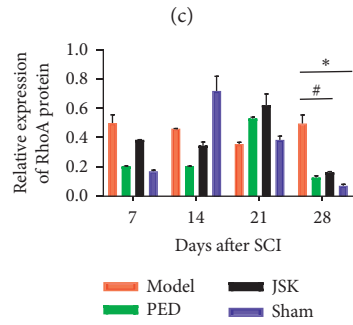
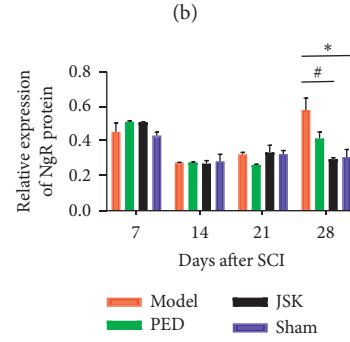
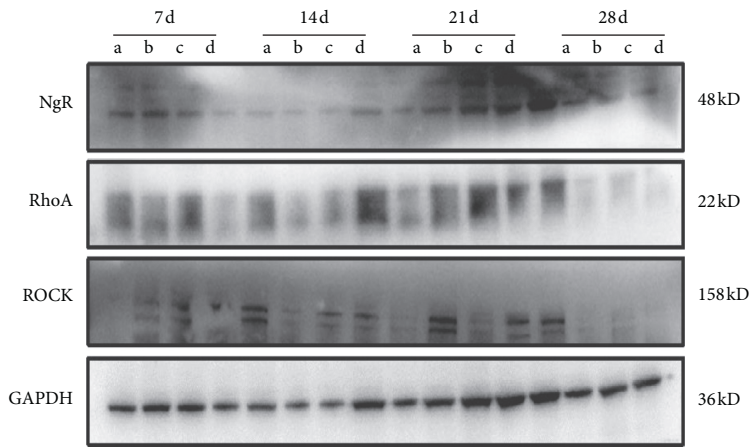
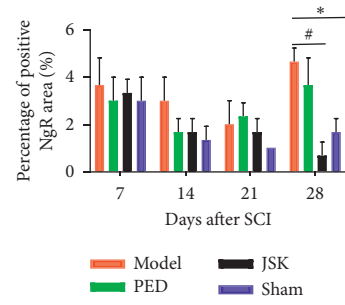
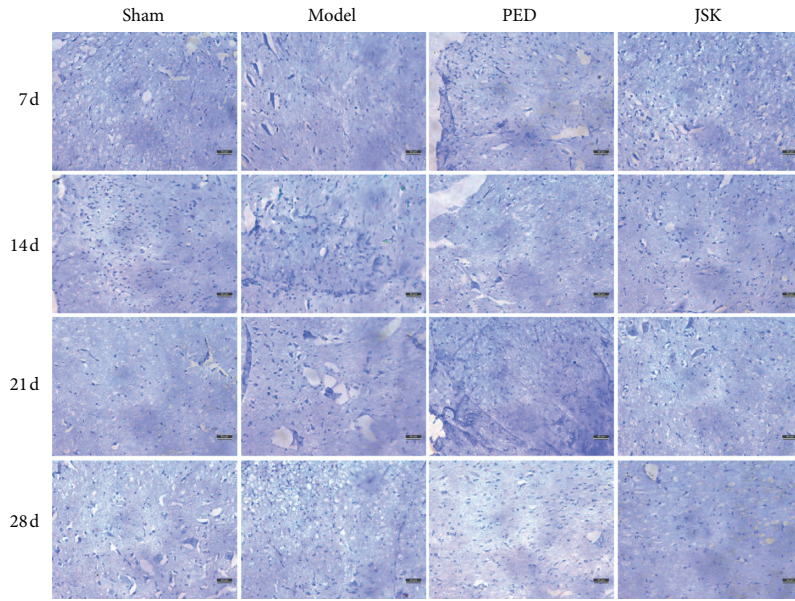


FIGURE 6: Continued.

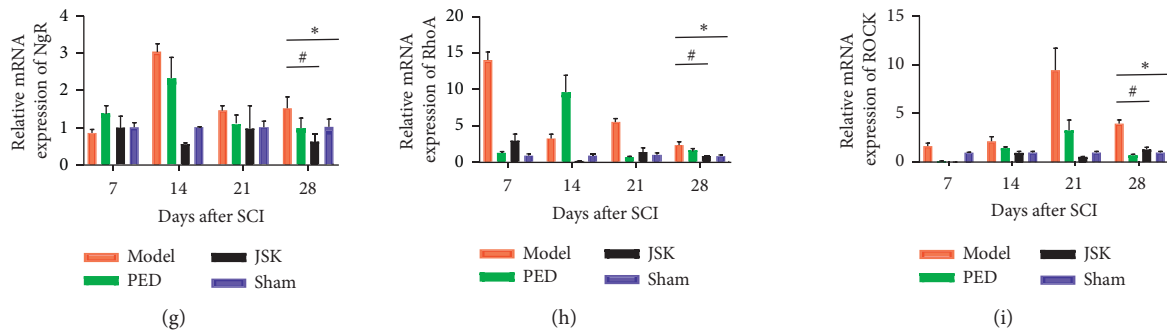


FIGURE 6: JSK could reduce the expression of NgR in the injured area of rats with SCI. (a) Representative images of immunohistochemistry. (b) Immunohistochemical statistics showed that, on the 28th day, the expression of NgR in the injured area of spinal cord increased but decreased after intervention of JSK. Compared with the sham group, the expression of NgR in the model group was significantly increased, and compared with the model group, JSK could significantly reduce the expression of NgR. (c) Representative images of western blot result. ((d), (e), (f), (g), (h), and (i)) The statistical results of western blot and qRT-PCR showed that, on the 28th day, the expression of NgR/RhoA/ROCK in the injured area of spinal cord increased but decreased after intervention of JSK. Compared with the sham group, the expression of NgR/RhoA/ROCK in the model group was significantly increased, and compared with the model group, JSK could significantly reduce the expression of NgR/RhoA/ROCK. NOTE: a is the model group, b is the prednisone group, c is the prednisone group, and d is the sham group. The data were presented as mean \pm SD; $n=3$ /group, * $P < 0.05$, and # $P < 0.05$.

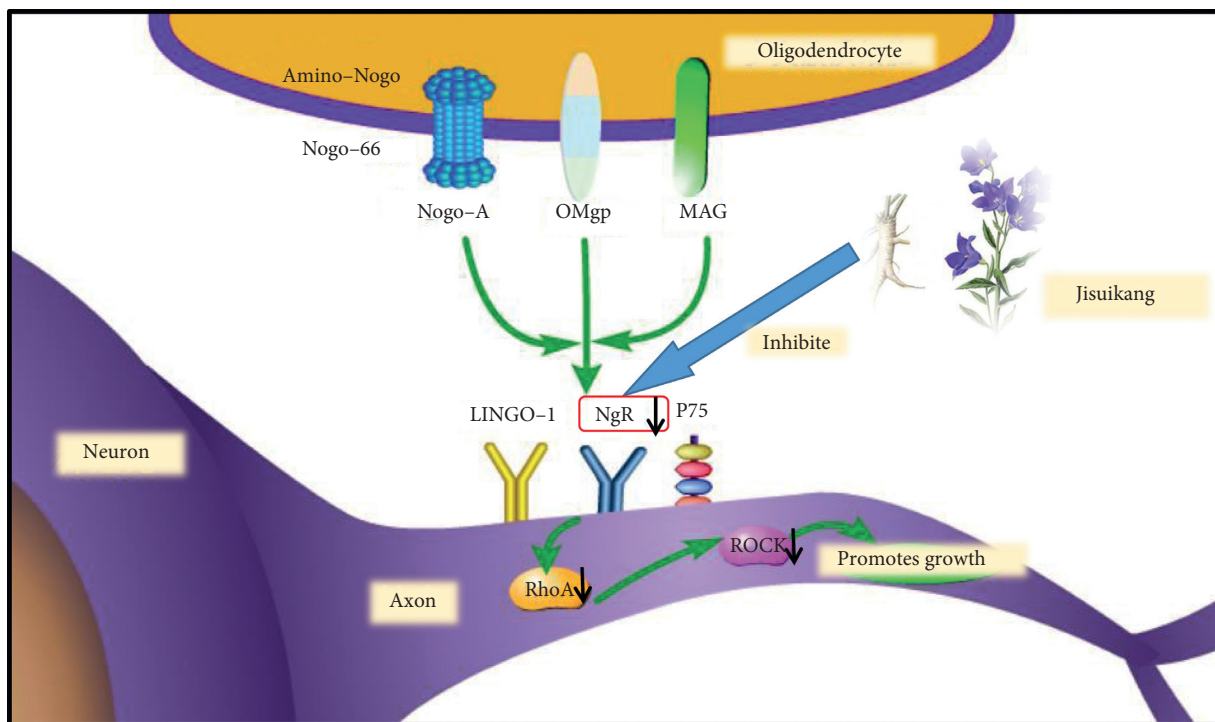


FIGURE 7: Jisuikang, a Chinese herbal formula, promotes the repair of spinal cord injury in rats by regulating the NgR/RhoA/ROCK signal pathway.

growth [47]. In addition, treatment with Y27632, a competitive antagonist of ROCK synthesis of ATP, could still promote neuronal axonal growth in the presence of MAIs [48, 49]. The NgR/RhoA/ROCK signal pathway is an important way to inhibit neuronal axonal regeneration, and NgR is the key to this pathway. The development of the NgR/RhoA/ROCK signal pathway in different periods after SCI should be studied.

In this experiment, the motor function and the expression of NgR/RhoA/ROCK in rats with SCI were studied. Compared with the model group on the 28th day, the BBB score and oblique board test showed that JSK could promote the recovery of motor function in rats with SCI, Golgi staining, and transmission electron microscope which suggested that JSK could improve the microstructure of neurons (mitochondria, endoplasmic reticulum, dendritic

spine, etc.) in rats with SCI. The double labeling of TUNEL and NeuN showed that JSK could reduce the apoptosis rate of neurons in rats with SCI, the double-labeling method of NeuN and NgR showed that JSK could inhibit the expression of NgR in neurons of rats with SCI; immunohistochemistry, western blot, and qRT-PCR all showed that JSK could inhibit the expression of NgR/RhoA/ROCK in the injured area of SCI rat (Figure 7).

In summary, the expression of NgR in the injured area of the spinal cord increased significantly and remained at a high level on the 7th day after SCI. However, on the 28th day, the expression of NgR/RhoA/ROCK in the PED group and JSK group was significantly lower than that in the model group, and JSK could significantly inhibit the expression of NgR/RhoA/ROCK in the injured area to promote nerve regeneration. This result is basically consistent with the results of Guo et al. [14, 50]. JSK can effectively inhibit the expression of NgR in the area of SCI, block the effect of myelin-derived nerve regeneration inhibitor and RhoA/ROCK, improve the microenvironment of axon regeneration, and promote the repair of SCI. In addition, it is worth noting that the motor function of rats with SCI basically recovered continuously before 28 days, and JSK could accelerate this process. The expression of NgR decreased to a certain extent, but the middle part of the results showed that the expression of NgR increased abruptly, which may be due to the fact that NgR is not only the receptor of Nogo-A but also the receptor of MAG and OMgp, while MAG and OMgp may be activated with Nogo-A, thus increasing the expression of NgR. At the same time, the expression of NgR may be increased due to the regulation of other neuronal signal pathways, so the mechanism of multipathway needs to be further studied.

Data Availability

The data sets used and/or analysed during the current study are available from the corresponding author on reasonable request.

Conflicts of Interest

The authors have declared that no conflicts of interest.

Acknowledgments

This article was supported by grants from the National Natural Science Foundation of China (81704100, 81573997, and 81973885), “Qing Lan Project” of Jiangsu University Funding Project (Su Teacher [2018] No. 12), and the project funded by the Priority Academic Program Development of Jiangsu Higher Education Institutions (Integration of Chinese and Western Medicine) [2018]87.

References

- [1] E. Hayta and H. Elden, “Acute spinal cord injury: a review of pathophysiology and potential of non-steroidal anti-inflammatory drugs for pharmacological intervention,” *Journal of Chemical Neuroanatomy*, vol. 87, pp. 25–31, 2018.
- [2] N. B. Jain, G. D. Ayers, E. N. Peterson et al., “Traumatic spinal cord injury in the United States, 1993–2012,” *JAMA*, vol. 313, no. 22, pp. 2236–2243, 2015.
- [3] M. Yong, W. Mao, and W. Jian-Wei, “28 cases of spinal cord injury treated with Jisuikang,” *Liaoning Journal of Traditional Chinese Medicine*, no. 4, p. 309, 2017.
- [4] M. Yong, W. Mao, and W. Jian-Wei, “Jisuikang in the treatment of 19 cases of dysuria after spinal cord injury,” *Jiangsu Journal of Traditional Chinese Medicine*, no. 4, p. 32, 2004.
- [5] L. Wang and D. M. Jiang, “Neuroprotective effect of Buyang Huanwu Decoction on spinal ischemia-reperfusion injury in rats is linked with inhibition of cyclin-dependent kinase 5,” *BMC Complementary and Alternative Medicine*, vol. 13, p. 309, 2013.
- [6] C. Hao, F. Wu, J. Shen et al., “Clinical efficacy and safety of buyang huanwu decoction for acute ischemic stroke: a systematic review and meta-analysis of 19 randomized controlled trials,” *Evidence-Based Complementary and Alternative Medicine*, vol. 2012, Article ID 630124, 10 pages, 2012.
- [7] L. Wang and D.-M. Jiang, “Neuroprotective effect of Buyang Huanwu decoction on spinal ischemia/reperfusion injury in rats,” *Journal of Ethnopharmacology*, vol. 124, no. 2, pp. 219–223, 2009.
- [8] L.-D. Zhao, J.-H. Wang, G.-R. Jin, Y. Zhao, and H.-J. Zhang, “Neuroprotective effect of Buyang Huanwu decoction against focal cerebral ischemia/reperfusion injury in rats—time window and mechanism,” *Journal of Ethnopharmacology*, vol. 140, no. 2, pp. 339–344, 2012.
- [9] P. Yang, A. Chen, Y. Qin et al., “Buyang huanwu decoction combined with BMSCs transplantation promotes recovery after spinal cord injury by rescuing axotomized red nucleus neurons,” *Journal of Ethnopharmacology*, vol. 228, pp. 123–131, 2019.
- [10] D. Xian-Hui, H. Xiao-Ping, and G. Wei-Juan, “Neuroprotective effects of the Buyang Huanwu decoction on functional recovery in rats following spinal cord injury,” *The Journal of Spinal Cord Medicine*, vol. 39, no. 1, pp. 85–92, 2016.
- [11] P. Ya-Lan, G. Yang, Z. Long-Yun, Y. Wen-Chao, M. Yong, and H. Gui-Cheng, “Effects of Chinese herbal compound “Jisuikang” on phagocytosis of microglia and regeneration of injured neurons in co-culture system,” *Chinese Journal of Immunology*, vol. 33, no. 11, pp. 1652–1657, 2017.
- [12] Y. Wen-Chao, W. Lei, Y. Ma, H. Gui-Cheng, Z. Long-Yun, and G. Yang, “Effect of Chinese herbal compound “Jisuikang” on engulfment of neuron debris by microglia,” *The Journal of Medical Practice*, vol. 33, pp. 3359–3363, 2017.
- [13] J. W. Wang, J. F. Yang, Y. Ma et al., “Nogo-A expression dynamically varies after spinal cord injury,” *Neural Regeneration Research*, vol. 10, no. 2, pp. 225–229, 2015.
- [14] Y. Guo, Y. Ma, Y. L. Pan, S. Y. Zheng, J. W. Wang, and G. C. Huang, “Jisuikang, a Chinese herbal formula, increases neurotrophic factor expression and promotes the recovery of neurological function after spinal cord injury,” *Neural Regeneration Research*, vol. 12, no. 9, pp. 1519–1528, 2017.
- [15] Z. Jie-Mei and T. Kou-Ming, “Neuroprotective function of astragalus injection on treatment of rats with acute spinal cord injury,” *Journal of Clinical Medical Practice*, vol. 18, no. 24, pp. 7–10, 2014.
- [16] R. Xian-Sheng, L. Xiang-Yang, Y. You-Geng, and X. Shen-Xiang, “Neuro-protective effect of astragalus root on

- experimental injury of spinal cord in rats," *Chinese Journal of Clinical Rehabilitation*, vol. 7, pp. 31–33, 2003.
- [17] L. Shiqing, M. Yonggang, P. Hao et al., "Neuroprotective effects of Astragalus root on experimentally spinal cord injury in rats," *China Journal of Orthopaedics and Traumatology*, vol. 8, pp. 20–22, 2003.
- [18] J. Hu, S. Liu, Y. Yang, and D. Xu, "Effect of salvia miltiorrhiza on spinal cord blood flow and motor function of lower limb in rats with spinal cord injury," *Chinese Journal of Integrated Traditional and Western Medicine*, vol. 1, pp. 167–169.
- [19] X. Xiang and J. Shu, "Experimental study on free radical change after spinal cord injury and the effect of salvia miltiorrhiza on free radical," *Chinese Journal of Traumatology*, vol. 5, pp. 14–16.
- [20] L. Wei, *Effect of Salvia Miltiorrhiza on Motor Function in Gray Matter of Acute Spinal Cord Injury in Rat and Its Mechanism*, Fujian University of Traditional Chinese Medicine, Fuzhou, China, 2013.
- [21] L. Fan, K. Wang, Z. Shi, J. Die, C. Wang, and X. Dang, "Tetramethylpyrazine protects spinal cord and reduces inflammation in a rat model of spinal cord ischemia-reperfusion injury," *Journal of Vascular Surgery*, vol. 54, no. 1, pp. 192–200, 2011.
- [22] L. H. Fan, K. Z. Wang, B. Cheng, C. S. Wang, and X. Q. Dang, "Anti-apoptotic and neuroprotective effects of Tetramethylpyrazine following spinal cord ischemia in rabbits," *BMC Neuroscience*, vol. 7, p. 48, 2006.
- [23] X. Xiao, Y. Liu, C. Qi et al., "Neuroprotection and enhanced neurogenesis by tetramethylpyrazine in adult rat brain after focal ischemia," *Neurological Research*, vol. 32, no. 5, pp. 547–555, 2010.
- [24] Z. Zhang, T. Wei, J. Hou, G. Li, S. Yu, and W. Xin, "Tetramethylpyrazine scavenges superoxide anion and decreases nitric oxide production in human polymorphonuclear leukocytes," *Life Sciences*, vol. 72, no. 22, pp. 2465–2472, 2003.
- [25] S. David and A. Aguayo, "Axonal elongation into peripheral nervous system "bridges" after central nervous system injury in adult rats," *Science*, vol. 214, no. 4523, pp. 931–933, 1981.
- [26] P. M. Richardson, U. M. McGuinness, and A. J. Aguayo, "Axons from CNS neurones regenerate into PNS grafts," *Nature*, vol. 284, no. 5753, pp. 264–265, 1980.
- [27] T. Savio and M. Schwab, "Rat CNS white matter, but not gray matter, is nonpermissive for neuronal cell adhesion and fiber outgrowth," *The Journal of Neuroscience*, vol. 9, no. 4, pp. 1126–1133, 1989.
- [28] C. Bandtlow, T. Zachleder, and M. Schwab, "Oligodendrocytes arrest neurite growth by contact inhibition," *The Journal of Neuroscience*, vol. 10, no. 12, pp. 3837–3848, 1990.
- [29] Z. Cao, Y. Gao, K. Deng, G. Williams, P. Doherty, and F. S. Walsh, "Receptors for myelin inhibitors: structures and therapeutic opportunities," *Molecular and Cellular Neuroscience*, vol. 43, no. 1, pp. 1–14, 2010.
- [30] S. Ping, *PirB Expression and Regulation on Axon Growth in Murine RGCs*, Third Military Medical University, Chongqing, China, 2014.
- [31] X. Wang, S.-J. Chun, H. Treloar, T. Vartanian, C. A. Greer, and S. M. Strittmatter, "Localization of Nogo-A and Nogo-66 receptor proteins at sites of axon-myelin and synaptic contact," *The Journal of Neuroscience*, vol. 22, no. 13, pp. 5505–5515, 2002.
- [32] T. Khan, R. M. Havey, S. T. Sayers, A. Patwardhan, and W. W. King, "Animal models of spinal cord contusion injuries," *Laboratory Animal Science*, vol. 49, no. 2, pp. 161–172, 1999.
- [33] D. M. Basso, M. S. Beattie, and J. C. Bresnahan, "A sensitive and reliable locomotor rating scale for open field testing in rats," *Journal of Neurotrauma*, vol. 12, no. 1, pp. 1–21, 1995.
- [34] S. Soares, Y. von Boxberg, and F. Nothias, "Repair strategies for traumatic spinal cord injury, with special emphasis on novel biomaterial-based approaches," *Revue Neurologique (Paris)*, vol. 176, 2020.
- [35] F. M. Bareyre, B. Haudenschild, and M. E. Schwab, "Long-lasting sprouting and gene expression changes induced by the monoclonal antibody IN-1 in the adult spinal cord," *The Journal of Neuroscience*, vol. 22, no. 16, pp. 7097–7110, 2002.
- [36] M. A. Kopp, T. Liebscher, A. Niedeggen et al., "Small-molecule-induced Rho-inhibition: NSAIDs after spinal cord injury," *Cell and Tissue Research*, vol. 349, no. 1, pp. 119–132, 2002.
- [37] U. Milbreta, Y. von Boxberg, P. Mailly, F. Nothias, and S. Soares, "Astrocytic and vascular remodeling in the injured adult rat spinal cord after chondroitinase ABC treatment," *Journal of Neurotrauma*, vol. 31, no. 9, pp. 803–818, 2014.
- [38] E. J. Bradbury and L. M. Carter, "Manipulating the glial scar: chondroitinase ABC as a therapy for spinal cord injury," *Brain Research Bulletin*, vol. 84, no. 4–5, pp. 306–316, 2011.
- [39] J. W. Fawcett, M. E. Schwab, L. Montani, N. Brazda, and H. W. Müller, "Defeating inhibition of regeneration by scar and myelin components," *Handbook of Clinical Neurology*, vol. 109, pp. 503–522, 2012.
- [40] K. Liu, Y. Lu, J. K. Lee et al., "PTEN deletion enhances the regenerative ability of adult corticospinal neurons," *Nature Neuroscience*, vol. 13, no. 9, pp. 1075–1081, 2010.
- [41] R. C. Assuncao-Silva, E. D. Gomes, N. Sousa, N. A. Silva, and A. J. Salgado, "Hydrogels and cell based therapies in spinal cord injury regeneration," *Stem Cells International*, vol. 2015, Article ID 948040, 24 pages, 2015.
- [42] A. Josephson, A. Trifunovski, H. R. Widmer, J. Widenfalk, L. Olson, and C. Spenger, "Nogo-receptor gene activity: cellular localization and developmental regulation of mRNA in mice and humans," *The Journal of Comparative Neurology*, vol. 453, no. 3, pp. 292–304, 2002.
- [43] G. Mei-ling and L. Xia-qing, "The roles and mechanism of myelin associated inhibitors," *Progress of Anatomical Sciences*, vol. 21, pp. 430–434, 2015.
- [44] T. Kubo, A. Yamaguchi, N. Iwata, and T. Yamashita, "The therapeutic effects of Rho-ROCK inhibitors on CNS disorders," *Therapeutics and Clinical Risk Management*, vol. 4, no. 3, pp. 605–615, 2008.
- [45] T. Kubo, K. Hata, A. Yamaguchi, and T. Yamashita, "Rho-ROCK inhibitors as emerging strategies to promote nerve regeneration," *Current Pharmaceutical Design*, vol. 13, no. 24, pp. 2493–2499, 2007.
- [46] T. Kubo and T. Yamashita, "Rho-ROCK inhibitors for the treatment of CNS injury," *Recent Patents on CNS Drug Discovery*, vol. 2, no. 3, pp. 173–179, 2007.
- [47] M. Lehmann, A. Fournier, I. Selles-Navarro et al., "Inactivation of Rho signaling pathway promotes CNS axon regeneration," *The Journal of Neuroscience*, vol. 19, no. 17, pp. 7537–7547, 1999.
- [48] P. Dergham, B. Ellezam, C. Essagian, H. Avedissian, W. D. Lubell, and L. McKerracher, "Rho signaling pathway targeted to promote spinal cord repair," *The Journal of Neuroscience*, vol. 22, no. 15, pp. 6570–6577, 2002.
- [49] B. Niederöst, T. Oertle, J. Fritsche, R. A. McKinney, and C. E. Bandtlow, "Nogo-A and myelin-associated glycoprotein mediate neurite growth inhibition by antagonistic regulation

- of RhoA and Rac1," *The Journal of Neuroscience*, vol. 22, no. 23, pp. 10368–10376, 2002.
- [50] G. Yang, M. Yong, F. Cheng, Y. L. Pan, and G. C. Huang, "Effect of Jisuikang on Nogo-66 receptor NgR expression in rats with spinal cord injury," *Chinese Journal of Tissue Engineering Research*, vol. 20, no. 18, pp. 2622–2627, 2016.

Research Article

The Protective Effects of the Ethyl Acetate Part of Er Miao San on Adjuvant Arthritis Rats by Regulating the Function of Bone Marrow-Derived Dendritic Cells

Jiemin Ding ^{1,2,3}, Min Liu,^{1,2,3} Zihua Xuan,^{1,2,3} Meng li Liu ^{1,2,3}, Ning Wang ^{1,2,3}, and Xiaoyi Jia ^{1,2,3}

¹School of Pharmacy, Anhui University of Chinese Medicine, Hefei 230012, China

²Anhui Province Key Laboratory of Chinese Medicinal Formula, Hefei, Anhui 230012, China

³Anhui Province Key Laboratory of Research & Development of Chinese Medicine, Hefei 230012, China

Correspondence should be addressed to Ning Wang; wnsnci123@163.com and Xiaoyi Jia; jiaxiaoyi78@126.com

Received 5 July 2020; Revised 5 October 2020; Accepted 28 October 2020; Published 12 November 2020

Academic Editor: Arham Shabbir

Copyright © 2020 Jiemin Ding et al. This is an open access article distributed under the Creative Commons Attribution License, which permits unrestricted use, distribution, and reproduction in any medium, provided the original work is properly cited.

Aims. The aim of this study was to evaluate the protective effects of Er Miao San (EMS) and the regulative function of bone marrow-derived dendritic cells (BMDCs) on adjuvant arthritis (AA) in rats. **Methods.** The ethyl acetate part of EMS (3 g/kg, 1.5 g/kg, and 0.75 g/kg) was orally administered from day 15 after immunization to day 29. The polyarthritis index and paw swelling were measured, the ankle joint pathological changes were observed using hematoxylin-eosin (HE) staining, and the spleen and thymus index were determined. Moreover, T and B cell proliferation were determined using the CCK-8 assay. The expression of BMDC surface costimulatory molecules and inflammatory factors were determined using flow cytometry and ELISA kits, respectively. **Results.** Compared with the AA model rats, the ethyl acetate fraction of EMS obviously reduced paw swelling (from 1.0 to 0.7) and the polyarthritis index (from 12 to 9) ($P < 0.01$) and improved the severity of histopathology ($P < 0.01$). The treatment using ethyl acetate fraction of EMS significantly reduced the spleen and thymus index ($P < 0.01$) and inhibited T and B cell proliferation ($P < 0.01$). Moreover, EMS significantly modulated the expression of surface costimulatory molecules in BMDCs, including CD40, CD80, CD86, and major histocompatibility complex class II (MHC-II) ($P < 0.01$). The results also showed that the ethyl acetate part of EMS significant inhibited the levels of proinflammatory cytokines interleukin- (IL-) 23 tumor necrosis factor- (TNF-) α and inflammatory factor prostaglandin (PG) E2 in the supernatant of BMDCs. However, the level of anti-inflammatory cytokine IL-10 was significantly increased ($P < 0.01$). **Conclusion.** These results suggest that the ethyl acetate part of EMS has better protective effects on AA rats, probably by regulating the function of BMDCs and modulating the balance of cytokines.

1. Introduction

Rheumatoid arthritis (RA) is an autoimmune disease characterized by joint synovial inflammation and cartilage damage [1]. An abnormal proliferation of fibroblast synovial cells is a typical feature of RA, which is correlated with over-activated immune cells, such as T-cells, B-cells, macrophages, and dendritic cells (DCs). A large number of infiltrated DCs are highly involved in the synovium of RA patients and arise to the occurrence of arthritic disease.

DCs are specialized antigen-presenting cells (APCs), which can take up processes, present antigens, and initiate T-cell-mediated immune responses [2]. DCs highly express surface costimulatory molecules, including CD40, CD80, CD86, and MHC-II, which present antigens to T-cells. Mature DCs can effectively activate the initial T cells, which are the center of initiation, regulation, and maintenance of immune responses [3]. Previous studies have confirmed the incidence and development of RA related to DCs. The synovial DCs of RA patients secrete chemokines and attract proinflammatory immune cells, including macrophages and

neutrophil monocytes [4, 5]. Compared with healthy controls, the concentration of proinflammatory cytokines (IL-1 β , IL-6, and IL-23) and inflammatory factors (PGE2) in RA patients have increased [6, 7]. This is one of the key factors of RA pathogenesis.

Er Miao San (EMS) is a traditional Chinese Medicine prescription, which is derived from «dan xi xin fa». It consists of Phellodendri Cortex and Atractylodis Rhizoma. We have previously reported that the ethyl acetate part of EMS could significantly reduce the pathological changes, having a therapeutic effect on adjuvant-induced arthritis (AA) rats [8]. Nevertheless, the immune mechanisms targeted by the ethyl acetate part of EMS are unclear. In this research, the aim was to investigate the antiarthritis mechanisms of EMS, whether its potential molecular mechanism was related to the regulation of the function of DCs.

2. Materials and Methods

2.1. Animals. Sprague Dawley rats (male, 180 ± 20 g) were purchased from the Animal Department of Anhui Medical University, China. Rats were adapted to standard laboratory conditions (under a controlled temperature of 22–26°C and a 12 h light and 12 h dark period) and to feed criterion forage and water daily during the experiment. All experiments were approved by the Experimental Animal Ethics Committee of Anhui University of Chinese Medicine (Identification number: 202005).

2.2. Reagents. Phellodendri Cortex and Atractylodis Rhizoma were purchased from Anhui herbal pieces Co., Ltd. (BoZou, Anhui Province, China). Petroleum ether was obtained from Shanghai SuYi Chemical Reagent Co., Ltd. Ethyl acetate was acquired from Jiangsu Qiangsheng Functional Chemical Co., Ltd. Methotrexate (MTX) was obtained from Xinyi Medical Limited Company (Shanghai, China). FITC-CD40, PE-CD80, PE-CD86, and PE-MHC-II were obtained from eBioscience, Inc. (CA, USA). Roswell Park Memorial Institute (RPMI)-1640 medium and fetal bovine serum (FBS) were obtained from Hyclone. TNF- α , IL-10, and PGE2 were obtained from the ELISA KIT (Multi Sciences Biotech, Co., Ltd), and IL-23 was obtained from the ELISA KIT (Cusabio Biotech, Co., Ltd).

2.3. Preparation of the Ethyl Acetate Part of EMS. Equal parts of Atractylodis rhizoma and Phellodendri cortex were mixed and crushed. The mixture was decocted with boiling water three times for 1.5, 1.0, and 0.5 h, and the suspension was condensed by means of evaporation in a water bath at a temperature of approximately 60°C. The suspension was concentrated to 500–800 mL and extracted five times with an equivalent volume of petroleum ether. The petroleum ether part of the EMS was discarded and extracted five times with an equivalent volume of ethyl acetate. The ethyl acetate part of the EMS was concentrated to a certain concentration (0.3 g/mL, 0.15 g/mL, and 0.075 g/mL) (calculated using the crude drug).

2.4. Induction of the AA Model and Treatment. The AA model was constructed in SD rats, as previously described [9]. Bacillus Calmette–Guerin (BCG) (80°C, 1 h) was adequately mingled with liquid paraffin, which was complete Freund's adjuvant (CFA, 10 mg/mL). The rat AA model was injected with 0.1 mL of CFA in the left hind plantar, and the normal group was injected with 0.1 mL of an equivalent volume of saline. On day 15 after immunization, rats were randomly divided into the following groups: the normal group, AA model group, EMS (3 g/kg, 1.5 g/kg, 0.75 g/kg), and MTX (0.5 mg/kg). EMS was administered via gavage for 14 days (once per day), and the MTX group was administered via gavage every 3 days for a total of five times [10]. Meanwhile, the normal and AA model groups were orally administered an equivalent volume of a carboxymethylcellulose aqueous solution (10 mL/kg).

2.5. Evaluation of Arthritis. All rat weights were recorded weekly using an electronic scale. The right hind paw volume was measured using a volume meter (PV-200, Chengdu Technology Market Co., Ltd.) before immunization (basic value, day 0) and after immunization on days 14, 17, 20, 23, 26, and 29. The polyarthritis index was graded from 0 points to 16 points, as described previously: 0, no swelling normally; 1, erythema and slight swelling of the ankle joint; 2, erythema and slight swelling of the ankle joint to the metatarsophalangeal or capsular joint; 3, erythema and moderate swelling of the ankle to the metatarsophalangeal or capsular joint; and 4, erythema and severe swelling of the ankle to the metatarsophalangeal joint [11].

2.6. Histopathological Examination of the Ankle Joints. The rats were sacrificed on day 29 after the first immunization. The right ankle joints and the surrounding soft tissues, such as muscles and tendons, were removed. The ankle joints were obtained and fixed in a 10% formalin solution. Additionally, the ankle tissues were decalcified in 5% nitric acid before being embedded in paraffin. Paraffin sections (5 mm thick) were stained with HE. Changes in the ankles were histopathologically appraised by two blinded observers. The severity of arthritis in the ankle joints was graded from 0 to 4, according to inflammatory cell infiltration, synovial proliferation, pannus formation, and bone erosion.

2.7. Spleen and Thymus Index. The rats were sacrificed on day 29 after the first immunization. The food was evacuated 12 h before. Spleen and thymus tissues were removed from the body, weighed, and recorded. The spleen and thymus index were calculated as the ratio of spleen and thymus to the rat body (mg/g).

2.8. T- and B-Lymphocyte Proliferation. The rat spleen and thymus tissues were aseptically removed, ground using a 120 nylon cloth, spread in RPMI 1640 supplemented with 10% FBS at a density of 1×10^6 cells/mL, and seeded into 96-well flat-bottom plates (1×10^5 cells/well). Furthermore, T- and

B-cells were separately stimulated with 5 mg/L concanavalin (Con) A (Sigma) or 4 mg/L lipopolysaccharides (LPS) (Sigma) and cultured for 48 h. Two hours before the end of culture, CCK-8 (10 μ L) was added to each well. The absorbance was read at 450 nm using a Microplate reader (EJ301, Thermo Fisher Scientific).

2.9. Culture of BMDCs. The femur and tibia were removed in a sterile environment, and the epiphysis of both ends was cut off to expose the bone marrow cavity. The bone marrow cavity was rinsed with RPMI-1640 medium and filtered using a 200 mesh nylon cloth. Cells were, then, cultured in RPMI 1640 supplemented with 10% FBS at a density of 1×10^6 cells/mL in normal conditions (37°C and 5% CO₂). The nonadherent cells were removed after 24 h of culture, and fresh culture medium, including human granulocyte-macrophage colony-stimulating factor (GM-CSF) and IL-4, both at a concentration of 20 ng/mL, was added. The culture medium was changed every two days and supplemented with sufficient cytokines. BMDCs were cultured until day 7.

2.10. Flow Cytometry. BMDCs were harvested and washed with 1 mL of phosphate-buffered saline (PBS). The cell suspensions were prepared using conventional methods, and 100 μ L of the fluorescently labeled monoclonal antibodies, CD40-FITC, CD80-PE, CD86-PE, and MHC-II-PE, were added, followed by incubation in the dark for 30 min at room temperature (20–25°C). After centrifugation, 1 mL of PBS buffer solution was aseptically added to wash the cells. Finally, the cells were subjected to flow cytometry (FC500, American Beckman Coulter Company), and the percentages of CD40, CD80, CD86, and MHC-II in BMDCs were analyzed using software.

2.11. ELISA. The supernatant of BMDCs was acquired after culture for 7 days using centrifugation (8 min, 2,000 rpm) and frozen at –80°C until detection. The levels of PGE2 (EK8103-01), IL-23 (CSB-E08462r), TNF- α (EK3823-01), and IL-10 (EK3101-01) in BMDCs were detected using ELISA kits, according to the manufacturer's instructions. Absorbance was read at 450 nm.

2.12. Statistical Analysis. Data are presented as the mean \pm SD. One-way analysis of variance (ANOVA) using SPSS software was used to define the significant differences among the control and the drug groups. A $P < 0.05$ with a 95% confidence interval was considered statistically significant.

3. Results

3.1. The Effects of the Ethyl Acetate Part of EMS on the Clinical Index in AA Rats. The paw swelling and polyarthritis index were defined to assess the severity of arthritis and the anti-inflammatory effects of medicines. According to Figure 1, the secondary inflammatory reaction appeared around days 14–17, culminating around days 20–23, and the weight of

AA rats increased slowly and obviously less compared with the normal rats ($P < 0.01$). On day 28, the ethyl acetate part of EMS treatment increased the weight of rats, and this change was faster compared with the model group. No significant difference in body weight was observed between the EMS and MTX groups during the administration period (Table 1). Compared with the AA model group, the ethyl acetate fraction of the EMS treatment not only ameliorated the effect on the paws of AA rats (Figure 1(a)) and obviously inhibited paw swelling (from 1.0 to 0.7) but also significantly reduced the polyarthritis index (from 12 to 9), $P < 0.01$ (Figures 1(b) and 1(c)). This result suggested that the ethyl acetate part of EMS treatment is effective and safe to use in AA rats.

3.2. The Effects of the Ethyl Acetate Part of EMS on Ankle Pathology in AA Rats. Histopathological analysis is considered a great index of clinical signs. To define the effectiveness of the ethyl acetate part of EMS, its antiarthritis effects were analyzed using histological analysis. As shown in Figure 2, the model group expressed severe arthritic symptoms, and synovial tissues infiltrated by many inflammatory cells, accompanied by synovial proliferation, bone erosion, and destruction (compared to the normal group, $P < 0.01$). The results suggested that EMS (3 g/kg) and MTX (0.5 mg/kg) all markedly reduced these histological severity scores (compared to the model group, $P < 0.01$). EMS (0.75 g/kg, 1.5 g/kg) also protected the tissues from histological damage ($P < 0.05$). The results showed that the ethyl acetate part of EMS has a protective effect in AA rats.

3.3. The Effects of the Ethyl Acetate Part of EMS on the Spleen and Thymus Index in AA Rats. The spleen and thymus index, a sign of organ changes in the body, accompanied the development of inflammation. As shown in Figure 3, compared to the normal group, model rats, spleen, and thymus index obviously increased ($P < 0.01$). EMS (3 g/kg) and MTX (0.5 mg/kg) significantly reduced the spleen and thymus index, compared to the AA group ($P < 0.01$). EMS at 0.75 and 1.5 g/kg reduced the thymus index, $P < 0.05$ (Figure 3(b)), and at 1.5 g/kg, it significantly reduced the spleen index compared to the AA group ($P < 0.01$; Figure 3(a)). These results suggest that EMS can inhibit the spleen and thymus index in AA rats.

3.4. The Effects of the Ethyl Acetate Part of EMS on T- and B-Cells Proliferation in AA Rats. T- and B-cells participate in human-specific immunity. The viability of T- and B-cells was determined using the CCK-8 assay (bestbio biological). As shown in Figure 4, compared to the normal group, both T- and B-cell proliferation increased in the model group. Furthermore, EMS (1.5 g/kg, 3 g/kg) and MTX (0.5 mg/kg) reduced Con A-induced T-lymphocyte proliferation and LPS-induced B-lymphocyte proliferation (compared to the model group, $P < 0.01$). In addition, EMS (0.75 g/kg) effectively suppressed T-lymphocyte proliferation (compared to the model group, $P < 0.05$) (Figure 4(a)). Additionally, the

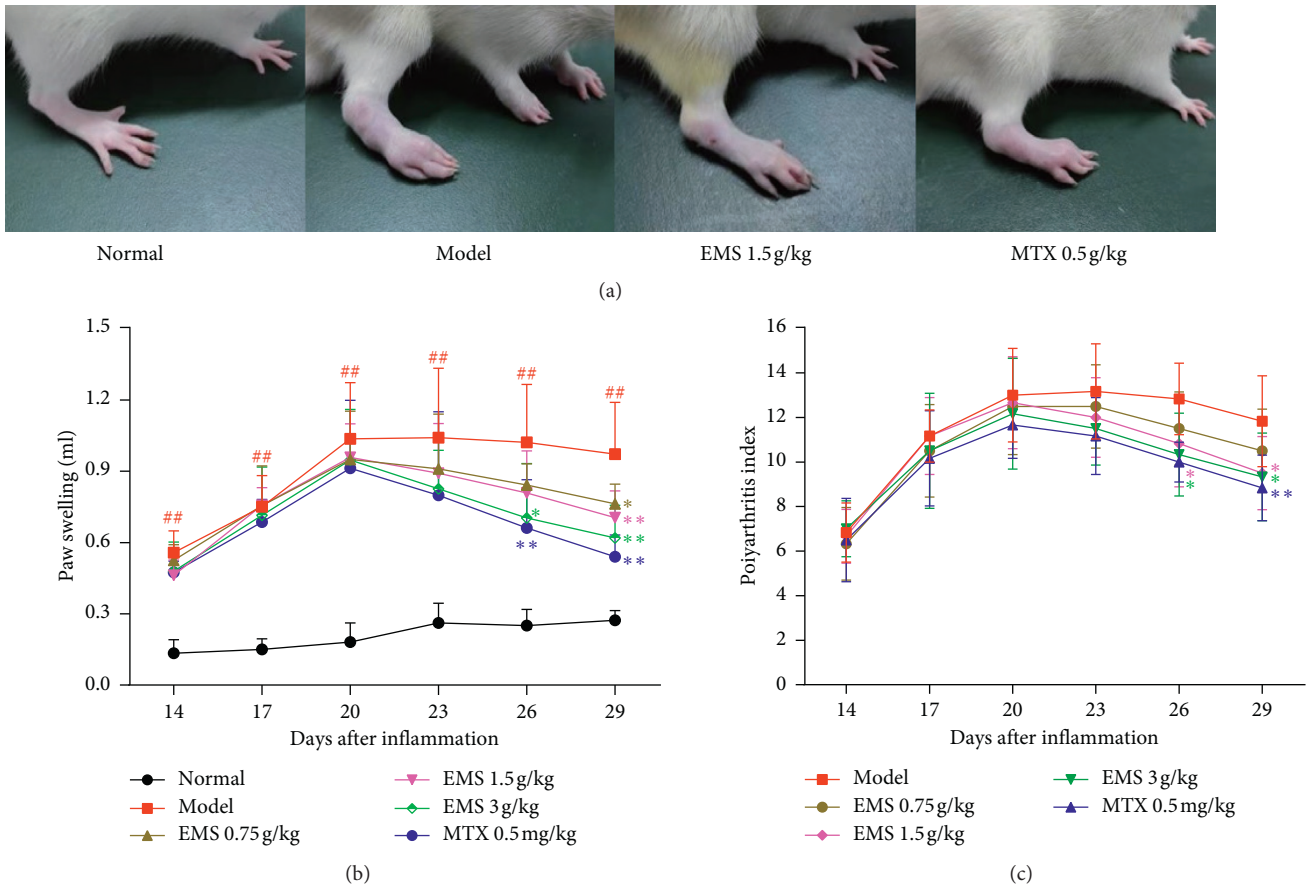


FIGURE 1: The effects of the ethyl acetate part of EMS on the clinical index in AA rats. (a) The effects of the ethyl acetate part of EMS on the paw in AA rats (day 29). The effects of the ethyl acetate part of EMS on paw swelling (b) and polyarthrititis index (c) in AA rats. $##P < 0.01$ versus the normal group, $*P < 0.05$, $**P < 0.01$ versus the model group ($n = 6$).

TABLE 1: The effects of the ethyl acetate part of EMS on the change of rat weight in AA rats.

| Groups | Dose (mg/kg) | d0 | d7 | d14 | d21 | d28 |
|--------|--------------|------------|-------------|--------------------------|---------------------------|---------------------------|
| Normal | — | 162 ± 2.95 | 218 ± 6.74 | 276 ± 18.97 | 308 ± 12.48 | 337 ± 19.00 |
| Model | — | 163 ± 2.66 | 215 ± 10.81 | 256 ± 19.71 [#] | 272 ± 12.24 ^{##} | 280 ± 22.59 ^{##} |
| EMS | 0.75 g/kg | 163 ± 3.50 | 222 ± 8.86 | 258 ± 19.80 | 291 ± 28.41 | 300 ± 19.07 [*] |
| EMS | 1.5 g/kg | 162 ± 3.08 | 211 ± 5.73 | 260 ± 6.66 | 286 ± 17.95 | 310 ± 26.72 |
| EMS | 3 g/kg | 163 ± 4.65 | 219 ± 10.35 | 263 ± 7.80 | 298 ± 23.33 | 309 ± 28.20 |
| MTX | 0.5 mg/kg | 162 ± 2.66 | 223 ± 4.58 | 258 ± 18.01 | 303 ± 27.77 | 309 ± 24.62 |

^{##} $P < 0.01$ versus the normal group, ^{*} $P < 0.05$ versus the model group ($n = 6$).

ethyl acetate part of EMS should regulate T- and B-cell function by inhibiting their viability.

3.5. The Effects of the Ethyl Acetate Part of EMS on the Expression of Surface Costimulatory Molecules in BMDCs. It is well known that DCs are specialized in antigen presenting, which plays an indispensable role in the onset of autoimmune diseases. To determine the effects of EMS on BMDC maturation and activation, CD40, CD80, CD86, and MHC-II were detected on DCs using flow cytometry. The morphology of BMDCs was observed using an inverted microscope (motic, AE2000LED) (Figure 5(a)). As shown in

Figure 5, flow cytometry results showed that the expression of CD40, CD80, CD86, and MHC-II were upregulated in the model group (compared to the normal group, $P < 0.01$). EMS (3 g/kg) treatment clearly suppressed the expression of CD80, CD86, and MHC-II ($P < 0.01$). In addition, EMS (0.75 g/kg) decreased the expression of CD86 compared with AA rats ($P < 0.01$). Moreover, EMS (1.5 g/kg) and MTX (0.5 mg/kg) suppressed the expression of CD40, CD80, CD86, and MHC-II in BMDCs compared with AA rats. The ethyl acetate part of EMS treatment inhibited the effect on BMDCs in AA rats in a dose-dependent manner. These results suggest that EMS inhibits BMDC maturation in AA rats.

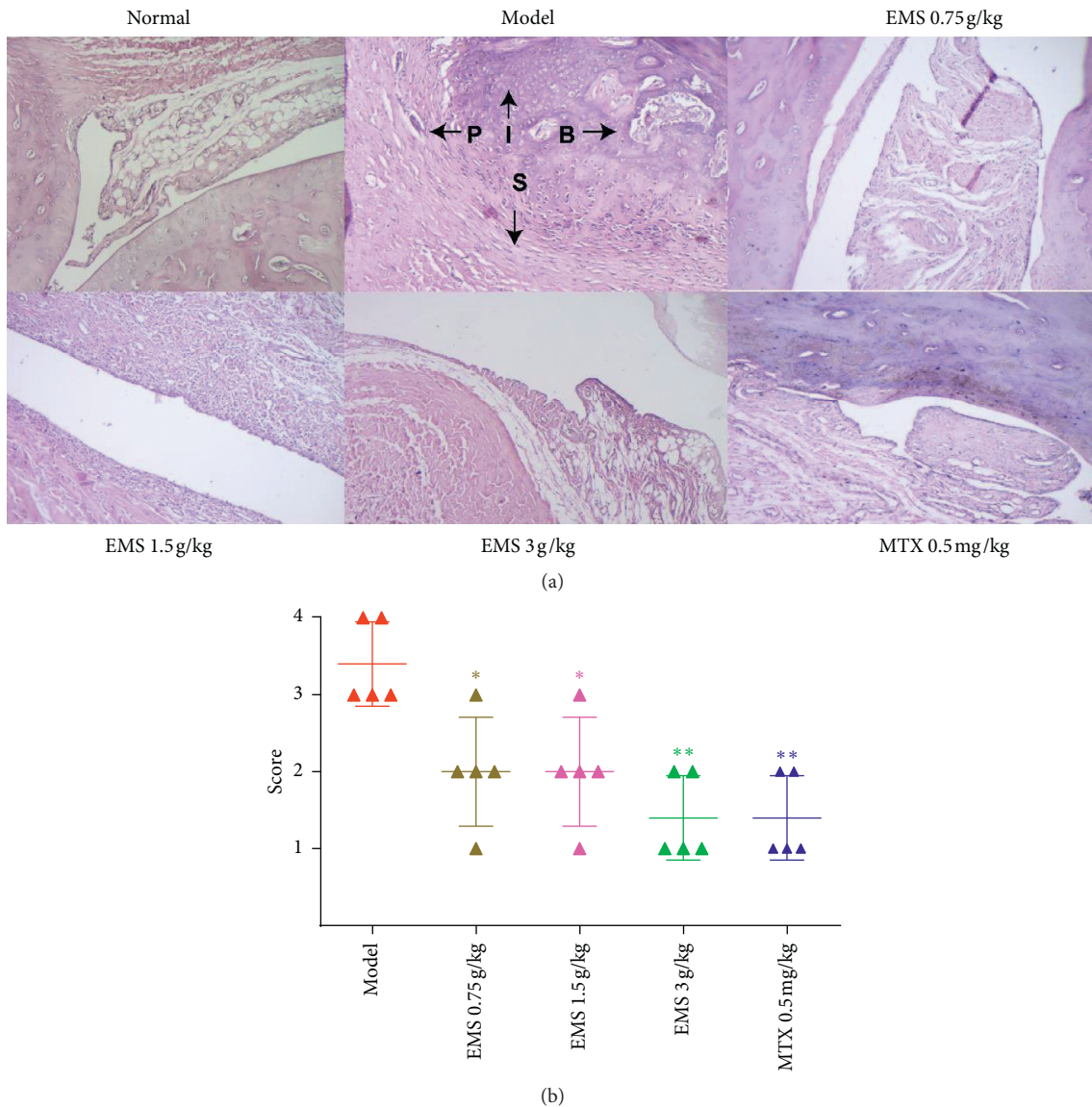


FIGURE 2: The ethyl acetate part of EMS effects on ankle pathology in AA rats was detected using HE staining. (a) Photographs of representative EMS effects on the ankle pathology in AA rats (HE, $\times 100$ magnification). P: pannus, B: bone erosion, S: synovial proliferation, and I: inflammatory cells infiltration. (b) The scores of histopathology in the rats were calculated. * $P < 0.05$, ** $P < 0.01$ versus the model group ($n = 5$).

3.6. The Effects of the Ethyl Acetate Part of EMS on BMDCs Supernatant Cytokines in AA Rats. With the development of RA, intracellular inflammatory factors have changed. To evaluate the ability of the ethyl acetate part of EMS to modulate cytokine production in BMDCs, proinflammatory cytokines (TNF- α and IL-23), inflammatory factors (PGE2), and anti-inflammatory cytokine (IL-10) were detected in the supernatant of BMDCs. As shown in Figure 6, compared with the normal group, the concentration of TNF- α , PGE2, and IL-23 in the supernatant of BMDCs increased in the model group ($P < 0.01$). By contrast, the concentration of IL-10 dramatically declined in the model group ($P < 0.01$) (Figure 6(d)). EMS (0.75, 1.5, and 3 g/kg) or MTX (0.5 mg/kg) significantly inhibited the concentration of proinflammatory cytokines (TNF- α and IL-23) and inflammatory

factors (PGE2) (compared to the model group, $P < 0.01$). Moreover, the levels of anti-inflammatory cytokine (IL-10) increased in a dose-dependent manner after EMS treatment ($P < 0.01$). These results suggest that EMS inhibits BMDC function to secrete inflammatory factors.

4. Discussion

Previous research has shown that EMS water extract has a therapeutic effect on AA rats, significantly reducing the pathological index and paw swelling in rats with arthritis [12]. In order to further study the effective antiarthritis parts of EMS, these were extracted using different organic solvents, such as dichloromethane, ethyl acetate, chloroform, and petroleum ether. Dichloromethane and ethyl acetate

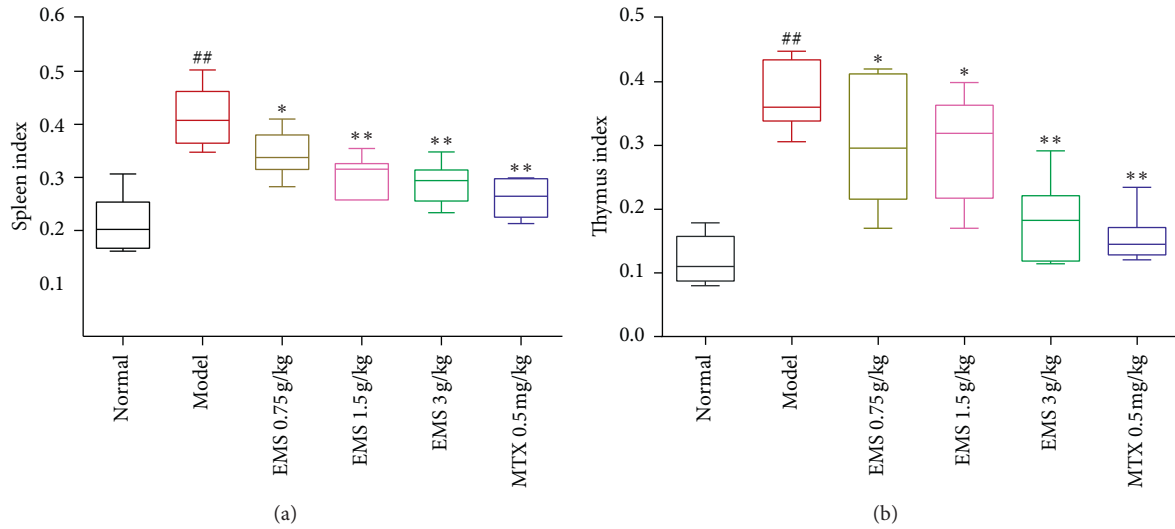


FIGURE 3: The effects of the ethyl acetate part of EMS on spleen and thymus index in AA rats. (a) Spleen index; (b) thymus index; ## $P < 0.01$ versus the normal group. * $P < 0.05$, ** $P < 0.01$ versus the model group ($n = 6$).

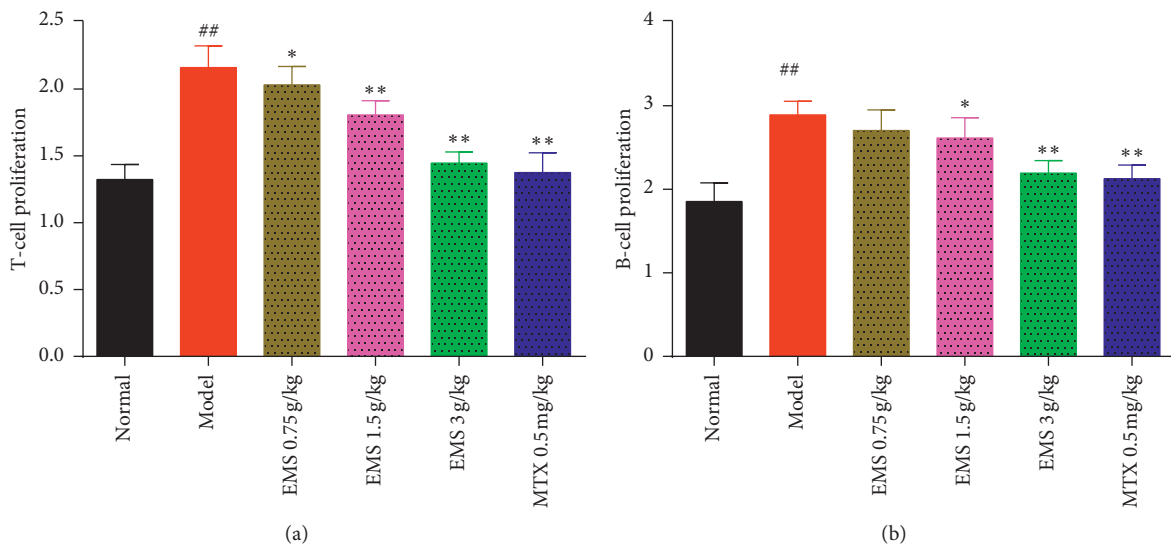


FIGURE 4: The effects of the ethyl acetate part of EMS on T- and B-cell proliferation in AA rats. (a) T-cell proliferation; (b) B-cell proliferation; ## $P < 0.01$ versus the normal group. * $P < 0.05$, ** $P < 0.01$ versus the model group ($n = 6$).

were the two parts of EMS treatment that had an effective effect on AA rats [8]. Through a comprehensive evaluation of the arthritic indicators, the ethyl acetate part of EMS might be an effective anti-inflammatory part. In this study, an aqueous solution of EMS was extracted with petroleum ether, which was directly extracted with ethyl acetate. Therefore, we obtained the ethyl acetate part of EMS. The ethyl acetate part of EMS (0.75, 1.5, and 3 g/kg) was administered to AA rats. The results showed that the ethyl acetate part of the EMS treatment obviously reduced paw swelling (Figure 1(b)) and the polyarthritis index (Figure 1(c)), improving the histological severity scores (Figure 2), which is consistent with our previous study [8]. However, the results provided the basis of pharmacodynamics and inspired us to continue exploring the

mechanism of ethyl acetate in EMS antiarthritis therapy. In addition, berberine and atracylodin were detected from the EMS ethyl acetate part using HPLC in a previous study [8]. Berberine has a positive effect in AA rats, reducing the concentration of proinflammatory cytokines (IL-1 β , IL-6, and IL-17) and increasing the concentration of anti-inflammatory cytokines (IL-10 and TGF- β) [13, 14]. Furthermore, berberine and atracylodin could protect collagen-induced arthritis rats by regulating the DC function by suppressing maturation or promoting apoptosis [15, 16]. Therefore, we speculate that the antiarthritis effect of EMS may be due to the regulation of DC maturation.

We found that the ethyl acetate part of EMS obviously reduced the spleen index and thymus index (Figure 3) and inhibited the proliferation of T- and B-cells (Figure 4). It has

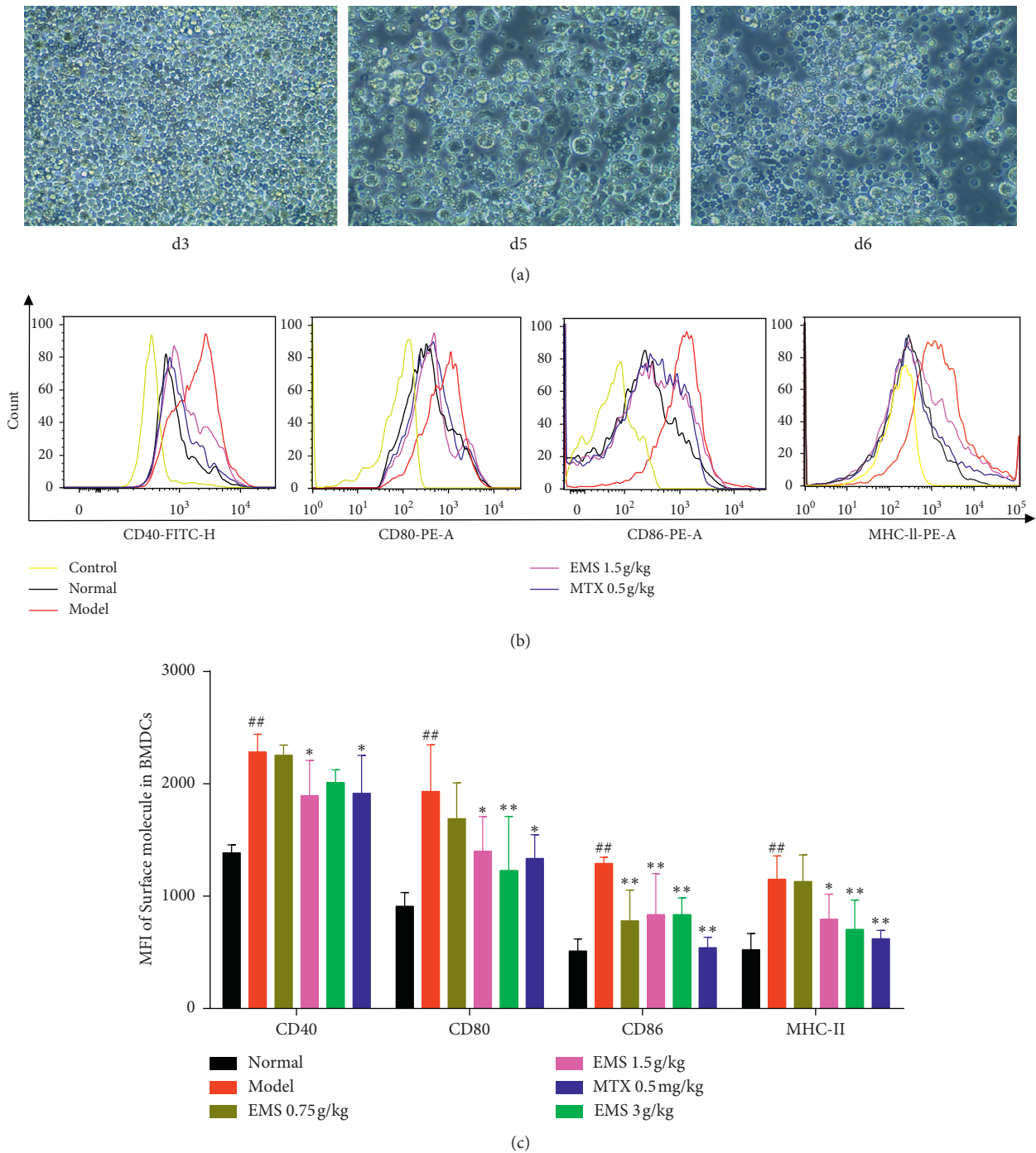


FIGURE 5: The effects of the ethyl acetate part of EMS on the expression of CD40, CD80, CD86, and MHC-II on BMDCs. (a) The morphology of bone marrow-derived dendritic cells (x200 magnification). (b) CD40, CD80, CD86, and MHC-II were detected by flow cytometry. (c) The MFI of CD40, CD80, CD86, and MHC-II in BMDCs were calculated. ## $P < 0.01$ versus the normal group. * $P < 0.05$, ** $P < 0.01$ versus the model group ($n = 4$).

been reported that cytotoxic T-lymphocyte-associated antigen-4 (CTLA-4) blocks the interaction between APC and T-cells, in which the mode of action is integrated with CD80 and CD86 receptors on APC, preventing CD28 on the surface of T-lymphocytes [17]. This protein receptor has been found to play a crucial role in autoimmune disease by blocking the interplay between B-cells, APC, and T-cells. It

was suggested that the fact that the ethyl acetate part of EMS alleviated arthritis may be related to the inhibition of T- and B-cells. As it has been reported, DCs are specialized in antigen presenting, which plays an indispensable role on the onset of autoimmune diseases. Mature DCs highly express surface stimulating molecules, such as CD40, CD80, CD86, and MHC-II. As an important indicator to identify DCs,

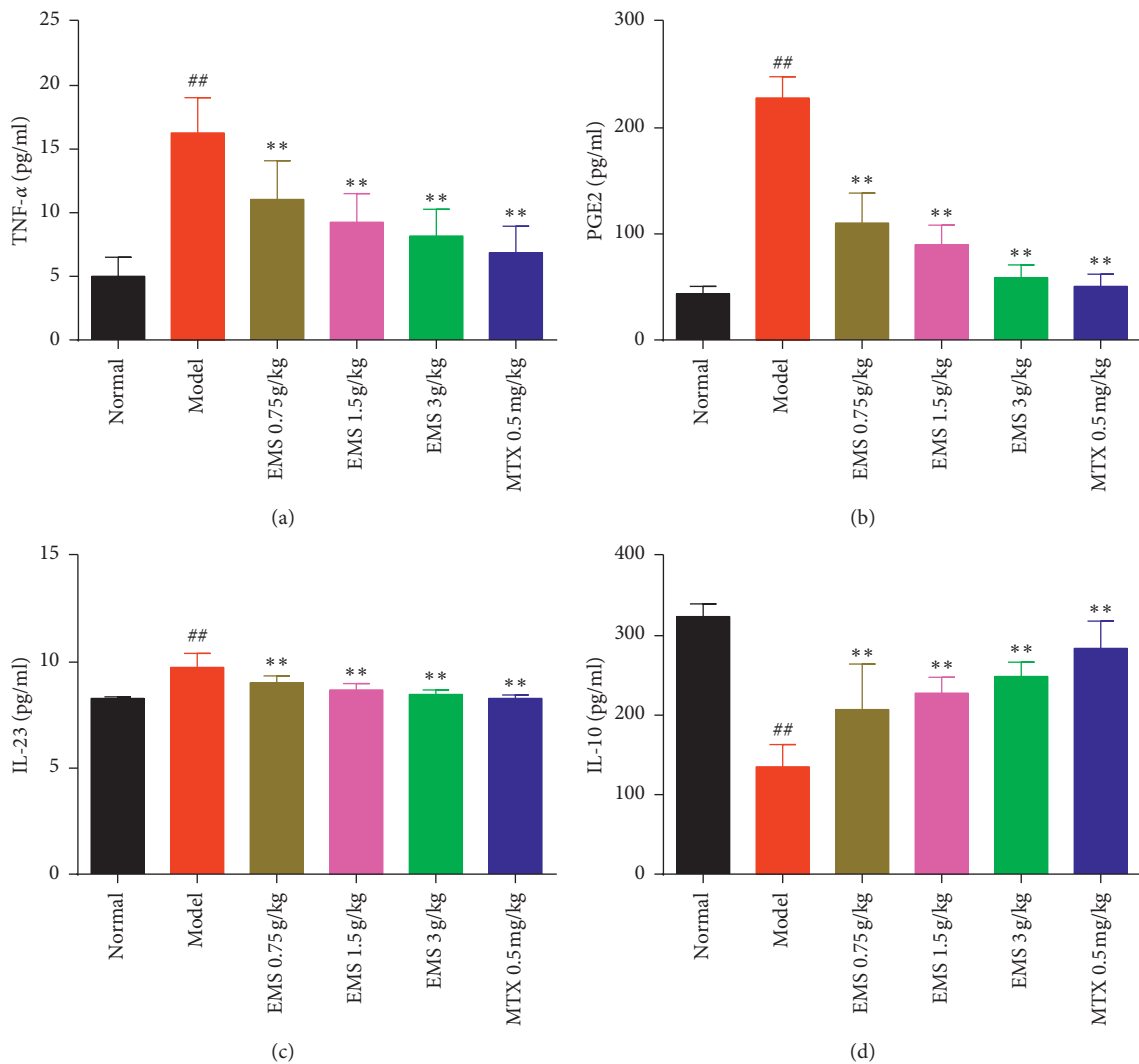


FIGURE 6: The effects of the ethyl acetate part of EMS on cytokines production in BMDCs of AA rats. The levels of TNF- α , PGE2, IL-23, and IL-10 in BMDCs were measured by ELISA. (a) TNF- α , (b) PGE2, (c) IL-23, and (d) IL-10, ^{##} $P < 0.01$, versus the normal group. ^{**} $P < 0.01$ versus the model group ($n = 6$).

flow cytometry can accurately and quickly detect the expression of CD40, CD80, CD86, and MHC-II on their surface. To determine the effects of EMS on BMDC maturation, CD40, CD80, CD86, and MHC-II were detected on DCs using flow cytometry. The results showed that the expression of CD40, CD80, CD86, and MHC-II was upregulated in AA rats. Treatment with EMS clearly suppressed the expression of CD40, CD80, CD86, and MHC-II in BMDCs compared with AA rats. Therefore, the ethyl acetate part of the EMS antiarthritis mechanism may be related to the inhibition of BMDC maturation.

IL-6 blocked tocilizumab and the IL-1 blocker anakinra have also been used to treat RA [18, 19]. DCs induce T-cell differentiation into Th1 and Th17 cells, which secrete IL-12 and IL-23 to exacerbate RA disease [20, 21]. IL-10 plays a crucial role in regulating Treg cell differentiation and enhancing the effect of Treg cell inhibition of TH17 cells to mitigate the degree of joint inflammation in AA mice [22, 23]. Meanwhile, we detected that the ethyl acetate part of

EMS effectively reduced the concentration of proinflammatory cytokines TNF- α (Figure 6(a)) and IL-23 (Figure 6(c)) and increased the level of anti-inflammatory cytokine IL-10 (Figure 6(d)). PGE2 is an important metabolite of arachidonic acid and plays an important regulatory role in the immune response. PGE2 was detectable in the synovium of patients with arthralgia [24]. It has been reported that PGE2 participates in the expression of prostaglandin E4 and nuclear factor kappa-B in DCs, which upregulate the level of cAMP protein by inducing IL-23 Subunit p19 in DCs [25, 26]. We found that the concentration of PGE2 in the supernatant of BMDCs increased in AA rats. EMS treatment significantly inhibited the concentration of PGE2 (Figure 6(b)). Therefore, the mechanism of alleviation of inflammation by inhibiting the expression of BMDCs may be related to a variety of signaling pathways. This might provide evidence to study the mechanism of the active pathway of DCs in RA. In future research, we will focus on the mechanism of the specific action of EMS

treatment on inhibiting the function of DC and its relationship with the participation of molecular signals.

5. Conclusions

These results suggest that the ethyl acetate part of EMS has better protective effects on AA rats, probably by regulating the maturation of BMDCs and modulating the balance of cytokines.

Data Availability

The data used to support the findings of this study are available from the corresponding author upon request.

Conflicts of Interest

The authors have no conflicts of interest to declare.

Authors' Contributions

XYJ and NW designed and performed experiments and revised the manuscript. JMD designed and performed experiments and wrote the manuscript. ZHX, ML, and MLL performed experiments. All authors read and approved the manuscript.

Acknowledgments

This work was supported by the National Natural Science Foundation of China (81603362) and by the Anhui Natural Science Foundation of China (1708085QC77).

References

- [1] M. Cojocaru, I. M. Cojocaru, I. Silosi, and C. D. Vrabie, "Metabolic syndrome in rheumatoid arthritis," *Maedica*, vol. 7, no. 2, pp. 148–152, 2012.
- [2] S.-W. Qiao, R. Iversen, M. Ráki, and L. M. Sollid, "The adaptive immune response in celiac disease," *Seminars in Immunopathology*, vol. 34, no. 4, pp. 523–540, 2012.
- [3] D. A. Horwitz, T. M. Fahmy, C. A. Piccirillo, and A. La Cava, "Rebalancing immune homeostasis to treat autoimmune diseases," *Trends in Immunology*, vol. 40, no. 10, pp. 888–908, 2019.
- [4] R. Thomas, L. S. Davis, and P. E. Lipsky, "Rheumatoid synovium is enriched in mature antigen-presenting dendritic cells," *Journal of Immunology*, vol. 152, no. 5, pp. 2613–2623, 1994.
- [5] M. B. Yu and W. H. R. Langridge, "The function of myeloid dendritic cells in rheumatoid arthritis," *Rheumatology International*, vol. 37, no. 7, pp. 1043–1051, 2017.
- [6] J. Alam, I. Jantan, and S. N. A. Bukhari, "Rheumatoid arthritis: recent advances on its etiology, role of cytokines and pharmacotherapy," *Biomedicine & Pharmacotherapy*, vol. 92, pp. 615–633, 2017.
- [7] H.-J. Yi and G.-X. Lu, "Adherent and non-adherent dendritic cells are equivalently qualified in GM-CSF, IL-4 and TNF- α culture system," *Cellular Immunology*, vol. 277, no. 1-2, pp. 44–48, 2012.
- [8] W. Zhang, Q. Zhang, Z. Xuan et al., "The protective effect of different polar solvent extracts of Er Miao san on rats with adjuvant arthritis," *Evidence-Based Complementary and Alternative Medicine*, vol. 2020, Article ID 5305278, 8 pages, 2020.
- [9] Z. Lingling, Y.-X. Shen, and W. Wei, "Relationship between clinical and animal models of rheumatoid arthritis," *Chinese Pharmacological Bulletin*, vol. 5, pp. 502–506, 2002.
- [10] X.-y. Jia, Y. Chang, F. Wei et al., "CP-25 reverses prostaglandin E4 receptor desensitization-induced fibroblast-like synoviocyte dysfunction via the G protein-coupled receptor kinase 2 in autoimmune arthritis," *Acta Pharmacologica Sinica*, vol. 40, no. 8, pp. 1029–1039, 2019.
- [11] I.-T. Chyuan, H.-F. Tsai, H.-J. Liao, C.-S. Wu, and P.-N. Hsu, "An apoptosis-independent role of TRAIL in suppressing joint inflammation and inhibiting T-cell activation in inflammatory arthritis," *Cellular & Molecular Immunology*, vol. 15, no. 9, pp. 846–857, 2018.
- [12] X. Dai, D. Yang, J. Bao et al., "Er Miao San, a traditional Chinese herbal formula, attenuates complete Freund's adjuvant-induced arthritis in rats by regulating Th17/Treg cells," *Pharmaceutical Biology*, vol. 58, no. 1, pp. 157–164, 2020.
- [13] X. Wang, X. He, C.-F. Zhang, C.-R. Guo, C.-Z. Wang, and C.-S. Yuan, "Anti-arthritis effect of berberine on adjuvant-induced rheumatoid arthritis in rats," *Biomedicine & Pharmacotherapy*, vol. 89, pp. 887–893, 2017.
- [14] P. Dinesh and M. K. Rasool, "Berberine mitigates IL-21/IL-21R mediated autophagic influx in fibroblast-like synoviocytes and regulates Th17/Treg imbalance in rheumatoid arthritis," *Apoptosis: An International Journal on Programmed Cell Death*, vol. 24, no. 7-8, pp. 644–661, 2019.
- [15] Z. Hu, Q. Jiao, J. Ding et al., "Berberine induces dendritic cell apoptosis and has therapeutic potential for rheumatoid arthritis," *Arthritis & Rheumatism*, vol. 63, no. 4, pp. 949–959, 2011.
- [16] C. H. Chuang, Y.-C. Cheng, S.-C. Lin et al., "Atractylodin suppresses dendritic cell maturation and ameliorates collagen-induced arthritis in a mouse model," *Journal of Agricultural and Food Chemistry*, vol. 67, no. 24, pp. 6773–6784, 2019.
- [17] T. L. Walunas, D. J. Lenschow, C. Y. Bakker et al., "Pillars article: CTLA-4 can function as a negative regulator of T cell activation. *Immunity*. 1994. 1: 405-413," *Journal of Immunology*, vol. 187, no. 7, pp. 3466–3474, 2011.
- [18] J. S. Smolen, A. Beaulieu, A. Rubbert-Roth et al., "Effect of interleukin-6 receptor inhibition with tocilizumab in patients with rheumatoid arthritis (OPTION study): a double-blind, placebo-controlled, randomised trial," *Lancet (London, England)*, vol. 371, no. 9617, pp. 987–997, 2008.
- [19] A. Chopra, M. Saluja, T. Kianifard, D. Chitre, and A. Venugopalan, "Long term effectiveness of RA-1 as a monotherapy and in combination with disease modifying anti-rheumatic drugs in the treatment of rheumatoid arthritis," *Journal of Ayurveda and Integrative Medicine*, vol. 9, no. 3, pp. 201–208, 2018.
- [20] S. Sozzani, A. Del Prete, and D. Bosisio, "Dendritic cell recruitment and activation in autoimmunity," *Journal of Autoimmunity*, vol. 85, pp. 126–140, 2017.
- [21] M. C. Lebre, S. L. Jongbloed, S. W. Tas, T. J. M. Smeets, I. B. McInnes, and P. P. Tak, "Rheumatoid arthritis synovium contains two subsets of CD83–DC–LAMP– dendritic cells with distinct cytokine profiles," *The American Journal of Pathology*, vol. 172, no. 4, pp. 940–950, 2008.
- [22] S. Nakachi, S. Sumitomo, Y. Tsuchida et al., "Interleukin-10-producing LAG3+ regulatory T cells are associated with disease activity and abatacept treatment in rheumatoid

- arthritis," *Arthritis Research & Therapy*, vol. 19, no. 1, p. 97, 2017.
- [23] M. J. Park, S. H. Lee, E. K. Kim et al., "Interleukin-10 produced by myeloid-derived suppressor cells is critical for the induction of Tregs and attenuation of rheumatoid inflammation in mice," *Scientific Reports*, vol. 8, no. 1, p. 3753, 2018.
- [24] M. J. de Hair, P. Leclerc, E. C. Newsum et al., "Expression of prostaglandin E2 enzymes in the synovium of arthralgia patients at risk of developing rheumatoid arthritis and in early arthritis patients," *PLoS One*, vol. 10, no. 7, p. e0133669, 2015.
- [25] V. P. Kocieda, S. Adhikary, F. Emig, J. H. Yen, M. G. Toscano, and D. Ganea, "Prostaglandin E2-induced IL-23p19 subunit is regulated by cAMP-responsive element-binding protein and C/AATT enhancer-binding protein β in bone marrow-derived dendritic cells," *The Journal of Biological Chemistry*, vol. 287, no. 44, pp. 36922–36935, 2012.
- [26] Y. Li, K. Sheng, J. Chen et al., "Regulation of PGE2 signaling pathways and TNF-alpha signaling pathways on the function of bone marrow-derived dendritic cells and the effects of CP-25," *European Journal of Pharmacology*, vol. 769, pp. 8–21, 2015.

Research Article

Amelioration of Rheumatoid Arthritis by *Anacardium occidentale* via Inhibition of Collagenase and Lysosomal Enzymes

Rabiya Naz,¹ Zaheer Ahmed ,² Muhammad Shahzad,³ Arham Shabbir ,⁴
and Faiza Kamal¹

¹Department of Home and Health Sciences, Allama Iqbal Open University Islamabad, Islamabad, Pakistan

²Department of Environmental Design, Health and Nutritional Sciences, Allama Iqbal Open University Islamabad, Islamabad, Pakistan

³Department of Pharmacology, University of Health Sciences Lahore, Lahore, Pakistan

⁴Institute of Pharmacy, Faculty of Pharmaceutical and Allied Health Sciences, Lahore College for Women University, Jail Road, Lahore, Pakistan

Correspondence should be addressed to Zaheer Ahmed; zaheer863@gmail.com

Received 25 August 2020; Revised 9 October 2020; Accepted 19 October 2020; Published 9 November 2020

Academic Editor: Francesca Mancianti

Copyright © 2020 Rabiya Naz et al. This is an open access article distributed under the Creative Commons Attribution License, which permits unrestricted use, distribution, and reproduction in any medium, provided the original work is properly cited.

Anacardium occidentale (cashew) has been used in the traditional system of medicine for curing many inflammatory disorders. The present study investigates the antiarthritic effects of cashew leaves extract using the rat model of FCA-induced rheumatoid arthritis. Arthritic rats were treated with 100 and 200 mg/kg b.w. ethanolic extract of cashew leaves. Animals were sacrificed at day 23, and before sacrificing the animals, gross pathological changes were observed. Histopathology of ankle joint was evaluated with hematoxylin and eosin staining, whereas the serum levels of C-reactive protein (CRP) were evaluated by the agglutination method. Inflammatory cells and other hematological parameters were assessed by employing an automated hemocytometer and chemistry analyzer. Rheumatoid factor (Rf) and lysosomal enzymes levels were determined in blood. Results indicated that *A. occidentale* significantly decreased the CPR levels, macroscopic arthritic score, and rheumatoid factor as compared to the diseased group. Histopathological evaluation showed significant attenuation in bone erosion, joint inflammation, and pannus formation by plant extract. Treatment with *A. occidentale* significantly suppressed the levels of acid phosphatase, β -galactosidase, β -glucuronidase, *N*-acetylglucosaminidase, and collagenase. Moreover, *A. occidentale* significantly raised the HB levels and RBCs counts which were found depleted in the diseased group. The raised counts of total leukocytes, platelets, neutrophils, lymphocytes, and monocytes were also significantly decreased by treatment with plant extract. Comparative analysis showed that higher dose of *A. occidentale* demonstrated superior amelioration of rheumatoid arthritis as compared to low dose. In conclusion, *A. occidentale* possesses significant antiarthritic potential, which may be attributed to the suppression of lysosomal enzymes and collagenase levels.

1. Introduction

Rheumatoid arthritis is an autoimmune disease that affects the joints but can also involve various extra-articular complications. It affects almost every diarthrodial joint and the hallmark features include persistent chronic inflammation, pannus formation, cartilage/bone erosion, and synovial proliferation. Extra-articular manifestations may implicate weight loss, rheumatoid nodules, vasculitis, serositis, etc. [1–3]. Globally, 1% of the population suffers from the rheumatoid arthritis and the age between 35 and 45 years is considered as the peak age for the onset of disease. RA significantly affects the quality of

life causing elevation in functional and work disability, morbidity rate, and economic burden [4–6].

Conventional medicines currently in use for arthritic treatment, such as disease-modifying antirheumatic agents, NSAIDs, steroids, and biological agents, have only limited success against RA and are linked with numerous side effects [7, 8]. Long-term use of these therapies is associated with well-known limitations like risks of hematological, gastrointestinal, cardiovascular, and kidney disorders and loss of response [9]. Plant-based medicines are gaining prime importance among patients suffering from RA due to the adverse effects associated with conventional therapy [10, 11].

Anacardium occidentale L. (Family: Anacardiaceae) has been traditionally used for curing many inflammatory diseases [12]. Previous studies have shown anti-inflammatory effects of *A. occidentale* in different models of inflammation. It is known to inhibit carrageenan-induced paw edema and formalin-induced paw licking in rats [13]. Treatment with *A. occidentale* also reduced ear edema and impaired leukocyte migration into the peritoneal cavity when tested using carrageenan-induced peritonitis [14]. Methanolic extract of *A. occidentale* showed protection against lipopolysaccharide-induced microvascular permeability [15, 16]. Treatment with *A. occidentale* significantly reduced prostaglandin-E2 production in the microglia. The plant showed anti-inflammatory property by inhibiting inflammation-associated cytokine production. Moreover, significant inhibition of COX-2 and iNOS gene production by blocking MAPK and NF- κ B pathways were observed [16]. The current study aimed to evaluate the antiarthritic effects of *Anacardium occidentale* using FCA-induced rat model of arthritis.

2. Materials and Methods

2.1. Experimental Animals. Male Wistar rats of age 6 to 8 weeks, weighing 225–250 g, were retained at standard conditions in animal house of the University of Punjab, Lahore. Animals were given distilled water and standard rat chow *ad libitum*. After development of arthritis, food was given on the lower portion of the cages as severely arthritic rats have problem in taking feed from the upper half of the cage. Standard temperature and humidity conditions (24–26°C and 40–60%, resp.) were maintained [17]. All the experiments and protocols were approved by the Allama Iqbal Open University, Islamabad (AIOU/283).

2.2. Preparation of Plant Extract. The leaves of the *Anacardium occidentale* were collected, identified by the Botanist, and shade-dried at room temperature. The leaves were ground to powdered form (yielding 300 g) and the powdered sample was macerated in 2 L of ethanol at room temperature for 24 h. Filtrate was collected by passing the mixture through muslin cloth and subsequently through filter paper (Whatman No. 1). The residue left was again macerated in ethanol and the procedure was repeated 3 times for the collection of filtrates. The resultant filtrate was evaporated in water bath (maintained at 40°C) to obtain a semisolid extract. The percentage yield was calculated as 6.67%. The extract was then kept in a refrigerator at 4°C for further use.

2.3. Experimental Design and Induction of Arthritis. Rats were distributed into 5 groups, having 6 rats in each group.

Group 1 (control): it included healthy rats serving as control group, injected with 0.1 ml normal saline at the subplantar region in hind paw.

Group 2 (arthritic): Freund's Complete Adjuvant (FCA) was used to induce arthritis. Normal saline was

administered to this group from day 8, once daily for 15 days.

Group 3 (AO 100 mg/kg): it included arthritic rats receiving low oral dose of *Anacardium occidentale* extract, i.e., 100 mg/kg b.w. Treatment was started from day 8, once daily for 15 days.

Group 4 (AO 200 mg/kg): arthritic rats were given high oral dose of *Anacardium occidentale* extract, i.e., 200 mg/kg b.w. Treatment was started from day 8, once daily for 15 days.

Group 5 (piroxicam): arthritic rats received 10 mg/kg b.w. piroxicam as standard drug [18]. Treatment was started from day 8, once daily intraperitoneally for 15 days.

For the induction of arthritis, 0.2 ml FCA (a suspension of heat-killed *Mycobacterium*) was injected in the subplantar region of the left hind rat paw on day 0 in all groups except control group. Treatment was started at the 8th day of arthritis induction for 15 days and all animals were sacrificed at day 23 [18].

2.4. Determination of Arthritic Development. Incidence and severity of arthritis was evaluated by arthritic scoring method. Presence of the detectable clinical arthritic features characterized by edema and/or erythema in the hind rat paws was observed. Through macroscopic evaluation, arthritic score was determined at days 13, 18, and 23. Scores 0–4 were given to normal-severe edema and/or erythema in ipsilateral paw. Arthritic score crossing 4 is the indication of involvement of contralateral paw [19].

2.5. Histopathological Examinations of Ankle Joints. The ankle joints of the ipsilateral paw were cut and fixed in 10% formalin for 36 hours. These separated joints were then submerged in decalcifying solution (a mixture of ethylenediamine tetra acetic acid, sodium tartrate, hydrochloric acid, and potassium sodium tartrate) for 48 hours. Collected tissues were further treated for implanting in paraffin blocks, sliced at 5 μ m thickness, and stained with hematoxylin and eosin (H&E). The histopathologist studied the slides in blinded fashion for the detection of bone erosion, inflammation, and pannus formation. A scale (0 to 4) was used for recording results, where 0 represents no pathological change whereas scores 1 to 4 refer to minimal, mild, moderate, and severe changes, respectively [17, 20].

2.6. Determination of Inflammatory Cell and Other Hematological Parameters in Blood. At the time of dissection, blood was collected in EDTA containing tubes by intracardiac puncture. Inflammatory cell counts like eosinophils, neutrophils, basophils, and lymphocytes were evaluated in Giemsa Wright stained blood smears under light microscope [21], and counts of RBCs, platelets, and total leukocytes along with Hb content were determined by using automated hemocytometer.

2.7. Evaluation of C-Reactive Protein Levels. On day 23, all the rats were sacrificed and blood was withdrawn by intracardiac puncture. Serum was collected after centrifugation for 10 min at 2380 g. The levels of CPR were determined by agglutination method using commercially available kits (Antec Diagnostic Products, UK). Significant agglutination is observed when high amount of CPR is present in the serum and it interacts with the antisera. CRP levels were semi-quantified according to the kit's protocol [3].

2.8. Determination of Rheumatoid Factor Levels. Rheumatoid factor is the autoantibody produced in arthritis. The level of rheumatoid factor (Rf) was estimated by means of the latex method. The complete procedure was followed according to the manufacturer's guidelines (Approach Bioscience). The concentration of rheumatoid factor was expressed as IU/ml [22].

2.9. Determination of Lysosomal Enzymes and Collagenase Levels. Acid phosphatase analysis was performed by utilizing a substrate known as disodium phenyl phosphate [23]. β -Glucuronidase was determined by the method of Kawai and Anno [24]. *p*-Nitrophenyl β -D-glucuronide was used as enzyme substrate in the reaction. *N*-Acetylglucosaminidase was measured by using the substrate 4-nitrophenyl *N*-acetylglucosaminide [25]. The activity of β -galactosidase was assessed by the method of [26] by utilizing the substrate 4-nitrophenyl *N*-acetyl galactopyranoside. Protein concentration was determined as described by [27]. Activity of collagenase was measured by the method of Van and Steinbrink [28], using *N*-(3-[2-furyl] acryloyl)-Leu-Gly-Pro-Ala as substrate.

2.10. Statistical Analysis. The data was analyzed using GraphPad version 5 software. Mean \pm standard deviation was used to represent the data. One-way analysis of variance and post hoc Tukey's test was applied to compare the quantitative variables and to analyze the difference among all groups. $P < 0.05$ was considered as statistically significant.

3. Results

3.1. *A. occidentale* Suppressed the Arthritic Development. The results indicated a significantly high arthritic score in arthritic rats as compared to control on day 13 (0.00 ± 0.00 vs. 3.750 ± 0.2739), day 18 (0.00 ± 0.00 vs. 4.667 ± 0.5164), and day 23 (0.00 ± 0.00 vs. 5.000 ± 0.4472). Although treatment with low dose of *A. occidentale* reduced the arthritic score on all these days, this reduction was not statistically significant as compared to the arthritic group. High dose of *A. occidentale* significantly reduced ($p < 0.001$) the arthritic score on day 13 (2.333 ± 0.2582 vs. 3.750 ± 0.2739), day 18 (3.00 ± 0.3162 vs. 4.667 ± 0.5164), and day 23 (2.833 ± 0.4082 vs. 5.00 ± 0.4472). Piroxicam also significantly decreased ($p < 0.001$) the arthritic score on these days as compared to the arthritic group (2.333 ± 0.4082 vs. 3.750 ± 0.2739), (2.833 ± 0.4082 vs. 4.667 ± 0.5164), and (2.750 ± 0.2739 vs. 5.000 ± 0.4472), respectively. There was

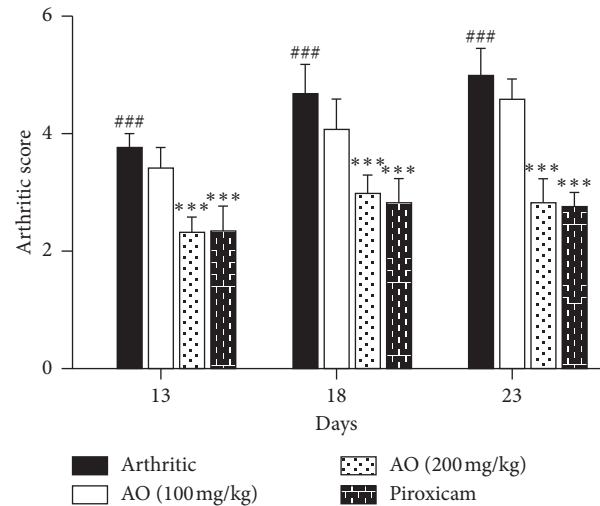


FIGURE 1: Treatment with *A. occidentale* showed significant reduction in arthritic score. The data is presented as mean \pm SD for $n = 6$. ### ($P < 0.001$) indicating significant difference compared to control group, while *** ($P < 0.001$) indicates significant difference compared to arthritic group.

no significant difference in the determined arthritic scores in high-dose plant extract-treated group and piroxicam-treated group on all days. The arthritic scores determined at days 13, 18, and 23 are presented Figure 1.

3.2. *A. occidentale* Significantly Suppressed C-Reactive Protein Levels. Administration of FCA resulted in increased CRP levels of arthritic group as compared to control group (24.48 ± 1.362 vs. 0.00 ± 0.00). Both low- and high-dose treatment of *A. occidentale* showed a significant reduction of CRP levels as compared to arthritic group (20.08 ± 1.931 vs. 24.48 ± 1.362) and (15.26 ± 1.727 vs. 24.48 ± 1.362), respectively. Similarly, piroxicam treatment also significantly decreased the CRP levels as compared to arthritic group (13.76 ± 1.172 vs. 24.48 ± 1.362). On comparing three treatment groups, we found that piroxicam showed a significantly higher capacity to alleviate C-reactive protein levels as compared to the low dose of *A. occidentale*, while no significant difference was seen when compared with the high dose of *A. occidentale* (Figure 2(a)).

3.3. *A. occidentale* Significantly Inhibited Rheumatoid Factor (RF). Increased levels of RF were found in arthritic group as compared to control group (119.7 ± 5.955 vs. 0.00 ± 0.00). Both high dose of *A. occidentale* and piroxicam showed a significant reduction in RF levels as compared to arthritic group (86.00 ± 4.099 vs. 119.7 ± 5.955) and (87.67 ± 4.546 vs. 119.7 ± 5.955), respectively. Low dose of *A. occidentale* did not show significant reduction in RF levels compared to arthritic group (112.0 ± 5.762 vs. 119.7 ± 5.955). We did not find any significant difference between the effect of high-dose *A. occidentale* and piroxicam (86.00 ± 4.099 vs. 119.7 ± 5.955) (Figure 2(b)).

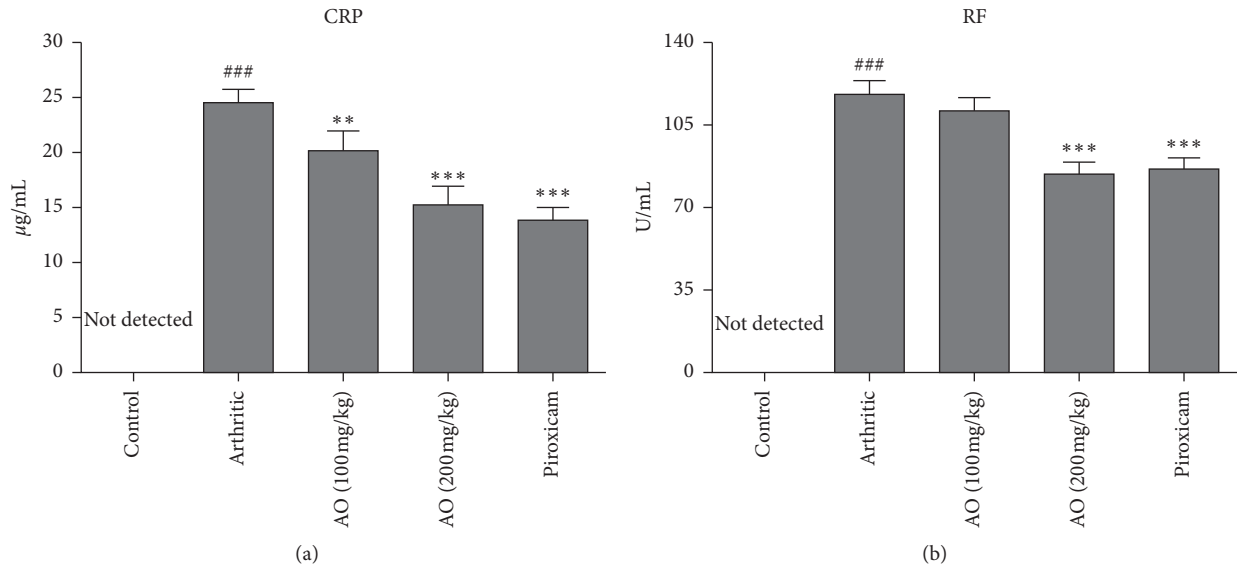


FIGURE 2: Treatment with *A. occidentale* extract caused significant suppression of levels of CRP and RF. The data is presented as mean \pm SD for $n=6$. ### ($P < 0.001$) indicating significant difference compared to control group, while ** ($P < 0.01$) and *** ($P < 0.001$) indicate significant difference compared to arthritic group.

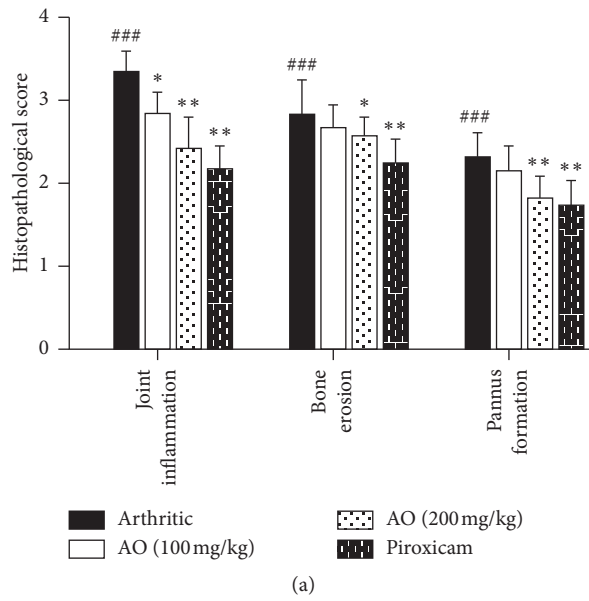


FIGURE 3: Continued.

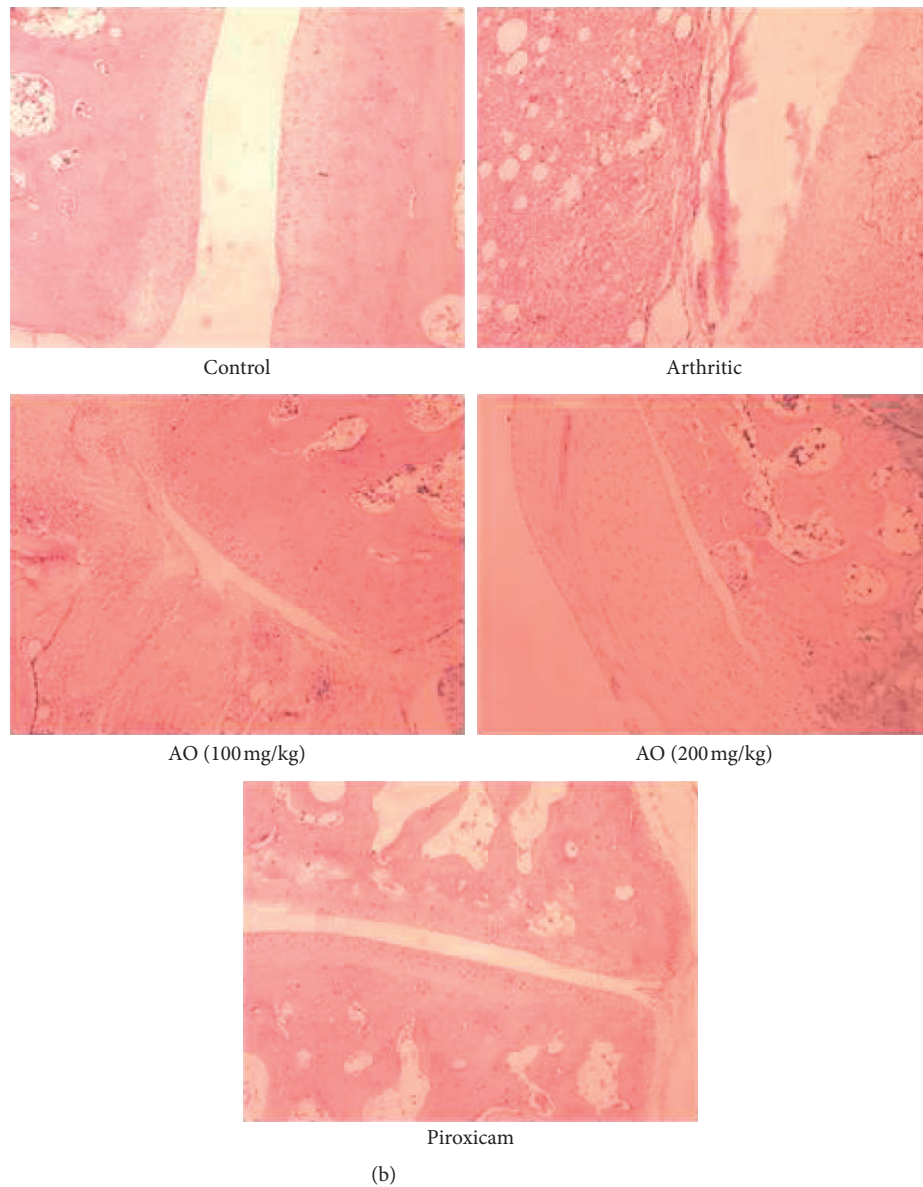


FIGURE 3: (a) Treatment with *A. occidentale* significantly reduced the histopathological score. The data is presented as mean \pm SD for $n = 6$. ### ($P < 0.001$) indicating significant difference compared to control group, while * ($P < 0.05$), ** ($P < 0.01$), and *** ($P < 0.001$) indicate significant difference compared to arthritic group. (b) H&E staining, showing normal ankle joint tissue, normal synovium, cartilage, bone, and no inflammation (control group); severe inflammation, pannus, and bony erosion (arthritic group); resolution of inflammation, pannus formation, and bony erosion (low-dose and high-dose AO group); and resolution of inflammation, pannus formation, and bony erosion (piroxicam group).

3.4. Effects of *A. occidentale* on Histopathological Changes in Ankle Joints. Severe inflammation along with massive joint inflammation, bone erosion, and pannus formation was observed in paw tissue of arthritic rats. Treatment with *A. occidentale* and piroxicam significantly decreased these histopathological changes (Figures 3(a) and 3(b)).

3.4.1. *A. occidentale* Significantly Attenuated Joint Inflammation. Significant joint inflammation was observed in arthritic group as compared with control group (3.333 ± 0.2582 vs. 0.0 ± 0.0). Treatment with low dose and high dose of

A. occidentale (2.833 ± 0.2582 vs. 3.333 ± 0.2582) and (2.417 ± 0.3764 vs. 3.333 ± 0.2582) and piroxicam (2.167 ± 0.2582) significantly reduced inflammation.

3.4.2. Treatment with *A. occidentale* Significantly Alleviated Bone Erosion. We observed significantly high bone erosion in arthritic group as compared to control group (2.833 ± 0.4082 vs. 0.0 ± 0.0). Although treatment with low dose of *A. occidentale* decreased the bone erosion, it was not significant (2.667 ± 0.2582 vs. 2.833 ± 0.4082). High-dose *A. occidentale* and piroxicam significantly reduced the bone

erosion (2.583 ± 0.2041 vs. 2.833 ± 0.4082) and (2.250 ± 0.2739 vs. 2.833 ± 0.4082), respectively.

3.4.3. *A. occidentale* Significantly Suppressed Pannus Formation. Results showed increased pannus formation in arthritic group (2.333 ± 0.2582) as compared to control group. Treatment with low dose of *A. occidentale* did not significantly decrease the pannus formation (2.167 ± 0.2582 vs. 2.333 ± 0.2582) while high dose of *A. occidentale* and piroxicam significantly reduced the pannus formation as compared to arthritic group (1.833 ± 0.2582 vs. 2.333 ± 0.2582) and (1.750 ± 0.2739 vs. 2.333 ± 0.2582), respectively.

3.5. *A. occidentale* Nearly Normalized the Total Leucocyte Count (TLC). The results showed an increase in TLC of arthritic group as compared to control group (9.293 ± 0.569 vs. 7.305 ± 0.3885) which means FCA-induced arthritis resulted in recruitment of leukocytes in arthritic group. Both low-dose and high-dose treatment of *A. occidentale* showed a significant decrease in TLC as compared to arthritic group (8.017 ± 0.3214 vs. 9.293 ± 0.569) and (7.900 ± 0.4801 vs. 9.293 ± 0.569), respectively. Similarly, piroxicam-treated group also showed a significant decrease in TLC as compared to arthritic group (7.807 ± 0.6639 vs. 9.293 ± 0.569). There was no significant difference in the TLC of low dose, high dose, and piroxicam groups when compared to each other (Table 1).

3.6. *A. occidentale* Significantly Suppressed the Raised Levels of DLC

3.6.1. *A. occidentale* Significantly Reduced Neutrophil Count. There was a significant increase in neutrophil count of arthritic group as compared to control group (66.78 ± 2.660 vs. 52.66 ± 3.369). Both low-dose and high-dose treatment of *A. occidentale* showed a significant decrease in neutrophil count as compared to arthritic group (60.43 ± 3.972 vs. 66.78 ± 2.660) and (57.94 ± 3.052 vs. 66.78 ± 2.660), respectively. Similarly, piroxicam-treated group also showed a significant decrease in TLC as compared to arthritic group (54.50 ± 3.355 vs. 66.78 ± 2.660). On comparing three treatment groups, we found that piroxicam showed a significantly higher capacity to alleviate neutrophil count as compared to low dose of *A. occidentale* while no significant difference was observed when compared with high dose of *A. occidentale* (Table 1).

3.6.2. *A. occidentale* Significantly Reduced the Elevated Lymphocytes Counts. We found a significant increase in lymphocyte counts of arthritic group as compared to control group (33.66 ± 0.7083 vs. 31.18 ± 0.6081) which indicates that FCA-induced arthritis resulted in recruitment of lymphocytes in arthritic group. Low dose of *A. occidentale* could not significantly reduce the lymphocyte count (33.27 ± 1.693 vs. 33.66 ± 0.7083), while high-dose treatment of *A. occidentale*, as well as

piroxicam, showed a significant decrease in lymphocyte count as compared to arthritic group (32.02 ± 0.5516 vs. 33.66 ± 0.7083) and (31.96 ± 0.5322 vs. 33.66 ± 0.7083), respectively. No significant difference was noted between the effects of high-dose *A. occidentale* and piroxicam when compared with one another (Table 1).

3.6.3. *A. occidentale* Ameliorated the Altered Monocyte Counts. A significant increase in monocyte counts of arthritic group was determined as compared to control group (2.412 ± 0.2001 vs. 1.610 ± 0.1336). Low dose of *A. occidentale* did not significantly reduce the lymphocyte count (2.303 ± 0.1720 vs. 2.412 ± 0.2001), while high-dose treatment of *A. occidentale*, as well as piroxicam, showed a significant decrease in monocyte count as compared to arthritic group (2.088 ± 0.1179 vs. 2.412 ± 0.2001) and (2.032 ± 0.1466 vs. 2.412 ± 0.2001), respectively. No significant difference was found between the effect of high dose *A. occidentale* and piroxicam when compared with one another (Table 1).

3.6.4. No Significant Change Was Observed in the Counts of Basophils. Results showed no significant change in basophil counts of arthritic group, low-dose *A. occidentale*, high-dose *A. occidentale*, and piroxicam-treated groups, when compared with each other (Table 1).

3.7. *A. occidentale* Reduced the Raised Platelet Counts. A significant increase in platelet count of arthritic group was observed as compared to control group (5.567 ± 0.3259 vs. 4.350 ± 0.2504). Low dose of *A. occidentale* did not significantly affect the platelet count (5.133 ± 0.1894 vs. 5.567 ± 0.3259), while high-dose treatment of *A. occidentale* (4.908 ± 0.3642 vs. 5.567 ± 0.3259), as well as piroxicam (4.882 ± 0.1847 vs. 5.567 ± 0.3259), showed a significant decrease in platelet count as compared to arthritic group. No significant difference was found between the effects of high-dose *A. occidentale* and piroxicam when compared with each other (Table 1).

3.8. *A. occidentale* Significantly Improved the RBC Count. Results indicated a significant decrease in RBC count of arthritic group as compared to control group (4.163 ± 0.4052 vs. 5.827 ± 0.3257). Low dose of *A. occidentale* did not significantly restore the RBC count (4.450 ± 0.4241 vs. 4.163 ± 0.4052), while high-dose treatment of *A. occidentale* and piroxicam showed a significant increase in RBC count as compared to arthritic group (5.057 ± 0.3642 vs. 4.163 ± 0.4052) and (4.963 ± 0.1445 vs. 4.163 ± 0.4052), respectively (Table 1).

3.9. *A. occidentale* Restored the Hemoglobin Content. There was a significant decrease in Hb content of arthritic group as compared to control group (11.67 ± 0.8179 vs. 14.66 ± 0.3985). Low dose and high dose of *A. occidentale* significantly restored the Hb content as compared to

TABLE 1: Treatment with *A. occidentale* nearly normalized all the hematological parameters.

| Parameters | Groups | | | | |
|---------------------------|----------------|-------------------------------|-----------------------------|-------------------------------|------------------------------|
| | Control | Arthritic | AO (100 mg/kg) | AO (200 mg/kg) | Piroxicam |
| TLC (10^3) | 7.305 ± 0.388 | 9.293 ± 0.569 ^{###} | 8.017 ± 0.321 ^{**} | 8.017 ± 0.321 ^{***} | 7.807 ± 0.663 ^{***} |
| Neutrophil (%) | 52.66 ± 3.369 | 66.78 ± 2.660 ^{###} | 60.43 ± 3.972 [*] | 57.94 ± 3.052 ^{***} | 54.50 ± 3.355 ^{***} |
| Lymphocytes (%) | 31.18 ± 0.608 | 33.66 ± 0.708 ^{###} | 33.27 ± 1.693 | 32.02 ± 0.551 [*] | 31.96 ± 0.532 [*] |
| Monocytes (%) | 1.610 ± 0.133 | 2.412 ± 0.200 ^{###} | 2.303 ± 0.1720 | 2.088 ± 0.117 [*] | 2.032 ± 0.146 ^{**} |
| Basophils (%) | 0.8050 ± 0.034 | 0.8500 ± 0.052 | 0.8400 ± 0.030 | 0.8267 ± 0.043 | 0.8117 ± 0.0256 |
| Platelet count (10^3) | 4.350 ± 0.250 | 5.567 ± 0.325 ^{###} | 5.133 ± 0.189 | 4.908 ± 0.364 ^{**} | 4.882 ± 0.184 ^{**} |
| RBC (10^6) | 5.827 ± 0.325 | 4.163 ± 0.405 ^{###} | 4.450 ± 0.424 | 5.057 ± 0.364 ^{**} | 4.963 ± 0.144 ^{**} |
| Hb (g/dL) | 14.66 ± 0.3985 | 11.67 ± 0.8179 ^{###} | 12.79 ± 0.3164 [*] | 13.36 ± 0.4298 ^{***} | 13.02 ± 0.6174 [*] |

^{###} $P < 0.001$ indicating significant difference compared to control group, ^{*} $P < 0.05$, ^{**} $P < 0.01$, and ^{***} $P < 0.001$ indicating significant difference compared to arthritic group.

arthritic group (12.79 ± 0.3164 vs. 14.66 ± 0.3985) and (13.36 ± 0.4298 vs. 14.66 ± 0.3985), respectively. Similarly, piroxicam also significantly improved the Hb content (13.02 ± 0.6174 vs. 14.66 ± 0.398). There was no significant difference in the effects of high dose of *A. occidentale* and piroxicam (Table 1).

3.10. Effects of *Anacardium occidentale* on Lysosomal Enzymes

3.10.1. Treatment with *A. occidentale* Significantly Reduced the Acid Phosphatase Levels. FCA resulted in increased acid phosphatase levels in arthritic group as compared to control group (0.8450 ± 0.0432 vs. 0.2233 ± 0.0463). Both high dose of *A. occidentale* and piroxicam showed a significant reduction in acid phosphatase levels as compared to arthritic group (0.4300 ± 0.0540 vs. 0.845 ± 0.0432) and (0.3583 ± 0.062 vs. 0.845 ± 0.043), respectively. Low dose of *A. occidentale* did not show any significant reduction in acid phosphatase levels compared to arthritic group (0.7667 ± 0.043 vs. 0.845 ± 0.0432). There was no significant difference between the effects of high-dose *A. occidentale* and piroxicam (0.430 ± 0.054 vs. 0.3583 ± 0.062) (Figure 4(a)).

3.10.2. *A. occidentale* Significantly Suppressed β -Galactosidase Levels. Elevated levels of β -galactosidase were found in arthritic group as compared to control group (3.500 ± 0.1814 vs. 1.867 ± 0.0778). Both high dose of *A. occidentale* and piroxicam showed a significant reduction in β -galactosidase levels as compared to arthritic group (2.542 ± 0.1532 vs. 3.500 ± 0.1814) and (2.372 ± 0.1038 vs. 3.500 ± 0.1814), respectively. Low dose of *A. occidentale* did not show any significant reduction in β -galactosidase levels compared to arthritic group (3.358 ± 0.1932 vs. 3.500 ± 0.1814). There was no significant difference between the effect of high-dose *A. occidentale* and piroxicam (2.542 ± 0.1532 vs. 2.372 ± 0.1038) (Figure 4(b)).

3.10.3. *A. occidentale* Significantly Attenuated β -Glucuronidase Levels. Results indicated high levels of β -glucuronidase in arthritic group as compared to control group (5.737 ± 0.2317 vs. 2.460 ± 0.2536). Both high dose of *A. occidentale* and piroxicam treatments resulted in a

significant reduction in β -glucuronidase levels as compared to arthritic group (2.918 ± 0.1569 vs. 5.737 ± 0.2317) and (3.163 ± 0.3574 vs. 5.737 ± 0.2317), respectively. Low dose of *A. occidentale* showed no significant reduction in β -glucuronidase levels comparing to arthritic group (5.327 ± 0.4614 vs. 5.737 ± 0.2317). There was no significant difference between the effect of high-dose *A. occidentale* and piroxicam (2.918 ± 0.1569 vs. 3.163 ± 0.3574) (Figure 4(c)).

3.10.4. *A. occidentale* Significantly Alleviated *N*-Acetyl Glucosaminidase Levels. Arthritic group showed increased levels of *N*-acetyl glucosaminidase as compared to control group (2.957 ± 0.0948 vs. 1.218 ± 0.0741). Both low dose and high dose of *A. occidentale* treatments resulted in a significant reduction in *N*-acetyl glucosaminidase levels as compared to arthritic group (2.707 ± 0.2229 vs. 2.957 ± 0.0948) and (2.047 ± 0.1211 vs. 2.957 ± 0.0948), respectively. Piroxicam also significantly reduced in *N*-acetyl glucosaminidase levels compared to arthritic group (2.257 ± 0.1618 vs. 2.957 ± 0.0948). There was no significant difference between the effect of high-dose *A. occidentale* and piroxicam (2.047 ± 0.1211 vs. 2.257 ± 0.1618) (Figure 4(d)).

3.10.5. *A. occidentale* Significantly Decreased Collagenase Levels. Results showed increased levels of collagenase in arthritic group as compared to control group (58.32 ± 3.308 vs. 31.25 ± 3.204). Both high dose of *A. occidentale* and piroxicam treatments resulted in a significant reduction in collagenase levels as compared to arthritic group (40.60 ± 2.109 vs. 58.32 ± 3.308) and (41.21 ± 3.967 vs. 58.32 ± 3.308), respectively. Low dose of *A. occidentale* showed no significant reduction in collagenase levels compared to arthritic group (52.28 ± 5.455 vs. 58.32 ± 3.308). There was no significant difference between the effect of high-dose *A. occidentale* and piroxicam (40.60 ± 2.109 vs. 41.21 ± 3.967) (Figure 5).

4. Discussion

Cashew leaves are known for their medicinal properties. The plant is used by the traditional practitioners as anti-inflammatory agent [29]. Various studies using different models of inflammation have validated the anti-

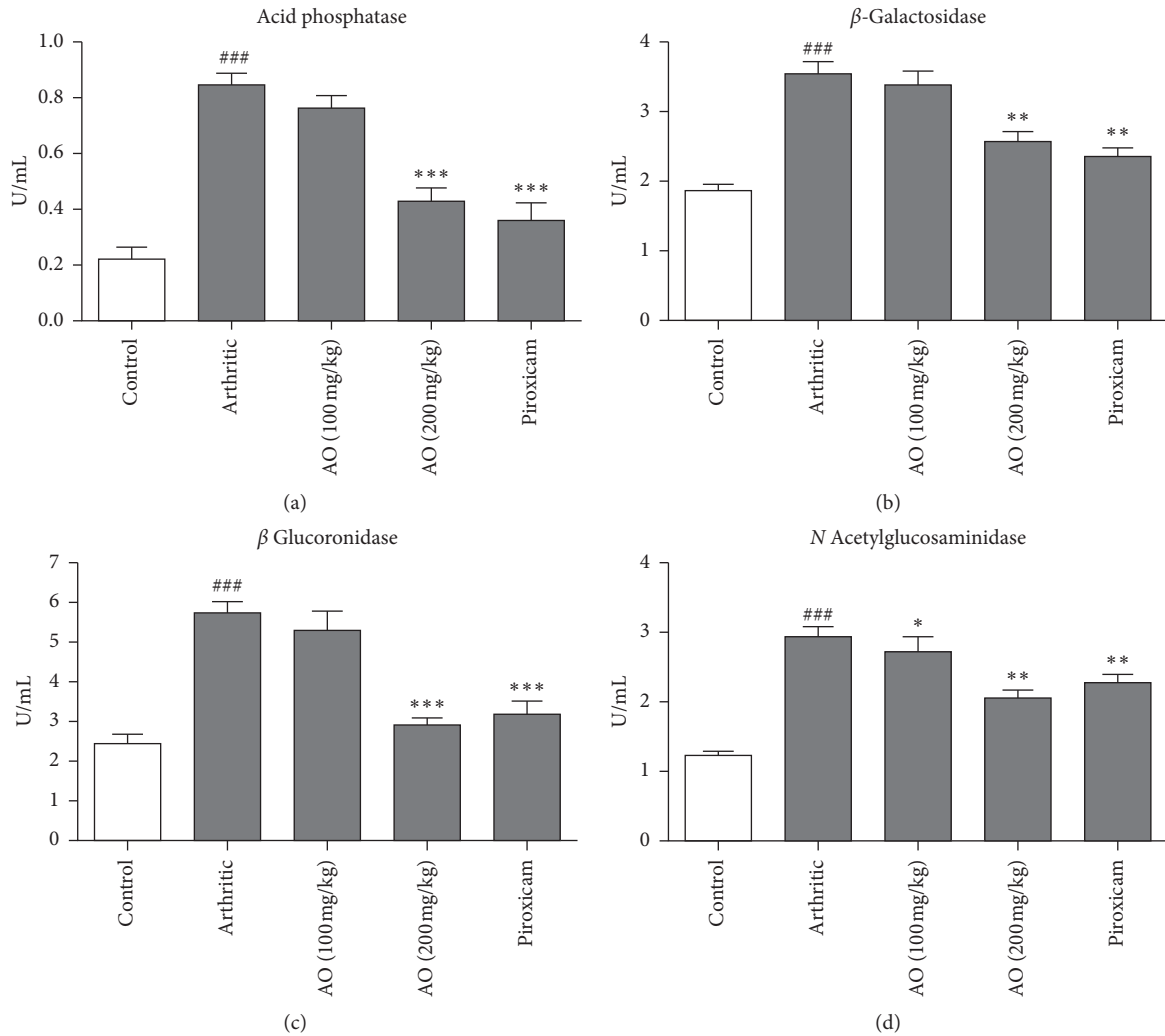


FIGURE 4: Treatment with *A. occidentale* leaves extract significantly reduced acid phosphatase, β -galactosidase, β -glucuronidase, and *N*-acetylglucosaminidase. The data is presented as mean \pm SD for $n = 6$. ### ($P < 0.001$) indicating significant difference compared to control group, while * ($P < 0.05$), ** ($P < 0.01$), and *** ($P < 0.001$) indicate significant difference compared to arthritic group.

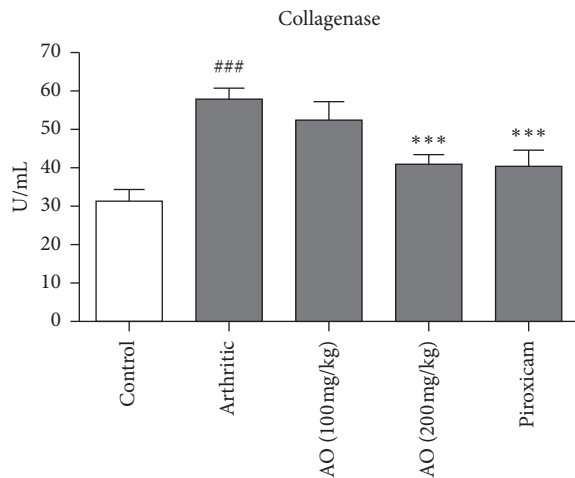


FIGURE 5: Treatment with *A. occidentale* leaves extract significantly reduced collagenase. The data is presented as mean \pm SD for $n = 6$. ### ($P < 0.001$) indicating significant difference compared to control group, while *** ($P < 0.001$) indicates significant difference compared to arthritic group.

inflammatory properties of cashew [14, 15]. Current study assessed the antiarthritic effect of cashew leaves extract using FCA-induced arthritic rat model. Adjuvant-induced arthritic model is a well-established model and has been used in several studies to determine the potential therapeutic targets and pathogenesis of RA. The role of inflammatory mediators and serological and pathological changes in adjuvant-induced arthritic model is considered similar to human rheumatoid arthritis [30, 31]. Synovial joints are particularly affected in rheumatoid arthritis. The development of synovial cell hyperplasia, inflammation, bone erosion, and pannus formation are considered as characteristic histopathological features of rheumatoid arthritis [3, 32]. Chronic inflammation of synovial tissues is the major reason for the damage inflicted to bone and cartilage [17]. Current study demonstrated that the treatment with higher dose of *A. occidentale* significantly attenuated arthritic development, bone erosion, and pannus formation which might be ascribed to anti-inflammatory effects of plant extracts. Reference drug used was piroxicam because it is

usually prescribed in the treatment of arthritis and is known to ameliorate adjuvant-induced arthritis through its immunomodulatory and anti-inflammatory activities [33, 34].

CRP is known as an acute phase protein and serves as an essential biomarker for different inflammatory, neoplastic, and degenerative disorders. Increased levels of CRP in blood are associated with almost all types of inflammatory disorders, especially in patients suffering from rheumatoid arthritis [35, 36]. RF is another important biomarker associated with various autoimmune and nonautoimmune diseases, especially rheumatoid arthritis. It is an antibody directed against the antigenic determinants on the Fc region of the immunoglobulin G [37]. RF has long been linked with the pathogenesis of RA and its induction is triggered by the formation of immune complexes during infection [38]. The elevated levels of CRP and RF in arthritic group in present study were found significantly reduced after treatment with both plant extract and piroxicam.

We found increase in TLC and platelet count in arthritic rats as compared with control group. This may be explained as the result of induction of immune response against attacking pathogen. Previous studies using adjuvant-induced arthritic model showed reduction in RBC count and Hb content in arthritic rats. This decline in hematological markers is an indicative of anemic condition. The anemia may be attributed to different reasons, e.g., failure of iron storage in reticuloendothelial system and synovial tissues and lack of adequate cell production due to failure of bone marrow functioning [18, 39, 40]. Treatment with *A. occidentale* normalized all the hematological parameters and no significant difference was found between the effects of plant extract and piroxicam.

We also evaluated the potential effects of *A. occidentale* extract on the levels of different lysosomal enzymes. Lysosomal enzymes have particular importance in rheumatoid arthritis. Lining cells of the synovial membrane and synovial fluid leucocytes were presumed to be the source of the lysosomal enzymes [41]. Acid phosphatase is one of the lysosomal enzymes and is considered responsible for the destruction of cartilage in arthritic condition. Levels of acid phosphatase are increased due to reduced stability of lysosomes in adjuvant-induced arthritis. The enhanced activity of acid phosphatase is an indicative of persistent inflammation [42, 43]. β -Galactosidase and β -glucuronidase are other lysosomal enzymes which cleave glycosidic bonds in proteoglycans and glycoproteins resulting in destruction of articular cartilage. A previous study showed that the activities of these exoglycosidase enzymes in both synovial fluid and serum of the arthritic patients were significantly increased [44]. *N*-acetylglucosaminidase is also a marker of inflammation and causes the hydrolysis of *N*-acetylglucosamine residues from *N*-acetylglucosaminides [45]. It normally exists in plasma and its levels are found increased in various inflammatory disorders like arthropathies and chronic obstructive pulmonary diseases. In addition, enhanced levels are found in liver disease, diabetes mellitus, and cancer [46]. These results are in accordance with the outcome of this study which

also showed enhanced levels of *N*-acetylglucosaminidase, β -glucuronidase, acid phosphatase, and β -galactosidase, and in rat serum after induction of arthritis. Treatment with plant extract significantly attenuated the levels of these lysosomal enzymes as compared with arthritic group.

Irreversible joint destruction is a characteristic of RA. Interstitial collagens are present in high content in joints and are critical structural targets of different enzymes. Although the presence of type-I collagen dominates in cartilaginous matrix, type-II collagen is largely found in extracellular matrix of bone, tendons, and ligaments. Collagenase acts by cleaving collagen within triple helical domains, thus playing an important role in RA-associated tissue destruction [47]. We found that treatment with *A. occidentale* extract significantly reduced collagenase levels as compared with arthritic group. The data showed that the amelioration of FCA-induced arthritis as evidenced by reduction in arthritic score and histopathological score might be attributed to the suppression of various tissue destructive enzyme levels.

A lot of studies have been conducted to evaluate the qualitative and quantitative phytochemical constituents of *A. occidentale* and are summarized in the form of a comprehensive review by [48]. Different vitamins and functional biofactors were reported in the cashew leaves, e.g., vitamin C, vitamins B2 and B3, thiamine, methyl gallate, leucocyanidin, leucodelphinidin, etc. The presence of fatty acids, like β -sitosterol, stigmasterol, etc., in cashew leaves has also been documented. Various studies revealed the presence of a number of phenolic compounds in the cashew leaves, e.g., 2-hydroxy-6-pentadecylbenzoic acid, hyperoside, amentoflavone derivate, myricetin-O-glycoside, kaempferol-3-O-xyloside, quercetin-3-O-xyloside, quercetin-3-O-arabinofuranoside, quercetin-3-O-arabinopyranoside, quercetin-3-O-rutinoside, etc. [48]. In another study, fresh cashew leaves were subjected to steam distillation for the evaluation of essential oils and found β -phellandrene + limonene (17.5%), methyl chavicol (11.4%), germacrene B (8%), and trans- α -bergamotene (7.9%) in the dominant quantities [49]. Many of these constituents are known to possess anti-inflammatory and antioxidant properties, which might be responsible for the amelioration of rheumatoid arthritis in current study.

5. Conclusion

The study suggests that ethanolic extract of leaves of *Anacardium occidentale* possesses significant antiarthritic properties in rats with FCA-induced arthritis and is attributed to the inhibition of lysosomal enzymes and collagenase. Notably, higher dose of *Anacardium occidentale* (200 mg/kg b.w.) exhibited better anti-inflammatory effects as compared to low dose (100 mg/kg b.w.).

Abbreviations

CRP: C-reactive protein
TLC: Total leukocyte count
DLC: Differential leukocyte count

Rf: Rheumatoid factor
 Hb: Hemoglobin
 RBC: Red blood cells
 FCA: Freund's complete adjuvant.

Data Availability

Data are available from the corresponding author upon request.

Conflicts of Interest

The authors declare that there are no conflicts of interest regarding the publication of this paper.

References

- [1] J. Chang and A. Kavanaugh, "Novel therapies for rheumatoid arthritis," *Pathophysiology*, vol. 12, no. 3, pp. 217–225, 2005.
- [2] R. Khurana and S. M. Berney, "Clinical aspects of rheumatoid arthritis," *Pathophysiology*, vol. 12, no. 3, pp. 153–165, 2005.
- [3] A. Shabbir, M. Shahzad, A. Ali, and M. Zia-Ur-Rehman, "Discovery of new benzothiazine derivative as modulator of pro- and anti-inflammatory cytokines in rheumatoid arthritis," *Inflammation*, vol. 39, no. 6, pp. 1918–1929, 2016.
- [4] J. A. Markenson, "Worldwide trends in the socioeconomic impact and long-term prognosis of rheumatoid arthritis," *Seminars in Arthritis and Rheumatism*, vol. 21, no. 2, pp. 4–12, 1991.
- [5] F. C. Breedveld and J. Kalden, "Appropriate and effective management of rheumatoid arthritis," *Annals of the Rheumatic Diseases*, vol. 63, no. 6, pp. 627–633, 2004.
- [6] B. Combe, "Early rheumatoid arthritis: strategies for prevention and management," *Best Practice & Research Clinical Rheumatology*, vol. 21, no. 1, pp. 27–42, 2007.
- [7] P. Kumar and S. Banik, "Pharmacotherapy options in rheumatoid arthritis," *Clinical Medicine Insights Arthritis Musculoskeletal Disorder*, vol. 6, pp. 35–43, 2013.
- [8] T. D. Wilsdon and C. L. Hill, "Managing the drug treatment of rheumatoid arthritis," *Australian Prescriber*, vol. 40, no. 2, pp. 51–58, 2017.
- [9] R. Payne, "Limitations of NSAIDs for pain management: toxicity or lack of efficacy?," *The Journal of Pain*, vol. 1, no. 3, pp. 14–18, 2000.
- [10] S. H. Venkatesha, R. Rajaiiah, B. M. Berman, and K. D. Moudgil, "Immunomodulation of autoimmune arthritis by herbal CAM," *Evidence-Based Complementary and Alternative Medicine*, vol. 2011, Article ID 986797, 13 pages, 2011.
- [11] H. Bliddal, R. Christensen, L. Højgaard et al., "Spiritual healing in the treatment of rheumatoid arthritis: an exploratory single centre, parallel-group, double-blind, three-arm, randomised, sham-controlled trial," *Evidence-Based Complementary and Alternative Medicine*, vol. 2014, Article ID 269431, 9 pages, 2014.
- [12] A. Baptista, R. V. Gonçalves, J. Bressan, and M. C. G. Pelúzio, "Antioxidant and antimicrobial activities of crude extracts and fractions of cashew (*Anacardium occidentale* L.), cajui (*Anacardium microcarpum*), and pequi (*Caryocar brasiliense* C.): a systematic review," *Oxidative Medicine and Cellular Longevity*, vol. 2018, Article ID 3753562, 13 pages, 2018.
- [13] S. A. Onasanwo, T. D. Fabiyi, F. S. Oluwole, and S. B. Olaleye, "Analgesic and anti-inflammatory properties of the leaf extracts of *Anacardium occidentale* in the laboratory rodents," *Nigerian Journal of Physiological Sciences*, vol. 27, no. 1, pp. 65–71, 2012.
- [14] F. A. Vanderlinde, H. F. Landim, E. A. Costa et al., "Evaluation of the antinociceptive and anti-inflammatory effects of the acetone extract from *Anacardium occidentale* L.," *Brazilian Journal of Pharmaceutical Sciences*, vol. 45, no. 3, pp. 437–442, 2009.
- [15] O. A. Galdino, M. A. Aderogba, A. D. Adedapo, and J. M. Makinde, "Effects of *Anacardium occidentale* stem bark extract on in vivo inflammatory models," *Journal of Ethnopharmacology*, vol. 95, no. 2-3, pp. 139–142, 2004.
- [16] O. A. Olajide, M. A. Aderogba, and B. L. Fiebich, "Mechanisms of anti-inflammatory property of *Anacardium occidentale* stem bark: inhibition of NF- κ B and MAPK signalling in the microglia," *Journal of Ethnopharmacology*, vol. 145, no. 1, pp. 42–49, 2013.
- [17] M. Uroos, Z. Abbas, S. Sattar et al., "Nyctanthes arbor-tristis ameliorated FCA-induced experimental arthritis: a comparative study among different extracts," *Evidence-Based Complementary and Alternative Medicine*, vol. 2017, Article ID 4634853, 13 pages, 2017.
- [18] A. Shabbir, M. Shahzad, A. Ali, and M. Zia-ur-Rehman, "Anti-arthritic activity of N'-[(2, 4-dihydroxyphenyl)methylidene]-2-(3, 4-dimethyl-5, 5-dioxidopyrazolo[4, 3-c][1, 2]benzothiazin-1(4H)-yl)acetohydrazide," *European Journal of Pharmacology*, vol. 738, pp. 263–272, 2014.
- [19] A. Shabbir, S. A. Batool, M. I. Basheer et al., "Ziziphora clinopodioides ameliorated rheumatoid arthritis and inflammatory paw edema in different models of acute and chronic inflammation," *Biomedicine & Pharmacotherapy*, vol. 97, pp. 1710–1721, 2018.
- [20] A. M. Uttra, Alamgeer, M. Shahzad, A. Shabbir, and S. Jahan, "Ephedra gerardiana aqueous ethanolic extract and fractions attenuate Freund complete adjuvant induced arthritis in Sprague Dawley rats by downregulating PGE2, COX2, IL-1 β , IL-6, TNF- α , NF- κ B and upregulating IL-4 and IL-10," *Journal of Ethnopharmacology*, vol. 224, pp. 482–496, 2018.
- [21] H. Aslam, M. Shahzad, A. Shabbir, and S. Irshad, "Immunomodulatory effect of thymoquinone on atopic dermatitis," *Molecular Immunology*, vol. 101, pp. 276–283, 2018.
- [22] S. Arjumand, M. Shahzad, A. Shabbir, and M. Z. Yousaf, "Thymoquinone attenuates rheumatoid arthritis by downregulating TLR2, TLR4, TNF- α , IL-1, and NF- κ B expression levels," *Biomedicine & Pharmacotherapy*, vol. 111, pp. 958–963, 2019.
- [23] J. King, "The hydrolases-acid and alkaline phosphatases," in *Practical Clinical Enzymology*, D. Van, Ed., pp. 191–208, Nostrand Company Limited, London, UK, 1965.
- [24] Y. Kawai and K. Anno, "Mucopolysaccharide-degrading enzymes from the liver of the squid, *ommatostephes sloani pacificus* I. hyaluronidase," *Biochimica et Biophysica Acta (BBA)—Enzymology*, vol. 242, no. 2, pp. 428–436, 1971.
- [25] D. Marhun, "Rapid colorimetric assay of β -galactosidase and N-acetyl- β -galactosaminidase in human urine," *Clinica Chimica Acta*, vol. 73, pp. 453–461, 1976.
- [26] P. D. Rosenblit, R. P. Metzger, and A. N. Wick, "Effect of streptozotocin diabetes on acid phosphatase and selected glycosidase activities of serum and various rat organs," *Experimental Biology and Medicine*, vol. 145, no. 1, pp. 244–248, 1974.
- [27] O. H. Lowry, N. J. Rosebrough, A. L. Farr, and R. J. Randall, "Protein measurement with the folin phenol reagent," *The*

- Journal of Biological Chemistry*, vol. 193, no. 1, pp. 265–275, 1951.
- [28] H. E. Van Wart and D. R. Steinbrink, “A continuous spectrophotometric assay for Clostridium histolyticum collagenase,” *Analytical Biochemistry*, vol. 113, no. 2, pp. 356–365, 1981.
- [29] T. J. N. Okonkwo, O. Okorie, J. Okonta, and C. Okonkwo, “Sub-chronic hepatotoxicity of *Anacardium occidentale* (Anacardiaceae) inner stem bark extract in rats,” *Indian Journal of Pharmaceutical Sciences*, vol. 72, no. 3, pp. 353–357, 2010.
- [30] P. B. Jacobson, S. J. Morgan, D. M. Wilcox et al., “A new spin on an old model: in vivo evaluation of disease progression by magnetic resonance imaging with respect to standard inflammatory parameters and histopathology in the adjuvant arthritic rat,” *Arthritis & Rheumatism*, vol. 42, no. 10, pp. 2060–2073, 1999.
- [31] Q. Nguyen, J. Shan, L. Di, L. Jiang, and H. Xu, “Therapeutic effects of daphnetin on adjuvant-induced arthritic rats,” *Journal of Ethnopharmacology*, vol. 120, no. 2, pp. 259–263, 2008.
- [32] D. M. Polireddy, “Evaluation of anti-arthritic activity of ethanolic extract of *Sida cardifolia*,” *International Journal of Science and Technology Research*, vol. 4, no. 11, pp. 86–96, 2015.
- [33] G. Akhtar and A. Shabbir, “*Urginea indica* attenuated rheumatoid arthritis and inflammatory paw edema in diverse animal models of acute and chronic inflammation,” *Journal of Ethnopharmacology*, vol. 238, Article ID 111864, 2019.
- [34] U. H. Hassan, Alamgeer, M. Shahzad et al., “Amelioration of adjuvant induced arthritis in Sprague Dawley rats through modulation of inflammatory mediators by *Ribes alpestre* Decne,” *Journal of Ethnopharmacology*, vol. 235, pp. 460–471, 2019.
- [35] M. B. Pepys and G. M. Hirschfield, “C-reactive protein: a critical update,” *Journal of Clinical Investigation*, vol. 111, no. 12, pp. 1805–1812, 2003.
- [36] G. Sindhu, M. Ratheesh, G. L. Shyni, B. Nambisan, and A. Helen, “Anti-inflammatory and antioxidative effects of mucilage of *Trigonella foenum graecum* (Fenugreek) on adjuvant induced arthritic rats,” *International Immunopharmacology*, vol. 12, no. 1, pp. 205–211, 2012.
- [37] F. Ingegnoli, R. Castelli, and R. Gualtierotti, “Rheumatoid factors: clinical applications,” *Disease Markers*, vol. 35, no. 5, pp. 727–734, 2013.
- [38] I. B. McInnes and G. Schett, “The pathogenesis of rheumatoid arthritis,” *New England Journal of Medicine*, vol. 365, no. 23, pp. 2205–2219, 2011.
- [39] A. G. Mowat, “Hematologic abnormalities in rheumatoid arthritis,” *Seminars Arthritis and Rheumatism*, vol. 1, no. 3, pp. 195–219, 1971.
- [40] S. Ekambaram, S. S. Perumal, and V. Subramanian, “Evaluation of anti-arthritic activity of *Strychnos potatorum* Linn seeds in Freund’s adjuvant induced arthritic rat model,” *BMC Complementary Alternative Medicine*, vol. 10, p. 56, 2010.
- [41] K. D. Muirden, “Lysosomal enzymes in synovial membrane in rheumatoid arthritis. Relationship to joint damage,” *Annals of the Rheumatic Diseases*, vol. 31, no. 4, pp. 265–271, 1972.
- [42] I. Olsen, S. Bon-Gharios, and D. Abraham, “The activation of resting lymphocytes is accompanied by the biogenesis of lysosomal organelles,” *European Journal of Immunology*, vol. 20, pp. 2161–2170, 1990.
- [43] N. K. Mishra, S. Bstia, G. Mishra, K. A. Chowdary, and S. Patra, “Anti-arthritic activity of *Glycyrrhiza glabra*, *Boswellia serrata* and their synergistic activity in combined formulation studied in Freund’s adjuvant induced arthritic rats,” *Journal of Pharmaceutical Education and Research*, vol. 2, no. 2, pp. 92–98, 2011.
- [44] S. Pancewicz, J. Popko, R. Rutkowski et al., “Activity of lysosomal exoglycosidases in serum and synovial fluid in patients with chronic Lyme and rheumatoid arthritis,” *Scandinavian Journal of Infectious Diseases*, vol. 41, no. 8, pp. 584–589, 2009.
- [45] M. Knaś, E. Albera, and M. Rózańska-Boczula, “Activities of N-acetyl- β -D-glucosaminidase and glutathione peroxidase in bovine colostrum and milk,” *Czech Journal of Animal Science*, vol. 55, no. 11, pp. 488–495, 2010.
- [46] M. P. Iqbal, K. A. Kazmi, H. R. Jafri, and N. Mehboobali, “N-Acetyl- β -D-glucosaminidase in acute myocardial infarction,” *Experimental & Molecular Medicine*, vol. 35, no. 4, pp. 275–278, 2003.
- [47] F. Sabeh, D. Fox, and S. J. Weiss, “Membrane-type I matrix metalloproteinase-dependent regulation of rheumatoid arthritis synovioocyte function,” *The Journal of Immunology*, vol. 184, no. 11, pp. 6396–6406, 2010.
- [48] B. Salehi, M. Gültekin-Özgüven, C. Kırkın et al., “*Anacardium* plants: chemical, Nutritional composition and biotechnological applications,” *Biomolecules*, vol. 9, no. 9, p. 465, 2019.
- [49] C. Silva, M. Moudachirou, V. Adjakidje, J.-C. Chalchat, and G. Figuéredo, “Essential oil chemical composition of *Anacardium occidentale* L. leaves from Benin,” *Journal of Essential Oil Research*, vol. 20, no. 1, pp. 5–8, 2008.

Research Article

Effects and Mechanism of Berberine on the Dexamethasone-Induced Injury of Human Tendon Cells

Shangjun Fu, Zongyun He, Yongfeng Tang, and Bo Lan 

Hand and Foot Surgery, Yiwu Central Hospital, Yiwu, 322000 Zhejiang, China

Correspondence should be addressed to Bo Lan; lanbo886@126.com

Received 6 September 2020; Revised 10 October 2020; Accepted 26 October 2020; Published 7 November 2020

Academic Editor: Arham Shabbir

Copyright © 2020 Shangjun Fu et al. This is an open access article distributed under the Creative Commons Attribution License, which permits unrestricted use, distribution, and reproduction in any medium, provided the original work is properly cited.

Objective. To investigate the effects of berberine (Berb) on dexamethasone- (Dex-) induced injury of human tendon cells and its potential mechanism. **Methods.** CCK-8 assay was used to explore the appropriate concentration of Dex-induced injury of tendon cells and the doses of Berb attenuates Dex cytotoxicity; cell wound healing assay was used to detect the effects ($P < 0.05$) of Berb and Dex on the migration ability of tendon cells; flow cytometry was used to measure cell apoptosis; DCF DA fluorescent probe was used to measure the ROS activity of cells. Western blotting was used to detect the expression of phenotype related factors including smooth muscle actin α (SMA- α), type I collagen (Col I), col III, apoptosis-related factors, caspase-3, cleaved caspase-3, caspase-9, cleaved caspase-9, and PI3K/AKT. **Results.** CCK-8 assay showed that 1–100 μ M Dex significantly inhibited the proliferation of tendon cells in a concentration-dependent manner ($P < 0.05$), where the inhibitory effect of 100 μ M Dex was most significant ($P < 0.005$), and the pretreatment of 150, 200 μ M Berb could reverse those inhibitions (all $P < 0.05$). Compared with the control group, Dex significantly inhibited cell migration ($P < 0.05$), while Berb pretreatment could enhance cell migration ($P < 0.05$). Flow cytometry and ROS assay showed that Dex could induce apoptosis and oxidative stress response of tendon cells (all $P < 0.05$), while Berb could reverse those responses ($P < 0.05$). Western blot showed that Dex could inhibit the expression of the col I and III as well as α -SMA (all $P < 0.05$) and enhance the expression of apoptosis-related factors including cleaved caspase-3 and cleaved caspase-9 (all $P < 0.05$). Besides, Dex could also inhibit the activation of the PI3K/AKT signaling pathway (all $P < 0.05$), thus affecting cell function, while Berb treatment significantly reversed the expression of those above proteins (all $P < 0.05$). **Conclusion.** Berb attenuated DEX induced reduction of proliferation and migration, oxidative stress, and apoptosis of tendon cells by activating the PI3K/AKT signaling pathway and regulated the expression of phenotype related biomarkers in tendon cells. However, further studies are still needed to clarify the protective effects of Berb in vivo.

1. Introduction

Tendinopathy includes all pain related to the tendon injury, and activity-related pain is its main clinical symptom [1]. It has been estimated that tendinopathy accounts for 30–50% of musculoskeletal diseases and can often affect the shoulder, elbow joint, patella, and Achilles tendon function [2, 3]. Although physical methods, such as local hot compress, massage, and infrared physiotherapy, are often used clinically to treat tendon injuries, the effect is often not satisfactory [4]. At present, the treatment of tendinopathy usually relies on limited scientific evidences [1], and clinical experts often disagree about the use of some of these methods. Among those, the application of glucocorticoids, such as the

commonly used dexamethasone (dexamethasone, Dex), is still very controversial and questionable [5]. Previous in vitro studies have shown that exposure to glucocorticoids has many negative effects on tendon cells [6]. For example, it can cause a decrease in the viability and proliferation of tendon cells and can reduce the level of total collagen (especially collagen 1 and proteoglycan) [7, 8]. The above effects can destroy the structure of the tendon, which is specifically shown as a decrease in the mechanical properties of the tendon [6] and can eventually lead to the occurrence of adverse events such as tendon rupture. Even given the side effects of glucocorticoid application on tendon cells, it is undeniable that hormones within glucocorticoid play a significant role when it comes to anti-inflammation.

Therefore, in the research of clinical treatment of tendinopathy, it is necessary to find an adjuvant drug that can reduce glucocorticoid-induced tendon cell injury.

Berberine (Berb), also known as berberine hydrochloride, has been used as a traditional medicine in China for thousands of years [9]. It has a variety of protective biological functions such as antioxidant, anti-inflammatory, and antiapoptosis [10, 11]. Currently, a large number of clinical trials have confirmed the effectiveness of Berb on nonalcoholic fatty liver, irritable bowel syndrome, insulin resistance, and other diseases [12]. Therefore, this study intends to establish a Dex-induced human tendon cell injury model and to observe whether Berb can exert a protective effect on tendon cell injury, and to further study its mechanism, ultimately aiming to reduce the adverse effects of glucocorticoid treatment of tendinopathy.

2. Materials and Methods

2.1. Materials and Reagents. Dulbecco's modified eagle medium (DMEM), fetal bovine serum, penicillin-streptomycin liquid, phosphate buffer, and trypsin-EDTA digestion solution were all purchased from Hyclone, USA. Cell Counting Kit-8 kit was purchased from Dojindo, Japan, and Annexin V-FITC/PI apoptosis kit was purchased from ThermoFisher, USA. Both Berb and Dex were purchased from Sigma-Aldrich, USA. RIPA protein lysate, antibody diluent, Tween-20, and ECL chemiluminescence reagents were all purchased from Shanghai Biyuntian Biotechnology Co., Ltd. Primary antibodies for smooth muscle actin α (smooth muscle actin α , α -SMA), type I collagen (Col I), col III, caspase-3, cleaved caspase-3, caspase-9, cleaved caspase-9, p-PI3K, PI3K, p-AKT, AKT, and β -actin were all purchased from Abcam, USA. The reactive oxygen species (ROS) detection kit was purchased from Shanghai Biyuntian Biotechnology Co., Ltd.

2.2. Method

2.2.1. Human Tenocyte Culture. This research protocol has been approved by the Human Research Ethics Committee of our hospital. Primary human tenocytes were prepared from the patellar tendons of healthy volunteers for culture by following [8]. After the volunteers signed the informed consent, when the anterior cruciate ligament was reconstructed with autologous bone-patellar tendon-bone transplantation, a tendon tissue block ($2 \times 2 \times 3$ mm) was cut from the central 1/3 of the healthy patellar tendon for primary cell culture. The tissue block was washed with a phosphate buffer solution containing 1% penicillin-streptomycin liquid (100 U/mL penicillin and 100 μ g/mL streptomycin) first before cutting the tissue block into 1 mm³ size under aseptic conditions. The tissue was then digested with trypsin-EDTA. After 5 minutes of digestion, the digested tissue pieces were then transferred to a 35 mm petri dish containing DMEM with 10% fetal bovine serum and 1% penicillin-streptomycin liquid and cultured in an incubator at 37°C with 5% CO₂. The medium was replaced twice a week. After observing the tendon cells and cell fusion in the tendon tissue under the microscope, the tendon fibroblasts

were then digested and cultured in the culture flask with the inoculation density of 10⁵ cells per flask under the same culture conditions for subculture. Subsequent experiments were conducted using the cells that were less than 5 passages.

2.2.2. Establishment of Dex-Induced Tendon Cell Injury Model. Dex was dissolved in absolute ethanol to prepare a storage solution with a concentration of 10 mM and stored in a refrigerator at -20°C. Before processing the tenocytes, the stock solution was diluted with DMEM supplemented with 10% fetal bovine serum and 1% penicillin-streptomycin liquid to a final concentration of 1, 10, and 100 μ M, respectively. Tendon cells were treated with the above concentrations for 48 h to induce cell damage, and the Dex concentrations that can significantly inhibit cell proliferation activity were selected for follow-up studies.

2.2.3. Detection of Cell Proliferation Activity by CCK-8

(1) *Test the Effect of Dex on the Proliferation Activity of Tenocytes.* For specific operations, see Method 1.2.2. Tenocytes were seeded in a 96-well plate at a density of 5×10^3 cells/well, cultured for 24 h under standard conditions and then treated with Dex at different concentrations (1, 10, and 100 μ M) for 48 h. After treatment, 10 μ L CCK-8 was added, and the cells were put in the incubator again and continued in culture for 2 h. After that, a spectrophotometer was used to measure the absorbance value (absorbance, A) at 450 nm wavelength to calculate the relative cell proliferation activity. Each group had 5 replicates. The value measured from the DMEM was used as the background value to eliminate the interference of the medium itself on the absorbance value. Relative cell proliferation activity = (A treatment group - A background group) / (A control group - A background group).

(2) *Detect the Effect of Berb on the Proliferation Activity of Dex-Induced Tenocytes.* First, different concentrations of Berb (0, 25, 50, 100, 150, 200, and 300 μ M) were used to pretreat tendon cells for 24 h, and then Dex was used to induce tendon cell injury for 48 h. For subsequent operations, see Method (1). The appropriate concentration that can effectively reduce the cell damage caused by Dex was selected for follow-up research.

2.2.4. Evaluation of Cell Migration Ability by the Scratch Test. Tenocytes were seeded in a six-well plate at a density of 2×10^5 cells/well, and they were divided into the control group (Control), Dex group, 150 Berb + Dex group (150 μ M Berb pretreatment), and 200 Berb + Dex group (200 μ M Berb pretreatment). After the inoculated cells were cultured for 24 h, the 150 Berb + Dex group and 200 Berb + Dex group were pretreated with 150 and 200 μ M Berb for 24 h, respectively, and then treated with Dex for 48 h. After the treatment, the cells were digested and reseeded in a six-well plate at a density of 1×10^6 cells/well. After 24 h of culture, a 200 μ L sterile pipette tip was used to draw 3 parallel lines that

were vertical to the plate. After washing the floating cells with PBS, normal DMEM was added, and pictures were then taken under an inverted microscope. After imaging, the cells were then returned to the incubator to continue culturing for 24 h, and then the pictures were taken again. Image J was then used to measure the width of the scratch (W), and the relative migration capacity of cells was calculated with formula $(W-0\text{ h}-W-24\text{ h})/W-0\text{ h}$.

2.2.5. Detection of ROS Level. The DCF-DA fluorescent probe was used to detect the ROS activity of cells. The cells were seeded in a 48-well plate at a density of 1×10^4 cells/well and processed as method 2.2.4 for specific operations. The cells were washed twice with PBS, and 200 μL of 25 μM DCF-DA was then added, and the cells were then put back in the incubator for 30 min. After the incubation, the cells were washed twice with PBS again, and then the relative fluorescence intensity of the sample was measured with the Synergy Mx multifunction microplate detector at the excitation and emission wavelengths of 485 and 528 nm, respectively.

2.2.6. Detection of Apoptosis by Flow Cytometry. Annexin V-FITC/PI double staining was used to detect cell apoptosis. First, the cells were inoculated in a six-well plate. After each group of cells was treated accordingly (see Method 2.2.4 for details), the cells were then digested with trypsin-EDTA digestion solution and centrifuged at 800 g for 5 min to obtain the cell pellet. 500 μL PBS was then added to wash the cell pellet before centrifuging again to collect the pellet. After repeating the washing 3 times, 500 μL of binding buffer was added to the cell pellet to resuspend the cells. After that, 15 μL of Annexin V-FITC and PI were added in sequence, and cells were then incubated at room temperature for 30 min in the dark. After the incubation, flow cytometry was then used for apoptosis detection.

2.2.7. Expression of Protein Detected by the Western Blotting

(1) Effects of Berb on the Protein Expression of Dex-Induced Tendon Cells. RIPA Lysis Buffer was used to lyse the treated cells on ice, cells were then centrifuged at 12,000 g/min for 20 min to take the cell lysate supernatant, and the BCA protein concentration determination kit was then used to determine the protein concentration. 30 μg protein sample was then taken and loaded on the SDS-PAGE gel, and the protein was separated by electrophoresis and transferred to the PVDF membrane. The membrane was blocked at room temperature for 1 h and then inoculated at 4°C with primary antibodies (SMA, col I, col III, caspase-3, cleaved caspase-3, caspase-9, cleaved caspase-9, p-PI3K, PI3K, P-AKT, AKT, and β -actin) overnight. After washing the membrane the next day, the membrane was then incubated in the corresponding secondary antibody for 1 h at room temperature. After washing the membrane again, enhanced chemiluminescence reagent was added for protein exposure and development, and Photoshop software was then used for protein grayscale analysis.

(2) Test the Effects of PI3K Inhibitors and Verify the Expression of PI3K/AKT Signaling Pathway Proteins. The cells were divided into 5 groups, namely, the control group (control), Dex group, LY294002 group, Berb + Dex group, and LY294002 + Berb + Dex group. After the corresponding treatment, the specific detection steps were conducted as shown in Method (1).

2.2.8. Statistical Analysis. The experimental data were analyzed and processed by SPSS 18.0. Quantitative data were expressed as mean \pm standard deviation. Under the same treatment condition, the difference between the groups was compared by one-way analysis of variance; the Dunnett *t*-test was used for the comparison between different groups and the control group. $P \leq 0.05$ was used for the statistically significant test. All experiments in the study were repeated independently at least three times.

3. Results

3.1. The Effect of Dex and Berb Treatment on the Proliferation Activity of Tenocytes. As shown in Figure 1(a), with the increase of Dex treatment concentration, the proliferation activity of tenocytes decreased in a dose-dependent manner ($P < 0.001$), so the follow-up study chose 100 μM Dex to treat tenocytes to induce cell damage. As shown in Figure 1(b), pretreatment of cells with different concentrations of Berb (0, 25, 50, 100, 150, 200, and 300 μM) before exposure to 100 μM Dex can reduce the damaging effect of Dex on cells in a dose-dependent manner ($P < 0.001$). The concentration of 150 and 200 μM Berb treatment was most obvious, so 150 and 200 μM were chosen as the Berb pretreatment concentration for follow-up research.

3.2. The Effect of Combined Treatment of Dex and Berb on the Migration Ability of Tenocytes. As shown in Figure 2, compared with the control group, Dex treatment can significantly reduce the cell migration ability (all $P < 0.05$), while, compared with the Dex group, it can be seen that Berb pretreatment can promote the recovery of cell migration ability (all $P < 0.05$). Moreover, with the extension of the scratch culture time, the promotion effect becomes more obvious.

3.3. The Combined Effect of Dex and Berb on the Induction of Apoptosis of Tendon Cells. As shown in Figure 3, flow cytometry showed that Dex can significantly induce apoptosis of tendon cells ($P < 0.05$), while Berb pretreatment can reduce the rate of apoptosis of tendon cells (all $P < 0.05$).

3.4. The Combined Treatment of Dex and Berb on the Induction of Oxidative Stress in Tendon Cells. As shown in Figure 4 (DCF-DA detection of ROS level), Dex can significantly induce oxidative stress in tendon cells, and ROS expression is significantly increased ($P < 0.05$), while Berb treatment can inhibit the production of ROS (all $P < 0.05$) indicating its inhibitory effects on the occurrence of oxidative stress.

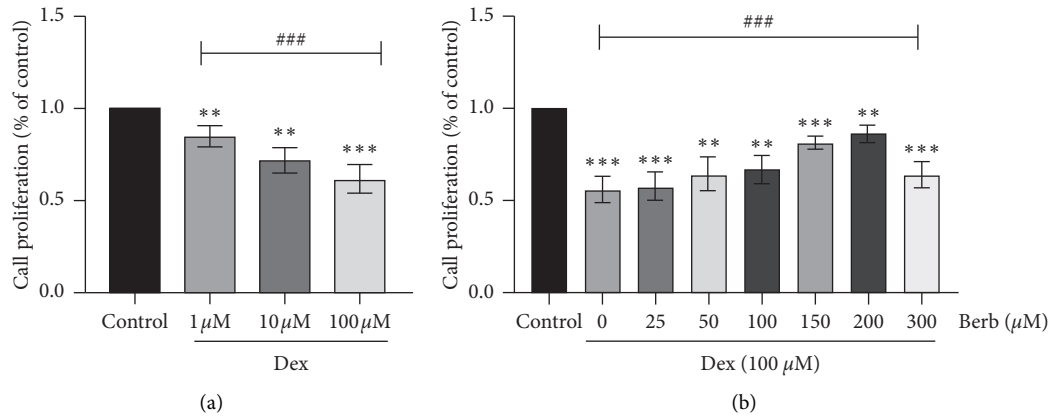


FIGURE 1: Effects of Dex and Berb on proliferation of tendon cells. (a) CCK-8 assay was used to detect the effects of various concentration of Dex (1, 10, and 100 μM) on the proliferation of tendon cells; (b) CCK-8 assay was used to measure the effects of Dex on the proliferation of tendon cells pretreated with different concentrations of Berb (0, 25, 50, 100, 150, 200, and 300 μM). *Note.* Compared with the control group, ** $P < 0.01$ and *** $P < 0.001$; compared within the treatment groups, ### $P < 0.001$.

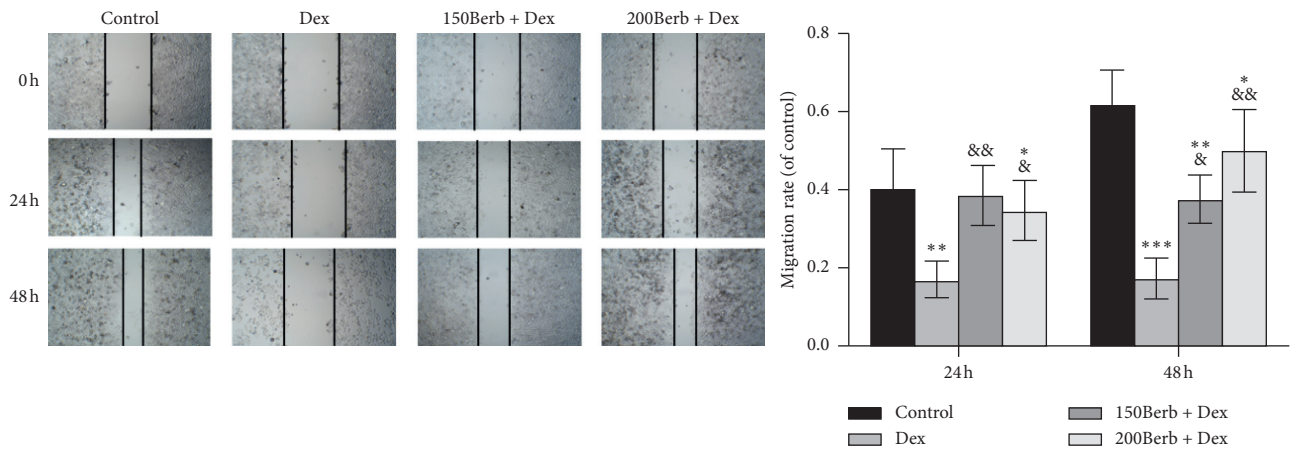


FIGURE 2: Berb attenuates the inhibitory effect of Dex on the migration of tendon cells. *Note.* Compared with the control group, * $P < 0.05$, ** $P < 0.01$, and *** $P < 0.001$; compared with Dex group, & $P < 0.05$ and && $P < 0.01$.

3.5. The Effect of Dex and Berb on the Expression of Apoptosis Factors in Tendon Cells. As shown in Figure 5, compared with the control group, Dex exposure can significantly increase the expression of cleaved caspase-3 and cleaved caspase-9 in cells (both $P < 0.05$) and induce the occurrence of apoptotic response, while Berb pretreatment can reverse the above changes (all $P < 0.05$) thus playing an anti-apoptotic effect.

3.6. The Combined Effect of Dex and Berb on the Expression of Phenotype-Related Biomarkers in Tendon Cells. As shown in Figure 6, compared with the control group, Dex treatment can significantly inhibit the expression of α -SMA, col I, and col III (all $P < 0.05$), thereby destroying cell function, while Berb pretreatment promoted the expression of α -SMA, col I, and col III (all $P < 0.05$), suggesting that Berb can contribute to the functional recovery of damaged tendon cells.

3.7. The Combined Effect of Dex and Berb on the Activation of PI3K/AKT Signaling Pathway. As shown in Figure 7, Dex

exposure can inhibit the activation of the PI3K/AKT signaling pathway in tendon cells (all $P < 0.05$), while Berb pretreatment can reverse this change (all $P < 0.05$). The addition of PI3K inhibitor LY294002 further confirmed this effect.

4. Discussion

The healing of tendon injuries involves many complex processes, which could span stages of inflammation, regeneration, and remodeling [13]. In this process, tendon cells migrate to the repair site, proliferate actively, and are responsible for depositing a large amount of extracellular matrix in the tissue. The normal progress of the above cell activities is the basis of tendon healing [14]. Previous studies have found that while Dex is anti-inflammatory, it can cause damage to the function of tendon cells, which may hinder the regeneration process of tendon healing [15]. Berb is the main isoquinoline alkaloid component of many common medicinal plants (such as barberry, coptis, etc.), due to its multiple biological activities, including antidiarrheal,

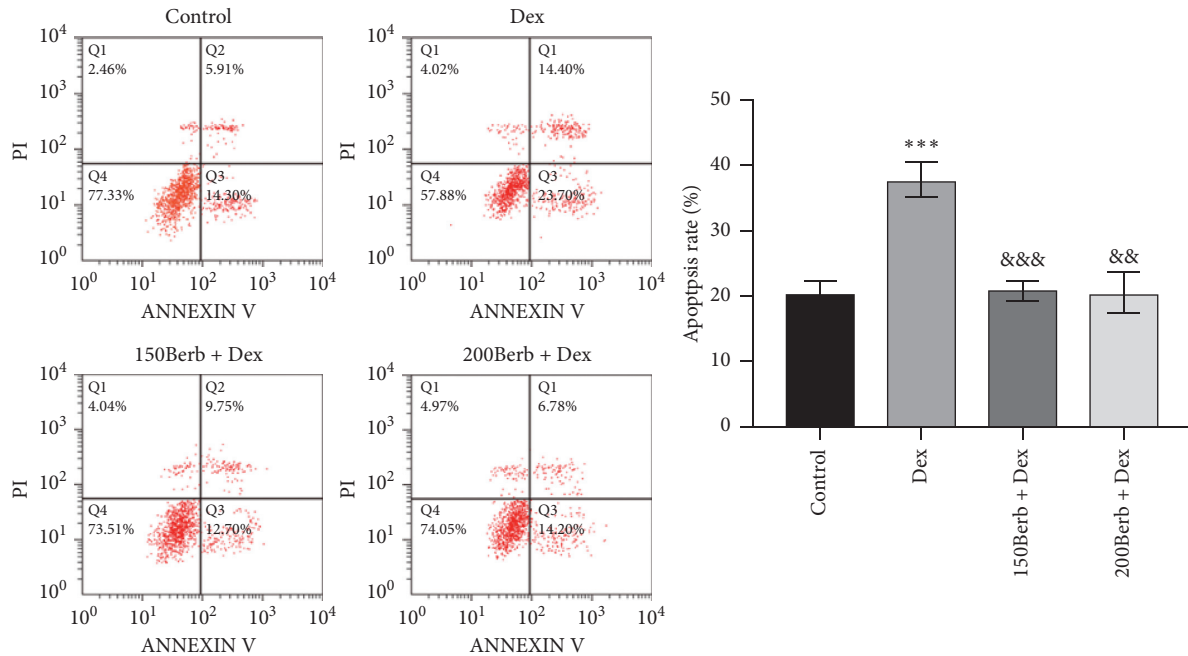


FIGURE 3: Berb attenuated Dex-induced apoptosis of tendon cells. Note. Compared with the control group, *** $P < 0.001$; compared with Dex group, &&& $P < 0.01$, && $P < 0.01$, and &&& $P < 0.001$.

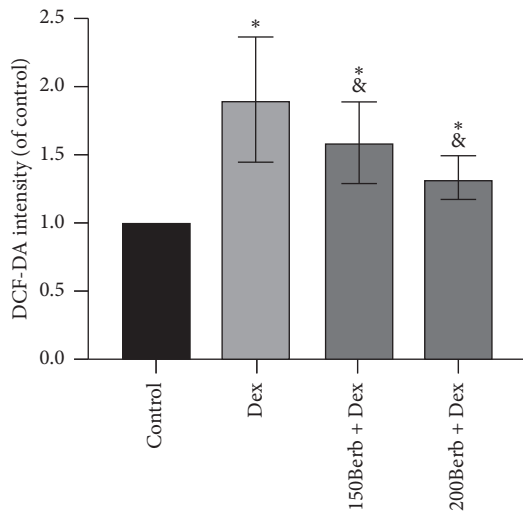


FIGURE 4: Effects of Dex and Berb on the oxidative stress response of tendon cells. Note. Compared with the control group, * $P < 0.05$; compared with the Dex group, & $P < 0.05$.

anticancer, antidiabetic, antihyperlipidemia, and heart protection, it has been widely used in traditional Chinese medicine [16]. Because of the bioprotective effect of Berb, this study aims to investigate whether Berb can reduce Dex-induced tendon cell damage and promote the recovery of cell function.

In this study, the proliferation and migration functions of tenocytes were studied by detecting cell proliferation activity, finding the appropriate concentration of Dex-induced damage and the intervention concentration of Berb that can inhibit Dex damage. The CCK-8 experiment found

that when 100 μM Dex is given to tenocytes, the proliferation activity of the cells can be significantly inhibited. This result is consistent with the results of Wong et al. [8]; that is, Dex can significantly reduce the viability of tenocytes and inhibit cell proliferation in a dose-dependent manner. Besides, this study also found that Berb can dose-dependently mitigate the reduction of cell proliferation induced by Dex in the concentration ranging from 25 to 200 μM . Furthermore, in the study on the change of the migration ability of damaged tenocytes, we found that Dex can significantly reduce the migration ability of cells; however, when cells were treated with Berb in advance and then exposed to Dex, the damaged migration ability of the cells can be significantly reversed, and, with the extension of the treatment time, the effect of improving cell migration ability is further enhanced. The above cell function experiments suggest that Berb can play a cytoprotective effect and reduce the damage of proliferation and migration ability caused by Dex.

This study also observed the inducing effect of Dex on the apoptosis and oxidation of tendon cells and the corresponding protective effect of Berb. By measuring cell apoptosis via flow cytometry, we found that Dex can significantly induce cell apoptosis. However, when cells were pretreated with 150 and 200 μM Berb, the rate of apoptosis was significantly reduced. We also confirmed the occurrence of apoptosis by detecting the protein expression levels of apoptosis-related factors including caspase-3 and caspase-9. It is known that caspase-3 can be activated by caspase-9 cleavage. The activation of the caspase signal and its downstream apoptotic response pathway is an important feature of the apoptotic cascade [17]. Cleaved caspase-3 and caspase-9 are important biomarkers for the progression of apoptosis. Besides the results of flow cytometry for the

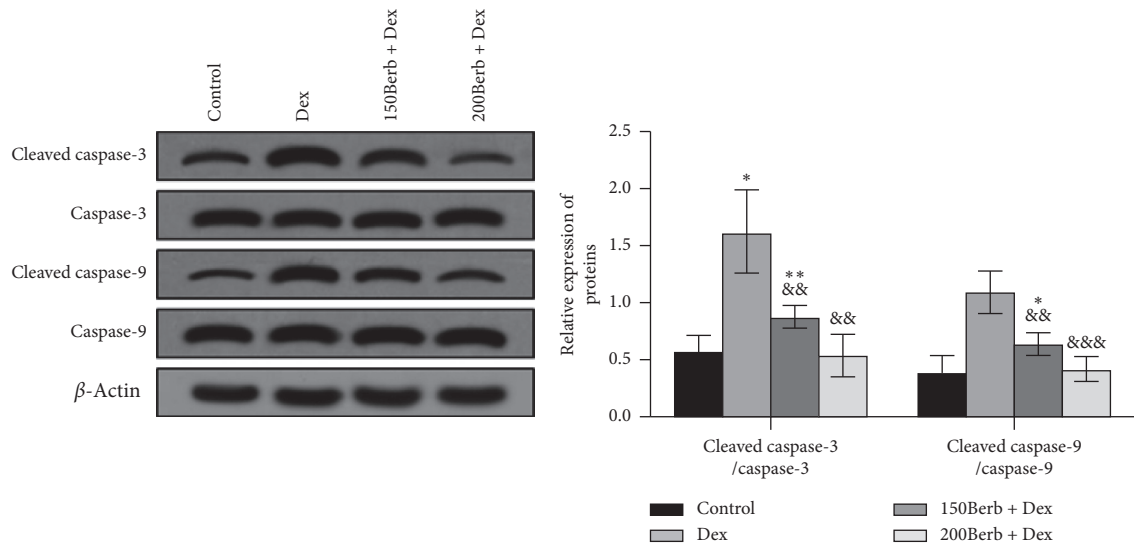


FIGURE 5: Berb inhibited Dex-induced expression of apoptosis related factors in tendon cells. *Note.* Compared with the control group, * $P < 0.05$, ** $P < 0.01$, and *** $P < 0.001$; compared with Dex group, && $P < 0.01$ and &&& $P < 0.001$.

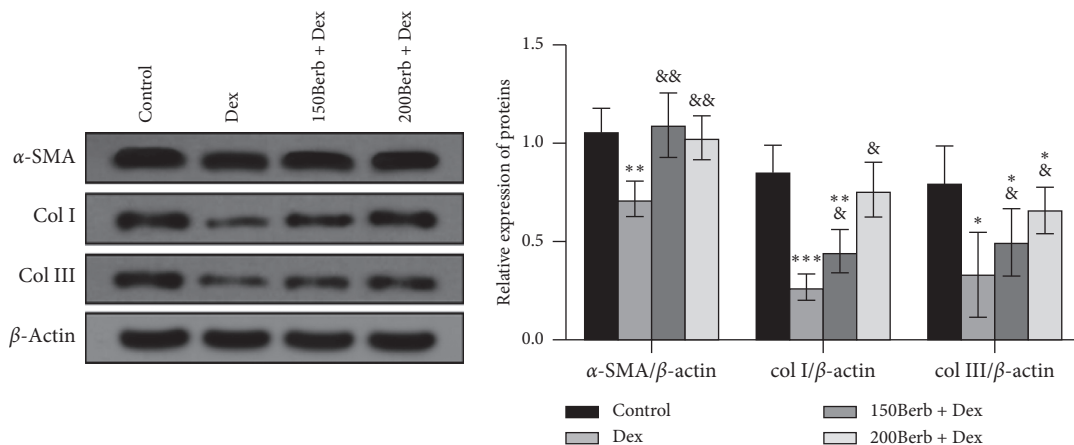


FIGURE 6: Effects of Dex and Berb on the expression of phenotype related biomarkers in tendon cells. *Note.* Compared with the control group, * $P < 0.05$, ** $P < 0.01$, and *** $P < 0.001$; compared with Dex group, & $P < 0.05$ and && $P < 0.01$.

detection of the apoptosis response, this study also found that Berb pretreatment can significantly reduce the increase in the expression of apoptotic proteins in tendon cells induced by Dex, thereby further verifying the antiapoptotic effect of Berb. Previously, Min et al. used Dex to induce human tendon cell injury. When studying the mechanism of vitamin D on tendon cells, they found that vitamin D can reduce the ROS produced by Dex [18]. In the oxidation reaction experiment, by detecting the strength of DCF-DA, which indicates the ROS level, it was found that Dex can increase the ROS level of tendon cells and cause cell oxidative damage, while the administration of Berb can reverse the occurrence of oxidation reaction, thereby exerting a protective effect. The above experiments suggest that Berb can not only promote the recovery of tenocyte function but

also reduce cell damage by inhibiting Dex-induced oxidation and apoptosis.

Collagen (col) is one of the important constituents of tendon cells, accounting for 70% of the dry weight of the tendon [19]. In the normal tendons, col I make up for about 90% of the collagen, and the rest is col III [20]. Col I usually form a tissue bundle by forming parallelly arranged fibers, while col III is normally confined to the inner membrane around the bundle formed by col I. When the injury occurs, tenocytes can produce col I and III to help tendon healing [21]. Studies have shown that, in human tendon tissues such as the anterior cruciate ligament, up to 50% of the cells contain α -SMA, which plays an important role in maintaining the structure of the extracellular matrix [22]. Given the evidence mentioned above, col I, col III, and α -SMA

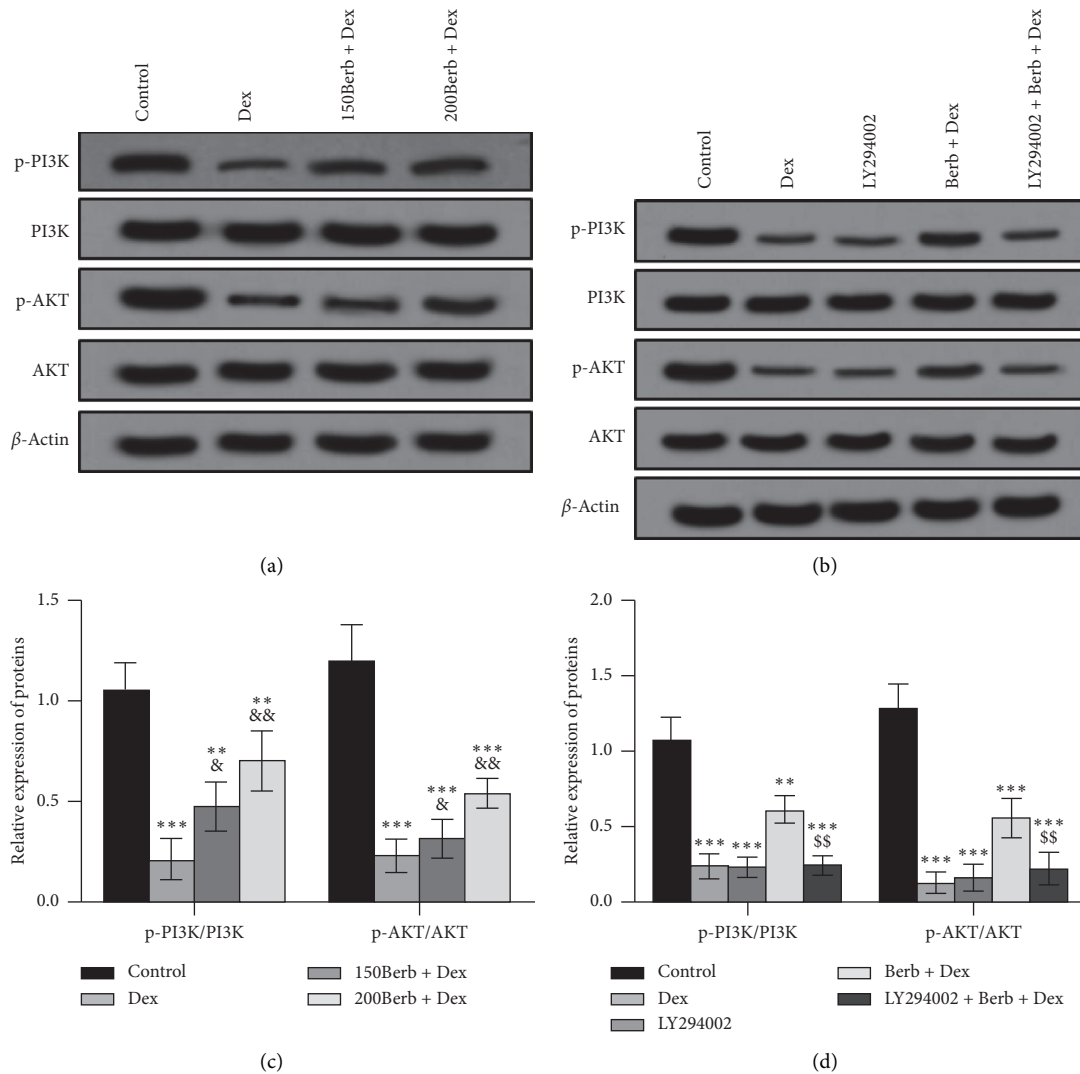


FIGURE 7: Berb treatment induced activation of PI3K/AKT signaling pathway in tendon cells. (a) Dex inhibited the activation of PI3K/AKT signaling pathway, which was reversed by Berb pretreatment; (b) PI3K inhibitor verified the activation of PI3K/AKT signaling pathway. *Note.* Compared with the control group, * $P < 0.05$, ** $P < 0.01$, and *** $P < 0.001$; compared with Dex group, & $P < 0.05$ and && $P < 0.01$; compared with Berb + Dex group, §§ $P < 0.01$.

were selected as the biological markers of tendon cell phenotype in this study, and the changes of their corresponding protein expressions were also measured to indicate the repair level of tendon cells. We found that the expression of these three proteins in the damaged cells induced by Dex was significantly reduced; however, treatment with Berb could reverse this change, suggesting the function of Berb in maintaining the phenotype of tenocytes and promoting its repairing.

It is known that AKT, as a mechanical conversion molecule, can affect the development and homeostasis of various musculoskeletal tissues, including muscle (stretch), cartilage (compression), and bone (shear force) [23]. Previous studies have confirmed that the PI3K/AKT signaling pathway plays an important role in the process of tendon differentiation and tendon formation [23]. Therefore, in the study of the mechanism of Berb's protective effect, this study measured the activation level of the PI3K/AKT signaling

pathway. The results showed that Dex can inhibit the activation of PI3K/AKT, while Berb pretreatment can promote the activation of this pathway. To confirm the relationship between PI3K/AKT signal transduction, Dex, and Berb, we used the PI3K inhibitor LY294002 in the combined action of Dex and Berb. We found that, based on Berb's activation of the PI3K/AKT signaling pathway, the addition of PI3K inhibitors can again inhibit the activation of this pathway suggesting that both Dex and Berb can inhibit and activate the PI3K/AKT signaling pathway, respectively.

5. Conclusion

This study found that pretreatment with Berb can regulate the activation of the PI3K/AKT signaling pathway and reverse the decrease in the proliferation and migration of tenocytes caused by Dex-induced injury. The pretreatment of Berb also decreased the occurrence of apoptosis and

oxidative stress caused by Dex, as well as restoring the expression of biological markers related to the phenotype of tenocytes. The above results suggest that Berb has a cytoprotective effect, but further in vivo studies are still needed to reveal the beneficial effects of Berb on tendons.

Data Availability

The data used to support the findings of this study are available from the corresponding author upon request.

Conflicts of Interest

The authors declare that there are no conflicts of interest regarding the publication of this paper.

Acknowledgments

This work was supported by 2017 Yiwu General Scientific Research Project (no. 17-1-13).

References

- [1] C. C. Skjong, A. K. Meininger, and S. S. W. Ho, "Tendinopathy treatment: where is the evidence?," *Clinics in Sports Medicine*, vol. 31, no. 2, pp. 329–350, 2012.
- [2] S. Dimitrios, "Exercise for tendinopathy," *World Journal of Methodology*, vol. 5, no. 2, pp. 51–54, 2015.
- [3] N. Maffulli, J. Wong, and L. C. Almekinders, "Types and epidemiology of tendinopathy," *Clinics in Sports Medicine*, vol. 22, no. 4, pp. 675–692, 2003.
- [4] P. Sharma and N. Maffulli, "Tendon injury and tendinopathy," *The Journal of Bone & Joint Surgery*, vol. 87, no. 1, pp. 187–202, 2005.
- [5] F. Buttgerit, C. M. Spies, and J. W. Bijlsma, "Novel glucocorticoids: where are we now and where do we want to go?," *Clinical and Experimental Rheumatology*, vol. 33, no. 4, pp. S29–S33, 2015.
- [6] B. J. F. Dean, E. Lostis, T. Oakley, I. Rombach, M. E. Morrey, and A. J. Carr, "The risks and benefits of glucocorticoid treatment for tendinopathy: a systematic review of the effects of local glucocorticoid on tendon," *Seminars in Arthritis and Rheumatism*, vol. 43, no. 4, pp. 570–576, 2014.
- [7] M. W. Wong, W. T. Lui, S. C. Fu, and K. M. Lee, "The effect of glucocorticoids on tendon cell viability in human tendon explants," *Acta Orthopaedica*, vol. 80, no. 3, pp. 363–367, 2009.
- [8] M. W. N. Wong, Y. Y. N. Tang, S. K. M. Lee, B. S. C. Fu, B. P. Chan, and C. K. M. Chan, "Effect of dexamethasone on cultured human tenocytes and its reversibility by platelet-derived growth factor," *The Journal of Bone and Joint Surgery-American Volume*, vol. 85, no. 10, pp. 1914–1920, 2003.
- [9] M. A. Neag, A. Mocan, J. Echeverría et al., "Berberine: botanical occurrence, traditional uses, extraction methods, and relevance in cardiovascular, metabolic, hepatic, and renal disorders," *Frontiers in Pharmacology*, vol. 9, p. 557, 2018.
- [10] X. Lin and N. Zhang, "Berberine: pathways to protect neurons," *Phytotherapy Research*, vol. 32, no. 8, pp. 1501–1510, 2018.
- [11] K. Wang, X. Feng, L. Chai, S. Cao, and F. Qiu, "The metabolism of berberine and its contribution to the pharmacological effects," *Drug Metabolism Reviews*, vol. 49, no. 2, pp. 139–157, 2017.
- [12] D.-Q. Liu, S.-P. Chen, J. Sun et al., "Berberine protects against ischemia-reperfusion injury: a review of evidence from animal models and clinical studies," *Pharmacological Research*, vol. 148, Article ID 104385, 2019.
- [13] T. J. Molloy, Y. Wang, A. Horner, T. M. Skerry, and G. A. C. Murrell, "Microarray analysis of healing rat Achilles tendon: evidence for glutamate signaling mechanisms and embryonic gene expression in healing tendon tissue," *Journal of Orthopaedic Research*, vol. 24, no. 4, pp. 842–855, 2006.
- [14] C. H. Chang, W. C. Tsai, M. S. Lin et al., "The promoting effect of pentadecapeptide BPC 157 on tendon healing involves tendon outgrowth, cell survival, and cell migration," *Journal of Applied Physiology*, vol. 110, no. 3, pp. 774–780, 2011.
- [15] C. Spang, J. Chen, and L. J. Backman, "The tenocyte phenotype of human primary tendon cells in vitro is reduced by glucocorticoids," *BMC Musculoskeletal Disorders*, vol. 17, no. 1, p. 467, 2016.
- [16] Y. Liang, C. Fan, X. Yan et al., "Berberine ameliorates lipopolysaccharide-induced acute lung injury via the PERK-mediated Nrf2/HO-1 signaling axis," *Phytotherapy Research*, vol. 33, no. 1, pp. 130–148, 2019.
- [17] R. Shakeri, A. Kheirollahi, and J. Davoodi, "Apaf-1: regulation and function in cell death," *Biochimie*, vol. 135, pp. 111–125, 2017.
- [18] K. Min, J. M. Lee, M. J. Kim et al., "Restoration of cellular proliferation and characteristics of human tenocytes by vitamin D," *Journal of Orthopaedic Research*, vol. 37, no. 10, pp. 2241–2248, 2019.
- [19] M. O'Brien, "Functional anatomy and physiology of tendons," *Clinics in Sports Medicine*, vol. 11, no. 3, pp. 505–520, 1992.
- [20] D. Amiel, S. D. Kuiper, C. D. Wallace, F. L. Harwood, and J. S. Vandeberg, "Age-related properties of medial collateral ligament and anterior cruciate ligament: a morphologic and collagen maturation study in the rabbit," *Journal of Gerontology*, vol. 46, no. 4, pp. B159–B165, 1991.
- [21] H.-N. Chang, J.-H. S. Pang, C. P. C. Chen et al., "The effect of aging on migration, proliferation, and collagen expression of tenocytes in response to ciprofloxacin," *Journal of Orthopaedic Research*, vol. 30, no. 5, pp. 764–768, 2012.
- [22] D. S. Torres, T. M. Freyman, I. V. Yannas, and M. Spector, "Tendon cell contraction of collagen-GAG matrices in vitro: effect of cross-linking," *Biomaterials*, vol. 21, no. 15, pp. 1607–1619, 2000.
- [23] T. Wang, C. Thien, C. Wang et al., "3D uniaxial mechanical stimulation induces tenogenic differentiation of tendon-derived stem cells through a PI3K/AKT signaling pathway," *The Federation of American Societies for Experimental Biology Journal*, vol. 32, no. 9, pp. 4804–4814, 2018.

Research Article

Integrated Network and Experimental Pharmacology for Deciphering the Medicinal Substances and Multiple Mechanisms of Duhuo Jisheng Decoction in Osteoarthritis Therapy

Wenyu Xiao , Weibing Sun , Hui Lian , and Juexin Shen 

Department of Orthopaedics, Shanghai Tenth People's Hospital Chongming Branch, School of Medicine, Tongji University, Shanghai 202157, China

Correspondence should be addressed to Juexin Shen; juexin_shen@163.com

Received 10 June 2020; Revised 16 September 2020; Accepted 21 October 2020; Published 4 November 2020

Academic Editor: Arham Shabbir

Copyright © 2020 Wenyu Xiao et al. This is an open access article distributed under the Creative Commons Attribution License, which permits unrestricted use, distribution, and reproduction in any medium, provided the original work is properly cited.

Osteoarthritis (OA) is currently the most common joint disorder worldwide. In last decades, herbal remedies have achieved a significant advancement in the treatment of OA. Duhuo Jisheng Decoction (DHJS), an herbal formula consisting of 15 medicinal herbs, has a long-time practice in OA therapy in China. However, its therapeutic mechanisms have not been comprehensively elucidated. In the present work, integrated network and experimental pharmacology were performed for investigating the therapeutic substances and mechanisms of DHJS. Based on network analysis, the contribution of each herb to OA therapy was evaluated. Furthermore, a series of potential targets and signaling pathways were enriched, which could be involved in the therapeutic effects and mechanisms of DHJS. Further experimental results indicated that DHJS attenuated TNF α , IL-6, MMP-1, MMP-9, MMP-13, and ADAMTs-5 expression, inhibited NF- κ B and p38 MAPK signaling pathway, activated AMPK-SIRT1 signaling pathway, and suppressed chondrocyte apoptosis, which synergistically contributed to OA therapy. Our work demonstrated that DHJS could be very promising for OA therapy through synergistically acting on multitargets and multipathways.

1. Introduction

Osteoarthritis (OA) is currently the most common joint disorder affecting about 250 million people worldwide [1]. With the combined epidemic of ageing and obesity, this syndrome has become a massive health and socioeconomic burden [2]. The pathophysiology of OA is characterized by articular cartilage degradation, subchondral bone remodeling, periarticular muscle weakness, synovial inflammation, and subchondral sclerosis [3]. These pathological changes caused the common symptoms including pain, swelling, and stiffness, which lead to instability and physical disability [4]. Therefore, OA severely impaired the quality of life for affected individuals. The complex pathogenesis of OA involves mechanical, inflammatory, and metabolic factors. For example, excessive production of proinflammatory mediators, including cytokines and chemokines, acts on the synovium

to induce inflammation [4]. Catabolic enzymes including matrix metalloproteinases (MMPs), which are released by chondrocytes, are involved in the degradation of extracellular matrix [1]. These factors could tilt the balance between anabolic and catabolic activities of joint tissues toward joint destruction, leading to OA pathogenesis and progression.

Currently, OA management focuses on ameliorating pain, minimizing disability, and enhancing life quality. The therapeutic options recommended in clinic include non-pharmacological and pharmacological interventions. Surgery is offered to those with severe symptoms and for whom conservative approaches have failed [4]. Common pharmacological therapies, such as nonsteroidal anti-inflammatory drugs (NSAIDs), are primarily symptomatic and faced with inefficacy and long-term adverse events [5, 6]. Intra-articular corticosteroids are recommended in case the OA patients have not responded to oral or topical analgesics

[7], but the evidence for clinically important benefits of corticosteroids still remains unclear [8]. In addition, the efficacy of glucosamine and chondroitin sulfate in cartilage repair is also controversial [9]. In summary, the limited efficacy and safety issues surrounding the existing medications necessitate other safe and effective treatments.

Herbal remedy, as an important branch of complementary and alternative medicine, has a long tradition in the treatment of OA. Duhuo Jisheng Decoction (DHJS), a traditional Chinese herbal recipe, has been developed and prescribed to treat OA in China for a long time [10]. This formula consists of 15 species of medicinal herbs: *Radix Angelicae pubescentis* (Duhuo), *Herba Taxilli* (Sangjisheng), *Radix Gentianae Macrophyllae* (Qinjiao), *Radix Saposhnikoviae* (Fangfeng), *Herba Asari* (Xixin), *Cortex Cinnamomi* (Rougui), *Poria Cocos* (Fuling), *Rhizoma Chuanxiong* (Chuanxiong), *Radix Paeoniae Alba* (Baishao), *Cortex Eucommiae Ulmoidis* (Duzhong), *Codonopsis Radix* (Dangshen), *Radix Glycyrrhizae* (Gancao), *Radix Angelicae Sinensis* (Danggui), *Radix Achyranthis Bidentatae* (Niuxi), and *Radix Rehmanniae Preparata* (Shudihuang). According to traditional Chinese medicine theory, *Radix Angelicae pubescentis* is monarch drug responding to dispelling wind and eliminating dampness; *Radix Gentianae Macrophyllae*, *Herba Asari*, and *Cortex Cinnamomi* are minister drugs responding to expelling wind, alleviating pain, and eliminating stagnation; *Herba Taxilli*, *Rhizoma Chuanxiong*, *Radix Achyranthis Bidentatae*, and *Cortex Eucommiae Ulmoidis* are assistant drugs responding to nourishing liver and kidney, strengthening the bone, and activating blood circulation; *Radix Glycyrrhizae* is guide drug responding to harmonizing other herbs. Therefore, DHJS can be mainly used to treat arthralgia syndrome, with the effects of eliminating stagnation, removing blood stasis, and also nourishing the liver and kidney [11].

In recent years, several clinical trials showed that DHJS could relieve OA-related symptoms [10, 12], and a latest meta-analysis paper demonstrated that DHJS combined with Western medicine or sodium hyaluronate injection appears to have beneficial outcomes for OA [13]. Based on modern biological techniques, research on the mechanisms of DHJS suggested that this decoction could alleviate OA through promoting chondrocyte proliferation and suppressing chondrocyte senescence and apoptosis [14–16]. However, DHJS is a multiherb formula containing plentiful bioactive ingredients, and its pharmacological efficacy could be derived from the synergistic actions of the multi-ingredients modulating multipathways in a whole system level. Although several studies have provided some clue to the pharmacological mechanism of DHJS, the comprehensive and precise mechanisms of DHJS on OA therapy have not been elucidated. Network pharmacology is an emerged cutting-edge methodology for revealing the synergism law of multicomponent drugs and seeking high efficacy and low toxicity of multiple-target medications [17]. In the present work, integrated network and experimental pharmacology were employed to pursue the scientific knowledge regarding the principle of formula combination and elucidate

the systematic and comprehensive mechanisms of DHJS on OA therapy.

2. Materials and Methods

2.1. Network Pharmacology-Based Analysis

2.1.1. Construction of DHJS Ingredient Library. The ingredients of each herb in DHJS formula were collected from TCMSP database. TCMSP database provides detailed information of various active ingredients related to traditional Chinese medicines (TCMs), including molecular weight, oral bioavailability, drug likeness, aqueous solubility, and drug targets [18]. In order to gather all reported ingredients in herbal formula, we also performed an extensive literature search for each herb.

2.1.2. Screening Strategy for Active Ingredients in DHJS. Oral bioavailability (OB) is one of the most important pharmacokinetic parameters for an oral administered drug. It is commonly used in drug screening cascades for screening candidate compounds [19]. Drug-likeness (DL) is a qualitative parameter representing how the pharmacokinetic and pharmaceutical properties of a compound correspond in the majority of available drugs [20]. In present work, $OB \geq 25\%$ and $DL \geq 0.18$ were set as a threshold for screening candidate ingredients from DHJS ingredient library. We set both of these variables because only those ingredients with OB and DL above the thresholds are likely the potential bioactive compounds contributing to the therapeutic effects [21, 22].

2.1.3. Collection of DHJS Putative Targets and OA Targets. Herbal formula with numerous bioactive ingredients could regulate multiple targets, so target identification is helpful to elucidate the therapeutic mechanism of DHJS. In this study, two specialized databases (TCMSP and STITCH) were used to search the putative targets of the candidate ingredients. Furthermore, considering that the databases are hard to realize real-time update and incorporate all latest studies, we also performed a large-scale text mining of PubMed using the each herbal ingredient as search term and manually extracted relevant targets from literatures ranging from the years 2015 to 2020. The official symbols of DHJS targets were generated through UniProtKB database (<https://www.uniprot.org/>) with the species limited to “*Homo sapiens*.” Finally, comprehensive ingredient-target interactome of DHJS was constructed in silico. The targets of OA were exported from the human gene database GeneCards (<http://www.genecards.org/>). The items “Symbol” and “Score” of each gene related to OA were reserved.

2.1.4. Pattern Recognition for Integrated Analysis of DHJS-OA Targets. For all DHJS targets, the repetition number of each target was counted as n , and then the same targets were merged. The values of n were normalized with the maximum n normalized to 1. For OA targets, the “Score” values of genes were normalized through being divided by the

maximum value. After normalization, the target scores ranged from 0 to 1, and the target with normalized score 1 was the most relevant target to OA. The number of interaction targets of DHJS and OA was generated with Venn diagram. The overlapped targets with corresponding values of herb targets and OA targets were extracted. Finally, the dataset containing herb targets and OA targets with corresponding values were constructed. After dataset construction, pattern recognition models including principal components analysis (PCA) and hierarchical cluster analysis (HCA) were used to resolve the relevance between herb targets and OA targets. The dataset was exported to the SIMCA-P software (version 12.0) and Heml (version 1.0.3) to perform PCA and HCA, respectively.

2.1.5. Network Construction and Analysis. To explore the multiscale mechanisms of therapeutic action of DHJS in OA, an integrated network consisting of “herb-ingredient network”, “ingredient-target network,” and “disease-target network” was constructed by Cytoscape 3.2.0. In the graphic network, herbal formula, ingredients, targets, and disease were described by nodes, and the intermolecular interactions were encoded by edges. The coverage scale of the targets of each herb and the contribution degree of the targets of each herb were applied to the analysis of the obtained network.

2.1.6. Protein-Protein Interaction Construction and Analysis. The DHJS-OA targets were imported into STRING web server (<http://www.string-db.org/>) for predicting protein-protein interaction (PPI). In PPI, the minimum required interaction score was set as 0.9 and max number of interactors was set as 5. Subsequently, gene ontology (GO) enrichment analysis was performed to extract the functional annotations of these targets.

2.1.7. Enrichment Analysis. Kyoto Encyclopedia of Genes and Genomes (KEGG) pathway enrichment analysis was performed to extract the canonical pathways and highly associated proteins. *p* values were given in enrichment analysis, and smaller *p* values suggested greater enrichment. To further characterize the molecular mechanism of DHJS on OA, the target-pathway network was generated using Cytoscape 3.2.0 based on the pathway data.

2.2. Experimental Validation

2.2.1. Preparation of DHJS Extract. The herbs in DHJS were purchased from Tongrentang (Shanghai, China). Then these herbs were identified by experts from School of Chinese Materia Medica, Shanghai University of Chinese Medicine (Shanghai, China). Herbs were mixed and extracted with the standard methods according to Chinese Pharmacopoeia 2015. Briefly, herbs were soaked in distilled water and boiled for 30 min twice and then the solution was filtered and concentrated with a rotary evaporator. The product was dissolved in DMSO to obtain a 1 g/mL stock solution. The

obtained solution was filtered twice (0.22 μ m) and the filtrate was stored at 4°C.

2.2.2. Cell Isolation and Culture. All animal procedures were approved by the Institutional Animal Care and Use Committee of Shanghai Tenth People’s Hospital Chongming Branch. Male Sprague-Dawley rats (8 weeks old, 200 \pm 20 g) were purchased from Super-BK Laboratory Animal Co. (Shanghai, China) and maintained under specific pathogen-free (SPF) conditions. Chondrocytes were isolated from rat articular cartilage and cultured as previously described [23]. The second-passages (P2) chondrocytes cultured until ~80% confluency were used in the study.

2.2.3. Cell Viability Assay. Briefly, chondrocytes were seeded in 96-well plates and then incubated with different concentrations of DHJS (20, 50, 100, 200, 500, and 1000 μ g/mL) in the presence or absence of recombinant rat IL-1 β (10 ng/mL) (Beyotime Institute of Biotechnology, Shanghai, China) for 24, 48, or 72 h. Subsequently, MTT assay was conducted to assess the effect of DHJS on cell viability.

2.2.4. Real-Time PCR. Chondrocytes were treated with different concentrations of DHJS (50, 100, and 200 μ g/mL) for 2 h, followed by stimulation with or without IL-1 β (10 ng/mL) for 24 h. Total RNA was extracted using Trizol reagent (Takara, Shiga, Japan) according to instructions and was reverse-transcribed to cDNA using a PrimeScript RT reagent kit (Takara, Shiga, Japan). Subsequently, real-time PCR was performed using SYBR[®] GreenER SuperMix (Takara, Shiga, Japan) and the results were analyzed using the $2^{-\Delta\Delta Ct}$ method. The primers used were as follows: β -actin: forward 5'-GGAGATTACTGCCCTGGCTCCTA-3', reverse 5'-GACTCATCGTACTCCTGCTTGCTG-3'; IL-6: forward 5'-ATTGTATGAACAGCGATGATGCAC-3', reverse 5'-CCA GGTAGAAACGGAAGTCCAGA-3'; TNF α : forward 5'-TCAGTTCATGGCCCAGAC-3', reverse 5'-GTTGTCT TTGAGATCCATGCCATT-3'; MMP-1: forward 5'-CTGAAGGTGATGAAGCAGCC-3', reverse 5'-AGTC-CAAGAGAATGGCCGAG-3'; MMP-13: forward 5'-TGAT GATGAAACCTGGACAAGCA-3', reverse 5'-GAACGT-CATCATCTGGGAGCA-3'; ADAMTs-5: forward 5'-AGAGTCCGAACGAGTTTACG-3', reverse 5'-GTGCCA GTTCTGTGCGTC-3'.

2.2.5. Western Blot. Proteins were extracted from cells using RIPA buffer and the protein concentration was determined using BCA protein assay kit (Thermo Scientific, IL, USA). Equal amounts of protein were separated by 10% SDS-PAGE and transferred onto PVDF membranes (Millipore, MA, USA). After blocking, PVDF membranes were incubated with primary antibodies against p65, p-p65, p38, p-p38, SIRT1, Bax, Bcl2, c-caspase3, and β -actin (Abcam Inc., MA, UK), followed by incubation with HRP-conjugated secondary antibody (Cell Signaling Technology Inc., MA, USA). The protein bands were visualized with Ultra Signal

chemiluminescence reagents (4A Biotech Co., Ltd., Beijing, China).

2.2.6. Statistical Analysis. Data was shown as mean \pm standard deviation (SD). Statistical differences of data were evaluated using the independent-samples *T*-test analysis or one-way analysis of variance using SPSS 16.0 software. *p* value <0.05 was considered statistically significant.

3. Results

3.1. Network Pharmacology-Based Analysis

3.1.1. Candidate Bioactive Ingredients in DHJS. A large number of ingredients in DHJS were obtained from TCMSP database (Table 1). Their corresponding properties were also collected to construct DHJS ingredient library. Subsequently, collected ingredients were subjected to OB and DL screening. As a result, total 77 ingredients were included and regarded as candidate compounds. The detailed information of 77 screened ingredients is shown in Table 1.

3.1.2. Collection of DHJS Putative Targets and OA Targets. Based on screening in TCMSP and STITCH databases, as well as supplemented text mining of PubMed, 77 candidate compounds yielded 359 targets after deleting duplicates. Total 2854 disease-related targets were extracted from GeneCards database. Finally, the library of DHJS targets and OA targets was constructed based on the procedures described in the above method.

3.1.3. Pattern Recognition for Integrated Analysis of DHJS-OA Targets. Total 359 DHJS targets were mapped with 2854 OA targets to generate 213 interaction targets (Figure 1(a)). Subsequently, the dataset containing DHJS targets with values and OA targets with values was imported into SIMCA and Heml software for pattern identification analysis. In SIMCA, PCA was used to obtain discrimination by predicting group membership. Scores scatter 3D plot from PCA showed that there was no clear separation between DHJS and OA, suggesting the high integration degree of DHJS targets and OA targets (Figure 1(b)). In addition, Dangshen, Sangjisheng, and Shudihuang showed obvious separation from other herbs, DHJS formula, and OA. Considering the distance of OA group to herb groups, Duhuo, Gancao, Niuxi, Duzhong, and Fangfeng were among the nearest groups to OA group. In Heml, heatmap from HCA analysis showed similar result to that from PCA analysis (Figure 1(c)). As expected, DHJS group and OA group were assigned into a near cluster since they shared similar target profile. Moreover, Dangshen was the farthest group from OA group, suggesting the obvious difference between their targets.

3.1.4. Network Construction and Analysis. 77 ingredients and 213 interaction targets were imported into Cytoscape software for network construction. The network linking the

candidate ingredients with their putative targets was plotted (Figure 2(a)). The affiliation of ingredients with herbs was also described. The ingredients with coexistence in several herbs were listed in only one herb based on the anticlockwise sort in network plot. As a result, the generated network diagram consisted of 288 nodes and 1985 edges. This diagram showed a complex interactive relationship between “one compound-multiple targets” and “one target-multiple compounds.” Additionally, there was no ingredient having affiliation with Danggui because the ingredients found in Danggui were also found in other herbs. Furthermore, all targets linked with verbascoside contained in Shudihuang were also linked with other ingredients in other herbs.

As depicted in Figure 2(b), the herb with more ingredients generated more targets and presented more probability to cover OA targets. Danggui contained the smallest number of ingredients and thus generated the least targets. The median of mapped percent of herbs was about 60%, and the herbs Danggui, Fuling, and Xixin were the top three at counting backward. Considering the contribution of each herb to DHJS-OA mapped targets, the herbs Niuxi, Gancao, and Duzhong were the top three, while the herbs Danggui, Fuling, and Qinjiao were the top three at counting backward (Figure 2(c)).

3.1.5. Protein-Protein Interaction Construction and Analysis. The PPI network was constructed in STRING as shown in Figure 3(a). The number of nodes was 213 and the number of edges was 1154. The nodes strongly linked with OA-related pathways were labeled with color. The GO information including biological process (BP), cellular component (CC), and molecular function (MF) terms was obtained. The top 5 significantly enriched terms in BP, CC, and MF categories are shown in Figure 3(b). The results indicated that DHJS could exert biological actions via protein binding, kinase binding, and transcription factor binding in organelle, cytosol, nucleoplasm, and extracellular space to exert its therapeutic effects. Figure 3(c) depicts the top 30 candidate targets according to the node degree which indicated the degree of importance to OA therapy. These targets were believed as crucial proteins involved in OA pathogenesis and pharmacologic therapeutic.

3.1.6. Pathway Enrichment Analysis. To further characterize the molecular mechanism of DHJS on OA treatment, we carried out pathway-based functional enrichment analysis. Total 70 KEGG pathways were systematically enriched and extracted. Among them, top 20 KEGG pathways are shown in Figure 4(a). Total 8 signaling pathways, including PI3K-AKT signaling pathway, FOXO signaling pathway, TNF signaling pathway, JAK-STAT signaling pathway, MAPK signaling pathway, AMPK-SIRT1 signaling pathway, IL-17 signaling pathway, TLR signaling pathway, and apoptosis signaling pathway, were assigned to be the positive pathways associated with OA. A representative enriched KEGG pathway, PI3K-AKT signaling pathway, is shown in Figure 4(b). Based on the extraction of labeled targets in these pathways, a target-pathway network was generated by

TABLE 1: Information for the ingredients of each herb in DHJS.

| No. | Herb | Number of ingredients | | | Name of ingredients |
|-----|-------------|-----------------------|-------------------|------------------|--|
| | | Total | OB & DL screening | Target screening | |
| 1 | Duhuo | 99 | 13 | 6 | Ammidin, beta-sitosterol, columbianadin, marmesin, nodakenin, and osthol |
| 2 | Sangjisheng | 46 | 4 | 3 | Beta-sitosterol, oleanolic acid, and quercetin |
| 3 | Qinjiao | 27 | | 4 | Beta-sitosterol, gentiopicrin, loganic acid, and oleanolic acid |
| 4 | Fangfeng | 173 | 26 | 8 | Ammidin, anomalin, beta-sitosterol, decursin, marmesin, phellopterin, prangenidin, and wogonin |
| 5 | Xixin | 192 | 10 | 3 | Asarinin, kaempferol, and sesamin |
| 6 | Rougui | 100 | 3 | 3 | Cinnamaldehyde, ethyl cinnamate, and procyanidin B1 |
| 7 | Fuling | 34 | 19 | 3 | Hederagenin, pachymic acid, and poricoic acid A |
| 8 | Chuanxiong | 189 | 12 | 4 | Beta-sitosterol, ferulic acid, myricanone, and tetramethylpyrazine |
| 9 | Baishao | 85 | 15 | 7 | Albiflorin, beta-sitosterol, (+)-catechin, kaempferol, mairin, oleanolic acid, and paeoniflorin |
| 10 | Duzhong | 147 | 39 | 13 | Beta-carotene, beta-sitosterol, (+)-cyclooolivil, cyclopamine, epicatechin, (+)-Eudesmin, kaempferol, mairin, (+)-medioresinol, pinoresinol diglucoside, quercetin, syringetin, and yangambin |
| 11 | Dangshen | 134 | 26 | 6 | Friedelin, glycitein, spinasterol, stigmasterol, tectorigenin, and luteolin |
| 12 | Gancao | 280 | 101 | 28 | Beta-sitosterol, calycosin, eurycarpin A, formononetin, glabridin, glabrone, glycyrol, glycyrrhizin, glypallichalcone, isolicoflavonol, isorhamnetin, jaranol, kaempferol, licochalcone A, licochalcone B, liquiritin, lupiwighteone, naringenin, oleanolic acid, pinocembrin, quercetin, and vestitol |
| 13 | Danggui | 125 | 3 | 3 | Beta-sitosterol, ferulic acid, and stigmasterol |
| 14 | Niuxi | 176 | 22 | 15 | Baicalin, baicalein, berberine, beta-ecdysterone, beta-sitosterol, coptisine, epiberberine, inophyllum E, kaempferol, oleanolic acid, palmatine, quercetin, spinasterol, stigmasterol, and wogonin |
| 15 | Shudihuang | 76 | 6 | 3 | Beta-sitosterol, stigmasterol, and verbascoside |

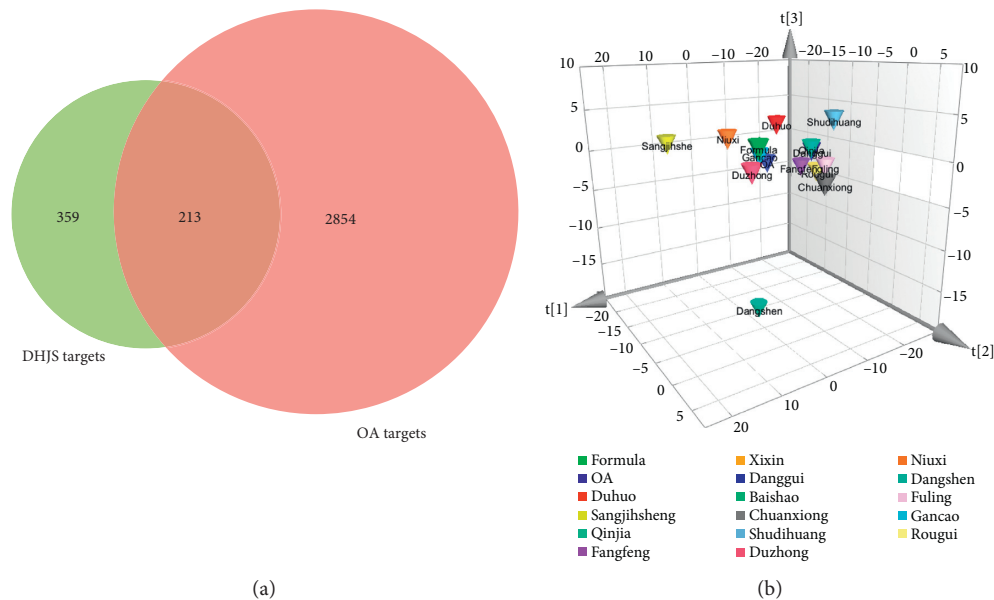


FIGURE 1: Continued.

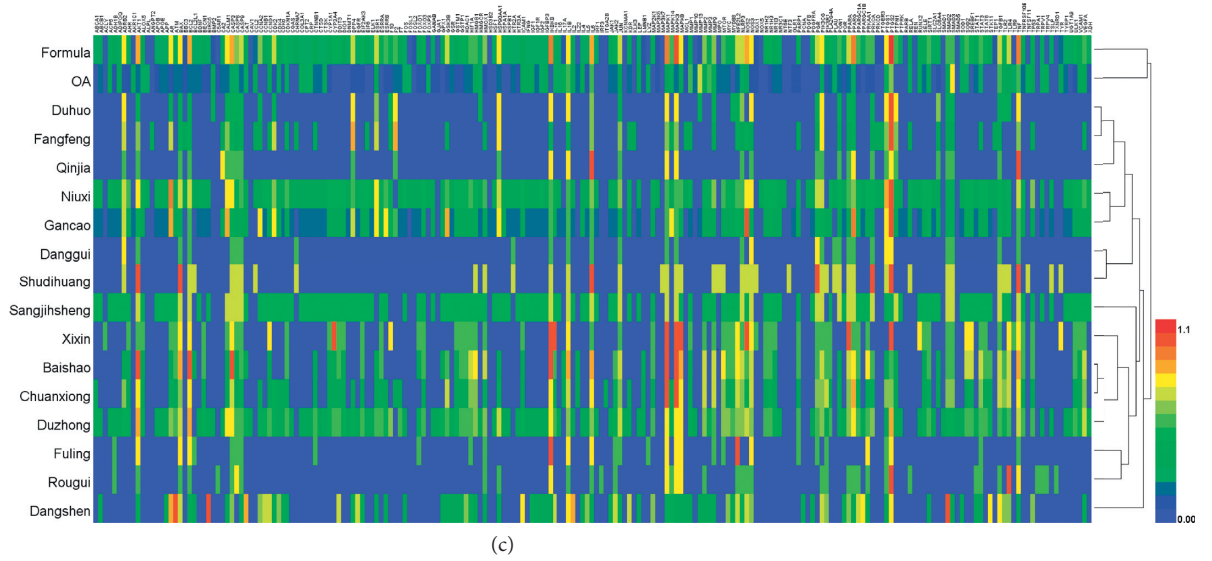


FIGURE 1: Integrated analysis of DHJS-OA targets. Venn diagram of DHJS and OA targets (a). Scores scatter 3D plot from PCA analysis of DHJS-OA target dataset (b). Heatmap from HCA analysis of DHJS-OA target dataset (c).

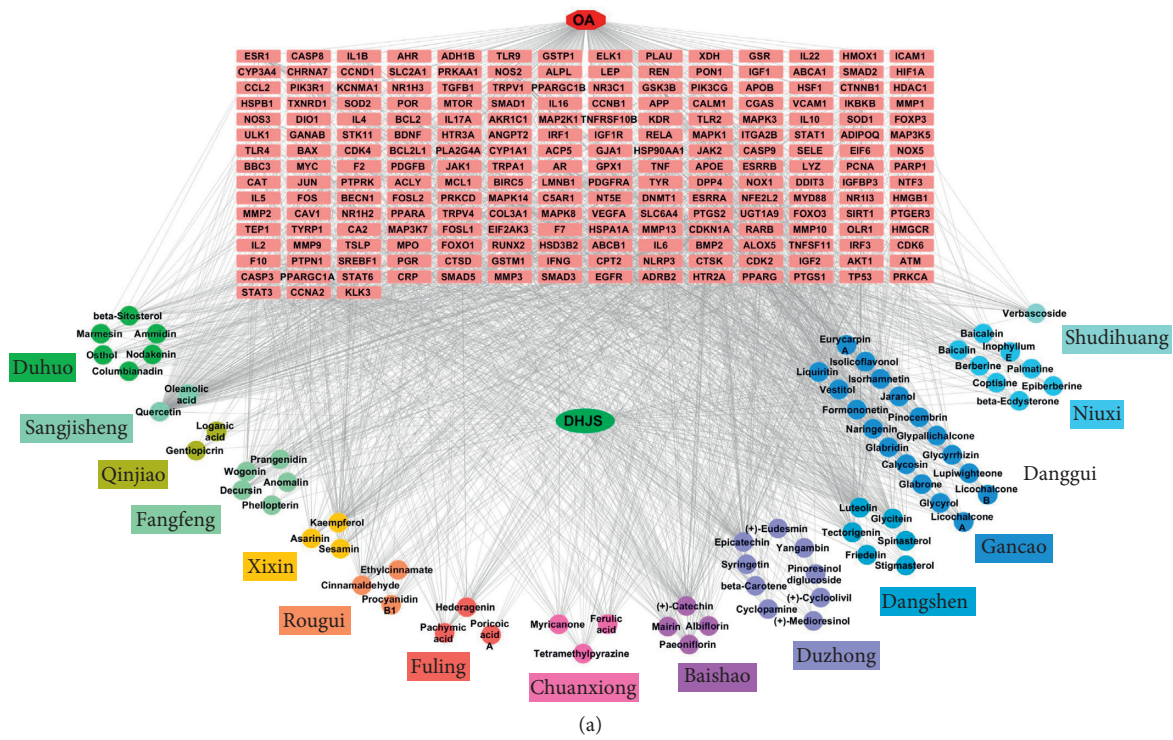


FIGURE 2: Continued.

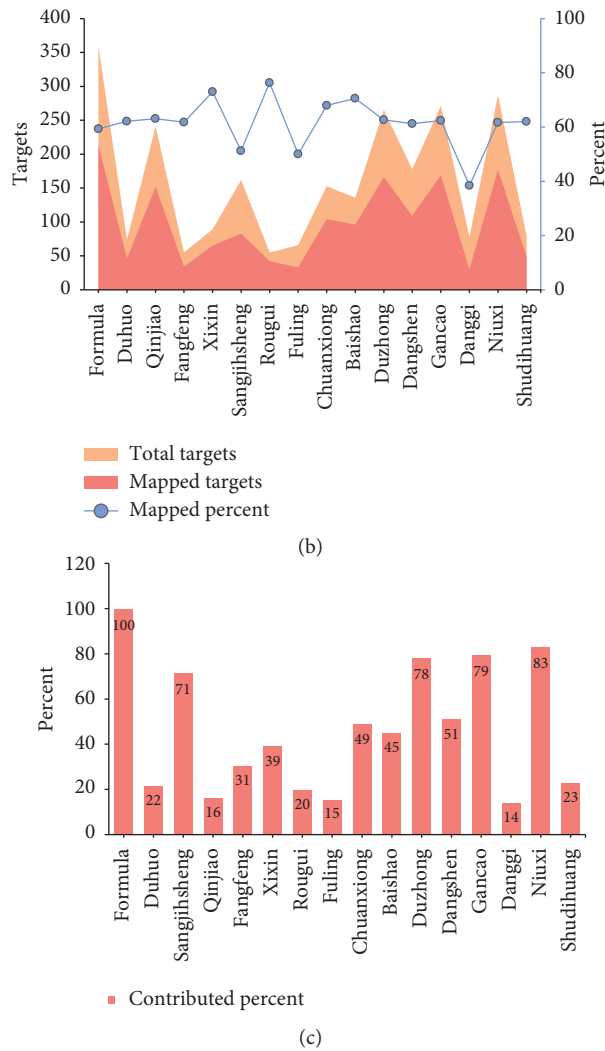


FIGURE 2: Network construction and analysis. Network diagram constructed by linking ingredient with putative targets (a). The nodes represent candidate compounds in DHJS which are shown as colorful circle, and the targets are indicated by light red fusiform. The total targets and DHJS-OA mapped targets generated by each herb (b). The contribution of each herb in DHJS formula to the interaction targets (c).

linking extracted targets with their corresponding significant signaling pathways (Figure 4(c)). This network illustrated the most potential targets and pathways which played a pivotal role in the therapeutic efficacy of DHJS formula for OA therapy.

3.2. Experimental Validation

3.2.1. Effect of DHJS on Chondrocyte Viability. Isolated primary chondrocytes were identified by toluidine blue staining. The primary chondrocytes were shaped like spindles with a protuberance, and proteoglycans in rat primary chondrocytes were stained purple by toluidine blue (Figure 5(a)). DHJS showed no significant cytotoxicity at doses ranging from 20 to 200 $\mu\text{g}/\text{mL}$, while higher dose of DHJS ($\geq 500 \mu\text{g}/\text{mL}$) significantly inhibited the cell viability (Figure 5(b)). Likewise, DHJS ($\leq 200 \mu\text{g}/\text{mL}$) exerted no

significant effect on the viability of IL-1 β -induced chondrocytes (Figure 5(c)).

3.2.2. DHJS Suppresses IL-1 β -Induced TNF α , IL-6, MMPs, and ADAMTs-5 Expression in Chondrocytes. In OA, large amounts of TNF α , IL-6, MMPs, and ADAMTs-5 are released with the occurrence of inflammation and resulted in ECM dissolution. In the present work, the effects of DHJS on the mRNA expression of these factors were examined in chondrocytes. As expected, IL-1 β treatment induced significant overexpression of TNF α , IL-6, MMP-1, MMP-9, MMP-13, and ADAMTs-5 genes in primary chondrocytes (Figures 5(d)–5(i)). Interestingly, DHJS pretreatment significantly alleviated the overexpression of TNF α , IL-6, MMP-1, MMP-9, MMP-13, and ADAMTs-5 genes in IL-1 β -induced chondrocytes (Figures 5(d)–5(i)).

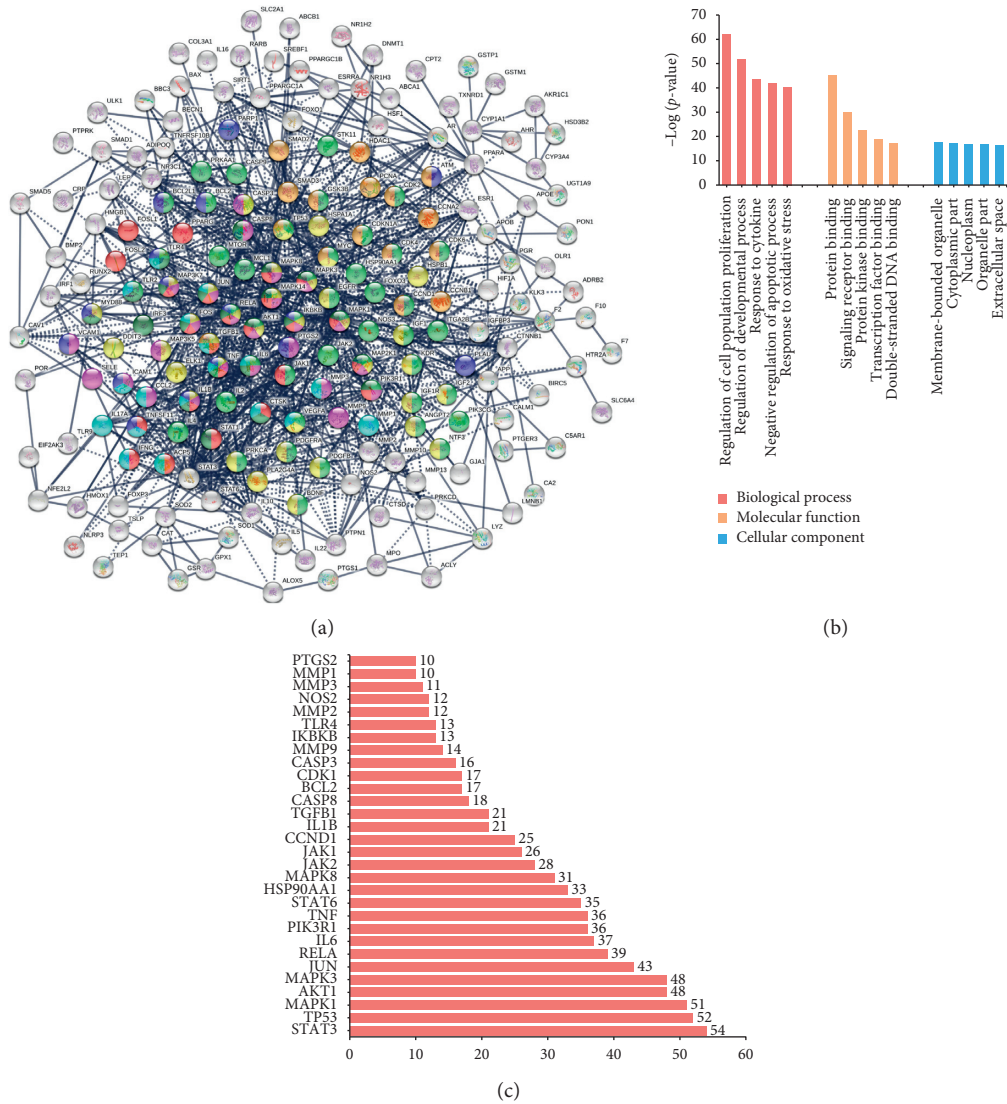


FIGURE 3: PPI construction and analysis. The PPI network generated on DHJS-OA mapped targets (a). The top 5 significantly enriched BP, CC, and MF categories based on gene ontology (b). The top 30 candidate targets extracted from PPI according to the node degree (c).

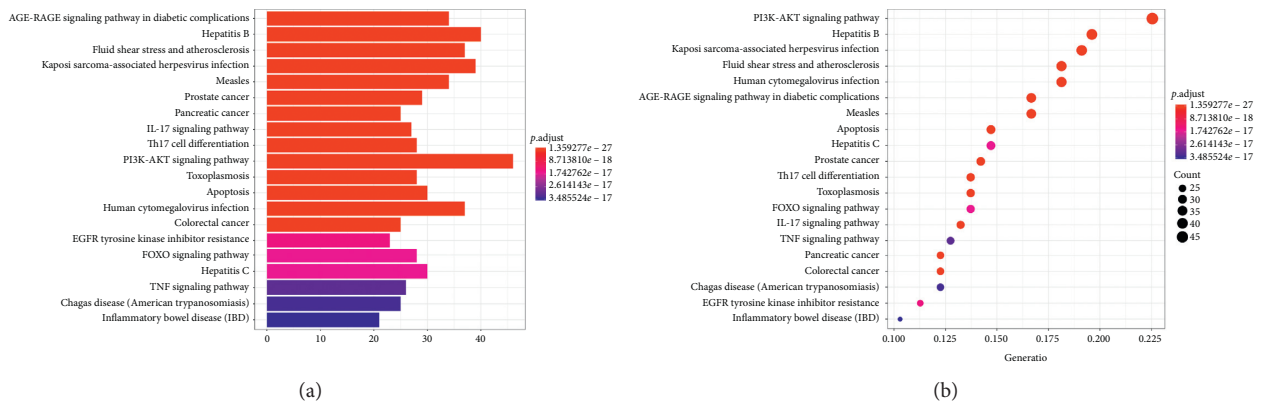


FIGURE 4: Continued.

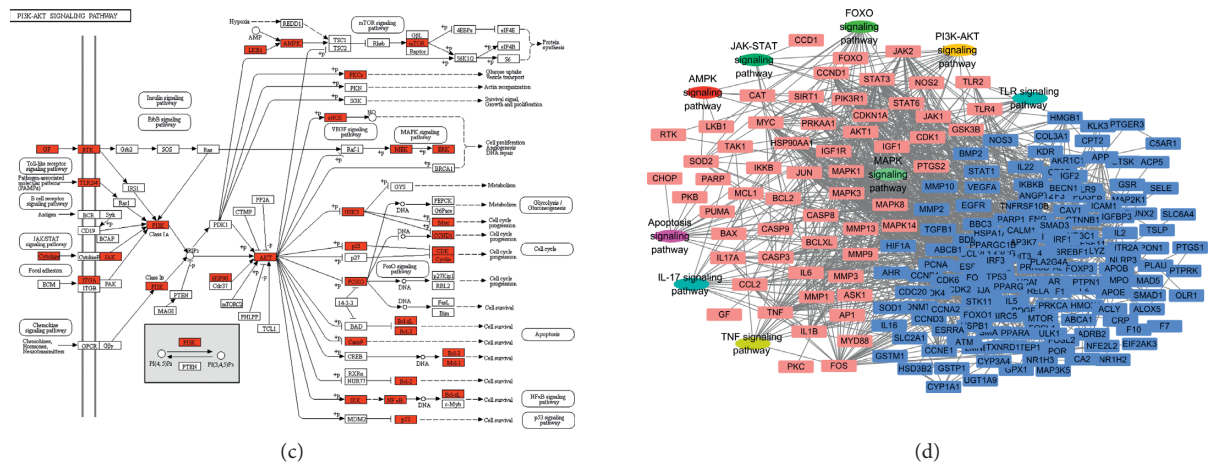


FIGURE 4: Pathway enrichment analysis. The top 20 pathways extracted based on KEGG enrichment analysis (a). The enriched PI3K-AKT pathway with mapped targets labeled red (b). The target-pathway network for DHJS on OA, in which the red nodes represent the most potential targets and the oval nodes represent the most potential pathways (c).

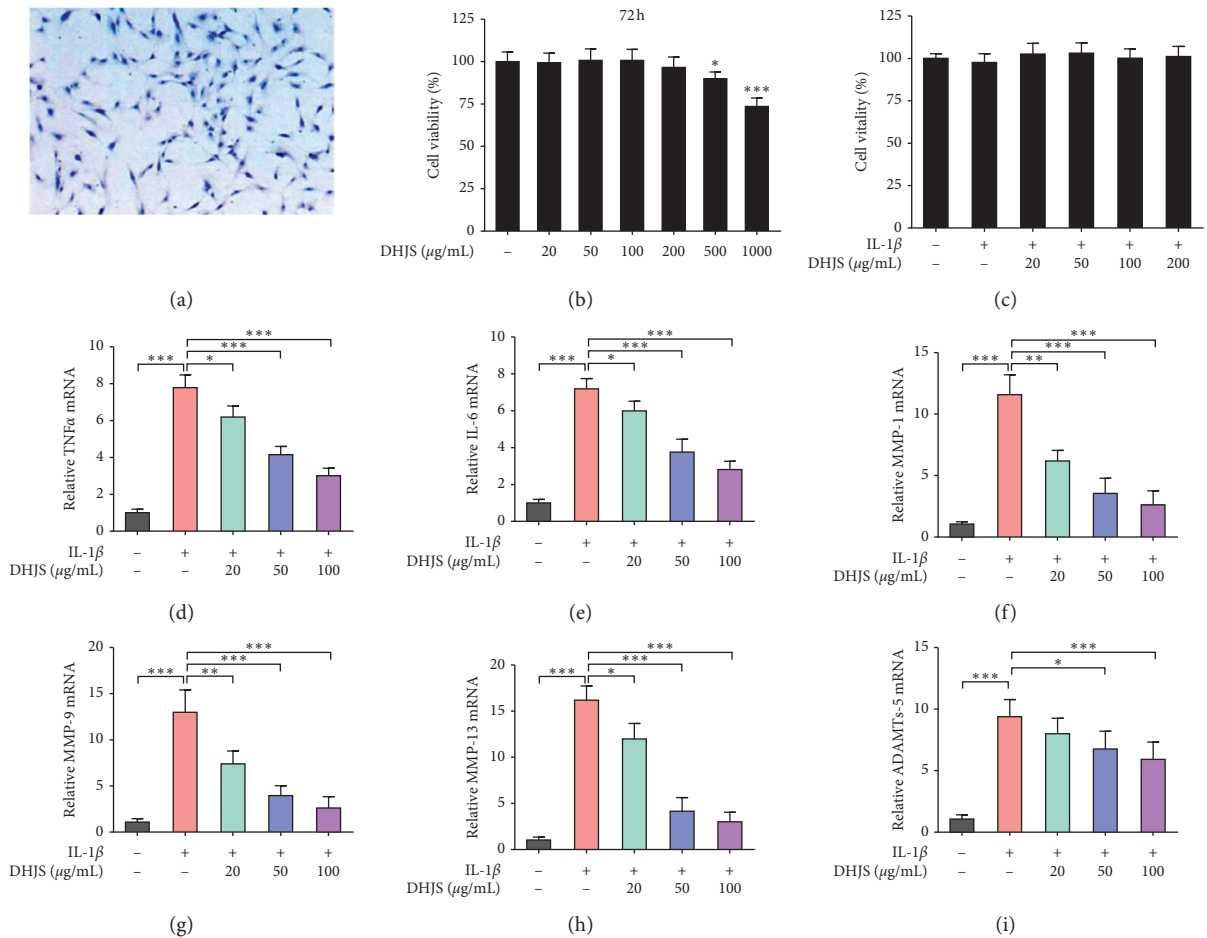


FIGURE 5: Effects of DHJS on cell viability and IL-1 β -induced expression of TNF α , IL-6, MMPs, and ADAMTs-5 in rat chondrocytes. Identification of rat primary chondrocytes (a). Rat chondrocytes were shaped like spindles with a protuberance, in which proteoglycans were stained purple by toluidine blue. Effects of DHJS on cell viability of chondrocytes (b). Effects of DHJS on cell viability of IL-1 β -induced chondrocytes (c). Effects of DHJS on IL-1 β -induced expression of TNF α (d), IL-6 (e), MMP-1 (f), MMP-3 (g), MMP-9 (h), and ADAMTs-5 (i) in rat chondrocytes. Data are expressed as mean \pm SD ($n = 3$). * $p < 0.05$, ** $p < 0.01$, and *** $p < 0.001$, compared between the marked groups.

3.2.3. Effect of DHJS on Dominating Signaling Pathways in IL-1 β -Induced Chondrocytes. To obtain insight into the mechanisms of DHJS on OA therapy, the expression levels of several key proteins involved in dominating signaling pathways were detected in IL-1 β -induced chondrocytes with or without DHJS pretreatment (Figures 6(a)–6(d)). As shown in Figure 6(a), IL-1 β inducement significantly increased the phosphorylation of NF- κ B in comparison with control group ($p < 0.001$), while DHJS pretreatment significantly inhibited the IL-1 β -induced phosphorylation of NF- κ B ($p < 0.05$). Likewise, significant p38 phosphorylation was found in IL-1 β -induced chondrocytes ($p < 0.001$), which was effectively alleviated by DHJS pretreatment (Figure 6(b)). In addition, IL-1 β inhibited the AMPK-SIRT1 pathway by suppressing AMPK phosphorylation and SIRT1 protein expression, which was also restored by DHJS pretreatment (Figure 6(c)). Furthermore, several apoptosis-related markers were evaluated. The results indicated that IL-1 β induced significant upregulation of proapoptotic c-caspase3 and Bax proteins and downregulation of antiapoptotic Bcl2 protein (Figure 6(d)). Fortunately, DHJS pretreatment abrogated IL-1 β -induced dysregulation of apoptosis-related proteins (Figure 6(d)). Taken together, the above results indicate that DHJS could suppress NF- κ B and p38 activation, activate AMPK-SIRT1 pathway, and inhibit apoptosis pathway.

4. Discussion

The pathophysiology of OA is still evolving, from being viewed as a cartilage-limited disease to a multifactorial disease [4]. It has been demonstrated that a wide range of underlying pathways lead to similar outcomes of joint destruction in OA [24]. The proposed mechanistic pathways include increased inflammatory components [25], mechanical overload [26], metabolic alterations [27], and cell senescence [28]. For detail, factors involved in inflammatory state include IL-1 β , IL-6, TNF α , PGE2, NO, and ROS; factors involved in matrix degradation include MMP-1, MMP-9, MMP-13, and ADAMTs-5; factors involved in osteoclast differentiation include receptor activator of nuclear factor- κ B ligand (TNFSF11) and sclerostin; factors involved in chondrocyte senescence include cytokines, chemokines, ROS, and HIF-1 α . Therefore, these factors play crucial roles in OA pathogenesis and also represent the potential targets to treat OA.

In last decades, herbal remedies have seen significant advancement against OA [29, 30]. DHJS formula consisting of 15 medicinal herbs has a clinical practice in OA therapy for a long time [11–13]. It was believed that the synergistic actions of bioactive ingredients respond to therapeutic efficacy of this formula for OA [14–16]. However, our study indicated that the ingredients contained in each herb and their corresponding targets showed some overlap. For instance, the candidate ingredients found in Danggui were also found in other herbs. The putative targets generated by the only candidate ingredient in Shudihuang were also found in other herbs. Furthermore, the herbs Danggui and Shudihuang showed much little contribution to DHJS-OA

mapped targets. Therefore, these results suggested that the ingredients and targets of Danggui and Shudihuang could be supplemented by other herbs which could be modified in DHJS formula for OA therapy. In addition, the contribution of each herb to OA therapy was different. PCA and HCA analysis indicated that Duhuo, Gancao, Niuxi, Duzhong, and Fangfeng were highly associated with OA therapy. It was consistent with that these herbs contributed the most DHJS-OA targets. Indeed, these herbs have also been widely reported to exert protective effects on joint cartilages in OA therapy [31–35]. However, the herbs Qinjiao and Fuling also showed much little contribution to DHJS-OA mapped targets, and there are few related reports about the using of Qinjiao and Fuling for OA therapy. These results suggested that the evidence of applying Qinjiao and Fuling for OA treatment was insufficient. In summary, in DHJS formula, the herbs including Duhuo, Gancao, Niuxi, Duzhong, and Fangfeng could exert greater contribution to OA therapy while herbs including Danggui, Shudihuang, Qinjiao, and Fuling might exert less contribution to OA therapy. However, further comparative pharmacological studies need to be carried out to validate such conclusion.

Although clinical trials demonstrated that DHJS could relieve OA-related symptoms [10, 12, 13] and a few reports indicated the relevant therapeutic mechanisms [14–16], the comprehensive and precise mechanisms of DHJS on OA therapy have not been elucidated. In the present work, a series of potential targets and interactive pathways were proposed based on enhanced network pharmacology, which were believed to play a pivotal role in the therapeutic efficacy of DHJS formula for OA therapy. IL-1 β is a key inflammation cytokine in OA pathogenesis and progression. IL-1 β stimulates the production of several inflammatory mediators, such as iNOS, TNF α , and IL-6, which contribute to chondrocytic dysfunction [36, 37]. Moreover, IL-1 β also promotes the secretion of MMPs such as MMP-1, MMP-13, and ADAMTs-5 in chondrocytes, which cause cartilage degeneration and ECM destruction [38, 39]. Based on network pharmacology, a series of key targets were enriched from network analysis, such as PTGS2, MMP-1, MMP-9, MMP-13, iNOS, IL-1 β , TNF α , and IL-6. These results suggested that DHJS could regulate these targets to exert beneficial effects on OA. As expected, DHJS apparently inhibited IL-1 β -induced TNF α , IL-6, MMP-1, MMP-9, MMP-13, and ADAMTs-5 expression in rat chondrocytes, which were basically consistent with the results of network analysis.

Next, we validated the therapeutic mechanisms of DHJS on OA. Several dominating signaling pathways were extracted from KEGG enrichment. Based on pathway enrichment, DHJS could regulate JAK-STAT signaling pathway for modulating G1/S phase transition to promote chondrocyte proliferation, which was consistent with a previous report [15]. However, DHJS at doses ranging from 20 to 200 μ g/mL showed no significant effect on chondrocyte viability, suggesting that DHJS might be hard to promote chondrocyte proliferation. NF- κ B pathway is profoundly involved in the regulation of inflammatory mediators in OA progression [40]. Upon stimulation, the activated NF- κ B

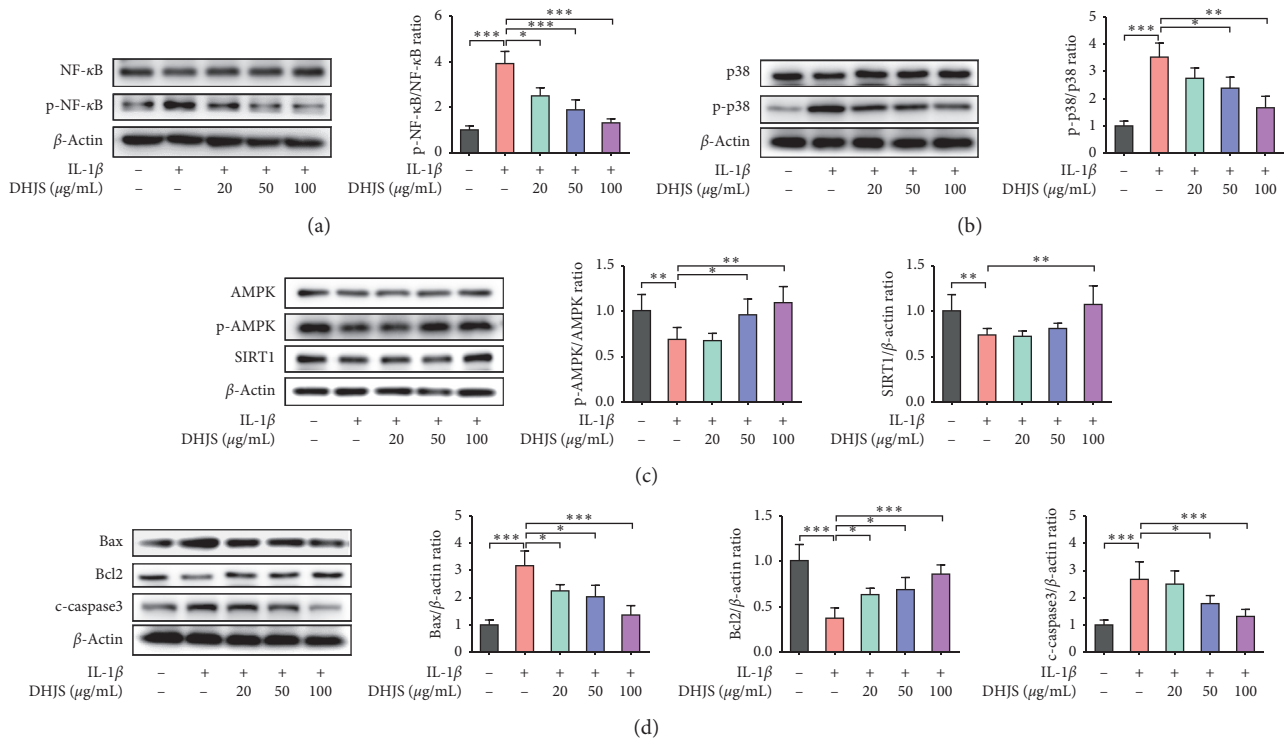


FIGURE 6: Effects of DHJS on protein expression of NF- κ B, p38, AMPK, SIRT1, Bax, Bcl2, and c-caspase3 in IL-1 β -induced chondrocytes. DHJS reduced IL-1 β -induced NF- κ B phosphorylation (a). DHJS reduced IL-1 β -induced p38 phosphorylation (b). DHJS increased AMPK phosphorylation and SIRT1 expression in IL-1 β -induced chondrocytes (c). DHJS reduced Bax and c-caspase3 expression and increased Bcl2 expression in IL-1 β -induced chondrocytes (d). Data are expressed as mean \pm SD ($n = 3$). * $p < 0.05$, ** $p < 0.01$, and *** $p < 0.001$, compared between the marked groups.

molecules trigger the expression of proinflammatory factors to induce the destruction of articular joint [40]. Therefore, inhibition of NF- κ B pathway could represent a promising therapeutic option for OA treatment. Pathway enrichment indicated that DHJS could target NF- κ B pathway, and in vitro experiment confirmed this conjecture in which DHJS significantly inhibited NF- κ B phosphorylation. Moreover, emerging evidence has demonstrated that p38 MAPK signal pathway was involved in OA development, and inhibiting the activation of p38 MAPK pathway may be a new target for OA treatment [41]. In the present work, the phosphorylation of p38 in IL-1 β -stimulated chondrocytes was significantly reduced by DHJS, suggesting that inhibiting p38 MAPK pathway represented one of the mechanisms of DHJS to treat OA. In addition, pathway enrichment indicated that DHJS could regulate AMPK-SIRT1 pathway to enhance oxidative defense, and cell experiment verified that DHJS activated AMPK-SIRT1 pathway in IL-1 β -induced chondrocytes. Moreover, Liu et al. reported that DHJS suppressed cell apoptosis to alleviate intervertebral disc degeneration [16]. Consistently, our study suggested DHJS could mediate apoptosis signaling pathway to protect chondrocyte against apoptosis, which was also confirmed by in vitro experiment. In summary, DHJS could have great potential in OA therapy through synergistic actions derived from acting on these multitargets and multipathways.

In conclusion, integrated network and experimental pharmacology were employed, which provided a comprehensive investigation to understand the medicinal substances and molecular mechanism of DHJS for OA treatment. The results demonstrated that DHJS could attenuate OA through decreasing TNF α , IL-6, MMP-1, MMP-9, MMP-13, and ADAMTs-5 levels, and the corresponding mechanisms could involve inhibiting NF- κ B and p38 MAPK signaling pathways, activating AMPK-SIRT1 signaling pathway, and reversing chondrocyte apoptosis. Due to the multifactorial pathogenesis of OA, DHJS with synergistic effects on multitargets and multipathways could have considerable potential in OA therapy.

Data Availability

The analyzed data sets generated during the present study are available from the corresponding author on reasonable request.

Conflicts of Interest

The authors declare that they have no conflicts of interest.

Authors' Contributions

Juexin Shen and Wenyu Xiao conceived and devised the research; Wenyu Xiao analyzed the data and wrote the

manuscript; Weibing Sun and Hui Lian revised the data and manuscript. All authors contributed to the interpretation of the data and critical revision of the manuscript. All authors have read and approved the final manuscript.

Acknowledgments

This work was supported by fund of the Science Foundation of Shanghai Chongming (CKY2015-16).

References

- [1] D. J. Hunter and S. Bierma-Zeinstra, "Osteoarthritis," *Lancet (London, England)*, vol. 393, pp. 1745–1759, Article ID 10182, 2019.
- [2] D. J. Hunter, D. Schofield, and E. Callander, "The individual and socioeconomic impact of osteoarthritis," *Nature Reviews Rheumatology*, vol. 10, no. 7, pp. 437–441, 2014.
- [3] J. R. Kim, J. J. Yoo, and H. A. Kim, "Therapeutics in osteoarthritis based on an understanding of its molecular pathogenesis," *International Journal of Molecular Sciences*, vol. 19, no. 3, 2018.
- [4] J. Martel-Pelletier, A. J. Barr, F. M. Cicuttini et al., "Osteoarthritis," *Nature Reviews Disease Primers*, vol. 2, Article ID 16072, 2016.
- [5] W. Zhang, G. Nuki, R. W. Moskowitz et al., "OARSI recommendations for the management of hip and knee osteoarthritis: part III: changes in evidence following systematic cumulative update of research published through January 2009," *Osteoarthritis and Cartilage*, vol. 18, no. 4, pp. 476–499, 2010.
- [6] J. Zhang, E. L. Ding, and Y. Song, "Adverse effects of cyclooxygenase 2 inhibitors on renal and arrhythmia events: meta-analysis of randomized trials," *JAMA*, vol. 296, no. 13, pp. 1619–1632, 2006.
- [7] A. E. Nelson, K. D. Allen, Y. M. Golightly, A. P. Goode, and J. M. Jordan, "A systematic review of recommendations and guidelines for the management of osteoarthritis: the chronic osteoarthritis management initiative of the U.S. bone and joint initiative," *Seminars in Arthritis and Rheumatism*, vol. 43, no. 6, pp. 701–712, 2014.
- [8] P. Jüni, R. Hari, A. W. S. Rutjes et al., "Intra-articular corticosteroid for knee osteoarthritis," *The Cochrane Database of Systematic Reviews*, vol. 10, Article ID CD005328, 2015.
- [9] M. C. Hochberg, J. Martel-Pelletier, J. Monfort et al., "Combined chondroitin sulfate and glucosamine for painful knee osteoarthritis: a multicentre, randomised, double-blind, non-inferiority trial versus celecoxib," *Annals of the Rheumatic Diseases*, vol. 75, no. 1, pp. 37–44, 2016.
- [10] S. Teekachunhatean, P. Kuanusorn, N. Rojanasthien et al., "Chinese herbal recipe versus diclofenac in symptomatic treatment of osteoarthritis of the knee: a randomized controlled trial ISRCTN70292892," *BMC Complementary and Alternative Medicine*, vol. 4, p. 19, 2004.
- [11] Y. Ma, J. Cui, M. Huang, K. Meng, and Y. Zhao, "Effects of Duhuo Jisheng Tang and combined therapies on prolapse of lumbar intervertebral disc: a systematic review of randomized control trials," *Journal of Traditional Chinese Medicine*, vol. 33, no. 2, pp. 145–155, 2013.
- [12] J. N. Lai, H. J. Chen, C. C. Chen, J. H. Lin, J. S. Hwang, and J. D. Wang, "Duhuo jisheng tang for treating osteoarthritis of the knee: a prospective clinical observation," *Chinese Medicine*, vol. 2, p. 4, 2007.
- [13] W. Zhang, S. Wang, R. Zhang et al., "Evidence of Chinese herbal medicine Duhuo Jisheng decoction for knee osteoarthritis: a systematic review of randomised clinical trials," *BMJ Open*, vol. 6, no. 1, Article ID e008973, 2016.
- [14] C. W. Chen, J. Sun, Y. M. Li, P. A. Shen, and Y. Q. Chen, "Action mechanisms of du-huo-ji-sheng-tang on cartilage degradation in a rabbit model of osteoarthritis," *Evidence-Based Complementary and Alternative Medicine*, vol. 2011, Article ID 571479, 2011.
- [15] G. Wu, H. Fan, Y. Huang, C. Zheng, J. Ye, and X. Liu, "Duhuo Jisheng Decoction-containing serum promotes proliferation of interleukin-1 β -induced chondrocytes through the p16-cyclin D1/CDK4-Rb pathway," *Molecular Medicine Reports*, vol. 10, no. 5, pp. 2525–2534, 2014.
- [16] W. Liu, S. Jin, M. Huang et al., "Duhuo jisheng decoction suppresses matrix degradation and apoptosis in human nucleus pulposus cells and ameliorates disc degeneration in a rat model," *Journal of Ethnopharmacology*, vol. 250, Article ID 112494, 2020.
- [17] A. L. Hopkins, "Network pharmacology," *Nature Biotechnology*, vol. 25, no. 10, pp. 1110–1111, 2007.
- [18] J. Ru, P. Li, J. Wang et al., "TCMSP: a database of systems pharmacology for drug discovery from herbal medicines," *Journal of Cheminformatics*, vol. 6, p. 13, 2014.
- [19] X. Xu, W. Zhang, C. Huang et al., "A novel chemometric method for the prediction of human oral bioavailability," *International Journal of Molecular Sciences*, vol. 13, no. 6, pp. 6964–6982, 2012.
- [20] W. P. Walters and M. A. Murcko, "Prediction of "drug-likeness"" *Advanced Drug Delivery Reviews*, vol. 54, no. 3, pp. 255–271, 2002.
- [21] H. Q. Pang, S. J. Yue, Y. P. Tang et al., "Integrated metabolomics and network pharmacology approach to explain possible action mechanisms of xin-sheng-hua granule for treating anemia," *Frontiers in Pharmacology*, vol. 9, p. 165, 2018.
- [22] F. Tang, Q. Tang, Y. Tian, Q. Fan, Y. Huang, and X. Tan, "Network pharmacology-based prediction of the active ingredients and potential targets of Mahuang Fuzi Xixin decoction for application to allergic rhinitis," *Journal of Ethnopharmacology*, vol. 176, pp. 402–412, 2015.
- [23] H. Li, X. Li, G. Liu et al., "Bauhinia championi (Benth.) Benth. polysaccharides upregulate Wnt/ β -catenin signaling in chondrocytes," *International Journal of Molecular Medicine*, vol. 32, no. 6, pp. 1329–1336, 2013.
- [24] L. A. Deveza and R. F. Loeser, "Is osteoarthritis one disease or a collection of many?" *Rheumatology (Oxford, England)*, vol. 57pp. iv34–iv42, 4, 2017.
- [25] C. R. Scanzello, "Role of low-grade inflammation in osteoarthritis," *Current Opinion in Rheumatology*, vol. 29, no. 1, pp. 79–85, 2018.
- [26] S. M. Bierma-Zeinstra and M. van Middelkoop, "Osteoarthritis: in search of phenotypes," *Nature Reviews Rheumatology*, vol. 13, no. 12, pp. 705–706, 2017.
- [27] A. Courties, J. Sellam, and F. Berenbaum, "Metabolic syndrome-associated osteoarthritis," *Current Opinion in Rheumatology*, vol. 29, no. 2, pp. 214–222, 2017.
- [28] O. H. Jeon, C. Kim, R.-M. Laberge et al., "Local clearance of senescent cells attenuates the development of post-traumatic osteoarthritis and creates a pro-regenerative environment," *Nature Medicine*, vol. 23, no. 6, pp. 775–781, 2017.
- [29] M. Cameron and S. Chrubasik, "Topical herbal therapies for treating osteoarthritis," *The Cochrane Database of Systematic Reviews*, vol. 5, Article ID CD010538, 2013.

- [30] M. Cameron and S. Chrubasik, "Oral herbal therapies for treating osteoarthritis," *The Cochrane Database of Systematic Reviews*, vol. 5, Article ID CD002947, 2014.
- [31] S. Lyu, B. Ji, W. Gao, X. Chen, X. Xie, and J. Zhou, "Effects of *Angelicae Pubescentis* and *Loranthi* Decotion on repairing knee joint cartilages in rats," *Journal of Orthopaedic Surgery and Research*, vol. 12, no. 1, p. 189, 2017.
- [32] C. Tu, Y. Ma, M. Song, J. Yan, Y. Xiao, and H. Wu, "Liquiritigenin inhibits IL-1 β -induced inflammation and cartilage matrix degradation in rat chondrocytes," *European Journal of Pharmacology*, vol. 858, Article ID 172445, 2019.
- [33] X. Weng, P. Lin, F. Liu et al., "Achyranthes bidentata polysaccharides activate the Wnt/ β -catenin signaling pathway to promote chondrocyte proliferation," *International Journal of Molecular Medicine*, vol. 34, no. 4, pp. 1045–1050, 2014.
- [34] G. P. Xie, N. Jiang, S. N. Wang et al., "Eucommia ulmoides Oliv. bark aqueous extract inhibits osteoarthritis in a rat model of osteoarthritis," *Journal of Ethnopharmacology*, vol. 162, pp. 148–154, 2015.
- [35] J. M. Chun, H. S. Kim, A. Y. Lee, S. H. Kim, and H. K. Kim, "Anti-inflammatory and antiosteoarthritis effects of *saposhnikovia divaricata* ethanol extract: in vitro and in vivo studies," *Evidence-Based Complementary and Alternative Medicine*, vol. 2016, p. 1984238, 2016.
- [36] G. Zheng, Y. Zhan, Q. Tang et al., "Monascin inhibits IL-1 β induced catabolism in mouse chondrocytes and ameliorates murine osteoarthritis," *Food & Function*, vol. 9, no. 3, pp. 1454–1464, 2018.
- [37] J. Chen, Y. T. Gu, J. J. Xie et al., "Gastrodin reduces IL-1 β -induced apoptosis, inflammation, and matrix catabolism in osteoarthritis chondrocytes and attenuates rat cartilage degeneration in vivo," *Biomedicine & Pharmacotherapy*, vol. 97, pp. 642–651, 2018.
- [38] C. Lu, Y. Li, S. Hu, Y. Cai, Z. Yang, and K. Peng, "Scoparone prevents IL-1 β -induced inflammatory response in human osteoarthritis chondrocytes through the PI3K/Akt/NF- κ B pathway," *Biomedicine & Pharmacotherapy*, vol. 106, pp. 1169–1174, 2018.
- [39] W. Zheng, Z. Tao, C. Chen et al., "Plumbagin prevents IL-1 β -induced inflammatory response in human osteoarthritis chondrocytes and prevents the progression of osteoarthritis in mice," *Inflammation*, vol. 40, no. 3, pp. 849–860, 2017.
- [40] S. Rigoglou and A. G. Papavassiliou, "The NF- κ B signalling pathway in osteoarthritis," *The International Journal of Biochemistry & Cell Biology*, vol. 45, no. 11, pp. 2580–2584, 2013.
- [41] F. Zhou, J. Mei, X. Han et al., "Kinsenoside attenuates osteoarthritis by repolarizing macrophages through inactivating NF-B/MAPK signaling and protecting chondrocytes," *Acta Pharmaceutica Sinica B*, vol. 9, no. 5, pp. 973–985, 2019.

Research Article

Integrating Network Pharmacology with Molecular Docking to Unravel the Active Compounds and Potential Mechanism of Simiao Pill Treating Rheumatoid Arthritis

Mengshi Tang ¹, Xi Xie ¹, Pengji Yi ², Jin Kang ¹, Jiafen Liao ¹, Wenqun Li ^{3,4}, and Fen Li ¹

¹Department of Rheumatology and Immunology, The Second Xiangya Hospital, Central South University, Changsha, Hunan 410011, China

²Department of Integrated Traditional Chinese & Western Medicine, The Second Xiangya Hospital, Central South University, Changsha, Hunan 410011, China

³Department of Pharmacy, The Second Xiangya Hospital, Central South University, Changsha, Hunan 410011, China

⁴Institute of Clinical Pharmacy, Central South University, Changsha, Hunan 410011, China

Correspondence should be addressed to Wenqun Li; liwq1204@csu.edu.cn and Fen Li; lifen0731@csu.edu.cn

Received 4 June 2020; Revised 5 September 2020; Accepted 20 October 2020; Published 4 November 2020

Academic Editor: Arham Shabbir

Copyright © 2020 Mengshi Tang et al. This is an open access article distributed under the Creative Commons Attribution License, which permits unrestricted use, distribution, and reproduction in any medium, provided the original work is properly cited.

Objective. To explore the main components and unravel the potential mechanism of simiao pill (SM) on rheumatoid arthritis (RA) based on network pharmacological analysis and molecular docking. **Methods.** Related compounds were obtained from TCMSP and BATMAN-TCM database. Oral bioavailability and drug-likeness were then screened by using absorption, distribution, metabolism, and excretion (ADME) criteria. Additionally, target genes related to RA were acquired from GeneCards and OMIM database. Correlations about SM-RA, compounds-targets, and pathways-targets-compounds were visualized through Cytoscape 3.7.1. The protein-protein interaction (PPI) network was constructed by STRING. Gene Ontology (GO) analysis and Kyoto Encyclopedia of Genes and Genomes (KEGG) pathway enrichment analysis were performed via R packages. Molecular docking analysis was constructed by the Molecular Operating Environment (MOE). **Results.** A total of 72 potential compounds and 77 associated targets of SM were identified. The compounds-targets network analysis indicated that the 6 compounds, including quercetin, kaempferol, baicalein, wogonin, beta-sitosterol, and eugenol, were linked to ≥ 10 target genes, and the 10 target genes (PTGS1, ESR1, AR, PGR, CHRM3, PPARG, CHRM2, BCL2, CASP3, and RELA) were core target genes in the network. Enrichment analysis indicated that PI3K-Akt, TNF, and IL-17 signaling pathway may be a critical signaling pathway in the network pharmacology. Molecular docking showed that quercetin, kaempferol, baicalein, and wogonin have good binding activity with IL6, VEGFA, EGFR, and NFKBIA targets. **Conclusion.** The integrative investigation based on bioinformatics/network topology strategy may elaborate on the multicomponent synergy mechanisms of SM against RA and provide the way out to develop new combination medicines for RA.

1. Introduction

Rheumatoid arthritis (RA) is a chronic polyarticular symmetric disease. It is characterized by chronic inflammation of the synovial membrane, which can destroy articular cartilage and juxta-articular bone [1]. RA affects 0.3%–1% of the population worldwide [2]. If insufficiently treated, it usually leads to persistent joint inflammation, progressive joint destruction, continuing functional decline, extra-articular

manifestations, disability, and increased mortality [3, 4]. Although current available therapeutic approaches against RA, including nonsteroidal anti-inflammatory drugs (NSAIDs), disease-modifying antirheumatic drugs (DMARDs), and corticosteroid, allow for excellent disease control, novel therapies are needed because RA remains incurable [5]. Furthermore, the long-term use of these drugs may cause multiple side effects and lead to limited therapeutic responses. Therefore, novel treatments are in urgent demand.

Traditional Chinese medicine (TCM) has been extensively applied for the treatment of RA for centuries in Asia and has been gradually accepted for worldwide clinical applications [6, 7]. Numerous studies have indicated that TCM can be served as complementary and alternative RA drugs for therapeutic effects and with fewer side effects [8, 9].

Simiao pill (SM), a traditional TCM formula, comprises four herbs, including Phellodendri Chinensis Cortex (Huang Bo), *Atractylodes lancea* (Thunb.) Dc. (Cang Zhu), *Achyranthis bidentatae radix* (Niu Xi), and Coicis Semen (Yi Yi Ren). Previous studies have indicated the anti-inflammation pharmacological effect of SM [10] and that SM reduced proinflammatory cytokine production by suppressing nuclear factor kappaB (NF- κ B)/pyrin domain containing 3 (NLRP3) inflammasome activation [11]. Recently, SM was demonstrated to exhibit anti-inflammatory and bone-protective effects by regulating autotaxin (ATX)-lysophosphatidic acid (LPA) and mitogen-activated protein kinase (MAPK) signaling pathways in collagen-induced arthritis (CIA) rats [12]. In addition, SM was recommended for the treatment of active RA (53.6%) in the expert consensus regarding the treatment of RA with various Chinese patent medicines (CPMs) [13]. However, because TCM formulas are characterized by multicomponents, multitargets, and multipathways [14], the therapeutic effect of SM against RA has not been fully elucidated. Therefore, it is necessary for further systematic investigation.

Nowadays, network pharmacology integrates network biology and polypharmacology based on existing databases, providing a novel approach for exploring the mechanisms and synergistic effect of TCM formulas as disease treatments [14–16]. Combining network science with ancient TCM formulas to investigate multiple molecular mechanisms has achieved successful attempts in the previous researches [17–20].

Therefore, in this study, a network pharmacology-based study was conducted to predict bioactive compounds and elucidate the comprehensive pharmacological mechanisms about the antirheumatic effect of SM. In addition, molecular docking analysis was performed to validate *in silico* to predict molecular interactions between compounds and targets.

2. Materials and Methods

Network pharmacology-based prediction of SM treating RA was constructed by the following (Figure 1): (1) data collection and preparation, including retrieving the ingredients list of SM formula, screening for candidate compounds, identifying SM and RA targets, and intersecting the identified targets of compounds and disease; (2) topological analysis of network and protein-protein interaction (PPI) network construction; (3) enrichment analysis; and (4) molecular docking analysis.

2.1. Data Collection and Preparation

2.1.1. Composite Compounds of SM. The related composite compounds of SM were obtained from the Traditional

Chinese Medicine Systems Pharmacology Database (TCMSP, <http://lsp.nwu.edu.cn/tcmsp.php>) and a Bioinformatics Analysis Tool for Molecular mechANism of Traditional Chinese Medicine (BATMAN-TCM, <http://bionet.ncpsb.org/batman-tcm/>).

2.1.2. Pharmacokinetic ADME Evaluation. The *in silico* integrative ADME (absorption, distribution, metabolism, and excretion) model administrated by TCMSP is employed for pharmaceutical research. As an oral drug, two related-ADME models, oral bioavailability (OB), and drug-likeness (DL) are applied to identify the potential bioactive compounds in this study. Only the compounds with $OB \geq 30$ and $DL \geq 0.18$ that satisfied the criteria suggested by the TCMSP database (removed the duplicated) are retained as the candidate compounds for further study [21]. In addition, among the compounds with $OB < 30$ or $DL < 0.18$, which are searched with “compound (name)” and “rheumatoid arthritis” [all fields] in PubMed databases to find relevant researches, the compounds in purified form focused on anti-RA mechanisms are also considered to be bioactive compounds (removed the duplicated) and included for further study.

2.1.3. Predictions of Target Genes Related to the Identified Compounds. All the potential compounds were input into TCMSP to capture the relationships between drugs and targets. Since the obtained targets include various biological species, all target names were also put into UniProt databases (<http://www.uniprot.org/>) to search for target gene names selected by human species.

2.1.4. Potential Disease Target Genes. Information of known RA-related therapeutic target genes was collected by keywords “rheumatoid arthritis” as queries from The Human Gene Databases (GeneCards, <https://www.genecards.org/>, ver.4.9.0) and Online Mendelian Inheritance in Man (OMIM, <http://www.omim.org/>, updated June 6, 2019), and only “*Homo sapiens*” target genes linked to RA are selected.

2.1.5. Venn Analysis. All target genes of identified compounds and RA are put into Bioinformatics and Evolutionary Genomics system (bioinformatics.psb.ugent.be/webtools/Venn/), respectively, to produce a Venn diagram, which indicates the intersection of identified targets of drug and disease.

2.2. Topological Analysis of Network and PPI Network Construction

2.2.1. Topological Network Analysis. SM-RA mechanism network, compounds-targets network, and pathways-targets-compounds network were visualized through Cytoscape (<https://cytoscape.org/>, ver. 3.7.1) to systemically explore the molecular mechanisms of SM treating RA.

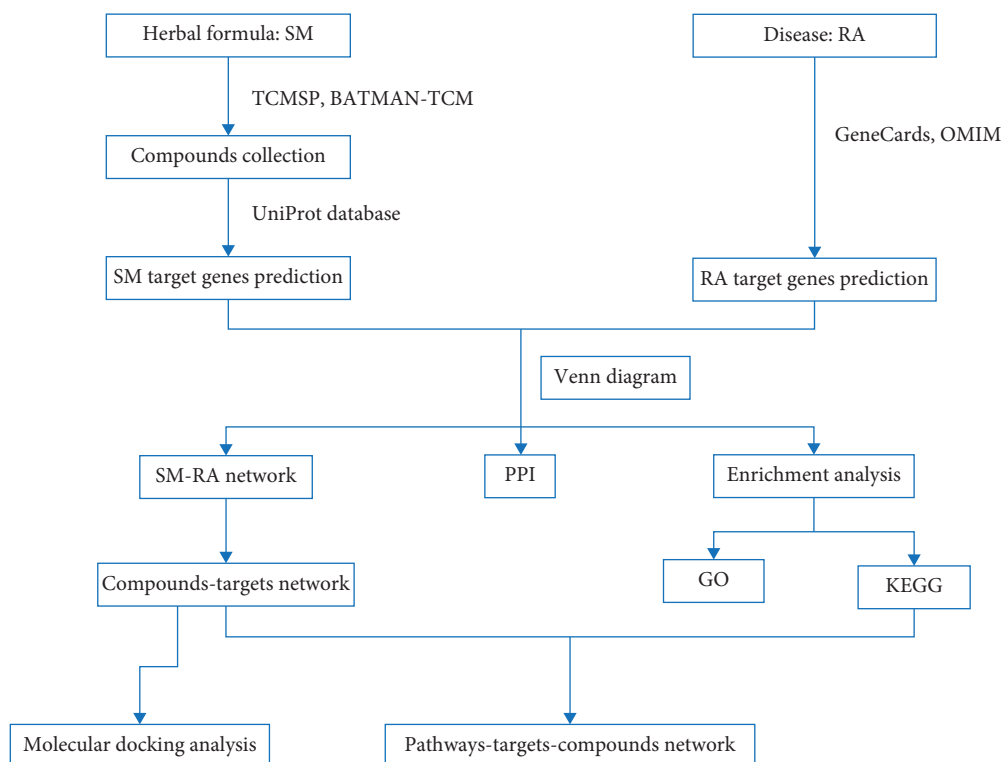


FIGURE 1: Workflow of network pharmacology analysis.

2.2.2. PPI Network Construction. The above 77 target genes acquired from the Venn diagram intersection were imported into STRING (<https://string-db.org/>, version 11.0) to construct a PPI network for understanding protein interaction systematically. The PPI network is constructed by setting the organism as “human sapiens”, setting the minimum required interaction score to “medium confidence (0.40)”, and excluding the disconnected protein nodes. In addition, statistics of protein interactions are figured out according to the PPI network, and a related bar plot diagram is constructed with R 3.6.0 subsequently.

2.3. Enrichment Analysis. R 3.6.0 and related R packages (colorspace, stringi, DOSE, clusterProfiler, and pathview) are applied to carry out Gene Ontology (GO) enrichment analysis and Kyoto Encyclopedia of Genes and Genomes (KEGG) pathway enrichment analysis of intersection target genes of SM-RA. P values < 0.05 and q values < 0.05 are considered statistically significant based on Fisher’s test.

2.4. Molecular Docking Analysis. The 3D structures of candidate targets were obtained from the PDB database (<http://www.rcsb.org/>) in PDB format by setting the organism to “Homo sapiens only”. The 3D conformers of candidate compounds are acquired from the PubChem database (<https://pubchem.ncbi.nlm.nih.gov/>) with SDF format. Subsequently, they were imported to the Molecular Operating Environment (MOE) to get the docking score. The greater the absolute value of the docking score, the better.

3. Results

3.1. Data Collection and Preparation

3.1.1. Identification of Compounds in SM. A total of 479 compounds were identified in SM, including 140 in *Phellodendri Chinensis Cortex* (Huang Bo), 49 in *Atractylodes lancea* (Thunb.) Dc. (Cang Zhu), 176 in *Achyranthis bidentatae radix* (Niu Xi), and 38 in *Coicis Semen* (Yi Yi Ren), and in TCMSP, also including 37 in *Phellodendri Chinensis Cortex* (Huang Bo), 26 in *Atractylodes lancea* (Thunb.) Dc. (Cang Zhu), 10 in *Achyranthis bidentatae radix* (Niu Xi), and 3 in *Coicis Semen* (Yi Yi Ren) in BATMAN-TCM.

3.1.2. Selection of Compounds Using ADME Screening and Related Targets. All the identified compounds were selected through ADME screening, with 90 of 479 compounds satisfying the suggested criteria $OB \geq 30$ and $DL \geq 0.18$ [18–20]. Of the 90 compounds, 25 were duplicated and removed, and the remaining 65 compounds were included for further study. Moreover, of the excluded compounds that do not meet the suggested criteria, 7 compounds, including ferulic acid, beta-elemene, eugenol, and paeonol in *Phellodendri Chinensis Cortex* (Huang Bo) and geniposide, rutin, and astragaloside in *Achyranthis bidentatae radix* (Niu Xi), are considered bioactive compounds and included for further analysis, and the effects of ferulic acid [22], beta-elemene [23], eugenol [24–26], paeonol [27–29], geniposide [30–32], rutin [33, 34], and astragaloside [35] on RA have been investigated. The final 72 compounds are selected from the four

herbal medicines (Table 1). A total of 386 target genes related to the final identified compounds are obtained from the UniProt databases.

3.1.3. Identified Disease Target Genes. The target genes related to RA were searched in GeneCards and OMIM databases, which include 3768 genes in GeneCards and 1 gene in OMIM, with no overlapping target gene.

3.1.4. Intersection of Identified Targets of Compounds and Disease. In the Venn diagram intersection of identified targets about identified compounds and of RA (Figure 2), a total of 77 target genes are acquired.

3.2. Topological and PPI Network

3.2.1. Topological Network Analysis. The SM-RA mechanism network (Figure 3) consists of 77 target genes nodes (shared gene of SM and RA), 41 compound nodes, and 349 edges. Among the 14 compounds (Dehydrotanshinone II A, Stigmasterol, beta-sitosterol, Isocorypalmine, beta-elemene, quercetin, eugenol, paeonol, (S)-Canadine, wogonin, baicalein, Inophyllum *E*, rutin, and kaempferol) that connected to more than four genes, 55 target genes are associated with quercetin, 22 target genes are associated with kaempferol, 15 target genes are associated with baicalein, 14 target genes are associated with wogonin, and 10 target genes are associated with beta-sitosterol and eugenol, respectively (Table 2). In addition, 10 genes, including PTGS1, ESR1, AR, PGR, CHRM3, PPARG, CHRM2, BCL2, CASP3, and RELA, are related to more than five compounds, as shown in the compounds-targets network (Figure 4). These compounds and genes may be the key nodes in the network.

3.2.2. PPI Network. The PPI network is established by setting the confidence level of more than 0.40 and hiding the independent target protein nodes. The PPI network nodes represent proteins and edges represent protein-protein interactions. The network has 75 nodes and 1604 edges (Figure 5). In addition, we analyzed the importance prioritization (adjacent nodes count of each protein) of proteins according to the network, and the leading 30 genes with higher connection were visualized by constructing a bar plot diagram (Figure 6), which indicates the 30 genes or proteins that may play a bridge role in connecting other nodes in the PPI network. These 30 genes or proteins include inflammation-associated genes (IL6 [36], NFKBIA [37]), cell proliferation-, differentiation-, and transformation-related genes (FOS [38], EGFR [39], MAPK8 [40], NR3C1 [41], RHOA [42], and PARP1 [43]), cell apoptosis-related genes (CASP3, CASP8 [44], CASP9 [45], MYC [46], CYCS [47], HIF1A [48], MCL1 [49], and GSK3B [50]), cell cycle-related gene (CCND1 [51]), hormone-related genes (INS [52], ESR1 [53], AR [54], and PGR [55]), angiogenesis-related gene (VEGFA [56]), and transcription factor (RELA [57]).

3.3. Enrichment Analysis

3.3.1. GO Enrichment Analysis. GO analysis consisted of biological process (BP), cellular component (CC), and molecular function (MF). As showed in Figure 7, the top 20 enrichment terms are visualized by the bar plot diagram. The results demonstrated that numerous targets are involved in various BPs associated with immune response and inflammation, such as the response to a steroid hormone, response to oxidative stress, and regulation of the apoptotic signaling pathway, which confirmed strongly the correlation with the pathogenesis in RA. The CC results showed that most of the targets are localized to the cellular membrane and nuclear chromatin part. The MF results indicated that many targets are associated with nuclear receptor activity and transcription factor activity.

3.3.2. KEGG Enrichment Analysis. The KEGG pathways are applied to examine the function and signaling pathways of the identified target genes, with the top 20 of the potential pathways ($P < 0.05$ and $q < 0.05$) shown by a bar plot diagram (Figure 8) and visualized with the pathways-targets-compounds network (Figure 9). The results showed that numerous targets are associated with certain virus infections (such as Epstein-Barr virus infection) and cancer, which are associated with the onset and prognosis of RA.

3.4. Molecular Docking Analysis. The selected targets, including IL6, VEGFA, EGFR, and NFKBIA, play a significant role in the SM-RA network. The candidate compounds, including quercetin, kaempferol, baicalein, and wogonin, are the top 4 compounds (ranking by related target genes count) in the SM-RA network. These 4 target genes and 4 compounds are imported into MOE for molecular docking verification. The docking scores are shown in Table 3. The action mode of NFKBIA and quercetin, kaempferol, baicalein, and wogonin and the action mode of wogonin and IL6, VEGFA, EGFR, and NFKBIA are shown in Figure 10.

4. Discussion

In the present network pharmacological analysis, a total of 479 compounds were identified in the four herbal medicines of SM, and 72 compounds were yielded by ADME criteria screening. A total of 386 targets related to potential compounds and 3769 targets associated with RA were identified, and 77 target genes were obtained from the interaction of targets about SM identified compounds and RA. SM-RA network analysis visualized the interaction of multicomponents and multitargets about SM on RA. The compounds-targets network analysis indicated that the 6 compounds, including quercetin, kaempferol, baicalein, wogonin, beta-sitosterol, and eugenol, were linked to ≥ 10 target genes, and the 10 target genes (PTGS1, ESR1, AR, PGR, CHRM3, PPARG, CHRM2, BCL2, CASP3, and RELA) were core target genes in the network. GO enrichment analysis indicated that numerous targets are involved in response to a steroid hormone, oxidative stress, and regulation of the

TABLE 1: 72 active compounds of SM.

| Mol id | Molecule name | OB (%) | DL | Herb |
|-----------|--|--------|------|---|
| MOL002636 | Kihadalactone A | 34.21 | 0.82 | Phellodendri Chinensis Cortex |
| MOL013352 | Obacunone | 43.29 | 0.77 | Phellodendri Chinensis Cortex |
| MOL002641 | Phellavin_qt | 35.86 | 0.44 | Phellodendri Chinensis Cortex |
| MOL002644 | Phellopterin | 40.19 | 0.28 | Phellodendri Chinensis Cortex |
| MOL002651 | Dehydrotanshinone II A | 43.76 | 0.40 | Phellodendri Chinensis Cortex |
| MOL002652 | delta7-dehydrosophoramine | 54.45 | 0.25 | Phellodendri Chinensis Cortex |
| MOL002656 | Dihydroniloticin | 36.43 | 0.81 | Phellodendri Chinensis Cortex |
| MOL002659 | Kihadanin A | 31.60 | 0.70 | Phellodendri Chinensis Cortex |
| MOL002660 | Niloticin | 41.41 | 0.82 | Phellodendri Chinensis Cortex |
| MOL002662 | Rutaecarpine | 40.30 | 0.60 | Phellodendri Chinensis Cortex |
| MOL002663 | Skimmianin | 40.14 | 0.20 | Phellodendri Chinensis Cortex |
| MOL002666 | Chelerythrine | 34.18 | 0.78 | Phellodendri Chinensis Cortex |
| MOL002668 | Worenine | 45.83 | 0.87 | Phellodendri Chinensis Cortex |
| MOL002670 | Cavidine | 35.64 | 0.81 | Phellodendri Chinensis Cortex |
| MOL002671 | Candletoxin A | 31.81 | 0.69 | Phellodendri Chinensis Cortex |
| MOL002672 | Hericenone H | 39.00 | 0.63 | Phellodendri Chinensis Cortex |
| MOL002673 | Hispidone | 36.18 | 0.83 | Phellodendri Chinensis Cortex |
| MOL000358 | Beta-sitosterol | 36.91 | 0.75 | Phellodendri Chinensis Cortex |
| MOL000622 | Magnograndiolide | 63.71 | 0.19 | Phellodendri Chinensis Cortex |
| MOL000762 | Palmidin A | 35.36 | 0.65 | Phellodendri Chinensis Cortex |
| MOL000787 | Fumarine | 59.26 | 0.83 | Phellodendri Chinensis Cortex |
| MOL000790 | Isocorypalmine | 35.77 | 0.59 | Phellodendri Chinensis Cortex |
| MOL001131 | phellamurin_qt | 56.60 | 0.39 | Phellodendri Chinensis Cortex |
| MOL001455 | (S)-canadine | 53.83 | 0.77 | Phellodendri Chinensis Cortex |
| MOL001771 | Poriferast-5-en-3beta-ol | 36.91 | 0.75 | Phellodendri Chinensis Cortex |
| MOL002894 | Berberrubine | 35.74 | 0.73 | Phellodendri Chinensis Cortex |
| MOL005438 | Campesterol | 37.58 | 0.71 | Phellodendri Chinensis Cortex |
| MOL006392 | Dihydroniloticin | 36.43 | 0.82 | Phellodendri Chinensis Cortex |
| MOL006401 | Melianone | 40.53 | 0.78 | Phellodendri Chinensis Cortex |
| MOL006413 | Phellochin | 35.41 | 0.82 | Phellodendri Chinensis Cortex |
| MOL006422 | Thalifendine | 44.41 | 0.73 | Phellodendri Chinensis Cortex |
| MOL002665 | Ferulic acid | 40.43 | 0.06 | Phellodendri Chinensis Cortex |
| MOL000908 | Beta-elemene | 25.63 | 0.06 | Phellodendri Chinensis Cortex |
| MOL000254 | Eugenol | 56.24 | 0.04 | Phellodendri Chinensis Cortex |
| MOL000874 | Paeonol | 28.79 | 0.04 | Phellodendri Chinensis Cortex |
| MOL000179 | 2-Hydroxyisoxypypropyl-3-hydroxy-7-isopentene-2,3-dihydrobenzofuran-5-carboxylic | 45.20 | 0.20 | <i>Atractylodes lancea</i> (Thunb.) Dc. |
| MOL000184 | NSC63551 | 39.25 | 0.76 | <i>Atractylodes lancea</i> (Thunb.) Dc. |
| MOL000186 | Stigmasterol 3-O-beta-D-glucopyranoside_qt | 43.83 | 0.76 | <i>Atractylodes lancea</i> (Thunb.) Dc. |
| MOL000188 | 3β-acetoxyatractylone | 40.57 | 0.22 | <i>Atractylodes lancea</i> (Thunb.) Dc. |
| MOL000088 | Beta-sitosterol 3-O-glucoside_qt | 36.91 | 0.75 | <i>Atractylodes lancea</i> (Thunb.) Dc. |
| MOL000092 | daucosterin_qt | 36.91 | 0.76 | <i>Atractylodes lancea</i> (Thunb.) Dc. |
| MOL000094 | daucosterol_qt | 36.91 | 0.76 | <i>Atractylodes lancea</i> (Thunb.) Dc. |
| MOL001006 | Poriferasta-7,22E-dien-3beta-ol | 42.98 | 0.76 | <i>Achyranthis bidentatae radix</i> |
| MOL012461 | 28-Norolean-17-en-3-ol | 35.93 | 0.78 | <i>Achyranthis bidentatae radix</i> |
| MOL012505 | bidentatoside, ii_qt | 31.76 | 0.59 | <i>Achyranthis bidentatae radix</i> |
| MOL012537 | Spinoside A | 41.75 | 0.40 | <i>Achyranthis bidentatae radix</i> |
| MOL012542 | β-ecdysterone | 44.23 | 0.82 | <i>Achyranthis bidentatae radix</i> |
| MOL002714 | Baicalein | 33.52 | 0.21 | <i>Achyranthis bidentatae radix</i> |
| MOL002776 | Baicalin | 40.12 | 0.75 | <i>Achyranthis bidentatae radix</i> |
| MOL002897 | Epiberberine | 43.09 | 0.78 | <i>Achyranthis bidentatae radix</i> |
| MOL003847 | Inophyllum E | 38.81 | 0.85 | <i>Achyranthis bidentatae radix</i> |
| MOL000422 | Kaempferol | 41.88 | 0.24 | <i>Achyranthis bidentatae radix</i> |
| MOL004355 | Spinasterol | 42.98 | 0.76 | <i>Achyranthis bidentatae radix</i> |
| MOL012516 | Geniposide | 8.40 | 0.44 | <i>Achyranthis bidentatae radix</i> |
| MOL000415 | Rutin | 3.20 | 0.68 | <i>Achyranthis bidentatae radix</i> |
| MOL000561 | Astragaln | 14.03 | 0.74 | <i>Achyranthis bidentatae radix</i> |
| MOL001323 | Sitosterol alpha1 | 43.28 | 0.78 | Coicis Semen |
| MOL001494 | Mandenol | 42.00 | 0.19 | Coicis Semen |

TABLE 1: Continued.

| Mol id | Molecule name | OB (%) | DL | Herb |
|-----------|--|--------|------|---|
| MOL002372 | (6 <i>Z</i> , 10 <i>E</i> , 14 <i>E</i> , 18 <i>E</i>)-2,6,10,15,19,23-hexamethyltetracos-2,6,10,14,18,22-hexaene | 33.55 | 0.42 | Coicis Semen |
| MOL002882 | [(2 <i>R</i>)-2,3-dihydroxypropyl] (Z)-octadec-9-enoate | 34.13 | 0.30 | Coicis Semen |
| MOL000359 | Sitosterol | 36.91 | 0.75 | Coicis Semen |
| MOL008118 | Coixenolide | 32.40 | 0.43 | Coicis Semen |
| MOL008121 | 2-Monoolein | 34.23 | 0.29 | Coicis Semen |
| MOL000953 | CLR | 37.87 | 0.68 | Coicis Semen |
| MOL001454 | Berberine | 36.86 | 0.78 | Phellodendri Chinensis Cortex, achyranthis bidentatae radix |
| MOL001458 | Coptisine | 30.67 | 0.86 | Phellodendri Chinensis Cortex, achyranthis bidentatae radix |
| MOL002643 | Delta 7-stigmastenol | 37.42 | 0.75 | Phellodendri Chinensis Cortex, achyranthis bidentatae radix |
| MOL000785 | Palmitine | 64.60 | 0.65 | Phellodendri Chinensis Cortex, achyranthis bidentatae radix |
| MOL000098 | Quercetin | 46.43 | 0.28 | Phellodendri Chinensis Cortex, achyranthis bidentatae radix |
| MOL000173 | Wogonin | 30.68 | 0.23 | <i>Atractylodes lancea</i> (Thunb.) Dc. Achyranthis bidentatae radix |
| MOL000085 | Beta-daucosterol_qt | 36.91 | 0.75 | <i>Atractylodes lancea</i> (Thunb.) Dc. Achyranthis bidentatae radix |
| MOL000449 | Stigmasterol | 43.83 | 0.76 | Phellodendri Chinensis Cortex, achyranthis bidentatae radix, Coicis Semen |

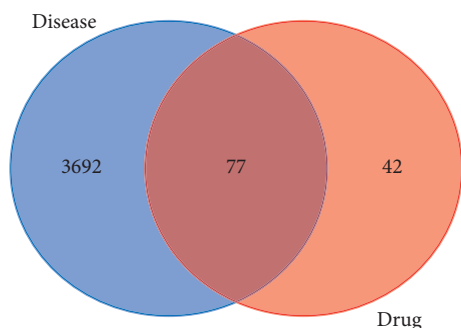


FIGURE 2: A Venn diagram showing intersection identified targets of identified compounds and RA.

apoptotic signaling pathway in BP, are localized to the cellular membrane and nuclear chromatin part in CC, and are associated with nuclear receptor activity and transcription factor activity in MF. KEGG pathways analysis results indicated that numerous targets are associated with certain virus infections and cancer. Molecular docking showed that quercetin, kaempferol, baicalein, and wogonin have good binding activity with IL6, VEGFA, EGFR, and NFKBIA targets.

About 72 identified compounds, particularly the 6 compounds, including quercetin, kaempferol, baicalein, wogonin, beta-sitosterol, and eugenol, were linked to more than 10 targets, indicating that these compounds might play a vital role in the process of RA treatment. Furthermore, certain compounds have exhibited the potential antirheumatic therapeutic activities except for wogonin (Table 4). For instance, quercetin has been reported to decrease levels of tumor necrosis factor- α (TNF- α), interleukin-1 β (IL-1 β), interleukin-17 (IL-17), and monocyte chemotactic protein-1

(MCP-1) [58] and significantly reduced damage to interchondral joints, infiltration of inflammatory cells, and pannus formation [59]. Besides, kaempferol suppresses the proliferation and migration of RAFLS and the release of activated T-cell-mediated inflammatory cytokines and reduces osteoclast differentiation through targeting on the fibroblast growth factor receptor 3- (FGFR3-) ribosomal S6 kinase 2 (RSK2) signaling axis [60]. In addition, baicalein inhibits human rheumatoid arthritis fibroblast-like synoviocytes (RAFLS) proliferation involving suppression of nuclear factor kappa B (NF- κ B) transcriptional activity and recombinant macrophage migration inhibitory factor-(MIF-) mediated signaling [61]. What's more, β -Sitosterol could modulate the functions of macrophages and attenuates rheumatoid inflammation in CIA mice [62]. For eugenol, it is reported to be effective in ameliorating oxidative stress and inflammation in arthritic rats [25, 26]. Moreover, among the other 66 compounds, some articles previously reported the antirheumatic effect. For example, ferulic acid is reported to suppress osteoclast differentiation and bone erosion via the inhibition of receptor activator of nuclear factor κ B ligand- (RANKL-) dependent NF- κ B signaling pathway [63], and berberine could attenuate adjuvant-induced arthritic fibroblast-like synoviocytes (AA-FLS) proliferation and regulate the Th17/Treg imbalance [64]. Collectively, these active components exhibit antirheumatic effects from various aspects, including anti-inflammatory, immunoregulatory, reducing bone erosion and destruction, and attenuating oxidative stress. Therefore, these might indicate the collective effectiveness and diversity of constituents in SM for treating RA.

Among the main target genes (top 30) in the PPI network is INS, ranking first with the highest connection, which may affect the local inflammatory process of joint in RA [52],

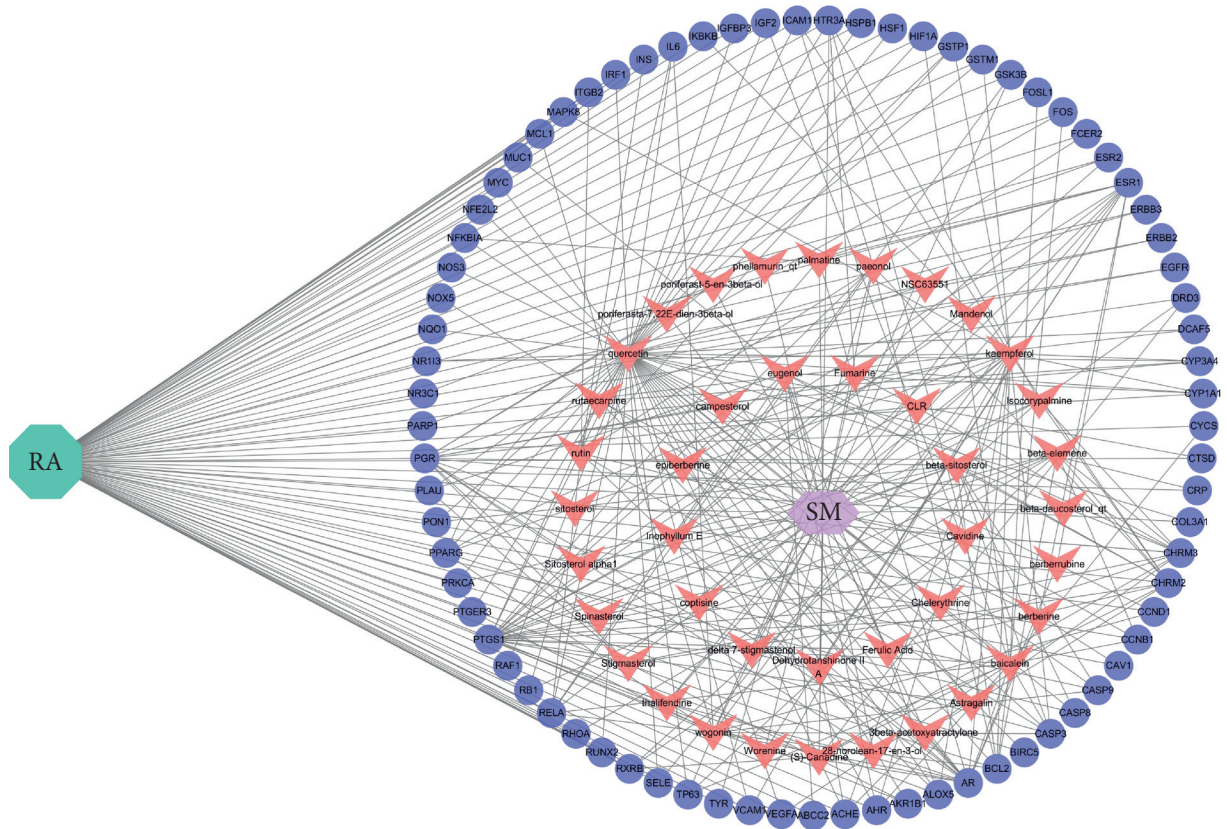


FIGURE 3: The SM-RA mechanism network. The green octagon represents rheumatoid arthritis (RA), the purple hexagon represents the herbal medicine simiao pill (SM), while pink V's represent compounds, and blue-purple ellipses represent genes.

TABLE 2: Target genes interacting with compounds in the SM-RA network.

| Compounds | Target genes |
|---------------------------------|---------------------------|
| Delta 7-stigmastenol | PGR |
| Poriferast-5-en-3beta-ol | PGR |
| Campesterol | PGR |
| NSC63551 | PGR |
| Beta-daucosterol_qt | PGR |
| Poriferasta-7,22E-dien-3beta-ol | PGR |
| 28-Norolean-17-en-3-ol | PGR |
| Spinasterol | PGR |
| Sitosterol alpha1 | PGR |
| Sitosterol | PGR |
| CLR | PGR |
| Chelerythrine | PTGS1 |
| Astragalin | PTGS1 |
| Mandenol | PTGS1 |
| Ferulic acid | PTGS1, CHRM2 |
| phellamurin_qt | ESR1, NR3C1 |
| Epiberberine | ESR1, AR |
| Berberine | PTGS1, ESR1, AR |
| Coptisine | PTGS1, ESR1, AR |
| Worenine | PTGS1, ESR1, AR |
| Berberrubine | PTGS1, ESR1, AR |
| Thalifendine | PTGS1, ESR1, AR |
| Fumarine | PTGS1, CHRM3, HTR3A |
| Rutaecarpine | PTGS1, AR, HTR3A, CYP3A4 |
| Cavidine | PTGS1, CHRM3, HTR3A, RXRB |

TABLE 2: Continued.

| Compounds | Target genes |
|------------------------|--|
| Palmatine | PTGS1, ESR1, AR, ESR2 |
| 3β-acetoxyatractylone | CHRM3, AR, ACHE, CHRM2 |
| Dehydrotanshinone II A | CHRM3, ESR1, AR, PPARG, ACHE |
| Inophyllum E | PTGS1, ESR1, AR, ESR2, GSK3B |
| Stigmasterol | PGR, PTGS1, AKR1B1, PLAU, CHRM3, CHRM2 |
| Isocorypalmine | PTGS1, CHRM3, HTR3A, CHRM2, DRD3, RXRB |
| (S)-canadine | PTGS1, CHRM3, HTR3A, CHRM2, DRD3, RXRB |
| Paeonol | PTGS1, CHRM2, RELA, BCL2, NFKBIA, ICAM1, TYR |
| Beta-elemene | CHRM2, PTGS1, CHRM3, BCL2, RB1, TP63, CCNB1, RHOA |
| Rutin | RELA, IL6, CASP3, ALOX5, GSTP1, INS, FCER2, ITGB2 |
| Beta-sitosterol | PGR, PTGS1, CHRM3, CHRM2, BCL2, CASP9, CASP3, CASP8, PRKCA, PON1 |
| Eugenol | PTGS1, CHRM3, CHRM2, PLAU, RELA, CYP1A1, ALOX5, AHR, ABCC2, MUC1 |
| Wogonin | PTGS1, ESR1, AR, PPARG, GSK3B, RELA, CCND1, BCL2, CASP9, IL6, CASP3, TP63, PTGER3, MCL1 |
| Baicalein | PTGS1, AR, RELA, VEGFA, BCL2, FOS, CASP3, TP63, HIF1A, FOSL1, CCNB1, AHR, IGF2, CYCS, NOX5 |
| Kaempferol | PTGS1, AR, PPARG, PGR, ACHE, CHRM2, RELA, IKKBK, BCL2, CASP3, MAPK8, PPARG, CYP3A4, CYP1A1, ICAM1, SELE, VCAM1, ALOX5, GSTP1, AHR, NR1I3, GSTM1 |
| Quercetin | PTGS1, AR, PPARG, AKR1B1, ACHE, RELA, EGFR, VEGFA, CCND1, BCL2, FOS, CASP9, PLAU, RB1, IL6, CASP3, TP63, NFKBIA, CASP8, RAF1, PRKCA, HIF1A, ERBB2, PPARG, CYP3A4, CAV1, MYC, CYP1A1, ICAM1, SELE, VCAM1, PTGER3, BIRC5, NOS3, HSPB1, CCNB1, ALOX5, GSTP1, NFE2L2, NQO1, PARP1, AHR, COL3A1, DCAF5, NR1I3, HSF1, CRP, RUNX2, CTSD, IGFBP3, IGF2, IRF1, ERBB3, PON1, GSTM1 |

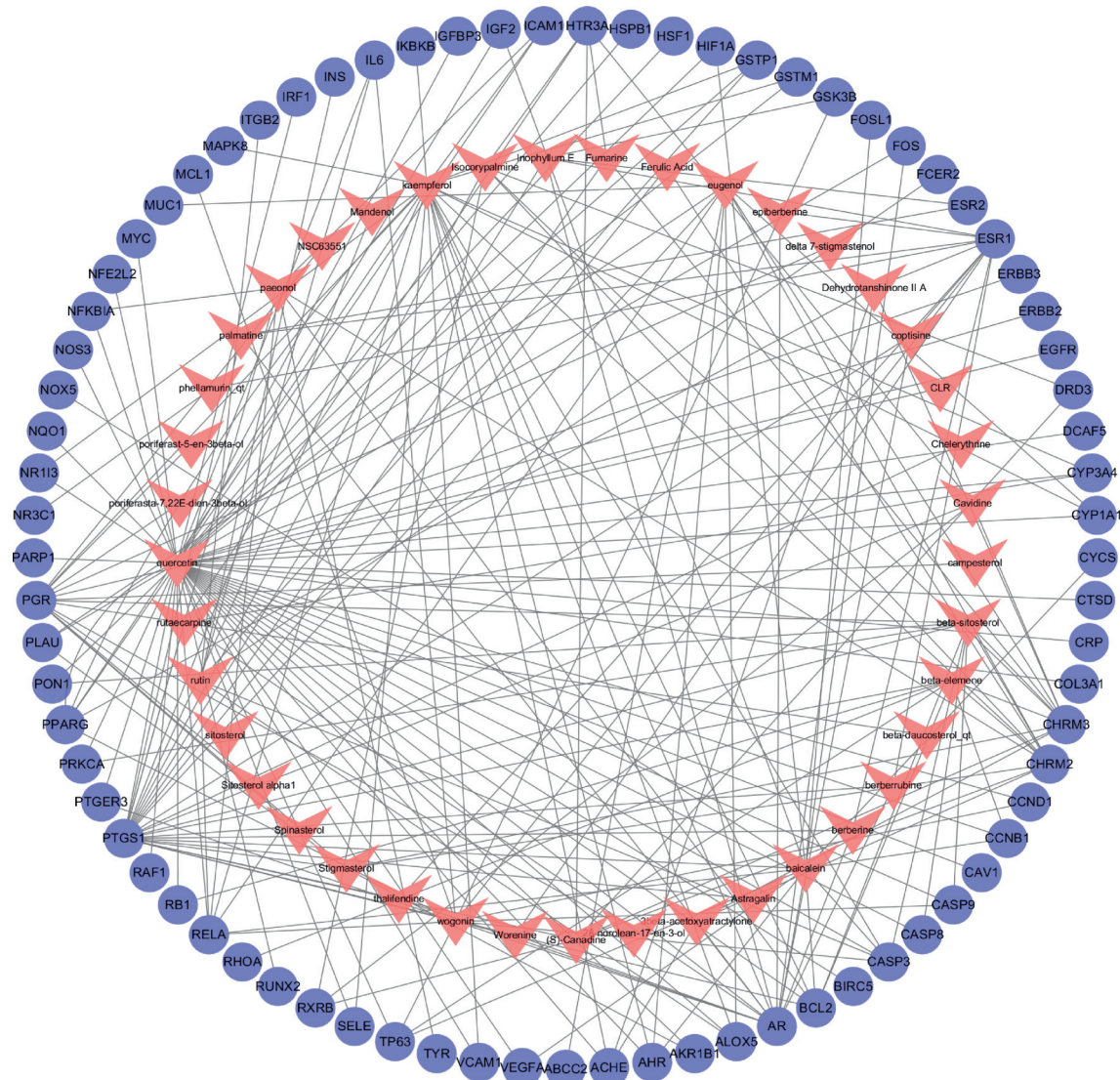


FIGURE 4: The compounds-targets network. The pink V's represent compounds and blue-purple ellipses represent target genes.

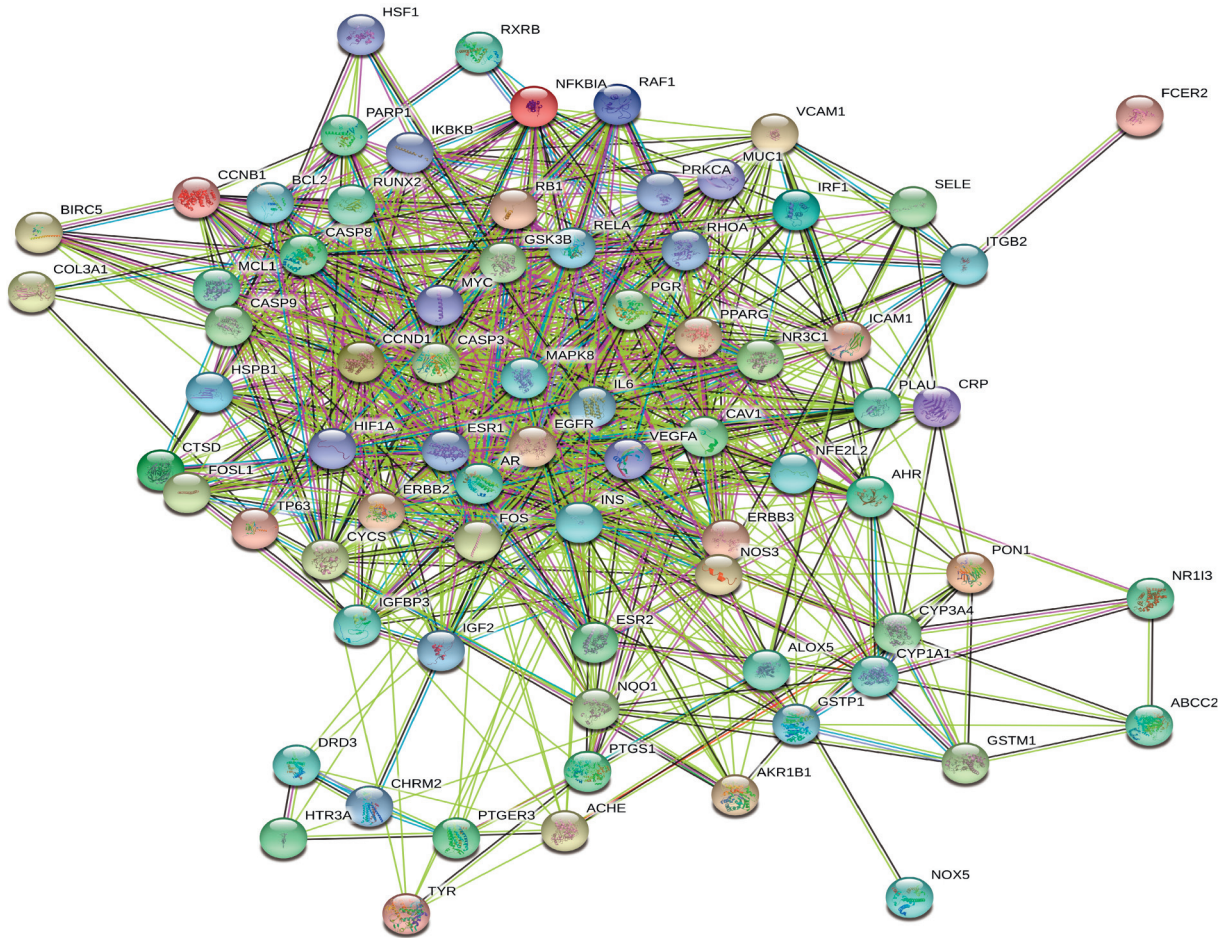


FIGURE 5: The PPI network of SM-RA. Each node represents the relevant gene, and the edges represent protein-protein associations.

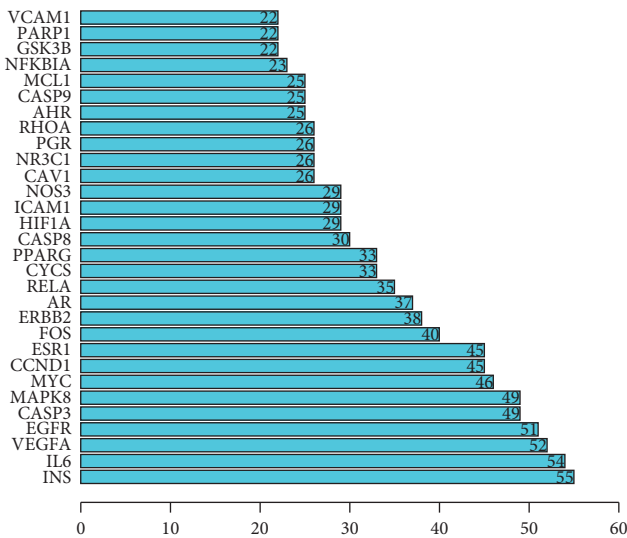


FIGURE 6: Hub top 30 genes of the PPI network. The y-axis displays significant top 30 genes, and the x-axis shows line counts of these genes.

though research about the role of INS in RA is rare. IL6 is involved in the regulation of the immune response, inflammation, and hematopoiesis and confirmed the

pathological roles in RA [65]. VEGFA contributes to promoting the angiogenic phenotype of RA [56]. EGFR is proved to be involved in the proliferation and cytokine production of synovial fibroblasts, the proliferation of endothelial cells, and the formation of osteoclasts [39]. CASP3, CASP8 [44], and CASP9 [45] are involved in the apoptosis of RA synoviocytes. NFKBIA is related to the inflammation of RA by regulating many genes for immune response, cell adhesion, differentiation, proliferation, angiogenesis, and apoptosis [37]. The antirheumatic effect of aforementioned baicalein, ferulic acid, etc. is partially associated with these target genes, indicating the interaction between multi-components and multitargets of SM treating RA.

KEGG pathway enrichment analysis indicated that certain types of virus infection and cancer might also be crucial in the network. The evidence that viral infection contributes to RA, such as Epstein-Barr virus infection [1], is strong, and RA is associated with an increased risk of cancer [66]. In addition, the KEGG pathway analysis also indicated that PI3K-Akt, TNF, and IL-17 signaling pathway may be a critical signaling pathway in the network pharmacology. The PI3K-Akt signaling pathway is involved in inflammatory cytokine production [67], proliferation and migration of RAFLS [68] and chondrocyte proliferation [69], and apoptosis and autophagy in RA [69]. Moreover, a pivotal role for

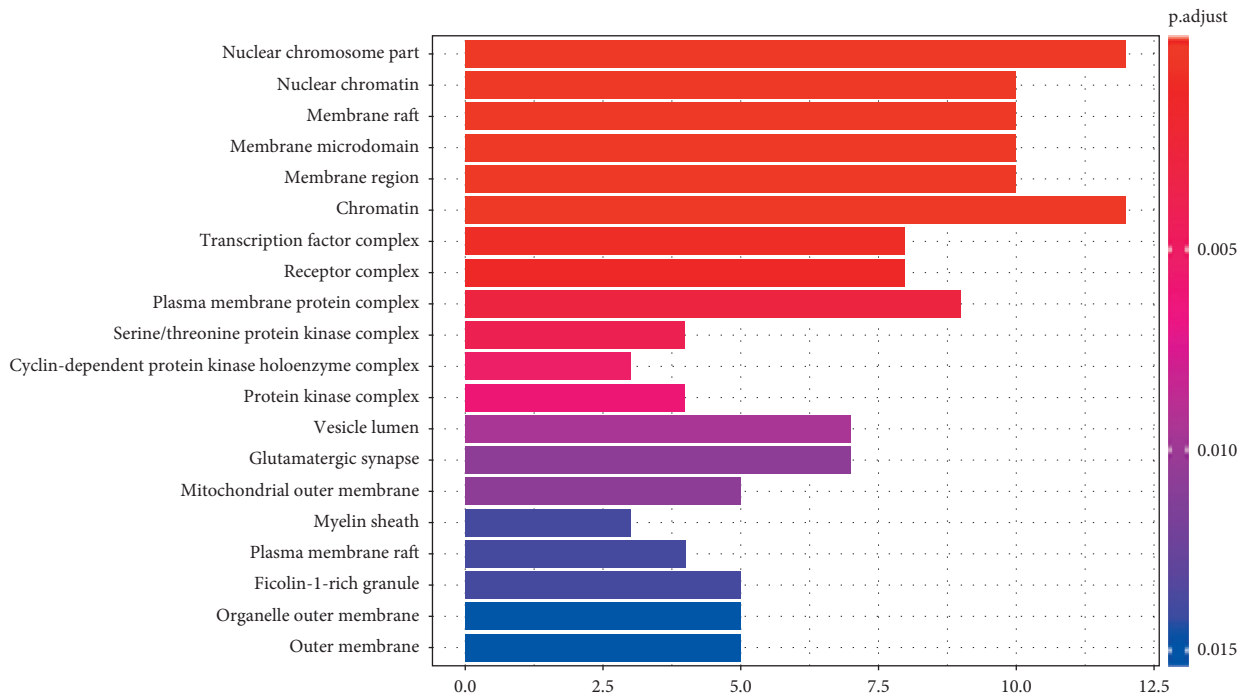
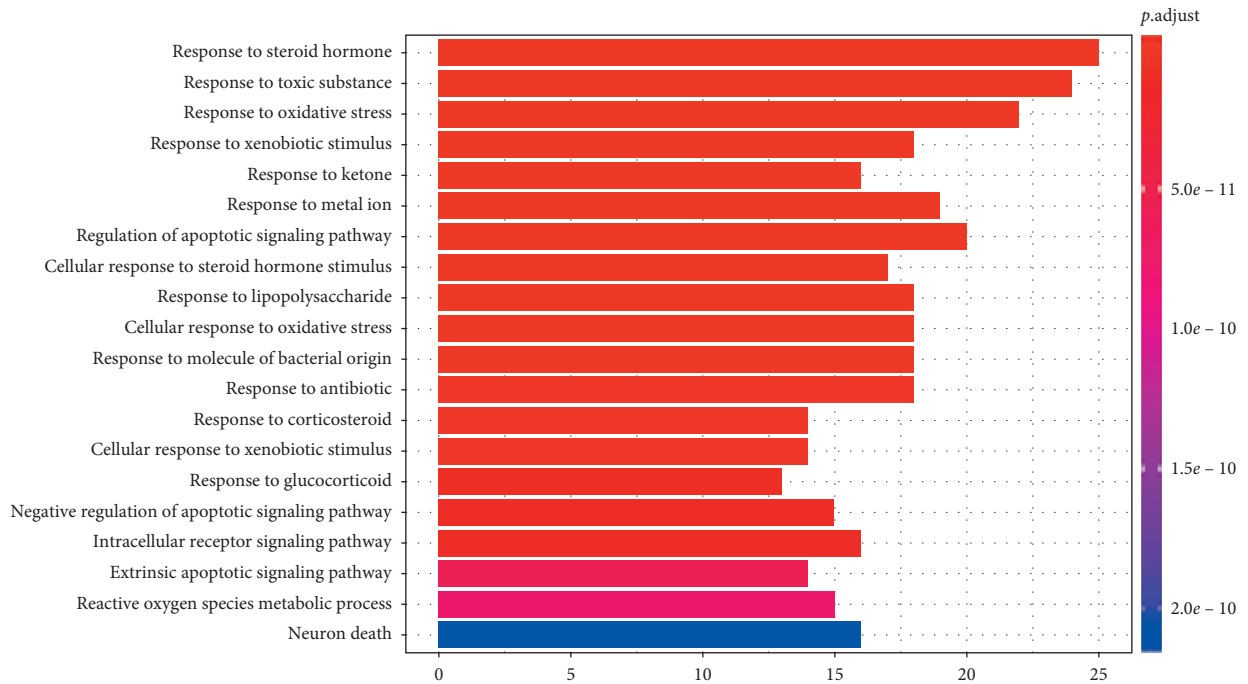


FIGURE 7: Continued.

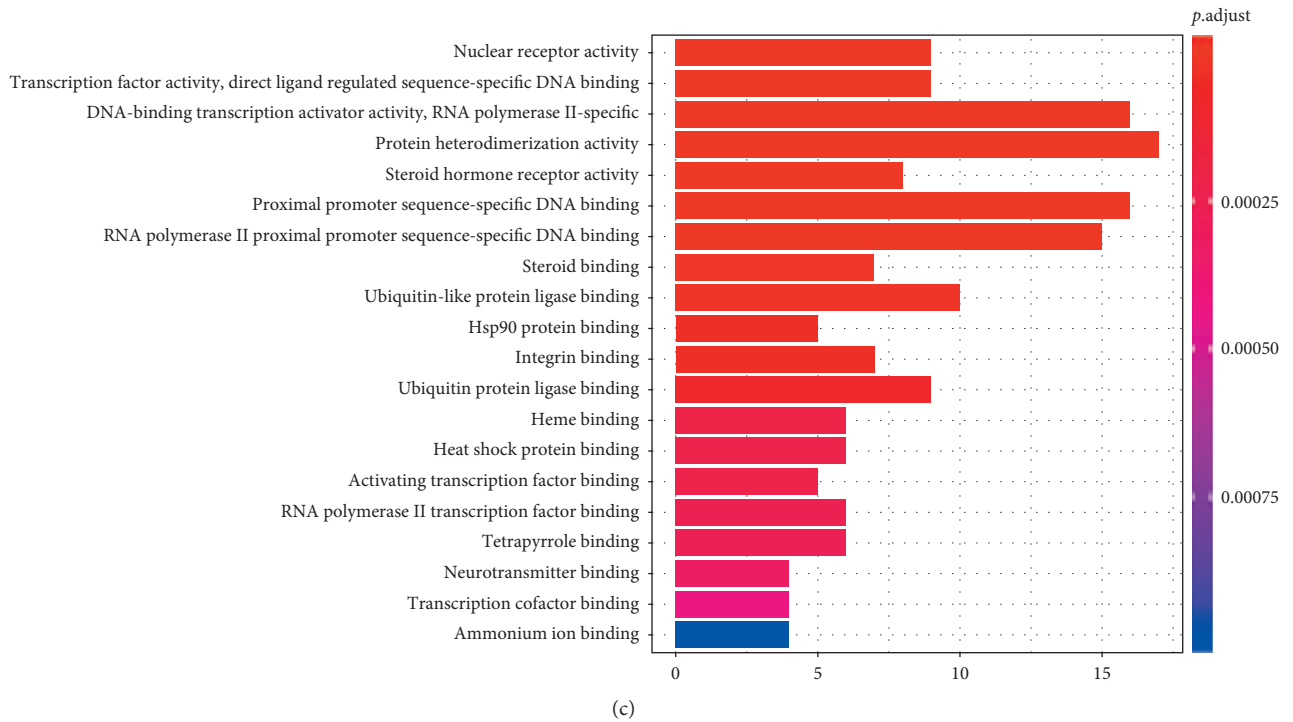


FIGURE 7: GO analysis of targets, the top 20 significant enrichment terms in BP (a), CC (b), and MF (c). The y-axis shows significantly enriched biological process, cellular component, and molecular function categories of the target genes, respectively. The redder the color, the lower the *P* value. The x-axis displays the enrichment scores of these terms, and the length of the bar indicates the number of target genes in each pathway.

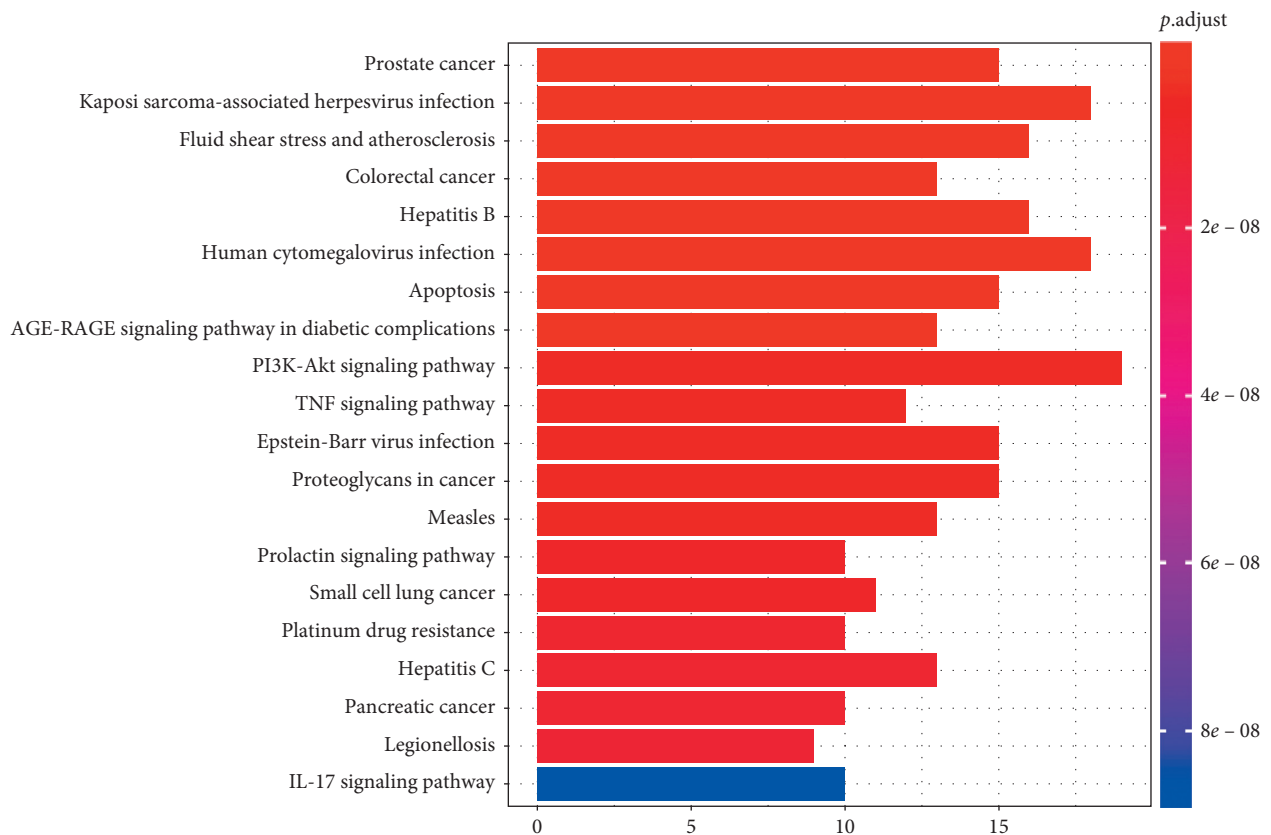


FIGURE 8: KEGG enrichment pathways (top 20). The y-axis displays the top 20 significantly enriched KEGG pathways of the target genes. The redder the color, the smaller the *P* value. The x-axis represents the target genes counts, and the length of the bar indicates the number of target genes in each pathway.

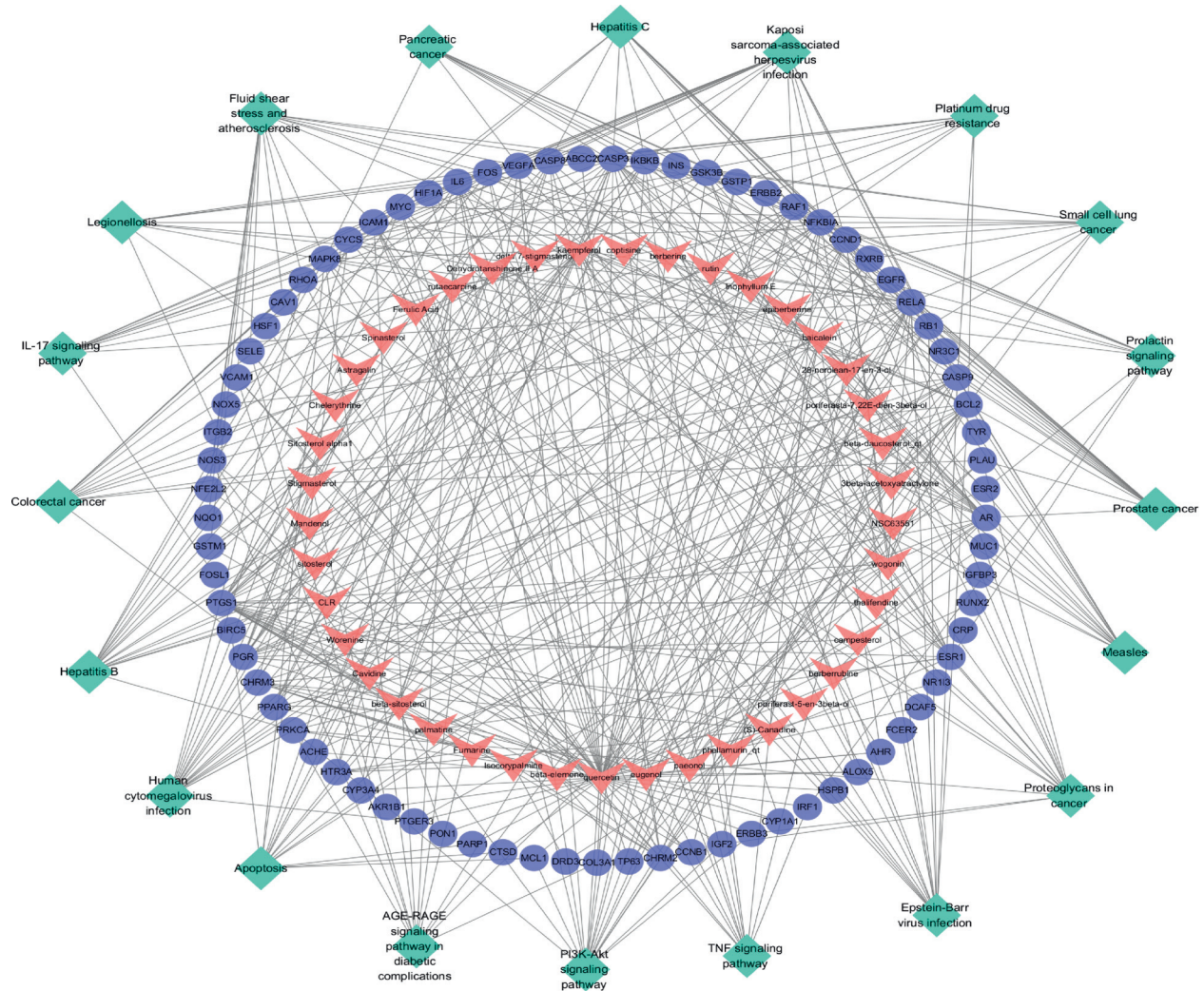


FIGURE 9: The pathways-targets-compounds network. The green diamonds represent pathways, the blue-purple ellipses represent genes, and the pink V's represent compounds.

TABLE 3: Molecular docking scores.

| | IL6 | VEGFA | EGFR | NFKBIA |
|------------|---------|---------|---------|---------|
| Quercetin | -4.7051 | -5.9131 | -6.0857 | -6.7291 |
| Kaempferol | -4.9898 | -5.4844 | -5.7466 | -6.5524 |
| Baicalein | -4.5010 | -5.5058 | -5.8372 | -6.2222 |
| Wogonin | -4.6678 | -5.6466 | -6.1084 | -6.6169 |

the proinflammatory cytokines, including tumor necrosis factor (TNF) [70] and interleukin- (IL-) 17 [71], in RA joint pathology has been identified.

Of the leading 30 target genes with a higher connection in the PPI network, IL6, VEGFA, EGFR, and NFKBIA play a critical role in the development of RA, which has been aforementioned. Besides, in the visualized pathways-targets network, IL6, VEGFA, EGFR, and NFKBIA are involved in numerous pathways, indicating that SM may exert anti-RA effects through multipathways and multitargets combined interaction. Furthermore, the molecular docking analysis

was constructed to investigate the interaction of some candidate compounds and targets. For example, the absolute value of docking scores about NFKBIA and quercetin, kaempferol, baicalein, and wogonin is the highest in each group, indicating that NFKBIA has a higher binding affinity than other target genes. For wogonin, although there have been no relevant studies about the effect in RA, the docking results indicated that wogonin performed good binding activity with IL6, VEGFA, EGFR, and NFKBIA. In brief, the high binding affinities of these active components indicated that the therapeutic effects of SM treating RA were probably through the modulation of several related targets.

As shown, the anti-RA effect of identified compounds (quercetin, kaempferol, baicalein, beta-sitosterol, and eugenol) is partially associated with the potential target genes, including NFKBIA, IL6, and MAPK, and potential signals, including PI3K-Akt, TNF, and IL-17, indicating the interaction between multicomponents, multitargets, and multi-signaling of SM treating RA.

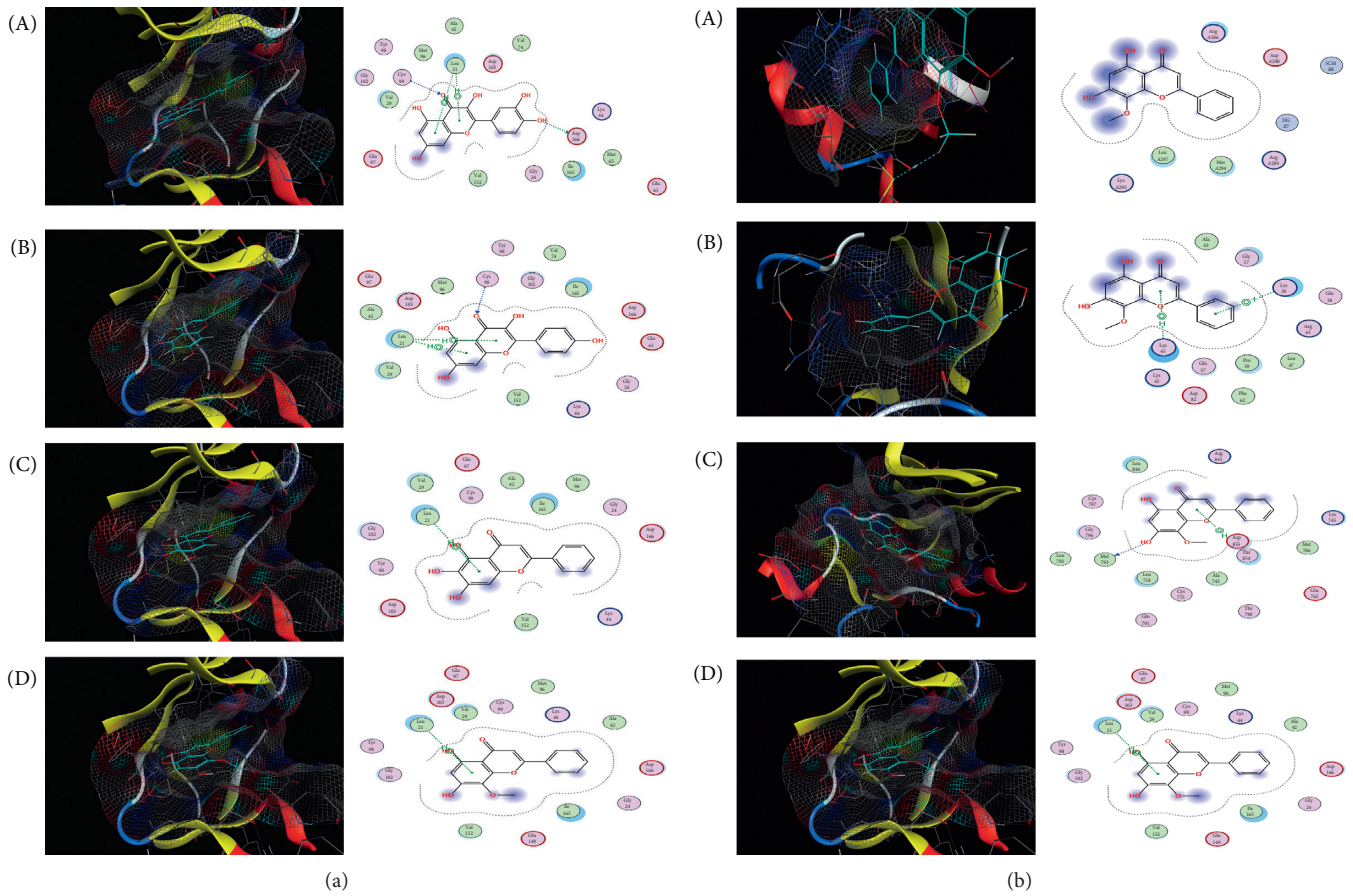


FIGURE 10: Molecular docking results. (a) The action mode of NFKBIA and quercetin, kaempferol, baicalein, and wogonin: (A) NFKBIA and quercetin; (B) NFKBIA and kaempferol; (C) NFKBIA and baicalein; (D) NFKBIA and wogonin. (b) The action mode of wogonin and IL6, VEGFA, EGFR, and NFKBIA: (A) wogonin and IL6; (B) wogonin and VEGFA; (C) wogonin and EGFR; (D) wogonin and NFKBIA.

TABLE 4: Potential anti-RA mechanisms of some compounds.

| Compound | Mechanism | Model | Reference |
|-----------------|---|--------------------------------|--------------------------|
| Quercetin | Decreased TNF- α , IL-1 β , IL-17, and MCP-1 | CIA mice | Haleagrahara et al. [58] |
| | Decreased TNF- α in joints, reduced interchondral joints damage, inflammatory cells infiltration, and pannus formation | CIA mice | Kawaguchi et al. [59] |
| | Promote RAFLS apoptosis by upregulating lncRNA metastasis-associated lung adenocarcinoma transcript 1 (MALAT1) and inhibiting PI3K/AKT signal activation subsequently | RAFLS | Pan et al. [72] |
| | Exerted anti-inflammatory, analgesic, and antioxidant effects by inhibiting NF- κ B and regulating nuclear factor erythroid 2-related factor (Nrf2)/home oxygenase (HO-1) signal | Zymosan-induced arthritis mice | Guazelli, et al. [73] |
| Kaempferol | Inhibited IL-17 and RANKL production, suppressed Th17 cell | RAFLS | Kim HR, et al. 2019 [74] |
| | Inhibited RAFLS proliferation and migration, suppressed inflammatory cytokines (IL-17, IL-21, and TNF- α) by targeting FGFR3-RSK2 signal | RAFLS | Lee, et al. [60] |
| | Inhibited RAFLS migration and invasion by blocking MAPK signal | RAFLS | Pan et al. [75] |
| Baicalein | Inhibited RAFLS proliferation, reduced MMPs, COX-2, and PGE2 production, inhibited NF- κ B activation | RAFLS | Yoon et al. [76] |
| Beta-sitosterol | Inhibited RAFLS proliferation by suppressing NF- κ B activation | RAFLS | Chen et al. [61] |
| Eugenol | Inhibited inflammatory cytokines (iNOS, IL-1 β), modulated macrophages functions | CIA mice | Liu et al. [62] |
| | Inhibited mononuclear infiltration, lowered TNF- α , TGF- β , and IFN- γ | CIA murine | Grespan et al. [24] |
| | Reduced inflammatory cytokines (TNF- α , IL-6, and IL-10) and oxidative stress | CIA rat | Mateen et al. [25] |
| | Reduced inflammatory cytokines (TNF- α , IL-6) and oxidative stress | RA patients | Mateen et al. [26] |

The anti-RA effect of identified compounds (quercetin, kaempferol, baicalein, beta-sitosterol, and eugenol) is partially associated with the potential target genes, including NFKBIA, IL6, and MAPK, and potential signals, including PI3K-AKT, TNF, and IL-17, indicating the interaction between multicomponents, multitargets, and multisignaling of SM treating RA.

5. Limitation

This study has some limitations. It provides only a predictive overview of the pharmacological mechanisms of SM against RA based on the existing database, and further experiment verification in vivo and in vitro is necessary to ensure the reliability and reasonability of predicted results. First, posttranscriptional processing, translation regulation, and posttranslational processing and regulation play a critical role in gene expression regulation, and most of the research on mechanisms about SM treating RA is gene level in this study; therefore, an in-depth study needs to explore the related mechanism. Second, the key proteins and KEGG pathways need to be verified. Third, the anti-RA effect needs to be further verified in the animal model.

Besides, for clinical applying of SM treating RA, owing to the ethnic, genetic, and possible etiological differences, potential mechanisms about the related therapeutic module coinciding with clinical applications are worthy of further experimental investigation. In addition, importantly, dosage exploration, oral bioavailability, water-solubility, pharmacokinetics, and potential side effects of SM will also need a thorough exploration.

6. Conclusion

In summary, a bioinformatics/topology-based strategy, including ADEM screening, bioinformatics, network topology, enrichment analysis, and molecular analysis, was applied for identification of the molecular mechanisms of SM against RA. The integrated strategy might make the decipherment of biological mechanisms more accurate and efficient. The SM-RA network, compounds-targets network, and pathways-targets network analysis visualized the interaction of multicomponents and multitargets about SM treating RA. In particular, quercetin, kaempferol, baicalein, wogonin, beta-sitosterol, and eugenol might be the candidate therapeutic agents, and PTGS1, ESR1, AR, PGR, CHRM3, PPARG, CHRM2, BCL2, CASP3, and RELA were identified as potential drug targets. The enrichment and PPI analysis revealed the biological functions of the grouping networks related to the pathogenesis of RA. The multi-component cosynergism of the herbal combinations about SM was elaborated. The study also revealed the multifunctional synergetic mechanisms of SM, including certain virus infection and cancer, and PI3K-Akt, TNF, and IL-17 signaling pathway.

Data Availability

The figures and tables used to support the findings of this study are included within the article, and the original data are available from the first author or corresponding author upon request.

Disclosure

This research did not receive any specific funding.

Conflicts of Interest

The authors declare that there are no conflicts of interest regarding the publication of this paper.

Acknowledgments

This research did not receive any specific funding.

References

- [1] D. Aletaha and J. S. Smolen, "Diagnosis and management of rheumatoid arthritis," *JAMA*, vol. 320, no. 13, pp. 1360–1372, 2018.
- [2] Y. Tanaka, T. Takeuchi, and S. Tanaka, "Efficacy and safety of peficitinib (ASP015K) in patients with rheumatoid arthritis and an inadequate response to conventional DMARDs: a randomised, double-blind, placebo-controlled phase III trial (RAJ3)," *Annals of the Rheumatic Diseases*, vol. 78, no. 10, pp. 1320–1332, 2019.
- [3] D. L. Scott, F. Wolfe, and T. W. Huizinga, "Rheumatoid arthritis," *The Lancet*, vol. 376, no. 9746, pp. 1094–1108, 2010.
- [4] I. B. McInnes and G. Schett, "Pathogenetic insights from the treatment of rheumatoid arthritis," *The Lancet*, vol. 389, no. 10086, pp. 2328–2337, 2017.
- [5] G. R. Burmester and J. E. Pope, "Novel treatment strategies in rheumatoid arthritis," *The Lancet*, vol. 389, no. 10086, pp. 2338–2348, 2017.
- [6] K. D. Moudgil and B. M. Berman, "Traditional Chinese medicine: potential for clinical treatment of rheumatoid arthritis," *Expert Review of Clinical Immunology*, vol. 10, no. 7, pp. 819–822, 2014.
- [7] S. Seca and G. Franconi, "Understanding Chinese medicine patterns of rheumatoid arthritis and related biomarkers," *Medicines (Basel)*, vol. 5, no. 1, 2018.
- [8] H.-Y. Yuan, X.-L. Zhang, X.-H. Zhang, L. Meng, and J.-F. Wei, "Analysis of patents on anti-rheumatoid arthritis therapies issued in China," *Expert Opinion on Therapeutic Patents*, vol. 25, no. 8, pp. 909–930, 2015.
- [9] S. Lü, Q. Wang, G. Li, S. Sun, Y. Guo, and H. Kuang, "The treatment of rheumatoid arthritis using Chinese medicinal plants: from pharmacology to potential molecular mechanisms," *Journal of Ethnopharmacology*, vol. 176, pp. 177–206, 2015.
- [10] Y. F. Liu, Y. Huang, C. Y. Wen et al., "The effects of modified simiao decoction in the treatment of gouty arthritis: a systematic review and meta-analysis," *Evidence Based Complementary and Alternative Medicine*, vol. 2017, Article ID 6037037, 2017.
- [11] C.-H. Ma, L.-L. Kang, H.-M. Ren, D.-M. Zhang, and L.-D. Kong, "Simiao pill ameliorates renal glomerular injury via increasing Sirt1 expression and suppressing NF- κ B/NLRP3 inflammasome activation in high fructose-fed rats," *Journal of Ethnopharmacology*, vol. 172, pp. 108–117, 2015.
- [12] P. Shen, S. Tu, H. Wang, K. Qin, and Z. Chen, "Simiao pill attenuates collagen-induced arthritis in rats through suppressing the ATX-LPA and MAPK signalling pathways," *Evidence Based Complementary and Alternative Medicine*, vol. 2019, Article ID 7498527, 2019.
- [13] J. Zhao, Q. Zha, M. Jiang, H. Cao, and A. Lu, "Expert consensus on the treatment of rheumatoid arthritis with Chinese patent medicines," *The Journal of Alternative and Complementary Medicine*, vol. 19, no. 2, pp. 111–118, 2013.

- [14] S. Li and B. Zhang, "Traditional Chinese medicine network pharmacology: theory, methodology and application," *Chinese Journal of Natural Medicines*, vol. 11, no. 2, pp. 110–120, 2013.
- [15] A. L. Hopkins, "Network pharmacology: the next paradigm in drug discovery," *Nature Chemical Biology*, vol. 4, no. 11, pp. 682–690, 2008.
- [16] T. T. Luo, Y. Lu, and S. K. Yan, "Network pharmacology in research of Chinese medicine formula: methodology, application and prospective," *Chinese Journal of Integrative Medicine*, vol. 26, no. 1, pp. 72–80, 2019.
- [17] Q. Guo, K. Zheng, and D. Fan, "Wu-Tou Decoction in Rheumatoid arthritis: integrating network pharmacology and in vivo pharmacological evaluation," *Frontiers in Pharmacology*, vol. 8, p. 230, 2017.
- [18] A. Y. Lee, W. Park, T.-W. Kang, M. H. Cha, and J. M. Chun, "Network pharmacology-based prediction of active compounds and molecular targets in Yijin-Tang acting on hyperlipidaemia and atherosclerosis," *Journal of Ethnopharmacology*, vol. 221, pp. 151–159, 2018.
- [19] G. Xie, W. Peng, and P. Li, "A network pharmacology analysis to explore the effect of astragali radix-radix angelica sinensis on traumatic brain injury," *Biomed Research International*, vol. 2018, Article ID 3951783, 2018.
- [20] P. Li, J. Chen, W. Zhang, H. Li, W. Wang, and J. Chen, "Network pharmacology based investigation of the effects of herbal ingredients on the immune dysfunction in heart disease," *Pharmacological Research*, vol. 141, pp. 104–113, 2019.
- [21] K. Tsaioun, B. J. Blaauboer, and T. Hartung, "Evidence-based absorption, distribution, metabolism, excretion (ADME) and its interplay with alternative toxicity methods," *Altex*, vol. 33, no. 4, pp. 343–358, 2016.
- [22] R. Ganesan and M. Rasool, "Ferulic acid inhibits interleukin 17-dependent expression of nodal pathogenic mediators in fibroblast-like synoviocytes of rheumatoid arthritis," *Journal of Cellular Biochemistry*, vol. 120, no. 2, 2018.
- [23] S. Zou, C. Wang, Z. Cui et al., " β -Elemene induces apoptosis of human rheumatoid arthritis fibroblast-like synoviocytes via reactive oxygen species-dependent activation of p38 mitogen-activated protein kinase," *Pharmacological Reports*, vol. 68, no. 1, pp. 7–11, 2016.
- [24] R. Grespan, M. Paludo, H. d. P. Lemos et al., "Anti-arthritis effect of eugenol on collagen-induced arthritis experimental model," *Biological and Pharmaceutical Bulletin*, vol. 35, no. 10, pp. 1818–1820, 2012.
- [25] S. Mateen, S. Shahzad, S. Ahmad et al., "Cinnamaldehyde and eugenol attenuates collagen induced arthritis via reduction of free radicals and pro-inflammatory cytokines," *Phytomedicine*, vol. 53, pp. 70–78, 2019.
- [26] S. Mateen, M. T. Rehman, S. Shahzad et al., "Anti-oxidant and anti-inflammatory effects of cinnamaldehyde and eugenol on mononuclear cells of rheumatoid arthritis patients," *European Journal of Pharmacology*, vol. 852, pp. 14–24, 2019.
- [27] Y. Li, P. Li, S.-H. Lin, Y.-Q. Zheng, and X.-X. Zheng, "Paeonol inhibited TNF- α -induced GM-CSF expression in fibroblast-like synoviocytes," *International Journal of Clinical Pharmacology and Therapeutics*, vol. 52, no. 11, pp. 986–996, 2014.
- [28] N. Liu, X. Feng, W. Wang, X. Zhao, and X. Li, "Paeonol protects against TNF- α -induced proliferation and cytokine release of rheumatoid arthritis fibroblast-like synoviocytes by upregulating FOXO3 through inhibition of miR-155 expression," *Inflammation Research*, vol. 66, no. 7, pp. 603–610, 2017.
- [29] K. F. Zhai, H. Duan, and L. Luo, "Protective effects of paeonol on inflammatory response in IL-1 β -induced human fibroblast-like synoviocytes and rheumatoid arthritis progression via modulating NF- κ B pathway," *Inflammopharmacology*, vol. 25, pp. 523–532, 2017.
- [30] F. Li, M. Dai, and H. Wu, "Immunosuppressive effect of geniposide on mitogen-activated protein kinase signalling pathway and their cross-talk in fibroblast-like synoviocytes of adjuvant arthritis rats," *Molecules*, vol. 23, no. 1, 2018.
- [31] R. Deng, F. Li, and H. Wu, "Anti-inflammatory mechanism of geniposide: inhibiting the hyperpermeability of fibroblast-like synoviocytes via the RhoA/p38MAPK/NF- κ B/F-actin signal pathway," *Frontiers in Pharmacology*, vol. 9, p. 105, 2018.
- [32] Y. Wang, L. Dai, H. Wu et al., "Novel anti-inflammatory target of geniposide: inhibiting Itg β 1/Ras-Erk1/2 signal pathway via the miRNA-124a in rheumatoid arthritis synovial fibroblasts," *International Immunopharmacology*, vol. 65, pp. 284–294, 2018.
- [33] C. L. Sun, J. Wei, and L. Q. Bi, "Rutin attenuates oxidative stress and proinflammatory cytokine level in adjuvant induced rheumatoid arthritis via inhibition of NF- κ B," *Pharmacology*, vol. 100, no. 1-2, pp. 40–49, 2017.
- [34] A. Gul, B. Kunwar, M. Mazhar et al., "Rutin and rutin-conjugated gold nanoparticles ameliorate collagen-induced arthritis in rats through inhibition of NF- κ B and iNOS activation," *International Immunopharmacology*, vol. 59, pp. 310–317, 2018.
- [35] Q. Jia, T. Wang, X. Wang et al., "Astragalins suppresses inflammatory responses and bone destruction in mice with collagen-induced arthritis and in human fibroblast-like synoviocytes," *Frontiers in Pharmacology*, vol. 10, p. 94, 2019.
- [36] F. Pandolfi, L. Franza, and V. Carusi, "Interleukin-6 in rheumatoid arthritis," *International Journal of Molecular Science*, vol. 21, no. 15, 2020.
- [37] X. F. Sun and H. Zhang, "NFKB and NFKBI polymorphisms in relation to susceptibility of tumour and other diseases," *Histology and Histopathology*, vol. 22, no. 12, pp. 1387–1398, 2007.
- [38] N. Hannemann, J. Jordan, S. Paul et al., "The AP-1 transcription factor c-jun promotes arthritis by regulating cyclooxygenase-2 and arginase-1 expression in macrophages," *The Journal of Immunology*, vol. 198, no. 9, pp. 3605–3614, 2017.
- [39] C. D. Swanson, E. H. Akama-Garren, E. A. Stein et al., "Inhibition of epidermal growth factor receptor tyrosine kinase ameliorates collagen-induced arthritis," *The Journal of Immunology*, vol. 188, no. 7, pp. 3513–3521, 2012.
- [40] G. L. Johnson and R. Lapadat, "Mitogen-activated protein kinase pathways mediated by ERK, JNK, and p38 protein kinases," *Science*, vol. 298, no. 5600, pp. 1911–1912, 2002.
- [41] L. Zhang, Y. Huang, and C. Wu, "Network pharmacology based research on the combination mechanism between escin and low dose glucocorticoids in anti-rheumatoid arthritis," *Frontiers in Pharmacology*, vol. 10, p. 280, 2019.
- [42] T. Laragione, C. Harris, and P. S. Gulko, "TRPV2 suppresses Rac1 and RhoA activation and invasion in rheumatoid arthritis fibroblast-like synoviocytes," *International Immunopharmacology*, vol. 70, pp. 268–273, 2019.
- [43] S. Garcia and C. Conde, "The role of poly(ADP-ribose) polymerase-1 in rheumatoid arthritis," *Mediators of Inflammation*, vol. 2015, Article ID 837250, 2015.
- [44] K. Okamoto, T. Kobayashi, T. Kobata et al., "Fas-associated death domain protein is a Fas-mediated apoptosis modulator in synoviocytes," *Rheumatology*, vol. 39, no. 5, pp. 471–480, 2000.

- [45] K. Itoh, H. Hase, H. Kojima, K. Saotome, K. Nishioka, and T. Kobata, "Central role of mitochondria and p53 in Fas-mediated apoptosis of rheumatoid synovial fibroblasts," *Rheumatology*, vol. 43, no. 3, pp. 277–285, 2004.
- [46] J. Lee, H. Jeong, E.-J. Park et al., "CIP2A facilitates apoptotic resistance of fibroblast-like synoviocytes in rheumatoid arthritis independent of c-Myc expression," *Rheumatology International*, vol. 33, no. 9, pp. 2241–2248, 2013.
- [47] A. Holmgren and J. Lu, "Thioredoxin and thioredoxin reductase: current research with special reference to human disease," *Biochemical and Biophysical Research Communications*, vol. 396, no. 1, pp. 120–124, 2010.
- [48] Y. Li, N. He, L. Shen, and M. Liu, "Apoptotic effect of *Aralia echinocaulis* extract on fibroblast-like synoviocytes in rats with adjuvant-induced arthritis via inhibiting the Akt/Hif-1 α signaling pathway in vitro," *Journal of Pharmacological Sciences*, vol. 139, no. 4, pp. 340–345, 2019.
- [49] Y. Jiao, H. Ding, and S. Huang, "Bcl-XL and Mcl-1 upregulation by calreticulin promotes apoptosis resistance of fibroblast-like synoviocytes via activation of PI3K/Akt and STAT3 pathways in rheumatoid arthritis," *Clinical and Experimental Rheumatology*, vol. 36, no. 5, pp. 841–849, 2018.
- [50] J. Sun, P. Yan, and Y. Chen, "MicroRNA-26b inhibits cell proliferation and cytokine secretion in human RASF cells via the Wnt/GSK-3 β /beta-catenin pathway," *Diagnostic Pathology*, vol. 10, p. 72, 2015.
- [51] X.-Y. Huang, X.-M. Zhang, F.-H. Chen et al., "Anti-proliferative effect of recombinant human endostatin on synovial fibroblasts in rats with adjuvant arthritis," *European Journal of Pharmacology*, vol. 723, pp. 7–14, 2014.
- [52] J. Zhou, R. Kvetnansky, and Z. Radikova, "Hormone concentrations in synovial fluid of patients with rheumatoid arthritis," *Clinical and Experimental Rheumatology*, vol. 23, no. 3, pp. 292–296, 2005.
- [53] V. Dziejdzijko, M. Kurzawski, K. Safranow, D. Chlubek, and A. Pawlik, "The effect of ESR1 and ESR2 gene polymorphisms on the outcome of rheumatoid arthritis treatment with leflunomide," *Pharmacogenomics*, vol. 12, no. 1, pp. 41–47, 2011.
- [54] M. R. Gubbels Bupp and T. N. Jorgensen, "Androgen-induced immunosuppression," *Frontiers in Immunology*, vol. 9, p. 794, 2018.
- [55] E. W. Karlson, L. B. Chibnik, M. McGrath et al., "A prospective study of androgen levels, hormone-related genes and risk of rheumatoid arthritis," *Arthritis Research & Therapy*, vol. 11, no. 3, p. R97, 2009.
- [56] Y. Zhang, H. Qiu, H. Zhang, L. Wang, C. Zhuang, and R. Liu, "Vascular endothelial growth factor A (VEGFA) polymorphisms in Chinese patients with rheumatoid arthritis," *Scandinavian Journal of Rheumatology*, vol. 42, no. 5, pp. 344–348, 2013.
- [57] E. Jimi, H. Fei, and C. Nakatomi, "NF-kappaB signaling regulates physiological and pathological chondrogenesis," *International Journal of Molecular Sciences*, vol. 20, no. 24, 2019.
- [58] N. Haleagrahara, S. Miranda-Hernandez, M. A. Alim, L. Hayes, G. Bird, and N. Ketheesan, "Inhibitory effect of quercetin in collagen-induced arthritis," *Biomedicine & Pharmacotherapy*, vol. 90, pp. 38–46, 2017.
- [59] K. Kawaguchi, M. Kaneko, R. Miyake, H. Takimoto, and Y. Kumazawa, "Potent inhibitory effects of quercetin on inflammatory responses of collagen-induced arthritis in mice," *Endocrine, Metabolic & Immune Disorders-Drug Targets*, vol. 19, no. 3, pp. 308–315, 2019.
- [60] C. J. Lee, S. J. Moon, and J. H. Jeong, "Kaempferol targeting on the fibroblast growth factor receptor 3-ribosomal S6 kinase 2 signaling axis prevents the development of rheumatoid arthritis," *Cell Death Diseases*, vol. 9, no. 3, p. 401, 2018.
- [61] S. Chen, Y. Yang, H. Feng, H. Wang, R. Zhao, and H. Liu, "Baicalein inhibits interleukin-1 β -induced proliferation of human rheumatoid arthritis fibroblast-like synoviocytes," *Inflammation*, vol. 37, no. 1, pp. 163–169, 2014.
- [62] R. Liu, D. Hao, W. Xu et al., " β -Sitosterol modulates macrophage polarization and attenuates rheumatoid inflammation in mice," *Pharmaceutical Biology*, vol. 57, no. 1, pp. 161–168, 2019.
- [63] H. M. Doss, S. Samarapita, R. Ganesan, and M. Rasool, "Ferulic acid, a dietary polyphenol suppresses osteoclast differentiation and bone erosion via the inhibition of RANKL dependent NF- κ B signalling pathway," *Life Sciences*, vol. 207, pp. 284–295, 2018.
- [64] P. Dinesh and M. Rasool, "Berberine mitigates IL-21/IL-21R mediated autophagic influx in fibroblast-like synoviocytes and regulates Th17/Treg imbalance in rheumatoid arthritis," *Apoptosis*, vol. 24, no. 7-8, pp. 644–661, 2019.
- [65] N. Nishimoto and T. Kishimoto, "Interleukin 6: from bench to bedside," *Nature Clinical Practice Rheumatology*, vol. 2, no. 11, pp. 619–626, 2006.
- [66] K. Elandt and D. Aletaha, "Treating rheumatic patients with a malignancy," *Arthritis Research & Therapy*, vol. 13, no. 3, p. 223, 2011.
- [67] J. Y. Lee, G. J. Kim, and J. K. Choi, "4-(Hydroxymethyl) catechol extracted from fungi in marine sponges attenuates rheumatoid arthritis by inhibiting PI3K/akt/NF-kappaB signaling," *Frontiers in Pharmacology*, vol. 9, p. 726, 2018.
- [68] B. Song, X.-F. Li, Y. Yao et al., "BMP9 inhibits the proliferation and migration of fibroblast-like synoviocytes in rheumatoid arthritis via the PI3K/AKT signaling pathway," *International Immunopharmacology*, vol. 74, Article ID 105685, 2019.
- [69] F.-B. Xu and H.-Y. Qiu, "Effects of artesunate on chondrocyte proliferation, apoptosis and autophagy through the PI3K/AKT/mTOR signaling pathway in rat models with rheumatoid arthritis," *Biomedicine & Pharmacotherapy*, vol. 102, pp. 1209–1220, 2018.
- [70] D. Wallach, "The cybernetics of TNF: old views and newer ones," *Seminars in Cell & Developmental Biology*, vol. 50, pp. 105–114, 2016.
- [71] W. B. van den Berg and P. Miossec, "IL-17 as a future therapeutic target for rheumatoid arthritis," *Nature Reviews Rheumatology*, vol. 5, no. 10, pp. 549–553, 2009.
- [72] F. Pan, L. Zhu, H. Lv, and C. Pei, "Quercetin promotes the apoptosis of fibroblast-like synoviocytes in rheumatoid arthritis by upregulating lncRNA malat1," *International Journal of Molecular Medicine*, vol. 38, no. 5, pp. 1507–1514, 2016.
- [73] C. F. S. Guazelli, L. Staurengo-Ferrari, A. C. Zarpelon et al., "Quercetin attenuates zymosan-induced arthritis in mice," *Biomedicine & Pharmacotherapy*, vol. 102, pp. 175–184, 2018.
- [74] H.-R. Kim, B.-M. Kim, J.-Y. Won et al., "Quercetin, a plant polyphenol, has potential for the prevention of bone destruction in rheumatoid arthritis," *Journal of Medicinal Food*, vol. 22, no. 2, pp. 152–161, 2019.
- [75] D. Lee, N. Li, Y. Liu et al., "Kaempferol inhibits the migration and invasion of rheumatoid arthritis fibroblast-like synoviocytes by blocking activation of the MAPK pathway," *International Immunopharmacology*, vol. 55, pp. 174–182, 2018.
- [76] H.-Y. Yoon, E.-G. Lee, H. Lee et al., "Kaempferol inhibits IL-1 β -induced proliferation of rheumatoid arthritis synovial fibroblasts and the production of COX-2, PGE2 and MMPs," *International Journal of Molecular Medicine*, vol. 32, no. 4, pp. 971–977, 2013.

Review Article

Acupotomy Therapy for Knee Osteoarthritis Pain: Systematic Review and Meta-Analysis

Jigao Sun ^{1,2}, Yan Zhao ², Ruizheng Zhu ¹, Qianglong Chen ³, Mengge Song ²,
Zhipeng Xue ¹, Rongtian Wang ¹ and Weiheng Chen ¹

¹The Third Affiliated Hospital of Beijing University of Chinese Medicine, Beijing, China

²Wangjing Hospital, China Academy of Chinese Medical Sciences, Beijing, China

³Guizhou University of Traditional Chinese Medicine, Guiyang, Guizhou, China

Correspondence should be addressed to Weiheng Chen; chenweiheng@yeah.net

Received 29 July 2020; Revised 8 October 2020; Accepted 14 October 2020; Published 31 October 2020

Academic Editor: Arham Shabbir

Copyright © 2020 Jigao Sun et al. This is an open access article distributed under the Creative Commons Attribution License, which permits unrestricted use, distribution, and reproduction in any medium, provided the original work is properly cited.

Background and Purpose. Knee osteoarthritis (OA) is a major public health problem, and currently, few effective medical treatments exist. Chinese acupotomy therapy has been widely used for the treatment of knee OA in China. We conducted this systematic review and meta-analysis to evaluate the efficacy of Chinese acupotomy in treating knee OA to inform clinical practice. **Methods.** We performed a comprehensive search on PubMed, the Cochrane Library, EMBASE, and four Chinese databases for articles published prior to June 2020. We included only randomized controlled trials (RCTs) that used acupotomy therapy as the major intervention in adults with knee OA, were published in either Chinese and English, included more than 20 subjects in each group, and included pain and function in the outcome measures. Knee OA was defined by the American College of Rheumatology or Chinese Orthopedic Association criteria in all studies. We extracted the visual analogue scale (VAS) pain score, the Western Ontario and McMaster Universities Osteoarthritis Index (WOMAC) pain score, the total effectiveness rate, the modified Japanese Orthopedic Association (JOA) activities of daily living score, and Lysholm's score. We calculated the mean difference (MD) or risk ratio (RR) for all relevant outcomes. Meta-analyses were conducted using random-effects models when appropriate. **Results.** We identified 1317 potentially relevant studies, thirty-two of which met the eligibility criteria and were conducted in China between 2007 and 2020. A total of 3021 knee OA patients (62.96% female, median age: 57 years, and median disease duration: 33 months) were included. The treatment duration ranged from 1 week to 5 weeks (median: 3 weeks). The typical acupotomy treatment involved releasing soft tissue adhesions and was performed once a week for 1–5 weeks until the pain was relieved. The control group treatments included acupuncture (8 studies), electroacupuncture (10 studies), sodium hyaluronate (8 studies), radio-frequency electrotherapy (1 study), and nonsteroidal anti-inflammatory drugs (NSAIDs, 5 studies). The results from the meta-analysis showed that acupotomy led to superior improvements in the VAS pain score (MD = -1.11; 95% confidence interval (CI), -1.51 to -0.71; $p < 0.00001$) and WOMAC pain score (MD = -2.32; 95% CI, -2.94 to -1.69; $p < 0.00001$), a higher total effectiveness rate (RR = 1.15; 95% CI, 1.09–1.21; $p < 0.00001$), and superior improvements in the JOA score (MD = 6.39; 95% CI, 4.11–9.76; $p < 0.00001$) and Lysholm's score (MD = 12.75; 95% CI, 2.61–22.89; $p = 0.01$) for overall pain and function. No serious adverse events were reported. **Conclusion.** Chinese acupotomy therapy may relieve pain and improve function in patients with knee OA. Furthermore, rigorously designed and well-controlled RCTs are warranted.

1. Introduction

Symptomatic osteoarthritis (OA) is the most frequent cause of dependency in lower limb tasks among ageing populations and is associated with substantial physical and psychosocial disability, a reduced quality of life, and

substantial healthcare costs [1]. At present, knee OA is considered a common health problem worldwide; in the United States, nearly 40% of adults over the age of 60 suffer from this disease [2]. Currently, no effective disease-modifying remedies are available to treat knee OA [3]. In the absence of effective disease-modifying treatments,

the current standards of care for knee OA are primarily aimed at pain relief and functional improvement [4].

Nonsteroidal anti-inflammatory drugs (NSAIDs) are important for treatment due to their widely reported efficacy but are restricted in clinical applications due to their side effects [5–9]. Therefore, only topical NSAIDs are strongly recommended for individuals with knee OA in the 2019 OARSI guidelines [10]. Due to the side effects of drugs, complementary and integrative therapies are favoured in the treatment of OA. Many complementary and integrative methods are used in China, such as traditional Chinese medications, and it has been reported that the prevalence of knee OA is 18% in China [11, 12]. In the latest 2019 American College of Rheumatology/Arthritis Foundation guidelines, tai chi, a traditional Chinese exercise, is strongly recommended, and acupuncture is conditionally recommended [13], but there is no mention of acupotomy therapy, which is also an important complementary and integrative therapy.

Acupotomy therapy is widely used in Chinese clinical practice and recommended in the Chinese medicine expert consensus for knee OA [14]. Acupotomy is a type of acupuncture used in traditional Chinese medicine (TCM), and it has both the characteristics of a “needle” in TCM and a “knife” in Western medicine [15]. Although it has been called feng zhen in ancient literature, acupotomy was reinvented and refined by professor Hanzang Zhu in China in 1976 [16]. Acupotomy is referred to by different names, such as needle-knife, small needle-knife, acupotome, and xiao zhen dao. The mechanism of acupotomy remains unclear and remains to be explored, but acupotomy can be used to release ligaments, joint sacs, and synovium [17]. Some studies have shown that acupotomy therapy can release adhesions, alter the mechanical balance of the knee joint, improve lymphatic circulation, and reduce abnormal tissue pressures [18–21].

Although acupotomy therapy has long been regarded as a key component of the treatment of OA in China and may be considered a safe and promising new treatment for knee OA, the quantitative evidence necessary to estimate its effects is still lacking. Two previous meta-analyses have reported that acupotomy is a safe and effective treatment for knee OA compared to intraarticular sodium hyaluronate and acupuncture [22, 23], but one meta-analysis included only 8 randomized controlled trials (RCTs), and the other meta-analysis included only 6 RCTs. One recent meta-analysis including 12 RCTs [24] attempted to assess the efficacy and safety of acupotomy compared to acupuncture. However, these meta-analyses have methodological flaws, including a lack of up-to-date RCTs data, insufficient sample sizes to make recommendations, and comparisons between acupotomy and only one specific intervention. Thus, these meta-analyses were unable to determine the overall efficacy of acupotomy in the treatment of knee OA. Therefore, we conducted an updated systematic review and meta-analysis to compare the efficacy of acupotomy with that of other treatments in treating patients with knee OA. This study has been registered on PROSPERO (CRD42020161293).

2. Methods

2.1. Search Strategy. We performed a comprehensive search in PubMed, the Cochrane Library, EMBASE and four Chinese databases (CNKI, Wan Fang, CBMdisc, and VIP) for articles published through June 2020. We included only RCTs that used acupotomy therapy as the main treatment for adults with knee OA. The Chinese and English search terms included acupotomy, acupotomies, acupuncture treatment, acupotomology, acupotome, needle-knife, needle scalpel, stiletto needle, sword-like needle, miniscalpel, small needle-knife, xiao zhen dao, pharmacopuncture, knee osteoarthritis, osteoarthritis of knee, osteoarthritis of the knee, pain, randomized controlled trial, and clinical trial.

2.2. Eligibility Criteria. Acupotomy was defined as a new type of minimally invasive surgical treatment for knee OA based on the traditional medical theory and modern surgery. We included RCTs that compared acupotomy therapy with acupuncture, electroacupuncture, or standard western treatment in adults with knee OA. Trials were eligible if the intervention included at least 1 acupotomy intervention, more than 20 subjects in each group, and original data. Studies that used the American College of Rheumatology (ACR) diagnostic criteria in 1995 were eligible [25]. We also considered studies that used the Chinese Orthopedic Association (COA) criteria of 2007 or 2018 [26, 27]. To evaluate the independent effects of the acupotomy intervention, we excluded treatment groups that received other major treatments, and we also excluded reviews, theoretical studies, case reports, and animal studies. There were no language restrictions in the literature search.

2.3. Study Selection. Two authors (QLC and RZZ) independently screened all the potentially eligible studies. The titles and abstracts were first screened to exclude irrelevant citations. The full texts of all the articles with potentially relevant abstracts were retrieved and screened according to the study eligibility criteria. Disagreements were resolved by consensus or discussion with a third author (YZ).

Pain intensity was measured using the visual analogue scale (VAS) or the Western Ontario and McMaster Universities Osteoarthritis Index (WOMAC). The VAS pain score and WOMAC pain score were the prespecified primary outcomes in this study. The total effectiveness rate was used to assess overall pain, physical performance, and wellness. The total effectiveness rate (%) was defined as the quotient of the number of patients who were clinically cured, exhibited significant improvement, or exhibited improvement divided by the total number of patients. The total effectiveness rate was assessed based on the number of patients in each of the following categories: “clinically cured” (the pain and swelling in the joints had disappeared, and the active functional state had returned to normal); “significant improvement” (the pain and swelling in the joints were alleviated, and the active functional state had improved significantly); “improvement” (the pain and swelling in the joints were partially alleviated, and the active functional state

had improved); and “not cured” (the pain and swelling in the joints remained unchanged, and there was no improvement in active function) [28]. The modified Japanese Orthopedic Association (JOA) activities of the daily living (ADL) score was used to assess pain when walking and pain when going up and down stairs. Lysholm’s score was used to assess overall pain and joint function. The total effectiveness rate, JOA score, and Lysholm’s score were also measured.

2.4. Data Extraction. One author (RZZ) extracted data from the selected studies using a predesigned data extraction table, which included publication information, the origin of study, the study setting, the time frame of the study, patient age, patient sex, the author’s definition of knee OA, detailed information on the interventions and controls, outcome measures, a summary of the results, the main conclusion, and adverse reactions (Table 1). The accuracy of the data extracted was verified by another author (ZPX).

2.5. Quality Assessment. Study quality was assessed in RevMan V5.3 (the Nordic Cochrane Centre, Cochrane Collaboration) using the Cochrane risk of bias tool [29]. The risk of bias for each of the following domains was assessed for each study: (1) random sequence generation, (2) allocation concealment, (3) blinding of the participants and personnel, (4) blinding of the outcome assessments, (5) incomplete outcome data, (6) selective reporting, and (7) other bias. Each study included was rated as having a high, low, or unclear risk of bias. Two authors (YZ and MES) evaluated all the data extracted and quality ratings for consistency and resolved disagreements. Disagreements were resolved by discussion with a third author (RTW).

2.6. Data Synthesis and Statistical Analysis. We qualitatively synthesized all the included studies (Table 1). The included studies on pain were synthesized based on the VAS pain score and the WOMAC pain score separately. The VAS score ranged from 0 points (no pain) to 10 points (worst possible pain). The WOMAC pain score ranged from 0 points to 20 points, with a lower score representing a better outcome. Lysholm’s score ranged from 0 points to 100 points, and the modified JOA score ranged from 0 points to 55 points, with a higher score representing a better outcome.

All analyses were conducted using RevMan V5.3. For the meta-analysis of the VAS pain score, WOMAC pain score, JOA score, and Lysholm’s score, we combined studies using the mean difference (MD); a positive MD indicated that the effect of acupotomy therapy was favourable compared with the control therapy. For the total effectiveness rate, we combined studies using the risk ratio (RR) in the meta-analysis, and an RR of the total effectiveness rate greater than 1 indicated that acupotomy was more effective than was the control therapy. We evaluated heterogeneity using the I^2 statistic. p values < 0.05 were considered to indicate statistical significance in all the results.

3. Results

3.1. Results of the Literature Search and Selection Processes. We screened a total of 1317 studies that were retrieved from 3 English databases and 4 Chinese databases. After initially screening 348 potentially relevant abstracts, we excluded 279 because they did not meet the inclusion criteria. Thirty-seven articles were excluded due to lack of randomization or the absence of a control group and insufficient data for the meta-analysis. Finally, 32 RCTs [19, 30–60], which included 3021 patients (62.96% female) and were published between 2007 and 2020, met our inclusion criteria. The details of the study selection process are summarized in Figure 1.

3.2. Included Studies. Table 1 describes the studies and patient characteristics of the included studies. All 32 RCTs [19, 30–60] were conducted in China, and the total sample size of the included RCTs ranged from 41 to 324 (median: 74). The mean age ranged from 47 to 66 years (median: 57 years), and the percentage of females ranged from 42.57% to 87.5% (median: 60%). The disease duration ranged from 4 to 152 months (median: 33 months).

The typical acupotomy therapy involved releasing soft tissue adhesions and was performed once a week for 1–5 weeks until the pain was relieved. Additional massage therapy after acupotomy was included in 2 studies, and functional training was included in 1 study. The control group treatments included acupuncture (8 studies), electroacupuncture (10 studies), sodium hyaluronate (8 studies), radiofrequency electrotherapy (1 study), and NSAIDs (5 studies). The NSAIDs used included oral NSAIDs (3 celecoxib and 1 diclofenac sodium) and topical NSAIDs (1 votalin emulsion). The treatment duration ranged from 1 to 5 weeks (median: 3 weeks).

The quality (risk of bias) of the trials was assessed using the Cochrane Collaboration tool, with modifications. Figure 2 describes the study quality, and Figure 3 describes the overall risk of bias distribution among the studies included. The overall bias quality for the trials was modest. The randomization process was adequate in 17 trials (53.13%), unclear in 14 trials (43.75%), and indicated a high risk of bias in 1 trial (3.13%). One trial (3.13%) reported appropriate allocation concealment methods, but 31 trials (96.88%) were at high risk of bias. Blinding of the participants and personnel occurred in 1 trial (3.13%), but 31 trials were considered to have a high risk of bias (96.88%). Blinding of the outcomes occurred in 1 trial (3.13%), but whether blinding was performed was unclear in 31 trials (96.88%). All studies reported the similarity of the study groups at baseline (100%).

3.3. Meta-Analysis. Among the thirty-two eligible RCTs, twenty-two trials [30–34, 36, 37, 39, 40, 42–47, 49, 50, 53, 55, 58–60] reported the VAS pain score for the individuals who underwent acupotomy therapy and controls. Nine trials [19, 35, 38, 41, 46, 48, 50, 52, 60] reported the WOMAC pain score. Furthermore, twenty-three trials [19, 30–42, 44–46, 48, 52, 55, 58–60] evaluated overall pain,

TABLE 1: Characteristics of the 32 included studies on Chinese acupotomy therapy for knee OA.

| Author (y) | Diagnostic criteria | N (female, %) | Age (%) | Disease duration (months) | Duration (wks) | Acupotomy therapy | Controls | Main outcomes | Results (treatment vs. control) | P value |
|-------------------|-----------------------------|---------------|---------|---------------------------|----------------|---|--|--|---|--------------------------|
| Li X. (2015) [30] | COA criteria (2007) | 324 (57.41%) | 64 | 61 | 3 | Release soft tissue adhesion, once/wk, 3 times | Acupuncture, 30 min, 6 times/wk, 3 wks | VAS pain Lysholm's score Total effectiveness rate | 2.83 vs. 3.94 89.55 vs. 80.64 87.65 vs. 85.80 | <0.05 <0.05 < 0.05 |
| Li S. (2015) [31] | ACR knee OA criteria (1995) | 67 (43.28%) | 55 | Not mentioned | 2 | Release soft tissue adhesion, once/wk, 2 times | Electroacupuncture, 20 min, once/day, 10 times | VAS pain Total effectiveness rate | 1.58 vs. 2.69 97.5 vs. 62.5 | <0.05 <0.01 |
| Sun (2019) [32] | Not mentioned | 60 (71.67%) | 59 | 152 | 4 | Release soft tissue adhesion, once/wk, 4 times | Sodium hyaluronate, 2 ml, once/wk, 4 wks | VAS pain Total effectiveness rate | 3.41 vs. 5.48, 96.67 vs. 66.67 | <0.01 <0.05 |
| Shi (2019) [33] | COA criteria (2018) | 120 (67.5%) | 58 | 21 | 4 | Release soft tissue adhesion, once/wk, 4 times | Sodium hyaluronate, 2.5 mg, once/6 days, 5 times | VAS pain Total effectiveness rate | 3.01 vs. 4.81, 90.91 vs. 77.78 | <0.05 <0.05 |
| Hong (2019) [34] | COA criteria (2007) | 61 (67.21%) | 58 | 15 | 3 | Release soft tissue adhesion, once/wk, 3 times | Acupuncture, 5 times/wk, 3 wks | VAS pain Total effectiveness rate | 1.81 vs. 2.7 96.7 vs. 73.3 | <0.05 <0.05 |
| Wang (2016) [35] | COA criteria (2007) | 230 (63.91%) | 52 | 14 | 2 | Release soft tissue adhesion, once | Acupuncture, 20 min, 1-2 times/wk, 2 wks | WOMAC pain Total effectiveness rate | 86.09 vs. 86.96 | <0.05 <0.05 |
| Jin (2020) [36] | ACR knee OA criteria | 60 (58.33%) | 57 | 89 | 4 | Release soft tissue adhesion, twice/wk, 8 times | Celecoxib capsules, 200 mg, twice/day, 4 wks | VAS pain Total effectiveness rate | 3.23 vs. 3.67 86.7 vs. 80 | <0.05 <0.05 |
| Xiu (2017) [37] | COA criteria (2007) | 80 (56.25%) | 53 | 73 | 2 | Release soft tissue adhesion, once/wk, 4 times; Massage therapy, once/2 days, 14 times | Acupuncture, 30 min, once every other day, 7 times; massage therapy, once/2 days, 14 times | VAS pain Lysholm's score Total effectiveness rate | 2.51 vs. 3.52 58.51 vs. 51.02 95 vs. 80 | <0.05 <0.01 <0.01 |
| Dai (2018) [38] | COA criteria (2007) | 200 (58.5%) | 53 | 17 | 2 | Release soft tissue adhesion, once | Acupuncture, 20 min, 1-2 times/wk, 2 wks | WOMAC Pain Total effectiveness rate | 8.52 vs. 10.81 98 vs. 78 | <0.05 < 0.01 |
| Jia (2017) [39] | COA criteria (2007) | 148 (42.57%) | 59 | 77 | 5 | Release soft tissue adhesion, once/wk, 5 times | Sodium hyaluronate, 25 mg, once/wk, 5 times | VAS pain Total effectiveness rate | 2.19 vs. 3.88 91.89 vs. 81.08 | <0.05 <0.05 |

TABLE 1: Continued.

| Author (y) | Diagnostic criteria | N (female, %) | Age (%) | Disease duration (months) | Duration (wks) | Acupotomy therapy | Controls | Main outcomes | Results (treatment vs. control) | <i>p</i> value |
|-------------------|-----------------------------|---------------|---------|---------------------------|----------------|--|---|--|--|-------------------------|
| Quan (2016) [40] | COA criteria (2007) | 50 (72%) | 56 | 78 | 2 | Release soft tissue adhesion, once/wk, 2 times | Electroacupuncture, 30 min, once/2 days, 7 times | VAS pain Total effectiveness rate | 1.28 vs. 3.71 96 vs. 76 | <0.01 <0.05 |
| Sun (2016) [41] | COA criteria (2007) | 73 (71.23%) | 56 | 11 | 4 | Release soft tissue adhesion, once/wk, 4 times | Acupuncture, 30 min, 5 times/wk, 4 wks | WOMAC Pain Total effectiveness rate | 3.95 vs. 7.46 94.44 vs. 91.89 | <0.05 <0.05 |
| Cheng (2015) [42] | COA criteria (2007) | 56 (44.64%) | 57 | 32 | 5 | Release soft tissue adhesion, once/wk, 4 times | Sodium hyaluronate, 2 ml, once/wk, 5 wks | VAS pain JOA assessment Total effectiveness rate | 2.15 vs. 3.52 46.37 vs. 39.81 78.57 vs. 50 | <0.05 <0.05 <0.05 |
| Zhou (2015) [43] | COA criteria (2007) | 100 (64%) | 58 | 12 | 4 | Release soft tissue adhesion, once/wk, 4 times | Sodium hyaluronate, 2 ml, once/wk, 4 wks | VAS pain | 1.52 vs. 1.49 | >0.05 |
| Sun (2012) [44] | COA criteria (2007) | 90 (73.33%) | 59 | 13 | 4 | Release soft tissue adhesion, once/wk, 1–4 times, until pain relieves | Diclofenac sodium, 75 mg, once/day, 20 days, oral pill | VAS pain Total effectiveness rate | 2.76 vs. 3.84 93.33 vs. 93.33 | <0.05 <0.05 |
| Chen (2011) [45] | ACR knee OA criteria (1995) | 120 (69.17%) | 60 | 45 | 2 | Release soft tissue adhesion, once/wk, 2 times; Massage therapy, once/2 days, 14 times | Electroacupuncture, 30 min, once every other day, 7 times; massage therapy, once/2 days, 14 times | VAS pain Total effectiveness rate | 1.27 vs. 3.64 96.7 vs. 90 | <0.01 <0.05 |
| Xiong (2020) [46] | COA criteria (2007) | 60 (56.67%) | 54 | 69 | 3 | Release soft tissue adhesion, once/wk, 3 times | Celecoxib capsules, 200 mg, once/day, 3 wks | VAS pain WOMAC pain Total effectiveness rate | 5.77 vs. 4.57 11.4 vs. 9.17 90 vs. 73.33 | <0.05 <0.05 <0.05 |
| Hu (2009) [47] | ACR knee OA criteria (1995) | 80 (50%) | 66 | 67 | 4 | Release soft tissue adhesion, once/wk, 4 times | Electroacupuncture, 30 min, once/day, 4 wks | VAS pain | 3.52 vs. 5.26 | <0.05 |
| Wang (2009) [48] | ACR knee OA criteria (1995) | 60 (66.67%) | 49 | 61 | 5 | Release soft tissue adhesion, 1 time | Sodium hyaluronate, 2 ml, once/wk, 5 wks | WOMAC pain Total effectiveness rate | 1.8 vs. 5.33 93.33 vs. 73.33 | <0.01 <0.05 |

TABLE 1: Continued.

| Author (y) | Diagnostic criteria | N (female, %) | Age (%) | Disease duration (months) | Duration (wks) | Acupotomy therapy | Controls | Main outcomes | Results (treatment vs. control) | <i>p</i> value |
|-------------------|-----------------------------|---------------|---------------|---------------------------|----------------|--|--|---|--|-------------------------|
| Zeng (2009) [49] | ACR knee OA criteria (1995) | 41 (68.29%) | Not mentioned | Not mentioned | 3 | Release soft tissue adhesion, once/wk, 1-3 times, until pain relieves | Electroacupuncture, 30 min, 3 times/wk, 3 wks | VAS pain | 1.49 vs. 2.85 | <0.01 |
| Zhang (2018) [50] | COA criteria (2007) | 80 (60%) | 58 | 59 | 1 | Release soft tissue adhesion, 2 times | Celecoxib, 400 mg, once/day, 1 wk Omeprazole, 20 mg, once/day, 1 wk | VAS pain WOMAC pain | 2.54 vs. 3.56 7.3 vs. 8.93 | <0.05 <0.05 |
| Xu (2018) [51] | ACR knee OA criteria | 82 (56.10%) | 58 | 34 | 3 | Release soft tissue adhesion, once/wk, 1-3 times | Electroacupuncture, 3 times/wk, 10 times | JOA assessment | 48.9 vs. 43.2 | <0.05 |
| Meng (2017) [52] | COA criteria (2007) | 69 (44.93%) | 56 | 54 | 4 | Release soft tissue adhesion, once/wk, 4 times | Sodium hyaluronate, 2 ml, once/wk, 4 wks | WOMAC pain Total effectiveness rate | 15.36 vs. 17.55 91.67 vs. 78.79 | <0.05 <0.05 |
| Gu (2016) [53] | ACR knee OA criteria (1995) | 75 (69.33%) | 57 | 28 | 2 | Release soft tissue adhesion, once/wk, 2 times | Votalin emulsion, 3 times/day, 2 wks | VAS pain | 2.06 vs. 2.64 | <0.05 |
| Liang (2015) [54] | ACR knee OA criteria (1995) | 60 (73.33%) | 59 | 10 | 3 | Release soft tissue adhesion, once/wk, 1-3 times; functional training, 3 wks | Electroacupuncture, 3 times/wk, 10 times; functional training, 3 wks | JOA assessment | 48.26 vs. 43.94 | <0.05 |
| Liu (2012) [55] | COA criteria (2007) | 60 (51.67%) | 63 | 38 | 4 | Release soft tissue adhesion, once/wk, 1 month | Acupuncture and moxibustion, once/day, 1 month | VAS pain Lysholm's score Total effectiveness rate | 2.01 vs. 3.32 23.3 vs. 48.35 80 vs. 60 | <0.05 <0.05 <0.05 |
| Guo (2012) [56] | ACR knee OA criteria (1995) | 180 (65.56%) | 60 | 62 | 3 | Release soft tissue adhesion, once/wk, 3 wks | Electroacupuncture, 3 times/wk, 3 wks | JOA assessment | 43.66 vs. 39.27 | <0.01 |

TABLE 1: Continued.

| Author (y) | Diagnostic criteria | N (female, %) | Age (%) | Disease duration (months) | Duration (wks) | Acupotomy therapy | Controls | Main outcomes | Results (treatment vs. control) | P value |
|-------------------|-----------------------------|---------------|---------|---------------------------|----------------|---|--|--|---|----------------|
| Zhang (2011) [57] | ACR knee OA criteria (1995) | 58 (53.45%) | 53 | 20 | 3 | Release soft tissue adhesion, once/wk, 1–3 times, until pain relieves | Electroacupuncture, 3 times/wk, 3 wks | JOA assessment | 41.33 vs. 31.79 | <0.01 |
| Zhang (2007) [19] | ACR knee OA criteria (1995) | 48 (87.50%) | 61 | 31 | 3 | Release soft tissue adhesion, once/wk, 1–3 times, until pain relieves | Electroacupuncture, twice/wk, 3 wks | WOMAC pain Total effectiveness rate | 3 vs. 4.13 95.8 vs. 91.7 | <0.01 >0.05 |
| Liu (2017) [58] | Not mentioned | 88 (54.55%) | 63 | 77 | 5 | Release soft tissue adhesion, once/wk, 4 times | Sodium hyaluronate 20–30 mg, once/wk, 5 times | VAS pain Total effectiveness rate | 1.5 vs. 1.9 97.7 vs. 88.4 | <0.05 <0.05 |
| An (2018) [59] | Not mentioned | 80 (53.75%) | 47 | 30 | 3 | Release soft tissue adhesion, once/wk, 3 times | Acupuncture, 20 min, once/wk, 3 wks | VAS pain Total effectiveness rate | 2.67 vs. 4.18 92.5 vs. 67.5 | <0.05 <0.01 |
| Zhu (2019) [60] | COA criteria (2007) | 60 (60%) | 53 | 4 | 2 | Release soft tissue adhesion, once/wk, 2 times | Medium frequency electrotherapy, 6 times/wk, 2 wks | VAS pain WOMAC pain Total effectiveness rate | 2.47 vs. 2.78 5.26 vs. 6.39 89.7 vs. 82.9 | <0.05 <0.05 |

* ACR, American College of Rheumatology; COA, Chinese Orthopedic Association; y, year; N, number of patients included; VAS, visual analogue scale; WOMAC, Western Ontario and McMaster Universities Osteoarthritis Index; JOA, Japanese Orthopedic Association.
 (1) VAS pain score: 0–10; lower score = better outcome. (2) WOMAC pain score: 0–20; it was assessed with the following five items: pain during walking, stair climbing, resting, weight bearing, and pain at night. Each subscale used the following descriptors: none (0 points), mild (1 point), moderate (2 points), severe (3 points), and extreme (4 points); lower score = better outcome. (3) The total effectiveness rate (%) was defined as the quotient of the number of patients who were clinically cured, exhibited significant improvement, and exhibited improvement divided by the total number of patients. It assesses overall pain, physical function, and wellness; a higher score = better outcome. (4) Lysholm's score: 0–100, 100 points indicated no symptoms, 80–99 indicated "excellent", 70–79 indicated "good", 60–69 indicated "medium", and less than 60 indicated "poor"; higher score = better outcome. (5) Modified JOA score [57]: 0–55, including pain when walking (30 points) and pain when going up and down stairs (25 points); higher score = better outcome.

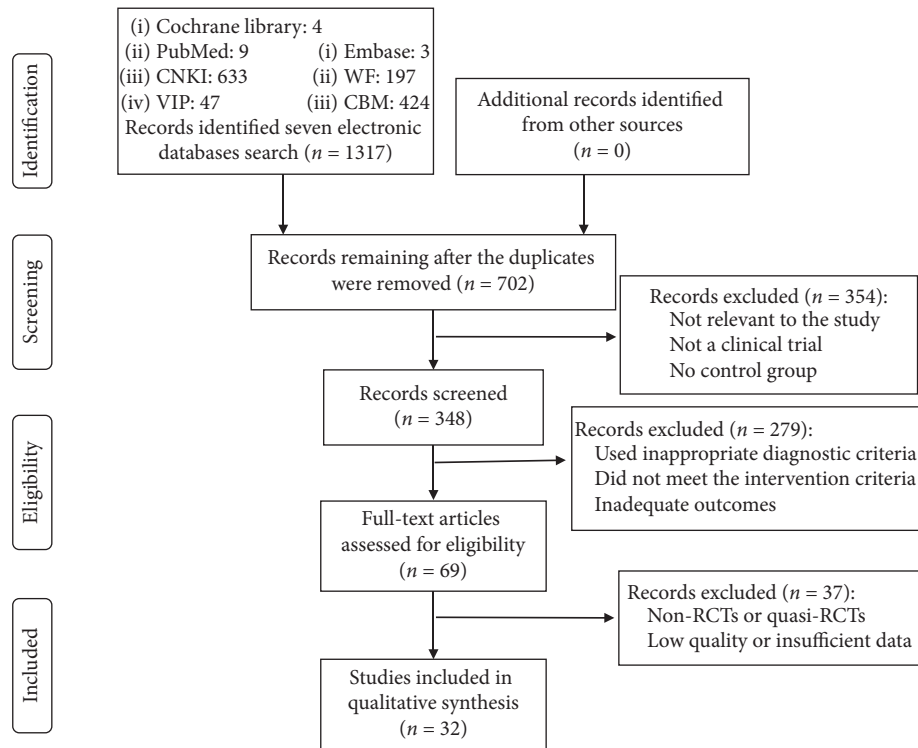


FIGURE 1: Study selection flow chart.

physical performance, and wellness using the total effectiveness rate. Three trials [30, 37, 55] used Lysholm's score and five trials [42, 51, 54, 56, 57] used the JOA score to evaluate overall pain and function.

3.3.1. VAS Pain Score. Twenty-two trials [30–34, 36, 37, 39, 40, 42–47, 49, 50, 53, 55, 58–60] involving 1969 patients were included in the meta-analysis of pain using the VAS pain score. The results of the random-effects meta-analysis indicated that the patients in the acupotomy groups had significantly lower pain scores than did those in the sodium hyaluronate injection, NSAID, acupuncture, electroacupuncture, and medium frequency electrotherapy control groups (MD = -1.11; 95% CI, -1.51 to -0.71; $p < 0.00001$) after 1–5 weeks of treatment. The level of heterogeneity (I^2) in the VAS score was 96% (Figure 4).

The subgroup analysis exploring the improvement in the VAS pain score among different control groups showed that acupotomy therapy has a larger effect than does acupuncture or electroacupuncture (MD = group analysis exploring the impro 0.0006), intraarticular sodium hyaluronate injection (MD = -1.21; 95% CI, -2.06 to -0.36; $p = 0.005$), NSAIDs (MD = -0.68; 95% CI, -0.99 to -0.37; $p < 0.0001$), and medium frequency electrotherapy (MD = -1.11; 95% CI, -1.51 to -0.71; $p = 0.01$) (Figure 4).

3.3.2. WOMAC Pain Score. Nine trials [19, 35, 38, 41, 46, 48, 50, 52, 60] involving 880 patients were included in the meta-analysis of pain using the WOMAC pain score. The results of the random-effects meta-analysis indicated that the patients

in the acupotomy groups had significantly lower pain scores than did those in the sodium hyaluronate, celecoxib, acupuncture, and electrotherapy control groups (MD = -2.32; 95% CI, -2.94 to -1.69; $p < 0.00001$) after 1–5 weeks of treatment. The level of heterogeneity (I^2) of the WOMAC pain score was 61% (Figure 5).

The subgroup analysis exploring the improvement in the WOMAC pain score among different control groups showed that acupotomy therapy had a larger effect than did acupuncture or electroacupuncture (MD = -2.44; 95% CI, -3.27 to -1.62; $p < 0.00001$), intraarticular sodium hyaluronate injection (MD = -2.57; 95% CI, -4.44 to -0.70; $p = 0.007$), NSAIDs (MD = -2.07; 95% CI, -4.62 to -0.48; $p = 0.11$), and medium frequency electrotherapy (MD = -2.10; 95% CI, -3.57 to -0.63; $p = 0.005$) (Figure 5).

3.3.3. The Total Effectiveness Rate. Twenty-three trials [19, 30–42, 44–46, 48, 52, 55, 58–60] involving 2276 patients were included in the meta-analysis of the total effectiveness rate of acupotomy compared to those of acupuncture, electroacupuncture, diclofenac sodium, intraarticular hyaluronate injection, and electrotherapy. The results from our meta-analysis with a random-effects model showed that acupotomy improved the clinical effectiveness rate by 15% (RR = 1.15; 95% CI, 1.09–1.21; $p < 0.00001$), with a moderate degree of heterogeneity ($I^2 = 54%$). Our meta-analysis showed that 2–5 weeks of acupotomy can improve clinical symptoms such as overall pain, physical performance, and wellness in patients with knee OA (Figure 6).

| | Random sequence generation (selection bias) | Allocation concealment (selection bias) | Blinding of participants and personnel (performance bias) | Blinding of outcome assessment (detection bias) | Incomplete outcome data (attrition bias) | Selective reporting (reporting bias) | Other bias |
|-------------|---|---|---|---|--|--------------------------------------|------------|
| An, 2018 | + | ? | - | ? | + | ? | ? |
| Chen, 2011 | ? | ? | - | ? | + | ? | ? |
| Cheng, 2015 | ? | ? | - | ? | + | ? | ? |
| Dai, 2018 | + | ? | - | ? | + | + | ? |
| Gu, 2016 | ? | ? | - | ? | + | + | ? |
| Guo, 2012 | + | + | + | + | + | + | ? |
| Hong, 2019 | + | ? | - | ? | + | ? | ? |
| Hu, 2009 | ? | ? | - | ? | + | ? | ? |
| Jia, 2017 | ? | ? | - | ? | + | ? | ? |
| Jin, 2020 | + | ? | - | ? | + | + | ? |
| Liang, 2015 | + | ? | - | ? | + | ? | ? |
| Li S, 2015 | + | ? | - | ? | + | ? | ? |
| Liu, 2012 | + | ? | - | ? | + | ? | ? |
| Liu, 2017 | ? | ? | - | ? | + | ? | ? |
| Li X, 2015 | ? | ? | - | ? | + | ? | ? |
| Meng, 2017 | + | ? | - | ? | + | ? | ? |
| Quan, 2016 | ? | ? | - | ? | + | ? | ? |
| Shi, 2019 | ? | ? | - | ? | + | + | ? |
| Sun, 2012 | + | ? | - | ? | + | ? | ? |
| Sun, 2016 | + | ? | - | ? | + | ? | ? |
| Sun, 2019 | ? | ? | - | ? | + | ? | ? |
| Wang, 2009 | + | ? | - | ? | + | ? | ? |
| Wang, 2016 | - | ? | - | ? | + | ? | ? |
| Xiong, 2020 | + | ? | - | ? | + | + | ? |
| Xiu, 2017 | + | ? | - | ? | + | + | ? |
| Xu, 2018 | ? | ? | - | ? | + | ? | ? |
| Zeng, 2009 | ? | ? | - | ? | + | + | ? |
| Zhang, 2007 | ? | ? | - | ? | + | ? | ? |
| Zhang, 2011 | + | ? | - | ? | + | ? | ? |
| Zhang, 2018 | ? | ? | - | ? | + | ? | ? |
| Zhou, 2015 | + | ? | - | ? | + | + | ? |
| Zhu, 2019 | + | ? | - | ? | + | ? | ? |

FIGURE 2: Risk of bias summary.

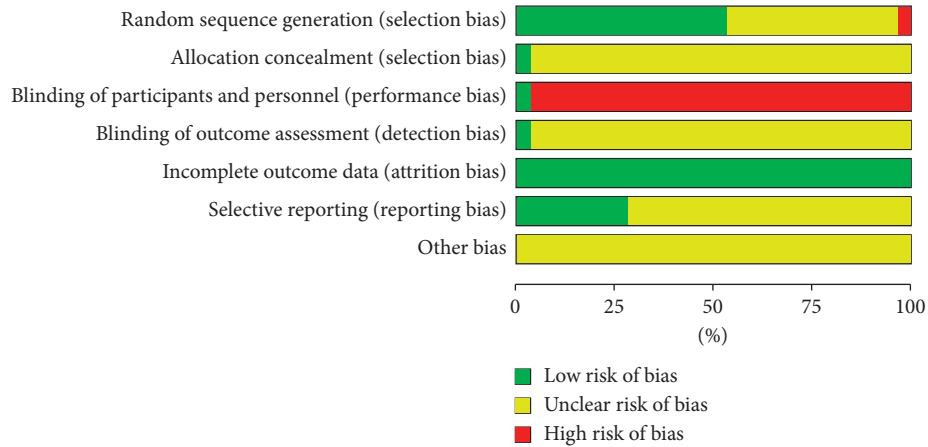


FIGURE 3: Risk of bias distribution graph.

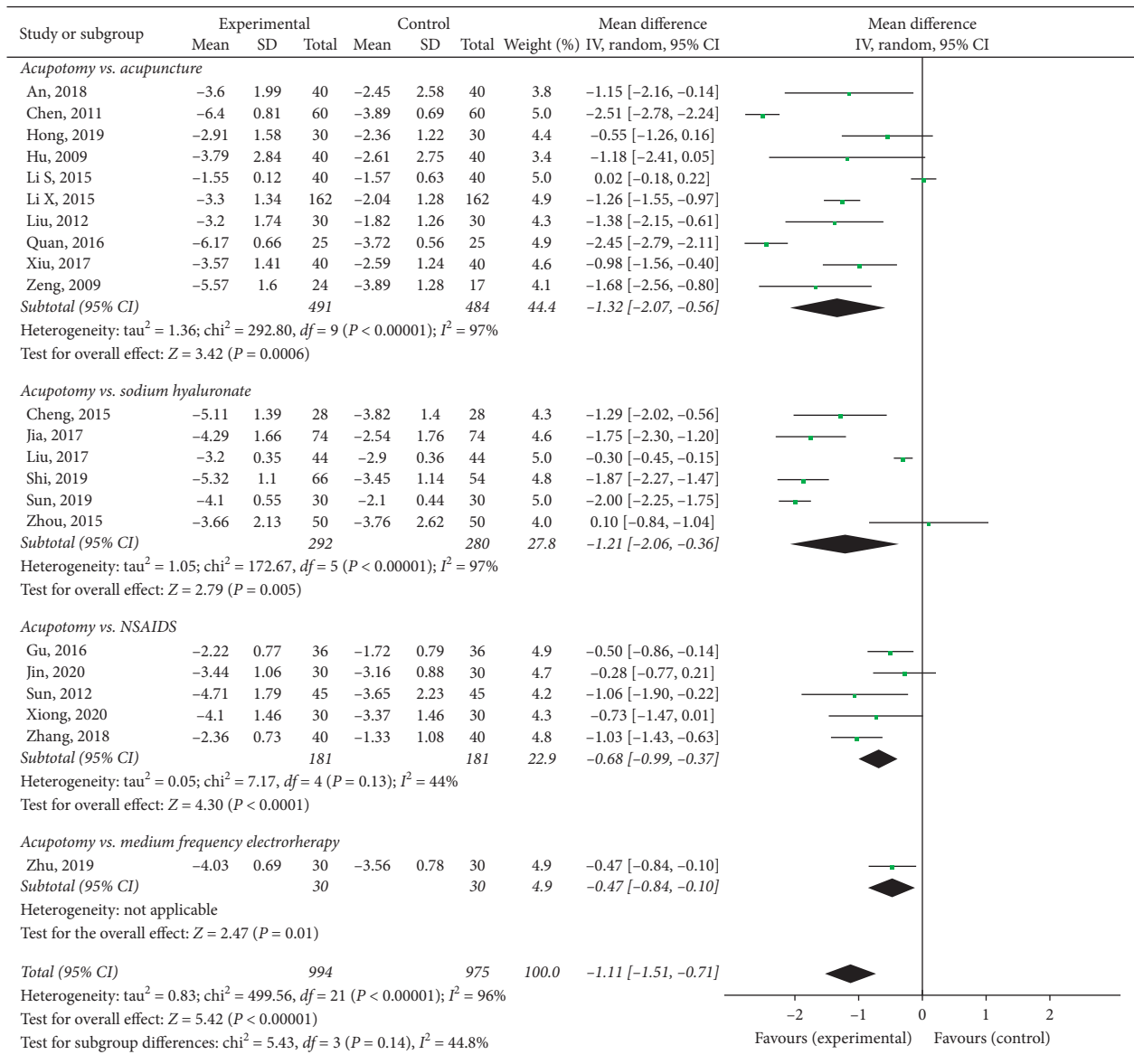


FIGURE 4: Effect of acupuncture therapy on the VAS pain score.

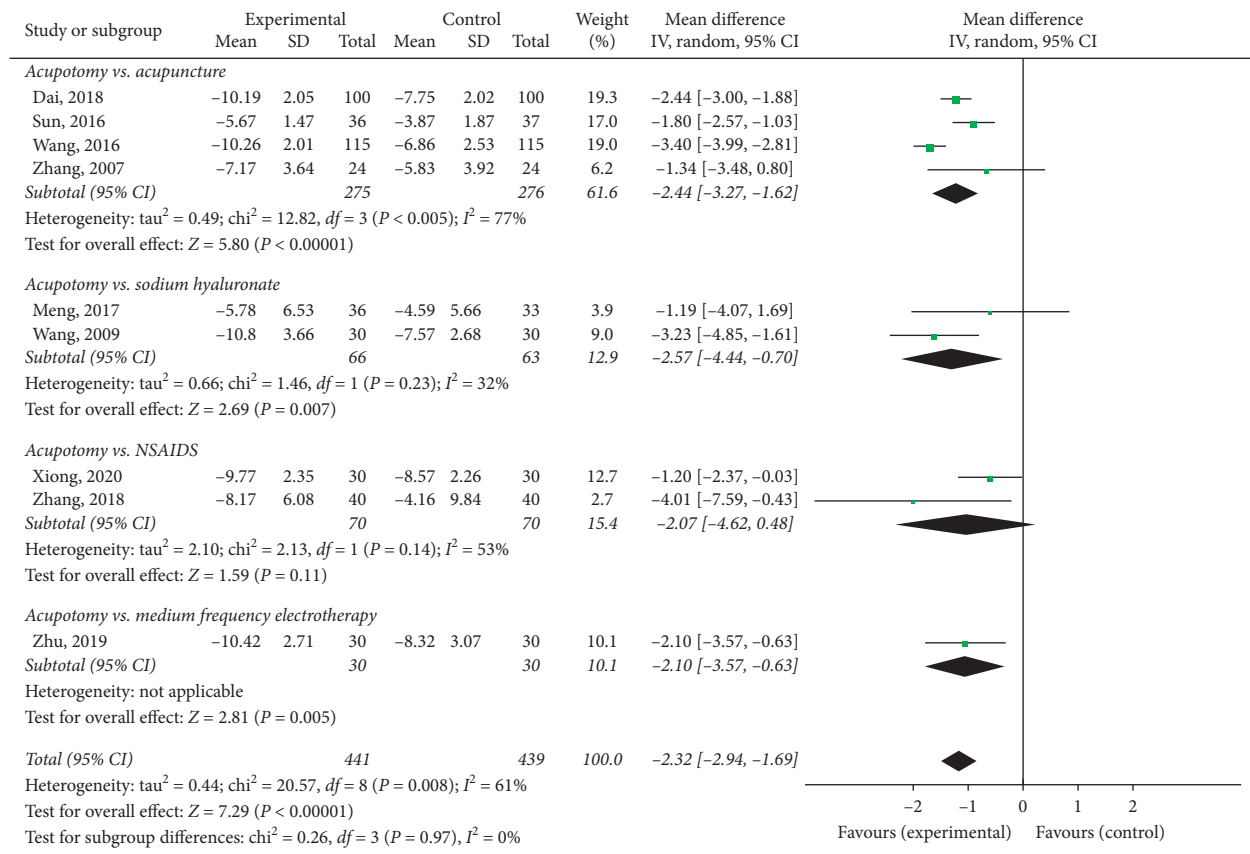


FIGURE 5: Effect of acupotomy therapy on the WOMAC pain score.

The subgroup analysis exploring the improvement in the total effectiveness rate among different control groups showed that acupotomy therapy had a larger effect than did acupuncture or electroacupuncture (RR = 1.15; 95% CI, 1.07–1.24; *p* = 0.0002), intraarticular sodium hyaluronate injection (RR = 1.18; 95% CI, 1.10–1.26; *p* < 0.00001), NSAIDs (RR = 1.06; 95% CI, 0.94–1.21; *p* = 0.34), and medium frequency electrotherapy (RR = 1.13; 95% CI, 0.89–1.44; *p* = 0.32) (Figure 6).

3.3.4. Lysholm’s Score. Three trials [30, 37, 55] involving 464 patients were included in the meta-analysis of the joint function outcomes using Lysholm’s score. The results of the random-effects meta-analysis indicated that the patients in the acupotomy groups had significantly better joint function than did those in the acupuncture control groups (MD = 12.75; 95% CI, 2.61–22.89; *p* = 0.01) after 2–4 weeks of treatment. The level of heterogeneity (*I*²) in Lysholm’s score was 98% (Figure 7).

3.3.5. JOA Score. Five trials [42, 51, 54, 56, 57] involving 436 patients were included in the meta-analysis of the pain outcomes using the JOA score. The results of the random-effects meta-analysis indicated that the patients in the acupotomy groups had significantly lower pain scores than did those in the sodium hyaluronate and acupuncture

control groups (MD = 6.39; 95% CI, 4.11–9.76; *p* < 0.00001) after 3–5 weeks of treatment. The level of heterogeneity (*I*²) in the JOA score was 78% (Figure 8).

The subgroup analysis exploring the improvement in the JOA score among different control groups showed that acupotomy therapy had a larger effect than did acupuncture or electroacupuncture (MD = 7.09; 95% CI, 3.89–10.29; *p* < 0.0001) and intraarticular sodium hyaluronate injection (RR = 5.82; 95% CI, 0.31–11.33; *p* = 0.04) (Figure 8).

4. Discussion

This systematic review and meta-analysis of 32 RCTs including 3021 individuals indicated that acupotomy therapy has larger beneficial effects than do standard Western medication, Chinese acupuncture, and electroacupuncture for knee OA. In addition, many studies have shown that acupuncture and electroacupuncture are beneficial for knee OA in alleviating pain and improving physical function [61–64]. Overall, acupotomy therapy appears to be a safe method for alleviating pain in people with knee OA.

Our findings are supported by the existing evidence. Zhao et al. [65] reported that according to 7 trials using acupotomy combined with sodium hyaluronate for 5 weeks, this combination therapy is more effective than sodium hyaluronate alone in treating knee OA. Another review of 12 RCTs by Fu et al. [66] suggested that acupotomy combined

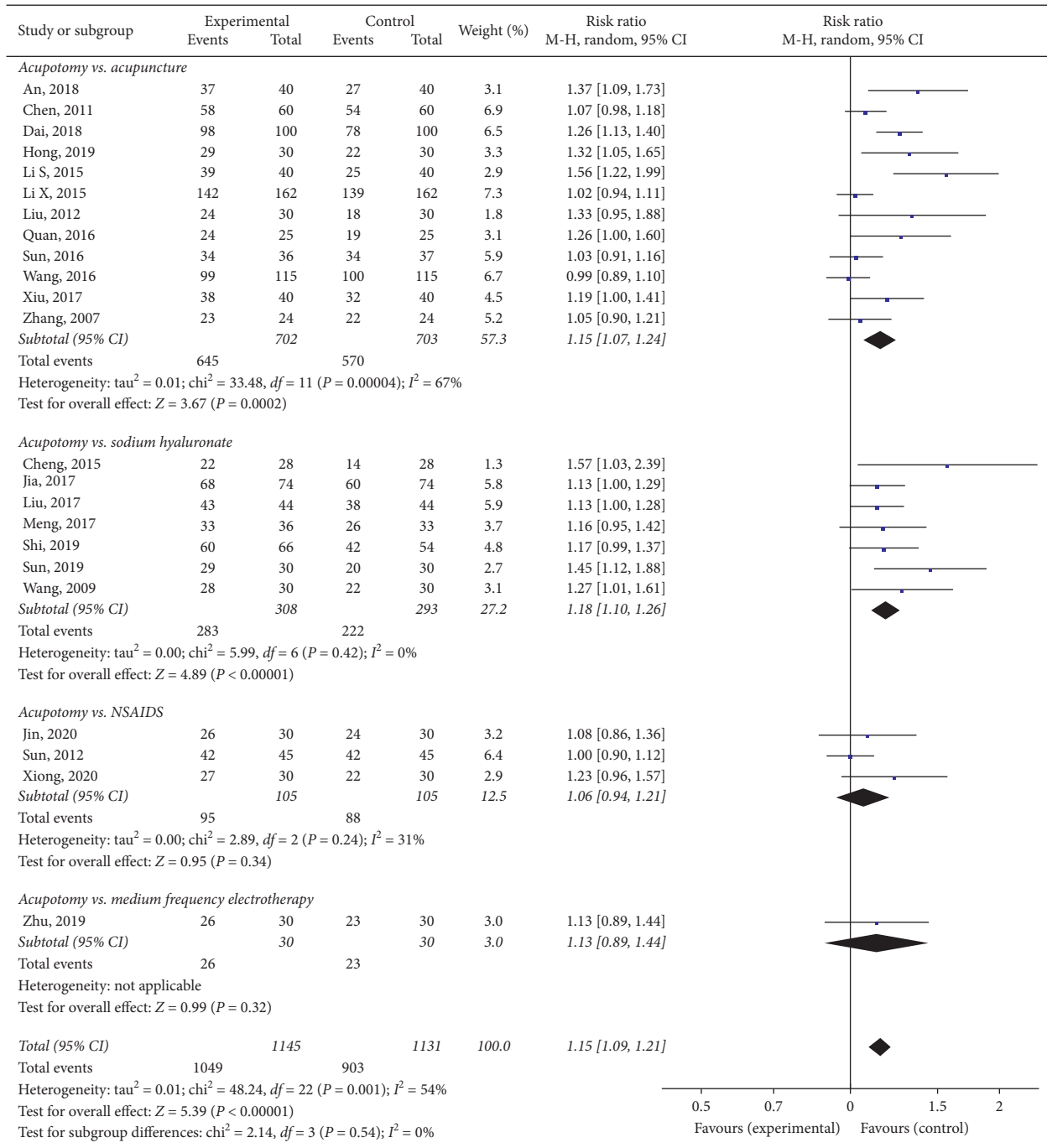


FIGURE 6: Effect of acupotomy therapy on the total effectiveness rate.

with ozone appears to have some advantages for treating knee OA. One study [67] reported that the combination of acupotomy therapy and an intraarticular injection showed better short-term and long-term effects than did the intraarticular injection only (control group). Furthermore, Cheng et al. [68] used acupotomy therapy and the bleeding method for knee OA patients, and the total effective rate reached 96.7%. The results of these reviews and studies agreed with our findings and indicated that acupotomy therapy is beneficial in reducing pain and improving the

physical function of individuals with knee OA. However, acupotomy was combined with other treatments in these reviews; so, it is hard to determine the exact effects of acupotomy alone. Our study included only RCTs that compared acupotomy with acupuncture, electroacupuncture, sodium hyaluronate, NSAIDs, or other treatments, so the effect of acupotomy on knee OA was clearer.

Despite the lack of knowledge about the biologic mechanisms of acupotomy therapy, it is likely to relieve

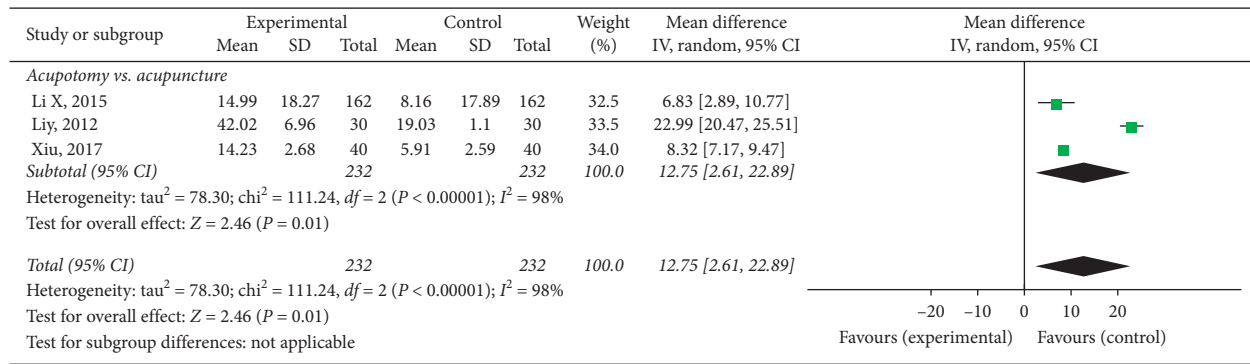


FIGURE 7: Effect of acupotomy therapy on Lysholm's score.

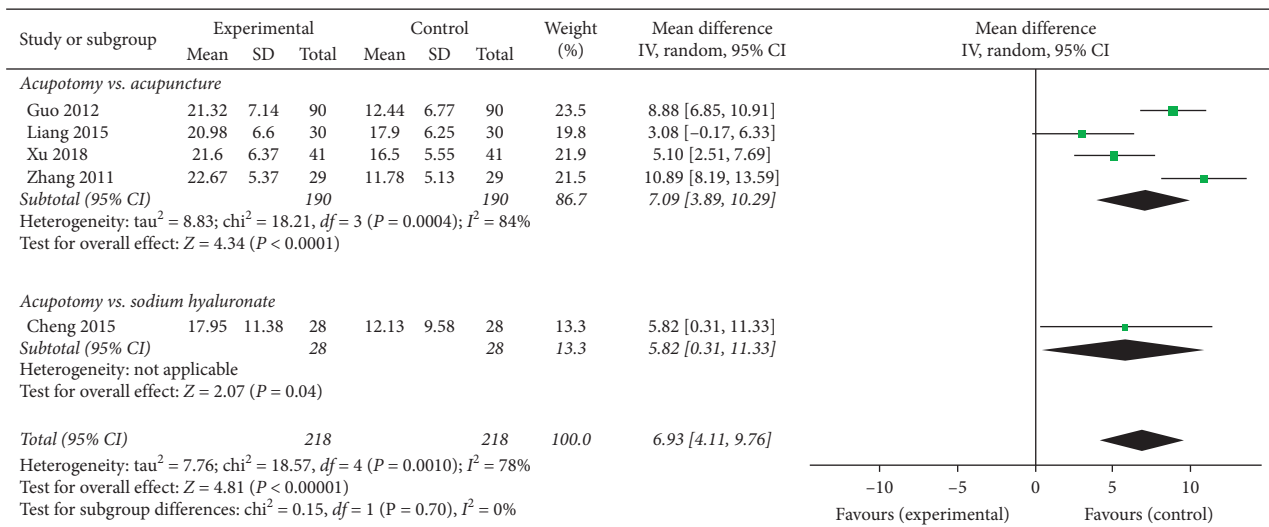


FIGURE 8: Effect of acupotomy therapy on the JOA score.

contractures in muscles and fasciae, relieve pain, and improve the function of the knee joint by releasing adhesive tissue [69]. The growing body of evidence is beginning to shed light on the potential mechanisms by which acupotomy therapy relieves the symptoms of knee OA. One study [70] showed that acupotomy can significantly reduce the magnitude of knee effusion and synovial thickness in patients with knee OA, as assessed by musculoskeletal ultrasound. One study [71] indicated that the centre of gravity is closer to the original point, and weight bearing is improved after acupotomy treatment. One animal study [72] showed that acupotomy can significantly change the behaviour and morphology and significantly improve the mechanical properties of the quadriceps femoris tendon. Recent studies [73–75] have suggested that acupotomy therapy can promote the repair of cartilage cells by activating the FAK-PI3K signalling pathway, promote cartilage cell metabolism, and regulate the PERK-eIF2 α -CHOP signalling pathway. Several studies [76, 77] have already shown an association between increases in the expression levels of the integrin β 1, col-II, and aggrecan proteins and decreases in the expression of BAX, caspase-3, and MMP-3 proteins. In addition,

acupotomy may also have an anti-inflammatory effect by suppressing the expression of inflammatory cytokines such as interleukin (IL)-1 β , IL-6, and TNF- α [20]. Overall, the mechanisms by which acupotomy relieves the symptoms of knee OA are still not clear, and there is accumulating evidence suggesting that acupotomy alters biomechanics, inhibits chondrocyte apoptosis, reduces inflammatory factors and anti-inflammation, inhibits pain signal transduction, and alleviates pain [78–80].

Our study has limitations. First, the overall methodological quality of the RCTs was moderate. Many of the included RCTs had a high risk of bias. Only one study reported double blinding and allocation concealment, and there were no placebo-controlled studies. Second, these studies were short-term, and their treatment did not exceed 6 weeks; therefore, a longer duration of follow-up is needed in future research. Third, the reporting of adverse events was insufficient. Only 1 trial [43] reported three cases of redness and swelling in a control group treated with sodium hyaluronate, and one trial [46] reported 3 cases of subcutaneous bruising after the acupotomy intervention and 2 cases of a stomach ache in the control group receiving a celecoxib capsule.

Three trials reported no adverse events, but 27 trials did not mention adverse events. Acupotomy therapy appears to be a safe method with no severe side effects, but it is important to assess adverse events in future studies. Fourth, despite the statistically significant and beneficial effects of acupotomy on pain and function in patients with knee OA, the clinically important benefits of acupotomy remain to be determined. Many challenges remain, and the potential benefits of acupotomy therapy for knee OA need to be further evaluated through clinical trials that employ more rigorous methodologies.

5. Conclusions

In summary, acupotomy therapy may be effective in reducing pain and improving the physical function of individuals with knee OA. Despite the limited quality of the trials included in this review, our study provides new and valuable information. Chinese acupotomy therapy may be effective in treating knee OA. More rigorous randomized controlled trial designs are needed in the future.

Disclosure

Jigao Sun and Yan Zhao are co-first authors.

Conflicts of Interest

The authors declare that they have no conflicts of interest.

Authors' Contributions

Weiheng Chen was involved in funding acquisition. Weiheng Chen and Jigao Sun were involved in conceptualization, review, and revision. Jigao Sun and Yan Zhao were involved in preparing original draft and in analyses. Ruizheng Zhu, Qianglong Chen, and Zhipeng Xue were involved in data extraction. Yan Zhao, Rongtian Wang, and Mengge Song were involved in quality assessment.

Acknowledgments

This study was supported by the National Science and Technology Support of China (2015BAI04B03), the China Association of Traditional Chinese Medicine (SATCM-2015-BZ402), and the Beijing Municipal Natural Science Foundation (No. 7182186).

Supplementary Materials

Additional file 1: VAS pain score funnel plot; additional file 2: WOMAC pain score funnel plot; additional file 3: the total effectiveness rate funnel plot; additional file 4: Lysholm's score funnel plot; additional file 5: JOA score funnel plot; additional file 6: image of acupotomy therapy, 0.8 mm × 80 mm (Huayou Medical Co., China). (*Supplementary Materials*)

References

- [1] D. T. Felson, "Clinical practice, osteoarthritis of the knee," *New England Journal of Medicine*, vol. 354, no. 8, pp. 841–848, 2006.
- [2] C. F. Dillon, E. K. Rasch, Q. Gu, and R. Hirsch, "Prevalence of knee osteoarthritis in the United States: arthritis data from the third national health and nutrition examination survey 1991–94," *Journal of Rheumatology*, vol. 33, no. 11, p. 2271, 2006.
- [3] Z. Jotanovic, R. Mihelic, B. Sestan, and Z. Dembic, "Emerging pathways and promising agents with possible disease modifying effect in osteoarthritis treatment," *Current Drug Targets*, vol. 15, no. 16, pp. 635–661, 2014.
- [4] R. R. Bannuru, M. C. Osani, F. Al-Eid, and C. Wang, "Efficacy of curcumin and boswellia for knee osteoarthritis: systematic review and meta-analysis," *Seminars in Arthritis and Rheumatism*, vol. 48, no. 3, pp. 416–429, 2018.
- [5] M. C. Osani, E. E. Vaysbrot, M. Zhou, T. E. McAlindon, and R. R. Bannuru, "Duration of symptom relief and early trajectory of adverse events for oral NSAIDs in knee osteoarthritis: a systematic review and meta-analysis," *Arthritis Care & Research*, vol. 72, no. 5, pp. 641–651, 2019.
- [6] M. Bally, N. Dendukuri, B. Rich et al., "Risk of acute myocardial infarction with NSAIDs in real world use: bayesian meta-analysis of individual patient data," *British Medical Journal*, vol. 357, Article ID j1909, 2017.
- [7] N. Bhalra, J. Emberson, A. Merhi, S. Abramson, N. Arber, J. A. Baron et al., "Vascular and upper gastrointestinal effects of non-steroidal anti-inflammatory drugs: meta-analyses of individual participant data from randomised trials," *Lancet (London, England)*, vol. 382, no. 9894, pp. 769–779, 2013.
- [8] C. Scarpignato, A. Lanas, C. Blandizzi, W. F. Lems, M. Hermann, and R. H. Hunt, "Safe prescribing of non-steroidal anti-inflammatory drugs in patients with osteoarthritis—an expert consensus addressing benefits as well as gastrointestinal and cardiovascular risks," *BMC Medicine*, vol. 13, p. 55, 2015.
- [9] C. Zeng, J. Wei, M. S. M. Persson et al., "Relative efficacy and safety of topical non-steroidal anti-inflammatory drugs for osteoarthritis: a systematic review and network meta-analysis of randomised controlled trials and observational studies," *British Journal of Sports Medicine*, vol. 52, no. 10, pp. 642–650, 2018.
- [10] R. R. Bannuru, M. C. Osani, E. E. Vaysbrot et al., "OARSI guidelines for the non-surgical management of knee, hip, and polyarticular osteoarthritis," *Osteoarthritis and Cartilage*, vol. 27, no. 11, pp. 1578–1589, 2019.
- [11] B. Chen, H. Zhan, J. Marszalek et al., "Traditional Chinese medications for knee osteoarthritis pain: a meta-analysis of randomized controlled trials," *The American Journal of Chinese Medicine*, vol. 44, no. 04, pp. 677–703, 2016.
- [12] B. Wang, D. Xing, S. J. Dong, R. Tie, and X. Wei, "Prevalence and disease burden of knee osteoarthritis in China: a systematic review," *Chinese Journal of Evidence-Based Medicine*, vol. 18, no. 2, pp. 134–142, 2018, in Chinese.
- [13] S. L. Kolasinski, T. Neogi, M. C. Hochberg et al., "2019 American College of rheumatology/arthritis foundation guideline for the management of osteoarthritis of the hand, hip, and knee," *Arthritis & Rheumatology*, vol. 72, no. 2, pp. 220–233, 2020.
- [14] W.-h. Callahan, X. X. Liu, X.-x. Liu, P.-j. Tong, and H.-s. Zhan, "Diagnosis and management of knee osteoarthritis: Chinese medicine expert consensus (2015)," *Chinese*

- Journal of Integrative Medicine*, vol. 22, no. 2, pp. 150–153, 2016.
- [15] H. J. Zhan, “Guiding significance of aponeurotic system theory for needle-knife in treating knee osteoarthritis,” *China Medical Herald*, vol. 13, no. 33, pp. 165–168, 2016, in Chinese.
 - [16] H. Z. Zhu, “Summarization of acupotomy system,” *Engineering Science*, vol. 8, no. 7, pp. 1–15, 2006, in Chinese.
 - [17] D. Y. Chen, J. He, X. Wang, M. C. Zhang, Y. C. Chen, and H. S. Zhan, “Clinical study of myofascial release therapy by acupotomy for nonspecific low back pain,” *Shanghai Journal of Traditional Chinese Medicine*, vol. 46, no. 6, pp. 53–54, 2012, in Chinese.
 - [18] Y. Ding, Y. Wang, X. Shi, Y. Luo, Y. Gao, and J. Pan, “Effect of ultrasound-guided acupotomy vs electro-acupuncture on knee osteoarthritis: a randomized controlled study,” *Journal of Traditional Chinese Medicine*, vol. 36, no. 4, pp. 450–455, 2016.
 - [19] Y. Zhang, C. Q. Guo, X. F. Zhang et al., “Study of the clinical efficacy of acupotomy for treating Knee Osteoarthritis: a randomized, controlled trial,” *China Science and Technology Information*, vol. 18, pp. 219–222, 2007, in Chinese.
 - [20] M. Lin, X. Li, W. Liang et al., “Needle-knife therapy improves the clinical symptoms of knee osteoarthritis by inhibiting the expression of inflammatory cytokines,” *Experimental and Therapeutic Medicine*, vol. 7, no. 4, pp. 835–842, 2014.
 - [21] J. Seungah, H. L. Jung, Mi. G. Han et al., “Efficacy and safety of miniscalpel acupuncture on knee osteoarthritis—a randomized controlled pilot trial,” *Journal of Pharmacopuncture*, vol. 21, no. 3, pp. 151–158, 2018.
 - [22] T. Fang, Q. Li, F. Zhou et al., “Effect and safety of acupotomy in treatment of knee osteoarthritis: a systematic review and Meta-analysis,” *Journal of Traditional Chinese Medicine = Chung I Tsa Chih Ying Wen pan*, vol. 40, no. 3, pp. 355–364, 2020.
 - [23] F. S. Xie, C. Q. Guo, Y. Zhang, and X. F. Jin, “Acupotomy versus intra-articular sodium hyaluronate for knee osteoarthritis: a systematic review and meta-analysis,” *China Journal of Traditional Chinese Medicine & Pharmacy*, vol. 27, no. 4, pp. 999–1003, 2012, in Chinese.
 - [24] F. S. Liu, D. Z. Jin, and X. Wu, “Acupotomy versus acupuncture for knee osteoarthritis: a Meta-analysis of randomized controlled trials,” *Chinese Journal of Tissue Engineering Research*, vol. 16, no. 44, pp. 8235–8239, 2012, in Chinese.
 - [25] M. C. Hochberg, R. D. Altman, K. D. Brandt et al., “Guidelines for the medical management of osteoarthritis,” *Arthritis & Rheumatism*, vol. 38, no. 11, pp. 1535–1540, 1995.
 - [26] Chinese Orthopaedic Association, “Diagnosis and treatment of osteoarthritis,” *Orthopaedic Surgery*, vol. 2, no. 1, pp. 1–6, 2010.
 - [27] Chinese Orthopaedic Association, “Guidelines for the diagnosis and treatment of osteoarthritis (2018 edition),” *Chinese Journal of Orthopaedics*, vol. 38, no. 12, pp. 705–715, 2018.
 - [28] X. Y. Moskowitz, *Guiding Principle of Clinical Research on New Drugs of Traditional Chinese Medicine*, pp. 349–353, ScienceOpen, Inc., Burlington, MA, USA, 2002.
 - [29] J. P. T. Higgins, D. G. Altman, J. A. C. Sterne et al., “Chapter 8: Assessing risk of bias in included studies,” *Higgins JPT, Green S. Cochrane Handbook for Systematic Reviews of Interventions Version 5.1.0*, The Cochrane Collaboration, London, UK, 2011, <http://www.cochrane-handbook.org>.
 - [30] X. J. Li and H. D. Wang, “Treating 162 cases of knee osteoarthritis by needle-knife lysis based on position differentiation and points fixed,” *Western Journal of Traditional Chinese Medicine*, vol. 28, no. 6, pp. 118–120, 2015, in Chinese.
 - [31] S. F. Li, Z. P. Lin, P. Lu, and X. Z. Chen, “Clinical research on treating knee osteoarthritis by small knife acupuncture,” *Clinical Journal of Chinese Medicine*, vol. 7, no. 34, pp. 39–40, 2015, in Chinese.
 - [32] X. J. Sun, “Clinical application of acupotomy in the treatment of knee osteoarthritis,” *World Latest Medicine Information*, vol. 19, no. 41, pp. 19–20, 2019, in Chinese.
 - [33] X. M. Shi and Y. D. Liu, “Short-term effect of needle-knife therapy on relieving symptoms of knee osteoarthritis,” *Journal of Guangzhou University of Traditional Chinese Medicine*, vol. 36, no. 1, pp. 74–78, 2019, in Chinese.
 - [34] H. Q. Hong, C. R. Zhang, D. C. Chen, Z. J. Hua, P. Wang, and Z. Z. Ruan, “Clinical effect of needle-knife in the treatment of knee osteoarthritis,” *China Medical Herald*, vol. 16, no. 9, pp. 162–169, 2019, in Chinese.
 - [35] X. Wang, S. Y. Liu, Y. Shi et al., “Clinical observation on acupotomy surgery for the treatment of knee osteoarthritis,” *China Journal of Orthopaedics and Traumatology*, vol. 29, no. 4, pp. 345–349, 2016, in Chinese.
 - [36] X. Jin, B. Nie, Y. Liu et al., “Clinical observation of acupotomy combined manipulation in the treatment of knee osteoarthritis,” *Guide to Traditional Chinese Medicine*, vol. 26, no. 7, pp. 35–37, 2020, in Chinese.
 - [37] Z. B. Xiu, C. X. Zhang, H. Liu, L. Z. Zhang, J. Liu, and A. H. Lu, “Clinical effect observation and mechanism discussion on needle knife release in treatment of knee osteoarthritis,” *Journal of Liaoning University of Traditional Chinese Medicine*, vol. 20, no. 1, pp. 15–18, 2018, in Chinese.
 - [38] D. F. Dai, C. S. Bao, F. Qin, and J. H. Yuan, “Clinical observation of acupotomy in the treatment of knee osteoarthritis,” *Chinese Journal of Primary Medicine and Pharmacy*, vol. 25, no. 12, pp. 1609–1611, 2018, in Chinese.
 - [39] M. Jai, “Clinical observation on acupotomy surgery for the treatment of knee osteoarthritis,” *Heilongjiang Medicine Journal*, vol. 30, no. 6, pp. 1391–1393, 2017, in Chinese.
 - [40] Ke. Quan, D. F. He, and M. T. Li, “Clinical analysis of needle-knife in the treatment of osteoarthritis in knee joint,” *China Practical Medicine*, vol. 11, no. 36, pp. 45–47, 2016, in Chinese.
 - [41] K. Sun, X. M. Bao, Y. C. Song, S. B. Wu, F. Zhang, and G. F. Hu, “Clinical efficacy evaluation on the treatment of knee osteoarthritis by acupotomy,” *Journal of Clinical Acupuncture & Moxibustion*, vol. 32, no. 10, pp. 44–47, 2016, in Chinese.
 - [42] W. Cheng and Y. H. Zhang, “Treating 28 cases of knee osteoarthritis by acupotomy surgery,” *Henan Traditional Chinese Medicine*, vol. 35, no. 7, pp. 1578–1579, 2015, in Chinese.
 - [43] L. Zhou and Y. Mu, “Clinical efficacy and safety evaluation of needle knife treatment for knee osteoarthritis,” *Journal of Clinical Acupuncture and Moxibustion*, vol. 31, no. 5, pp. 34–36, 2015, in Chinese.
 - [44] K. Sun, D. C. Liu, S. B. Wu, Y. C. Song, and Z. L. Zhou, “Clinical study of acupotomy in treating pain and dysfunction of knee osteoarthritis,” *Clinical Journal of Traditional Chinese Medicine*, vol. 24, no. 5, pp. 416–418, 2012, in Chinese.
 - [45] M. Chen, X. Y. Shi, Y. H. Gu, B. Xu, and L. F. Xu, “Clinical study on acupotomy in treating 60 cases of knee osteoarthritis,” *Journal of Nanjing University of Traditional Chinese Medicine*, vol. 27, no. 4, pp. 384–386, 2011, in Chinese.
 - [46] Y. Z. Xiong, J. C. Zhu, C. Wang et al., “Clinical efficacy of needle-knife combined with Celecoxib in treating knee

- osteoarthritis,” *Chinese Journal of Orthopedics and Traumatology*, vol. 28, no. 2, pp. 19–23, 2020, in Chinese.
- [47] S. R. Hu, L. H. Yin, and W. Y. Li, “Clinical study on the improvement of Knee osteoarthritis by acupotomy surgery,” *Jiangxi Medical Journal*, vol. 44, no. 11, pp. 1093–1095, 200, in Chinese.
- [48] L. K. Wang and J. L. Qiao, “A randomized controlled clinical study of acupotomy and sodium hyaluronate injection in the treatment of knee osteoarthritis-Annex: a report of 60 cases,” *Journal of Chengdu University of Traditional Chinese*, vol. 32, no. 1, pp. 22–25, 2009, in Chinese.
- [49] G. G. Zeng, X. F. Zhang, W. C. Quan, W. L. Qin, Y. Y. Fu, and Q. G. Liu, “Effects of needle knife relaxing therapy on stress stimulation and clinical symptoms of knee osteoarthritis,” *Chinese Archives of Traditional Chinese Medicine*, vol. 27, no. 1, pp. 66–68, 2009, in Chinese.
- [50] Z. Q. Zhang, B. Q. Zhang, J. W. Liu, and D. Guo Clinical, “Effects of injection needle scalpel therapy on knee osteoarthritis at early stage,” *Modern Hospital*, vol. 18, no. 7, pp. 1052–1054, 2018, in Chinese.
- [51] X. Xu, “Effect of acupotomy on the early pain of knee osteoarthritis,” *Shenzhen Journal of Integrated Traditional Chinese and Western Medicine*, vol. 28, no. 6, pp. 60–62, 2018, in Chinese.
- [52] F. Meng, Y. Yin, T. F. Wang, and L. Feng, “Therapeutic effects of small needle knife on knee osteoarthritis and its effects on the expression levels of TNF- α , MMPs in joint synovial fluid of patients,” *Hebei Medical Journal*, vol. 39, no. 2, pp. 168–172, 2017, in Chinese.
- [53] L. J. Gu, W. H. Li, B. Zhang, Y. Tang, W. K. Qin, and F. H. Dong, “Observation on the short-term clinical curative effect of release with stiletto needle versus knife needle for treatment of early-middle knee osteoarthritis,” *The Journal of Traditional Chinese Orthopedics and Traumatology*, vol. 28, no. 9, pp. 30–34, 2016, in Chinese.
- [54] C. Liang, J. Y. Cai, L. Yan et al., “Evaluation of the curative effect of needle-knife therapy for relieving knee pain in patients with early knee osteoarthritis,” *The Journal of Traditional Chinese Orthopedics and Traumatology*, vol. 27, no. 9, pp. 9–14, 2015, in Chinese.
- [55] M. R. Liu, L. Li, and Z. W. He, “Efficacy observation on osteoarthritis of the knee treated with the ultrastructural acupotomy therapy at the counter-Ashi points,” *Chinese Acupuncture & Moxibustion*, vol. 32, no. 7, pp. 621–624, 2012, in Chinese.
- [56] C. Q. Guo, T. Si, J. M. Wen et al., “Effects of acupotomy therapy on the pain symptoms in patients with knee osteoarthritis: a randomized controlled clinical trial,” *Tianjin Journal of Traditional Chinese Medicine*, vol. 29, no. 1, pp. 35–38, 2012, in Chinese.
- [57] X. F. Zhang, W. C. Quan, S. Peng, Y. B. Wang, T. J. Chen, and L. H. Li, “Effects of acupotomy on the footplate pressure and X ray manifestations in the treatment of knee osteoarthritis,” *Medical Journal of the Chinese People’s Armed Police Forces*, vol. 109, no. 44, pp. 21028–21039, 2011, in Chinese.
- [58] Z. L. Liu, “Research on pathogenesis of knee joint osteoarthritis and study on curative effect of needle knife therapy,” *China & Foreign Medical Treatment*, vol. 36, no. 20, pp. 33–37, 2017, in Chinese.
- [59] J. H. An, Q. H. Hua, and H. D. Wang, “Effect of acupotomy on pain relief and joint function improvement in patients with knee joint disease,” *Internal Medicine*, vol. 13, no. 4, pp. 565–567, 2018, in Chinese.
- [60] F. F. Zhu, B. Dong, P. W. Yuan et al., “Clinical study on treatment of early knee osteoarthritis with small needle knife therapy Modern,” *Journal of Integrated Traditional Chinese and Western Medicine*, vol. 28, no. 31, pp. 3421–3425, 2019, in Chinese.
- [61] M. S. Corbett, S. J. C. Rice, V. Madurasinghe et al., “Acupuncture and other physical treatments for the relief of pain due to osteoarthritis of the knee: network meta-analysis,” *Osteoarthritis and Cartilage*, vol. 21, no. 9, pp. 1290–1298, 2013.
- [62] Q. Zhang, J. Yue, B. Golianu, Z. Sun, and Y. Lu, “Updated systematic review and meta-analysis of acupuncture for chronic knee pain,” *Acupuncture in Medicine*, vol. 35, no. 6, pp. 392–403, 2017.
- [63] H. MacPherson, E. Vertosick, G. Lewith et al., “Influence of control group on effect size in trials of acupuncture for chronic pain: a secondary analysis of an individual patient data meta-analysis,” *PLoS One*, vol. 9, no. 4, Article ID e93739, 2014.
- [64] N. Chen, J. Wang, A. Mucelli, X. Zhang, and C. Wang, “Electro-acupuncture is beneficial for knee osteoarthritis: the evidence from meta-analysis of randomized controlled trials,” *The American Journal of Chinese Medicine*, vol. 45, no. 5, pp. 965–985, 2017.
- [65] J. Zhao, Q. F. Wang, Y. F. Ma et al., “Meta-analysis on efficacy of acupotomy combined with sodium hyaluronate versus sodium hyaluronate in treating knee osteoarthritis,” *Chinese Journal of Traditional Medical Traumatology & Orthopedics*, vol. 22, no. 2, pp. 15–20, 2014, in Chinese.
- [66] F. Y. Fu, H. L. Ye, Z. X. Jia, M. G. Song, and W. H. Chen, “Meta-analysis of efficacy of acupotomy combined with ozone in treatment of knee osteoarthritis,” *Journal of Hainan Medical University*, vol. 25, no. 23, pp. 1811–1817, 2019, in Chinese.
- [67] S. F. Chen, K. Q. Wang, and H. M. Zhang, “Clinical study of articular cavity injection combined with needle knife for the knee osteoarthritis,” *Guiding Journal of Traditional Chinese Medicine & Pharmacy*, vol. 23, no. 23, pp. 87–90, 2017, in Chinese.
- [68] Y. Cheng, K. Wu, Z. Cheng et al., “Randomized controlled study on the treatment of knee osteoarthritis with different acupuncture methods at different stages,” *Zhongguo Zhen Jiu*, vol. 33, no. 6, pp. 508–512, 2013, in Chinese.
- [69] G. Li, B. Zhu, X. Li, and X. Chen, “Acupotomy therapy’s effect and mechanism in knee osteoarthritis,” *World Chinese Medicine*, vol. 11, no. 6, pp. 1077–1081, 2016, in Chinese.
- [70] J. Y. Li, “Objective to investigate the soft tissue changes of knee osteoarthritis treated by acupotomy with musculoskeletal ultrasound,” *Hubei Journal of Traditional Chinese Medicine*, vol. 37, no. 8, pp. 51–52, 2015, in Chinese.
- [71] L. J. Gu, B. Zhang, W. H. Li, Y. Tang, and F. H. Dong, “Stiletto needle and needle-knife for influence of gravity index in treating knee osteoarthritis,” *Zhongguo Gu Shang*, vol. 30, no. 12, pp. 1091–1096, 2017.
- [72] L. J. Wang, X. W. Shi, W. Zhang, T. Wang, S. Zhou, and C. Q. Guo, “Effect of needle knife intervention on tensile mechanics of femoral quadriceps tendon in rabbits with knee osteoarthritis,” *Zhongguo Gu Shang*, vol. 32, no. 5, pp. 462–468, 2019.
- [73] S. N. Ma, Z. G. Xie, Y. Guo et al., “Effect of acupotomy on FAK-PI3K signaling pathways in KOA rabbit articular cartilages,” *Evidence-Based Complementary and Alternative Medicine*, vol. 2017, Article ID 4535326, 11 pages, 2017.

- [74] N. G. Liu, J. N. Yu, B. Hu, Y. Guo, and C. Q. Guo, "Phosphorylated focal adhesion kinase, phosphoinositides 3 kinase and aggrecan genes and proteins in cartilage cells are probably involved in needle knife intervention induced improvement of knee osteoarthritis in rabbits," *Zhen Ci Yan Jiu*, vol. 43, no. 4, pp. 221–225, 2018.
- [75] Y.-h. Yang, T.-h. Liu, L.-d. Zhang, Z.-y. Chen, and X.-s. Huang, "Role of the PERK-eIF2 α -CHOP signaling pathway in the effect of needle knife therapy on knee joint chondrocyte apoptosis," *Evidence-Based Complementary and Alternative Medicine*, vol. 2019, Article ID 7164916, 7 pages, 2019.
- [76] C. X. Liang, Y. Guo, L. Tao et al., "Effects of acupotomy intervention on regional pathological changes and expression of cartilage-mechanics related proteins in rabbits with knee osteoarthritis," *Zhen Ci Yan Jiu*, vol. 40, no. 2, pp. 119–124, 2015.
- [77] Y. R. Huang, Y. L. Jin, N. Li et al., "Effects of acupotomy, electroacupuncture or round-sharp acupuncture needle interventions on expression of Bcl-2, Bax, Caspase-3 proteins of rectus femoris in rabbits with knee osteoarthritis," *Zhen Ci Yan Jiu*, vol. 39, no. 2, pp. 100–105, 2014.
- [78] M. L. Zhao, Y. H. Bai, Y. Zhang, and W. M. Shi, "Advances in the treatment of knee osteoarthritis with small needle knife," *Hebei Journal of Traditional Chinese Medicine*, vol. 39, no. 12, pp. 1908–1912, 2017, in Chinese.
- [79] Z. J. Niu, W. Shen, and L. M. Xie, "Parallel control study of needle-knife combined with traditional Chinese medicine hot compress and simple needle knife in the treatment of knee osteoarthritis with cold-damp blocking syndrome," *Journal of Clinical and Experimental Medicine*, vol. 18, no. 12, pp. 1297–1301, 2019, in Chinese.
- [80] A. C. Niu, J. M. Wu, and N. Li Research, "Progress of the effect and mechanisms of needle-knife on knee osteoarthritis," *Asia-Pacific Traditional Medicine*, vol. 12, no. 7, pp. 76–78, 2016, in Chinese.

Research Article

***In Vitro* Antiosteoporosis Activity and Hepatotoxicity Evaluation in Zebrafish Larvae of Bark Extracts of *Prunus jamasakura* Medicinal Plant**

Richard Komakech,^{1,2,3} Ki-Shuk Shim,⁴ Nam-Hui Yim,⁵ Jun Ho Song,¹ Sun Kyu Yang,¹ Goya Choi,¹ Jun Lee,^{1,2} Yong-goo Kim,¹ Francis Omujal,³ Moses Agwaya,³ Grace Kyeyune Nambatya,³ Hyemin Kan,⁶ Kyu-Seok Hwang,⁶ Gilbert Matsabisa Motlalepula,⁷ and Youngmin Kang^{1,2}

¹Herbal Medicine Resources Research Center, Korea Institute of Oriental Medicine (KIOM), 111 Geonjae-ro, Naju-si, Jeollanam-do 58245, Republic of Korea

²University of Science & Technology (UST), Korean Convergence Medicine Major, KIOM, 1672 Yuseongdae-ro, Yuseong-gu, Daejeon 34054, Republic of Korea

³Natural Chemotherapeutics Research Institute (NCRI), Ministry of Health, P.O. Box 4864, Kampala, Uganda

⁴Korea Institute of Oriental Medicine (KIOM), 1672 Yuseongdae-ro, Yuseong-gu, Daejeon 34054, Republic of Korea

⁵Korean Medicine Application Center, Korea Institute of Oriental Medicine, 70 Cheomdan-ro, Dong-gu, Daegu 41062, Republic of Korea

⁶Bio & Drug Discovery Division, Korea Research Institute of Chemical Technology, Daejeon, Republic of Korea

⁷IKS Research Group, Department of Pharmacology, Faculty of Health Sciences, University of the Free State, Bloemfontein 9301, Free State, South Africa

Correspondence should be addressed to Youngmin Kang; ymkang@kiom.re.kr

Received 15 July 2020; Revised 25 August 2020; Accepted 3 September 2020; Published 24 September 2020

Academic Editor: Arham Shabbir

Copyright © 2020 Richard Komakech et al. This is an open access article distributed under the Creative Commons Attribution License, which permits unrestricted use, distribution, and reproduction in any medium, provided the original work is properly cited.

Osteoporosis is one of the main health problems in the world today characterized by low bone mass and deterioration in bone microarchitecture. In recent years, the use of natural products approach to treat it has been in the increase. In this study, *in vitro* antiosteoporosis activity and hepatotoxicity of *P. jamasakura* bark extracts were evaluated. *Methods.* Mouse bone marrow macrophage (BMM) cells were incubated with tartrate-resistant acid phosphate (TRAP) buffers and *p*-nitrophenyl phosphate and cultured with different *P. jamasakura* bark extracts at concentrations of 0, 6.25, 12.5, 25, and 50 $\mu\text{g}/\text{ml}$ in the presence of the receptor activator of nuclear factor kappa-B ligand (RANKL) for 6 days. The osteoclast TRAP activity and cell viability were measured. Nitric oxide (NO) assay was conducted using murine macrophage-like RAW 264.7 cells treated with *P. jamasakura* ethanolic and methanolic bark extracts at concentrations of 0, 6.25, 12.5, 25, 50, 100, and 200 $\mu\text{g}/\text{ml}$. For hepatotoxicity assessment, zebrafish larvae were exposed to *P. jamasakura* bark extracts, 0.05% dimethyl sulfoxide as a negative control, and 5 μM tamoxifen as a positive control. The surviving larvae were anesthetized and assessed for hepatocyte apoptosis. *Results.* TRAP activity was significantly inhibited ($p < 0.001$) at all concentrations of *P. jamasakura* extracts compared to the control treatment. At 50 $\mu\text{g}/\text{ml}$, both ethanolic and methanolic extracts of *P. jamasakura* exhibited significant ($p < 0.01$) BMM cell viability compared to the control treatment. *P. jamasakura* ethanolic and methanolic extracts had significant inhibitory ($p < 0.01$) effects on lipopolysaccharide (LPS)-induced NO production at 200 $\mu\text{g}/\text{ml}$ and exhibited significant ($p < 0.01$) and ($p < 0.05$) stimulative effects, respectively, on RAW 264.7 cell viability. No overt hepatotoxicity was observed in the liver of zebrafish larvae in any of the treatments. *Conclusion.* The TRAP activity of *P. jamasakura* bark gives a foundation for further studies to enhance future development of antiosteoporosis drug.

1. Introduction

Osteoporosis is a major global public health problem characterized by low bone mass and a deterioration of bone microarchitecture [1]. People suffering from an osteoporosis have increased risk of fractures [2, 3]. It is one of the major causes of morbidity in older people [4] due to imbalance between the bone formation and resorption rate [3]. Several factors have been associated with an increased risk of osteoporosis, including menopause, sex steroid deficiency, and aging [2, 3]. Chronic inflammation has long been associated with a broad range of noninfectious diseases [5], and recent studies suggest that inflammation is one of the key factors that influence bone turnover, leading to osteoporosis [4, 6]. In fact, proinflammatory cytokines have been implicated as primary mediators of accelerated bone loss during menopause [7]. Currently, the treatment of osteoporosis focuses on inhibition of bone resorption by osteoclasts and/or increase in bone formation by osteoblasts [1]. A number of conventional treatment options for osteoporosis are available such as bisphosphonates and estrogen but their adverse effects including burning sensation and gastrointestinal tract disturbances associated with these therapies limit their use [8]. Consequently, exploring the use of natural products in the treatment of osteoporosis may offer a better alternative to avoid the side effects of the conventional therapies [8]. Over the years, herbal medicines have been used to treat osteoporosis [1, 9] and as a crucial substitute of anti-inflammatory drugs [10]. The plants used in traditional medicine for the treatment of inflammation- and osteoporosis-related conditions are those of *Prunus* (family Rosaceae), including *Prunus jamasakura* f. *hortensis* (Maxim.) (Koidz) (Scientific synonym *Prunus x lannesiana* (Carrière) E. H. Wilson) [11]. *P. jamasakura* is native to Korea and Japan and has been used to treat several diseases in folk medicine including inflammatory diseases [12], cough, and food poisoning [11]. These medicinal activities have been attributed to several compounds including sakuranetin, sakuranin, naringenin, and genistein, found in its stem bark (Pruni cortex) [11].

Despite its myriad therapeutic uses, there are currently no studies on the antiosteoporosis activity of *P. jamasakura*. Hence, this study evaluated the *in vitro* antiosteoporosis activity of the ethanolic and methanolic bark extracts of *P. jamasakura*. In addition, we evaluated the hepatotoxicity of the extracts in zebrafish (*Danio rerio*) larvae and conducted the HPLC chemical profiling of the compounds in the extracts. This study may therefore provide the foundation for further studies regarding *P. jamasakura* for future drug development to treat and manage osteoporosis.

2. Materials and Methods

2.1. Chemicals. All of the chemicals and solvents used in this study were of analytical grade. Acetonitrile (Fisher Scientific,

UK) and trifluoroacetic acid (Sigma-Aldrich, USA) were of HPLC grade. Ultrapure water from a Milli-Q system (Millipore, USA) was used for the mobile phase preparation. Naringenin, genistein, and sakuranetin were purchased from ChemFaces (Wuhan, Hubei, China) and were used as the standard components.

2.2. Plant Material and Preparation of Extract. The stem bark of *P. jamasakura* (Pruni cortex) was procured from Daejeon, South Korea. The voucher specimen number KIOM201501013821A was deposited in the Korean Herbarium of Standard Herbal Resources (Index Herbarium Code: KIOM) at the Korea Institute of Oriental Medicine (KIOM), South Korea. The stem bark of the sample was ground using a steel pulverizing machine (250G New Type Pulverizing Machine, Model RT-N04-2V, Taiwan) at 25,000 rpm to obtain a fine powder. The maceration and concentration process was done following the previous method [13]. 30 g of the fine powder was extracted via maceration using 600 ml of 100% methanol, 100% ethanol, and distilled water. The extracts were filtered using Whatman filter no. 1 after 24 h and concentrated under a vacuum reduced pressure at 40°C, 70 rpm, using an EYELA N-1200B (Tokyo Rikakikai Co. Ltd., Japan) efficient rotary evaporator. The concentrated extract was then vacuum dried. The resultant dried extract was used for subsequent HPLC phytochemical analysis, nitric oxide (NO) assay, tartrate-resistant acid phosphatase (TRAP) assay, and hepatotoxicity evaluation.

2.3. HPLC Chemical Profiles of *Prunus jamasakura*. The method used was modified from that of the previous study [13]. The chemical standards naringenin, genistein, and sakuranetin used in this study were each dissolved in methanol at 1 mg/ml to make a stock solution and then further diluted to 20 µg/ml in methanol for the HPLC analysis. Similarly, *P. jamasakura* extracts were dissolved in methanol at 10 mg/ml and filtered using a 0.2 mm syringe membrane filter (Whatman Ltd., Maidstone, UK) for analysis. Separation was performed using an HPLC system (Dionex Ultimate 3000; Thermo Fisher Scientific, Sunnyvale, CA, USA) comprising a pump, an auto sampler, a column oven, and a diode array UV/VIS detector. The chromatograms were analyzed using the Chromeleon software system (version 7). The components of the *P. jamasakura* extracts were separated using a Gemini C₁₈ column (4.6 × 250 mm, 5 µm) (Phenomenex, Torrance, CA, USA) at 40°C. An injection volume of 10 µl was used at a detection wavelength of 280 nm. The mobile phase, consisting of ultrapure water with 0.1% trifluoroacetic acid (A) and acetonitrile (B), was eluted at a flow rate of 1.0 ml/min. The gradient elution program used was as follows: 3% (v/v) B at 0–2 min; 3–35% (B) at 2–30 min; 35–50% (B) at 30–31 min; 50% (B) at 31–35 min; 50–100% (B) at 35–40 min; and 100% (B) at 40–45 min.

2.4. Inhibitory Effect of *P. jamasakura* on No Generation and Osteoclastogenesis

2.4.1. Cell Culture. Murine macrophage-like RAW 264.7 cells (ATCC; Manassas, VA, USA) were cultured in Dulbecco's modified Eagle medium supplemented with 10% fetal bovine serum (FBS) and 1% antibiotics following previously described method [13]. Mouse bone marrow macrophages (BMMs) were cultured in a proliferation medium (an α -MEM medium with 10% FBS and macrophage-colony stimulating factor (M-CSF) (60 ng/ml)) following the previously described method [14, 15]. To differentiate the osteoclasts, BMMs were cultured in a proliferation medium with RANKL (100 ng/ml) for 6 days.

2.4.2. NO Assay. Murine macrophage-like RAW 264.7 cells were treated with the ethanolic and methanolic extracts of *P. jamasakura* samples at various concentrations of 0, 12.5, 25, 50, 100, and 200 μ g/ml and cultured for 1 h prior to lipopolysaccharide (LPS) stimulation for 24 h following a previously described method [13]. The nitrite levels in the culture media were determined by incubation with Griess reagent (1% sulfanilamide, 0.1% naphthylethylenediamine dihydrochloride, and 2.5% phosphoric acid) for 5 min. The absorbance was measured at 570 nm using a microplate reader (VersaMax, Molecular Devices). The quantity of nitrite in the samples was calculated using the concentration of sodium nitrite as a standard.

Cell viability was analyzed using a cell counting kit assay (Dojindo). Cells were plated in a 96-well plate and treated with different concentrations of *P. jamasakura* extracts at concentrations of 0, 12.5, 25, 50, 100, and 200 μ g/ml for ethanolic and methanolic extracts for 24 h. After incubating with the cell counting kit (CCK) solutions and the cells for 1 h, the absorbance was measured at 450 nm using a microplate reader (VersaMax). The results are presented as a percentage of the control.

2.4.3. TRAP Assay and BMM Cell Viability. The measurement of osteoclast TRAP activity was based on the generation of absorbance by incubating BMM cells with TRAP buffer (50 mM sodium tartrate, 0.12 M sodium acetate, and pH 5.2) and *p*-nitrophenyl phosphate (1 mg/ml) for 15 min based on method previously described [14]. For TRAP staining, the cells were incubated with TRAP buffer containing naphthol AS-MX phosphate (0.1 mg/ml) and Fast Red Violet (0.5 mg/ml). The BMM cells were then cultured with the different ethanolic and methanolic *P. jamasakura* extracts at different concentrations of 0, 6.25, 12.5, 25, and 50 μ g/ml in the presence of RANKL for 6 days. The osteoclast TRAP activity was determined using a colorimetric assay with *p*-nitrophenyl phosphate as a substrate. The cell viability was determined using cell counting kit-8 (WST-8/CCK8; Dojindo), according to the manufacturer's instructions.

For the measurement of cell viability, cells were plated in 96-well plates and treated with ethanolic and methanolic *P. jamasakura* extracts at different concentrations of 0, 6.25,

12.5, 25, and 50 μ g/ml for 24 h. After incubating with the CCK solutions and the cells for 1 h, the absorbance was measured at 450 nm using a microplate reader (Versa Max). The results are presented as a percentage of the control.

2.5. Hepatotoxicity Assay in Zebrafish (*Danio rerio*) Larvae. Zebrafish larvae were bred under standard conditions as previously described [16] (Westerfield, 2000). At 90 h postfertilization (hpf), the larvae were transferred to a transparent 24-well plate ($N=10$ /well) with 1 ml of an embryonic medium. The larvae were then exposed to water, ethanolic, and methanolic *P. jamasakura* extracts at various concentrations of 50, 100, and 200 μ g/ml for ethanolic and methanolic, and water extracts from 96 to 120 hpf. Dimethyl sulfoxide (DMSO) was used as a negative control while 5 μ M of tamoxifen (Sigma-Aldrich, St. Louis, MO, USA) was used as a positive control. To obtain images, the larvae were anesthetized in tricaine (Sigma-Aldrich), mounted in 3% methyl cellulose (Sigma-Aldrich), and observed under a Leica MZ10F stereomicroscope equipped with a Leica DFC425 camera and Leica application Suite software (version 4.5).

2.6. Statistical Analysis. Data are represented as the mean \pm standard deviation. Statistical significance between groups was analyzed using Student's *t*-test. *p* values <0.05 were considered statistically significant.

3. Results and Discussion

3.1. HPLC Chemical Profiles of *Prunus jamasakura*. HPLC is a versatile, reproducible chromatographic technique for the estimation and detection of secondary metabolites in plants [17]. In this study, the phytochemical components of *P. jamasakura* based on the HPLC fingerprinting of their methanol, ethanol, and water extracts at 203, 254, 280, and 320 nm UV wavelengths (data not shown) were conducted. Among the four types of UV wavelengths, good separation and selectivity were observed at 280 nm. The distinct profiling patterns of the components were confirmed regardless of the type of solvent used in Figure 1(a).

Three chemical compounds, namely, naringenin [18], genistein [19], and sakuranetin [1], were selected as the standard components of *P. jamasakura*, according to a previous study [11]. The UV wavelength of the chromatograms was adjusted to 280 nm according to the maximum UV absorption of the three standard components (Figure 1(b)). The identification of the three standard components in *P. jamasakura* was based on a comparison between their retention times (t_R), UV absorption, and chromatograms and those of each standard. The mixed standard components were identified at retention times of 34.350 min (1), 34.547 min (2), and 38.457 min (3) in the chromatogram. Under the same conditions, three component standards were detected at similar retention times, 34.337 min (1), 34.533 min (2), and 38.433 min (3) in the *P. jamasakura* ethanol extract (Figure 1(c)). Therefore, this HPLC result showed the presence of naringenin, genistein,

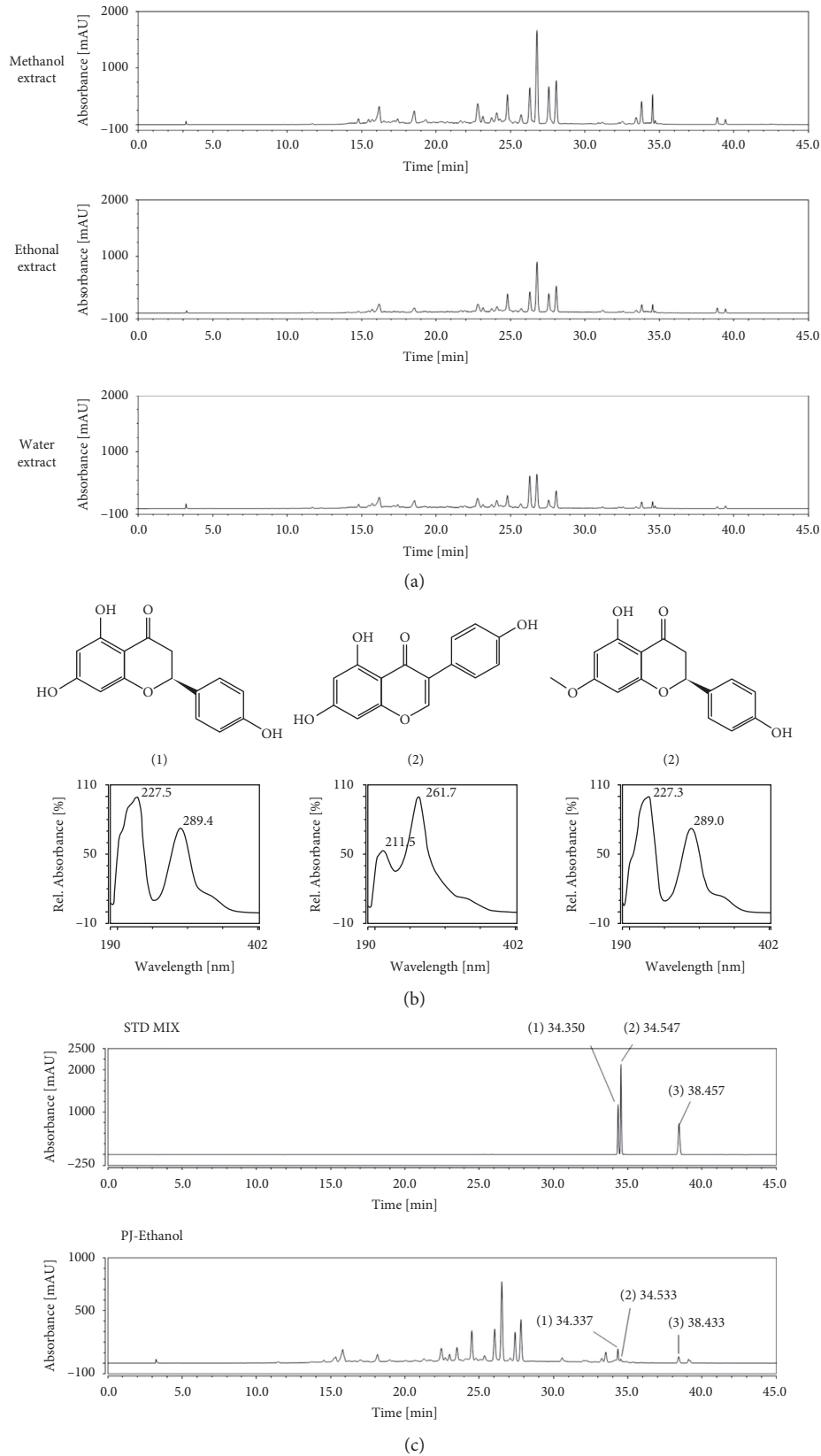


FIGURE 1: HPLC-DAD analysis of phytochemical components of *P. jamasakura*. (a) HPLC fingerprint of the ethanolic, methanolic, and water extracts of *P. jamasakura* at 280 nm. (b) Chemical structures and UV spectrum of three standard components: (1) naringenin, (2) genistein, and (3) sakuranetin. (c) Determination of naringenin (1), genistein (2), and sakuranetin (3), in *P. jamasakura* ethanol extracts at 280 nm.

and sakuranetin compounds in the stem bark of *P. jamasakura*.

3.2. NO Assay and RAW264.7 Cell Viability. NO plays a key role in the immune system defense against extracellular organisms [20]. However, when produced in excess, it is known to play an important role in the pathogenesis of inflammatory disorders of the joint, gut, and lungs [13, 21, 22]. A previous study also showed that increased NO production contributes to the pathogenesis of osteoporosis [23]. Therefore, the inhibition of NO production represents a potential therapeutic pathway for the management of inflammatory diseases [21]. In this study, the *P. jamasakura* extracts exhibited inhibitory effects on NO production (Figure 2). At 100 $\mu\text{g/ml}$ and 200 $\mu\text{g/ml}$, the ethanolic and methanolic *P. jamasakura* extracts showed significant ($p < 0.05$) and ($p < 0.01$) inhibition of the LPS-induced NO production in RAW264.7 cells, respectively, compared to the control (Figure 2(a)). At concentrations of 50, 100, and 200 $\mu\text{g/ml}$, the ethanolic and methanolic extracts exhibited significant cell ($p < 0.001$) and ($p < 0.05$) simulative effect, respectively, on cell viability (Figure 2(b)).

A previous study reported the downregulation of NO production by sakuranetin and naringenin compounds [12], and hence the presence of these compounds in *P. jamasakura* may somewhat explain its ability to inhibit LPS-mediated NO production in RAW 264.7 cells in this study.

3.3. TRAP Assay and BMM Viability. TRAP activity is a vital cytochemical marker of osteoclasts. As such, its concentration in the serum is utilized as a biochemical and histochemical marker of osteoclast function and degree of bone resorption [24, 25]. A previous study showed that the levels of serum TRAP were higher in patients with osteoporosis than in the control group. Furthermore, a negative linear correlation was previously found between serum TRAP and bone mineral content in women with osteoporosis, suggesting that TRAP concentration is a useful marker for bone loss [26]. Indeed, all forms of acquired osteoporosis reflect increased osteoclast function relative to that of osteoblasts, such that the pharmacological arrest of osteoclasts is a mainstay in the treatment of systemic bone loss [27]. TRAP initiates osteoclast differentiation, activation, and proliferation [18] and has been observed to play a vital role in many biological processes, including skeletal development, collagen synthesis and degradation, and bone mineralization [25, 28]. In this study, the ethanolic and methanolic *P. jamasakura* extracts at different concentrations of 0, 6.25, 12.5, 25, and 50 $\mu\text{g/ml}$ all significantly ($p < 0.001$) inhibited TRAP activity compared to the control (Figure 3(a)).

At 12.5 and 25 $\mu\text{g/ml}$, *P. jamasakura* methanolic and ethanolic extracts had a significant effect ($p < 0.05$) simulative effect on the cell viability of BMM cells (Figure 3(b)). At a higher concentration of 50 $\mu\text{g/ml}$ for both ethanolic and methanolic extracts, the cell viability increased significantly ($p < 0.01$) compared to the control. The significant viability of the BMM cells treated with all provides an indication of

the noncytotoxicity of the stem bark of *P. jamasakura* within a given dose range.

The suppression of TRAP activity by *P. jamasakura* may also be attributed to the various chemicals in it including naringenin and genistein. Naringenin has been observed to inhibit osteoclastogenesis and osteoclastic bone resorption [29, 30]. Genistein also showed direct inhibitory effect on osteoclasts *in vitro* [31] and suppressed TRAP activity [32]. Previous studies have also shown the antiosteoporosis activity of other *Prunus* species [33, 34]. The bioactive compounds in the fruit of *P. mume* were found to significantly stimulate the differentiation of preosteoblastic MC3T3-E1 cells to increase collagen synthesis or mineralization functions of osteoblasts and suppress TRAP activity in the receptor activator of nuclear factor- κB ligand-induced osteoclastic RAW 264.7 cells [35]. Additionally, terpenes and sterols in the fruit of *P. mume* were found to inhibit osteoclast differentiation by suppressing TRAP activity [36]. These results further validates the potential of *Prunus* species as an anti-osteoporosis medicinal plant.

3.4. Hepatotoxicity in Zebrafish Larvae. The hepatotoxicity results for a given drug are vital for understanding its potential effects on the liver and the potential induction of liver injury [37]. Herbal medicines have been previously associated with various complications, such as liver damage, which result in high incidences of mortalities and morbidities [19]. Hence, the screening of herbal medicines for their hepatotoxicity is a key step during the development of herbal medicines. Zebrafish larvae represent an important model system for the study of the effects of toxicant exposure on liver function and development [38, 39], as well as changes in red fluorescence intensity and size, making it a useful model for hepatotoxicity studies [40]. Liver organogenesis in zebrafish initiates at 30 hpf on the left-hand side of the embryo. In this study, the liver bud was enlarged, connected with the intestine, and functionally matured until 72 hpf [41]. At 96 hpf, treatment with liver toxicants (tamoxifen or acetaminophen) induced a reduction in liver transparency, indicating liver cell death in the zebrafish larvae [42]. In this study, the exposure of the zebrafish larvae from 96 to 120 hpf (Figure 4(a)) to DMSO did not result in the liver cell death (Figure 4(b)). However, treatment with tamoxifen resulted in liver cell death (Figure 4(c)). In *P. jamasakura* bark water and ethanolic extract at the concentrations of 50, 100, and 200 $\mu\text{g/ml}$, 100% of the zebrafish larvae survived at 120 hpf and hepatocyte death was not observed. Similarly, there was 100% survival of the zebrafish larvae exposed to *P. jamasakura* bark methanolic extract at concentrations at 50 $\mu\text{g/ml}$ with no hepatocyte death observed at 120 hpf (Figures 4(d) and 4(e)). However, at higher concentrations of 100 and 200 $\mu\text{g/ml}$ *P. jamasakura* bark methanolic extract, only 30% and 20% of the zebrafish larvae, respectively, survived but hepatocyte death was not observed in them (Figure 4(f)).

Hepatotoxicity observed in the zebrafish larvae model system correlates with that in humans [43], an indication that *P. jamasakura* extracts may have a low hepatotoxic effect on other vertebrates, including humans.

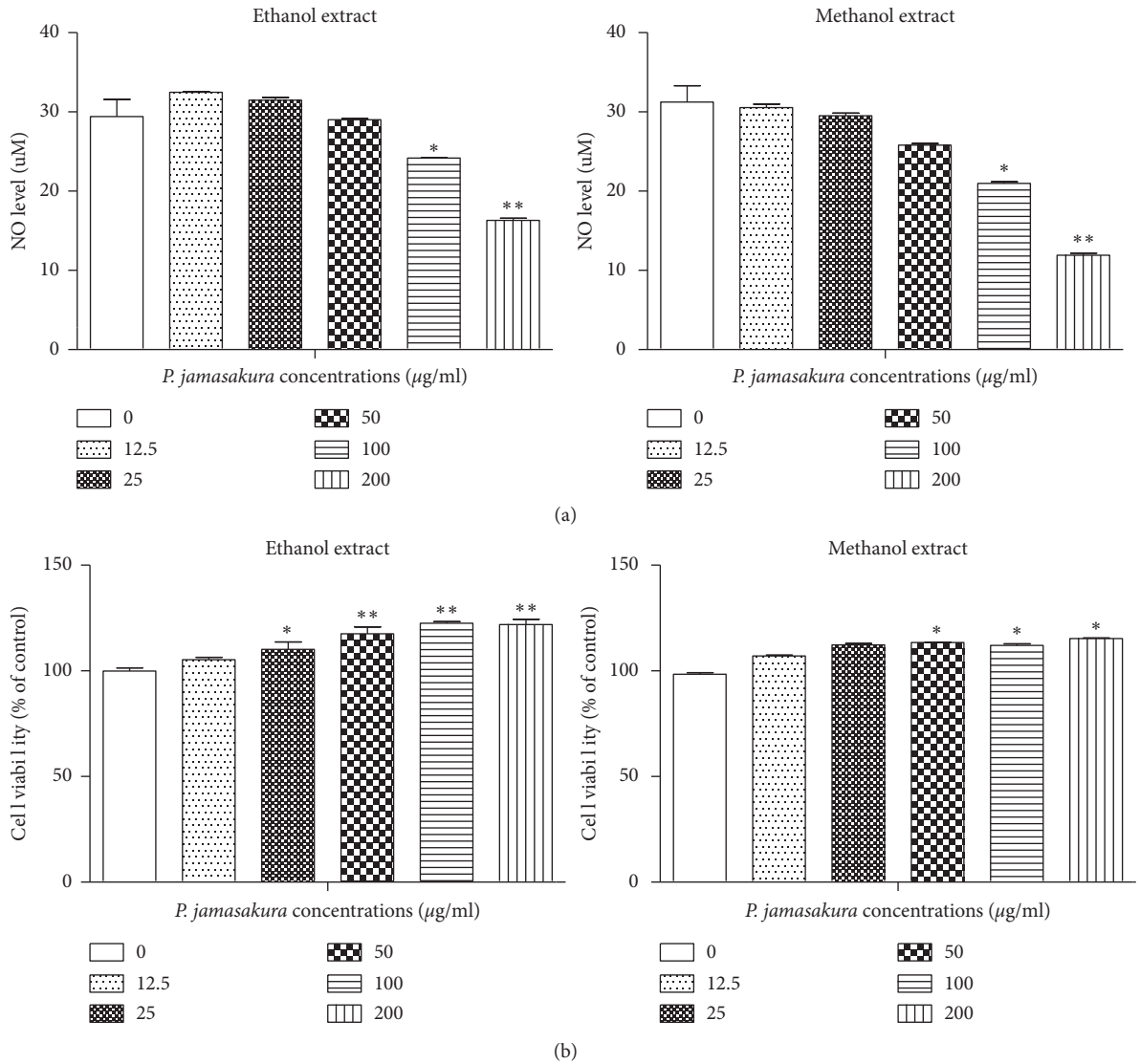


FIGURE 2: Effect of *P. jamasakura* on LPS-induced NO production in raw 264.7 cells. RAW264.7 cells were pretreated with *P. jamasakura* for 1 h before LPS treatment. (a) After 24 h incubation with LPS, the culture supernatant was collected for measurement of nitrite concentration. (b) Cell viability was determined using cell counting kit-8 following the manufacturer's instructions. * $p < 0.05$, ** $p < 0.01$, and *** $p < 0.001$.

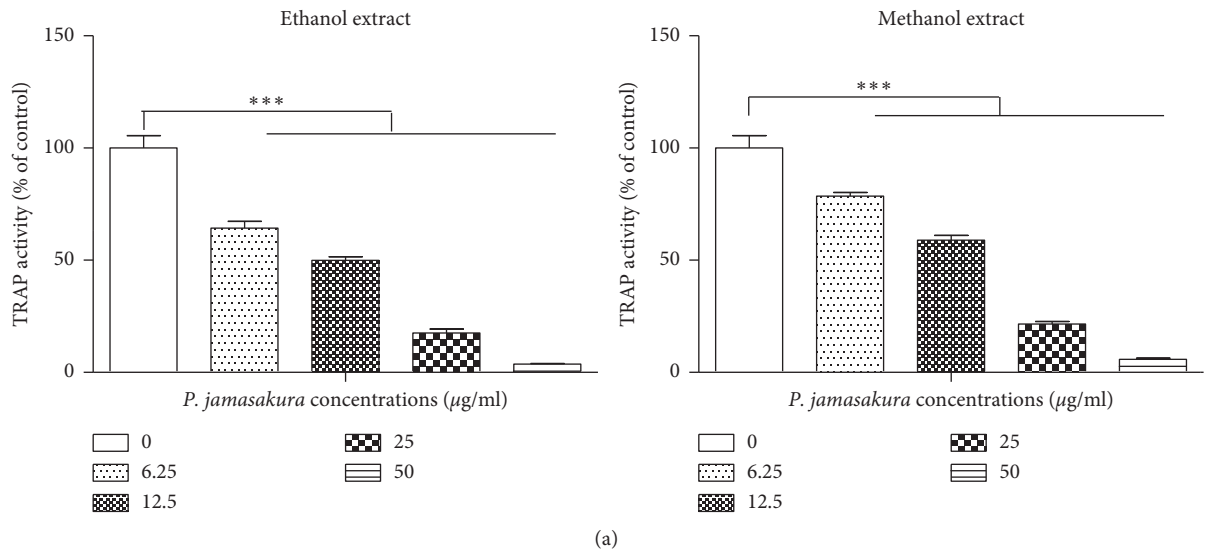


FIGURE 3: Continued.

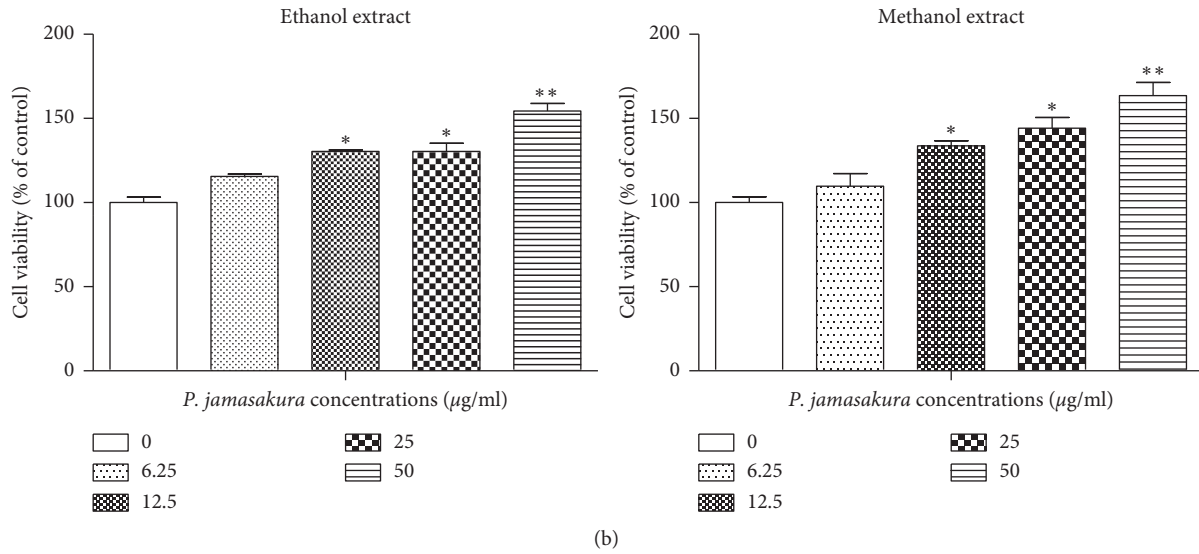


FIGURE 3: Effect of *P. jamasakura* on trap activity in BMM. The BMM was cultured with *P. jamasakura* in the presence of RANKL for 6 days. (a) TRAP activity of osteoclasts was measured by colorimetric assay using *p*-nitrophenyl phosphate as a substrate. (b) Cell viability was determined using cell counting kit-8 following the manufacturer’s instructions. * $p < 0.05$, ** $p < 0.01$, and *** $p < 0.001$.

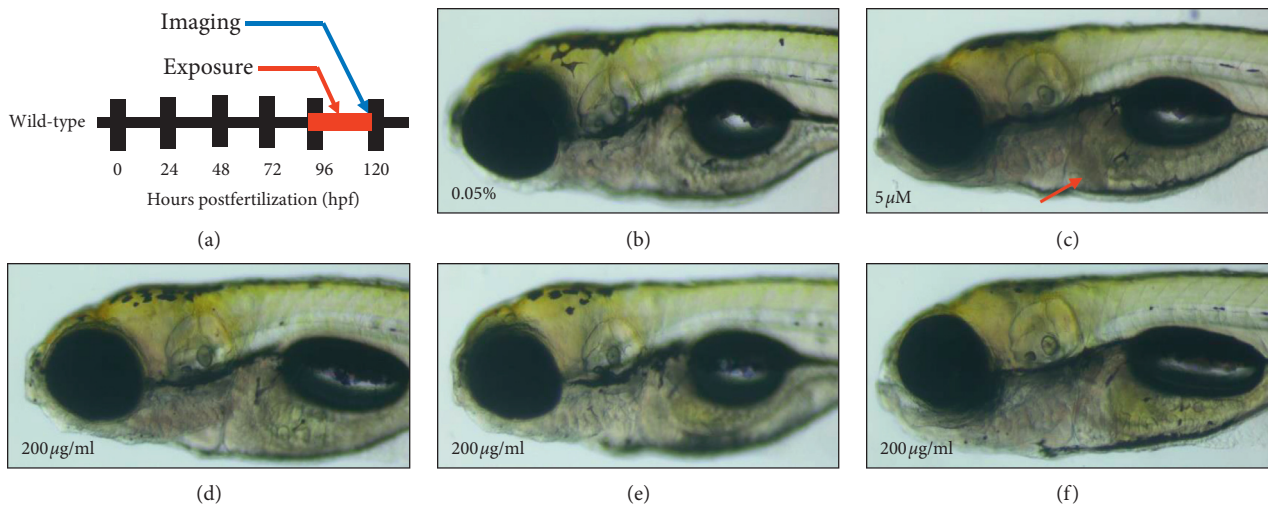


FIGURE 4: Hepatotoxicity assay in zebrafish larvae. (a) Schematic diagram of hepatotoxicity assay in zebrafish. (b) Treatment with DMSO did not show liver cell death. (c) Tamoxifen treatment induced liver cell death (red arrow). (d) No liver cell death was observed at concentration of 200 µg/ml of water extract. (e) No liver cell death was observed at concentration of 200 µg/ml of ethanolic extract. (f) No liver cell death was observed at concentration of 200 µg/ml of methanolic extract.

4. Conclusion

The use of medicinal plants to treat myriad of conditions including osteoporosis and inflammation has been in existence since time immemorial. This present study has demonstrated the antiosteoporosis, anti-inflammatory, and nonhepatotoxic activities of *P. jamasakura*. And as such, the study provides a basis for clinical studies and a foundation upon which *P. jamasakura* antiosteoporosis drugs can be developed in the future.

Abbreviations

- BMMs: Bone marrow macrophages
- CCK: Cell counting kit
- FBS: Fetal bovine serum
- HPLC: High-performance liquid chromatography
- LPS: Lipopolysaccharide
- M-CSF: Macrophage-colony stimulating factor
- NO: Nitric oxide
- TRAP: Tartrate-resistant acid phosphatase.

Data Availability

The raw data supporting the results of this article will be made available through the corresponding author upon request.

Conflicts of Interest

The authors declare no conflicts of interest.

Authors' Contributions

RK conceived the original research plans, collected test materials, and wrote this manuscript. KS conducted the experiments on NO and TRAP assays. NHY and JL conducted the extractions of the samples and carried out the UPHLC chemical profiling. SKY, JHS, and GC carried out the botanical authentication of the sample of *P. jamasakura* used in this study and wrote the manuscript. YGK performed the statistical analysis and wrote this manuscript. FO, AM, and GNK wrote and revised the manuscript. HK and KSH conducted the hepatotoxicity assay on zebrafish. MGM conducted experiments on phytochemical profiling and revised the manuscript. YK technically supervised all the experiments and is the corresponding author.

Acknowledgments

This study was supported under the framework of International Cooperation Program (Korea-South Africa Cooperative Research Project for Excavation of Candidate Resources of Complementary and Alternative Medicine) managed by National Research Foundation of Korea (grant nos. 2017093655 and KIOM: D17470). Additionally, this work was also supported by the Development of Foundational Techniques for the Domestic Production of Herbal Medicines (K18405), Development of Sustainable Application for Standard Herbal Resources (KSN2012320), and Korea Institute of Oriental Medicine through the Ministry of Science and ICT, Republic of Korea. Partially, this work was also supported by a grant from the Ministry of Trade, Industry and Energy, Republic of Korea (grant no. 2019-10063396).

References

- [1] J. An, H. Yang, Q. Zhang et al., "Natural products for treatment of osteoporosis: the effects and mechanisms on promoting osteoblast-mediated bone formation," *Life Sciences*, vol. 147, pp. 46–58, 2016.
- [2] A. Prentice, "Diet, nutrition and the prevention of osteoporosis," *Public Health Nutrition*, vol. 7, no. 1, pp. 227–243, 2004.
- [3] T. Sözen, L. Ozisik, and N. Calik Basaran, "An overview and management of osteoporosis," *European Journal of Rheumatology*, vol. 4, no. 1, pp. 46–56, 2017.
- [4] L. Ginaldi, M. Di Benedetto, and M. De Martinis, "Osteoporosis, inflammation and ageing," *Immunity & Ageing*, vol. 2, no. 1, p. 14, 2005.
- [5] R. Komakech, Y.-G. Kim, G. M. Matsabisa, and Y. Kang, "Anti-inflammatory and analgesic potential of *Tamarindus*

- indica* linn. (fabaceae): a narrative review," *Integrative Medicine Research*, vol. 8, no. 3, pp. 181–186, 2019.
- [6] D. Mitra, D. M. Elvins, D. J. Speden, and A. J. Collins, "The prevalence of vertebral fractures in mild ankylosing spondylitis and their relationship to bone mineral density," *Rheumatology*, vol. 39, no. 1, pp. 85–89, 2000.
- [7] G. R. Mundy, "Osteoporosis and inflammation," *Nutrition Review*, vol. 65, no. 12, pp. S147–S151, 2007.
- [8] V. Suvarna, M. Sarkar, P. Chaubey et al., "Bone health and natural products-an insight," *Frontiers in Pharmacology*, vol. 9, p. 981, 2018.
- [9] K. Senthilkumar, J. Venkatesan, and S.-K. Kim, "Marine derived natural products for osteoporosis," *Biomedicine & Preventive Nutrition*, vol. 4, no. 1, pp. 1–7, 2014.
- [10] Y. Wang and K. Zeng, "Natural products as a crucial source of anti-inflammatory drugs: recent trends and advancements," *Traditional Medicine Research*, vol. 4, no. 5, pp. 257–268, 2019.
- [11] K. Watanabe, V. Karuppagounder, S. Arumugam et al., "Pruni cortex ameliorates skin inflammation possibly through HMGB1-NF κ B pathway in house dust mite induced atopic dermatitis NC/Nga transgenic mice," *Journal of Clinical Biochemistry and Nutrition*, vol. 56, no. 3, pp. 186–194, 2015.
- [12] Y. Yamauchi, T. Okuyama, T. Ishii, T. Okumura, Y. Ikeya, and M. Nishizawa, "Sakuranetin downregulates inducible nitric oxide synthase expression by affecting interleukin-1 receptor and CCAAT/enhancer-binding protein β ," *Journal of Natural Medicines*, vol. 73, no. 2, pp. 353–368, 2019.
- [13] J. Choi, M. J. Kim, R. Komakech, H. Jung, and Y. Kang, "Anti-inflammatory activities of astringent persimmons (*diospyros kaki* thunb.) stalks of various cultivar types based on the stages of maturity in the gyeongnam province," *BMC Complementary and Alternative Medicine*, vol. 19, no. 1, 2019.
- [14] K. Shim, B. Lee, and Y. J. Ma, "Water extract of *Rumex crispus* prevents bone loss by inhibiting osteoclastogenesis and inducing osteoblast mineralization," *BMC Complementary and Alternative Medicine*, vol. 17, no. 1, p. 483, 2017.
- [15] K.-S. Shim, T. Kim, H. Ha et al., "Hwangryun-haedok-tang fermented with *Lactobacillus casei* suppresses ovariectomy-induced bone loss," *Evidence-Based Complementary and Alternative Medicine*, vol. 201212 pages, Article ID 325791, 2012.
- [16] M. Westerfield, *The Zebrafish Book: A Guide for the Laboratory Use of Zebrafish (Danio Rerio)*, University of Oregon Press, Eugene, OR, USA, 4th edition, 2000.
- [17] A. A. Boligon and M. L. Athayde, "Importance of HPLC in analysis of plants extracts," *Austin Chromatography*, vol. 1, no. 3, 2014.
- [18] S. M. Abdelmagid, G. R. Sondag, F. M. Moussa et al., "Mutation in osteoactivin promotes receptor activator of NF κ B ligand (rankl)-mediated osteoclast differentiation and survival but inhibits osteoclast function," *Journal of Biological Chemistry*, vol. 290, no. 33, pp. 20128–20146, 2015.
- [19] C. Amadi and O. Orisakwe, "Herb-induced liver injuries in developing nations: an update," *Toxics*, vol. 6, no. 2, p. 24, 2018.
- [20] T. V. Rajan, P. Porte, J. A. Yates, L. Keefer, and L. D. Shultz, "Role of nitric oxide in host defense against an extracellular, metazoan parasite, *Brugia malayi*," *Infection and Immunity*, vol. 64, no. 8, pp. 3351–3353, 1996.
- [21] J. N. Sharma, A. Al-Omran, and S. S. Parvathy, "Role of nitric oxide in inflammatory diseases," *Inflammopharmacology*, vol. 15, no. 6, pp. 252–259, 2007.
- [22] S.-B. Yoon, Y.-J. Lee, S. K. Park et al., "Anti-inflammatory effects of *Scutellaria baicalensis* water extract on LPS-activated

- RAW 264.7 macrophages,” *Journal of Ethnopharmacology*, vol. 125, no. 2, pp. 286–290, 2009.
- [23] K. E. Armour, R. J. Van’T Hof, P. S. Grabowski, D. M. Reid, and S. H. Ralston, “Evidence for a pathogenic role of nitric oxide in inflammation-induced osteoporosis,” *Journal of Bone and Mineral Research*, vol. 14, no. 12, pp. 2137–2142, 1999.
- [24] P. Ballanti, S. Minisola, M. T. Pacitti et al., “Tartrate-resistant acid phosphate activity as osteoclastic marker: sensitivity of cytochemical assessment and serum assay in comparison with standardized osteoclast histomorphometry,” *Osteoporosis International*, vol. 7, no. 1, pp. 39–43, 1997.
- [25] F. J. M. Blumer, B. Hausott, C. Schwarzer, R. A. Hayman, J. Stempel, and H. Fritsch, “Role of tartrate-resistant acid phosphatase (trap) in long bone development,” *Mechanisms of Development*, vol. 129, no. 5–8, pp. 162–176, 2012.
- [26] C. De La Piedra, R. Torres, A. Rapado, M. Diaz, and N. Castro, “Serum tartrate-resistant acid phosphatase and bone mineral content in postmenopausal osteoporosis,” *Calcified Tissue International*, vol. 45, no. 1, pp. 58–60, 1989.
- [27] S. L. Teitelbaum, “Osteoclasts: what do they do and how do they do it?” *The American Journal of Pathology*, vol. 170, no. 2, pp. 427–435, 2007.
- [28] A. R. Hayman, “Tartrate-resistant acid phosphatase (trap) and the osteoclast/immune cell dichotomy,” *Autoimmunity*, vol. 41, no. 3, pp. 218–223, 2008.
- [29] V. D. La, S. Tanabe, and D. Grenier, “Naringenin inhibits human osteoclastogenesis and osteoclastic bone resorption,” *Journal of Periodontal Research*, vol. 44, no. 2, pp. 193–198, 2009.
- [30] X. Lü, Y. Zhou, K. M. Chen, Z. Zhao, J. Zhou, and X. N. Ma, “Inhibitory effect of 8-prenylnaringenin on osteoclastogenesis of bone marrow cells and bone resorption activity,” *Acta Pharmaceutica Sinica B*, vol. 48, no. 3, pp. 347–351, 2013.
- [31] Y. H. Gao and M. Yamaguchi, “Suppressive effect of genistein on rat bone osteoclasts: apoptosis is induced through Ca^{2+} signaling,” *Biological & Pharmaceutical Bulletin*, vol. 22, no. 8, pp. 805–809, 1999.
- [32] S.-H. Lee, J.-K. Kim, and H.-D. Jang, “Genistein inhibits osteoclastic differentiation of raw 264.7 cells via regulation of ros production and scavenging,” *International Journal of Molecular Sciences*, vol. 15, no. 6, pp. 10605–10621, 2014.
- [33] Y. H. Kim, Y. Xi-Tao, H. S. Lee, and D. H. Jang, “Potential anti-osteoporotic and antioxidant components from *Artemisia iwayomogi* and *Prunus mume*,” *Planta Medica*, vol. 81, no. 5, 2015.
- [34] T. Wallace, “Dried plums, prunes and bone health: a comprehensive review,” *Nutrients*, vol. 9, no. 4, p. 401, 2017.
- [35] X.-T. Yan, S.-H. Lee, W. Li, H.-D. Jang, and Y.-H. Kim, “Terpenes and sterols from the fruits of *Prunus mume* and their inhibitory effects on osteoclast differentiation by suppressing tartrate-resistant acid phosphatase activity,” *Archives of Pharmacal Research*, vol. 38, no. 2, pp. 186–192, 2015.
- [36] X.-T. Yan, S.-H. Lee, W. Li et al., “Evaluation of the antioxidant and anti-osteoporosis activities of chemical constituents of the fruits of *Prunus mume*,” *Food Chemistry*, vol. 156, pp. 408–415, 2014.
- [37] E. Björnsson, “Hepatotoxicity by drugs: the most common implicated agents,” *International Journal of Molecular Sciences*, vol. 17, no. 2, p. 224, 2016.
- [38] K. Bambino, J. Morrison, and J. Chu, “Hepatotoxicity in zebrafish larvae,” *Methods in Molecular Biology*, vol. 1965, pp. 129–138, 2019.
- [39] S. Scholz, “Zebrafish embryos as an alternative model for screening of drug-induced organ toxicity,” *Archives of Toxicology*, vol. 87, no. 5, pp. 767–769, 2013.
- [40] X. Zhang, C. Li, and Z. Gong, “Development of a convenient in vivo hepatotoxin assay using a transgenic zebrafish line with liver-specific DsRed expression,” *PLoS One*, vol. 9, no. 3, Article ID e91874, 2014.
- [41] S. Korzh, X. Pan, M. Garcia-Lecea et al., “Requirement of vasculogenesis and blood circulation in late stages of liver growth in zebrafish,” *BMC Developmental Biology*, vol. 8, no. 1, p. 84, 2008.
- [42] H. S. Nam, K. S. Hwang, Y. M. Jeong et al., “Expression of miRNA-122 induced by liver toxicants in zebrafish,” *BioMed Research International*, vol. 20167 pages, Article ID 1473578, 2016.
- [43] M. Pandya, D. Patel, J. Rana, M. Patel, and N. Khan, “Hepatotoxicity by acetaminophen and amiodarone in zebrafish embryos,” *Journal of Young Pharmacists*, vol. 8, pp. 50–52, 2016.

Research Article

Efficacy of Acupoints Dual-Frequency Low-Level Laser Therapy on Knee Osteoarthritis

Fang-Yin Liao,¹ Chien-Lin Lin,^{1,2} Sui-Foon Lo,^{1,2} Chun-Ching Chang,³ Wen-Yen Liao,¹ and Li-Wei Chou ^{1,4,5}

¹Department of Physical Medicine and Rehabilitation, China Medical University Hospital, Taichung 40432, Taiwan

²School of Chinese Medicine, College of Chinese Medicine, China Medical University, Taichung 40433, Taiwan

³Department of Rehabilitation, New Bodhi Hospital, Taichung 41222, Taiwan

⁴Department of Physical Therapy and Graduate Institute of Rehabilitation Science, China Medical University, Taichung 40433, Taiwan

⁵Department of Physical Medicine and Rehabilitation, Asia University Hospital, Asia University, Taichung 41350, Taiwan

Correspondence should be addressed to Li-Wei Chou; chouliwe@gmail.com

Received 30 May 2020; Revised 30 July 2020; Accepted 4 August 2020; Published 24 September 2020

Guest Editor: Arham Shabbir

Copyright © 2020 Fang-Yin Liao et al. This is an open access article distributed under the Creative Commons Attribution License, which permits unrestricted use, distribution, and reproduction in any medium, provided the original work is properly cited.

Background. Knee osteoarthritis (OA) presented with knee pain and limitation of mobility is common, and it may become a chronic problem resulting in major loss of function, with related impaired activity of daily living. Current traditional therapy for knee OA includes pharmacological treatment and physiotherapy, but the efficacies are limited. An alternative noninvasive treatment low-level laser therapy (LLLT) applied to acupoints is still contradictory and the efficacy needs to be assessed. **Methods and Materials.** We conduct the randomized double-blind control study to investigate the efficacy of a dual-frequency LLLT (combines red light (780 nm) and near-infrared light (830 nm)) in patients suffering knee OA. Participates were randomly assigned into active laser therapy (ALT) and placebo laser therapy (PLT) groups. Subjects in the ALT group were separately treated by laser apparatus at the three acupoints (SP9, SP10, and EX-LE2) on their knee joints under continuous radiation for 15 min at the maximum intensity, three times per week for four weeks. The PLT group used laser apparatus of the same model according to similar procedures without laser light emission. Outcome Measurements including visual analog scale (VAS), pain pressure threshold (PPT), and Lequesne index were used. **Results.** A total of 30 subjects with two-sided knee OA in both groups completed the experiment. Statistically significant decreases were observed in the Lequesne index (5.27 ± 3.26 vs. 10.83 ± 3.83), conscious VAS 4 weeks after treatment (moving: 2.87 ± 1.13 vs. 5.67 ± 1.72 ; resting: 0.33 ± 0.62 vs. 2.67 ± 1.29), and the increase was noted in PPT (21.23 ± 1.82 kg vs. 13.02 ± 1.46 kg) in the ALT group compared with the PLT group. **Conclusion.** It appears that the knee OA pain and disability can be decreased after a dual-frequency LLLT applied to acupoints (SP9, SP10, and EX-LE2). The clinical efficacy of LLLT is highly related to the therapeutic settings of the laser apparatus; hence, more clinical trials with different parameter settings are needed to be further clarified.

1. Introduction

In the modern society, degenerative arthritis is one of the common diseases prevalent among the population over age 45; the incidence of this disease is twice more prominent in females than in male [1–7]. Damages to peripheral soft tissues, including the bursa, tendon, and ligament around the joint, are probable sources of pain in patients with

degenerative arthritis, which is a joint deformity, caused by articular cartilage wear and tear. In imaging, knee osteoarthritis (OA) can be divided into four levels by severity. However, the results of X-ray examination are not exactly the same as the clinical manifestations [1, 8, 9]. Therefore, the American College of Rheumatology (ACR) formulated diagnostic criteria for knee OA: over age 50; early morning stiffness for less than 30 minutes; a sudden bursting sound as

the ball joint moves; knee pain or tenderness; and joint space narrowing, spur proliferation, and bone hypertrophy as revealed by X-ray imaging [10].

Degenerative arthritis is manifested with joint pain and impaired physical mobility, belonging to the category of arthromyodynia in traditional Chinese medicine. According to Huangdi Neijing, although clinical manifestations of arthromyodynia vary with depth and location, the blocked or unbalanced Qi or blood circulation through the body's meridians can be relieved by acupuncture at certain points, mainly involving five-point acupuncture of knee, Yangming stomach channel of foot, Shaoyang gall bladder channel of foot, and Taiyin spleen channel of foot.

Traditional therapeutic options for degenerative arthritis mainly include medication and physiotherapy in rehabilitation department [11, 12]. However, the former is prone to side effects, whereas the latter makes little effects in some severe cases. Thus, low-level laser therapy (LLLT), a non-invasive substitutive therapy, is adopted in the present study [13–15]. Laser therapy in animal experiments can adjust the proliferation of chondrocytes and the synthesis of DNAs in cartilage-specific proteoglycan and collagen/noncollagen proteins (NCPs) [16–18], relieve pain, accelerate the release of serotonin from the body [19], and produce an anti-inflammatory effect [20]. In the present study, bichromatic laser-emitting dual-frequency laser beams in an alternating way can achieve deeper laser penetration, which may produce a better curative effect despite variation of lesion depth from person to person and from spot to spot [21]. Based on the literature, three acupoints, which are commonly used to treat knee OA, including SP9 (yīnlíngquán, Taiyin spleen channel of foot), SP10 (xùèhǎi, Taiyin spleen meridian of foot), and EX-LE2 (hèdǐngxué) [22–24], were chosen in the present study. A double-blind trial was conducted to determine the curative effect of acupoints dual-frequency LLLT on knee osteoarthritis.

2. Materials and Methods

This study involved patients diagnosed with knee OA at rehabilitation clinics. This study was approved by the Institutional Review Board of the China Medical University Hospital (DMR99-IRB-136). Patients gave their written informed consent to participate in this study, and the research was conducted in accordance with the principles of the Declaration of Helsinki.

The inclusion criteria were (1) knee OA patients who meet the criteria established by the ACR on 1986; (2) those with knee OA as revealed by X-ray imaging, having the severity above Level II as rated by the Kellgren–Lawrence grading scale; (3) those over the age of 50; (4) those with knee OA pain lasting clinically for more than six months; and (5) those who are willing to cooperate and sign informed consents after being fully apprised of procedures and its purposes of the clinical trial. The exclusion conditions were (1) those suffering from malignant tumors and/or acute medical diseases, motor or sensory nerve defect, mental disorders, dementia, mental retardation, and/or any other organic mental abnormality; (2) those who have received

intra-articular steroids or hyaluronic acid in their knees over the past three months; (3) those who have ever undergone knee surgeries, or whose knees have been wounded and suffer from congenital knee deformation, severe knee varus or valgus deformity, or secondary knee OA to endocrinopathy, metabolic disorders, infectious and inflammatory diseases, and/or rheumatic autoimmune diseases; and (4) those with contraindications for LLLT, such as malignant tumors, pregnancy, and photosensitization. After the screening, the eligible subjects were completely randomly assigned to the treatment group ($n=16$) and the control group ($n=17$) by means of random number table. The randomization procedure was performed by a researcher who was not involved in data collection, and assignments were held in sealed opaque envelopes to ensure randomization concealment. During the follow-up course, there were one or two patients walking out from the treatment group and the control group, respectively. Thus, the two groups included 15 subjects each at the completion of the course, which was conducted three times per week for four weeks.

In the present study, multiband laser therapeutic apparatuses (TI-816-2, Transverse Inc., Taiwan) were adopted as the active laser treatment (ALT) group, with the output wavelengths of 780 nm (power: 50 mW) and 830 nm (power: 30 mW), and the maximum cumulative energy of 216 J under the continuous irradiation for 15 min at the maximum intensity. The clinical trial was designed as a randomized, double-blind, and controlled trial. Subjects were separately treated by laser apparatus at the three points (SP9, SP10, and EX-LE2) on their knee joints under continuous radiation for 15 min at the maximum intensity, three times per week for four weeks. The control group (placebo laser treatment (PLT)) in the experiment used laser apparatus of the same model according to similar procedures, but without laser light emission. The flowchart of this study is shown in Figure 1.

The efficacy was assessed by three outcome measurements: chief complaint about pain intensity (both moving and resting knee), pain pressure threshold (PPT), and knee OA severity scale. The chief complaint about pain intensity is expressed by the visual analog scale (VAS). This method is represented with a straight line of 10 cm, both ends of which are marked with “0” and “10” (“0”: completely painless; “10”: intolerable pain), which allows patients to mark and identify their pain levels by measuring the distance between the point of “0” and the corresponding markers, indicating their respective pain index values. Pressure algometry was applied to measure the PPT three times at a certain sore spot of each patient's pes anserinus tendon, with an interval of 60 seconds, and the value of pressure algometry at which pain became unbearable was recorded. Additionally, the median of the three measured values was defined as the pain pressure threshold. The Lequesne index [25] was measured by the knee osteoarthritis severity scale. By summing up, the score for the lowest severity level was 0 point, and that of the highest severity level was 24 points.

The results from the present study were statistically analyzed using Statistical Package for Social Science (SPSS 18.0) for Windows. Data are expressed as mean \pm standard

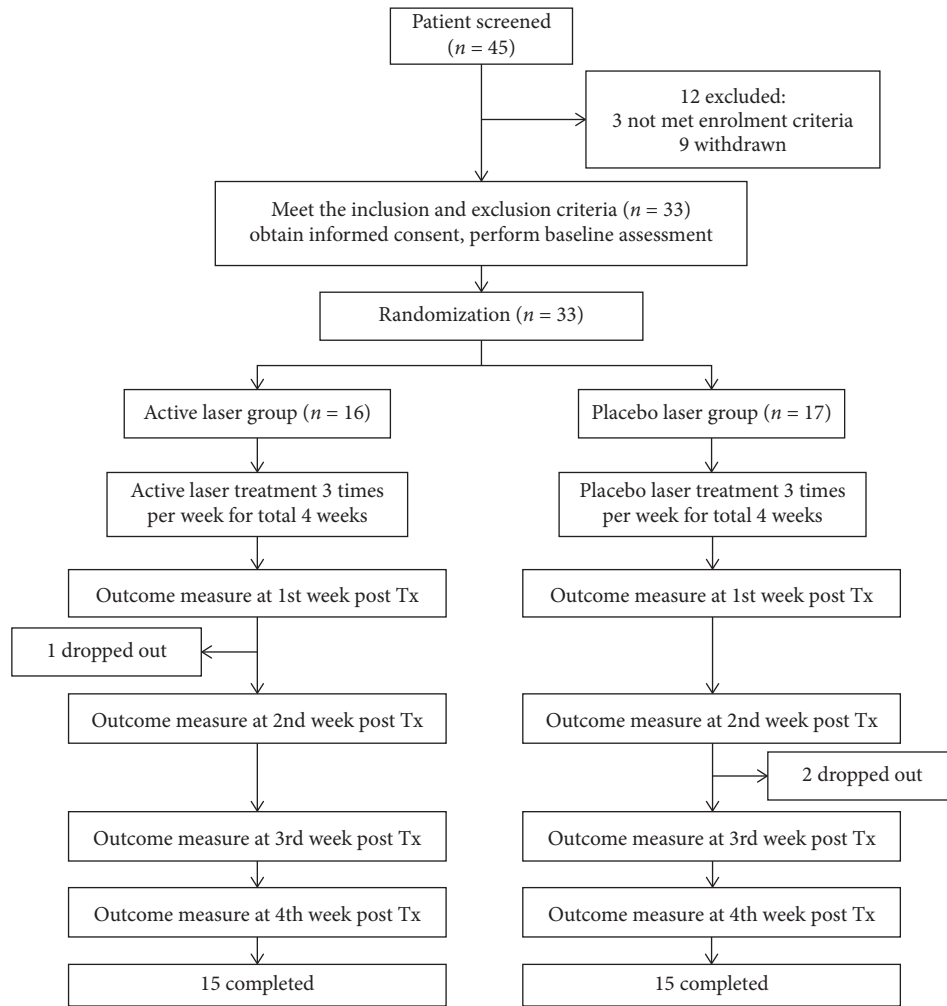


FIGURE 1: Flowchart of this study.

deviation (SD). As for descriptive statistics, the between-group analysis of all variables was conducted by independent two-sample *t*-test and chi-square test, thereby obtaining the curative effects. For inferential statistics, the within-group analysis of all variables was conducted by the paired sample *t*-test while the between-group analysis of the variables was conducted by the independent two-sample *t*-test. As revealed in the present study, there were statistically significant differences among the results ($P < 0.05$).

3. Results

In the present study, a total of 33 subjects were randomized into two groups (ALT and PLT). The ALT group consisted of 16 subjects while the PLT group was of 17 subjects. However, one or two subjects had withdrawn from the ALT and PLT groups, respectively, in the middle of the study period; thus, the two groups had 15 subjects at the completion of the therapy for four weeks (see Figure 1). A total of 30 patients with two-sided knee OA completed the study. After diagnosis, a total of 60 knee OA samples were collected. Statistically, the mean values of clinical index data of every subject's left and right knees

were taken for clinical assessment. There were no statistically significant differences between the two groups in basic data (Table 1). In terms of clinical evaluation indicators before therapy, including knee OA severity index, conscious VAS for moving knee, conscious VAS for resting knee, and pes anserinus tendon PPT (Table 1), there were no statistically significant differences between the two groups in those clinical evaluation indicators before therapy (independent two-sample *t*-test).

3.1. Severity Index of Knee OA Severity (Lequesne Index).

The variations of the two groups in the knee OA severity index before experiment and within the 1st, 2nd, 3rd, and 4th weeks after treatment are shown as Figure 2. Comparison of the ALT group before LLLT and within the 1st, 2nd, 3rd, and 4th weeks after treatment showed that the knee OA severity index was significantly improved with statistically significant differences. By contrast, the Lequesne index of the PLT group after the four-week course did not significantly decrease, and the therapeutic regimen for the PLT group produced little curative effect on knee OA from the Lequesne index.

TABLE 1: Baseline characteristics and clinical evaluation indicators of the subjects in the two groups.

| | ALT group | PLT group | P value |
|--------------------------------|-----------------|----------------|------------|
| Age (year) | 70.53 ± 6.89 | 69.73 ± 6.91 | $P > 0.05$ |
| BMI (kg/m ²) | 26.61 ± 4.33 | 25.98 ± 2.71 | $P > 0.05$ |
| Duration of knee pain (month) | 136.40 ± 84.08 | 129.20 ± 57.23 | $P > 0.05$ |
| Sex | Male (number) | 2 | $P > 0.05$ |
| | Female (number) | 14 | $P > 0.05$ |
| K-L grade | 2 (number) | 11 | $P > 0.05$ |
| | 3 (number) | 16 | $P > 0.05$ |
| | 4 (number) | 3 | $P > 0.05$ |
| Lequesne index | 11.93 ± 4.55 | 12.23 ± 4.14 | $P > 0.05$ |
| Conscious VAS for moving knee | 6.67 ± 2.16 | 6.93 ± 1.79 | $P > 0.05$ |
| Conscious VAS for resting knee | 3.00 ± 1.93 | 3.33 ± 1.68 | $P > 0.05$ |
| Pes anserinus tendon PPT (Kg) | 11.71 ± 1.86 | 11.81 ± 1.89 | $P > 0.05$ |

Data are expressed as mean ± SD; ALT, active laser treatment; PLT, placebo laser treatment; BMI, body mass index; K-L grade, Kellgren—Lawrence radiographic grade of knee OA; VAS, visual analog scale; PPT, pain pressure threshold.

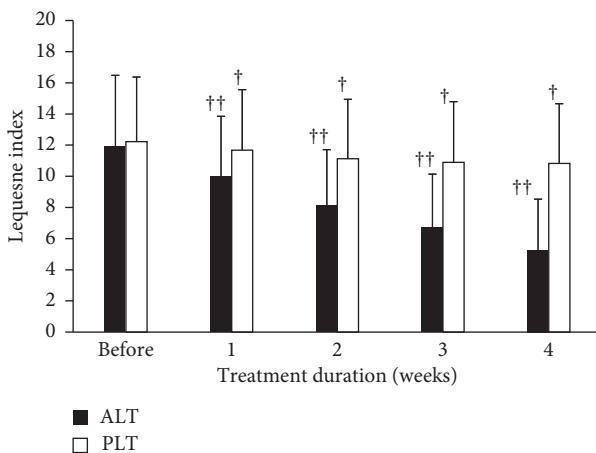


FIGURE 2: The variations of the two groups in the knee OA severity index before experiment and 4 weeks after treatment. Data are expressed as bar plot (mean) with error bars (SD) ($†P < 0.001$, $††P < 0.0001$) (ALT: active laser treatment; PLT: placebo laser treatment).

3.2. Conscious VAS for Moving Knee. Considering the conscious VAS for moving knees, the results of the two groups before experiment and within the 1st, 2nd, 3rd, and 4th weeks after it are shown in Figure 3. Results showed that, for the ALT group before LLLT and within the 1st, 2nd, 3rd, and 4th weeks after it, the conscious VAS for moving knee significantly decreased (6.67 ± 2.16 , before; 2.87 ± 1.13 , within the 4th week after). However, the conscious VAS of the PLT group after the four-week therapy did not drop significantly (6.93 ± 1.79 , before; 5.67 ± 1.72 , within the 4th week after). Significant differences were found between the two groups in the experimental results.

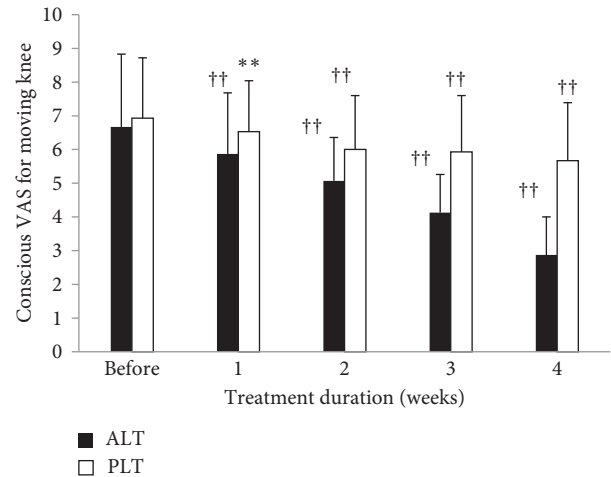


FIGURE 3: The variations of the two groups in the conscious VAS for moving knees before experiment and 4 weeks after treatment. Data are expressed as bar plot (mean) with error bars (SD) ($**P < 0.01$, $††P < 0.0001$) (ALT: active laser treatment; PLT: placebo laser treatment).

3.3. Conscious VAS for Resting Knee. The variations of the two groups in the conscious VAS for resting knee before experiment and within the 1st, 2nd, 3rd, and 4th weeks after it are shown in Figure 4. By comparing the ALT group before LLLT and within the 1st, 2nd, 3rd, and 4th weeks after it, the conscious VAS for resting knee was significantly improved (3.00 ± 1.93 , before; 0.33 ± 0.62 , within the 4th week after), having statistically significant differences. For the PLT group, the conscious VAS for resting knee was not significantly improved (3.33 ± 1.68 , before; 2.67 ± 1.29 , within the 4th week after).

3.4. Pes Anserinus Tendon Pain Pressure Threshold. The variations of the two groups before experiment and within the 1st, 2nd, 3rd, and 4th weeks after it in the pes anserinus tendon PPT are shown as Figure 5. Results showed that, for the ALT group before LLLT and within the 1st, 2nd, 3rd, and 4th weeks after it, the pes anserinus tendon PPT was significantly improved (11.71 ± 1.86 , before; 21.23 ± 1.82 , within the 4th week after), having statistically significant differences. The PPT of the PLT group was 12–13, indicating that the therapeutic regimen for the PLT group failed to effectively improve the pain pressure threshold.

4. Discussion

In the present study, 33 patients with two-sided knee OA were randomized into the ALT group (16 subjects) and the PLT group (17 subjects). In the course of the experiment, one subject of the treatment group withdrew after one week treatment, and two of the control group also quitted after two weeks treatment. The patients refused to continue because they felt unsure of the painless treatment and felt no effect at all. Thus, the two groups just had 15 subjects each upon completion of the four-week treatment course. These patients were with two-sided knee OA pain. However,

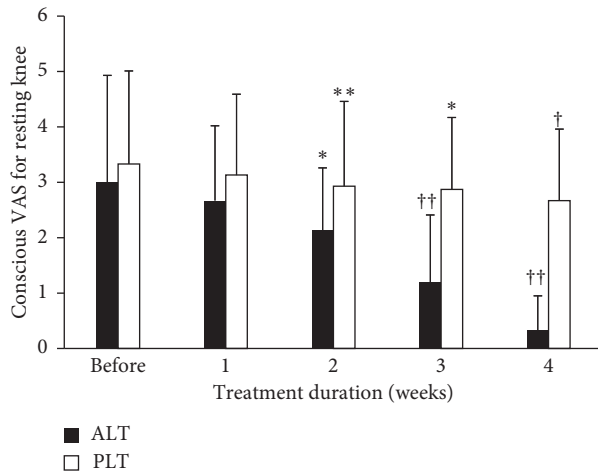


FIGURE 4: The variations of the two groups in the conscious VAS for resting knees before experiment and 4 weeks after treatment. Data are expressed as bar plot (mean) with error bars (SD) (* $P < 0.05$, ** $P < 0.01$, † $P < 0.001$, †† $P < 0.0001$) (ALT: active laser treatment; PLT: placebo laser treatment).

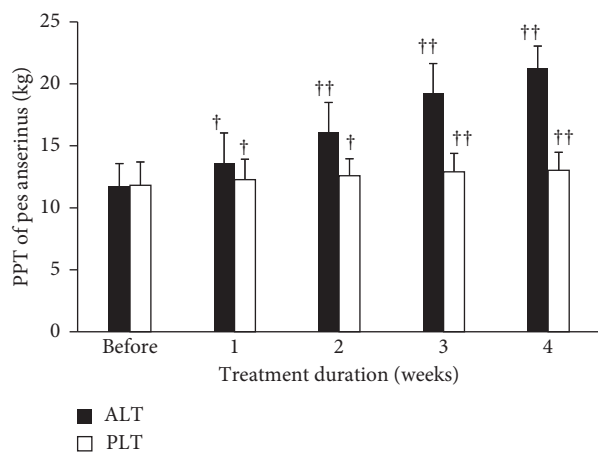


FIGURE 5: The variations of the two groups in the pes anserinus tendon pain pressure threshold before experiment and 4 weeks after treatment. Data are expressed as bar plot (mean) with error bars (SD) († $P < 0.001$, †† $P < 0.0001$) (ALT: active laser treatment; PLT: placebo laser treatment).

neither traditional physiotherapy nor drug-assisted treatment produced good curative effect. After LLLT for three times per week for four weeks, the curative effect for the ALT group was better than that of the PLT group in terms of knee OA severity index, conscious pain index for moving knee, conscious pain index for knee resting still, and pes anserinus tendon PPT with statistically significant differences.

Degenerative arthritis initially affects the medial articular surface, so degenerated articular cartilage often occurs in the medial tibia and/or on the articular surface of the femur [26]. For patients with knee OA, these acupoints, SP9 and SP10, which anatomically correspond to vastus medialis oblique muscle and pes anserinus tendon, respectively, are the most susceptible to soreness. SP9 and SP10 are found at the points on the spleen channel. According to the

acupuncture principle of “tracking and treating a disease along the appropriate meridian course,” stimulating points of the spleen channel in the vicinity of the knee joint produces curative effect on degenerative arthritis. EX-LE2 (hèdǐngxuè) is the most popular extraordinary point used for managing the knee problem in traditional Chinese medicine. The acupoint is located in the center of the upper border of the patella and needled with the patient’s knee slightly flexed. In the neuroanatomy of western medicine, the point is innervated via the intermediate femoral cutaneous nerve of the thigh (L2-L3).

Pain of knee OA involves arthralgias, articular cartilage impairment, peripheral soft tissue damages, etc. LLLT can facilitate tissue repair and proliferation by promoting blood circulation, thereby relieving joint pain and improving pain pressure threshold [27–29]. Hegedus et al. [27] indicated that degenerative arthritis patients could be treated with the LLLT apparatus, twice per week for four weeks. Results showed that the treatment group showed significant improvements in terms of pain index, pressure sensitivity, and joint bending angle after LLLT. In addition, lesions were detected using the infrared apparatus and the temperature at the targeted spots of knee joints slightly increased, thus indicating that LLLT can improve the blood circulation of the irradiated spots.

Laser penetration in human tissues varies with wavelength; that is, red laser penetrates more deeply than violet light, green light, or yellow light. Infrared ray with longer wavelength is invisible and it penetrates human tissues more deeply than visible red light. The laser apparatuses used in the present study have bichromatic laser needles alternating, having broader penetration range. Laser penetration often varies with lesion depth, and the broader penetration range can produce a better curative effect. The first bichromatic laser apparatus (685 nm/785 nm) was developed by the University of Paderborn, Germany, and the earliest related scientific research was conducted and published by Medical University of Graz, Austria, in 2002. Bichromatic laser is often a combination of two different wavelengths. For instance, the dual-frequency LLLT apparatus used in the present study combines red light (780 nm) and near-infrared light (830 nm), having deeper penetration (2–3 cm) than any laser of a single wavelength in human tissues [30].

The findings of this study have to be seen in light of two limitations. First, the sample size of this study is small and it may affect statistical power. The second limitation concerns the lack of long-term follow-up for evaluation of clinical efficacy after LLLT. Therefore, if there are sufficient resources, future research is required to follow up longer for better understanding of the subsequent responses.

5. Conclusions

In this study, patients with knee OA received LLLT at the three points, namely, SP9, SP10, and EX-LE2. Results showed that a diode laser (TL-816-2, Transverse Inc., Taiwan) produced a dual-frequency laser beams (combines red light (780 nm) and near-infrared light (830 nm)) and a good curative effect on knee OA, with significant improvements in

the severity index (Lequesne index), conscious pain index, and pain pressure threshold. Nonetheless, the clinical efficacy of LLLT and the parameter setting of the laser apparatus need further investigation.

Data Availability

The original data used to support the findings of this study are available from the corresponding author upon request.

Disclosure

No commercial party having a direct financial interest in the results of the research supporting this article has or will confer a benefit upon the authors or upon any organization with which the authors are associated.

Conflicts of Interest

The authors declare that they have no conflicts of interest.

Acknowledgments

This work was supported in part by China Medical University Hospital (CRS-108-047, DMR-109-094) and Asia University Hospital (10751003).

References

- [1] L. S. Cunningham and J. L. Kelsey, "Epidemiology of musculoskeletal impairments and associated disability," *American Journal of Public Health*, vol. 74, no. 6, pp. 574–579, 1984.
- [2] D. T. Felson, A. Naimark, J. Anderson, L. Kazis, W. Castelli, and R. F. Meenan, "The prevalence of knee osteoarthritis in the elderly: the Framingham osteoarthritis study," *Arthritis & Rheumatism*, vol. 30, no. 8, pp. 914–918, 1987.
- [3] D. T. Felson, "The epidemiology of knee osteoarthritis: results from the Framingham osteoarthritis study," *Seminars in Arthritis and Rheumatism*, vol. 20, no. 3, pp. 42–50, 1990.
- [4] D. T. Felson, Y. Zhang, M. T. Hannan et al., "The incidence and natural history of knee osteoarthritis in the elderly, the Framingham osteoarthritis study," *Arthritis & Rheumatism*, vol. 38, no. 10, pp. 1500–1505, 1995.
- [5] G. Peat, R. McCauley, and P. Croft, "Knee pain and osteoarthritis in older adults: a review of community burden and current use of primary health care," *Annals of the Rheumatic Diseases*, vol. 60, no. 2, pp. 91–97, 2001.
- [6] I. F. Petersson, "Occurrence of osteoarthritis of the peripheral joints in European populations," *Annals of the Rheumatic Diseases*, vol. 55, no. 9, pp. 659–661, 1996.
- [7] H. J. Cho, V. Morey, J. Y. Kang, K. W. Kim, and T. K. Kim, "Prevalence and risk factors of spine, shoulder, hand, hip, and knee osteoarthritis in community-dwelling Koreans older than age 65 years," *Clinical Orthopaedics and Related Research*, vol. 473, no. 10, pp. 3307–3314, 2015.
- [8] D. J. Hart and T. D. Spector, "Definition and epidemiology of osteoarthritis of the hand: a review," *Osteoarthritis and Cartilage*, vol. 8, no. Suppl A, pp. S2–S7, 2000.
- [9] J. H. Kellgren and J. S. Lawrence, "Radiological assessment of osteo-arthrosis," *Annals of the Rheumatic Diseases*, vol. 16, no. 4, pp. 494–502, 1957.
- [10] R. Altman, E. Asch, D. Bloch et al., "Development of criteria for the classification and reporting of osteoarthritis: classification of osteoarthritis of the knee," *Arthritis & Rheumatism*, vol. 29, no. 8, pp. 1039–1049, 1986.
- [11] L. E. Miller, M. J. Sloniewsky, T. E. Gibbons, J. G. Johnston, K. D. Vosler, and S. Nasir, "Long-term clinical benefit and cost-effectiveness of an 8-week multimodal knee osteoarthritis management program incorporating intra-articular sodium hyaluronate (Hyalgan®) injections," *Journal of Pain Research*, vol. 10, pp. 1045–1054, 2017.
- [12] D. Ip and N.-Y. Fu, "Two-year follow-up of low-level laser therapy for elderly with painful adhesive capsulitis of the shoulder," *Journal of Pain Research*, vol. 8, pp. 247–252, 2015.
- [13] E. F. Youssef, Q. I. Muaidi, and A. A. Shanb, "Effect of laser therapy on chronic osteoarthritis of the knee in older subjects," *Journal of Lasers in Medical Sciences*, vol. 7, no. 2, pp. 112–119, 2016.
- [14] T. Nakamura, S. Ebihara, I. Ohkuni et al., "Low level laser therapy for chronic knee joint pain patients," *Laser Therapy*, vol. 23, no. 4, pp. 273–277, 2014.
- [15] T. A. Ammar, "Monochromatic infrared photo energy versus low level laser therapy in patients with knee osteoarthritis," *Journal of Lasers in Medical Sciences*, vol. 5, no. 4, pp. 176–182, 2014.
- [16] J. H. Herman and R. C. Khosla, "In vitro effects of Nd:YAG laser radiation on cartilage metabolism," *The Journal of Rheumatology*, vol. 15, no. 12, pp. 1818–1826, 1988.
- [17] R. J. Schultz, S. Krishnamurthy, W. Thelmo, J. E. Rodriguez, and G. Harvey, "Effects of varying intensities of laser energy on articular cartilage: a preliminary study," *Lasers in Surgery and Medicine*, vol. 5, no. 6, pp. 577–588, 1985.
- [18] T.-C. Pan, Y.-H. Tsai, W.-C. Chen, and Y.-L. Hsieh, "The effects of laser acupuncture on the modulation of cartilage extracellular matrix macromolecules in rats with adjuvant-induced arthritis," *PLoS One*, vol. 14, no. 3, Article ID e0211341, 2019.
- [19] J. Walker, "Relief from chronic pain by low power laser irradiation," *Neuroscience Letters*, vol. 43, no. 2-3, pp. 339–344, 1983.
- [20] A. A. Matulis, V. V. Vasilenkaitis, I. L. Raistenskii, E. N. Cheremnykh-Alekseenko, and B. A. Gaigalene, "Laser therapy and laser puncture in rheumatoid arthritis, osteoarthritis deformans and psoriatic arthropathy," *Terapevticheski Arkhiv*, vol. 55, no. 7, pp. 92–97, 1983.
- [21] K. H. Beckmann, G. Meyer-Hamme, and S. Schröder, "Low level laser therapy for the treatment of diabetic foot ulcers: a critical survey," *Evidence-Based Complementary and Alternative Medicine*, vol. 2014, Article ID 626127, 9 pages, 2014.
- [22] K. Itoh, S. Hirota, Y. Katsumi, H. Ochi, and H. Kitakoji, "A pilot study on using acupuncture and transcutaneous electrical nerve stimulation (TENS) to treat knee osteoarthritis (OA)," *Chinese Medicine*, vol. 3, no. 1, p. 2, 2008.
- [23] M. E. Suarez-Almazor, C. Looney, Y. Liu et al., "A randomized controlled trial of acupuncture for osteoarthritis of the knee: effects of patient-provider communication," *Arthritis Care & Research*, vol. 62, no. 9, pp. 1229–1236, 2010.
- [24] S. Lee, K. H. Kim, T.-H. Kim et al., "Moxibustion for treating knee osteoarthritis: study protocol of a multicentre randomized controlled trial," *BMC Complementary and Alternative Medicine*, vol. 13, no. 1, p. 59, 2013.
- [25] M. G. Lequesne, C. Mery, M. Samson, and P. Gerard, "Indexes of severity for osteoarthritis of the hip and knee: validation-value in comparison with other assessment tests," *Scandinavian Journal of Rheumatology*, vol. 16, no. sup65, pp. 85–89, 1987.

- [26] S. Ahlback, "Osteoarthritis of the knee: a radiographic investigation," *Radiology*, vol. 93, no. 1, p. 134, 1969.
- [27] B. Hegedus, L. Viharos, M. Gervain, and M. Gálfi, "The effect of low-level laser in knee osteoarthritis: a double-blind, randomized, placebo-controlled trial," *Photomedicine and Laser Surgery*, vol. 27, no. 4, pp. 577–584, 2009.
- [28] Z. Huang, J. Chen, J. Ma, B. Shen, F. Pei, and V. B. Kraus, "Effectiveness of low-level laser therapy in patients with knee osteoarthritis: a systematic review and meta-analysis," *Osteoarthritis and Cartilage*, vol. 23, no. 9, pp. 1437–1444, 2015.
- [29] S. M. Rayegani, S. A. Raeissadat, S. Heidari, and M. Moradi-Joo, "Safety and effectiveness of low-level laser therapy in patients with knee osteoarthritis: a systematic review and meta-analysis," *Journal of Lasers in Medical Sciences*, vol. 8, no. Suppl 1, pp. S12–S19, 2017.
- [30] G. Litscher, "Integrative laser medicine and high-tech acupuncture at the medical university of Graz, Austria, Europe," *Evidence-Based Complementary and Alternative Medicine*, vol. 2012, no. 1, 21 pages, Article ID 103109, 2012.

Research Article

Effect of Qing'e Decoction on Leptin/Leptin Receptor and Bone Metabolism in Naturally Aging Rats

Pan Sun ¹, Yuanyuan Zhang,² Zhenpu Wei,³ Zhiqiang Wang,³ Shiming Guo,⁴ and Yanping Lin ¹

¹Academy of Integrative Medicine, Fujian University of Traditional Chinese Medicine, Fuzhou, Fujian 350122, China

²Institute of Traditional Chinese Medicine, Fujian University of Traditional Chinese Medicine, Fuzhou, Fujian 350122, China

³Institute of Acupuncture and Moxibustion, Fujian University of Traditional Chinese Medicine, Fuzhou, Fujian 350122, China

⁴Zhangzhou Hospital of Traditional Chinese Medicine, Zhangzhou, Fujian 363000, China

Correspondence should be addressed to Yanping Lin; linyanping1966@163.com

Received 11 June 2020; Accepted 5 September 2020; Published 19 September 2020

Academic Editor: Arham Shabbir

Copyright © 2020 Pan Sun et al. This is an open access article distributed under the Creative Commons Attribution License, which permits unrestricted use, distribution, and reproduction in any medium, provided the original work is properly cited.

Senile osteoporosis (SOP) is a common disease that has decreased bone strength as its main symptom. There is currently no medication that can treat SOP, and traditional Chinese medicine has advantages in slowing down bone aging. The present study aimed to observe the effects of Qing'e decoction on leptin, leptin receptor, sex hormone, and biochemical markers of bone metabolism in naturally aging rats and to explore its mechanism in regulating bone metabolism. The results revealed that, with the increase in age, the bone mineral density (BMD), bone strength, bone trabecula sparse, serum levels of leptin receptor (LEP-R), estradiol (E2), testosterone (T), core binding-factor α -1 (Cbf α -1), collagen-I (COL-I) and osteocalcin (OC), and the mRNA levels of leptin (LEP) and LEP-R in bone tissue decreased, while serum LEP levels increased in the female and male NS groups. The serum levels of LEP, LEP-R, E2, T, osteoprotegerin, Cbf α -1, COL-I, OC and bone alkaline phosphatase, and the mRNA levels of LEP and LEP-R in bone tissue in the female and male QED groups were higher than those in the same age and sex NS group, while the BMD, bone trabecular area percentage, maximum load, and maximum stress in the female and male QED groups were significantly higher than those in the same age and sex NS group. In conclusion, with the increase in age, the bone quality of naturally aging rats decreased gradually. Qing'e decoction can regulate the bone metabolism and increase the bone quality and delay bone aging, which may be achieved by increasing sex hormone, LEP, and LEP-R levels.

1. Introduction

Osteoporosis (OP), which is called a 'silent killer', is a common degenerative disease characterized by reduced bone mass and bone microstructural changes, decreased bone strength, and increased risk of fracture. Senile osteoporosis (SOP) is a type of primary OP with a low conversion rate of bone metabolism [1]. With the increase in human life expectancy, the world is gradually entering an aging society, and the incidence and morbidity of OP are also increasing year by year [2]. However, there is currently a lack of an ideal treatment for SOP.

LEP, which is a peptide hormone synthesized and secreted by fat cells, is an endocrine protein mainly expressed

in adipose tissue. In recent years, studies have shown that LEP plays a key role in regulating bone metabolism [3, 4]. It has been proved that leptin receptors are widely present in a variety of tissues, including bone tissue. Leptin receptors are expressed in bone marrow mesenchymal stem cells, osteoblasts, and other osteocytes [5, 6]. Studies on the pathogenesis of osteoporosis have found that an increase in adipocytes in the bone marrow can affect osteoblast differentiation and function, increase osteoclast activity, and influence bone mineralization, so leptin production by adipocytes may be an important regulator of the pathogenesis of osteoporosis [4]. However, its specific mechanism of action, especially in the aging process, needs further clarification.

Qing'e pills originated from *Prescriptions of the Bureau of Taiping People's Welfare Pharmacy* [7] and consist of *Eucommia ulmoides*, *Psoralea corylifolia* L, *Semen Juglandis*, and *Allium sativum* L. In the theory of Traditional Chinese Medicine, SOP is mainly caused by deficiency of spleen-kidney Yang, so tonifying the kidney and strengthening the spleen can treat SOP; Qing'e pills have the functions of invigorating the kidney and strengthening the spleen, bones, waist, and knee. Clinical research has confirmed that Qing'e pills have significant efficacy on SOP; Qing'e Pills can improve bone quality and bone density and relieve low back pain in different syndrome types of SOP [8, 9]. However, the mechanism of Qing'e pills in the treatment of osteoporosis is still unclear. Therefore, this study intended to use aging rats as an SOP model to observe changes in LEP, leptin receptor (LEP-R) and serum bone metabolism markers with age, and the mechanism of action of the drug. Since rats cannot swallow pills, instead of Qing'e pills, oral decoction was used, which was called Qing'e decoction (QED).

2. Materials and Methods

2.1. Preparation of QED. According to the dosage of Chinese medicines in the 2000 edition of the Pharmacopoeia of the People's Republic of China (edited by the National Pharmacopoeia Commission) [10], the ratio of *Eucommia ulmoides*, *Psoralea corylifolia* L, *Semen Juglandis*, and *Allium sativum* L was 16 : 8 : 5 : 4. All herbs (from Good Agricultural Practice planting base) were purchased from the Chinese Medicine Hall of Fujian University of Traditional Chinese Medicine. All ingredients were identified by the Department of Pharmacy of the Second People's Hospital of Fujian Province to fulfil the quality requirements of the Pharmacopoeia of the People's Republic of China. The extract was also prepared by the aforementioned department. All the ingredients were soaked for 20 min, and the mixture was then decocted in boiling water for 45 min and vacuum-dried to yield a final concentration of 4.71 g crude drug/g. The conversion ratio between 200 g rats and 70 kg adults is 0.018, and the daily oral crude drug consumption for adults is 99 g; thus, the daily dose for rats was calculated to be $99 \times 0.018 / 0.2 = \sim 9$ g/kg/day, which is equivalent to 1.91 g extract.

2.2. Animals. All animal experiments were conducted in strict accordance with the *Guide for the Care and Use of Laboratory Animals* and were approved by the Animal Care and Use Committee of Fujian University of Traditional Chinese Medicine (Approval No. 2020012). In total, 162 healthy, SPF-grade 6-month-old Sprague Dawley (SD) rats were purchased from Shanghai Slac Laboratory Animal Co., Ltd. (license no. SCXK (Shanghai) 2012-0002; certificate no. 2007000562039). SD rats were fed in the Experimental Animal Center of Fujian University of Traditional Chinese Medicine. The rats were fed with unified standard feed, which contained crude protein, crude fat, crude fiber, and other components. Each kilogram of feed contained 10–18 g calcium, 6–12 g phosphorus, and vitamin D ≥ 800 IU. The

feeding conditions of each group were the same, which would not affect the experimental results.

2.3. Experiment Design and Treatment. There were 81 male and 81 female SD rats of 6 months of age. A total of 9 male and female SD rats were randomly selected, and their tissues were collected after 1 week of adaptive feeding. In total, 36 rats (18 males and 18 females) were randomly selected from the remaining rats and divided into four groups: (i) female rats fed with QED (female QED group; $n = 9$); (ii) female rats fed with normal saline (female NS group; $n = 9$); (iii) male rats fed with QED (male QED group; $n = 9$); and (iv) male rats fed with normal saline (male NS group; $n = 9$). The remaining rats were fed normally and were grouped again at the age of 9, 12, and 15 months. The grouping method was the same as that described above. The gavage dose was calculated according to the body surface area, and the dose was adjusted weekly according to weight. Rats in the QED group were administered 1.91 g/kg/day QED extract dissolved with 2 ml normal saline. The saline group was administered normal saline (2 ml/day). After 3 months of continuous intervention, rats were euthanized with an overdose of pentobarbital (200 mg/kg), and their tissues were collected.

Blood was collected from the abdominal aorta, and the serum was centrifuged at 990 g for 15 min after standing for 4 h to separate the serum. The serum was separated and stored in the refrigerator at -80°C . The left tibia was separated, fixed in paraformaldehyde solution and EDTA decalcified. Next, Masson staining sections were prepared. The right tibia was separated for detection of bone density and bone biomechanics. The lumbar were subjected to LEP and LEP-R protein and mRNA detection.

2.4. Reagents. The following reagents were used in our study: RIPA protein lysate, protease inhibitor (Solarbio Science and Technology) (Beyotime Institute of Biotechnology); color prestained protein marker (Thermo Fisher Scientific, 26616); BCA protein concentration assay kit and TRIzol (Beyotime Institute of Biotechnology); estradiol (E2), testosterone (T), osteoporogeterin (OPG), receptor activator of nuclear factor- κ B ligand (RANKL), core-binding factor subunit α -1 (Cbf α -1), collagen-I (COL-I), osteocalcin (OC), bone alkaline phosphatase (BALP), and tartrate-resistant acid phosphatase 5b (TRACP-5b) ELISA kits (Wuhan Cusabio Bioengineering Co., Ltd.); reverse transcription kit and SYBR Premix Ex TaqTM PCR Kit (Takara Bio, Inc.); PCR primers (Shanghai Bioengineering Technology Co., Ltd.); anti-LEP antibody (1 : 1000; Abcam, cat. no. ab3583); anti-LEP-R antibody (1 : 1000; Abcam, cat. no. ab104403); anti- β -actin antibody (1 : 1000; Cell Signaling Technology, Inc., cat. no. #4970); and anti-mouse IgG (H + L) (1 : 5000; Proteintech Group, Inc. cat. no. SA00001-1).

2.5. Measurement of Bone Mineral Density (BMD) and Bone Biomechanics. The BMD of the right tibia of rats was measured by a dual-energy X-ray 4500W BMD instrument.

The maximum load (KN) and the maximum stress (n/mm²) were measured in an ig-a1000n universal material testing machine.

2.6. Morphology. The metaphyses of the left proximal tibia of the rats in each group were isolated and fixed with 4% paraformaldehyde solution for 48 h. Then, they were decalcified in EDTA-decalcified solution for 90 days and embedded in paraffin. A tissue slicer was used to prepare slices of 5 mm thickness along the longitudinal section of the long axis of the tibia. After Masson staining, changes in morphology and structure of the metaphyses of the proximal tibia (excluding tibial plateau) were observed with a microscope. The percentage of trabecular area (trabecular area in visual field/total area measured) was measured using a Motic Med 6.0 digital medical image analysis system (Motic Instruments).

2.7. ELISA. Frozen serum was incubated at room temperature for 30 min. Then, 100 μ l standard at different concentrations and serum were added to the well. Then, 50 μ l enzyme-linked affinity was added to each well and incubated at 37°C for 60 min. Next, the solution was removed from inside the well and washed thoroughly. Then, substrates I and II were added to the wells and mixed and allowed to react for 15 min at room temperature in the dark. The reaction was stopped, and 30 mins later, the optical density (OD) of each well was measured using a microplate reader set to 450 nm. A standard curve was created to calculate the LEP, LEP-R, E2, T, BALP, TRACP-5b, OC, Cbfa-1, OPG, and RANKL contents in serum.

2.8. Reverse Transcription-Quantitative PCR (RT-qPCR). Total RNA was extracted from the tissue according to the TRIzol method, and the RNA concentration and OD were measured with a UV spectrophotometer. An OD260/OD280 between 1.8 and 2.0 indicated that the RNA concentration was appropriate. A total of 1 μ g RNA was used for the reaction, alongside 4 μ l 5X PrimeScriptTM Buffer (for Real Time), 1 μ l PrimeScriptTM RT Enzyme Mix 1, 1 μ l Oligo dT Primer, 1 μ l/concentration total RNA, and DECP water (20 μ l). RT was performed on a PCR instrument, and cDNA was obtained for PCR. The primers used were as follows: LEP primer (F) 5'-TCACACACGCAGTCGGTATC-3' and reverse (R) 5'-GAGGAGGTCTCGCAGGTCT-3'; LEP-R F 5'-TTGCGTATGGAAGTCACAGATG-3' and R 5'-CACCTGGACCTCGTATGAAGAC-3'; and GAPDH F 5'-GGCACAGTCAAGGCTGAGAATG-3' and R 5'-ATGGTGGTGAAGACGCCAGTA-3'.

According to SYBR GREEN instructions, the reaction system was set up as follows: SYBR Premix Ex TaqTM II (2X), 10 μ l; ROX Reference Dye II (50X), 0.4 μ l; F primer (10 μ mol/l), 0.8 μ l; R primer (10 μ mol/l), 0.8 μ l; 2 μ l cDNA template; and 6 μ l DECP water. The reaction conditions were as follows: Predenaturation at 95°C for 30 sec, denaturation at 95°C for 5 sec, annealing and extension at 60°C for 34 sec (40 cycles to obtain the amplification curve

and Cq value), and 95°C for 30 sec, 95°C for 3 sec, and 60°C for 30 sec (40 cycles to obtain the dissolution curve).

2.9. Western Blotting. After extracting total protein from bone tissue, the BCA method was used for protein quantification. Gels were prepared according to the instructions of the SDS-PAGE kit (Solarbio Science & Technology, P1200) and 5 μ l marker, and 40 μ g protein samples were loaded. The initial voltage was 20 V for 10 min, 80 V for 30 min, and 120 V for 90 min. After electrophoresis, the proteins were transferred to a PVDF membrane, and membranes were blocked by 5% nonfat milk for 2 h and incubated with the primary antibodies overnight at 4°C. TBST was used to wash the membranes, and the goat peroxidase-conjugated secondary antibody was incubated at room temperature for 1 h before chemiluminescence imaging.

2.10. Statistical Analysis. Statistical analysis was performed using SPSS software (version 23.0; IBM Corp.). Data were analyzed using one-way ANOVA with the post hoc Tukey's test was used to compare multiple groups. Data are presented as the mean \pm standard deviation. $P < 0.05$ was considered to indicate a statistically significant difference. The correlation between LEP, LEP-R, BMD, E2, T, OPG, RANKL, Cbfa-1, COL-I, OC, BALP, and TRACP-5b was analyzed by bivariate correlation test.

3. Results

3.1. QED Can Improve the Bone Quality of Aging Rats. The bone density of male rats reached the highest peak at 15 months of age, while that of female rats reached the highest peak at 12 months of age and then it gradually decreased. The decrease in bone density in the QED group was slower than that in the NS group (Figure 1(a)). The maximum load and stress of tibia of male and female rats decreased gradually after 12 months of age. The rate of decrease in the QED group was slower than that in the NS group (Figures 1(b) and 1(c)). The results showed that the loss of bone mass and the decrease in bone strength occurred after 12 months of age. The bone density and bone strength of rats in QED group were higher than those of the NS group. This indicates that QED can slow down the loss of bone mass, improve the bone quality, and delay the aging of bones.

3.2. Morphology. In this experiment, the bone trabeculae of the upper tibia were stained with Masson staining after conventional paraffin-embedded sectioning. The bone trabeculae were colored blue/green, and the bone marrow cells were red. The results showed that the bone trabeculae of the upper tibia of 6-month-old rats were arranged regularly and closely, distributed evenly, connected in a network shape, and continuous without fracture and had small interstices. With the increase in age, the number of bone trabeculae decreased gradually; the morphology and structure became

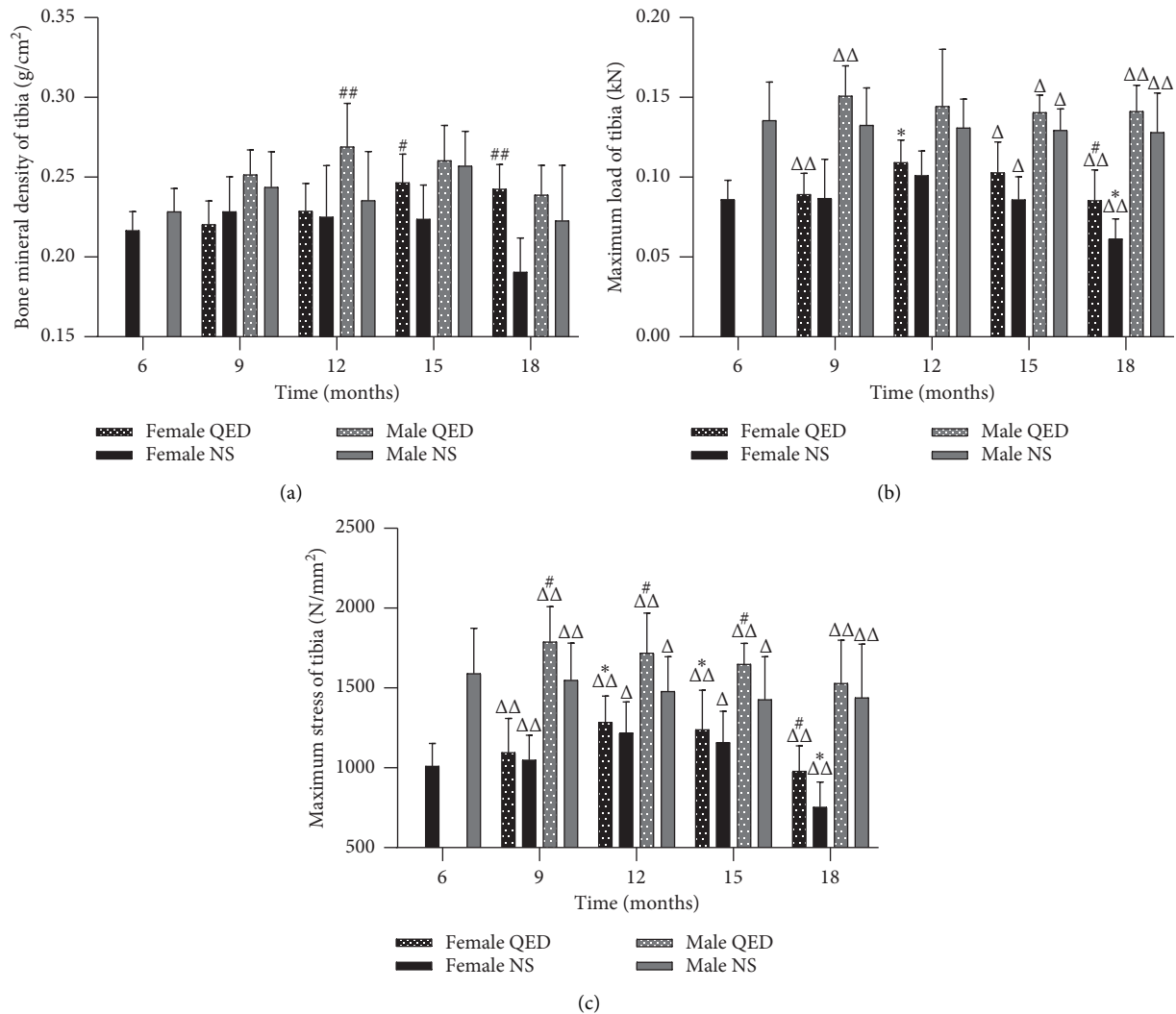


FIGURE 1: Qing'e decoction can improve the bone quality of aging rats. (a) Bone mineral density of tibia. (b) Maximum load of tibia. (c) Maximum stress of tibia. * $P < 0.05$, ** $P < 0.01$ vs. same-sex 6-month-old group; # $P < 0.05$, ## $P < 0.01$ vs. same-age and sex normal saline group but different intervention group; ΔΔ $P < 0.05$, ΔΔΔ $P < 0.01$ vs. same-intervention and age group but different sex.

sparse and thin; the distribution of trabeculae was scattered and irregular; the coincidence between trabeculae decreased; the porosity increased; the spacing increased; and there were fractures. Compared with that of the NS group of the same age and sex, the bone trabeculae in the QED group had better morphological and structural integrity, higher number, smaller spacing, and less fractures. The results showed that, with the increase in age, the percentage of trabecular area in the female and male groups decreased gradually, which was significantly different from that observed in the same sex groups ($P < 0.01$). Compared with the same-sex NS group, the percentage of bone trabecular area in both the female and male QED groups increased significantly ($P < 0.05$ and $P < 0.01$, respectively). In the same age and intervention group, the male was higher than the female in different genders. There were significant differences between the 12-, 15-, and 18-month-old QED group and the NS group ($P < 0.05$ and $P < 0.01$) (Figures 2(a) and 2(b)).

3.3. Effect of QED on Serum LEP, LEP-R, and Bone Metabolism Biomarkers. The serum LEP levels in the female and male NS groups gradually increased with age, while the serum LEP-R levels exhibited the opposite trend. Serum LEP and LEP-R levels in the female and male QED groups were higher than those in the same age and sex NS groups, but there was no significant difference. The levels of serum LEP and LEP-R in males were higher than those in females in the same age and the same-intervention group. The male 15-month-old QED group and the 12- and 15-month-old NS groups were significantly different from the female group ($P < 0.05$, $P < 0.01$) (Figures 3(a) and 3(b)).

With the increase in age, the serum E2 and T levels in both the female and male NS groups decreased significantly ($P < 0.05$). The E2 levels of the female QED groups were higher than those of the NS groups of the same sex and age ($P < 0.05$ and $P < 0.01$, respectively). The T levels of the male QED groups at 9 and 15 months of age were higher than

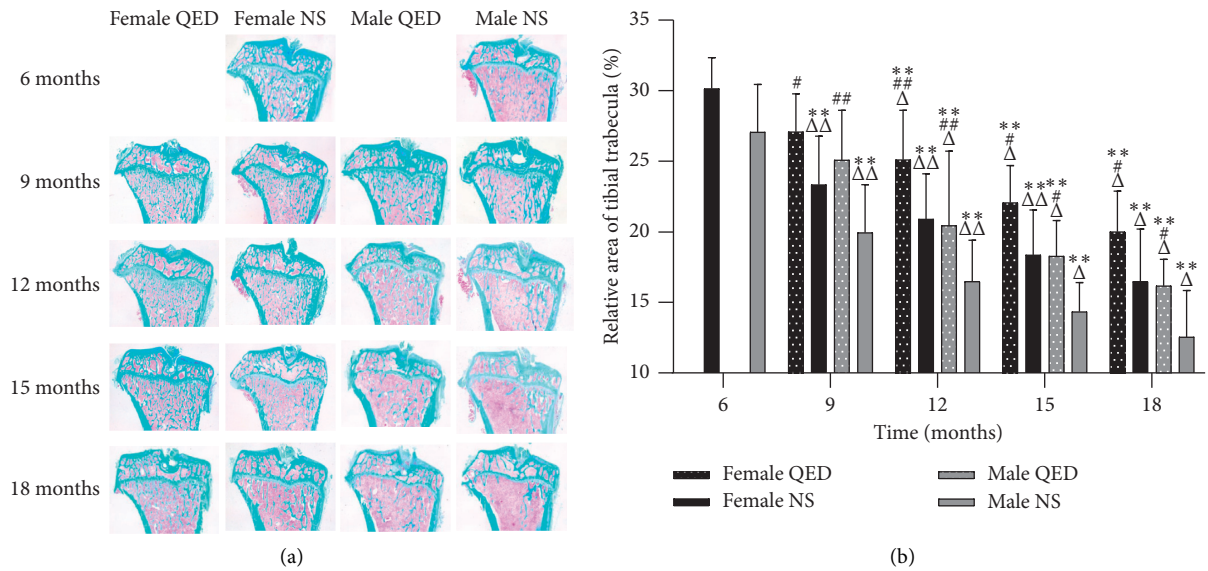


FIGURE 2: QED can increase the trabecular bone area. (a) Compared with that in the same-sex NS group of the same age, the bone trabeculae in the QED group had better morphological and structural integrity, higher number, and smaller spacing and less fracture phenomenon (magnification, $\times 20$). (b) Measurement results of trabecular area (%) of tibia in each group. * $P < 0.05$, ** $P < 0.01$ vs. same-sex 6-month-old rats; # $P < 0.05$, ## $P < 0.01$ vs. same-age and sex NS group but different intervention group; $\Delta P < 0.05$, $\Delta\Delta P < 0.01$ vs. same-intervention and age group but different sex. QED, Qing'e decoction; NS, normal saline.

those of the NS groups at the same sex and age ($P < 0.05$ or $P < 0.01$) (Figures 3(c) and 3(d)).

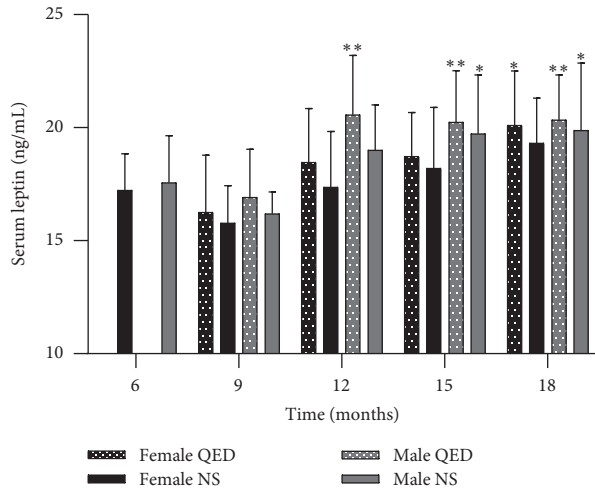
Serum OPG and RANKL levels were significantly increased from 6 to 9 months in both the male and female NS groups ($P < 0.01$) and were significantly decreased from 9 to 18 months of age ($P < 0.05$ or $P < 0.01$). Compared with those of the NS groups of the same age and sex, the serum OPG levels were increased, while the RANKL levels were decreased in the female and male QED groups ($P < 0.05$ or $P < 0.01$). The serum OPG levels in males were higher than those in females, while the serum RANKL levels were lower (Figures 3(e) and 3(f)).

The serum Cbfa-1, COL-I, and OC levels of the female and male NS groups decreased gradually, and the Cbfa-1 and COL-I levels were significantly different from the 6 months of the same gender ($P < 0.05$ or $P < 0.01$). However, OC levels did not differ significantly. The serum levels of Cbfa-1, COL-I and OC in the female and male QED groups were higher than those in the same-age NS group, and Cbfa-1 was significantly different in QED groups regardless of age ($P < 0.01$). COL-I exhibited significant differences in the 18-month-old QED groups ($P < 0.05$), whereas there was no significant difference in OC. Compared with those in the different sex and the same intervention group of the same age, the serum COL-I levels in the male groups were higher than those in the female groups, while the opposite was observed for OC. Serum Cbfa-1 in the 6- to 12-month-old male groups was higher than that in the female groups, while it was lower in the 12- to 15-month-old male groups, and had significant differences at each age ($P < 0.05$ or $P < 0.01$). The serum COL-I of the 12-, 15-, and 18-month-old QED groups were significantly different from those of the NS groups ($P < 0.01$). OC was significantly different only in the 15-month-old QED group ($P < 0.01$) (Figures 3(g) and 3(i)).

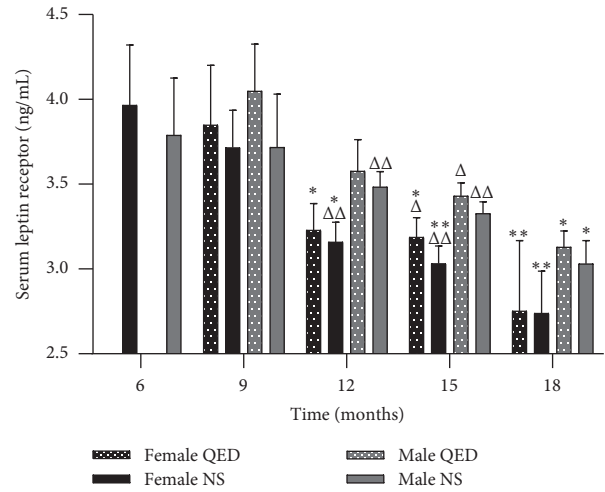
The serum BALP level of the female and male NS groups increased from 6 to 9 months, while it decreased from 9 to 18 months. The serum TRACP-5b level decreased with age. BALP and TRACP-5b in female and male QED groups were higher than those in the same-sex NS groups. The serum BALP and TRACP-5b levels in the male groups were higher than those in the female groups, and BALP was significantly different in the 18-month-old QED and the 12-, 15-, and 18-month-old NS groups ($P < 0.01$), while TRACP-5b was significantly different in the 9-month-old QED and NS groups ($P < 0.05$ and $P < 0.01$) (Figures 3(j) and 3(k)).

3.4. LEP and LEP-R mRNA and Protein Expression. With the increase in age, the expression level and protein content of LEP and LEP-R mRNA in bone tissue of the male and female NS groups decreased gradually. The expression of LEP and LEP-R mRNA and protein in the same-age and sex groups was higher than that in the NS group, but there was no significant difference. No significant differences were found males and females of the same-age and intervention groups (Figures 4(a)–4(e)).

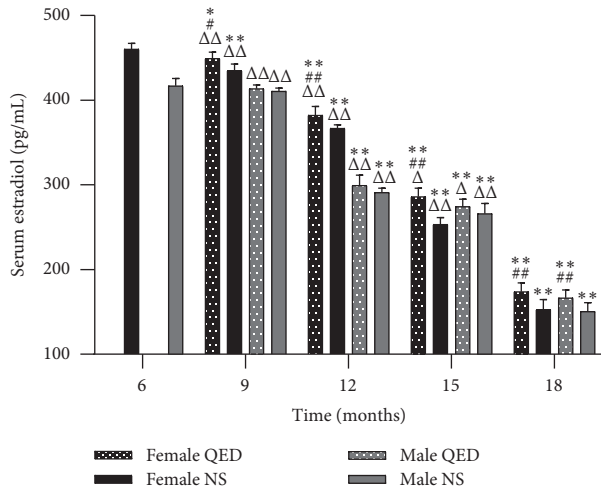
3.5. Correlation between Serum LEP, LEP-R, BMD, and Other Serum Bone Metabolic Markers. The correlation between LEP, LEP-R, BMD, E2, T, OPG, RANKL, Cbfa-1, COL-I, OC, BALP, and TRACP-5b was analyzed by the bivariate correlation test, with Pearson as the correlation coefficient. The results showed that serum LEP was negatively correlated with E2, T, OPG, RANKL, Cbfa-1, COL-I, and OC but not with BMD, serum BALP, or TRACP-5b. Serum LEP-R was positively correlated with, E2, T, OPG, RANKL, Cbfa-1,



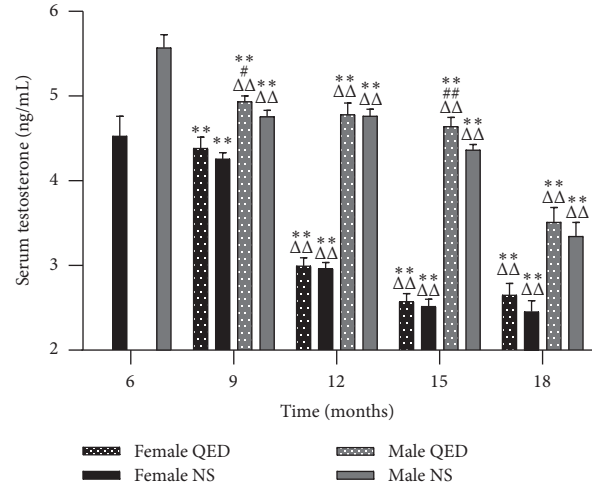
(a)



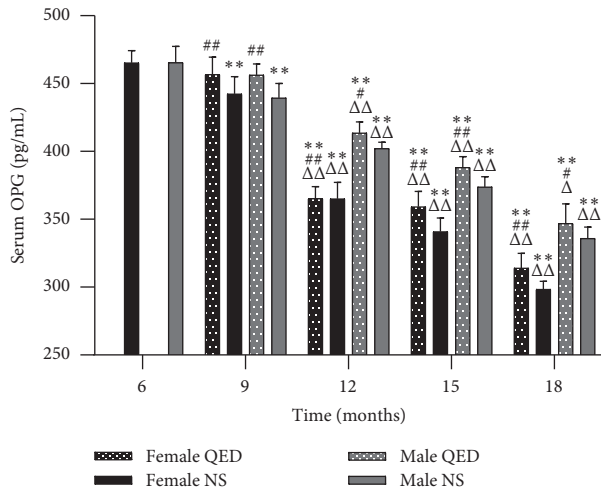
(b)



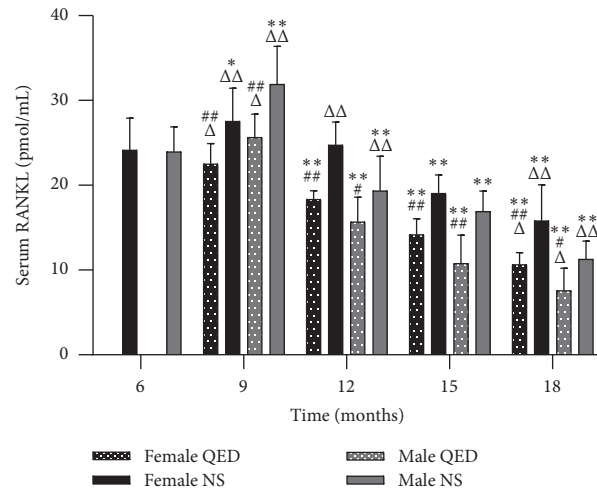
(c)



(d)



(e)



(f)

FIGURE 3: Continued.

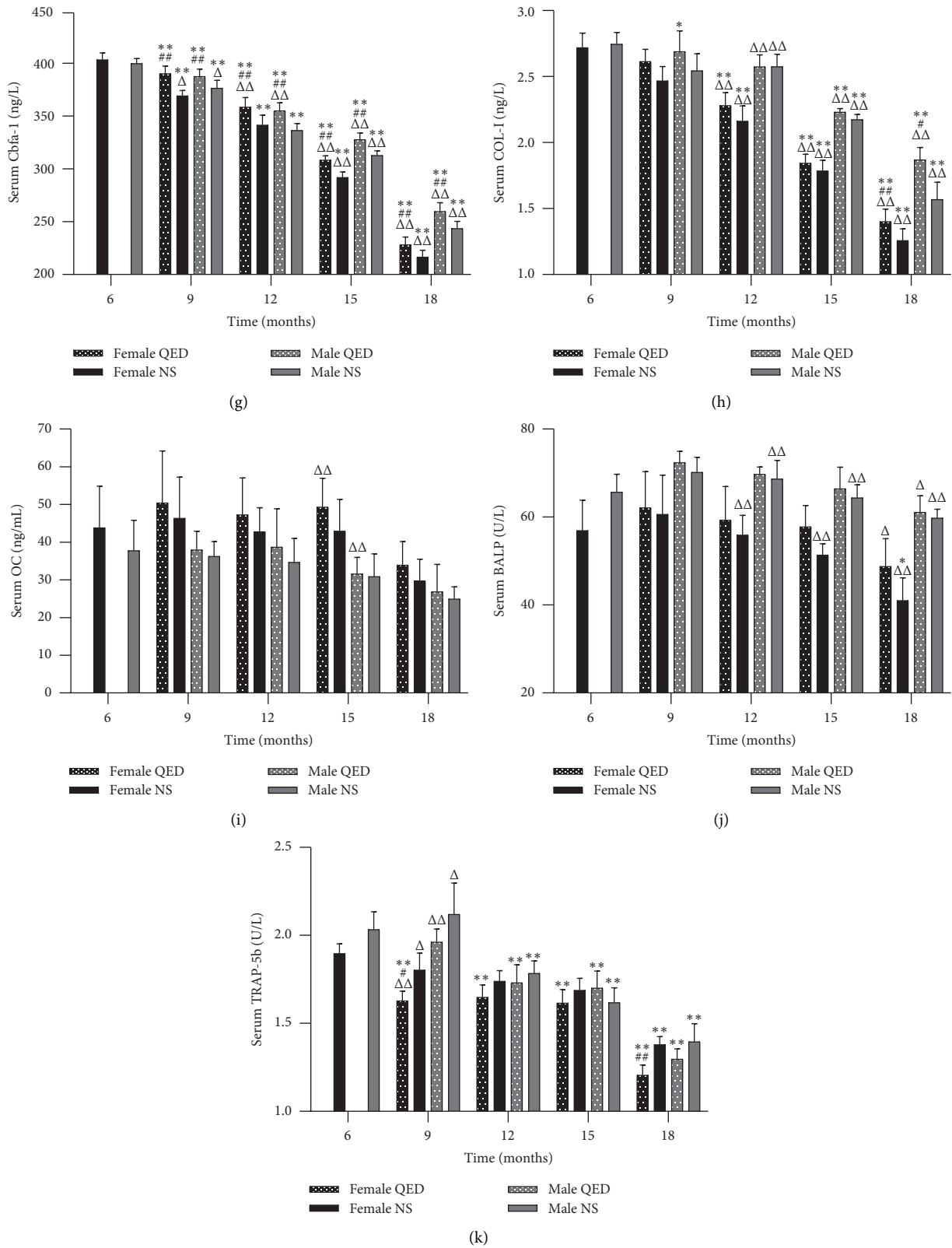


FIGURE 3: Qing'e decoction can affect serum leptin, leptin receptor, and bone metabolism markers. These biomarkers were detected by ELISA. * $P < 0.05$, ** $P < 0.01$ vs. same-sex 6-month-old rats; $P < 0.05$, ## $P < 0.01$ vs. same-age and sex NS group but different intervention group; $\Delta P < 0.05$, $\Delta\Delta P < 0.01$ vs. same-intervention and age group but different sex. OPG, osteoprotegerin; RANKL, receptor activator of nuclear factor- κ B ligand; Cbfa-1, core-binding factor subunit α -1; COL-I, collagen-I; OC, osteocalcin; BALP, bone alkaline phosphatase; TRACP-5b, tartrate-resistant acid phosphatase 5b.

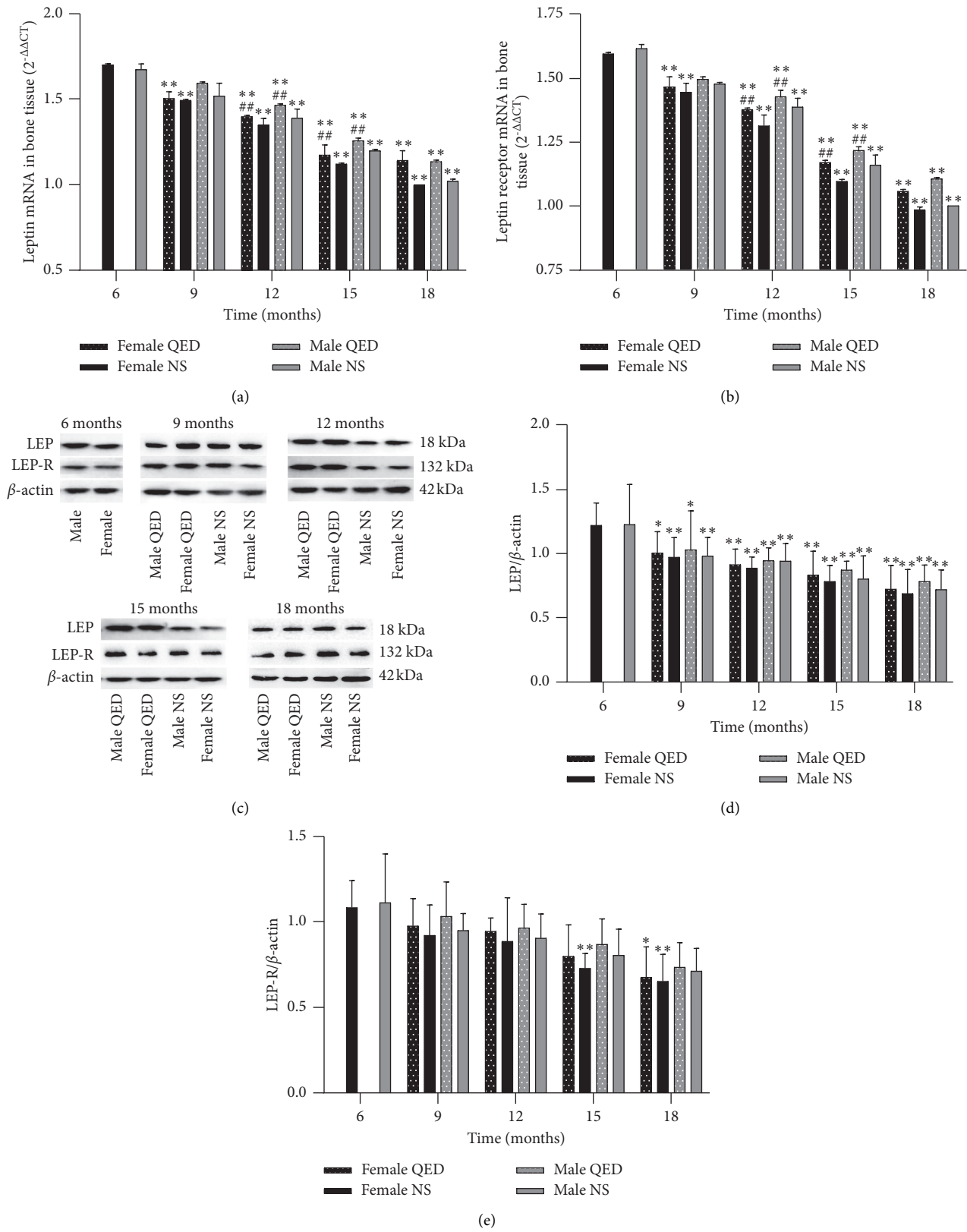


FIGURE 4: Effect of Qing'e decoction on bone tissue LEP and LEP-R mRNA and protein expression. Results of reverse transcription-quantitative PCR indicating the relative mRNA expression levels of (a) LEP and (b) LEP-R. (c) Images of protein expression analyzed by western blot assay. Relative protein expression levels of (d) LEP and (e) LEP-R. * $P < 0.05$, ** $P < 0.01$ vs. same-age 6-month-old rats; # $P < 0.05$, ## $P < 0.01$ vs. same-age and sex normal saline group but different intervention group. LEP, leptin; LEP-R, leptin receptor.

COL-I, OC, BALP, and TRACP-5b but not with BMD (Table 1).

4. Discussion

The bone remodeling process of normal people is maintained by the 'bone formation and resorption' coupling mechanism. As age increases, the uncoupling of bone formation and resorption is the main cause of bone loss. The results of BMD, biomechanics (Figures 1(a)–1(c)), and bone histomorphology (Figures 2(a) and 2(b)) showed that age-related bone loss begins to appear in female rats at 12 months of age and in male rats at 15 months of age, and the age-related bone loss in male rats is relatively slow, while the decrease in BMD is later and slower than in female rats. The reduction in bone metabolism leads to bone formation and bone resorption uncoupling, and osteoblast cell function is decreased while osteoclast functional activity is enhanced, eventually resulting in bone resorption greater than bone formation; thus, bone density is reduced, thereby causing bone aging. The morphological changes and biochemical markers of naturally aging rats at 18 months of age were similar to those of OP, which established a theoretical basis for further research in this subject.

Multiple factors are involved in the bone remodeling process, and LEP is one of them. Previous studies have shown that serum LEP levels increase with age in normal rats, while LEP-R levels decrease with age [11]. The soluble LEP-R is the major conjugate of LEP in the peripheral circulation and is an important factor in determining the total amount of LEP in the peripheral circulation. It can be used as a measure of the total quantity of bioactive LEP [12, 13]. Excessive LEP cannot play a role in inhibiting fat synthesis, indicating that there may be a 'LEP resistance' effect during aging, and this effect gradually increases with age [14]. Recent studies have shown that LEP plays a critical role in regulating bone metabolism [3, 4]. However, since the mechanism of the effect of LEP on bone metabolism involves numerous aspects, there is no convincing conclusion.

With the increase in age, the serum LEP levels of the female and male NS groups gradually increased, whereas the serum LEP-R levels decreased. The male serum LEP and LEP-R levels were higher in the same-intervention group than in the same-age group (Figures 3(a) and 3(b)). In bone tissue, we can see a gradual decrease in LEP mRNA and protein levels (Figures 4(a)–4(e)). As the expression of LEP-R decreased with age, the total LEP in serum increased but did not play a role with increasing age, probably due to "LEP resistance". The serum test results of bone metabolism-related biomarkers showed that serum E2, T, OPG, RANKL, Cbfa-1, COL-I, OC, and BALP levels in the female and male NS groups decreased significantly with age, while TRACP-5b significantly increased. There was a significant difference between the age of each month and the age of 6 months ($P < 0.05$ or $P < 0.01$) (Figures 3(a)–3(k)). In this experiment, the bivariate correlation test was used to analyze the correlation between biomarkers. The results showed that serum LEP was negatively correlated with E2, T, OPG, Cbfa-1, COL-I, and BALP, while serum LEP-R was

positively correlated with the levels of E2, T, OPG, RANKL, Cbfa-1, COL-I, OC, BALP, and TRACP-5b, indicating that serum LEP and LEP-R were closely associated with bone metabolism. In addition, the secretion of sex hormones decreased with age, and E2 and T were positively correlated with LEP-R but negatively correlated with LEP, indicating that the secretion of sex hormones was closely associated with the expression of LEP and LEP-R (Table 1).

OP is a disease of "guku," "guwei," and "gubi" in Traditional Chinese Medicine, mostly a spleen-kidney yang deficiency syndrome. In the theory of Traditional Chinese Medicine, the kidney includes the endocrine, urinary and reproductive systems, while the spleen includes the digestive system. Traditional Chinese Medicine considers that the kidney is involved in generating marrow and dominating bone, which means that the kidney plays an important role in the growth and development of bones. As age increases, kidney essence deficient, cannot generate marrow to raise bone, which leads to atrophic debility of the bone, namely OP. Therefore, the clinical treatment methods mostly rely on tonifying the kidney and strengthening the spleen. QED consists of *Eucommia* (fried salt), *Psoralea corylifolia L* (fried salt), *Semen Juglandis* (fried), and *Allium sativum L*. Decocting these four herbs together helps to warming up the yang, tonifying the kidney, warming up the middle, and strengthening the spleen, muscles, and bones. Previous studies have shown that QED can significantly regulate the bone metabolism-related factors, promote the bone formation, inhibit the bone absorption, and play an active role in the prevention and treatment of OP [15–18].

Our results showed that the serum LEP level increased and the serum LEP-R level decreased with age. In serum and bone tissue, LEP and LEP-R levels of the female and male QED groups were higher than those of the same-sex NS group, although the difference was not significant (Figures 3(a) and 3(b), (Figures 4(a)–4(e)). The serum LEP and LEP-R levels were higher in males than in females. Compared with the findings in the same-sex NS group of the same age, the shape and structure of bone trabeculae in the QED group were more complete, higher in number and smaller in spacing, and exhibited less fractures. The BMD, percentage of trabecular area, maximum load, and maximum stress in the female and male QED groups were higher than those in the same-age group. This result suggests that, with the increase in age, LEP may affect the bone metabolism, improve the bone quality, and delay the bone aging in various ways.

Some studies have shown that LEP can significantly increase the expression of Cbfa-1, COL-I, OC, and BALP [19, 20], which play key roles in the proliferation, differentiation, and maturation of osteoblasts [21–27], indicating that LEP can enhance bone formation. The experimental results showed that, with the increase in age, the levels of Cbfa-1, COL-I, and OC in the serum of female and male QED groups were significantly higher than those of the same-sex NS groups, and there were significant differences in Cbfa-1 at different ages ($P < 0.01$). COL-I levels exhibited a significant difference at 18 months of age ($P < 0.05$ or $P < 0.01$), but there was no significant difference in OC

TABLE 1: Correlation analysis of LEP, LEP-R, and bone metabolism markers.

| | BMD | E2 | T | OPG | RANKL | Cbfa1 | Col-I | OC | BALP | TRACP-5b |
|-------|-------|----------|---------|----------|----------|----------|----------|---------|---------|----------|
| LEP | 0.136 | -0.480** | -0.170* | -0.405** | -0.442** | -0.407** | -0.330** | -0.198* | -0.095 | -0.058 |
| LEP-R | 0.132 | 0.744** | 0.738** | 0.840** | 0.540** | 0.793** | 0.808** | 0.224** | 0.580** | 0.242** |

**Significant correlation at 0.01 level (bilateral), *Significant correlation at 0.05 level (bilateral). BMD: bone mineral density, E2: estradiol, T: testosterone, OPG: osteoporogeterin, RANKL: receptor activator of nuclear factor- κ B ligand, Cbfa-1: core-binding factor subunit alpha-1, COL-1: collagen?, OC: osteocalcin, BALP: bone alkaline phosphatase, TRACP-5b: tartrate-resistant acid phosphatase 5b.

levels, while serum LEP-R levels were positively correlated with Cbfa-1, COL-I, and OC. Furthermore, the serum BALP levels in the female and male QED groups were higher than those in the same-sex NS group. These findings suggested that QED can increase the concentration of Cbfa-1 in serum and then increase the concentration of COL-I, OC, and BALP, which may be caused by the increase in LEP-R in serum, which promotes the differentiation and maturation of osteoblasts, increases the functional activity of osteoblasts, and adjusts the uncoupling of bone absorption and bone formation caused by aging, thus effectively preventing and treating primary OP (Figures 3(g)–3(j)).

LEP can inhibit the differentiation, development, maturation, and function of osteoclasts through the regulation of RANKL/RANK/OPG, a signaling pathway closely associated with osteoclast functional activity [28–30]. The ratio of OPG to RANKL is negatively correlated with osteoclast differentiation [31]. LEP can increase the expression of OPG in osteoblasts and bone marrow stromal cells and inhibit the expression of RANKL, thus inhibiting the differentiation of osteoclasts, reducing the generation of osteoclasts, and inhibiting the bone absorption [32]. The results showed that, with the increase in age, the levels of serum OPG and RANKL in the female and male QED groups were significantly higher than those in the same-sex NS group ($P < 0.05$ or $P < 0.01$). It has been suggested that QED can increase the expression of OPG, enhance the competition with RANKL, reduce the concentration of RANKL, and decrease the binding rate of RANKL and RANKL, which may be associated with the increase in expression of LEP-R and the upregulation of the expression of LEP with biological activity, which increases the ratio of OPG/RANKL, inhibits the differentiation and maturation of osteoclasts, reduces the expression of Tracp-5b (an effective marker of osteoclast number and functional activity), and inhibits bone resorption and delays bone aging (Figures 3(e), 3(f) and 3(k)).

In the aging process, an important feature is the decrease in gonadal function. There is a close association between sex hormones and LEP. Some studies have shown that the expression level of sex hormones increases with the increase in LEP, and there is a positive correlation between the two [33, 34]. LEP can increase the estrogen concentration by increasing aromatase activity through LEP-R and STAT3, thus promoting bone formation. Moreover, estrogen can affect STAT3 phosphorylation levels through binding to the estrogen receptor and then acting on LEP and LEP-R [35, 36]. In conclusion, LEP is closely associated with sex hormones. LEP can regulate bone metabolism by affecting the expression of sex hormones. The results showed that,

with the increase in age, the serum E2 and T levels of the female and male QED groups were significantly higher than those of the same-sex NS groups, and the E2 levels of the female and male QED groups were significantly higher than those of males of 18 months of age, while the T levels of males at 9 and 15 months of age were significantly different ($P < 0.05$ or $P < 0.01$). This suggested that serum E2 and T levels in the female and male NS groups decreased significantly with increasing age, while QED could increase the expression of E2 and T by upregulating the expression of LEP-R, which may involve proteins of the LEP pathway such as STAT3, thus regulating bone metabolism and adjusting the uncoupling of bone absorption and bone formation due to aging in order to effectively prevent and treat primary OP (Figures 3(c) and 3(d)).

5. Conclusion

With the increase in age, the level of serum sex hormones decreased and the expression of serum LEP increased and the expression of LEP-R decreased, which led to the decrease of the OPG/RANKL ratio, disorder of bone metabolism, greater bone absorption than bone formation, and decrease in bone quality.

QED can regulate the bone metabolism, improve the bone quality, delay the bone aging, and prevent the and cure primary OP. This effect may be achieved by increasing the level of sex hormones, the expression of LEP and LEP-R, and the OPG/RANKL ratio.

Data Availability

The data used to support the findings of this study are available from the corresponding author upon request.

Conflicts of Interest

The authors declare that they have no conflicts of interests.

Authors' Contributions

LY and GS designed and directed the experiments. SP and ZY performed the experiments and wrote the manuscript. WeZ collected the data. WaZ analyzed the data. All authors read and approved the final manuscript.

Acknowledgments

This work was supported by the Natural Science Foundation of China (grant no. 81574003), Fujian Provincial Health and Family Planning Personnel Training Project (grant no. 2018-

ZQN-78), and Zhangzhou Natural Science Foundation (grant no. ZZ2018J33).

References

- [1] Z. Zhang, Z. Liu, S. Shi et al., "A retrospective study on the incidence of osteoporosis diagnosed by-2.5 SD in mainland China," *Chinese Journal of Osteoporosis*, vol. 24, no. 1, pp. 1-7, 2015.
- [2] Z. A. Cole, E. M. Dennison, and C. Cooper, "Osteoporosis epidemiology update," *Current Rheumatology Reports*, vol. 10, no. 2, pp. 92-96, 2008.
- [3] Y. Fujita, K. Watanabe, and K. Maki, "Serum leptin levels negatively correlate with trabecular bone mineral density in high-fat diet-induced obesity mice," *Journal of Musculoskeletal & Neuronal Interactions*, vol. 12, no. 2, pp. 84-94, 2012.
- [4] K. Gunaratnam, C. Vidal, J. M. Gimble, and G. Duque, "Mechanisms of palmitate-induced lipotoxicity in human osteoblasts," *Endocrinology*, vol. 155, no. 1, pp. 108-116, 2014.
- [5] M. Cheng and L. Xu, "Research progress of leptin and postmenopausal bone metabolism," *Chinese Journal of Osteoporosis*, vol. 22, no. 7, pp. 929-933, 2016.
- [6] M. Han, T. Yan, and D. Wang, "The development and prospect of leptin in bone metabolism regulation," *Progress in Modern Biomedicine*, vol. 15, no. 14, pp. 2766-2769, 2015.
- [7] D. Song, *Prescriptions of the Bureau of Taiping People's Welfare Pharmacy*, People's Medical Publishing House, Beijing, China, 2007.
- [8] X. Xu, L. Shen, Y. Yang et al., "Effect of Qinge Pill on bone density and bone conversion markers in postmenopausal osteoporosis patients," *Chinese Journal of Traditional Medical Traumatology & Orthopedics*, vol. 21, no. 6, pp. 8-10, 2013.
- [9] L. Shen, J. Du, J. Yang et al., "Observation of 52 cases of senile osteoporosis treated by Jiawei Qinge Pill," *Hubei Journal of Traditional Chinese Medicine*, vol. 16, no. 3, pp. 16-18, 1994.
- [10] National Pharmacopoeia Commission, *Chinese Medicines in the 2000 Edition of the Pharmacopoeia of the People's Republic of China*, National Pharmacopoeia Commission, Ghaziabad, India, 2000.
- [11] X. Chen, "Effect of aging on serum leptin and soluble leptin receptor," *Shanxi Medical Journal*, vol. 35, no. 12, pp. 1611-1612, 2006.
- [12] M. Maamra, M. Bidlingmaier, M.-C. Postel-Vinay, Z. Wu, C. J. Strasburger, and R. J. M. Ross, "Generation of human soluble leptin receptor by proteolytic cleavage of membrane-anchored receptors," *Endocrinology*, vol. 142, no. 10, pp. 4389-4393, 2001.
- [13] J. Sun and Z. Wang, "Research progress of soluble leptin receptor," *Foreign Medical Sciences (Clinical Biochemistry and Laboratory Credits)*, vol. 24, no. 2, pp. 87-88, 2003.
- [14] J. Li and Q. Li, "Research progress of leptin resistance," *Foreign Medical Sciences (Genetics Fascicles)*, vol. 26, no. 3, pp. 166-169, 2003.
- [15] J. Wang and Y. Lin, "Research Progress of Qing'e Pill in the treatment of Postmenopausal Osteoporosis," *China Journal of Orthopedics and Traumatology*, vol. 21, no. 10, pp. 70-72, 2013.
- [16] J. Wang, Y. Lin, Y. Wu et al., "Effect of Qing'e Decoction on bone tissue MMP-9 and serum TRACP in osteoporosis model rats," *Rehabilitation Medicine*, vol. 24, no. 3, pp. 11-14, 2014.
- [17] W. Luo, "Study on the effect of Qing'e Decoction on OPN, BSP and integrin $\alpha\beta 3$ in bone tissue cells," *Doctoral dissertation*, Fujian University of Traditional Chinese Medicine, Fuzhou, China, 2015.
- [18] S. Guo, "Experimental study on the effect of Qing'e Fang on Bone resorption based on FAK/SRC/p130Cas Pathway," *Rehabilitation Medicine*, Doctoral dissertation, Fujian University of Traditional Chinese Medicine, Fuzhou, China, 2015.
- [19] J. O. Gordeladze and J. E. Reseland, "A unified model for the action of leptin on bone turnover," *Journal of Cellular Biochemistry*, vol. 88, no. 4, pp. 706-712, 2003.
- [20] M. Zhang and J. Dong, "Effects of leptin on proliferation and expression of Collagen I and Cbfa1mRNA of osteoblasts," *Chinese Journal of Osteoporosis*, vol. 16, no. 3, pp. 177-180, 2010.
- [21] T. Komori, H. Yagi, S. Nomura et al., "Targeted disruption of Cbfa1 results in a complete lack of bone formation owing to maturational arrest of osteoblasts," *Cell*, vol. 89, no. 5, pp. 755-764, 1997.
- [22] Z. S. Xiao, T. K. Hinson, and L. D. Quarles, "Cbfa1 isoform overexpression upregulates osteocalcin gene expression in non-osteoblastic and pre-osteoblastic cells," *Journal of Cellular Biochemistry*, vol. 74, no. 4, pp. 596-605, 1999.
- [23] T. Alliston, L. Choy, R. Deryneck et al., "TGF-beta-induced repression of CBFA1 by Smad3 decreases cbfa1 and osteocalcin expression and inhibits osteoblast differentiation," *The EMBO Journal*, vol. 20, no. 9, pp. 2254-2272, 2001.
- [24] H. Drissi, Q. Luc, R. Shakoobi et al., "Transcriptional autoregulation of the bone related CBFA1/RUNX2 gene," *Journal of Cellular Physiology*, vol. 184, no. 3, pp. 341-350, 2000.
- [25] A. Javed, G. L. Barnes, B. O. Jasanya et al., "Runt homology domain transcription factors (runx, cbfa, and AML) mediate repression of the bone sialoprotein promoter: evidence for promoter context-dependent activity of cbfa proteins," *Molecular and Cellular Biology*, vol. 21, no. 8, pp. 2891-2905, 2001.
- [26] J. Yu and X. Yu, "The using of markers of bone metabolism and bone mineral density in patients with osteoporosis," *Journal of Clinical Department of Internal Medicine*, vol. 26, no. 3, 2009.
- [27] D. J. DeFranco, J. Glowacki, K. A. Cox et al., "Normal bone particles are preferentially resorbed in the presence of osteocalcin-deficient bone particles in vivo," *Calcified Tissue International*, vol. 49, no. 1, pp. 43-50, 1991.
- [28] W. R. Holloway, F. M. Collier, C. J. Aitken et al., "Leptin inhibits osteoclast generation," *Journal of Bone and Mineral Research*, vol. 17, no. 2, pp. 200-209, 2002.
- [29] Unit of Hematology, University of Bari, "Osteoprotegerin and RANKL in the pathogenesis of osteoporosis in patients with thalassaemia major," *Panminerva Medica*, vol. 51, no. 1, pp. 17-23, 2009.
- [30] S. Jia and X. Jia, "Study on the relationship between osteoporosis and OPG, RANKL and ApoE in postmenopausal women," *Maternal and Child Health Care of China*, vol. 22, no. 32, pp. 105-107, 2007.
- [31] S. Jabbar, J. Drury, J. N. Fordham, H. K. Datta, R. M. Francis, and S. P. Tuck, "Osteoprotegerin, RANKL and bone turnover in postmenopausal osteoporosis," *Journal of Clinical Pathology*, vol. 64, no. 4, pp. 354-357, 2011.
- [32] A. Liu and J. Dong, "Effect of leptin on proliferation and OPG/RANKL mRNA expression of mouse osteoblast MC3T3-E1," *Chinese Journal of Osteoporosis*, vol. 14, no. 8, pp. 552-555, 2008.
- [33] S. Sharma, V. Tandon, S. Mahajan, V. Mahajan, and A. Mahajan, "Obesity: friend or foe for osteoporosis," *Journal of Mid-life Health*, vol. 5, no. 1, pp. 6-9, 2014.

- [34] X. Liu, Z. Wen, and N. Li, "Effects of leptin changes on sex hormones in male rats during catch-up sexual growth," *The Journal of Practical Medicine*, vol. 26, no. 2, pp. 206-207, 2010.
- [35] J.-H. Choi, K.-T. Lee, and P. C. K. Leung, "Estrogen receptor alpha pathway is involved in leptin-induced ovarian cancer cell growth," *Carcinogenesis*, vol. 32, no. 4, pp. 589-596, 2011.
- [36] N. A. Binai, A. Damert, G. Carra et al., "Expression of estrogen receptor alpha increases leptin-induced STAT3 activity in breast cancer cells," *International Journal of Cancer*, vol. 127, no. 1, pp. 55-66, 2009.

Research Article

Antiarthritic and Antihyperalgesic Properties of Ethanolic Extract from *Gomphrena celosioides* Mart. (Amaranthaceae) Aerial Parts

Luis Fernando Benitez Macorini,^{1,2} Joyce Alencar Santos Radai,¹ Rafael Souza Maris ^{1,2},
Saulo Euclides Silva-Filho,³ Maicon Matos Leitao,^{1,2} Sérgio Faloni de Andrade,⁴
Dayanna Isabel Araque Gelves,⁵ Marcos Jose Salvador,⁵ Arielle Cristina Arena,^{1,6}
and Cândida Aparecida Leite Kassuya ¹

¹School of Health Sciences, Federal University of Grande Dourados (UFGD), Dourados, MS, Brazil

²School of Health Sciences, University Center of Grande Dourados (UNIGRAN), Dourados, MS, Brazil

³College of Pharmaceutical Sciences, Food and Nutrition, Federal University of Mato Grosso do Sul (UFMS), Campo Grande, MS, Brazil

⁴Research Center for Biosciences and Health Technologies (CBIOS), Lusofona University, Lisbon, Portugal

⁵Institute of Biology, Department of Plant Biology, PPG BTPB, PPG BCE, University of Campinas (UNICAMP), Campinas, São Paulo, Brazil Institute of Biology, Brazil

⁶Department of Structural and Functional Biology, Institute of Biosciences of Botucatu, UNESP—University Estadual Paulista—Botucatu, São Paulo State, Botucatu, Brazil

Correspondence should be addressed to Cândida Aparecida Leite Kassuya; candida2005@gmail.com

Received 18 June 2020; Revised 14 August 2020; Accepted 7 September 2020; Published 15 September 2020

Academic Editor: Arham Shabbir

Copyright © 2020 Luis Fernando Benitez Macorini et al. This is an open access article distributed under the Creative Commons Attribution License, which permits unrestricted use, distribution, and reproduction in any medium, provided the original work is properly cited.

Gomphrena celosioides Mart. (Amaranthaceae) is used in folk medicine as a natural analgesic, and in Brazil, the species of genus *Gomphrena* is used for rheumatism. However, scientific evidence which supports its popular use as an analgesic is scarce. This study assessed the antiarthritic and antihyperalgesic activities of the ethanolic extract obtained from *G. celosioides* aerial parts on Swiss or C57BL/6 mice. The antiarthritic and antihyperalgesic potential of *Gomphrena celosioides* was evaluated using paw edema, mechanical hyperalgesia, cold allodynia, carrageenan-induced pleurisy, articular inflammation zymosan-induced, Freund's complete adjuvant-induced inflammation zymosan-induced peritonitis, and carrageenan-induced adhesion and rolling experiment models. All doses of *G. celosioides* (300, 700, and 1000 mg/kg) significantly reduced edema formation in all the intervals evaluated, whereas the mechanical hyperalgesia was reduced 3 hours after the carrageenan injection. The cold hyperalgesia was significantly decreased 3 (700 mg/kg) and 4 hours (700 and 1000 mg/kg) after the carrageenan injection. Ethanolic extract of *G. celosioides* at 1000 mg/kg reduced the total leukocyte number, without interfering in the protein extravasation in carrageenan-induced pleurisy model. Ethanolic extract of *G. celosioides* (300 mg/kg) was also able to reduce significantly the leukocyte migration in zymosan-induced articular edema, while a reduction of the adhesion and migration and leukocyte rolling was induced by the ethanolic extract of *G. celosioides* (300 mg/kg) in zymosan-induced peritonitis. In Freund's complete adjuvant-induced inflammation model, an edema formation and mechanical hyperalgesia reduction were induced by the ethanolic extract of *G. celosioides* on day 22, whereas the cold allodynia was reduced on day 6 of treatment with the extract. These results show that ethanolic extract of *G. celosioides* has antihyperalgesic and antiarthritic potential in different acute and persistent models, explaining, at least in part, the ethnopharmacological relevance of this plant as a natural analgesic agent.

1. Introduction

Scientific evidence has demonstrated that products from natural sources, including medicinal plants, are promising for the development of safe alternatives for the treatment of pain management and inflammatory diseases [1]. Thus, the ethnopharmacologically guided research has contributed with the identification of new therapeutic agents obtained from plants [2], which often have fewer adverse effects, and is important for patients who use medications for long periods.

Gomphrena celosioides Mart. (synonyms *G. serrata* and *G. decumbens*), an annual herb known popularly as “Perpétua Brava,” belongs to the Amaranthaceae family [3] and can be found in America, Australia, and Indomalaysia. In Brazil, this species occurs in savanna vegetation, napeadic grassland, high altitude grassland, and caatinga [4]. This plant is used for several folk medicinal purposes, such as for the treatment of several liver-related and dermatological diseases, dysmenorrhea, bronchial infections, renal disorders, and also as an analgesic [4–8].

Several chemical compounds with high therapeutic potential, such as hydrocarbons, alcohol, steroids, terpenes, ecdysteroids, flavonoids, saponins, butacyanine, and ketoses, have already been isolated from *G. celosioides* [9]. De Moura et al. [10] identified and isolated chemical compounds from *G. celosioides* aerial parts, including vanillic acid, 4-hydroxy-benzoic acid, and 4-hydroxy-3-methoxybenzoic acid, in addition to stigmasterol, sitosterol, and campesterol. Dosumu et al. [11] identified and isolated 3-(4-hydroxyphenyl)methylpropenoate from the methanol extract of *G. celosioides*. These same authors also found aurantiamide and aurantiamide acetate from the *n*-hexane extract of *G. celosioides* [12].

Despite its importance in folk medicine, there are few scientific studies which validate its therapeutic effects, especially the analgesic activity. Some studies using the aerial parts of *G. celosioides* extract have already reported its antihypertensive [8], antitumor, antimicrobial [10], cytotoxic, anti-inflammatory, and analgesic properties [13]. In a study carried out by Vasconcelos et al. [8], the ethanolic extract of *G. celosioides* showed diuretic effect and reduced the blood pressure in rats, demonstrating potential as an antihypertensive drug. Oluwabunmi and Abiola [6] showed a gastroprotective effect of the methanolic extract obtained from leaves, while De Moura et al. [10] found an antimicrobial effect of the crude extract of the plant against *Staphylococcus aureus* and *Salmonella typhi*. In another study, the ethyl acetate and methanol extracts were active against *Fasciola gigantica*, *Taenia solium*, and *Pheretima posthuma*, corroborating the popular use of *G. celosioides* in the treatment of infectious diseases [11].

Although *G. celosioides* is a species widely used in folk medicine with important bioactive compounds, few scientific studies are found in the literature to confirm its popular indication, especially regarding its antiarthritic and antihyperalgesic potential. Thus, this study aimed to evaluate the analgesic and antiarthritic activities of the ethanolic extract of the *G. celosioides* aerial parts in different acute and persistent inflammation models.

2. Materials and Methods

2.1. Plant Material and Preparation of Ethanolic Extract

G. celosioides aerial parts were collected (lat: -19.666667; long: -51.183333 WGS84) and identified by Dr. Josafá Carlos de Siqueira. A voucher specimen (SCAB 4051) is deposited in the herbarium of Pontifical Catholic University, Rio de Janeiro. The preparation of ethanolic extract of *G. celosioides* (EEGC) was performed according to Vasconcelos et al. [8].

2.2. Animals. Male and female Swiss or C57BL6 mice (weighing 20–30 g; 60–65 days of age) were provided by the Central Animal House of the Federal University of Grande Dourados/Mato Grosso do Sul, Brazil. The animals were housed at $22 \pm 2^\circ\text{C}$ under a 12/12 h light/dark cycle with free access to food and water. Prior to the experiments, the animals were fasted overnight, with water provided *ad libitum*. The experimental protocols were in accordance with the Ethical Principles in Animal Research adopted by the Brazilian College of Animal Experimentation and were approved by the Ethical Committee in Animal Experimentation of the Federal University of Grande Dourados (protocol number: 09/2018). The experimental design is shown in Figure 1.

2.3. Reagents. Carrageenan, dexamethasone, zymosan, indomethacin, acetone, and Bradford reagent were purchased from Sigma-Aldrich Co. LLC. (St. Louis, MO, USA).

2.4. Paw Edema, Mechanical Hyperalgesia, and Cold Allodynia Induced by Carrageenan. Swiss male mice were allocated into five groups: negative control group (treated with saline 0.9%, p.o.), positive control group (Dexa; dexamethasone 1 mg/kg, s.c.), and three groups treated with different doses of ethanolic extract of *G. celosioides* (EEGC) (300, 700, or 1000 mg/kg, p.o.). One hour after the treatment, all animals received 50 μL of carrageenan (300 μg /paw, s.c.) in the right hind paw and saline solution in the left hind paw (used as a control). The paw volume was measured in time intervals (1, 2, and 4 h) using a plethysmometer device. Mechanical hyperalgesia was evaluated by the electronic Von Frey pressure-increasing test at time intervals 3 and 4 h [14]. Sensitivity to cold was performed by the acetone drop test described by Decosterd et al. [15], at time intervals 3 and 4 h. Acetone (30 μL) was released over the right paw of the animals. Right after, the number of times in which the paw rising reaction occurred was evaluated. Minimum and maximum cutoff points were assigned at 5 and 20 s, respectively.

2.5. Model of Carrageenan-Induced Pleurisy in Mice. Swiss female mice (50 days of age) were treated and allocated into five groups: negative control group (saline solution 0.9% p.o.), positive control group (Dexa, 1 mg/kg, s.c.), and three groups treated with different doses of EEGC (300, 700, or

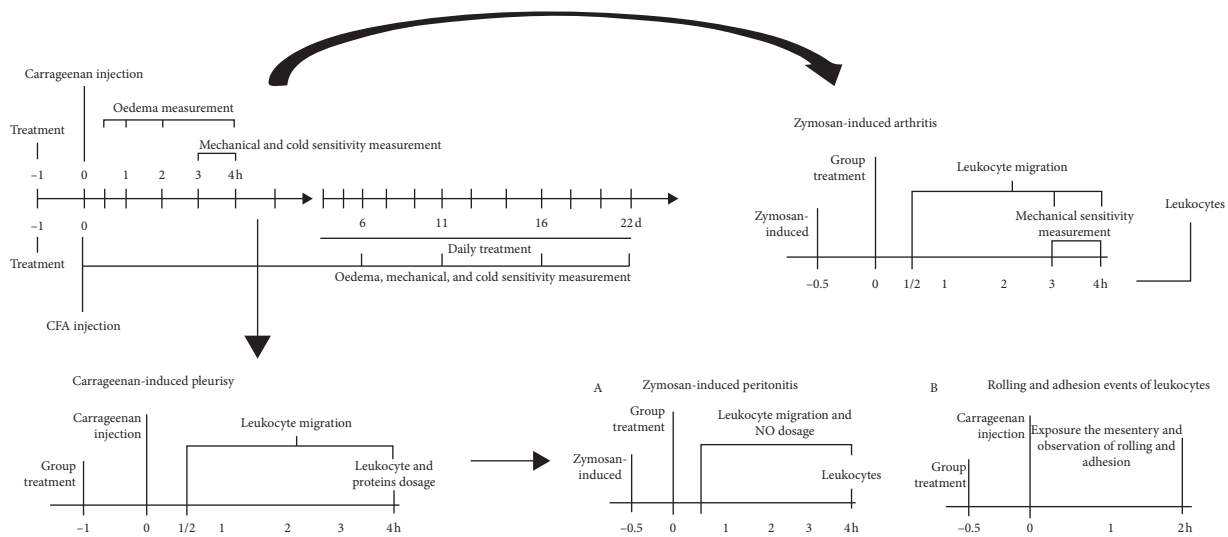


FIGURE 1: The experimental design.

1000 mg/kg p.o.). One hour after the treatment, 1 mL of carrageenan (300 $\mu\text{g}/\text{cavity}$, diluted in sterile saline) was injected into the animals by the intrapleural pathway, as described by Vinegar et al. [16]. After 4 h of the carrageenan injection, the animals were anesthetized and euthanized (ketamine/xylazine solution 1:1). The exudate was collected by aspiration and put into tubes. The leukocyte count was performed in the Neubauer chamber, and the total protein was determined by the Bradford method using a commercial kit Bioagency®.

2.6. Leukocyte Recruitment and Mechanical Hyperalgesia Evaluation in Experimental Model of Zymosan-Induced Arthritis. The experimental model of zymosan-induced arthritis was carried out as previously reported [17]. The right knee joints of the animals received 200 $\mu\text{g}/\text{cavity}$ of zymosan (in 10 μL sterile saline; intra-articularly injected), while the contralateral knee joint received an equal volume of saline. Thirty minutes before zymosan injection, the mice were treated orally with vehicle (saline) or EEGC (300 mg/kg). The additional mice group received only saline in the articular cavity and was treated with vehicle (naive group). At times of 3 and 4 h after zymosan injection, the mechanical hyperalgesia was evaluated using a digital analgesimeter (Von Frey, Insight®), a pressure transducer which records the applied force (in grams) in paw until the moment of paw withdrawal. At a time of 6 h after zymosan injection, the animals were anesthetized and euthanized, and the knee joint was exposed by surgical incision and washed twice with 5 μL of phosphate-buffered saline (PBS) containing ethylenediaminetetraacetic acid (EDTA). The supernatant was diluted to a final volume of 50 μL with PBS/EDTA to determine the total cells counts.

2.7. Zymosan-Induced Peritonitis. Swiss male mice were allocated into four groups: naive group (saline 0.9%, p.o.), negative control group (saline 0.9%, p.o.), positive control

group (Dexa, 1 mg/kg s.c.), and EEGC (300 mg/kg, p.o.). Peritonitis was induced by 1 mg/kg of zymosan administered intraperitoneally 30 min after the treatment in each animal [18]. The naive group received saline solution for control. The zymosan-induced peritonitis was assessed 6 h after the administration. After this period, the animals were euthanized, and their peritoneal cavity was washed with 1 mL of PBS/EDTA. Then, the solution containing the wash was centrifuged, and the supernatant was used for the nitric oxide (NO) dosage, and the precipitate was resuspended in 1 mL of PBS/EDTA for the total leukocyte analysis using the KX-21n Roche® equipment. The nitric oxide determination nitrite was measured by methods of Griess. A Griess solution was prepared, where 50 μL of the solution and 50 μL of the sample were added in a 96-well microplate; after a 15 min wait, the reading was performed in a spectrophotometer at 580 nm. A nitrite curve using sodium nitrite at 5, 10, 30, and 60 μM concentrations was also performed [19].

2.8. In Situ Intravital Microscopy Analysis for Rolling and Adhesion Events of Leukocytes in the Mesenteric Microcirculation. The leukocyte rolling and adhesion were performed after the induction of leukocyte migration by an injection of carrageenan (500 $\mu\text{g}/\text{cavity}$, i.p.) in sterile saline. The mice were treated orally with EEGC (300 mg/kg), vehicle (saline), or indomethacin (5 mg/kg) as a reference drug, 30 min before the carrageenan injection. The additional mice group was injected only with saline in the peritoneal cavity. After 2 h of carrageenan or saline injection, the animals were anesthetized (ketamine/xylazine solution 1:1). A lateral surgical incision was performed in the abdominal wall to the exposure of the mesentery and observation of *in situ* microcirculation. The mice were kept on a heated plate, with temperature maintained at 37°C, adapted to the chariot of an optical microscope with a video camera and monitor to project and record the images. The preparation was kept moist and warm with Ringer Locke's solution that contained 1% gelatin. The vessels considered the postcapillary venules

with 10–18 μm diameter. The number of rolling and adherent leukocytes was counted as 10 min intervals. Leukocyte adherence was determined when cells remained static in the endothelium for 30 s or more [20].

2.9. Paw Edema and Mechanical Hyperalgesia Induced by Freund's Complete Adjuvant (CFA). The persistent model of edema and mechanical hyperalgesia induced by Freund's complete adjuvant (CFA) in male C57BL6 mice was performed to study the analgesic and anti-inflammatory properties with prolonged treatment with EEGC. The animals were allocated into three groups: control group (saline 0.9%, p.o.), EEGC group (100 mg/kg, p.o.), and positive control group (Dexa, 1 mg/kg s.c.).

At time zero, 20 μL of a suspension containing dead *Mycobacterium tuberculosis* and added in paraffin oil (85%) and monooleate (15%) was injected into the right hind paw. The nociceptive threshold was estimated at 3 and 4 h after CFA and was then analyzed on days 6, 11, 16, and 22 using the Von Frey electronic test [21]. In addition, CFA-induced edema was resolved at 2 and 4 h intervals on days 6, 11, 16, and 22 after CFA injection with a plethysmometer.

Cold sensitivity was measured by the acetone drop test as described by Eliav et al. [22]. A blind needle attached to a syringe was used to release 30 μL of acetone in the paw of CFA animals from the CFA model experiment on days 6, 11, 16, and 22, and the duration (in s) of paw withdrawal was evaluated. The minimum and maximum cutoff points were assigned to be 0.5 and 20 s, respectively. Paw removals due to locomotion or weight change were not counted.

2.10. Statistical Analysis. The data are presented as the mean \pm SEM (standard error of the mean). Differences among means were evaluated by one-way analysis of variance (ANOVA), followed by the Newman–Keuls post hoc test, using GraphPad Prism software. Statistical differences were considered significant when $P < 0.05$.

3. Results

3.1. Effects of EEGC on the Paw Edema, Mechanical Hyperalgesia, and Cold Allodynia Induced by Carrageenan. All doses of EEGC (300, 700, and 1000 mg/kg) reduced the edema formation in the first, second, and fourth hours after the carrageenan administration with a maximum inhibition of $61 \pm 5\%$, $53 \pm 6\%$, and $68 \pm 5\%$ for at 300, 700, and 1000 mg/kg, respectively. The values were similar to those of the animals treated with dexamethasone, which had its maximum antiedematogenic activity in the fourth hour reducing $68 \pm 4\%$ paw edema (Figures 2(a)–2(c)).

Furthermore, the treatment with all doses of extract (300, 700, and 1000 mg/kg) after 3 h of the carrageenan injection reduced the mechanical hyperalgesia (Figure 3). EEGC exhibited maximal activity on the mechanical hyperalgesia at 300 mg/kg with $91 \pm 22\%$, a reduction similar to those observed with dexamethasone treatment ($87 \pm 8\%$). However, it was not possible to observe the same reduction after the fourth hour (Figures 3(a) and 3(b)). In

relation to cold allodynia, EEGC treatment promoted a reduction at 700 mg/kg of EEGC in the third hour and in the fourth hour occurred the allodynia reduction in the doses of 700 and 1000 mg/kg with a maximum inhibition of $58 \pm 14\%$ (Figures 3(c) and 3(d)).

3.2. Effects of EEGC on Carrageenan-Induced Pleurisy. The EEGC treatment at the dose of 300 mg/kg showed a significant reduction ($58 \pm 14\%$) of the leukocyte migration compared to the control group, indicating a possible reduction of the inflammatory process (Figure 4(a)). However, the treatment with the extract did not show reduction in the protein extravasation to the pleural cavity (Figure 4(b)).

3.3. Effects of EEGC on Zymosan-Induced Articular Inflammation and Peritonitis. In another model of articular inflammation, EEGC treatment at a dose of 300 mg/kg promoted a reduction of hyperalgesia and leukocyte migration compared to the control group with a maximum inhibition of $52 \pm 3\%$ and $81 \pm 4\%$, respectively (Figures 5 and 6). There was a significant reduction of $46 \pm 10\%$ induced by EEGC in the total leukocytes migration in peritonitis at 300 mg/kg dose (Figure 7); therefore, EEGC did not alter significantly the nitric oxide (NO) levels (figure not shown). The dexamethasone group inhibited significantly the hyperalgesia and leukocyte migration in articular injection (Figures 5 and 6) and also the leukocyte migration in peritonitis (Figure 7).

A significant reduction in cell adhesion to the endothelium and in cells rolling provoked by EEGC administration (300 mg/kg) was observed with $40 \pm 7\%$ and $48 \pm 6\%$ of inhibition, respectively. As expected, the reference drug (indomethacin) at a dose of 5 mg/kg decreased the adhesion ($45 \pm 5\%$ of inhibition) and consequently the rolling of leukocytes ($65 \pm 4\%$ of inhibition) (Figures 8(a) and 8(b)).

3.4. Effects of EEGC on CFA Inflammatory Model. The dose of 100 mg/kg of EEGC was tested in the CFA model of chronic inflammation for 22 days, and the oral EEGC treatment was able to reduce significantly the edema volume (a maximal inhibition of $25 \pm 18\%$) after this period. The dexamethasone reference drug showed a reduction in the paw edema on the sixteenth day, when compared to the control group (Figure 9(a)).

EEGC (100 mg/kg) and dexamethasone groups blocked the development of the mechanical hyperalgesia by induced CFA on day 22 of the treatment (Figure 8(b)), while the cold allodynia had an inhibition of sensitivity until the 16th day, possessing its maximum effect both by EEGC ($44 \pm 21\%$) and dexamethasone ($67 \pm 11\%$) on the sixth day of treatment (Figure 9(c)).

4. Discussion

Despite the therapeutic benefit, nonsteroidal anti-inflammatory (NSAIDs) and disease-modifying antirheumatoid drugs have important adverse effects [23], which reinforce

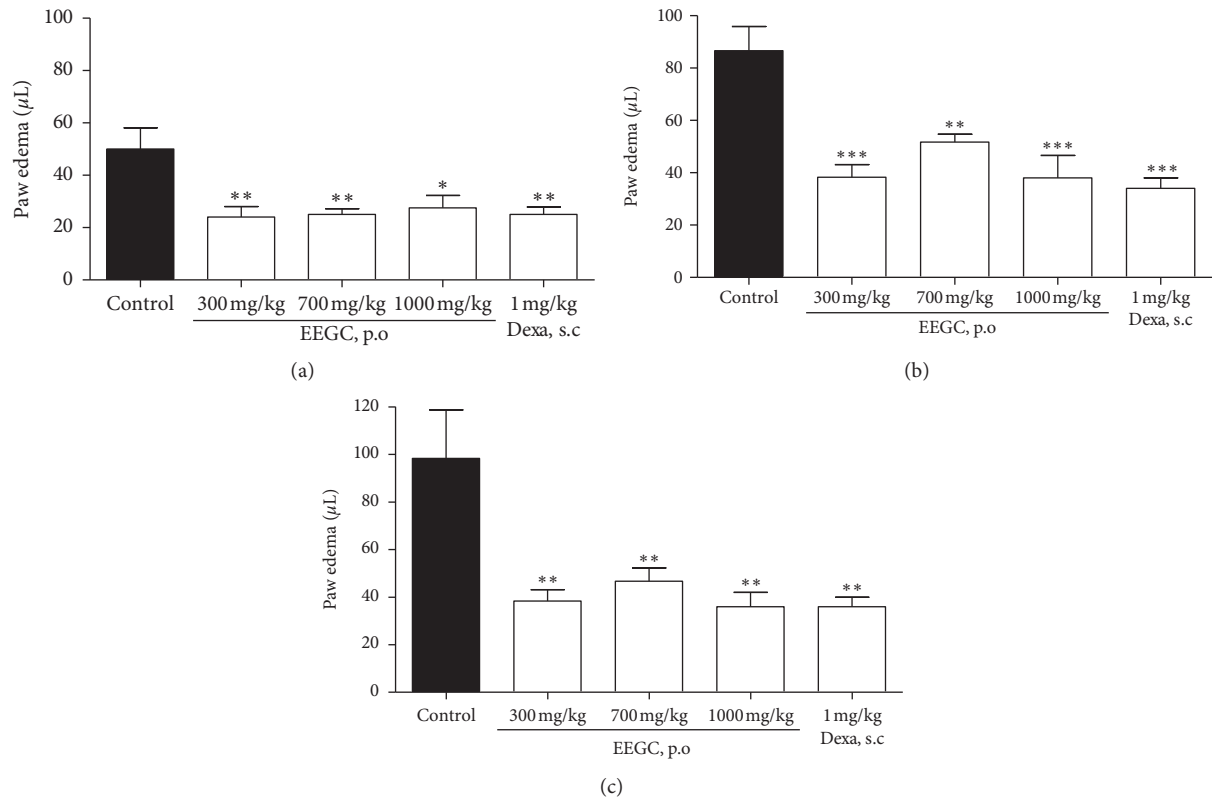


FIGURE 2: Effect of oral administration of EEGC at 1 (a), 2 (b), and 4 (c) hours after carrageenan-induced edema. The control (saline 0.9%, p.o.), EEGC (300, 700, or 1000 mg/kg, p.o.), and DEXA (dexamethasone 1 mg/kg, i.p.) groups were treated after 1 hour with carrageenan. The bars express the mean \pm SEM compared to the control group. * $P < 0.05$; ** $P < 0.01$; *** $P < 0.001$. One-way analysis of variance followed by the Newman-Keuls test.

the need to search for other safe and efficient therapeutic alternatives. The results of this study contribute with this search showing that EEGC has great antiarthritic and antihyperalgesic potential, corroborating the popular use already reported.

In the carrageenan-induced acute paw edema model, all doses of EEGC exhibited a similar result to the dexamethasone (a reference drug), demonstrating an anti-edematogenic potential of this extract. This model is associated with an acute inflammatory process and has several mediators for inflammatory response induction. In the first and second hours, the inflammatory effect is mediated by histamine, serotonin, and kinins, while in the next phase (3 to 6 hours), it is mediated by an increase in the prostaglandin production and COX-2 activation [24, 25]. The EEGC showed great potential in reducing the peripheral inflammatory process, the mechanical hyperalgesia, and the cold allodynia in the paw edema model, actions which may be related to the direct action of the cytokine expression and release of NO in the tissues.

Studies show that the release of proinflammatory cytokines activates the expression of cyclooxygenases, such as COX-1 and COX-2 [26]. These enzymes play an important role in the production of prostaglandins and leukotrienes from arachidonic acid [27]. Several physiological functions such as gastric mucosa protection, regulation of gastric juice

release, vascular tone control, and metabolism are related to the action of these molecules [28]. However, physiological effects of COX action such as hyperalgesia, increased body temperature (fever), and inflammatory processes are also found. Studies also show that COX-1 is traditionally known as the constitutive or inducible isoform, while COX-2 is known as inducible isoform in the inflammatory process. The selective COX-2 NSAIDs drugs did not frequently show gastric ulcer induction, which is a common adverse effect observed by traditional NSAIDs. The carrageenan-induced edema was inhibited by EEGC in this study and may be related with an inhibition of the prostaglandin production [29, 30].

The main anti-inflammatory and analgesic drugs used by the population are within the class of NSAIDs. However, the majority of these drugs are not characterized by the selectivity to cyclooxygenases, except for coxibes, which acts in the selective inhibition of COX-2 [31]. Some studies show that coxibes drugs, after prolonged use, have adverse effects such as direct action on the cardiovascular system [32]. The anti-inflammatory effect was also evaluated in an acute model of pleurisy induced by carrageenan. The carrageenan administration induces the formation of exudate, changes in colloid osmotic pressure, and infiltration of polymorphonuclear leukocytes in the pleural cavity, in addition to the release of proinflammatory mediators [33]. Doses of 700 and

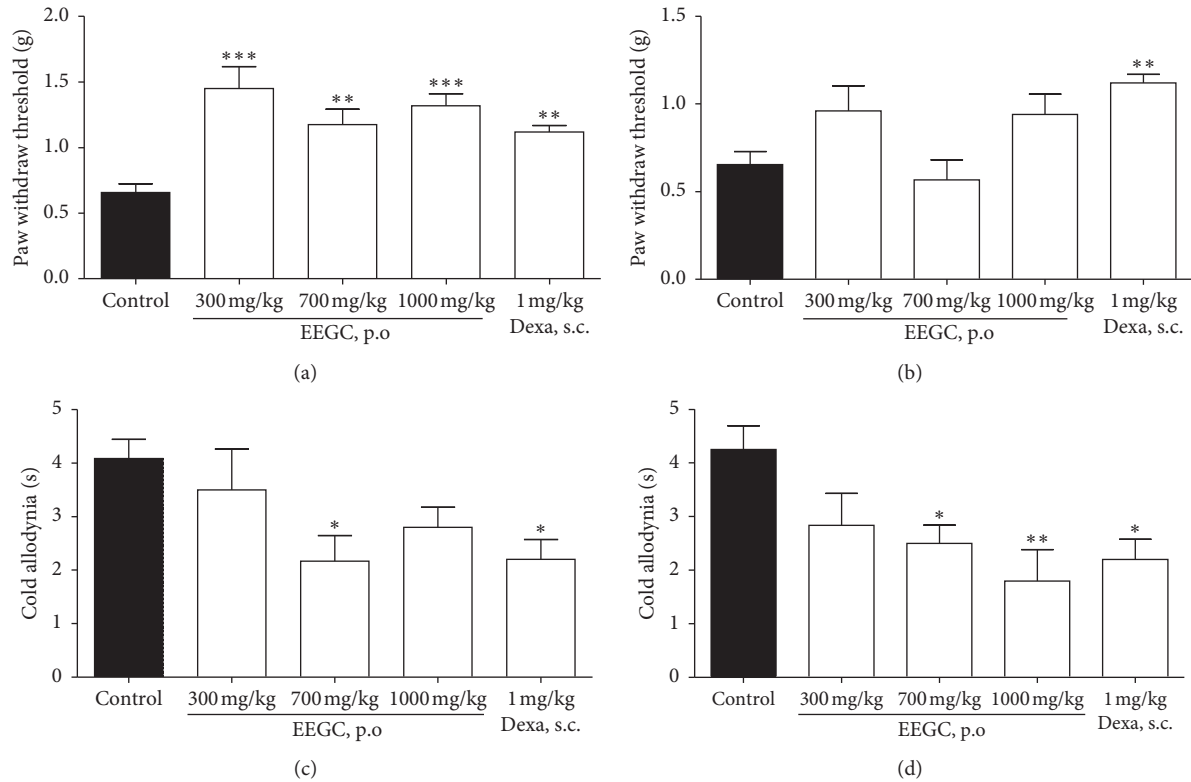


FIGURE 3: Effect of oral administration of EEGC at 3 h and 4 h after carrageenan-induced mechanical sensitivity (a, b) and cold hypersensitivity (c, d). The control (saline 0.9%, p.o.), EEGC (300, 700, or 1000 mg/kg, p.o.), and dexa (dexamethasone 1 mg/kg, s.c.) groups were treated after 1 hour with carrageenan. The bars express the mean \pm SEM compared to the control group. ** $P < 0.01$, * $P < 0.05$, and *** $P < 0.001$. One-way analysis of variance followed by the Newman-Keuls test.

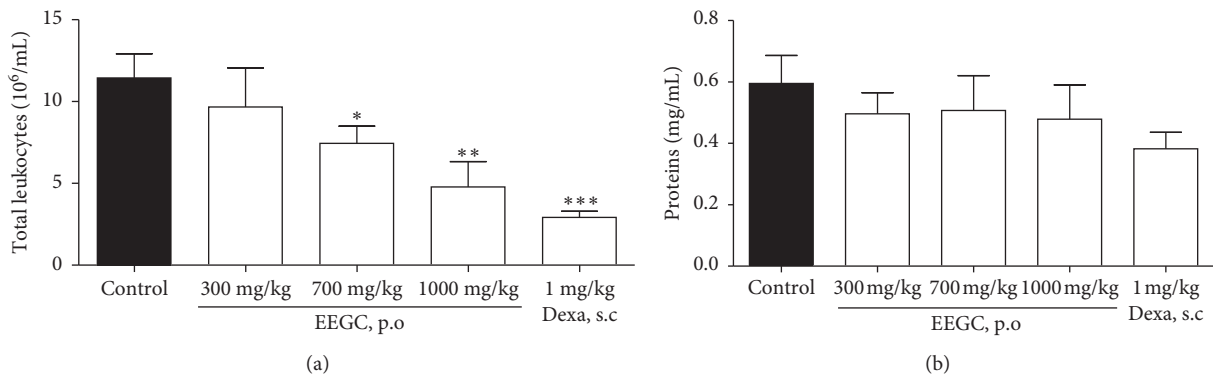


FIGURE 4: Effect of the oral administration of EEGC on acute inflammation induced by intrapleural injection of carrageenan in mice. In (a), leukocyte migration $\times 10^6$ cells/cavity and (b) proteins (mg/ml). The control group received saline solution (0.9%), and the EEGC groups received 300, 700, or 1000 mg/kg. The bars express the mean \pm SEM compared to the control versus treated group. * $P < 0.05$, ** $P < 0.01$, and *** $P < 0.001$. One-way analysis of variance followed by the Newman-Keuls test.

1000 mg/kg of EEGC reduced the total leukocyte migration in the pleural cavity and however did not reduce the protein extravasation.

The antiarthritic activity of EEGC was evaluated by zymosan-induced arthritis in mice. Zymosan is an isolate from the cell wall of the yeast *Saccharomyces cerevisiae* characterized as a polysaccharide that acts in macrophage toll-like 2 (TLR2) receptors and subsequently in the

activation of proinflammatory mechanisms [21, 34]. The EEGC decreased the total leukocytes of the articular lavage, indicating a reduction in diapedesis [35].

Our research group identified caffeic acid, ferulic acid, vanillic acid, and catechin in EEGC [8]. Among the biologically active compounds contained in this extract, we point out important anti-inflammatory agents such as caffeic acid, ferulic acid, vanillic acid, and catechin [36] that can be

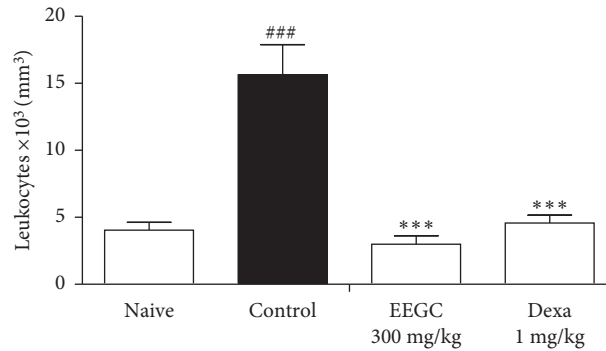


FIGURE 5: Effect of the oral administration of EEGC on the leukocyte recruitment in articular inflammation induced by the zymosan model in mice. The figures show the values after the induction of arthritis in the naive, control (saline, 0.9%, p.o.), EEGC (300 mg/kg, p.o.), and dexa (dexamethasone 1 mg/kg, s.c.) groups. The bars express the mean \pm SEM. ### or *** $P < 0.001$. ### Control versus naive. *** EEGC versus control. One-way analysis of variance followed by the Newman-Keuls test.

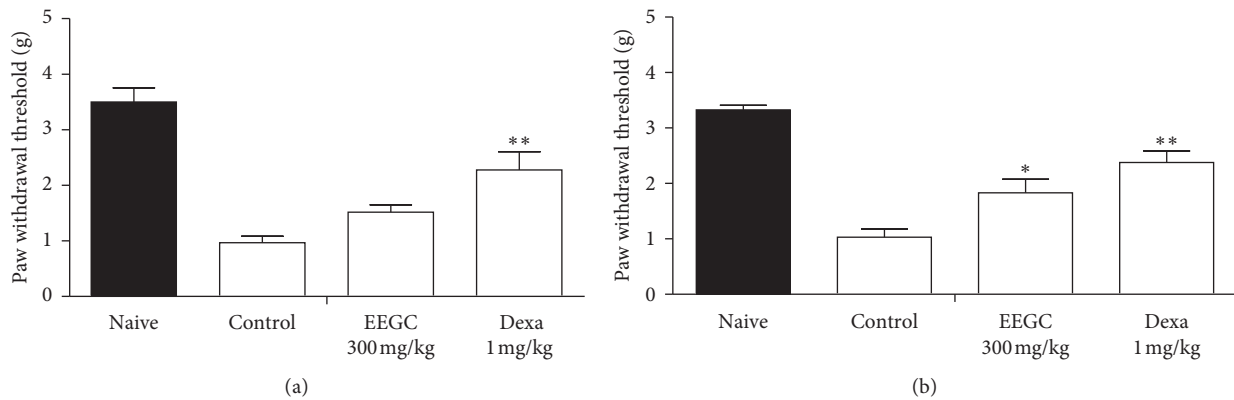


FIGURE 6: Effect of the oral administration of EEGC on the increase in mechanical sensitivity (paw withdrawal threshold) in articular inflammation induced by the zymosan model in mice. The figures show the values at 3 (a) and 4 h (b) after the procedure of induction of articular inflammation in the naive, control up (saline 0.9%, p.o.), EEGC (100 mg/kg, p.o.), and dexa (1 mg/kg, s.c.) groups. The bars express the mean \pm SEM compared with the control vs. treated group. * $P < 0.05$; ** $P < 0.01$; One-way analysis of variance followed by the Newman-Keuls test.

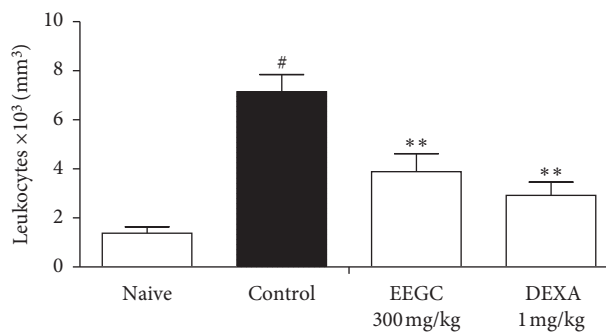


FIGURE 7: Effect of the oral administration of EEGC on leukocyte migration after peritoneal injection of carrageenan in mice. Mice were pretreated with EEGC (300 mg/kg, p.o.), dexamethasone (dexa, 1 mg/kg, i.p.), or vehicle (saline solution, 0.9%, p.o.). After 60 min, naive mice were injected with saline i.p., while all other groups received zymosan. The bars express the mean \pm SEM compared with the control vs. treated group; # or ** $P < 0.001$. # Control versus naive. ** EEGC versus control. One-way analysis of variance followed by the Newman-Keuls test.

related to the therapeutic effects exhibited by EEGC. Calixto-Campos et al. [37] showed that the anti-inflammatory effect of vanillic acid is related to the inhibition of the neutrophil

recruitment and also to the NF κ B activation. Vanillic acid can also inhibit the COX-2 and NO expression induced by LPS *in vitro* [38].

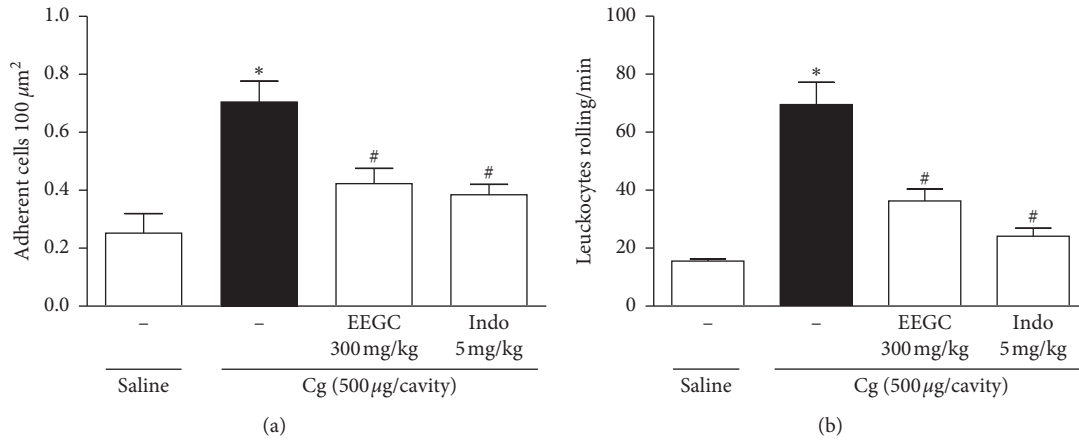


FIGURE 8: Effect of EEGC on leukocyte rolling (a) and adhesion (b) induced by carrageenan. Mice were orally pretreated with EEGC (300 mg/kg), indomethacin (indo 5 mg/kg), or vehicle. After 60 min, saline or carrageenan was injected i.p. leukocyte rolling, and adhesion was evaluated by intravital microscopy in the mesentery 2 h later. The bars express the mean ± SEM compared with the control vs. treated group; # or **P* < 0.001. # Control versus naive; *EEGC versus control. One-way analysis of variance followed by the Newman-Keuls test.

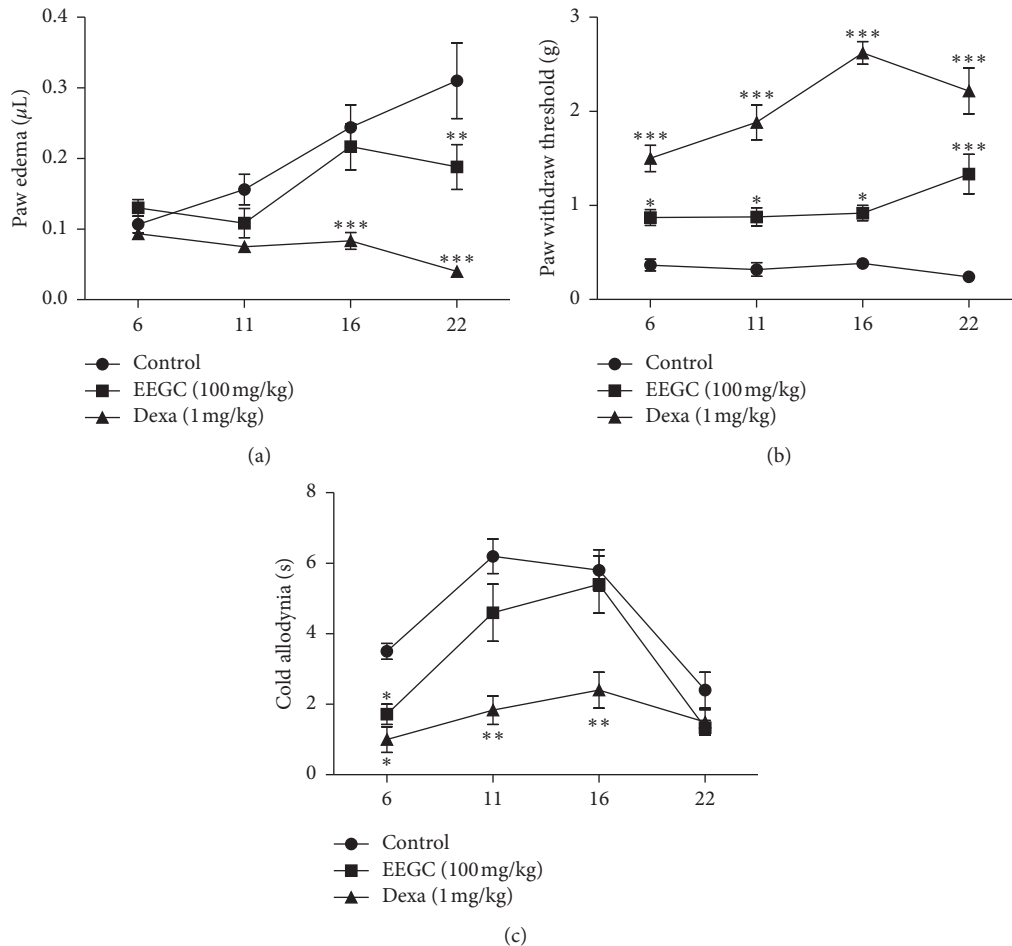


FIGURE 9: Effect of the oral administration of EEGC on increase in paw edema (a), mechanical sensitivity (paw withdrawal threshold) (b), and cold hypersensitivity (c) in persistent inflammation induced by the CFA model. Mice were treated once/day for 21 days with saline (0.9%, p.o., control), EEGC (100 mg/kg, p.o.), and dexamethasone (1 mg/kg, i.p.) after CFA. The points are expressed as the mean ± SEM compared with the control vs. treated group. **P* < 0.05; ***P* < 0.01 or ****P* < 0.001. One-way analysis of variance followed by the Newman-Keuls test.

Zymosan-induced peritonitis was also evaluated in this study. The adhesion, rolling, and leukocyte migration to the peritoneal cavity were decreased by EEGC, with a similar reduction produced by the reference drug indomethacin. Indomethacin decreases the expression of adhesion molecules such as L-selectin, E-selectin, I-CAM, and VCAM [20, 39]. These molecules play important role in the leukocyte adhesion and in the rolling to the focus of the inflammatory process although others factors are important to the leukocyte migration phenomenon. NO is an important mediator in the leukocyte migration, promoting vasodilation and reducing the recruitment, adhesion, rolling, and leukocyte migration during inflammatory response favoring diapedesis [40, 41]. Since EEGC did not increase the NO levels induced by zymosan, it led us to conclude that the EEGC mechanism of action was not involved in the NO pathway. EEGC maybe act by the same pathway of indomethacin.

Based on the results obtained in acute models, the oral dose of 100 mg/kg EEGC was tested in the CFA model to evaluate EEGC antiarthritic and antihyperalgesic properties. EEGC was effective against mechanical and cold hyperalgesia induced by CFA confirming the popular use of *G. celosioides* as an analgesic. In addition, it is possible to report that the mechanical hyperalgesia and cold hyperalgesia processes are characterized as pain indicators since they result from the sensitization and the pain pathway and type C nerve fiber caused by the CFA inflammatory persistent process [42, 43].

In conclusion, the ethanolic extract of *G. celosioides* aerial parts showed antiarthritic and antihyperalgesic activities in different evaluated models, decreasing leukocyte recruitment, rolling, adhesion, and migration to the inflammatory focus. Although these results corroborate the popular statement, other studies should be conducted to evaluate the mechanisms of action and to identify the compound responsible for these effects.

Abbreviations

| | |
|----------------|---|
| ANOVA: | Analysis of variance |
| C57BL/6: | C57 black 6 |
| CFA: | Freund's complete adjuvant |
| COX: | Cyclooxygenase |
| DEXA: | Dexamethasone |
| EDTA: | Ethylenediaminetetraacetic acid |
| EDTA: | Ethylenediaminetetraacetic acid |
| EEGC: | Ethanolic extract of <i>Gomphrena celosioides</i> |
| ESI-MS: | Electrospray ionisation mass spectrometry |
| ICAM: | Intercellular adhesion molecule |
| IL-1 β : | Interleukin 1 β |
| Indo: | Indomethacin |
| NF κ B: | Factor nuclear kappa B |
| NO: | Nitric oxide |
| NSAIDs: | Nonsteroidal anti-inflammatory |
| PBS: | Phosphate-buffered saline |
| TLR2: | Toll-like 2 |
| TNF: | Tumor necrosis factor |
| VCAM: | Vascular cell adhesion molecule. |

Data Availability

The data used to support the findings of this study are available from the corresponding author upon request.

Disclosure

The authors declare that the work did not receive a specific funding.

Conflicts of Interest

The authors declare that they have no conflicts of interest in this work.

Acknowledgments

The authors are grateful to the CAPES, FUNDECT, CNPq, FAPESP, UFGD, and FAEPEX-UNICAMP for the financial support.

References

- [1] T. Yue, X. Fan, Z. Zhang et al., "Downregulation of lncRNA ITSNI-2 correlates with decreased disease risk and activity of rheumatoid arthritis (RA), and reduces RA fibroblast-like synoviocytes proliferation and inflammation via inhibiting NOD2/RIP2 signaling pathway," *American Journal of Translational Research*, vol. 11, no. 8, pp. 4650–4666, 2019.
- [2] A. W. K. Yeung, M. Heinrich, and A. G. Atanasov, "Ethnopharmacology—a bibliometric analysis of a field of research meandering between medicine and food science?" *Frontiers in Pharmacology*, vol. 9, p. 215, 2018.
- [3] M. M. Sangare, J. R. Klotoe, V. Dougnon et al., "Evaluation of the hepatoprotective activity of *Gomphrena celosioides* (Amaranthaceae) on wistar rats intoxicated with tetrachloride carbon," *International Journal of Current Research*, vol. 4, pp. 67–72, 2012.
- [4] C. C. J. Vieira, H. Mercier, E. P. Chu, and R. C. L. Figueiredo-Ribeiro, "*Gomphrena* species (globe amaranth): *in vitro* culture and production of secondary metabolites," *Medicinal and Aromatic Plants VII*, vol. 2, pp. 257–270, 1994.
- [5] F. Takim, O. Olawoyin, and W. Olanrewaju, "Growth and development of *Gomphrena celosioides* mart under screen house conditions in ilorin, southern Guinea savanna zone of Nigeria," *Agrosearch*, vol. 13, no. 2, pp. 59–66, 2013.
- [6] I. J. Oluwabunmi and T. Abiola, "Gastroprotective effect of methanolic extract of *Gomphrena celosioides* on indomethacin induced gastric ulcer in Wistar albino rats," *International Journal of Applied and Basic Medical Research*, vol. 5, no. 1, p. 41, 2015.
- [7] K. N. Nandini, M. N. Palaksha, and D. A. Gnanasekaran, "A review of *Gomphrena serrata*," *International Journal of Science and Research Methodology*, vol. 11, no. 1, pp. 104–110, 2018.
- [8] D. P. Vasconcelos, P. C. Tirloni, and C. A. S. Palozzi, "Diuretic herb *Gomphrena celosioides* Mart. (Amaranthaceae) promotes sustained arterial pressure reduction and protection from cardiac remodeling on rats with renovascular hypertension," *Journal of Ethnopharmacology*, vol. 224, pp. 126–133, 2018.
- [9] S. Botha and V. D. V. L. M. Gerritsma, "Pharmacochemical study of *Gomphrena celosioides* (Amaranthaceae)," *Suid-Afrikaanse Tydskrif vir Natuurwetenskap en Tegnologie*, vol. 5, no. 1, pp. 40–45, 1986.

- [10] R. M. X. De Moura, P. S. Pereira, A. H. Januário, S. C. França, and D. A. Dias, "Antimicrobial screening and quantitative determination of benzoic acid derivative of *Gomphrena celosioides* by tlc-densitometry," *Chemical and Pharmaceutical Bulletin*, vol. 52, no. 11, pp. 1342–1344, 2004.
- [11] O. O. Dosumu, O. Ekundayo, P. A. Onocha, and P. A. Idowu, "Isolation of 3-(4-hydroxyphenyl) methylpropenoate and bioactivity evaluation of *Gomphrena celosioides* extracts," *EXCLI Journal*, vol. 9, pp. 173–180, 2010.
- [12] O. O. Dosumu, P. Onocha, O. Ekundayo, and M. Ali, "Isolation of aurantiamides from *Gomphrena celosioides* C. Mart," *Iranian Journal of Pharmaceutical Research*, vol. 13, no. 1, p. 143, 2014.
- [13] G. M. Oladele, M. O. Abatan, J. O. Olukunle, and B. S. Okediran, "Anti-inflammatory and analgesic effects of aqueous leaf extracts of *Gomphrena celosioides* and *Momordica charantia*," *JSME International Journal Series B*, vol. 8, no. 2, pp. 1–8, 2009.
- [14] D. F. De Santana Aquino, A. C. Piccinelli, F. L. Soares et al., "Anti-hyperalgesic and anti-inflammatory activity of *Alternanthera maritima* extract and 2'-O- α -L-rhamnopyranosylvitexin in mice," *Inflammation*, vol. 38, no. 6, pp. 2057–2066, 2015.
- [15] I. Decosterd, A. Allchorne, and C. J. Woolf, "Progressive tactile hypersensitivity after a peripheral nerve crush: non-noxious mechanical stimulus-induced neuropathic pain," *Pain*, vol. 100, no. 1-2, pp. 155–162, 2002.
- [16] R. Vinegar, J. F. Traux, and J. L. Selph, "Some quantitative temporal characteristic of carrageenin-induced pleurisy in the rat," *Experimental Biology and Medicine*, vol. 143, no. 3, pp. 711–714, 1973.
- [17] K. A. Möller, B. Johansson, and O. G. Berge, "Assessing mechanical allodynia in the rat paw with a new electronic algometer," *Journal of Neuroscience Methods*, vol. 84, no. 1-2, pp. 41–47, 1998.
- [18] S. Pace, A. Rossi, V. Krauth et al., "Sex differences in prostaglandin biosynthesis in neutrophils during acute inflammation," *Scientific Reports*, vol. 7, no. 1, pp. 1–10, 2017.
- [19] K. B. Menaka, A. Ramesh, B. Thomas, and N. S. Kumari, "Estimation of nitric oxide as an inflammatory marker in periodontitis," *Journal of Indian Society of Periodontology*, vol. 13, no. 2, p. 75, 2009.
- [20] S. E. Silva-Filho, L. A. M. Würlzler, H. A. O. Cavalcante et al., "Effect of patchouli (*Pogostemon cablin*) essential oil on in vitro and in vivo leukocytes behavior in acute inflammatory response," *Biomedicine & Pharmacotherapy*, vol. 84, pp. 1697–1704, 2016.
- [21] Á. M. Kuraoka-Oliveira, J. A. S. Radai, M. M. Leitão, C. A. Lima Cardoso, S. E. Silva-Filho, and C. A. Leite Kassuya, "Anti-inflammatory and anti-arthritis activity in extract from the leaves of *Eriobotrya japonica*," *Journal of Ethnopharmacology*, vol. 249, Article ID 112418, 2020.
- [22] E. Eliav, U. Herzberg, M. A. Ruda, and G. J. Bennett, "Neuropathic pain from an experimental neuritis of the rat sciatic nerve," *Pain*, vol. 83, no. 2, pp. 169–182, 1999.
- [23] A. Gaffo, K. G. Saag, and J. R. Curtis, "Treatment of rheumatoid arthritis," *American Journal of Health-System Pharmacy*, vol. 63, no. 24, pp. 2451–2465, 2006.
- [24] M. L. Di Rosa, J. P. Giroud, and D. A. Willoughby, "Studies of the mediators of the acute inflammatory response induced in rats in different sites by carrageenan and turpentine," *The Journal of Pathology*, vol. 10, no. 1, pp. 15–29, 1971.
- [25] I. Posadas, M. Bucci, F. Roviezzo et al., "Carrageenan-induced mouse paw oedema is biphasic, age-weight dependent and displays differential nitric oxide cyclooxygenase-2 expression," *British Journal of Pharmacology*, vol. 142, no. 2, pp. 331–338, 2004.
- [26] J. A. Mitchell, M. G. Belvisi, P. Akaraseenont et al., "Induction of cyclo-oxygenase-2 by cytokines in human pulmonary epithelial cells: regulation by dexamethasone," *British Journal of Pharmacology*, vol. 113, no. 3, pp. 1008–1014, 1994.
- [27] T. Hoffman, E. F. Lizzio, J. Suissa et al., "Dual stimulation of phospholipase activity in human monocytes: role of calcium-dependent and calcium-independent pathways in arachidonic acid release and eicosanoid formation," *The Journal of Immunology*, vol. 140, no. 11, pp. 3912–3918, 1988.
- [28] M. A. Khan and M. J. Khan, "Nano-gold displayed anti-inflammatory property via NF- κ B pathways by suppressing COX-2 activity," *Artificial Cells Nanomedicine, and Biotechnology*, vol. 46, no. 1, pp. 1149–1158, 2018.
- [29] W. A. Carvalho, R. D. S. Carvalho, and F. Rios-santos, "Specific cyclooxygenase-2 inhibitor analgesics: therapeutic advances," *Revista Brasileira de Anestesiologia*, vol. 54, no. 3, pp. 448–464, 2004.
- [30] N. Kiruthiga, M. Alagumuthu, C. Selvinthanuja, K. Srinivasan, and T. Sivakumar, "Molecular modelling, synthesis and evaluation of flavone and flavanone scaffolds as anti-inflammatory agents," *Anti-Inflammatory & Anti-Allergy Agents in Medicinal Chemistry*, vol. 19, 2020.
- [31] A. Ibrahim, A. Karim, J. Feldman, and E. Kharasch, "The influence of parecoxib, a parenteral cyclooxygenase-2 specific inhibitor, on the pharmacokinetics and clinical effects of midazolam," *Anesthesia & Analgesia*, vol. 95, no. 3, pp. 667–673, 2002.
- [32] C. Patrono, "Cardiovascular effects of cyclooxygenase-2 inhibitors: a mechanistic and clinical perspective," *British Journal of Clinical Pharmacology*, vol. 82, no. 4, pp. 957–964, 2016.
- [33] A. M. D. Oliveira, L. M. Conserva, J. N. De Souza Ferro, F. D. A. Brito, R. P. L. Lemos, and E. Barreto, "Antinociceptive and anti-inflammatory effects of octacosanol from the leaves of *Sabicea grisea* var. *grisea* in mice," *International Journal of Molecular Sciences*, vol. 13, no. 2, pp. 1598–1611, 2012.
- [34] N. K. Jain, T. O. Ishikawa, I. Spigelman, and H. R. Herschman, "COX-2 expression and function in the hyperalgesic response to paw inflammation in mice," *Prostaglandins, Leukotrienes and Essential Fatty Acids*, vol. 79, no. 6, pp. 183–190, 2008.
- [35] T. Rath, U. Billmeier, F. Ferrazzi et al., "Effects of anti-integrin treatment with vedolizumab on immune pathways and cytokines in inflammatory bowel diseases," *Frontiers in Immunology*, vol. 9, p. 1700, 2018.
- [36] D. Paula Vasconcelos, P. C. Spessotto, and D. R. Marinho, "Mechanisms underlying the diuretic effect of *Gomphrena celosioides* mart (amaranthaceae)," *Journal of Ethnopharmacology*, vol. 202, pp. 85–91, 2017.
- [37] C. Calixto-Campos, T. T. Carvalho, M. S. Hohmann et al., "Vanillic acid inhibits inflammatory pain by inhibiting neutrophil recruitment, oxidative stress, cytokine production, and NF- κ B activation in mice," *Journal of Natural Products*, vol. 78, no. 8, pp. 1799–1808, 2015.
- [38] M. C. Kim, S. J. Kim, D. S. Kim et al., "Vanillic acid inhibits inflammatory mediators by suppressing NF- κ B in lipopolysaccharide-stimulated mouse peritoneal macrophages," *Immunopharmacology and Immunotoxicology*, vol. 33, no. 3, pp. 525–532, 2011.
- [39] F. Díaz-González and F. Sánchez-Madrid, "Inhibition of leukocyte adhesion: an alternative mechanism of action for anti-inflammatory drugs," *Immunology Today*, vol. 19, no. 4, pp. 169–172, 1998.

- [40] C. In-Ho, K. Byung-Woo, P. Yun-Jae, L. Han-Joo, P. Sok, and L. Namju, "Ginseng berry extract increases nitric oxide level in vascular endothelial cells and improves cGMP expression and blood circulation in muscle cells," *Journal of Exercise Nutrition & Biochemistry*, vol. 22, no. 3, pp. 6–13, 2018.
- [41] B. Csoma, A. Bikov, L. Nagy et al., "Dysregulation of the endothelial nitric oxide pathway is associated with airway inflammation in COPD," *Respiratory Research*, vol. 20, no. 1, p. 156, 2019.
- [42] D. Andrew and J. D. Greenspan, "Mechanical and heat sensitization of cutaneous nociceptors after peripheral inflammation in the rat," *Journal of Neurophysiology*, vol. 82, no. 5, pp. 2649–2656, 1999.
- [43] J. H. Curfs, J. F. Meis, and J. A. Hoogkamp-Korstanje, "A primer on cytokines: sources, receptors, effects, and inducers," *Clinical Microbiology Reviews*, vol. 10, no. 4, pp. 742–780, 1997.

Research Article

Jingui Shenqi Pills Regulate Bone-Fat Balance in Murine Ovariectomy-Induced Osteoporosis with Kidney Yang Deficiency

Qi Shang ^{1,2}, Wenhua Zhao,^{1,2} Gengyang Shen,^{2,3} Xiang Yu,^{2,3} Zhida Zhang,^{1,2} Xuan Huang,^{1,2} Weicheng Qin,^{1,2} Guifeng Chen,^{1,2} Fuyong Yu,^{1,2} Kai Tang,^{1,2} Honglin Chen,^{2,3} Juanmin Li,^{2,3} De Liang,^{2,3} Jingjing Tang ^{2,3}, Xiaobing Jiang ^{2,3} and Hui Ren ^{2,3}

¹Guangzhou University of Chinese Medicine, Guangzhou 510405, China

²Lingnan Medical Research Center of Guangzhou University of Chinese Medicine, Guangzhou 510405, China

³Department of Spinal Surgery, The First Affiliated Hospital of Guangzhou University of Chinese Medicine, Guangzhou 510405, China

Correspondence should be addressed to Xiaobing Jiang; spinedrjxb@sina.com and Hui Ren; renhuispine@163.com

Received 24 May 2020; Revised 16 August 2020; Accepted 27 August 2020; Published 7 September 2020

Academic Editor: Arham Shabbir

Copyright © 2020 Qi Shang et al. This is an open access article distributed under the Creative Commons Attribution License, which permits unrestricted use, distribution, and reproduction in any medium, provided the original work is properly cited.

Jingui Shenqi Pills (JGSQP) have been a staple of traditional Chinese medicine for thousands of years, used primarily as a treatment for kidney yang deficiency (KYD). *In vitro* analyses of JGSQP revealed strong induction of osteogenic differentiation and inhibition of adipogenic differentiation in bone-marrow-derived mesenchymal stem/stromal cells. However, the mechanisms by which JGSQP regulate the bone-fat balance in murine ovariectomy-induced osteoporosis with KYD have not been reported. **Materials and Methods.** Two-month-old female C57BL/6 mice were divided randomly into three groups: those receiving a sham operation (Sham); those undergoing bilateral ovariectomy and selection of KYD syndrome (Model); and those subjected to both bilateral ovariectomy and KYD syndrome selection for 8 weeks, followed by JGSQP treatment for 4 weeks (JGSQP). In the Sham and Model groups, mice were given the same dose of distilled water orally for 4 weeks. Animals from all three groups were euthanised at the 12th week. Vertebral microarchitecture and histomorphology were examined by micro-CT and H&E staining, respectively. In addition, we examined the mRNA expression of *Akt*, *Wnt10b*, *Osterix (Osx)*, *Fndc5*, *PPAR γ* , and *Fabp4*, as well as the protein of AKT, phosphorylation-AKT (p-AKT), BMP2, COL1A1, and FNDC5. **Results.** JGSQP treatment improved bone microarchitecture and mitigated histomorphological damage relative to the Model group. The osteoblast number (Ob.N/BS) and area (Ob.S/BS) were increased, whereas adipocyte number (adipocyte/tissue area) and area (adipocyte area/tissue area) were decreased in the JGSQP group. JGSQP treatment reduced the mRNA expression of *Akt* and adipogenesis-related genes (*Fndc5*, *PPAR γ* , and *Fabp4*) while promoting osteogenesis-related genes (*Wnt10b* and *Osx*) mRNA expression. Additionally, the expression of p-AKT, BMP2, and COL1A1 proteins was increased and FNDC5 protein expression was decreased after JGSQP treatment. **Conclusions.** JGSQP treatment reversed murine ovariectomy-induced osteoporosis with KYD by controlling bone-fat balance via AKT pathway.

1. Introduction

Postmenopausal osteoporosis (PMOP) is brought on by a dramatic drop in oestrogen among postmenopausal women, leading to decreases in bone mass and density and an increase in the risk of fragility fracture [1]. With the gradual ageing of the population throughout the world, the

incidence of PMOP and associated fractures continues to increase annually, posing a serious threat to public health. Worldwide, 30–50% of postmenopausal women have osteoporosis [2], with significant differences based on ethnicity and nationality. White women aged >50 years were shown to have a 50% lifetime risk of fragility fracture [1], and ~40% of postmenopausal women in Europe and the United States are

diagnosed with osteoporosis [3]. Disability rates of up to 50% and a mortality rate of 20% have been reported in association with fragility fracture [4]. Medical expenses associated with fragility fractures in China are predicted to be as high as 163 billion yuan in 2050 [5]. Traditional Chinese medicine (TCM) has been shown to offer unique advantages in the treatment of PMOP, although the mechanisms underlying its therapeutic benefits remain poorly understood, which limits its clinical application.

TCM practitioners hold the view that kidney dominates bone, and kidney yang deficiency (KYD) is a key pattern underlying osteoporosis treatment based on the TCM practice of syndrome differentiation [6, 7]. Modern medical studies have shown that KYD is characterised by multiple disorders, including hypofunction of the pituitary–adrenal axis, decreases in antioxidation capacity, hyp immunity, and age-related conditions [8, 9], all of which are related closely to osteoporosis [10–13]. Furthermore, analysis of serum taken from patients with PMOP revealed decreased osteogenic differentiation and mineralisation in a human osteoblastic cell line [14]. Thus, KYD is related closely to the occurrence of osteoporosis.

PMOP is characterised by reduced osteogenesis and enhanced adipogenesis [15]. These changes correlate with reduced trabecular bone volume and increased adipocyte cell size and number [16]. Previous studies have shown that osteoporosis can be induced in mice using a classical method of ovariectomy [17, 18]. These models have been further adapted to establish a KYD model from ovariectomised mice [19, 20]. Jingui Shenqi Pills (JGSQP), a Chinese herbal compound prescription, have been used in TCM for warming and to invigorate the kidney yang [21]. It has been shown to attenuate decreases in the testosterone level and androgen receptor gene expression in mice with KYD [22–24] and to improve the function of damaged ovaries and increase testis telomerase activity [25, 26]. Furthermore, efforts to tonify the kidney yang were shown to more effectively promote osteogenic differentiation and inhibit adipogenic differentiation in bone-marrow-derived mesenchymal stem/stromal cells (BMSCs) than did tonification of the kidney yin [27]. Although these findings suggest interaction between JGSQP and PMOP, little is known regarding the role of JGSQP in pathological bone metabolism. In this study, we sought to better understand the role of JGSQP and its effects on the bone-fat balance in a murine model of ovariectomy-induced osteoporosis with KYD and to evaluate JGSQP as a potential option for the treatment and prevention of PMOP.

2. Material and Methods

2.1. Experimental Animals and Groups. Eight-week-old female C57/BL6 mice (18–22 g) were obtained from the experimental animal center of Guangzhou University of Chinese Medicine (License no. SCXK (Yue) 2018–0034). The mice were raised under conditions of 22–25°C temperature and 25 kPa atmospheric pressure with a 12 h light/dark cycle in the First Affiliated Hospital of Guangzhou University of Chinese Medicine (SYXK (Yue) 2018–0092). Food and water

were accessible throughout the experiment. After 1 week of adaptive feeding, the mice were divided randomly into three groups: the Sham group, which received a sham operation in which the fat around the bilateral ovaries was removed; the Model group, which underwent bilateral ovariectomy (OVX) followed by artificial selection of mice with KYD syndrome; and the JGSQP group, which was subjected to OVX and artificial selection of mice with KYD syndrome 8 weeks thereafter, followed by JGSQP treatment for 4 weeks. In the Sham and Model groups, mice were given the same dose of distilled water orally for 4 weeks (Figure 1). All experimental protocols were approved by the ethics committee of the First Affiliated Hospital of Guangzhou University of Chinese Medicine (License no. TCMF1-2019030).

2.2. Establishment of the PMOP with KYD Model. The PMOP with KYD model was established as described previously [19, 20]. Briefly, mice were subjected to OVX and allowed to recover for 8 weeks, after which mice exhibiting symptoms of KYD syndrome according to the *Reference Standard for Syndrome Differentiation of TCM Deficiency Syndrome* were selected. Features of KYD syndrome include thin and erect hair, reluctance to move, reduced resistance to scraping, listlessness, unresponsiveness, decreased water consumption, increased sleeping, dark-purple tongue and tail, and dark red eyes. Mice exhibiting three or more of these symptoms were considered to have KYD syndrome.

2.3. Preparation of Freeze-Dried JGSQP Powder. Freeze-dried JGSQP powder was prepared as described previously [28]. The single ingredient of JGSQP, conforming to the Drug Standards of National Medical Products Administration of People's Republic of China, was purchased from the First Affiliated Hospital of Guangzhou University of Chinese Medicine (Guangzhou, China). The prescription formula was composed of eight herbs: Processed Radix Aconiti Lateralis (Fuzi, 3.0 g), Cassia Twig (Guizhi, 3.0 g), Dried Rehmannia (Dihuang, 24.0 g), *Dioscorea opposita* (Shanyao, 12.0 g), *Cornus officinalis* (Shanzhuyu, 12.0 g), Alisma Orientalis (Zexie, 9.0 g), *Poria cocos* (Fuling, 9.0 g), and Cortex Moutan (Danpi, 9.0 g). The drugs were soaked in eight volumes of pure water, boiled for 30 min, and filtered. They were then concentrated to 1 g/mL at 80°C and 0.09 MPa. The resulting liquid was then further concentrated by rotary evaporator at 60°C until no droplets remained, frozen at –80°C for 48 h, and lyophilised for 72 h. The resulting powder was stored at –20°C until needed for intragastric administration. The *in vivo* concentration was 0.5 g/mL, representative of the human equivalent dose calculated based on body surface area, consistent with previous studies [28].

2.4. Micro-CT. Micro-CT images were analysed as described previously [29, 30]. Briefly, the L4 vertebral bodies were separated, fixed in 4% paraformaldehyde for 24 h, and placed in a rigid plastic tube to ensure that they did not move. Then, the vertebral bodies were analysed using a micro-CT

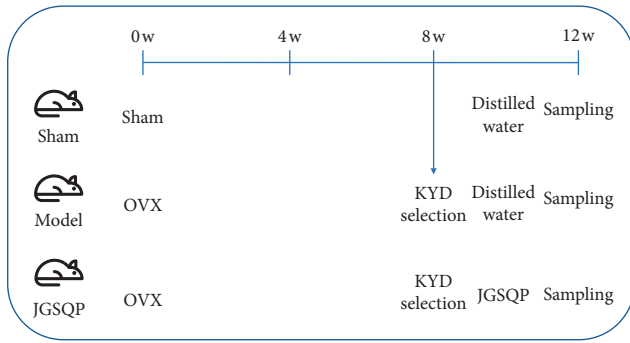


FIGURE 1: Schematic diagram of the experimental design. w: week; OVX: ovariectomy; and KYD: kidney yang deficiency.

imaging system (SkyScan, Kontich, Belgium) with a 55 kV scanning voltage, 145 mA current, and 4 μm slice thickness. Next, the μCT 80 evaluation programme was used to analyse the volume of interest of the L4 vertebrae. Bone microstructure features were characterised using the following parameters: bone volume/tissue volume (BV/TV), bone surface/tissue volume (BS/TV), trabecular number (Tb.N), trabecular thickness (Tb.Th), trabecular separation (Tb.Sp), and structural model index (SMI).

2.5. Bone Histomorphometric Analysis. Histomorphometric analysis of the L4 vertebrae was performed as described previously [30]. Briefly, the L4 vertebrae were fixed in 4% paraformaldehyde for 24–48 h and then placed in ethylenediaminetetraacetic acid (EDTA) decalcification solution for 3–5 weeks. Next, the samples were placed in the distilled water for gradient alcohol dehydration and paraffin-embedded. After trimming of the paraffin blocks, 5- μm -thick slices were cut using a paraffin slicer and visualised by hematoxylin and eosin staining (H&E; Solarbio, Beijing, China). Histomorphometric measurements, including the osteoblast surface ratio (Ob.S/BS, %), number of osteoclasts (Ob.N/BS, 1/mm), adipocyte number/tissue area (mm^2), and adipocyte area/tissue area (%), were analysed using the Image J software (Wayne Rasband, National Institutes of Health, USA).

2.6. RNA Isolation and qRT-PCR. For RNA isolation, 50 mg fresh lumbar vertebrae was snap frozen in liquid nitrogen and ground using a tissue-grinding pestle. Total RNA was then extracted using a MiniBEST Universal extraction Kit (Takara). RNA concentrations and sample purity were assessed using an ultraviolet spectrophotometer (Thermo Fisher). cDNA synthesis was performed using PrimeScript RT Master Mix (Takara). qRT-PCR was performed using SYBR Premix Ex Taq (Takara) in a Bio-Rad CFX96 device for two-step quantitative analysis (40 cycles of 95°C for 30 s, 95°C for 5 s, and 60°C for 1 min). Primer sequences are shown in Table 1. Gene expressions were assessed using the $2^{-\Delta\Delta\text{Ct}}$ method.

2.7. Western Blot Analysis. Total proteins were extracted from the mice lumbar vertebrae using RIPA lysis buffer (Thermo Fisher) and then quantified using a BCA protein assay kit (Beyotime). Proteins were resolved by electrophoresis on a 10% SDS-PAGE gel then transferred to PVDF membranes (Millipore, Shanghai, China). The membranes were blocked in 5% bovine serum albumin for 2 h at room temperature then incubated in the presence of primary antibodies. Primary antibodies against phosphorylation-AKT (p-AKT; 1:1000; rabbit; ab192623), AKT (1:10000; rabbit; ab179463), BMP2 (1:500; rabbit; ab14933), COL1A1 (1:1000; rabbit; ab34710), FNDC5 (1:1000; rabbit; ab174833), and GAPDH (1:10000; rabbit; ab181602) were incubated for 24 h at 4 °C. The membranes were then washed three times for 5 min each with TBST followed by treatment with a secondary antibody (goat anti-rabbit IgG, 1:3000, ab6939) for another 2 hours at room temperature. Protein levels were evaluated by enhanced chemiluminescence (Bio-Rad, Hercules, CA, USA) following the manufacturer's instructions. The Image J software was used to determine the gray values of the protein electrophoresis bands, which indicates the relative protein expression levels.

2.8. Statistical Analysis. SPSS 19.0 (IBM, Chicago, IL, USA) was used for data analysis. All data analysed were quantitative, and comparison among groups was performed by one-way ANOVA followed by Tukey's test for multiple comparisons. P values <0.05 were considered to be significant.

3. Results

3.1. JGSQP Treatment Improved Bone Microarchitecture of Murine OVX-Induced Osteoporosis with KYD. Reconstructed micro-CT images of the L4 vertebrae from the model group revealed reduced, thinning trabeculae and increased Tb.Sp relative to the Sham group. Treatment with JGSQP significantly attenuated damage to the bone microarchitecture. Accordingly, JGSQP treatment created a strong bone-protecting phenotype in mice with OVX-induced osteoporosis and KYD, as evidenced by decreased Tb.Sp and increased Tb.Th, Tb.N, and BV/TV ($P < 0.05$ for all; Figure 2).

3.2. JGSQP Attenuated Histomorphological Damage in Murine OVX-Induced Osteoporosis with KYD. H&E staining of the L4 vertebrae revealed thinner, smaller trabeculae with more lipid droplets and microfractures in the Model group relative to Sham controls. The Ob.N/BS and Ob.S/BS were consistently decreased in the Model group, whereas the adipocyte number and area were increased relative to Sham controls. As before, JGSQ treatment significantly attenuated histomorphological damage in the murine model of OVX-induced osteoporosis with KYD (Figure 3).

TABLE 1: Quantitative PCR primer sequences.

| Gene | Forward (5'-3') | Reverse (5'-3') |
|--------------------------------|--------------------------|--------------------------|
| <i>Akt</i> | ATGAACGACGTAGCCATTGTG | TTGTAGCCAATAAAGGTGCCAT |
| <i>Wnt10b</i> | GCGGGTCTCCTGTTCTTGG | CCGGGAAGTTTAAGGCCAG |
| <i>Osx</i> | AAAGGAGGCACAAAGAAGC | CAGGAAATGAGTGAGGGAAG |
| <i>Fndc5</i> | TTGCCATCTCTCAGCAGAAGA | GGCCTGCACATGGACGATA |
| <i>PPARγ</i> | TCGCTGATGCACTGCCTATG | GAGAGTCCACAGAGCTGATT |
| <i>GAPDH</i> | ATGTTCCAGTATGACTCCACTCAC | GAAGACACCAGTAGACTCCACGAC |

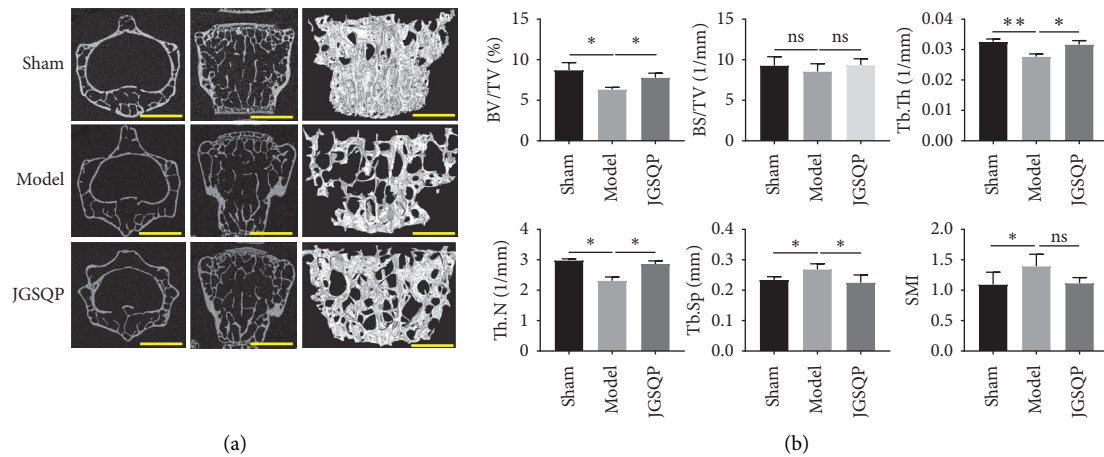


FIGURE 2: JGSQP improved bone microarchitecture of murine ovariectomy-induced osteoporosis with KYD. (a) Representative 2D and 3D micro-CT images (scale bars = 250 μ m); (b) BV/TV, BS/TV, Tb.Th, Tb.N, Tb.Sp, and SMI were calculated based on micro-CT results. Data are expressed as means \pm SDs. * P < 0.05, ** P < 0.01 (one-way ANOVA with Tukey's multiple comparison test); ns: not significant.

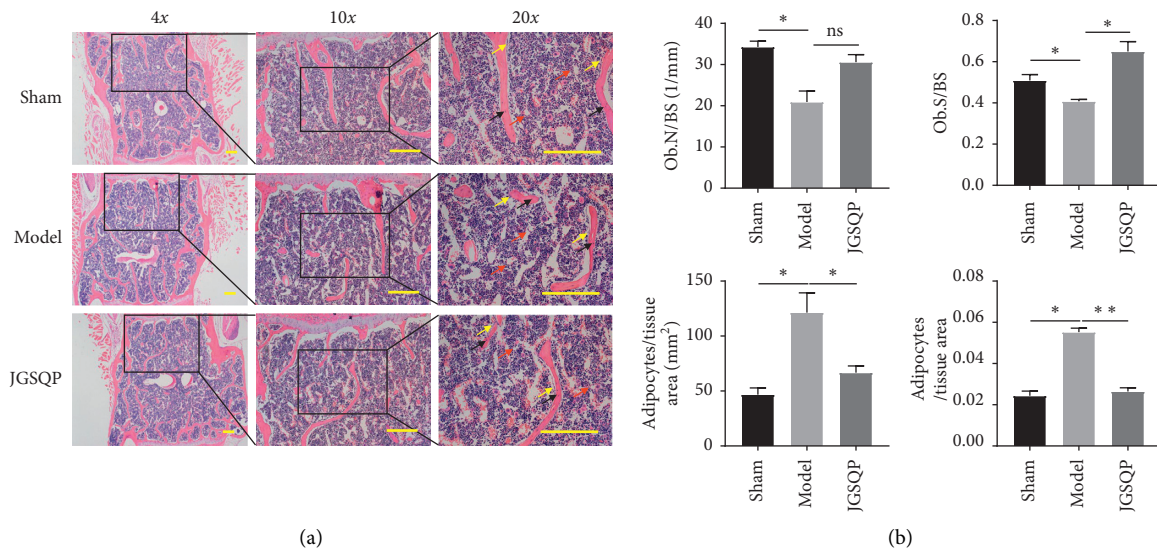


FIGURE 3: JGSQP attenuated histomorphological damage of murine ovariectomy-induced osteoporosis with KYD. (a) Representative images of H&E staining. (b) The quantifications of Ob.N/BS, Ob.S/BS, adipocyte/tissue area, and adipocyte area/tissue area were calculated based on H&E staining and analysed using the Image J software. Data are expressed as means \pm SDs. * P < 0.05, ** P < 0.01 (one-way ANOVA with Tukey's multiple comparison test); ns: not significant.

3.3. JGSQP Reduced *Akt* and Adipogenesis-Related Gene (*Fndc5*, *PPAR γ* , and *Fabp4*) Expression and Promoted the Expression of Osteogenesis-Related Genes (*Wnt10b* and *Osx*).

Gene expression analyses were conducted using tissues from the L1-L3 vertebrae of all mice (Figure 4). The Model group showed significant downregulation of *Wnt10b* and *Osx* and

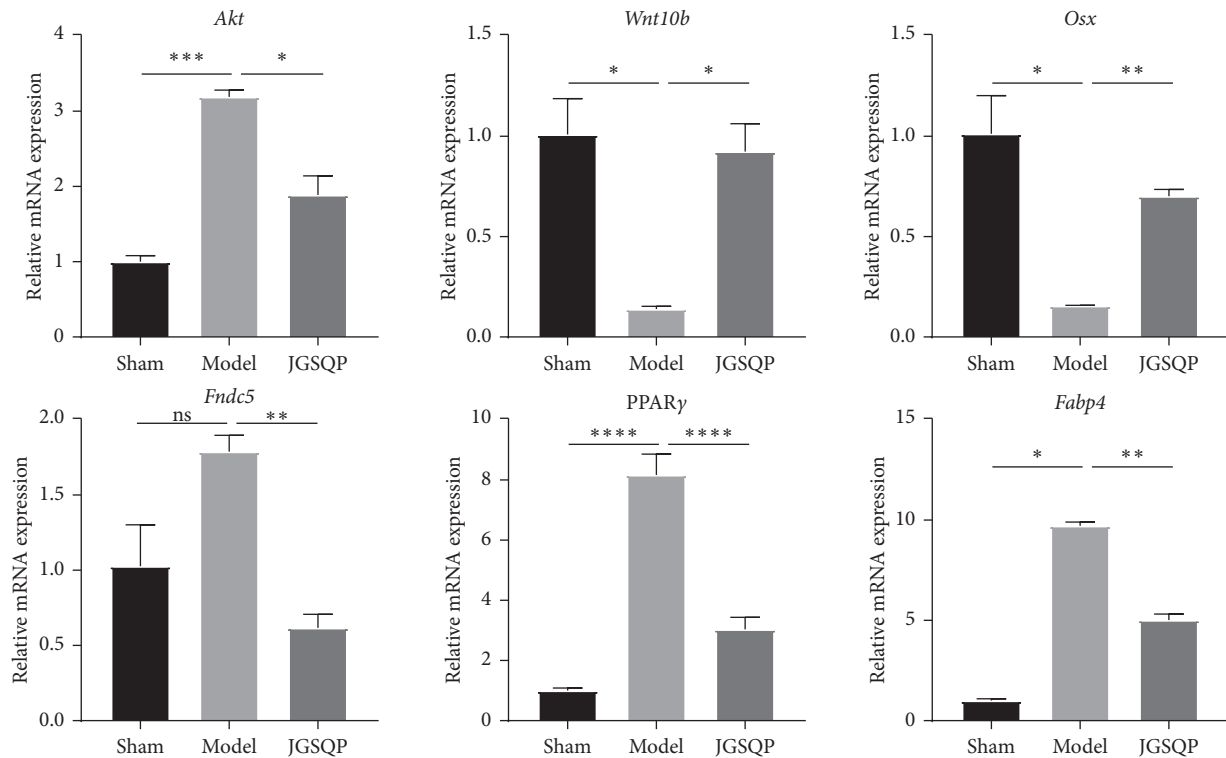


FIGURE 4: Effect of JGSQP treatment on the mRNA expression of *Akt*, adipogenic (*Fndc5*, *PPARγ*, and *Fabp4*) and osteogenesis-specific genes (*Wnt10b* and *Osx*). Data are expressed as means \pm SDs. * $P < 0.05$, ** $P < 0.01$, *** $P < 0.001$, and **** $P < 0.0001$ (one-way ANOVA with Tukey's multiple comparison test); ns: not significant.

upregulation of *Akt*, *PPARγ*, and *Fabp4* expressions compared with the Sham group. Although *Fndc5* expression did not differ significantly between groups, a strong tendency toward increased expression was observed in the Model group. After JGSQP treatment, the expression of *Akt* and adipogenesis-related genes (*Fndc5*, *PPARγ*, and *Fabp4*) was downregulated, whereas osteogenesis-related genes (*Wnt10b* and *Osx*) were upregulated.

3.4. JGSQP Increased p-AKT, BMP2 Protein Expressions and Reduced FNDC5 Protein Expression. Protein levels were analysed by western blot. The Model group exhibited significantly reduced p-AKT, BMP2, and COL1A1 expression and significantly increased FNDC5 expression relative to Sham controls. Compared with the Model group, the JGSQP group exhibited significantly greater p-AKT, BMP2 expressions and significantly reduced FNDC5 expression. COL1A1 protein expression did not differ significantly after JGSQP treatment (Figure 5).

4. Discussion

An increasing number of studies have focused on the role of bone-fat imbalance in the context of PMOP. Previously, clinical cross-sectional studies showed that bone marrow fat content was positively correlated with the risks of osteoporosis and fracture [31, 32], and other studies have shown that increased bone marrow fat tissue limits the regeneration

of damaged bone [16, 33]. Bone and fat interact with each other through endocrine and paracrine forms. Bone marrow fat cells express endocrine factors (ADIPOQ, IGF1, IGF1BP2, etc.) and paracrine factors (*Wnt10b*, BMP4, ANGPT2, etc.) to regulate bone regeneration. Bone secretion factors (OCN, SOST, BMP, PTHrp, etc.) can also regulate fat tissue metabolism [33, 34]. Together, these results show that bone and fat exist in a complex regulatory environment, suggesting that control of the bone-fat balance is important for the prevention and treatment of PMOP.

JGSQP is a TCM prescription used to treat KYD syndrome and many other diseases. It has been shown to play important roles in the regulation of ageing [35], tissue repair [36], and apoptosis [37] and to help prevent acute and critical diseases, including heart failure [38], diabetes [35, 39], asthma [40], neonatal hypoxic-ischemia [41], adrenal insufficiency [42], and hypertension [43–45]. Research conducted using metabolomic and proteomic approaches has demonstrated that JGSQP effectively treats kidney impairment with KYD syndrome involved in Wnt, chemokine, PPAR, and MAPK signaling pathways [36]. Furthermore, tonification of the kidney yang more effectively facilitates osteogenic differentiation and suppresses adipogenic differentiation of BMSCs than does tonification of the kidney yin [27]. However, the effect of JGSQP in terms of bone-fat balance control in an *in vivo* murine model of OVX-induced osteoporosis with KYD has not been reported previously. In the present study, we demonstrated that JGSQP could ameliorate changes to bone microarchitecture in such a model, as confirmed by

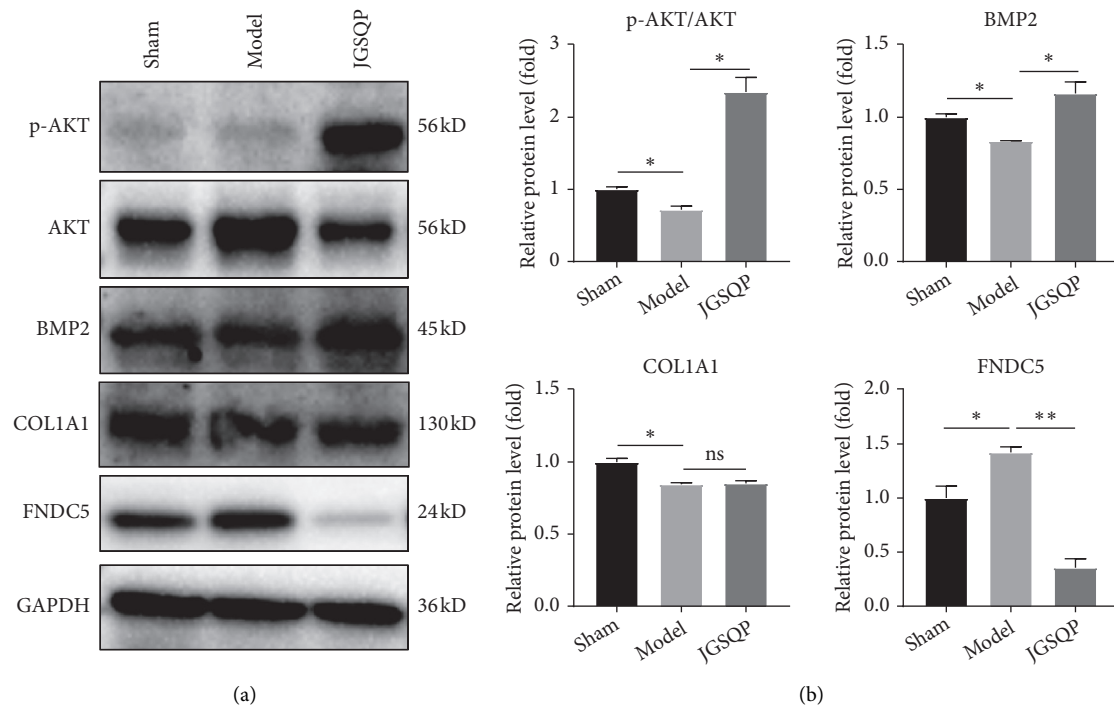


FIGURE 5: Changes in adipogenesis- and osteogenesis-related protein expressions. (a) Representative images of western blot results. (b) Quantifications of western blot electrophoretograms performed with Image J software. Data are expressed as means \pm SDs. * $P < 0.05$, ** $P < 0.01$ (one-way ANOVA with Tukey's multiple comparison test); ns: not significant.

histomorphological assessment by micro-CT and H&E staining. Furthermore, the quantification of bone histomorphological parameters revealed that JGSQP promoted increases in osteoblast number and surface area while inhibiting such increases in the adipocyte number and area, consistent with the *in vitro* findings of Cheng et al. [27].

To further elucidate the pathogenetic molecular mechanisms possibly underlying these effects, the mRNA and protein expression levels of several genes involved in bone and fat metabolism in the lumbar spine were analysed. *Wnt10b*, *Osx*, and *BMP2* are defined broadly as positive regulators of bone formation [46–48], whereas *PPAR γ* and *Fabp4* are generally considered to be upregulators of adipogenesis [49, 50]. The role of *Fndc5* in bone formation and adipogenesis remains controversial. *Fndc5* knockout has been shown to block OVX-induced bone loss, suggesting that this gene plays a positive role in adipogenesis [51, 52]. In our study, the bone formation-specific genes *Wnt10b* and *Osx* were upregulated, whereas the adipogenesis-related genes *Fndc5*, *PPAR γ* , and *Fabp4* were downregulated in the JGSQP group compared with the Model group, indicating that JGSQP promoted bone formation and inhibited bone marrow lipogenesis, thereby controlling the bone-fat balance in mice with OVX-induced osteoporosis and KYD. In accordance with the results, in protein expressions, the osteogenesis-specific protein *BMP2* was increased, whereas the adipogenesis-related protein *FNDC5* was decreased in the JGSQP group relative to the Model group.

AKT signaling remains a key pathway that regulates the balance of bone and fat metabolism [53–55]. Increases in p-AKT contributed to the inactivation of *GSK-3 β* , which increased downstream β -catenin transcription to the nucleus, promoted osteogenic differentiation (e.g., of *Osx*, *Runx2*), and inhibited lipogenic differentiation (e.g., of *Fabp4*, *PPAR γ*) [56–58]. In our study, JGSQP activated the expression of p-AKT along with multiple bone formation and adipogenesis-related genes (*Wnt10b*, *Osx*, *BMP2*, *PPAR γ* , *Fabp4*, and *Fndc5*), suggesting that it may ameliorate murine OVX-induced osteoporosis with KYD by controlling the bone-fat balance via the AKT pathway. Our investigations demonstrated that JGSQP is an important regulator of the bone-fat balance, and thus that it may be an attractive option for the treatment of PMOP.

5. Conclusion

JGSQP treatment reversed murine ovariectomy-induced osteoporosis with KYD through controlling bone-fat balance via the AKT pathway. Thus, this study provides evidence supporting the effectiveness of JGSQP for the treatment of PMOP with KYD.

Although we successfully demonstrated the protective effect of JGSQP treatment on murine ovariectomy-induced osteoporosis with KYD and also gained insight into its underlying mechanism concerning regulating bone-fat balance, this study had several limitations. First, the

evaluation of ovariectomy-induced osteoporosis with KYD model lacked precise quantitative index. Second, although some differentially expressed genes were found, advanced techniques such as high-throughput sequencing, gene knockout, and overexpression studies were not employed to explore potentially underlying mechanisms in this study. Third, the findings of this study should be further verified by additional clinical and experimental investigations.

Abbreviations

| | |
|----------------------|---|
| PMOP: | Postmenopausal osteoporosis |
| OVX: | Ovariectomy |
| JGSQP: | Jingui Shenqi Pills |
| KYD: | Kidney yang deficiency |
| BV: | Bone volume |
| BS: | Bone surface |
| Ob.N/BS: | Osteoblast number/bone surface |
| Ob.S/BS: | Osteoblast surface/bone surface |
| TV: | Tissue volume |
| Tb.Th: | Trabecular bone thickness |
| Tb.N: | Trabecular bone number |
| Tb.Sp: | Trabecular bone space |
| Osx: | Osterix |
| Phosphorylation-AKT: | p-AKT |
| GAPDH: | Glyceraldehyde 3-phosphate dehydrogenase. |

Data Availability

The data used to support the findings of our study are available from the correspondence author upon request.

Conflicts of Interest

The authors declare that there are no potential conflicts of interest to disclose regarding the publication of this paper.

Authors' Contributions

Qi Shang, Wenhua Zhao, and Gengyang Shen contributed equally to this work. All authors listed in the current study carried out the experiments, participated in the design of the study, performed the statistical analysis, conceived the study, and helped to draft the manuscript.

Acknowledgments

This work was generously supported by National Natural Science Foundation of China (81904225, 81674000, 81774338, and 81503591), Guangdong Province Universities and Colleges Pearl River Scholar Funded Scheme (2018), Science and Technology Program of Guangzhou (201707010298), the Youth Scientific Research Training Project of GZUCM (2019QNPY04), Key Project of Basic Research and Applied Basic Research of the Department of Education of Guangdong Province (2018KZDXM021), and Guangdong Natural Science Foundation (2018A030310615).

References

- [1] R. Eastell, T. W. O'Neill, L. C. Hofbauer et al., "Postmenopausal osteoporosis," *Nature Reviews Disease Primers*, vol. 2, Article ID 16069, 2016.
- [2] J. Thulkar, S. Singh, S. Sharma, and T. Thulkar, "Preventable risk factors for osteoporosis in postmenopausal women: systematic review and meta-analysis," *Journal of Mid-life Health*, vol. 7, no. 3, pp. 108–113, 2016.
- [3] T. Sozen, L. Ozisik, and N. Calik Basaran, "An overview and management of osteoporosis," *European Journal of Rheumatology*, vol. 4, no. 1, pp. 46–56, 2017.
- [4] J. E. M. Sale, D. Beaton, and E. Bogoch, "Secondary prevention after an osteoporosis-related fracture," *Clinics in Geriatric Medicine*, vol. 30, no. 2, pp. 317–332, 2014.
- [5] L. Si, T. M. Winzenberg, Q. Jiang, M. Chen, and A. J. Palmer, "Projection of osteoporosis-related fractures and costs in China: 2010–2050," *Osteoporosis International*, vol. 26, no. 7, pp. 1929–1937, 2015.
- [6] Y. M. Xie, F. Z. Zhang, and W. Q. Zhou, "Clinical study of bugu shengsui capsule in treating primary osteoporosis with kidney-yang deficiency syndrome," *Zhongguo Zhong Xi Yi Jie He Za Zhi*, vol. 17, no. 9, pp. 526–530, 1997.
- [7] S. An, E. Li, and X. Tong, "Study on relationship between estrogen receptor gene polymorphism and syndrome differentiation typing of female postmenopausal osteoporosis in Traditional Chinese medicine," *Zhongguo Zhong Xi Yi Jie He Za Zhi*, vol. 20, no. 12, pp. 907–910, 2000.
- [8] W. Xiufeng, Z. Lei, H. Rongbo et al., "Regulatory mechanism of hormones of the pituitary-target gland axes in kidney-Yang deficiency based on a support vector machine model," *Journal of Traditional Chinese Medicine*, vol. 35, no. 2, pp. 238–243, 2015.
- [9] B. H. Lin, S. Q. Fang, and Y. Ye, "Exploration on essence of spleen-kidney deficiency in middle-aged patients," *Zhongguo Zhong Xi Yi Jie He Za Zhi*, vol. 22, no. 1, pp. 33–36, 2002.
- [10] H. Schacke, W. D. Docke, and K. Asadullah, "Mechanisms involved in the side effects of glucocorticoids," *Pharmacology & Therapeutics*, vol. 96, no. 1, pp. 23–43, 2002.
- [11] E. Ambrogini, X. Que, S. Wang et al., "Oxidation-specific epitopes restrain bone formation," *Nature Communications*, vol. 9, no. 1, p. 2193, 2018.
- [12] P. W. G. Mallon, "Aging with HIV," *Current Opinion in HIV and AIDS*, vol. 9, no. 4, pp. 428–435, 2014.
- [13] M. Hayashi, T. Nakashima, N. Yoshimura, K. Okamoto, S. Tanaka, and H. Takayanagi, "Autoregulation of osteocyte Sema3A orchestrates estrogen action and counteracts bone aging," *Cell Metabolism*, vol. 29, no. 3, pp. 627–637, 2019.
- [14] Y. Li, W. Liang, X. Li et al., "Effect of serum from postmenopausal women with osteoporosis exhibiting the Kidney-Yang deficiency pattern on bone formation in an hFOB 1.19 human osteoblastic cell line," *Experimental and Therapeutic Medicine*, vol. 10, no. 3, pp. 1089–1095, 2015.
- [15] Y. Fu, R. Li, J. Zhong et al., "Adipogenic differentiation potential of adipose-derived mesenchymal stem cells from ovariectomized mice," *Cell Proliferation*, vol. 47, no. 6, pp. 604–614, 2014.
- [16] B. Yu, L. Huo, Y. Liu et al., "PGC-1 α controls skeletal stem cell fate and bone-fat balance in osteoporosis and skeletal aging by inducing TAZ," *Cell Stem Cell*, vol. 23, no. 2, pp. 193–209, 2018.
- [17] M. Ishii, J. G. Egen, F. Klauschen et al., "Sphingosine-1-phosphate mobilizes osteoclast precursors and regulates bone homeostasis," *Nature*, vol. 458, no. 7237, pp. 524–528, 2009.

- [18] G. Shen, H. Ren, Q. Shang et al., "Foxf1 knockdown promotes BMSC osteogenesis in part by activating the Wnt/beta-catenin signalling pathway and prevents ovariectomy-induced bone loss," *EBioMedicine*, vol. 52, Article ID 102626, 2020.
- [19] B. Xu, H. Liu, H. T. Jin, J. L. Fang, L. W. Xiao, and P. J. Tong, "Research on osteoporosis model rats with kidney deficiency syndrome," *Zhongguo Gu Shang*, vol. 25, no. 9, pp. 766–770, 2018.
- [20] X. R. Tang, J. X. Wang, L. Fu et al., "Effects of total flavonoids in Astragali Complanati Semen on liver lipid level and ERalpha expression on liver in hyperlipidemia rats with kidney-Yang deficiency pattern," *Zhongguo Zhong Yao Za Zhi*, vol. 43, no. 11, pp. 2365–2371, 2018.
- [21] Y. Zhang, S. Y. Xu, M. N. Liu et al., "Comparative studies on chemical contents and effect in kidney-yang deficiency rats of salt-processed product and wine-processed product of cuscuteae semen," *Evid Based Complement Alternat Med*, vol. 2019, Article ID 2049497, 13 pages, 2019.
- [22] J. Yang, Y. Wang, Y. Bao, and J. Guo, "The total flavones from Semen cuscuteae reverse the reduction of testosterone level and the expression of androgen receptor gene in kidney-yang deficient mice," *Journal of Ethnopharmacology*, vol. 119, no. 1, pp. 166–171, 2008.
- [23] W. J. Che, X. Z. He, J. P. Jiang, W. Y. Cai, and S. J. Xie, "Preliminary study on treatment of partial androgen deficiency in aging males with Jingui Shenqi Pill," *Chinese Journal of Integrative Medicine*, vol. 11, no. 4, pp. 300–302, 2005.
- [24] J. Y. Chen, Y. Y. Zhang, and Q. Wu, "Effect of jingui shenqi pills on sex hormone in aged rats," *Zhongguo Zhong Yao Za Zhi*, vol. 18, no. 10, pp. 619–620, 1993.
- [25] Y. L. Long and Z. M. Li, "Effect of jingui shenqi pill and its disassembled recipes on ovarian functions in shen yang deficiency female rats," *Zhongguo Zhong Xi Yi Jie He Za Zhi*, vol. 33, no. 7, pp. 967–971, 2015.
- [26] C. P. Xu, Q. J. Zhu, J. Song, Z. Li, and D. Zhang, "Acceleration of Jingui Shenqi Pill on the testis telomerase activity in mice of Shen-yang deficiency," *Zhongguo Zhong Xi Yi Jie He Za Zhi*, vol. 33, no. 2, pp. 252–255, 2013.
- [27] Z. A. Cheng, L. Han, J. A. Wei, J. Sun, and X. D. Duan, "Regulation effects of liuwe dihuang pill, jingui shenqi pill, jiangou erxian pill containing serums on adipogenic and osteogenic differentiation-related genes expressions in the differentiation process of preadipocytes to osteoblasts," *Zhongguo Zhong Xi Yi Jie He Za Zhi*, vol. 33, no. 2, pp. 261–265, 2018.
- [28] S.-T. Kao, S.-D. Wang, C.-C. Lin, and L.-J. Lin, "Jin Gui Shen Qi Wan, a traditional Chinese medicine, alleviated allergic airway hypersensitivity and inflammatory cell infiltration in a chronic asthma mouse model," *Journal of Ethnopharmacology*, vol. 227, pp. 181–190, 2018.
- [29] J. Li, A. Ayoub, Y. Xiu et al., "TGFbeta-induced degradation of TRAF3 in mesenchymal progenitor cells causes age-related osteoporosis," *Nature Communications*, vol. 10, no. 1, p. 2795, 2019.
- [30] G. Shen, H. Ren, Q. Shang et al., "miR-128 plays a critical role in murine osteoclastogenesis and estrogen deficiency-induced bone loss," *Theranostics*, vol. 10, no. 10, pp. 4334–4348, 2020.
- [31] A. V. Schwartz, "Marrow fat and bone: review of clinical findings," *Front Endocrinol (Lausanne)*, vol. 6, p. 40, 2015.
- [32] J. Li, X. Chen, L. Lu, and X. Yu, "The relationship between bone marrow adipose tissue and bone metabolism in postmenopausal osteoporosis," *Cytokine & Growth Factor Reviews*, vol. 52, pp. 88–98, 2020.
- [33] P. Boroumand and A. Klip, "Bone marrow adipose cells-cellular interactions and changes with obesity," *Journal of Cell Science*, vol. 133, no. 5, 2020.
- [34] A. N. Tikhonova, I. Dolgalev, H. Hu et al., "The bone marrow microenvironment at single-cell resolution," *Nature*, vol. 569, no. 7755, pp. 222–228, 2019.
- [35] B. Pang and Q. Ni, "Application of classical formula in treatment of diabetes," *Zhongguo Zhong Yao Za Zhi*, vol. 44, no. 18, pp. 3895–3898, 2019.
- [36] A. Zhang, X. Zhou, H. Zhao et al., "Metabolomics and proteomics technologies to explore the herbal preparation affecting metabolic disorders using high resolution mass spectrometry," *Molecular BioSystems*, vol. 13, no. 2, pp. 320–329, 2017.
- [37] H.-T. Shin, S.-H. Chung, J.-S. Lee et al., "Protective effect of shenqi-wan against H₂O₂-induced apoptosis in hippocampal neuronal cells," *The American Journal of Chinese Medicine*, vol. 31, no. 5, pp. 675–686, 2003.
- [38] X. J. Xiong, H. You, and K. L. Su, "Application of cream formula in treatment of severe heart failure," *Zhongguo Zhong Yao Za Zhi*, vol. 44, no. 18, pp. 3903–3907, 2019.
- [39] J. Wang, Q. Wang, Z. Z. Wang et al., "Comparative study on hypoglycemic effects of different traditional Chinese medicine treatments in rats with diabetes mellitus induced by alloxan," *Journal of Chinese Integrative Medicine*, vol. 8, no. 8, pp. 781–784, 2010.
- [40] B. Ji, Y. Y. Li, W. J. Yang et al., "Jinkui shenqi pills ameliorate asthma with kidney yang deficiency by enhancing the function of the hypothalamic-pituitary-adrenal Axis to regulate T helper 1/2 imbalance," *Evidence-Based Complementary and Alternative Medicine*, vol. 2018, Article ID 7253240, 10 pages, 2018.
- [41] H. N. Kim, M. E. Pak, M. J. Shin et al., "Beneficial effects of Jiawei Shenqi-wan and treadmill training on deficits associated with neonatal hypoxic-ischemia in rats," *Experimental and Therapeutic Medicine*, vol. 13, no. 5, pp. 2134–2142, 2017.
- [42] L. Zhao, A. Zhao, T. Chen et al., "Global and targeted metabolomics evidence of the protective effect of Chinese patent MedicineJinkui ShenqiPill on adrenal insufficiency after acute glucocorticoid withdrawal in rats," *Journal of Proteome Research*, vol. 15, no. 7, pp. 2327–2336, 2016.
- [43] X. D. Liu, J. Fu, M. Z. Feng, and Z. H. Zhang, "Effect of Jingui Shenqi pill combined with nifedipine for the treatment of elderly hypertensive patients with spleen-kidney Yang deficiency syndrome," *Zhongguo Zhong Yao Za Zhi*, vol. 40, no. 24, pp. 4908–4913, 2015.
- [44] X. Xiong, P. Wang, X. Li, and Y. Zhang, "Shenqi pill, a traditional Chinese herbal formula, for the treatment of hypertension: a systematic review," *Complementary Therapies in Medicine*, vol. 23, no. 3, pp. 484–493, 2015.
- [45] L. Y. Wang, K. W. Chan, Y. Yuwen, N. N. Shi, X. J. Han, and A. Lu, "Expert consensus on the treatment of hypertension with Chinese patent medicines," *Evidence-Based Complementary and Alternative Medicine*, vol. 2013, Article ID 510146, 8 pages, 2013.
- [46] A. M. Tyagi, M. Yu, T. M. Darby et al., "The microbial metabolite butyrate stimulates bone formation via T regulatory cell-mediated regulation of WNT10B expression," *Immunity*, vol. 49, no. 6, pp. 1116–1131, 2018.
- [47] L. Z. Ding, X. Teng, Z. B. Zhang, C. J. Zheng, and S. H. Chen, "Mangiferin inhibits apoptosis and oxidative stress via BMP2/Smad-1 signaling in dexamethasone-induced MC3T3-E1 cells," *International Journal Of Molecular Medicine*, vol. 41, no. 5, pp. 2517–2526, 2018.

- [48] N. Yin, L. Zhu, L. Ding et al., "MiR-135-5p promotes osteoblast differentiation by targeting HIF1AN in MC3T3-E1 cells," *Cellular & Molecular Biology Letters*, vol. 24, no. 1, 2019.
- [49] T. Garin-Shkolnik, A. Rudich, G. S. Hotamisligil, and M. Rubinstein, "FABP4 attenuates PPAR and adipogenesis and is inversely correlated with PPAR in adipose tissues," *Diabetes*, vol. 63, no. 3, pp. 900–911, 2014.
- [50] A. Briot, P. Decaunes, F. Volat et al., "Senescence alters PPAR γ (peroxisome proliferator-activated receptor gamma)-dependent fatty acid handling in human adipose tissue microvascular endothelial cells and favors inflammation," *Arteriosclerosis, Thrombosis, and Vascular Biology*, vol. 38, no. 5, pp. 1134–1146, 2018.
- [51] A. B. Crujeiras, M. Pardo, and F. F. Casanueva, "Irisin: "fat" or artefact," *Clinical Endocrinology*, vol. 82, no. 4, pp. 467–474, 2015.
- [52] H. Kim, C. D. Wrann, M. Jedrychowski et al., "Irisin mediates effects on bone and fat via α V integrin receptors," *Cell*, vol. 175, no. 7, pp. 1756–1768.e17, 2018.
- [53] B. D. Manning and A. Toker, "AKT/PKB signaling: navigating the network," *Cell*, vol. 169, no. 3, pp. 381–405, 2017.
- [54] C. Schreiber, S. Saraswati, S. Harkins et al., "Loss of ASAP1 in mice impairs adipogenic and osteogenic differentiation of mesenchymal progenitor cells through dysregulation of FAK/Src and AKT signaling," *PLoS Genet*, vol. 15, no. 6, Article ID e1008216, 2019.
- [55] F. Zhang, J. Ye, Y. Meng et al., "Calcium supplementation enhanced adipogenesis and improved glucose homeostasis through activation of camkii and PI3K/Akt signaling pathway in porcine bone marrow mesenchymal stem cells (pBMSCs) and mice fed high fat diet (HFD)," *Cellular Physiology and Biochemistry*, vol. 51, no. 1, pp. 154–172, 2018.
- [56] L. Song, M. Liu, N. Ono, F. R. Bringhurst, H. M. Kronenberg, and J. Guo, "Loss of wnt/ β -catenin signaling causes cell fate shift of preosteoblasts from osteoblasts to adipocytes," *Journal of Bone and Mineral Research*, vol. 27, no. 11, pp. 2344–2358, 2012.
- [57] V. Krishnan, H. U. Bryant, and O. A. Macdougald, "Regulation of bone mass by Wnt signaling," *Journal of Clinical Investigation*, vol. 116, no. 5, pp. 1202–1209, 2006.
- [58] L. Huang, X. Wang, H. Cao et al., "A bone-targeting delivery system carrying osteogenic phytomolecule icaritin prevents osteoporosis in mice," *Biomaterials*, vol. 182, pp. 58–71, 2018.

Research Article

Deciphering the Molecular Targets and Mechanisms of HGWD in the Treatment of Rheumatoid Arthritis via Network Pharmacology and Molecular Docking

Wei Liu ¹, Yihua Fan ^{1,2}, Chunying Tian ², Yue Jin ¹, Shaopeng Du ¹, Ping Zeng,^{2,3}
and Aihua Wang¹

¹Department of Rheumatism and Immunity, First Teaching Hospital of Tianjin University of Traditional Chinese Medicine, Tianjin 300193, China

²Tianjin University of Traditional Chinese Medicine, Tianjin 301617, China

³GuiZhou University of Traditional Chinese Medicine, Guiyang 550025, Guizhou, China

Correspondence should be addressed to Wei Liu; fengshiliuwei@163.com

Received 7 July 2020; Accepted 18 August 2020; Published 26 August 2020

Academic Editor: Arham Shabbir

Copyright © 2020 Wei Liu et al. This is an open access article distributed under the Creative Commons Attribution License, which permits unrestricted use, distribution, and reproduction in any medium, provided the original work is properly cited.

Background. Huangqi Guizhi Wuwu Decoction (HGWD) has been applied in the treatment of joint pain for more than 1000 years in China. Currently, most physicians use HGWD to treat rheumatoid arthritis (RA), and it has proved to have high efficacy. Therefore, it is necessary to explore the potential mechanism of action of HGWD in RA treatment based on network pharmacology and molecular docking methods. **Methods.** The active compounds of HGWD were collected, and their targets were identified from the Traditional Chinese Medicine Systems Pharmacology Database (TCMSP) and DrugBank database, respectively. The RA-related targets were retrieved by analyzing the differentially expressed genes between RA patients and healthy individuals. Subsequently, the compound-target network of HGWD was constructed and visualized through Cytoscape 3.8.0 software. Protein-protein interaction (PPI) network was constructed to explore the potential mechanisms of HGWD on RA using the plugin BisoGenet of Cytoscape 3.8.0 software. Gene ontology (GO) analysis and Kyoto Encyclopedia of Genes and Genomes (KEGG) were performed in R software (Bioconductor, clusterProfiler). Afterward, molecular docking was used to analyze the binding force of the top 10 active compounds with target proteins of VCAM1, CTNNA1, and JUN. **Results.** Cumulatively, 790 active compounds and 1006 targets of HGWD were identified. A total of 4570 differentially expressed genes of RA with a p value < 0.05 and $|\log_2(\text{fold change})| > 0.5$ were collected. Moreover, 739 GO entries of HGWD on RA were identified, and 79 pathways were screened based on GO and KEGG analysis. The core target gene of HGWD in RA treatment was JUN. Other key target genes included FOS, CCND1, IL6, E2F2, and ICAM1. It was confirmed that the TNF signaling pathway and IL-17 signaling pathway are important pathways of HGWD in the treatment of RA. The molecular docking results revealed that the top 10 active compounds of HGWD had a strong binding to the target proteins of VCAM1, CTNNA1, and JUN. **Conclusion.** HGWD has important active compounds such as quercetin, kaempferol, and beta-sitosterol, which exert its therapeutic effect on multiple targets and multiple pathways.

1. Introduction

Rheumatoid arthritis (RA), a common chronic systemic autoimmune disease, is characterized by synovial hyperproliferation and inflammatory/immune cell infiltration [1, 2]. Typical clinical symptoms of RA include tender and swelling of the joints, accompanied by morning stiffness of

the affected joints. In severe cases, large joints can be injured leading to joint deformity and loss of function. The current global incidence of RA is 0.24%, and it is expected to increase [3–6]. Besides, RA is ranked 74th as a social burden and 42nd as a disability [3–6]. Current international guidelines for the management of RA recommend the use of disease-modifying antirheumatic drugs (DMARDs), with methotrexate

(MTX) as the first-line drug [7, 8]. However, MTX is not an ideal therapeutic agent. It has damaging side effects on the neuronal, gastrointestinal, and immune systems [9]. Therefore, it is imperative to explore safe and effective clinical treatment for RA.

The traditional Chinese medicine (TCM) is based on the theory of syndrome differentiation and has long been established as an effective treatment of RA. Huangqi Guizhi Wuwu Decoction (HGWD), a classical prescription described in *Jingui Yaolue*, has been used over 1000 years in China to treat joint pain. HGWD was formulated by Zhang Zhongjing during the Han dynasty. It is a mixture of five Chinese medicines including *Astragalus membranaceus* (Huangqi), Cassia Twig (Guizhi), *Radix Paeoniae Alba* (Baishao), ginger (Shengjiang), and Chinese date (Dazao). HGWD is considered to have the ability to reinforce Qi and nourish blood, warm and smoothen meridian, and dredge arthritic pain traditionally [10]. In a study of rats with RA, HGWD administration reduced joint inflammation, synovial hyperplasia, and cartilage damage [11]. Previous studies have revealed that HGWD improves the clinical symptoms and signs, as well as laboratory indices, in RA patients [12]. Moreover, a systematic review and meta-analysis showed that when HGWD was combined with Western medicine therapy to treat RA, better efficacy, improved morning stiffness, reduced C-reactive protein, and rheumatoid factor content were achieved compared to Western medicine only [13]. However, the mechanisms of HGWD in RA treatment are not clear, a major limiting factor for its extensive application.

Network pharmacology is partly bioinformatics and was first proposed by Hopkins [14]. It has been successfully used to study complex TCM formulations. This is because it not only combines system network analysis and pharmacology but is also based on the connotation of holistic theory, multicomponents, multitargets, and multipathways of Chinese medicine [15, 16]. Network pharmacology can elucidate the mechanisms of HGWD in the RA treatment at the molecular level via compound-compound network, compound-target network, and target-disease network.

In the present study, network pharmacology was used to establish a compound-target-disease network for exploring the potential HGWD mechanism of action in RA treatment. This study provides a reference for future pharmacological studies and clinical applications. The flow diagram of the network is shown in Figure 1.

2. Methods

2.1. Collection of Active HGWD Compound Information. Information on the HGWD compounds was retrieved from the Traditional Chinese Medicine Systems Pharmacology Database (TCMSP, <http://tcmsp.com/tcmsp.php>) [17]. TCMSP is a unique system pharmacology database of Chinese herbal medicines with data on absorption, distribution, metabolism, and excretion (ADME)-related parameters of herbal ingredients as well as the relationships

between diseases, targets, ingredients, and drugs [18]. The active compounds of HGWD were primarily screened based on oral bioavailability (OB) and drug-like (DL) properties, the two important indicators for bioinformatics evaluation of ADME characteristics [19]. The OB is a major pharmacokinetic parameter of oral drugs and is the proportion of oral drug dose in the systemic circulation [20]. DL properties are the physical and chemical properties that qualitatively evaluate whether a compound is similar to existing drugs [21]. Subsequently, the compounds with $OB \geq 30\%$ and $DL \geq 0.18$ were chosen as the candidate compounds for further analysis.

2.2. Identification of HGWD Potential Targets. Target identification is an important aspect of drug exploration [22]. The target candidate compounds were imported into the DrugBank database (<https://www.drugbank.ca/>) to identify the corresponding potential targets of HGWD [23].

2.3. Known RA-Related Targets. The differentially expressed genes in RA were retrieved from the GEO database (<https://www.ncbi.nlm.nih.gov>; series: GSE21959; samples: there were 36 samples, 18 for healthy individuals and 18 for those with rheumatoid arthritis). The genes with a p value < 0.05 and $|\log_2(\text{fold change})| > 0.5$ were regarded as differentially expressed genes and RA-related targets.

2.4. Network Construction. The compound-target network of HGWD was constructed and visualized via Cytoscape 3.8.0 software [24]. Protein-protein interaction (PPI) networks were constructed to explore the potential mechanisms of HGWD on RA using the plugin BisoGenet of Cytoscape 3.8.0 software [25]. Afterward, the topological importance of each node by calculating degree centrality (DC), betweenness centrality (BC), closeness centrality (CC), eigenvector centrality (EC), local average connectivity-based method (LAC), and network centrality (NC) was evaluated with a Cytoscape plugin CytoNCA. Their definitions and computational formulas have been reported and are the topological importance representative of each node [26].

2.5. Gene Ontology and Pathway Enrichment Analysis. Gene ontology (GO) analysis and Kyoto Encyclopedia of Genes and Genomes (KEGG) are important methods that describe the features of candidate targets. The two were performed in R software (Bioconductor, clusterProfiler) with the standard p value cutoff of 0.05 and the q value of 0.05 [27, 28]. The GO analysis was applied for target protein analysis, and the top 20 functional categories in biological process (BP), cellular component (CC), and molecular function (MF) were chosen. Based on the targets of HGWD in RA treatment, KEGG enrichment analysis was carried out. The top 20 KEGG pathways were selected for plotting a histogram. Meanwhile, the network diagram of the gene pathway was drawn.

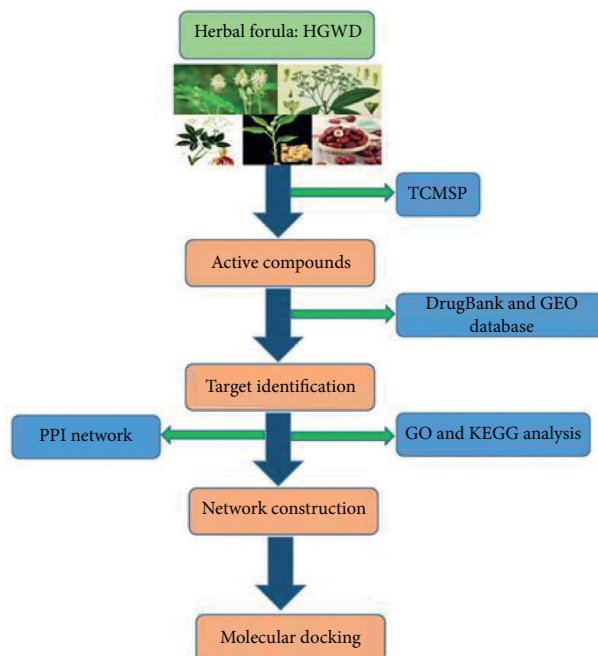


FIGURE 1: The flow diagram of network pharmacology analysis.

2.6. Molecular Docking of the Main Active Constituents of HGWD and Core Proteins. The 3D protein structure of the three core proteins corresponding to the core targets, VCAM1, CTNBN1, and JUN, was downloaded from the UniProt database. Subsequently, the structure of the active ingredient in HGWD (the top 10 places in the number of targets) was downloaded from the PubChem database and saved in the PDB format. Using PyMOL software, the three proteins were virtually dehydrated and hydrogenated, the original ligands were extracted in each protein, and then were stored separately. AutoDockTools 1.5.6 was utilized to convert compounds, ligands, and proteins into the “pdbqt” format and to define if the location of each protein or its ligands was the active pocket of the protein. Finally, Vina 1.5.6 was run to assess molecular docking. At a binding energy value <0 , the molecular proteins were considered to spontaneously bind and interact with each other. Accordingly, the lower the energy is, the more stable the molecular conformation is.

3. Results

3.1. Target Screening of HGWD and RA. A total of 790 compounds of the five herb medicines in HGWD were retrieved from the TCMSP database. This included 87 compounds in Huangqi, 220 in Guizhi, 85 in Baishao, 265 in Shengjiang, and 133 in Dazao. Among them, 74 compounds passed $OB \geq 30\%$ and $DL \geq 0.18$ filtering. Specifically, the numbers of candidate compounds in Huangqi, Guizhi, Baishao, Shengjiang, and Dazao were 20, 7, 13, 5, and 29, respectively. The candidate compounds in HGWD used for further analysis are shown in Table 1. The DrugBank database retrieval predicted a total of 1006 potential targets. The potential targets linked to Huangqi, Guizhi, Baishao, Shengjiang, and Dazao were 405, 57, 104, 60, and 380,

respectively. Moreover, a total of 4570 differentially expressed genes in RA were collected from the GEO database. As shown in Figure 2, a volcano plot was drawn to show the distribution of the differentially expressed genes. The genes are represented by the red and green dots in the plot. We compared the target genes regulated by the active compounds in HGWD, and different genes in RA were compared, obtaining 49 common target genes. These 49 target genes were found to be regulated by 28 active compounds.

3.2. Compound-Target Network Analysis. The compound-target network of HGWD was established with the collected compounds and their targets as shown in Figure 3. The network contains 77 nodes (28 compounds in HGWD and 49 compound targets) and 130 edges elucidating the compound-target interactions. Quercetin, kaempferol, and beta-sitosterol acted on 33, 14, and 8 targets, respectively. The OB of quercetin, kaempferol, and beta-sitosterol was 43.43, 41.88, and 36.91%, respectively. Therefore, they are potential key active compounds due to their relative positioning in the network. Besides, it has been revealed that Guizhi, Baishao, and Dazao share a common component (+)-catechin (ID: MOL000492); Shengjiang and Dazao have the same ingredient stigmasterol (ID: MOL000449); Guizhi, Baishao, Shengjiang, and Dazao share a common ingredient beta-sitosterol (ID: MOL000358); Huangqi and Baishao share the same constituent kaempferol (ID: MOL000422); and Huangqi and Dazao share the same component quercetin (ID: MOL000098).

3.3. The Candidate Targets for HGWD against RA. To elucidate the mechanism by which HGWD ameliorates RA, the potential target network was merged with the RA-related

TABLE 1: Basic information of the active compounds in the HGWD formula.

| Molecule ID | Name | OB | DL | Source |
|-------------|---|--------|------|------------------------------------|
| MOL000211 | Mairin | 55.38 | 0.78 | Huangqi, Baishao, Dazao |
| MOL000239 | Jaranol | 50.83 | 0.29 | Huangqi |
| MOL000296 | Hederagenin | 36.91 | 0.75 | Huangqi |
| MOL000033 | (3S,8S,9S,10R,13R,14S,17R)-10,13-Dimethyl-17-[(2R,5S)-5-propan-2-yl]-2,3,4,7,8,9,11,12,14,15,16,17-dodecahydro-1H-cyclopenta[a]phenanthren-3-ol | 36.23 | 0.78 | Huangqi |
| MOL000354 | Isorhamnetin | 49.6 | 0.31 | Huangqi |
| MOL000371 | 3,9-Di-O-methylisolin | 53.74 | 0.48 | Huangqi |
| MOL000374 | 5'-Hydroxyiso-muronulatol-2',5'-di-O-glucoside | 41.72 | 0.69 | Huangqi |
| MOL000378 | 7-O-Methylisomucronulatol | 74.69 | 0.3 | Huangqi |
| MOL000379 | 9,10-Dimethoxypterocarpan-3-O-β-D-glucoside | 36.74 | 0.92 | Huangqi |
| MOL000380 | (6aR,11aR)-9,10-Dimethoxy-6a,11a-dihydro-6H-benzofuro[3,2-c]chromen-3-ol | 64.26 | 0.42 | Huangqi |
| MOL000387 | Bifendate | 31.1 | 0.67 | Huangqi |
| MOL000392 | Formononetin | 69.67 | 0.21 | Huangqi |
| MOL000398 | Isoflavanone | 109.99 | 0.3 | Huangqi |
| MOL000417 | Calycosin | 47.75 | 0.24 | Huangqi |
| MOL000422 | Kaempferol | 41.88 | 0.24 | Huangqi, Baishao |
| MOL000433 | FA | 68.96 | 0.71 | Huangqi |
| MOL000438 | (3R)-3-(2-Hydroxy-3,4-dimethoxyphenyl)chroman-7-ol | 67.67 | 0.26 | Huangqi |
| MOL000439 | Isomucronulatol-7,2'-di-O-glucoside | 49.28 | 0.62 | Huangqi |
| MOL000442 | 1,7-Dihydroxy-3,9-dimethoxy pterocarpene | 39.05 | 0.48 | Huangqi |
| MOL000098 | Quercetin | 46.43 | 0.28 | Huangqi, Dazao |
| MOL001736 | (-)-Taxifolin | 60.51 | 0.27 | Guizhi |
| MOL000358 | Beta-sitosterol | 36.91 | 0.75 | Guizhi, Baishao, Shengjiang, Dazao |
| MOL000359 | Sitosterol | 36.91 | 0.75 | Guizhi, Baishao |
| MOL000492 | (+)-Catechin | 54.83 | 0.24 | Guizhi, Baishao, Dazao |
| MOL000073 | ent-Epicatechin | 48.96 | 0.24 | Guizhi |
| MOL004576 | Taxifolin | 57.84 | 0.27 | Guizhi |
| MOL011169 | Peroxyergosterol | 44.39 | 0.82 | Guizhi |
| MOL001928 | Albiflorin_qt | 66.64 | 0.33 | Baishao |
| MOL001918 | Paeoniflorgenone | 87.59 | 0.37 | Baishao |
| MOL001910 | 11alpha,12alpha-Epoxy-3beta-23-dihydroxy-30-norolean-20-en-28,12beta-olide | 64.77 | 0.38 | Baishao |
| MOL001925 | Paeoniflorin_qt | 68.18 | 0.4 | Baishao |
| MOL001919 | (3S,5R,8R,9R,10S,14S)-3,17-Dihydroxy-4,4,8,10,14-pentamethyl-2,3,5,6,7,9-hexahydro-1H-cyclopenta[a]phenanthrene-15,16-dione | 43.56 | 0.53 | Baishao |
| MOL001930 | Benzoyl paeoniflorin | 31.27 | 0.75 | Baishao |
| MOL001924 | Paeoniflorin | 53.87 | 0.79 | Baishao |
| MOL001921 | Lactiflorin | 49.12 | 0.8 | Baishao |
| MOL006129 | 6-Methylgingediacetate2 | 48.73 | 0.32 | Shengjiang |
| MOL000449 | Stigmasterol | 43.83 | 0.76 | Shengjiang, Dazao |
| MOL001771 | Poriferast-5-en-3beta-ol | 36.91 | 0.75 | Shengjiang |
| MOL008698 | Dihydrocapsaicin | 47.07 | 0.19 | Shengjiang |
| MOL012921 | Stepharine | 31.55 | 0.33 | Dazao |
| MOL012940 | Spiradine A | 113.52 | 0.61 | Dazao |
| MOL012946 | Zizyphus saponin I_qt | 32.69 | 0.62 | Dazao |
| MOL012961 | Jujuboside A_qt | 36.67 | 0.62 | Dazao |
| MOL012976 | Coumestrol | 32.49 | 0.34 | Dazao |
| MOL012980 | Daechuine S6 | 46.48 | 0.79 | Dazao |
| MOL012981 | Daechuine S7 | 44.82 | 0.83 | Dazao |
| MOL012986 | Jujubasaponin V_qt | 36.99 | 0.63 | Dazao |
| MOL012989 | Jujuboside C_qt | 40.26 | 0.62 | Dazao |
| MOL012992 | Mauritine D | 89.13 | 0.45 | Dazao |
| MOL001454 | Berberine | 36.86 | 0.78 | Dazao |
| MOL001522 | (S)-Coclaurine | 42.35 | 0.24 | Dazao |
| MOL003410 | Ziziphin_qt | 66.95 | 0.62 | Dazao |
| MOL004350 | Ruvoside_qt | 36.12 | 0.76 | Dazao |
| MOL005360 | Malkangunin | 57.71 | 0.63 | Dazao |
| MOL000627 | Stepholidine | 33.11 | 0.54 | Dazao |
| MOL007213 | Nuciferin | 34.43 | 0.4 | Dazao |

TABLE 1: Continued.

| Molecule ID | Name | OB | DL | Source |
|-------------|---|-------|------|--------|
| MOL000783 | Protoporphyrin | 30.86 | 0.56 | Dazao |
| MOL000787 | Fumarine | 59.26 | 0.83 | Dazao |
| MOL008034 | 21302-79-4 | 73.52 | 0.77 | Dazao |
| MOL008647 | Moupinamide | 86.71 | 0.26 | Dazao |
| MOL002773 | Beta-carotene | 37.18 | 0.58 | Dazao |
| MOL000096 | (-)-Catechin | 49.68 | 0.24 | Dazao |
| MOL013357 | (3S,6R,8S,9S,10R,13R,14S,17R)-17-[(1R,4R)-4-Ethyl-1,5-dimethylhexyl]-10,13-dimethyl-2,3,6,7,8,9,11,12,14,15,16,17-dodecahydro-1H-cyclopenta[a]phenanthrene-3,6-diol | 34.37 | 0.78 | Dazao |

Note. OB, oral bioavailability; DL, drug-likeness.

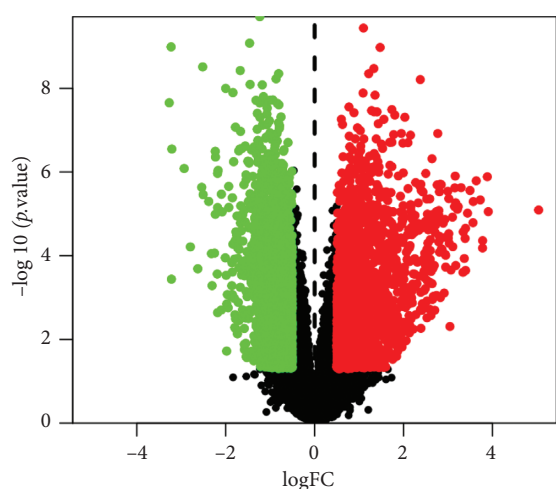


FIGURE 2: Volcano plot of differentially expressed genes. The red and green dots represent the significant differentially expressed genes.

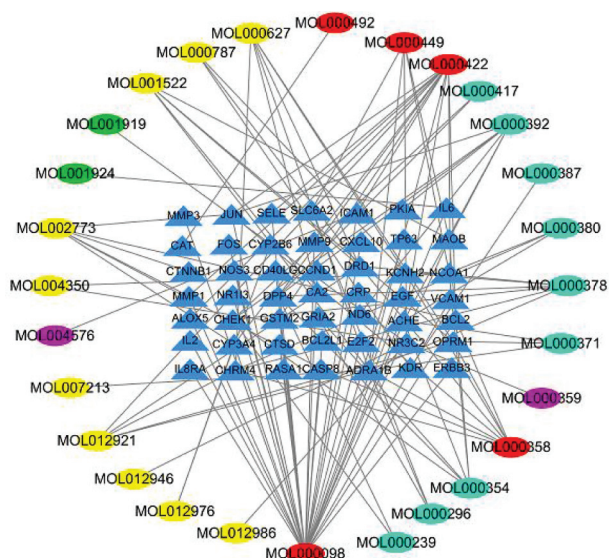


FIGURE 3: Compound-target network of the HGWD formula. The blue triangles represent the targets, and the ellipses represent active compounds. The green, yellow, amaranth, wathet, and red colors represent compounds from Baishao, Dazao, Guizhi, Huangqi, and multidrug, respectively.

target network to form a core PPI network of 2284 nodes and 53,119 edges (Figure 4(a)). The previous research showed that the median degree of all nodes was more than 74 degrees which were identified as significant targets [29]. Accordingly, a network of the significant targets for HGWD against RA with 426 nodes and 17,112 edges with a $DC \geq 74$ was constructed (Figure 4(b)).

During the second screening, since the number of genes was limited, only BC average value was used. The candidate targets were further identified, and 111 targets with $BC \geq 348.07$ (BC average value) were chosen (Figure 4(c)). Eventually, 111 HGWD target genes against RA were identified. VCAM1 (degree: 452), CTNNB1 (degree: 390), and JUN (degree: 274) might be the most important among 111 target genes for HGWD against RA.

3.4. GO and KEGG Pathway Enrichment Analysis. To further confirm the biological responses from RA treatment with HGWD, GO analysis of the 49 RA-related potential therapeutic target genes was performed based on BP, CC, and MF. The analysis results revealed a total of 739 entries. In BP enrichment analysis, 666 entries were obtained including response to antibiotic, response to alcohol, and response to steroid hormone. In CC enrichment analysis, 34 entries involved in membrane raft, membrane microdomain, membrane region, etc. were obtained. The MF enrichment analysis revealed 39 entries, including kinase regulator activity, protein kinase regulator activity, and serine hydrolase activity. The top 20 terms are shown in Figure 5.

To further show the biological processes of these targets, the KEGG pathway analysis was performed. The analysis results showed that these targets were enriched in 79 pathways with an adjusted p value < 0.05 . The top 20 KEGG pathways' enrichment analysis is shown in Figure 6. Among these pathways, the top three were fluid shear stress and atherosclerosis, TNF signaling pathway, and IL-17 signaling pathway based on the number of the pathway target genes.

3.5. The Gene-Pathway Network. The gene-pathway network analysis was constructed according to the significantly enriched pathways and genes which regulate these pathways as shown in Figure 7. The diagram shows the network relationship between the top 20 pathways and their regulated target genes. According to the network analysis, JUN had the

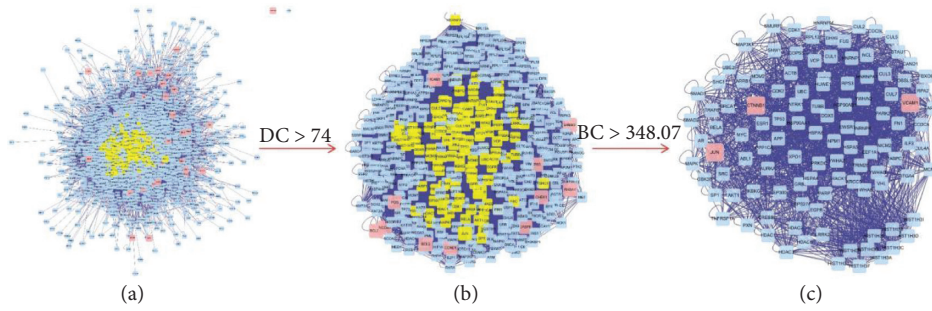


FIGURE 4: Protein interaction network of the HGWD formula.

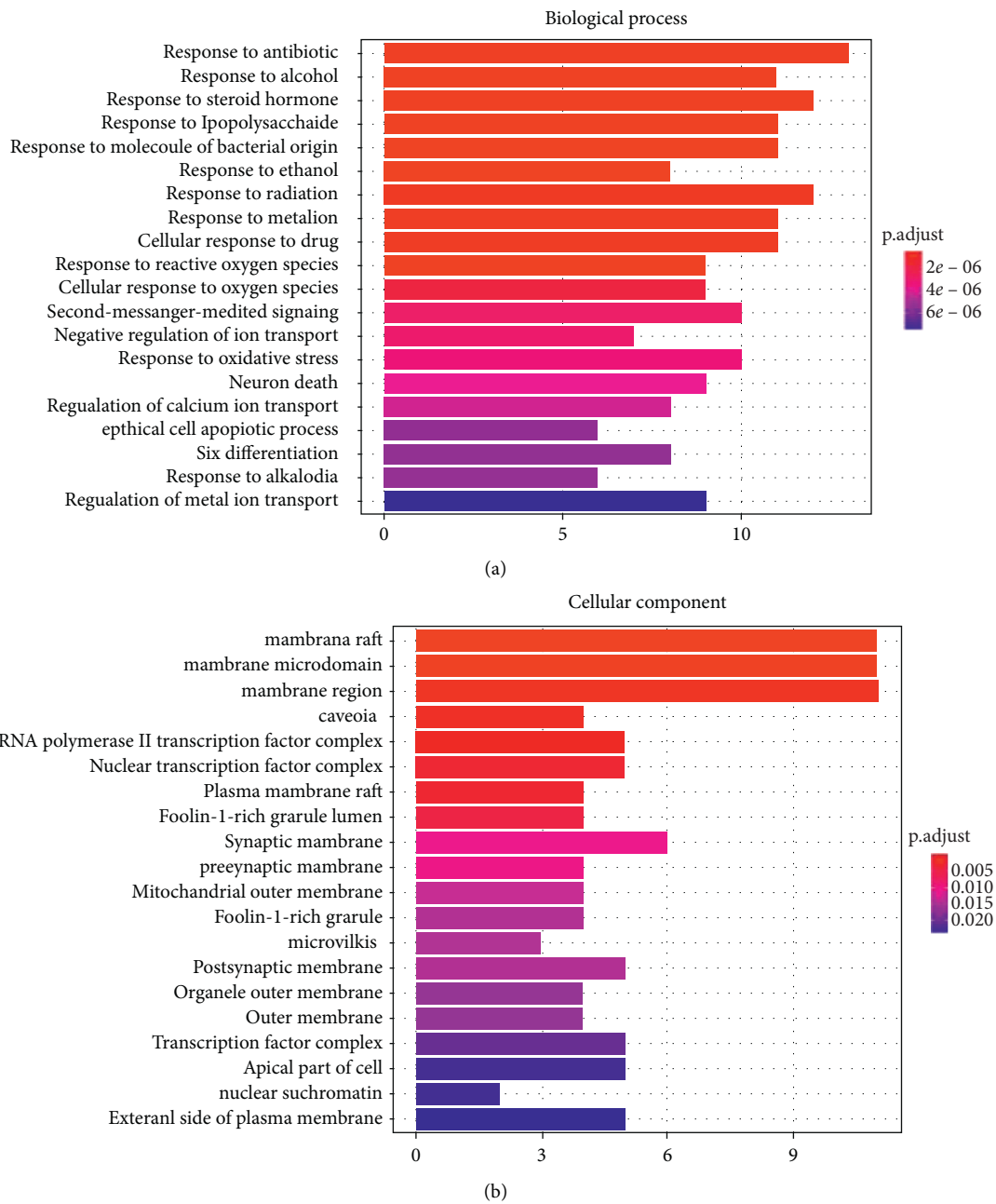


FIGURE 5: Continued.

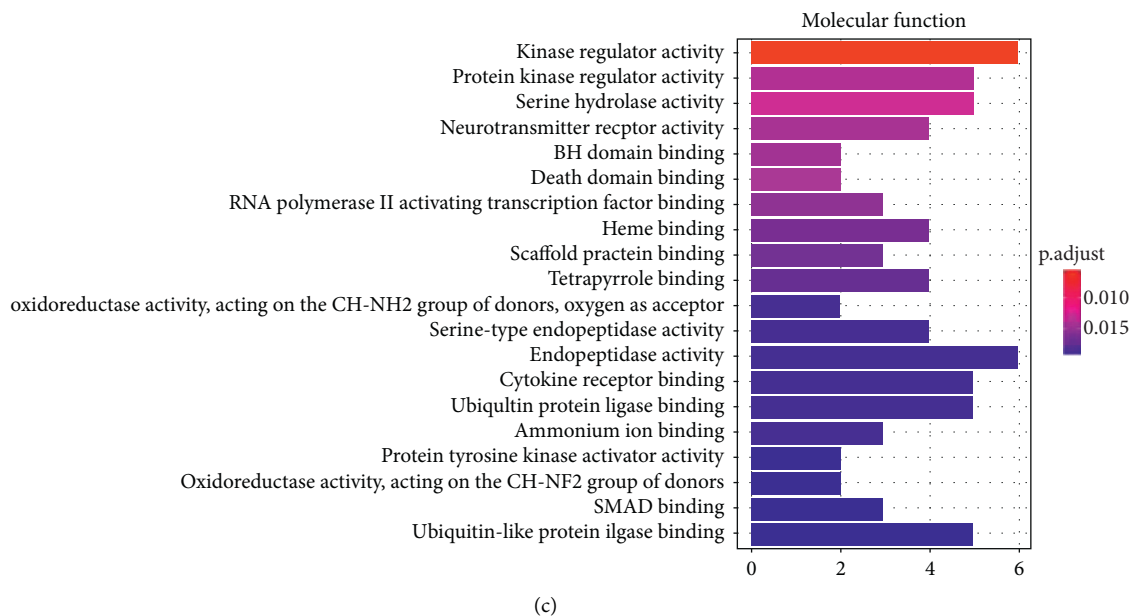


FIGURE 5: Gene ontology terms of the candidate targets of the HGWD formula against RA. (a) Biological process. (b) Cellular component. (c) Molecular function.

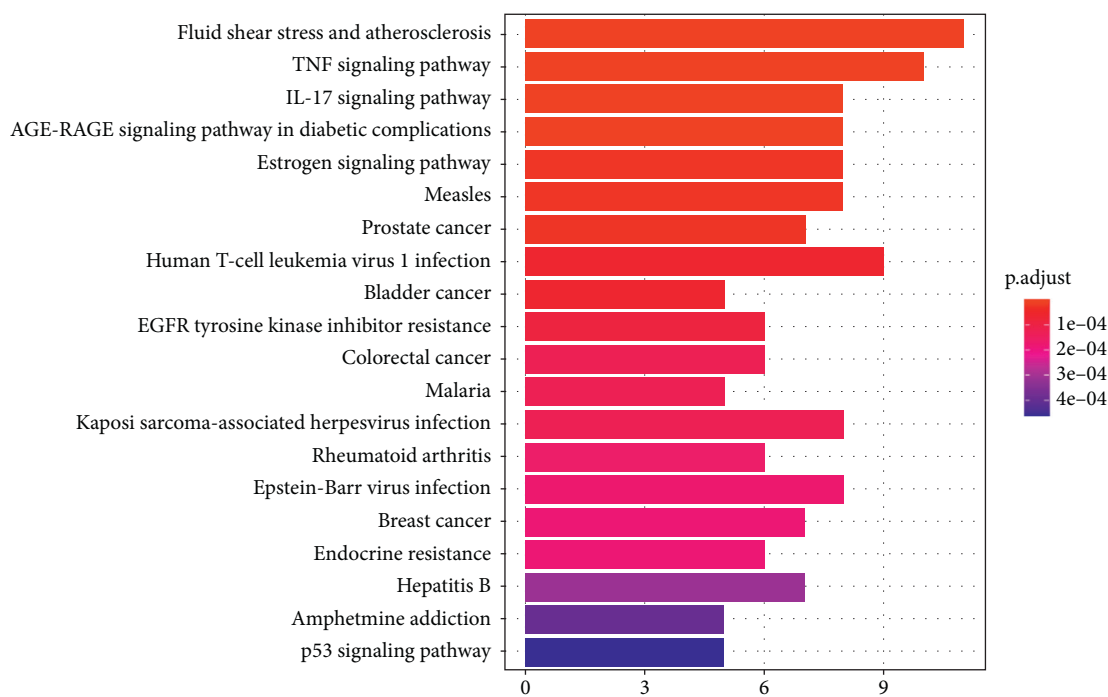


FIGURE 6: KEGG pathway enrichment of the candidate targets of the HGWD formula against RA.

highest volume, hence the core target gene. Additionally, other genes had a relatively high volume including FOS, CCND1, IL6, E2F2, and ICAM1. These genes are potential key target genes involved in the HGWD treatment of RA.

3.6. The Molecular Docking of the Main Active Constituents of HGWD and Core Proteins. Normally, high connectivity compounds are associated with more targets. According to

the number of related targets, the top 10 active compounds in HGWD with high connectivity in the compound-target network were selected for molecular docking (Table 2, binding energy of the main potential active ingredients in HGWD). Based on the binding energy value, the lower the binding energy value, the stronger the binding to the target protein. Among them, stigmasterol and stepholidine had the strongest binding force with VCAM1 (PDB: 1ij9), beta-carotene and quercetin had the strongest binding force with

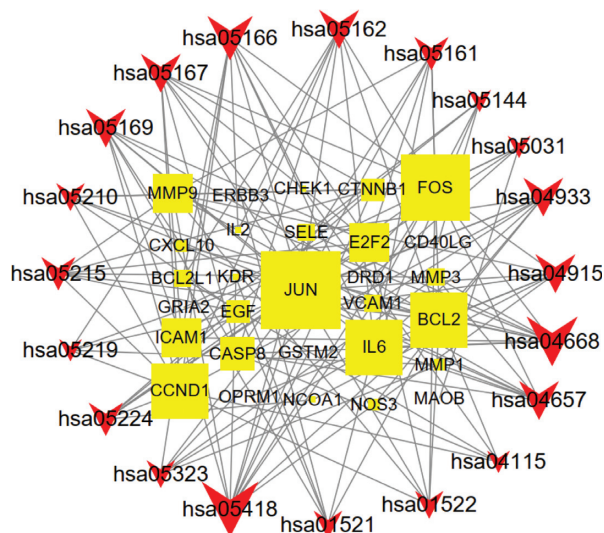


FIGURE 7: Gene-pathway network of the HGWD formula against RA. The yellow squares represent the target genes, and the red v-shapes represent pathways. The large size represents the larger betweenness centrality.

TABLE 2: The binding energy of the main potential active ingredients in the HGWD formula.

| Compound | Molecular formula | Binding energy (VCAM1) | Binding energy (CTNNB1) | Binding energy (JUN) |
|---------------------------|--------------------|------------------------|-------------------------|----------------------|
| Quercetin | $C_{15}H_{10}O_7$ | -7.1 | -7.3 | -7.3 |
| Kaempferol | $C_{15}H_{10}O_6$ | -7.1 | -6.5 | -7.4 |
| Beta-sitosterol | $C_{29}H_{50}O$ | -7.3 | -7.1 | -7.8 |
| Formononetin | $C_{16}H_{12}O_4$ | -7 | -6.3 | -6.9 |
| 7-O-Methylisomucronulatol | $C_{18}H_{20}O_5$ | -6.7 | -6 | -6.9 |
| Isorhamnetin | $C_{16}H_{12}O_7$ | -6.9 | -6.5 | -7.5 |
| Beta-carotene | $C_{40}H_{56}$ | -6.5 | -7.9 | -8.1 |
| Stepholidine | $C_{19}H_{21}NO_4$ | -7.5 | -6.7 | -6.9 |
| (S)-Coclaurine | $C_{17}H_{19}NO_3$ | -7.1 | -6.3 | -7.1 |
| Stigmasterol | $C_{29}H_{48}O$ | -7.6 | -7 | -8.1 |

CTNNB1 (PDB: 1jdh), and beta-carotene and stigmasterol had the strongest binding force with JUN (PDB: 2g01). The corresponding molecular docking diagram of stepholidine, stigmasterol, and VCAM1, beta-carotene, quercetin and CTNNB1, and beta-carotene, stigmasterol, and JUN is illustrated in Figure 8.

4. Discussion

TCM, characterized by multicomponent and multitarget medicines, cures diseases via multiple targets, multiple pathways, and multiple links. Due to the complex chemical ingredients of TCM, conventional research methods such as clinical and pharmacological research are not capable of fully elucidating the mechanism of action of TCM. Fortunately, network pharmacology provides a solution to this challenge since it is suitable for multicomponent and multitarget research. In the present study, the mechanism of action of HGWD on RA was explored via network pharmacology methods. This provided a clear direction for further basic and clinical research.

Modern pharmacology has shown that HGWD has a specific therapeutic effect on RA, where it elicits obvious anti-inflammatory and analgesic effects [30]. Specifically,

Huangqi has an anti-inflammatory effect and improves the immunity [31]. The volatile oil of Guizhi has good anti-inflammatory, immunological, and chondrocyte proliferation effects [32]. The total glycosides, the main components of Baishao, have anti-inflammatory, analgesic, and auto-immunological effects [33]. Shengjiang resists oxidation, scavenges free radicals, and relieves pain [34]. The polysaccharide of Dazao can significantly inhibit proinflammatory cytokines, such as IL-6 and TNF, with anti-inflammatory activity [35]. It is suggested that this prescription has anti-inflammatory, antioxidation, analgesic, and autoimmune reaction pharmacological effects, thus providing specific pharmacological basis for its clinical function in the treatment of RA.

In this study, the compound-target network of HGWD was constructed using 28 compounds and their 49 targets. The network diagram demonstrated that most of the HGWD compounds affected multiple targets. For instance, quercetin, kaempferol, and beta-sitosterol acted on 33, 14, and 8 targets, respectively. Therefore, they were the likely key active compounds for HGWD. Quercetin is a common active component of Huangqi and Dazao. Kaempferol is a common active component of Huangqi and Baishao. Beta-sitosterol is a common active component of Guizhi, Baishao,

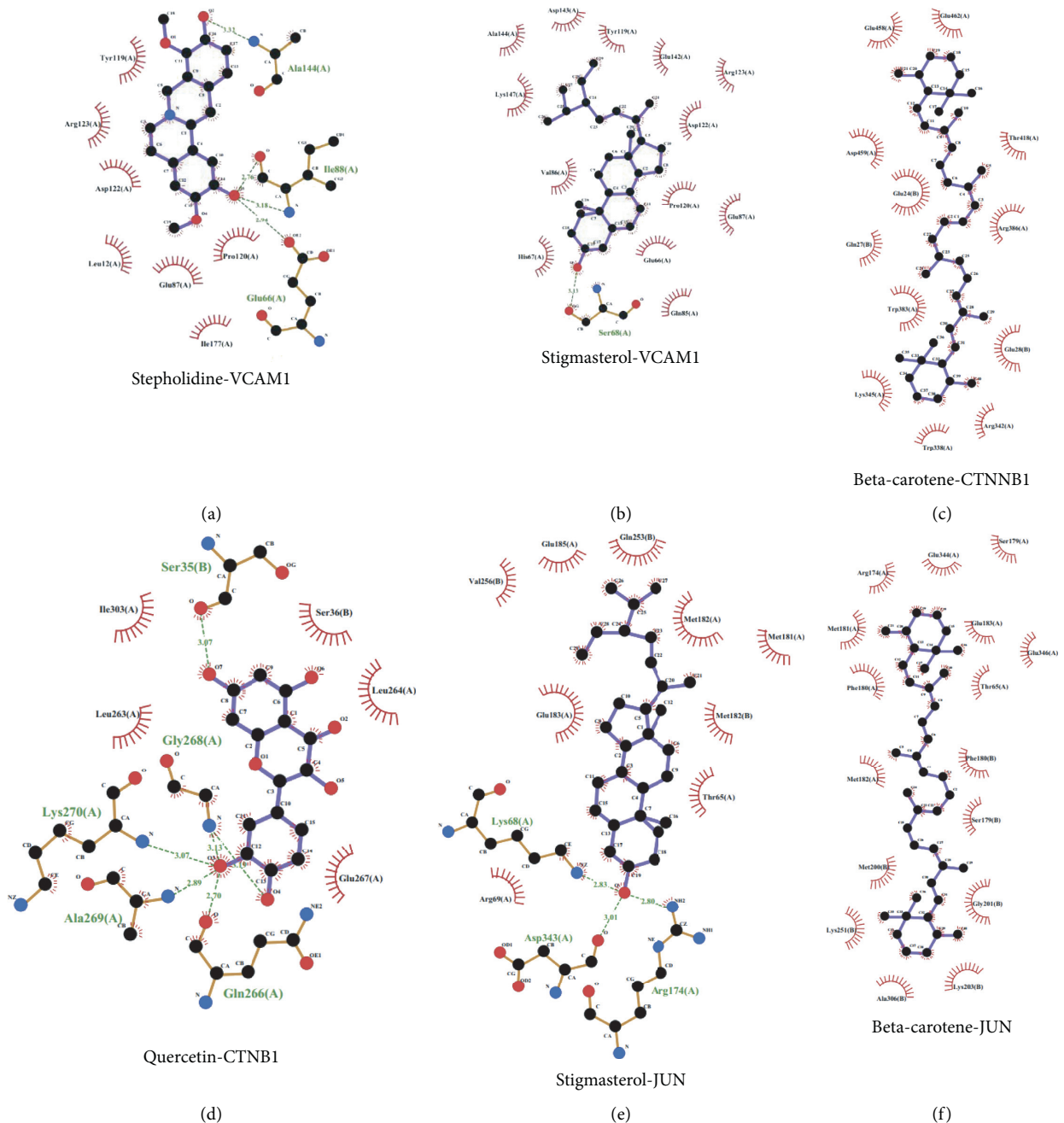


FIGURE 8: Molecular docking diagram. (a) Stepholidine-VCAM1. (b) Stigmasterol-VCAM1. (c) Beta-carotene-CTNNB1. (d) Quercetin-CTNNB1. (e) Stigmasterol-JUN. (f) Beta-carotene-JUN.

Shengjiang, and Dazao. These drugs have been mainly used together in Chinese medical history. It indicates that the compatibility between these drugs has a synergistic effect and increases their efficacy.

Quercetin is a flavonol that has unique therapeutic biological properties including anticarcinogenic, anti-inflammatory, antioxidant, antiviral, and psychostimulant activities [36, 37]. Kaempferol, a representative flavonoid, has been known to exert a range of pharmacological actions including the mediation of antioxidant, antimicrobial, and anti-inflammatory effects [38, 39]. Kaempferol is a potent immunosuppressant that reduces the harmful immune responses including autoimmunity and chronic inflammation

[40]. Beta-sitosterol, a main constituent of plants and vegetables, has versatile activities that impact cell activities including anti-inflammatory effect [41, 42]. In this study, quercetin, kaempferol, and beta-sitosterol regulated most RA-related targets and exhibited anti-inflammatory effects. Besides, they have a high oral bioavailability. Therefore, they were identified as the representative compounds of HGWD.

The PPI networks of HGWD targets and RA-related targets were constructed and merged to identify the candidate targets of HGWD against RA. To accurately obtain the targets, two parameters including DC and BC were set to construct a new network. Through PPI analysis, VCAM1, CTNNB1, and JUN were established as the important targets in RA

treatment. VCAM-1 is a glycoprotein expressed in vascular endothelial cells, whose serum is positively correlated with RA [43]. Studies have found that [44] TNF- α upregulates the expression of VCAM-1 in the endothelial cell membrane at the small joint synovium. VCAM-1 binds to $\alpha 4\beta 1$ on the surface of free immune cells in the blood vessels, inducing the migration of immune cells to inflammatory joints thus expanding the inflammatory response cascade and aggravating small joint injury. Proliferation and invasion of fibroblast synovial cells are important mechanisms that result in the thickened synovial lining, increased secretion of inflammatory cytokines, and cartilage and bone injury [45]. Studies have shown that inhibition of CTNFB1 transcription reduces the proliferation of fibroblast synovial cells and the levels of proinflammatory cytokines such as interleukin-6 (IL-6), IL-10, and TNF- α [46]. Elsewhere, it has been shown that CD44 can activate the transcription factor AP-1 (the whole is a protein) expressed by the gene JUN, thus promoting the activation of T cells and aggravating RA synovitis [47].

The targets of HGWD against RA were enriched in BP, CC, and MF through GO analysis. Results suggested that HGWD mainly regulated response to antibiotics, response to steroid hormones, and response to radiation. Furthermore, it was shown to affect some cellular components and molecular functions including membrane raft, membrane microdomain, membrane region, and kinase regulator activity. In the present study, 79 KEGG pathways including TNF signaling pathway and IL-17 signaling pathway were significantly enriched. IL-17 and TNF- α are classic proinflammatory cytokines. IL-17 is mainly secreted by helper T-cells type 17 and has strong proinflammatory effects. Analysis of synovial fluid in patients with RA found that IL-17 content was significantly increased and positively correlated with Disease Activity Score-28 (DAS28) [48]. This was a confirmation that IL-17 is involved in the occurrence of RA. Fischer et al. [49] found that, after IL-17 treatment of fibroblast synovial cells, the expression of proinflammatory cytokines such as IL-6, IL-8, and granulocyte-macrophage colony-stimulating factor (GM-CSF) increases, aggravating the inflammatory damage of fibroblast synovial cells. Besides, IL-17 can also induce joint bone and cartilage damages [50]. It has been revealed that IL-17 upregulates the levels of nuclear factor-kappa B (NF- κ B) receptor activator ligand RANKL. Consequently, this increases the content of matrix metalloproteinases, possibly promoting cartilage degradation, inhibiting chondrogenitor cell formation, and stimulating osteoclast bone damaging [51–53].

TNF- α plays an important role in the development of RA. On the one hand, it can bind to the TNFR1 receptor on fibroblast synovial cells, promoting the release of inflammatory cytokines such as IL-1, IL-6, and IL-8 and aggravating the damage of the articular cartilage and bone [54]. On the other hand, TNF- α can stimulate immune cells in blood to enter the joint through VCAM-1, aggravating the joint injury [44]. Besides, the other pathways in the first 20 pathways have not been reported to be related to RA, providing new ideas and clues for future research.

The gene-pathway network was constructed to explore the main target genes of HGWD against RA. The results

revealed that JUN, FOS, CCND1, IL6, E2F2, and ICAM1 are important target genes. A study found that the ERK-JNK-P38 signaling pathways in autoimmune disease are activated, leading to high levels of downstream JUN and Fos protein. Subsequently, the two combine to form dimer transcription factor-activating protein 1 (AP-1), which is involved in the occurrence and development of RA. It regulates the transformation of initial T cells into effector T cells, hence regulating the immune response and inflammatory process [55–58]. Inflammatory response runs throughout RA. The proinflammatory cytokines such as TNF- α , IL-6, and IL-17 play a crucial role in synovial fibroblast inflammation. Studies have demonstrated that TNF- α upregulates the E2F2 expression by activating the nuclear transcription factor NF- κ B pathway. This enhances synovial cell proliferation and synovial tissue thickening leading to joint injury [59]. The serum level of intercellular adhesion molecule-1 (ICAM-1) is high in RA patients. It has been found that ICAM-1 induces inflammatory cell aggregation and promotes synovial cell inflammation once it combines with ligand lymphocyte function antigen-1 (LFA-1) [60]. Through the molecular docking analysis of the effects of the chief active components in HGWD and the core target proteins of RA, the molecular mechanism of the treatment of RA by the active components of TCM can be predicted. This is of great reference significance for subsequent research and development of targeted drugs. The results showed that the main compounds in HGWD have a strong binding force to the core proteins VCAM1, CTNFB1, and JUN. Among them, stigmasterol and stepholidine closely link to VCAM1 through hydrogen bonds and hydrophobic forces. Beta-carotene and quercetin closely link to CTNFB1 through hydrogen bonds and hydrophobic interactions. Stigmasterol closely links to JUN through hydrogen bonds and hydrophobic interactions. Beta-carotene closely links to JUN only through hydrophobic interactions. Based on this, it can be concluded that stigmasterol, stepholidine, beta-carotene, and quercetin are the key compounds in the treatment of RA.

5. Conclusion

Our study systematically elucidated the mechanisms of action and molecular targets of HGWD against RA via the network pharmacology approach. Quercetin, kaempferol, and beta-sitosterol regulated most of the targets related to RA. The HGWD can regulate gene function through their related pathways including TNF signaling pathway and IL-17 signaling pathway. The key target genes in the gene-pathway network of HGWD against RA were JUN, FOS, CCND1, IL6, E2F2, and ICAM1. Furthermore, according to molecular docking analysis, important compounds such as stepholidine, stigmasterol, beta-carotene, quercetin, and the core protein CTNFB1, VCAM1, and JUN all have good binding ability. The network pharmacology is a promising suitable approach for the study of TCM formulations.

Abbreviations

RA: Rheumatoid arthritis
DMARDs: Disease-modifying antirheumatic drugs

| | |
|-----------------|--|
| MTX: | Methotrexate |
| TCM: | Traditional Chinese medicine |
| HGWD: | Huangqi Guizhi Wuwu Decoction |
| TCMSP: | Traditional Chinese Medicine Systems Pharmacology Database |
| ADME: | Absorption, distribution, metabolism, and excretion |
| OB: | Oral bioavailability |
| DL: | Drug-like properties |
| PPI: | Protein-protein interaction |
| DC: | Degree centrality |
| BC: | Betweenness centrality |
| CC: | Closeness centrality |
| EC: | Eigenvector centrality |
| LAC: | Local average connectivity-based method |
| NC: | Network centrality |
| GO: | Gene ontology |
| KEGG: | Kyoto Encyclopedia of Genes and Genomes |
| BP: | Biological process |
| CC: | Cellular component |
| MF: | Molecular function |
| IL-6: | Interleukin-6 |
| DAS28: | Disease Activity Score-28 |
| GM-CSF: | Granulocyte-macrophage colony-stimulating factor |
| NF- κ B: | Nuclear factor-kappa B |
| AP-1: | Activating protein-1 |
| ICAM-1: | Intercellular adhesion molecule-1 |
| LFA-1: | Lymphocyte function antigen-1. |

Data Availability

The data supporting the findings of this study are available from the corresponding author upon request.

Disclosure

Wei Liu and Yihua Fan are the co-first authors.

Conflicts of Interest

The authors declare that they have no conflicts of interest.

Authors' Contributions

Wei Liu and Yihua Fan contributed equally to this work.

Acknowledgments

The authors would like to thank FreeScience (www.home-for-researchers.com) for the help with the English language. This research was financially supported by the National Natural Science Foundation of China (no. 81673927), the National Key Research and Development Project (no. 2018YFC1705201), the Twelfth Five-Year Plan Key Disciplines of Traditional Chinese Medicine, organized by the State Administration of Traditional Chinese Medicine of China (no. 2018ZDXK001), the Tianjin Science and

Technology Commission Program (2019ZD12), and Tianjin Key Specialty Program (20200602-1).

References

- [1] E. Zampeli, P. G. Vlachoyiannopoulos, and A. G. Tzioufas, "Treatment of rheumatoid arthritis: unraveling the conundrum," *Journal of Autoimmunity*, vol. 65, pp. 1-18, 2015.
- [2] Q. Guo, Y. Wang, D. Xu, J. Nossent, N. J. Pavlos, and J. Xu, "Rheumatoid arthritis: pathological mechanisms and modern pharmacologic therapies," *Bone Research*, vol. 6, no. 1, p. 15, 2018.
- [3] M. Cross, E. Smith, D. Hoy et al., "The global burden of rheumatoid arthritis: estimates from the global burden of disease 2010 study," *Annals of the Rheumatic Diseases*, vol. 73, no. 7, pp. 1316-1322, 2014.
- [4] J. S. Smolen, D. Aletaha, M. Koeller, M. H. Weisman, and P. Emery, "New therapies for treatment of rheumatoid arthritis," *The Lancet*, vol. 370, no. 9602, pp. 1861-1874, 2007.
- [5] D. Symmons, G. Turner, R. Webb et al., "The prevalence of rheumatoid arthritis in the United Kingdom: new estimates for a new century," *Rheumatology*, vol. 41, no. 7, p. 793, 2002.
- [6] S. E. Gabriel, C. S. Crowson, and M. O'Fallon, "The epidemiology of rheumatoid arthritis in rochester, minnesota, 1955-1985," *Arthritis & Rheumatism*, vol. 42, no. 3, pp. 415-420, 1999.
- [7] J. S. Smolen, R. Landewe, J. Bijlsma et al., "Eular recommendations for the management of rheumatoid arthritis with synthetic and biological disease-modifying antirheumatic drugs: 2016 update," *Annals of the Rheumatic Diseases*, vol. 76, no. 6, pp. 960-977, 2017.
- [8] A. Mian, F. Ibrahim, and D. L. Scott, "A systematic review of guidelines for managing rheumatoid arthritis," *BMC Rheumatology*, vol. 3, p. 42, 2019.
- [9] V. C. Romão, A. Lima, M. Bernardes, H. Canhão, and J. E. Fonseca, "Three decades of low-dose methotrexate in rheumatoid arthritis: can we predict toxicity?" *Immunologic Research*, vol. 60, no. 2-3, pp. 289-310, 2014.
- [10] B. Chen, P. W. Yuan, W. L. Kang et al., "Application of HGWD in orthopedics," *Chinese Journal of Traditional Medical Traumatology*, vol. 23, pp. 71-74, 2015.
- [11] J. W. Liu, Y. H. Wang, Y. Y. Li et al., "Effect of HGWD on JAK-STAT signal pathway in rheumatoid arthritis CIA model rats," *Shizhen Guoyi Guoyao*, vol. 4, pp. 811-814, 2019.
- [12] Q. W. Yang, X. L. Li, Q. C. Huang et al., "Therapeutic effect of HGWD on rheumatoid arthritis," *World Traditional Chinese Medicine*, vol. 4, pp. 861-864, 2018.
- [13] Z. Jiang, F. Tang, W. Ma et al., "Meta analysis of the clinical effect of HGWD on rheumatoid arthritis," *Rheumatism and Arthritis*, vol. 8, no. 5, pp. 33-38, 2019, in Chinese.
- [14] A. L. Hopkins, "Network pharmacology: the next paradigm in drug discovery," *Nature Chemical Biology*, vol. 4, no. 11, pp. 682-690, 2008.
- [15] J.-S. You, C.-Y. Li, W. Chen et al., "A network pharmacology-based study on alzheimer disease prevention and treatment of qiong yu gao," *BioData Mining*, vol. 13, no. 1, 2020.
- [16] Y. Jiang, N. Liu, S. Zhu, X. Hu, D. Chang, and J. Liu, "Elucidation of the mechanisms and molecular targets of yiqi shexue formula for treatment of primary immune thrombocytopenia based on network pharmacology," *Frontiers in Pharmacology*, vol. 10, p. 1136, 2019.
- [17] J. Ru, P. Li, J. Wang et al., "TCMSP: a database of systems pharmacology for drug discovery from herbal medicines," *Journal of Cheminformatics*, vol. 6, p. 13, 2014.

- [18] W.-Y. Lee, C.-Y. Lee, Y.-S. Kim, and C.-E. Kim, "The methodological trends of traditional herbal medicine employing network pharmacology," *Biomolecules*, vol. 9, no. 8, p. 362, 2019.
- [19] B. Gong, Y. Kao, C. Zhang, F. Sun, and H. Zhao, "Systematic investigation of scutellariae barbatae herba for treating hepatocellular carcinoma based on network pharmacology," *Evidence-Based Complementary and Alternative Medicine*, vol. 2018, Article ID 4365739, 12 pages, 2018.
- [20] X. Xu, W. Zhang, C. Huang et al., "A novel chemometric method for the prediction of human oral bioavailability," *International Journal of Molecular Sciences*, vol. 13, no. 6, pp. 6964–6982, 2012.
- [21] W. Wang, T. Liu, L. Yang et al., "Study on the multi-targets mechanism of triphala on cardio-cerebral vascular diseases based on network pharmacology," *Biomedicine & Pharmacotherapy*, vol. 116, Article ID 108994, 2019.
- [22] M. Xu, J. Shi, Z. Min, H. Zhu, and W. Sun, "A network pharmacology approach to uncover the molecular mechanisms of herbal formula kang-Bai-ling for treatment of vitiligo," *Evidence-Based Complementary and Alternative Medicine*, vol. 2019, Article ID 3053458, 11 pages, 2019.
- [23] V. Law, C. Knox, Y. Djoumbou et al., "Drugbank 4.0: shedding new light on drug metabolism," *Nucleic Acids Research*, vol. 42, no. 1, pp. D1091–D1097, 2014.
- [24] P. Shannon, A. Markiel, O. Ozier et al., "Cytoscape: a software environment for integrated models of biomolecular interaction networks," *Genome Research*, vol. 13, no. 11, pp. 2498–2504, 2003.
- [25] A. Martin, M. E. Ochagavia, L. C. Rabasa, J. Miranda, J. Fernandez-de-Cossio, and R. Bringas, "Bisogenet: a new tool for gene network building, visualization and analysis," *BMC Bioinformatics*, vol. 11, no. 1, p. 91, 2010.
- [26] Y. Tang, M. Li, J. Wang, Y. Pan, and F.-X. Wu, "CytoNCA: a cytoscape plugin for centrality analysis and evaluation of protein interaction networks," *Biosystems*, vol. 127, pp. 67–72, 2015.
- [27] R. Wang and J. Lin, "Analysis of the mechanism of zhi-chuanling oral liquid in treating bronchial asthma based on network pharmacology," *Evidence-Based Complementary and Alternative Medicine*, vol. 2020, Article ID 1875980, 10 pages, 2020.
- [28] W. D. Lu, L. Li, Y. J. Shen et al., "Network pharmacology study of xiaoxuming decoction based on vasodilatory and vasoconstrictory related GPCR targets," *Zhongguo Zhong Yao Za Zhi*, vol. 43, no. 23, pp. 4698–4708, 2018, in Chinese.
- [29] Y. Zhang, Z. Li, M. Yang et al., "Identification of GRB2 and GAB1 coexpression as an unfavorable prognostic factor for hepatocellular carcinoma by a combination of expression profile and network analysis," *PLoS One*, vol. 8, no. 12, Article ID e85170, 2013.
- [30] Z. Huang, X. Shi, W. Zhu, Z. Zhao, and Z. Wang, "A comparative study on HGWD and its compatibility with anti inflammation and analgesia," *New Chinese Medicine and Clinical Pharmacology*, vol. 2, pp. 93–96, 2005, in Chinese.
- [31] Y. Xiang, L. Xiao, J. Zhang et al., "Research progress on the effect and mechanism of *Astragalus polysaccharides* in the treatment of nervous system diseases," *Chinese Journal of Hospital Pharmacy*, vol. 8, pp. 687–691, 2016, in Chinese.
- [32] L. Zhang, D. Ma, J. Cheng, and L. Ni, "Comparison of cell anti-inflammatory, immune and bone cell repair activities of volatile oil/water extract of traditional Chinese medicine," *New Chinese Medicine and Clinical Pharmacology*, vol. 1, pp. 34–39, 2015, in Chinese.
- [33] L. Li, D. Zhang, and F. Kunmiao, "Research progress of pharmacological action and mechanism of TGP in the treatment of rheumatoid arthritis," *Shandong Medicine*, vol. 59, no. 26, pp. 111–113, 2019, in Chinese.
- [34] L. Zhou, J. Zhao, H. Xu, M. Shi, D. Chen, and Y. Luo, "Comparative study on antioxidant effect of turmeric extract of different commodity specifications and grades," *Pharmacology and Clinical of Traditional Chinese Medicine*, vol. 1, pp. 110–112, 2016, in Chinese.
- [35] X. Ji, Q. Peng, H. Li et al., "Chemical characterization and anti-inflammatory activity of polysaccharides from *Zizyphus jujube* cv. muzao," *International Journal of Food Engineering*, vol. 13, no. 7, 2017.
- [36] J. M. Davis, E. A. Murphy, and M. D. Carmichael, "Effects of the dietary flavonoid quercetin upon performance and health," *Current Sports Medicine Reports*, vol. 8, no. 4, pp. 206–213, 2009.
- [37] Y. Li, J. Yao, C. Han et al., "Quercetin, inflammation and immunity," *Nutrients*, vol. 8, no. 3, p. 167, 2016.
- [38] M.-S. Tsai, Y.-H. Wang, Y.-Y. Lai et al., "Kaempferol protects against propacetamol-induced acute liver injury through CYP2E1 inactivation, UGT1A1 activation, and attenuation of oxidative stress, inflammation and apoptosis in mice," *Toxicology Letters*, vol. 290, pp. 97–109, 2018.
- [39] J. M. Calderón-Montaño, E. Burgos-Morón, C. Pérez-Guerrero, and M. López-Lázaro, "A review on the dietary flavonoid kaempferol," *Mini-Reviews in Medicinal Chemistry*, vol. 11, pp. 298–344, 2011.
- [40] M.-K. Lin, Y.-L. Yu, K.-C. Chen et al., "Kaempferol from semen *cuscutae* attenuates the immune function of dendritic cells," *Immunobiology*, vol. 216, no. 10, pp. 1103–1109, 2011.
- [41] M. Valerio and A. B. Awad, " β -Sitosterol down-regulates some pro-inflammatory signal transduction pathways by increasing the activity of tyrosine phosphatase SHP-1 in J774A. 1 murine macrophages," *International Immunopharmacology*, vol. 11, no. 8, pp. 1012–1017, 2011.
- [42] M. S. Bin Sayeed and S. S. Ameen, "Beta-sitosterol: a promising but orphan nutraceutical to fight against cancer," *Nutrition and Cancer*, vol. 67, no. 8, pp. 1214–1220, 2015.
- [43] L. Wang, Y. Ding, X. Guo, and Q. Zhao, "Role and mechanism of vascular cell adhesion molecule-1 in the development of rheumatoid arthritis," *Experimental and Therapeutic Medicine*, vol. 10, no. 3, p. 1229, 2015.
- [44] D. H. Kong, Y. K. Kim, M. R. Kim, J. H. Jang, and S. Lee, "Emerging roles of vascular cell adhesion molecule-1 (VCAM-1) in immunological disorders and cancer," *International Journal of Molecular Sciences*, vol. 19, no. 4, p. 1057, 2018.
- [45] B. Bartok and G. S. Firestein, "Fibroblast-like synoviocytes: key effector cells in rheumatoid arthritis," *Immunological Reviews*, vol. 233, no. 1, p. 233, 2010.
- [46] G.-Q. Li, Y.-X. Fang, Y. Liu et al., "MALAT1-driven inhibition of wnt signal impedes proliferation and inflammation in fibroblast-like synoviocytes through CTNBN1 promoter methylation in rheumatoid arthritis," *Human Gene Therapy*, vol. 30, no. 8, p. 1008, 2019.
- [47] K. Fujii, Y. Tanaka, S. Hubscher et al., "Cross-linking of CD44 on rheumatoid synovial cells up-regulates VCAM-1," *The Journal of Immunology*, vol. 167, no. 3, pp. 2391–2398, 1999.
- [48] G. Liu and L. Deng, "Correlation between IL-17 content in synovial fluid and inflammatory injury in patients with rheumatoid arthritis," *Chinese Journal of Experimental Diagnostics*, vol. 20, no. 4, pp. 669–670, 2016, in Chinese.

- [49] J. A. A. Fischer, A. J. Hueber, S. Wilson et al., "Combined inhibition of tumor necrosis factor α and interleukin-17 as a therapeutic opportunity in rheumatoid arthritis: development and characterization of a novel bispecific antibody," *Arthritis & Rheumatology*, vol. 67, no. 1, pp. 51–62, 2015.
- [50] X. Wang, X. Lu, Y. Lu et al., "Correlation between IL-17 level and bone and joint damage in early rheumatoid arthritis patients," *Shandong Medical Journal*, vol. 51, no. 1, pp. 102–103, 2011, in Chinese.
- [51] J. Yao, G. Han, and M. Hu, "The effect of IL-17 on the expression of MMP-9 in osteoclasts and its significance," *Journal of Jilin University*, vol. 42, no. 3, pp. 462–466, 2016, in Chinese.
- [52] B. Schminke, S. Trautmann, B. Mai et al., "Interleukin 17 inhabits progenitor cells in rheumatoid arthritis cartilage," *European Journal of Immunology*, vol. 46, no. 2, pp. 400–405, 2016.
- [53] M. I. Koenders, R. J. Marijnissen, I. Devesa et al., "Tumor necrosis factor-interleukin-17 interplay induces S100A8, interleukin-1 β , and matrix metalloproteinases, and drives irreversible cartilage destruction in murine arthritis: rationale for combination treatment during arthritis," *Arthritis & Rheumatism*, vol. 63, no. 8, pp. 2329–2339, 2011.
- [54] H. Zhang and W. Xiao, "TNFR1 and TNFR2 differentially mediate TNF- α -induced inflammatory responses in rheumatoid arthritis fibroblast-like synoviocytes," *Cell Biology International*, vol. 41, no. 4, p. 415, 2017.
- [55] R. Eferl and E. F. Wagner, "AP-1: a double-edged sword in tumorigenesis," *Nature Reviews Cancer*, vol. 3, no. 11, p. 859, 2003.
- [56] E. F. Wagner and Á. R. Nebreda, "Signal integration by JNK and p38 MAPK pathways in cancer development," *Nature Reviews Cancer*, vol. 9, no. 8, p. 537, 2009.
- [57] H. Bazzazi, M. Aghaei, A. Memarian, H. Asgarian-Omran, N. Behnampour, and Y. Yazdani, "Th1–Th17 ratio as a new insight in rheumatoid arthritis disease," *Iranian Journal of Allergy, Asthma and Immunology*, vol. 17, no. 1, pp. 68–77, 2018.
- [58] A. Tanel, S. G. Fonseca, B. Yassine-Diab et al., "Cellular and molecular mechanisms of memory T-cell survival," *Expert Review of Vaccines*, vol. 8, no. 3, p. 299, 2009.
- [59] R. Zhang, L. Wang, and J. Pan, "Expression of E2F2 in rheumatoid arthritis synovial fibroblast like cells," *Journal of Medical Research*, vol. 3, pp. 73–77, 2017.
- [60] L. Xie, D. Ou, W. Wang et al., "Study on the change characteristics and clinical significance of serum sICAM-1 in patients with rheumatoid arthritis related interstitial lung disease," *Modern Medicine and Health*, vol. 20, pp. 3117–3119, 2019.

Review Article

The Effect of Kinesitherapy on Bone Mineral Density in Primary Osteoporosis: A Systematic Review and Meta-Analysis of Randomized Controlled Trial

Shanxi Wang,¹ Shuzhen Li ,¹ Xing Xie,² and Juying Xie¹

¹College of Rehabilitation, Xiangnan University, Chenzhou 423000, China

²Affiliated Hospital of Xiangnan University, Chenzhou 423000, China

Correspondence should be addressed to Shuzhen Li; 308634590@qq.com

Received 20 May 2020; Accepted 26 June 2020; Published 5 August 2020

Guest Editor: Arham Shabbir

Copyright © 2020 Shanxi Wang et al. This is an open access article distributed under the Creative Commons Attribution License, which permits unrestricted use, distribution, and reproduction in any medium, provided the original work is properly cited.

Objective. Osteoporosis (OP) is a well-established age-related disease, pathologically characterized by bone microarchitectural deterioration, increased fragility, and low BMD. Primary osteoporosis (POP) is the most common type of OP. **Methods.** Publications pertaining to the effectiveness of kinesitherapy on BMD in POP from PubMed, SCI, Cochrane Library, Embase, VIP, CNKI, and Wanfang Database were retrieved from their inception to October 2019. **Results.** A total of 21 studies with 1840 participants were included. The results of the meta-analysis revealed that kinesitherapy plus antiosteoporosis medications had a positive effect on lumbar spine BMD when the duration of intervention was 6 months (MD = 0.11 g/cm²; 95% CI: 0.06–0.15; $P < 0.0001$) or >6 months (MD = 0.04 g/cm²; 95% CI: 0.02–0.06; $P < 0.0001$) compared with antiosteoporosis medications alone. Additional kinesitherapy plus antiosteoporosis medications were associated with improved femoral neck BMD compared with antiosteoporosis medications alone (MD = 0.09 g/cm²; 95% CI: 0.03–0.16; $P = 0.004$). **Conclusions.** Kinesitherapy plus antiosteoporosis medications significantly improved lumbar spine and femoral neck BMD in the current low-quality evidence. Additional high-quality evidence is required to confirm the effect of kinesitherapy on BMD in patients with POP.

1. Introduction

With age, bone mass declines, and an accelerated loss of bone mineral density (BMD) occurs by 50 years of age [1]. Osteoporosis (OP) is a well-established age-related disease pathologically characterized by bone microarchitectural deterioration, increased fragility, and low BMD [2]. The diagnosis of OP is based on measurements of BMD and is defined by the World Health Organization as BMD ≥ 2.5 standard deviations (SD) below the average value for young healthy individuals [3]. Moreover, OP is associated with high morbidity and mortality, as well as reduced quality of life, which in turn increases the rate of fractures, healthcare costs, and social economic stress [4–9]. In North America [10, 11], over 55 million people are at risk of developing OP or osteopenia. OP is typically classified into three main categories: (1) primary; (2) secondary; and (3) idiopathic.

Primary osteoporosis (POP) refers to the natural aging process of human tissue and organ systems, and the symptoms are associated with degenerative changes in the skeletal system. Moreover, POP is the most common type of OP, accounting for 90% of OP cases, and includes women with postmenopausal osteoporosis (PMOP) and senile osteoporosis (SOP) [12, 13]. PMOP is primarily related to postmenopausal estrogen deficiency, whereas SOP is associated with increased age [14]. Thus, as the proportion of elderly populations increases throughout the world, the number of POP cases will also increase gradually. In the European Union, according to relevant statistics [15, 16], 22 million women and 5.5 million men over the age of 50 suffer from osteoporosis. And that number is expected to increase by 23 percent by 2025, according to a study. One study found that the overall prevalence rate of osteoporosis was 32.1% in at least one measurement site (28.5% in the lumbar and

14.5% in the femoral region), while 49.7% of elderly people suffer from decreased bone mass (osteopenia) in Amirkola, north of Iran [17]. According to the latest epidemiological results of osteoporosis in China, the prevalence of osteoporosis at the age of 40~49 is 3.2%, including 2.2% in males and 4.3% in females. The prevalence rate of osteoporosis over the age of 50 was 19.2%, including 6.0% in males and 32.1% in females. And the prevalence of osteoporosis over the age of 65 was 2.0%, with 0.7% of men and 51.6% of women [18].

POP treatment is a long-term process and may not 100% prevent the development or reverse the symptoms of the disease [19]. In addition, exercise is one of the key recommendations for the prevention and treatment of bone loss [20, 21]. Several studies have demonstrated that exercise can prevent bone loss [22] and improve calcium absorption, bone formation [23], and the secretion of sex hormones [24, 25], which then promotes BMD [26]. Kinesiotherapy, as a part of physical therapy, is a comprehensive exercise that represents one of the most important aspects of medical rehabilitation. Kinesiotherapy involves the movement of various parts of the body or the entire body using exercises to maintain, establish, develop, and change the function of the locomotor apparatus and organs in locomotion. Kinesiotherapy for the treatment of POP primarily includes routine static training, walking training, grip training, outbreak and endurance exercise training, push-ups, stretching, or isometric exercise. In addition, multiple reviews have confirmed that exercise reduces bone loss and increases BMD in postmenopausal women or PMOP [27–29]. A meta-analysis also demonstrated that exercise can improve functional outcomes, including mobility, balance, and self-reported measures of functioning in persons with OP [30]. However, there was no systematic review to evaluate the effect of kinesiotherapy on BMD in patients with POP. Therefore, the aim of this study was to conduct a systematic review and meta-analysis to assess the effect of kinesiotherapy in persons with POP on lumbar spine and femoral neck BMD via conducting a maximal search of both Chinese and English databases.

2. Methods

2.1. Eligibility Criteria. Available human, clinical, or community studies with a randomized controlled trial published in English or Chinese were included in this review. The participants consisted of patients with POP who had no thoracolumbar vertebral fracture and other complications such as heart, vein, lung, liver, and kidney as well as metabolic diseases and were not taking drugs affecting bone metabolism. The age and gender of the subjects were not limited. The included studies focused on the effect of kinesiotherapy plus antiosteoporosis medications therapy as a kinesiotherapy group compared with antiosteoporosis medications therapy as a control group for the BMD of POP (SOP and SMOP). Those which compared kinesiotherapy alone with another exercise or any other antiosteoporosis intervention were excluded. The kinesiotherapy should include weight-bearing, impact, resistance, endurance

training, or a combination of these types of training, and only single-motion experiments will be ruled out. Health education can be added to all patients, and all inpatients can be given routine care. The outcomes included at least lumbar spine or femoral neck BMD.

2.2. Data Sources and Searches. The original research articles were obtained after a search of six electronic English and Chinese databases, which included PubMed, Science Citation Index (SCI), EMBASE, Chinese Scientific Journal Database (VIP), China National Knowledge Information (CNKI) database, and Wanfang from their inception to October 3, 2019. We used the following search strategy ([kinesiotherapy OR exercise] AND osteoporosis AND bone mineral density) in all the English and Chinese databases.

2.3. Study Identification and Quality Assessment. Two reviewers (WSX and LSZ) independently screened and reviewed the title and abstract of the searched studies using NoteExpress V3.2.0.6992 software. The full text of the studies that potentially met the eligibility criteria was obtained, and any potentially relevant references were retrieved according to predefined eligibility criteria. The data were extracted by one reviewer (WSX) using the prepared forms and checked for accuracy by the second reviewer (LSZ). The details extracted from the eligible literature included the language of publication, participant characteristics, sample size, methodological information, participant demographics, experimental and control interventions (category, intensity, frequency, duration, and details of antiosteoporosis medication treatment), outcomes, and adverse effects [31]. Studies published in multiple reports were only included once to avoid duplication in this review. Disagreements were resolved through discussion, and the original author was contacted if an agreement could not be reached. The primary outcomes were lumbar spine BMD and femoral neck BMD, which were expressed as g/cm^2 assessed by dual X-ray absorptiometry or dual photo absorptiometry. The baseline and follow-up data pertaining to BMD were calculated. If follow-up data could not be obtained, the data at the end of the intervention were used instead.

The quality of the studies was independently evaluated by two reviewers (WSX and LSZ) using the Cochrane Collaboration's tool for assessing the risk of bias [32]. The following recommended domains were considered: selection bias (random sequence generation and allocation concealment); performance bias (blinding of participants and personnel); detection bias (blinding of outcome assessment); attrition bias (incomplete outcome data); reporting bias (selective reporting); and other bias, each of which was rated according to the level of bias and categorized as either low, high, or unclear.

2.4. Data Analysis. Review Manager 5.2 software from the Cochrane Collaboration was applied for the data analysis. Statistical heterogeneity among the studies was assessed using a chi-square test or by calculating Higgins I^2 values

[33]. The results were pooled using a fixed effect model when the I^2 value was less than 40%. Otherwise, a random effect model was applied. However, if the I^2 value among the studies was greater than 75%, the heterogeneity was considered to be substantive and the overall meta-analysis was not appropriate to conduct, but a sensitivity analysis was considered to measure the pooled effect. Subgroup analysis was used to explore the source of heterogeneity if the duration of the intervention exhibited variability. The continuous outcomes were calculated for the mean difference (MD) with standard deviations (SDs) with a corresponding 95% confidence interval (CI), and all P values were two sided.

3. Results

3.1. Description of Studies. A detailed screening flowchart depicting the generation of eligible articles is presented in Figure 1. A total of 791 records were identified via database searches. After removing duplicates, 507 remained to be screened for eligibility. Consequently, 21 studies met the inclusion criteria and were included in the meta-analysis.

Table 1 presents the sample, intervention, and outcome characteristics. This review involved a total of 1840 POP patients (including SOP and PMOP). Part of the subjects were from outpatient clinics, inpatient settings, and community or physical examination centers, with the exception of eleven subjects for whom the sources were unknown. In the included studies, the subject type consisted of eleven PMOP patients, five POP patients, and five SOP patients. In one RCT, the diagnostic criteria for the study were in accordance with the WHO diagnostic criteria for osteoporosis. In the seven RCTs, the reference diagnostic criteria for osteoporosis were Chinese, with one diagnostic criterion for osteoporosis in Japan; the Chinese diagnostic criteria included the Chinese recommended diagnostic criteria for osteoporosis, the Chinese medical association osteoporosis diagnosis and treatment guidelines (a second draft) and a primary bone guide formulated by Chinese Medical Association Osteoporosis and Bone Mineral Disease Branch; one RCT used Western diagnostic criteria for disease; four RCTs only mentioned the diagnostic criteria in accordance with the diagnostic criteria of PMOP or POP; and five RCTs used the laboratory examination in which the T value of was less than or equal to -2.5 SD in at least one site; the diagnostic criteria in the remaining RCT did not elaborate. The whole RCTs compared kinesitherapy plus medication treatment with medication treatment alone. Kinesitherapy involves comprehensive exercises rather than individual exercises. Of those RCTs, only one RCT used traditional Chinese medicine (e.g., kidney method), and the remaining RCTs were treated with Western medicine. All of the RCTs included a measure of lumbar spine BMD, and five of the RCTs included lumbar spine and femoral neck BMD.

3.2. Methodological Quality. As shown in Figure 2, twelve studies described the generation of random sequences. Five of these studies used a random number table, three of these

used simple random methods, three studies used computer-generated random numbers, and the remaining one trial used the method of lottery. Three trials involve allocation concealment. However, the blind intervention associated with the intervention exercises cannot be implemented blindly. One study described that the data analysis was based on the author's own statistics. One study described an exit from the case, but did not explain the reason. There were no dropouts indicated or explanations for withdrawal in the remaining studies. All of the included studies were considered to have a high risk of bias.

3.3. Meta-Analysis of Lumbar Spine BMD. All the controls in the literatures were kinesitherapy plus antiosteoporosis drugs versus antiosteoporosis drugs. According to the duration of the intervention, the subgroups were divided into three groups based on an intervention duration of (1) less than 6 months; (2) 6 months; and (3) longer than 6 months.

3.3.1. Intervention Duration < 6 Months. Two trials [35, 53] compared the effect of kinesitherapy plus antiosteoporosis medications with antiosteoporosis medications alone on lumbar spine BMD when the duration of intervention was less than 6 months. The meta-analyses indicated that there was no significant difference between the two groups (MD = 0.02; 95% CI: -0.00 – 0.05 ; $P = 0.10$) (Figure 3).

3.3.2. Intervention Duration = 6 Months. Ten studies [37, 38, 41, 46, 51, 54] involving 699 participants reported that after 6 months, kinesitherapy had significantly increased lumbar BMD (MD = 0.11 g/cm²; 95% CI: 0.06 – 0.15 ; $P < 0.0001$). However, the heterogeneity among the studies was substantial with $I^2 = 83\%$, and no obvious changes were observed after the sensitivity analysis when any one or two of the studies were removed (Figure 4).

3.3.3. Intervention Duration > 6 Months. Eleven studies [34, 36, 39, 40, 42–44, 48–50, 52] involving 1019 participants revealed that when the duration of treatment was longer than 6 months, the lumbar spine BMD in the kinesitherapy group significantly increased compared with the control group (MD = 0.04 g/cm²; 95% CI: 0.02 – 0.06 ; $P < 0.0001$) with high heterogeneity ($I^2 = 73\%$) (Figure 5). The heterogeneity was $I^2 = 23\%$ after the sensitivity analysis when one study [40] was removed.

3.4. Meta-Analysis of Femoral Neck BMD. Five trials [43–45, 47, 53] involving 439 participants compared effect of kinesitherapy plus antiosteoporosis medications with antiosteoporosis medications alone on lumbar spine BMD. The meta-analysis revealed a significant antiosteoporosis effect on lumbar spine BMD (MD = 0.09 g/cm²; 95% CI: 0.03 – 0.16 ; $P = 0.004$) but with high heterogeneity ($I^2 = 90\%$) (Figure 6). It showed low heterogeneity ($I^2 = 0\%$) after the sensitivity analysis when two studies were removed [45, 47].

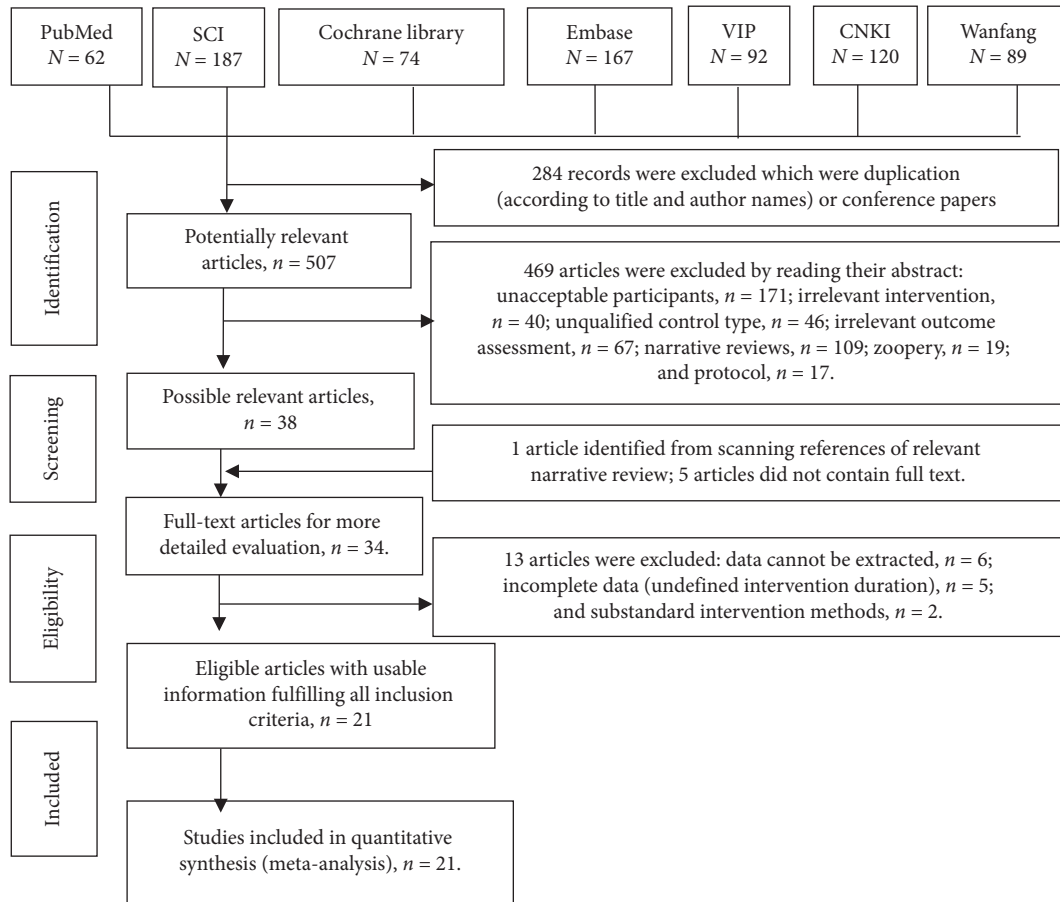


FIGURE 1: Details of literature search and selection. SCI: Science Citation Index; VIP: Chinese Scientific Journal Database; CNKI: China National Knowledge Information database.

TABLE 1: The characteristics of all the trails.

| Author, year | Participants (type, source, age, sample) | Duration (months) | Intervention | | Outcomes |
|---------------------------|--|-------------------|--|---|------------------|
| | | | Kinesitherapy group | Control group | |
| Iwamoto et al., 2001 [34] | PMOP, unspecified, 53–77 years, 28 (KT: 8, CON: 20) | 24 | Brisk walking (1000 steps in the first 7 days, increase the step count by 30%/week) + gymnastic training (no details provided) + CON | Calcium lactate (2.0 g, Qd) and 1 α -hydroxyvitamin D3 (1 μ g, Qd) | Lumbar spine BMD |
| Shen, 2003 [35] | POP, outpatient and inpatient, 45–80 years, 60 (KT: 30, CON: 30) | 3 | Aerobics, tai chi, dance, yangko, jogging, walking etc. (30–60 min/time, 5–7 times/week) + CON | Tonifying kidney granules (3 times/day, 1 dose/time) | Lumbar spine BMD |
| Zhu, 2007 [36] | SOP, outpatient, 60–72 years, 96 (KT: 48, CON: 48) | 12 | Walking, jogging, tai chi (30–60 min/time, 3–5 times/week) + CON | Calcium (600 mg/d) | Lumbar spine BMD |
| Liu et al., 2007 [37] | PMOP, outpatient, 48–61 years, 68 (KT: 36, CON: 32) | 6 | Draft movement, abdominal isometric exercises, flexion, and extension of the upper limbs (20 minutes each time, once every 3 days) + CON | Caltrate D (600 mg, Qd) | Lumbar spine BMD |
| Li et al., 2008 [38] | PMOP, unspecified, 48–61 years, 70 (KT: 38, CON: 32) | 6 | Draft movement, abdominal isometric exercises, flexion, and extension of the upper limbs (20 min/time, once every four days) + CON | Ossotide injection (50 mg, Qd, 20 days in total) | Lumbar spine BMD |
| Liu et al., 2009 [39] | SOP, outpatient service, 60–94 years, 60 (KT: 30, CON: 30) | 12 | Walking, jogging, tai chi (60 min/time, 1 time/day) + CON | Fosamax (10 mg, once a day) and calcium (600 mg/d) | Lumbar spine BMD |

TABLE 1: Continued.

| Author, year | Participants (type, source, age, sample) | Duration (months) | Intervention | | Outcomes |
|------------------------------|---|-------------------|--|---|-----------------------------------|
| | | | Kinesitherapy group | Control group | |
| Liu and Wang, 2012 [40] | SOP, unspecified, 60–81 years, 320 (KT: 162, CON: 158) | 12 | Tai chi and jogging (no less than 30 min/time, no less than 4 times/week) + CON | Calcium carbonate D ₃ (600 mg, Qd) | Lumbar spine BMD |
| Li et al., 2013 [41] | SOP, hospital, 67 ± 4 years, 86 (KT:43, CON: 43) | 6 | Progressive lumbar dorsal muscle function exercise includes sitting training, swallow training and five-point support training (1-2 times/day) + CON | Lorelli calcium capsule (1 capsules, 1 time/d for 2 consecutive months) | Lumbar spine BMD |
| Ming, 2013 [42] | SOP, hospital, 60–78 years, 96 (KT: 48, CON: 48) | 12 | Walking, aerobics, running, and tai chi (5 to 7 times a week for 45 to 60 minutes) + CON | Calcium gluconate (20 ml/time, 3 times/day) and vitamin D (400 units, 2 times/day) | Lumbar spine BMD |
| Chen, 2015 [43] | PMOP, clinic, 53–years, 57 (KT: 27, CON: 30) | 12 | Brisk walking (15–30 minutes), resistance strength exercises (15–20 minutes), and balance and flexibility exercises (simplify tai chi and five birds, 15–20 min) + CON | Alendronate (70 mg, Qd), caltrate D (600 mg, Qd), and alfacalcidol soft capsules (0.25 µg, Qd) | Lumbar spine and femoral neck BMD |
| Dischereit et al., 2016 [44] | PMOP, unspecified, 68 years, 42(KT: 25, CON: 17) | 24 | Endurance and strength training program (3 sessions once weekly, 65 min) + CON | Adequate calcium and vitamin D supplementation and bisphosphonate therapy | Lumbar spine and femoral neck BMD |
| Li et al., 2016 [45] | PMOP, unspecified, 52–76 years, 188 (KT: 94, CON: 94) | 6 | Mainly includes walking, aerobics, running, and tai chi (30–60 min/time, more than 3 times/week) + CON | Caltrate D (1000 mg, Qd), derivatives, vitamin D, and raloxifene (1 pill, Qd) | Lumbar spine and femoral neck BMD |
| Chen, 2016 [46] | PMOP, unspecified, 53–77 years, 65(KT: 33, CON:32) | 6 | Brisk walking and tai chi (30–50 min/time, 2-3 times/week) + CON | Alendronate (70 mg, Qd), caltrate D (600 mg, Qd), and alfacalcidol soft capsules(0.25 µg, Qd) | Lumbar spine BMD |
| Xu, 2017 [47] | PMOP, unspecified, 51–67 years, 100 (KT:50, CON:50) | 6 | Aerobics, tai chi, and jogging (more than 30 min, more than 3 times/week) + CON | Calcine D (2 times/day, 2pills/time) + estrogen (1 time/day, 60 mg/time) | Lumbar spine and femoral neck BMD |
| Chang, 2017 [48] | POP, unspecified, 60–79 years, 84 (KT: 42, CON: 42) | 12 | Aerobics, walking, swimming, jogging, and cycling (3–4 times, not less than 2 times, each exercise 30–60 minutes) + CON | Calcine D 600 (1 tablet once, 2 times a day) and health education | Lumbar spine BMD |
| Qi, 2017 [49] | PMOP, community healthcare center, 45–65 years, 56 (KT: 28, CON:28) | 12 | Aerobic exercise resistance group, load bearing, and stretching (30 min/time, 3–5 times/week, more than 1 h) + CON | Conventional treatment | Lumbar spine BMD |
| Wen, 2017 [50] | POP, unspecified, 60–78 years, 96 (KT: 48, CON: 48) | 12 | Jogging, tai chi, etc. (daily) + CON | Routine prevention and taking medicine | Lumbar spine BMD |
| Liu and Yang, 2018 [51] | POP, unspecified, 36–79 years, 80 (KT: 40, CON: 40) | 6 | Walking, fitness running, ballroom dancing, and swimming (at least 12 times a month, each time ≥30 min) + CON | Calcium and vitamin D ₃ | Lumbar spine BMD |
| Zheng et al., 2019 [52] | POP, unspecified, 53–77 years, 84 (KT: 42, CON: 42) | 12 | Walking, jogging, alternate running, cycling, etc. (3 to 4 times per week, the minimum 2 times, 30–60 min) + CON | Calcium (300 mg/tablet, 2 times/d, 1 tablet/time) | Lumbar spine BMD |
| Li et al., 2019 [53] | PMOP, unspecified, 50–65 years, 52 (KT: 26, CON: 26) | 3 | Brisk walking (30 min, once a day, 4d/week) and resistance training (week 1, 2 weekly complete 1 set (15 times/set), and then add 1 set every 2 weeks) + CON | Calcium carbonate D ₃ (600 mg, 1 time/d), alfacalcidol soft capsule (0.5 g, 1time/d), and sodium alendronate (70 mg, 1 time/d/ weeks) for 3 months | Lumbar spine and femoral neck BMD |
| Yan et al., 2019 [54] | POP, unspecified, 53–77 years, 52 (KT: 26, CON: 26) | 6 | Flexible resistance exercise therapy to exercise the lumbar and dorsal muscles (5 times/week) + CON | Calcium carbonate D ₃ (600 mg), vitamin D ₃ (0.25 UG), health education, and routine nursing | Lumbar spine BMD |

PMOP, postmenopausal osteoporosis; POP, primary osteoporosis; SOP, senile osteoporosis; KT, kinesitherapy group; CON, control group; BMD, bone mineral density.

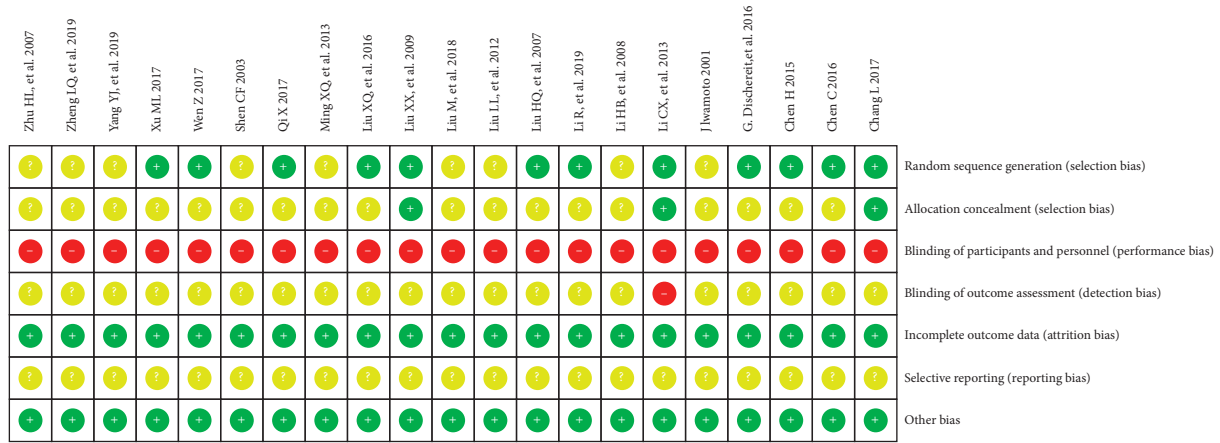


FIGURE 2: Risk of bias summary for each included study.

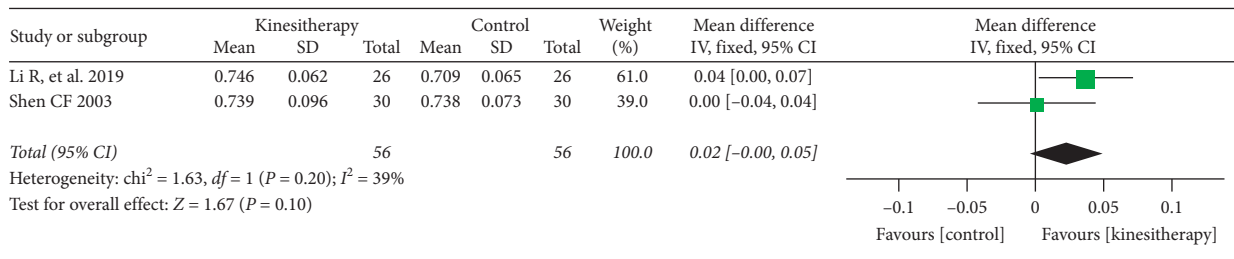


FIGURE 3: Kinesitherapy plus antiosteoporosis medications versus antiosteoporosis medications on lumbar spine BMD (intervention duration < 6 months).

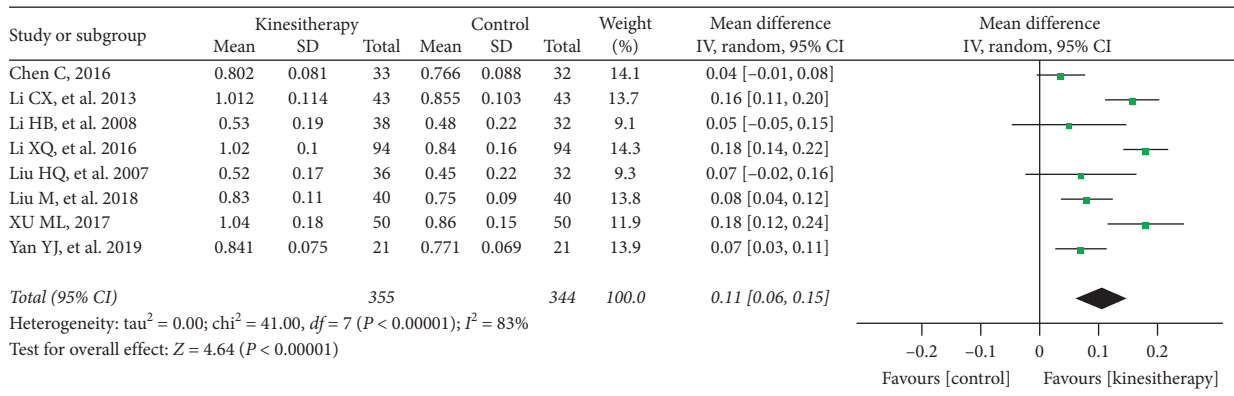


FIGURE 4: Kinesitherapy plus antiosteoporosis medications versus antiosteoporosis medications on lumbar spine BMD (intervention duration = 6 months).

4. Discussion

4.1. Summary. POP is a worldwide health problem that primarily impacts postmenopausal women and senile individuals. Moreover, POP is often related to physical frailty, an increased risk of falls, substantial morbidity, mortality, and impairment in quality of life [55]. The aim of OP treatment is to improve BMD and prevent fractures. Nonpharmacological treatment includes a healthy diet, prevention of falls, and physical exercise programs. Pharmacological treatment involves calcium, vitamin D, and

medications for activating bone tissue (e.g., antiresorptives, bone formers, and mixed agents) [56]. In addition, exercise is considered important for maintaining bone health. Individuals with OP are strongly recommended to regularly engage in multicomponent exercise programs [57]. Moreover, several studies have confirmed that exercise can increase BMD at the femoral neck and the lumbar spine in elderly women with osteoporosis [58, 59]. This review is the first systematic review and meta-analysis to evaluate the effect of kinesitherapy on BMD on the lumbar spine and femoral neck in persons with POP from RCTs. This study

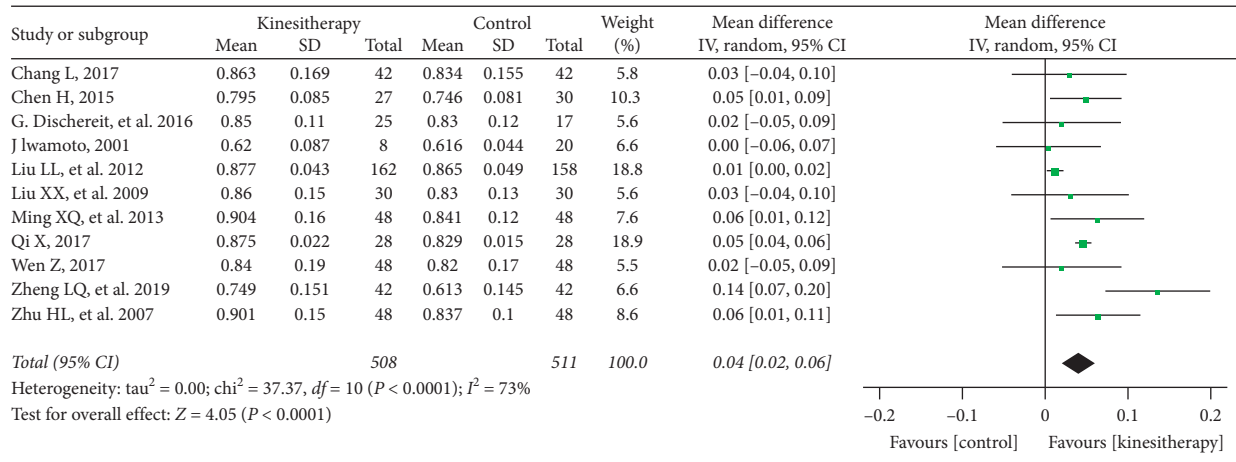


FIGURE 5: Kinesitherapy plus antiosteoporosis medications versus antiosteoporosis medications on lumbar spine BMD (intervention duration > 6 months).

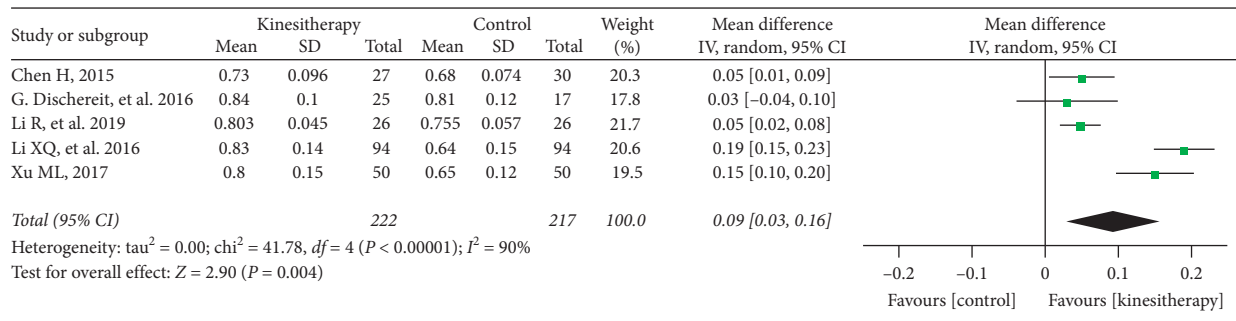


FIGURE 6: Meta-analysis of femoral neck BMD.

involved 21 RCTs that included a total of 1840 subjects with POP (including SOP and PMOP). The duration of treatment varied from 3 to 24 months. The outcome measures primarily consisted of lumbar spine and femoral neck BMD. The results of the meta-analysis showed that there were no statistically significant differences between kinesitherapy plus antiosteoporosis medications versus antiosteoporosis medications alone on lumbar spine BMD when the duration of intervention was less than 6 months (MD = 0.02; 95% CI: -0.00-0.05; P = 0.10). However, kinesitherapy had a positive effect on lumbar spine BMD when the duration of intervention was 6 months (MD = 0.11 g/cm²; 95% CI: 0.06-0.16; P < 0.0001) or more than 6 months (MD = 0.04 g/cm²; 95% CI: 0.02-0.06; P < 0.0001) compared with antiosteoporosis medications alone. Furthermore, kinesitherapy had a remarkable effect on femoral neck BMD (MD = 0.09 g/cm²; 95% CI: 0.03-0.16; P < 0.004) when compared with antiosteoporosis medications alone.

4.2. Limitations and Suggestions for Future Research. A total of 21 RCTs were included in this review, which showed that kinesitherapy had a favourable effect on lumbar spine and femoral neck BMD in patients with POP. Nevertheless, the

interpretation and generalization of this systematic review and meta-analysis are subject to some limitations. According to the Cochrane Collaboration’s tool, low-quality evidence, which included studies with a high risk of bias, resulted in a high heterogeneity of the meta-analysis results and favoured the positive effect of kinesitherapy on BMD in patients with POP. There were eleven RCTs that did not report the random sequence generation, and the remaining RCTs were lacking detailed descriptions of randomization, which could result in selection bias. The performance bias was high since the blinding of participants and personnel was not implemented. In all of the included trials, whether the blinding of the outcome assessment was used or not is not mentioned except for one study which states explicitly that the blinding of the outcome assessment was not applied and the statistics of outcome operated by the author. Although one trial reported reasons for withdrawal and dropout, an intention-to-treat analysis was not performed in the data analysis phase for which attrition bias was inevitable. In addition, all of the study protocols from the trials could not be obtained. Furthermore, a specific exercise was not designed for the analysis, which suggests that such an analysis is problematic due to the diversity of interventions. Only five trials included the outcome of femoral neck BMD in the currently available

studies; thus, the reliability of the treatment effects of kinesitherapy on femoral neck BMD is reduced. Therefore, more multicenter, larger sample, long-term, single-blind RCTs are required to assess the effect of kinesitherapy on BMD in patients with POP.

5. Conclusion

The meta-analyses in this study suggest that kinesitherapy plus antiosteoporosis medications can significantly improve lumbar spine BMD when the duration of intervention is longer than 6 months compared with antiosteoporosis medications alone in the current low-quality evidence. More high-quality evidence in the form of multicenter, larger sample, long-term, single-blind, randomized controlled trials is required to confirm the effect of kinesitherapy on BMD in patients with POP.

Conflicts of Interest

The authors have no conflicts of interest to declare.

Acknowledgments

This study was supported by the Youth Program of the Department of Education, Hunan Province, China (grant no. 17B246).

References

- [1] Y. Jiang, Y. Pei, X. Y. Miao et al., "Relationship among aging, body composition, body mass index, and bone mass density in elderly men over 50-year-old," *Chinese Journal of Osteoporosis & Bone Mineral Research*, vol. 9, no. 2, pp. 122–128, 2016.
- [2] K. S. Park, J. I. Yoo, H. Y. Kim et al., "Education and exercise program improves osteoporosis knowledge and changes calcium and vitamin D dietary intake in community dwelling elderly," *Bmc Public Health*, vol. 17, no. 1, p. 966, 2017.
- [3] M. R. McClung, "Prevention and management of osteoporosis," *Best Practice & Research Clinical Endocrinology & Metabolism*, vol. 17, no. 1, pp. 53–71, 2003.
- [4] H. J. Choi, C. S. Shin, Y.-C. Ha et al., "Burden of osteoporosis in adults in Korea: a national health insurance database study," *Journal of Bone and Mineral Metabolism*, vol. 30, no. 1, pp. 54–58, 2012.
- [5] C. García-Gomáriz, J. M. Blasco, C. Macián-Romero, E. Guillem-Hernández, and C. Igual-Camacho, "Effect of 2 years of endurance and high-impact training on preventing osteoporosis in postmenopausal women," *Menopause*, vol. 25, no. 3, pp. 301–306, 2018.
- [6] L. Sung-Rak, H. Yong-Chan, H. Kang et al., "Morbidity and mortality in jeju residents over 50-years of age with hip fracture with mean 6-year follow-up: a prospective cohort study," *Journal of Korean Medical Science*, vol. 28, no. 7, pp. 1089–1094, 2013.
- [7] J. L. Porter and S. S. Bhimji, *Osteoporosis. Treasure Island*, StatPearls Publishing, Treasure Island, FL, USA, 2017.
- [8] E. Gielen, D. Vanderschueren, F. Callewaert, and S. Boonen, "Osteoporosis in men," *Best Practice & Research Clinical Endocrinology & Metabolism*, vol. 25, no. 2, pp. 321–335, 2011.
- [9] D. Bliuc, N. D. Nguyen, D. Alarkawi, T. V. Nguyen, J. A. Eisman, and J. R. Center, "Accelerated bone loss and increased post-fracture mortality in elderly women and men," *Osteoporosis International*, vol. 26, no. 4, pp. 1331–1339, 2015.
- [10] N. C. Wright, A. C. Looker, K. G. Saag et al., "The recent prevalence of osteoporosis and low bone mass in the United States based on bone mineral density at the femoral neck or lumbar spine," *Journal of Bone and Mineral Research*, vol. 29, no. 11, pp. 2520–2526, 2014.
- [11] W. D. Leslie, L. M. Lix, G. S. Finlayson, C. J. Metge, S. N. Morin, and S. R. Majumdar, "Direct healthcare costs for 5 years post-fracture in Canada," *Osteoporosis International*, vol. 24, no. 5, pp. 1697–1705, 2013.
- [12] R. Liu and B. K. Zhao, "The drug treatment of Osteoporosis," *Chinese Journal of Ethnomedicine & Ethnopharmacy*, vol. 4, no. 7, pp. 58–60, 2014.
- [13] W. Wang, N. I. Li-Gang, L. I. Chun-Wen et al., "Research progress of osteoporotic hip fracture in old age," *Chinese Archives of Traditional Chinese Medicine*, vol. 30, no. 5, pp. 1069–1072, 2012.
- [14] K. Sundeeep and P. Roberto, *Osteoporosis*, Elsevier, Amsterdam, Netherlands, 4th edition, 2013.
- [15] A. Svedbom, E. Hernlund, M. Ivergård et al., "Osteoporosis in the European Union: a compendium of country-specific reports," *Archives of Osteoporosis*, vol. 8, no. 1-2, p. 136, 2013.
- [16] S. Maria and P. A. Witt-Enderby, "Melatonin effects on bone: potential use for the prevention and treatment for osteopenia, osteoporosis, and periodontal disease and for use in bone-grafting procedures," *Journal of Pineal Research*, vol. 56, no. 2, pp. 115–125, 2014.
- [17] Z. Porhashem, M. Biani, H. Noreddini et al., "Prevalence of osteoporosis and its association with serum vitamin D level in older people in Amirkola, North of Iran," *Caspian Journal of Internal Medicine*, vol. 3, no. 1, pp. 347–353, 2012.
- [18] Z. M. Hu and C. Liu, "Epidemiology and associated risk factors of osteoporosis," *World Latest Medicine Information*, vol. 19, no. 42, pp. 55–57, 2019.
- [19] I. R. Reid, D. M. Black, R. Eastell et al., "Reduction in the risk of clinical fractures after a single dose of zoledronic acid 5 milligrams," *Bone*, vol. 48, no. 2, pp. 557–563, 2011.
- [20] T. E. Howe, B. Shea, L. J. Dawson et al., "Exercise for preventing and treating osteoporosis in postmenopausal women," *The Cochrane Database of System Reviews*, vol. 6, no. 7, Article ID CD000333, 2011.
- [21] J. Iwamoto, "A role of exercise and sports in the prevention of osteoporosis," *Clinical Calcium*, vol. 27, no. 1, pp. 17–23, 2017.
- [22] R. Zhao, M. Zhang, and Q. Zhang, "The effectiveness of combined exercise interventions for preventing postmenopausal bone loss: a systematic review and meta-analysis," *Journal of Orthopaedic & Sports Physical Therapy*, vol. 47, no. 4, pp. 241–251, 2017.
- [23] L. Cheng, S. Yan, J. Zhu, P. Cai, T. Wang, and Z. Shi, "Exercise enhance the ectopic bone formation of calcium phosphate biomaterials in muscles of mice," *Materials Science and Engineering: C*, vol. 77, pp. 136–141, 2017.
- [24] W. A. van Gemert, A. J. Schuit, J. van der Palen et al., "Effect of weight loss, with or without exercise, on body composition and sex hormones in postmenopausal women: the shape-2 trial," *Breast Cancer Research*, vol. 17, p. 120, 2015.
- [25] M. de Roon, A. M. May, A. McTiernan et al., "Effect of exercise and/or reduced calorie dietary interventions on breast cancer-related endogenous sex hormones in healthy postmenopausal women," *Breast Cancer Research*, vol. 20, no. 1, p. 81, 2018.

- [26] R. Armamento-Villareal, L. Aguirre, D. L. Waters et al., "Effect of aerobic or resistance exercise, or both, on bone mineral density and bone metabolism in obese older adults while dieting: a randomized controlled trial," *Journal of Bone and Mineral Research*, vol. 35, no. 3, pp. 430–439, 2019.
- [27] C. F. Dionello, D. Sá-Caputo, H. V. Pereira et al., "Effects of whole body vibration exercises on bone mineral density of women with postmenopausal osteoporosis without medications: novel findings and literature review," *Journal of Musculoskeletal & Neuronal Interactions*, vol. 16, no. 3, pp. 193–203, 2016.
- [28] R. Zhao, Z. Xu, and M. Zhao, "Antiresorptive agents increase the effects of exercise on preventing postmenopausal bone loss in women: a meta-analysis," *Plos One*, vol. 10, no. 1, Article ID e0116729, 2015.
- [29] D. Segev, D. Hellerstein, and A. Dunskey, "Physical activity—does it really increase bone density in postmenopausal women? A review of articles published between 2001–2016," *Current Aging Science*, vol. 11, no. 1, pp. 4–9, 2018.
- [30] A. Varahra, I. B. Rodrigues, J. C. Macdermid et al., "Exercise to improve functional outcomes in persons with osteoporosis: a systematic review and meta-analysis," *Osteoporosis International*, vol. 29, no. 1, pp. 1–22, 2018.
- [31] J. Savović, L. Weeks, J. A. Sterne et al., "Evaluation of the cochrane collaboration's tool for assessing the risk of bias in randomized trials: focus groups, online survey, proposed recommendations and their implementation," *Systematic Reviews*, vol. 3, p. 37, 2014.
- [32] G. Zheng, S. Li, M. Huang et al., "The effect of tai chi Training on cardiorespiratory fitness in healthy adults: a systematic review and meta-analysis," *Plos One*, vol. 10, no. 2, Article ID e0117360, 2015.
- [33] J. P. T. Higgins, S. G. Thompson, J. J. Deeks et al., "Measuring inconsistency in meta-analyses," *Bmj*, vol. 327, no. 7414, pp. 557–560, 2003.
- [34] J. Iwamoto, T. Takeda, and S. Ichimura, "Effect of exercise training and detraining on bone mineral density in postmenopausal women with osteoporosis," *Journal of Orthopaedic Science*, vol. 6, no. 2, pp. 128–132, 2001.
- [35] C. F. Shen, "Clinical study on the treatment of primary osteoporosis (POP) by combined method of move and nourish the kidney," *Hunan College of Traditional Chinese Medicine*, 2003.
- [36] H. L. Zhu, "Effects of exercise on bone mass and bone metabolism in elderly patients with osteoporosis," *Maternal and Child Health Care of China*, vol. 9, pp. 1251–1252, 2007.
- [37] H. Q. Liu, J. J. Qin, and H. J. Liu, "Effect of combined kinesiotherapy on bone mineral density in postmenopausal osteoporosis," *The Journal of Traditional Chinese Orthopedics and Traumatology*, vol. 19, no. 3, p. 14, 2007.
- [38] H. B. Li, Q. Mei, X. L. Yin, and R. Chang, "Clinical observation of exercise and bone peptide preparation on bone mineral density in patients of osteoporosis," *Journal of Henan Medical College*, vol. 20, no. 5, pp. 446–447, 2008.
- [39] X. X. Liu, Y. Zhou, and Y. P. Han, "Effects of community intervention on bone density in elderly patients with osteoporosis," *Guangzhou Medical Journal*, vol. 40, no. 3, pp. 67–68, 2009.
- [40] L. L. Liu and J. Wang, "Observation of the efficacy of oral supplying compound calcium and exercise prescription for the treatment of senile osteoporosis," *Journal of Clinical Research*, vol. 29, no. 4, pp. 743–745, 2012.
- [41] C. X. Li, Y. J. Tang, F. Y. Huang et al., "The effect of progressive psoas muscle functional exercise on bone density and low back pain in patients with osteoporosis," *Chinese Journal of Gerontology*, vol. 33, no. 15, pp. 3623–3624, 2013.
- [42] Q. X. Ming, "Analysis on the effect of exercise rehabilitation on senile osteoporosis," *China Health Care & Nutrition*, vol. 23, no. 10, pp. 5735–5736, 2013.
- [43] H. Chen, *Exercise Therapy Has the Influence of Bone Mineral Density and Biochemical Index for Patients of Postmenopausal with Osteoporosis*, Nanjing University of Chinese Medicine, Nanjing, China, 2015.
- [44] G. Dischereit, U. Müller-Ladner, and U. Lange, "Effects of osteoporosis specific standardized physical therapy on functional capacity, bone mineral density and bone metabolism—a 2-year prospective and randomized study," *Physikalische Medizin, Rehabilitationsmedizin, Kurortmedizin*, vol. 26, no. 3, pp. 124–129, 2016.
- [45] X. Q. Li, L. N. Tao, and H. Y. Ren, "Effect of estrogen replacement therapy combined with kinesiotherapy on postmenopausal osteoporosis in women," *Laboratory Medicine and Clinic*, vol. 13, no. 21, pp. 3099–3101, 2016.
- [46] C. Chen, *Effect of Exercise Therapy on Bone Mineral Density, lean Body Mass and Fat Mass of Postmenopausal Osteoporosis*, Nanjing University of Chinese Medicine, Nanjing, China, 2016.
- [47] M. L. Xu, "Effect of hormone replacement combined with exercise therapy on osteoporosis in postmenopausal women," *Chinese And Foreign Medical Research*, vol. 15, no. 22, pp. 50–51, 2017.
- [48] L. Chang, "Effect of alternating exercise therapy on the rehabilitation of senile osteoporosis patients," *Chinese Journal of Geriatric Care*, vol. 15, no. 5, pp. 79–80, 2017.
- [49] X. Qi, "The preventive effect of exercise therapy on osteoporosis fracture in postmenopausal women," *China Reflexology*, vol. 26, no. 10, pp. 158–159, 2017.
- [50] Z. Wen, "The role of exercise therapy in the prevention of osteoporosis fracture in elderly women," *World Latest Medicine Information*, vol. 17, no. 39, p. 156, 2017.
- [51] M. Liu and J. Q. Yang, "Effect of long-term aerobic exercise on estrogen level and bone composition in female patients with osteoporosis," *Journal of Hainan Medical University*, vol. 24, no. 18, pp. 71–77, 2018.
- [52] L. Q. Zheng, X. A. N. Pan, and Y. Q. Zheng, "Effect of alternating exercise therapy on the rehabilitation of senile osteoporosis patients," *Jilin Medical Journal*, vol. 40, no. 6, pp. 1320–1321, 2019.
- [53] R. Li, Z. Yang, W. Han et al., "Effects of combined exercise therapy on bone metabolism in postmenopausal patients with osteoporosis," *International Journal of Orthopaedics*, vol. 40, no. 1, pp. 56–66, 2019.
- [54] Y. Yan and F. Zhao, "Effect of exercise intervention on clinical effect, back pain and bone metabolism of osteoporosis patients," *Investigacion Clinica*, vol. 60, no. 5, pp. 1219–1231, 2019.
- [55] C. L. Lai, S. Y. Tseng, C. N. Chen et al., "Effect of 6 months of whole body vibration on lumbar spine bone density in postmenopausal women: a randomized controlled trial," *Clinical Interventions in Aging*, vol. 8, pp. 1603–1609, 2013.
- [56] S. S. Maeda and M. Lazaretti-Castro, "An overview on the treatment of postmenopausal osteoporosis," *Arquivos Brasileiros de Endocrinologia & Metabologia*, vol. 58, no. 2, pp. 162–171, 2014.
- [57] L. M. Giangregorio, A. Papaioannou, N. J. Macintyre et al., "Too fit to fracture: exercise recommendations for individuals with osteoporosis or osteoporotic vertebral fracture," *Osteoporosis International*, vol. 25, no. 3, pp. 821–835, 2014.

- [58] Al-S. A. ShanbE. F. Youssef et al., "The effect of magnetic therapy and active exercise on bone mineral density in elderly women with osteoporosis," *Journal of Musculoskeletal Research*, vol. 15, no. 3, pp. 65–70, 2012.
- [59] E. Angın, Z. Erden, and F. Can, "The effects of clinical pilates exercises on bone mineral density (BMD), physical performance and quality of life of women with postmenopausal osteoporosis," *Journal of Back & Musculoskeletal Rehabilitation*, vol. 28, no. 4, p. 849, 2015.

Research Article

***Zingiber officinale* Roscoe Prevents DNA Damage and Improves Muscle Performance and Bone Integrity in Old Sprague Dawley Rats**

**Suzana Makpol ¹, Nur Fathiah Abdul Sani ¹, Nur Haleeda Hakimi ¹,
Nazirah Ab Rani ¹, Siti Nor Asyikin Zakaria ¹, Ahmad Fais Abd Rasid ¹,
Geetha Gunasekaran ¹, Nur Fatin Nabilah Mohd Sahardi ¹, Jen Kit Tan ¹,
Norzana Abd Ghafar ² and Mariam Firdhaus Mad Nordin ³**

¹Department of Biochemistry, Faculty of Medicine, Level 17 Preclinical Building, UKM Medical Center, Jalan Yaacob Latif, Bandar Tun Razak, Cheras, Kuala Lumpur 56000, Malaysia

²Department of Anatomy, Faculty of Medicine, Level 18 Preclinical Building, UKM Medical Center, Jalan Yaacob Latif, Bandar Tun Razak, Cheras, Kuala Lumpur 56000, Malaysia

³Department of Chemical Process Engineering, Universiti Teknologi Malaysia (UTM) Kuala Lumpur, Jalan Sultan Yahya Petra, Kuala Lumpur 54100, Malaysia

Correspondence should be addressed to Suzana Makpol; suzanamakpol@ppukm.ukm.edu.my

Received 26 May 2020; Accepted 16 July 2020; Published 5 August 2020

Guest Editor: Arham Shabbir

Copyright © 2020 Suzana Makpol et al. This is an open access article distributed under the Creative Commons Attribution License, which permits unrestricted use, distribution, and reproduction in any medium, provided the original work is properly cited.

Age-related loss of skeletal muscle mass and strength or sarcopenia is attributed to the high level of oxidative stress and inadequate nutritional intake. The imbalance in oxidative status with increased production of free radicals results in damage to the DNA which leads to cell dysfunction. This study aimed to determine the effect of *Zingiber officinale* Roscoe (ginger) on muscle performance and bone integrity in Sprague Dawley (SD) rats. SD rats aged three (young), nine (adult), and twenty-one (old) months old were treated with either distilled water or ginger extract at a concentration of 200 mg/kg body weight (BW) daily for 3 months via oral gavage. Muscle performance was assessed at 0, 1, 2, and 3 months of treatment by measuring muscle strength, muscle function, and bone integrity while DNA damage was determined by comet assay. Muscle cell histology was analyzed by hematoxylin and eosin (H&E) staining. Young and adult ginger-treated rats showed a significant improvement in muscle strength after 3 months of supplementation. Bone mineral density (BMD) and bone mineral content (BMC) were increased while fat free mass (FMM) was decreased after 3 months of ginger supplementation in young rats but not changed in adult and old ginger supplemented groups. Interestingly, supplementation of ginger for 3 months to the old rats decreased the level of damaged DNA. Histological findings showed reduction in the size of muscle fibre and fascicles with heterogenous morphology of the muscle fibres indicating sarcopenia was evident in old rats. Treatment with ginger extract improved the histological changes even though there was evidence of cellular infiltration (mild inflammation) and dilated blood vessels. In conclusion, *Z. officinale* Roscoe prevents DNA damage and improves muscle performance and bone integrity in SD rats indicating its potential in alleviating oxidative stress in ageing and thus delaying sarcopenia progression.

1. Introduction

Sarcopenia is a common disease that occurs among the elderly which normally affect people aged 60 years old and above. This disease is related to the loss of skeletal muscle

mass and strength which occurs with advancing age [1]. Statistics has shown that 5 to 13% of elderly, aged 60 to 70 years, are affected by sarcopenia [2]. This number increases to 11 to 50% for those aged 80 years and above. A previous study showed that this muscle deterioration commonly

occurred among older males as compared to females [3] which could be characterized by the decrement of muscle mass, muscle strength, and physical performance [4]. Currently, sarcopenia has become a greater problem among the elderly because this disease contributes to the reduction of life expectancies by increasing the risk of frailty, fall, morbidity, and mortality. The cause of sarcopenia is multifactorial which involves genetic, physiological, and environmental factors. It can be attributed to the high level of oxidative stress, hormonal changes, sedentary lifestyle, and inadequate nutritional intake [5]. However, high level of oxidative stress is the main contributor to this muscle deterioration disease [6].

Oxidative stress refers to the imbalance between reactive oxygen species (ROS) production and antioxidant defence [7]. ROS including hydrogen peroxide (H_2O_2), hydroxyl radical ($\cdot OH$), nitric oxide (NO), and superoxide anion ($O_2^{\cdot -}$) can be produced from endogenous sources such as mitochondria, endoplasmic reticulum, and cytochrome c as well as from exogenous sources such as pollution, ultra violet (UV) light, and heavy metals [8, 9]. Excessive production of ROS in the body will result in oxidative damage to several types of biological molecules such as proteins, DNA, carbohydrates, and lipids. Oxidative damage to DNA and protein could cause alteration of DNA transcription as well as loss of DNA repair capacity [10]. Meanwhile, oxidative damage to lipids results in increment of lipid peroxidation [11]. The accumulation of these molecular damages could lead to mitochondrial dysfunction, mutation, alteration of cell growth, and differentiation as well as apoptosis. Finally, the accumulation of these damages could alter the balance between synthesis and degradation of skeletal muscle protein which contributes to the pathogenesis of loss of muscle mass disease including sarcopenia [12]. Currently, several strategies have been introduced in order to combat these conditions such as nutritional supplements, hormonal therapy, and physical exercise which have shown positive effects on muscle mass and strength [13–15].

Ginger (*Zingiber officinale* Roscoe) is one of the traditional herbs or spices that has been studied as an antioxidant agent against oxidative stress in the pathogenesis of degenerative diseases. Ginger consists of several bioactive compounds such as 6-gingerol, 6-shogaol, 10-gingerol, gingerdiones, gingerdiols, paradols, 5 diacetoxy-6-gingerdial, and 12-gingerol that contribute to many therapeutic effects including antioxidant, antibacterial, anticancer, anti-inflammatory, antidiabetic, neuroprotective, and gastro-protective [16–18].

A previous study showed that ginger extract could exhibit inhibitory effect against α -amylase, α -glucosidase, and angiotensin-converting enzyme (ACE) activity in type 2 diabetes mellitus rats [19]. Ginger extract also prevented lipid peroxidation, inhibited ACE activity, and reversed the expression of inflammatory cytokines and lipid in cardiovascular rats [20, 21]. A study carried out by Park et al. [22] found that 6-shogaol in ginger extract had the ability to improve the formation of synapse in the brain and inhibit components of inflammatory pathway such as tumour necrosis alpha (TNF- α), nitric oxide (NO), cyclooxygenase-2

(COX-2), and inducible nitric oxide synthase (iNOS) in the *in vivo* Parkinson disease model. This finding was similar to the result from another study performed by Ha et al. [23].

However, no study has been reported which investigated the effect of ginger extract in improving muscle performance in ageing. Thus, this study aimed to elucidate the effect of *Z. officinale* Roscoe in improving muscle performance in Sprague Dawley (SD) rats.

2. Materials and Methods

2.1. *Zingiber officinale* Roscoe Preparation. Fresh ginger was harvested from Bentong, Pahang, Malaysia. The extraction process was carried out at Department of Chemical Process Engineering, Universiti Teknologi Malaysia (UTM, Kuala Lumpur, Malaysia), and ERP Two One Technologies & Innovations Sdn Bhd (Subang, Malaysia). Standardized ginger extract was isolated by using the subcritical water extraction method at optimum temperature of 130°C for 30 min with the solvent to solid ratio at 28/2 ml/mg [24]. The extract contains 6-gingerol and 6-shogaol at concentrations of 289.531 mg/mL and 15.466 mg/mL, respectively. Ginger was freeze-dried to form powder and stored at -20°C before use.

2.2. Animals. For the main study, the SD rats were divided into three groups: 18 male young 3-month-old SD rats, 18 male adult 9-month-old SD rats, and 18 male aged 21-month-old SD rats. The rats were purchased from Universiti Kebangsaan Malaysia Laboratory Animal Resource Unit (LARU). Each age group of rats was further allotted into two groups: Group 1 was control group which was given 1 ml of distilled water ($n = 8$) and Group 2 was given 200 mg/kg/body weight (BW) daily of *Z. officinale* Roscoe ($n = 10$) for three months. Each rat was randomly kept in individual Sealsafe® Plus Rat IVC Green Line (TECHNIPLAST, Varese, Italy) cage in animal care facility and allowed to acclimatize for one week before administration of the treatment. Throughout the study, the rats were maintained in animal care facilities with temperature of 24°C and 12 h of light and dark cycle. The rats were also provided with rat pellet (Gold Coin, Malaysia) and water ad libitum. The rat pellet is composed of minimum 22.0% crude protein content, maximum 5.0% crude fibre content, minimum 3.0% crude fat content, maximum 13.0% moisture, maximum 8.0% ash, 0.8%–1.2% calcium, 0.6%–1.0% phosphorus, and approximately 49.0% nitrogen-free extract. Kenaff (Muhaaz Enterprise, Terengganu Malaysia) was used as the bedding of the rats which was changed twice per week. The animals were tested based on their groups, starting from Group 1 and followed by Group 2 for each test performed. The experimental design was consented by the Universiti Kebangsaan Malaysia Animal Ethics Committee (UKMAEC Approval Number: BIOD/PP/2018/SUZANA/14-MAY/924-JUNE-2018-MAY-2020). The experimental protocol for this research is depicted in Figure 1. The number of animals was chosen based on previous study that used seven rats for control and eight rats for the treated group to study the effect

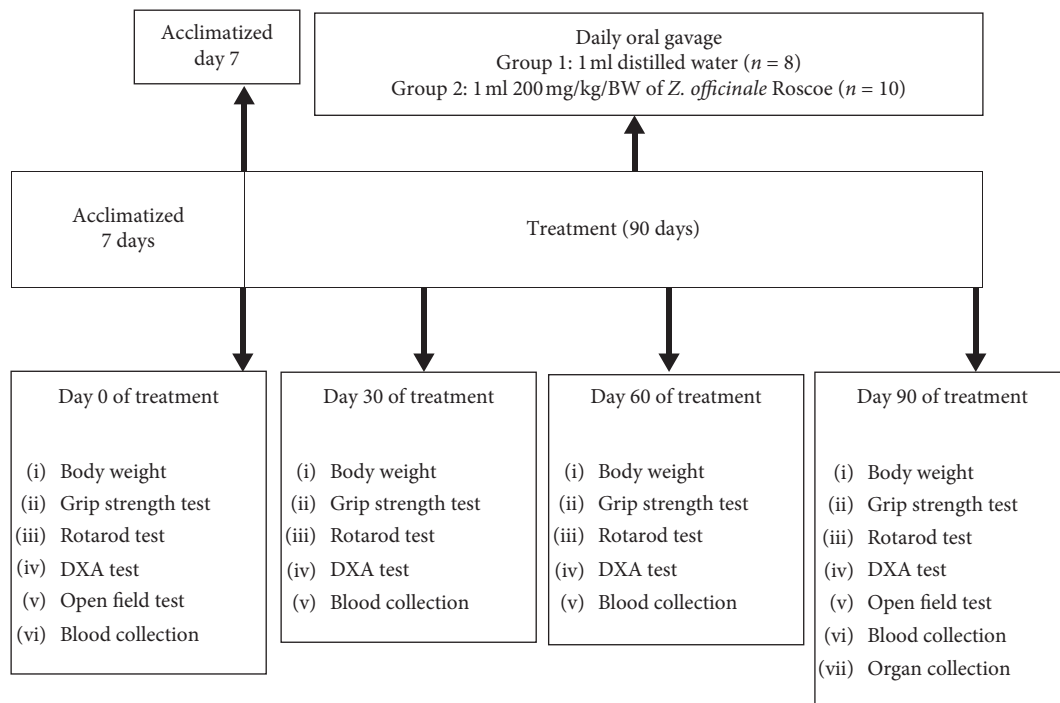


FIGURE 1: The timeline for the experimental protocol.

of gelam honey and ginger, along with the approval from UKMAEC [25].

2.3. Pilot Study. In the pilot study, three female rats were used. The main purpose of this pilot study was to select the optimum dosage to be used in the main study and to minimize the number of rats to be used. The starting dosage of *Z. officinale* Roscoe in this pilot study was 5 mg/kg/BW followed by 50, 300, and 2000 mg/kg/BW sequentially for every five days. Blood was drawn on days 6, 11, 16, and 21 for liver function test.

2.4. Clinical Observations. The rats were observed individually at 0.5, 1, 2, 3, and 4 h after administration of *Z. officinale* Roscoe extract. The rats were then observed after 24 h, followed by observation twice daily thereafter for the duration of 21 days for mortality and clinical toxicity signs. The signs of clinical toxicity include changes on skin, fur, eyes, and mucous membrane, behavioural pattern, tremors, salivation, diarrhoea, occurrence of secretion, excessive grooming, repetitive circling, and bizarre behaviour such as self-mutilation and walking backwards. Throughout the experimentation, the rats were also closely monitored for any signs of pain which include excessive licking or scratching, redness and swelling at any site, anorexia which was indicated by the absence of faeces, struggling, squealing, convulsions, twitching, tremors, weakness, teeth grinding, hunched up, unwilling to move, and favouring a limb. The other signs of pain include decrease in appetite which were evidence by few faeces, biting of affected body part, reluctant to move, increased respiration, change in bowel or urinary activities, and porphyrin discharge which was shown

by red-brown pigment around eyes and nostrils. The BW for each rat was recorded on days 0 (prior to dosing), 6, 11, 16, and 21.

2.5. Acute Toxicity Study. Twelve female SD rats were used in the toxicity study. From the pilot study, it was found that the highest dose of 2000 mg/kg/BW *Z. officinale* Roscoe extract did not cause mortality and toxicity signs. Thus, the dosage of 200 mg/kg/BW *Z. officinale* Roscoe extract was selected for the main study. Thus, this dose was used for acute toxicity study and treatment was given either orally once (single unrepeatable dose) or orally daily (repeated dose) for 14 days. The extract was freshly prepared before administration and calculated based on the current BW of the rat. The rats were then observed individually at 0.5, 1, 2, 3, 4, and 24 h, followed by observation twice daily thereafter for the duration of 14 days for mortality and clinical toxicity signs. The BW for each rat was recorded on days 0 (prior to dosing), 7, and 14. Blood was also collected on days 0, 7, and 14 for liver function test. After the animals were sacrificed, all organs were then collected, weighted, and observed for any sign of toxicity.

2.6. Grip Strength Test. The front paws and hind paws grip strength were measured using Bioseb's Grip Strength Test (USA) machine. The grip strength was used to determine the maximal peak force developed by a rat when it pulled out the metal bar. The machine was set up on a strong and stable table. The rat was allowed to grasp the metal bar by its front paws when it was pulled by the tail backwards in horizontal plane. Peak tension, the force applied to the bar just before it loses grip, was recorded in grams unit. The rats were pulled

three times and the machine would record the highest peak tension. Then, the same procedure was repeated for the hind paw grip strength measurement.

2.7. Rotarod Test. An automated rotarod (Med Associates, St. Albans, VT, USA) was used to assess muscle function by evaluating grip strength and balance. Each rat was placed on the rotating cylinder with a constant speed rotation (16 rpm) over 300 s where they had to walk to maintain their position on the cylinder. Test ended when rat fell from the rod, and the latency to fall was recorded (max 300 s). Each rat was tested three times with 10 min of rest between each test. Data are presented as the average of the three tests. The test was performed at 0, 1, 2, and 3 months of supplementation.

2.8. Measurement of Bone Mineral Density, Bone Mineral Content, and Lean Bone Mineral Content. For the analysis of computerized tomography of bone density, the entire body of the rat was scanned by applying dual energy X-ray absorptiometry (DXA) (Hologic Discovery W, Bedford, USA). The rat was first anesthetized and left for 10 to 15 min for its sedative effect. The sedated rat was then laid down on the X-ray platform and scanning was performed within 3 min duration. As scanning was performed, a large radiating scanning arm was moved over the rats and a low-dose X-ray beam was passed through the rats. These radiation changes were converted to the quantification of bone mineral density (BMD), bone mineral content (BMC), lean BMC, and percentage of fat free mass (FFM) of each rat by the Hologic software.

2.9. Open Field Test. The rat was carried to the test room in its home cage and was handled by the base of their tails at all times. The open field test was carried out in a square and black painted wooden box of 60 cm × 60 cm. The rat was placed into one of the four corners facing towards the wall of the box and allowed to explore the field for 5 minutes in which its movement was recorded by a video camera mounted to the ceiling. The rat was simultaneously assessed using HVS Image Software 2017, based on the parameters of interest which include total path length and percentage of time moving. After the 5-minute test, the rat was returned to its home cage and the wooden box was wiped with 70% ethanol and permitted to dry between tests.

2.10. Blood Collection. Blood was withdrawn from each rat on days 0, 30, 60, and 90 of treatment by orbital sinus collection methodology. The rat was anesthetized prior to blood collection and was handled with thumb and forefinger of the left hand. Skin around the rat's eye was pulled out until the eye bulged out and a capillary tube was inserted with slight thumb pressure into the medial canthus of the eye at 30° angle to the nose. Blood was flown through the capillary tube after puncturing through the tissue and plexus/sinus. A total of 3 ml of blood was collected into EDTA tube before gently removing the capillary tube. Bleeding was then stopped by applying a gentle pressure by the finger and

wiped with sterile cotton. The collected blood was later centrifuged and plasma was kept in -80°C freezer for further analysis.

2.11. Analysis of Damaged DNA by Comet Assay. Comet assay was performed as described by Singh et al. [26] with slight modification. Fully frosted microscope slides were coated with a thin layer of 0.6% normal melting point agarose (Sigma-Aldrich, St. Louise, MO, USA) and placed at room temperature for 10 minutes. Once the first agarose layer was solidified, a mixture of 5 µL of whole blood with 0.6% low melting point agarose (Sigma-Aldrich, St. Louise, USA) was applied as the second layer. Then, the slides were immersed in chilled fresh lysing solution (2.5 M NaCl, 100 mM Na₂EDTA-2H₂O, 10 mM Tris at pH 10, 1% sodium N-lauroylsarcosinate, 1% Triton X-100, and 10% dimethylsulfoxide) for 1 h at 4°C. After lysis, the slides were placed in a horizontal electrophoresis tank filled with chilled fresh buffer (0.3 M NaOH and 1 mM Na₂ EDTA) for 20 minutes to allow unwinding of the DNA followed by 20 minutes electrophoresis at 25 V with the current adjusted to 300 mA. After electrophoresis, the slides were rinsed twice with neutralization buffer (0.4 M Tris Base, pH 7.5) to neutralize the excess alkali and were stained with ethidium bromide (20 µg/mL) (Sigma-Aldrich, St. Louise, MO, USA). Then, the slides were kept at room temperature to dry for later analysis. The slide was examined at 40x magnifications using a fluorescence microscope (Olympus, UK) where photomicrographs of 500 randomly selected nonoverlapping cells on each slide were captured. The slides of each rats were made in triplicate. All of the above procedures were performed in the dark. Comet images were analyzed using CASP software (CASP, Wroclaw, Poland). Percentages of tail DNA, tail length, tail moment, and olive tail moment were recorded to evaluate DNA damage.

2.12. Euthanization of Animals. The anaesthesia agents used in this study were KTX agents which are the combination of ketamine, xylazine, and zoletil-50 (tiletamine and zolazepam). The KTX agents were administered based on 0.1 ml/250 g of rat BW for each rat by intraperitoneal injection, at the lower right quadrant of the abdomen due to its rapidity, efficacy, and minimal pain, fear, and distress. The rats were then left for about 30 min for the KTX agents to give their sedative effect. This was observed by clinical signs, including disorientation and loss of consciousness, depression of respiration or rapid irregular breathing, progressively declined heart rate and blood pressure, urination, and defecation. Later, the rats were euthanized by decapitation method using decapitator (Modiezhham Sdn. Bhd., Kuala Lumpur, Malaysia).

2.13. Collection of Organs. All rats were fastened overnight on day 90 before sacrificing for necropsy examination. The organs such as the heart, liver, kidneys, brain, and quadriceps muscle were dissected from the sacrificed rats. All organs were washed with 90% normal saline to remove any

adherent tissue and later weighted. The weight of the organs was taken as quickly as possible to avoid drying, and they were analyzed in relative to the BW of the animals.

2.14. Histological Analysis. Quadriceps muscle tissues were fixated in 10% neutral formalin to preserve it permanently. The tissue was cut into small section and placed inside plastic cassette to hold the tissue while being processed by automated vacuum tissue processor (STP 120 Spin Tissue Processor, Thermo Fisher Scientific, Massachusetts, USA). Then, the tissue was embedded to be made as block of paraffin (Surgipath® Paraplast® from Leica Biosystems Richmond Inc., Illinois, USA). The tissue was later cut into section of 5 μ m by using Leica RM2135 Manual Rotary Microtome (Leica, Nussloch, Germany). The cut sections were then floated on a 38°C preheated warm water bath (Leica HI1210 Water Bath, Leica, Nussloch, Germany), before picking it up on glass microscopic slide. The glass slide with tissue section attached was further warmed at 50°C for 30 min in Memmert UN50 Universal Oven (Memmert, Buechenbach, Germany). Haematoxylin and eosin (H&E) staining was then performed. The stained section of the slide was mounted by DPX mountant (VWR International Ltd., Poole, England) and covered with thin cover slides. The staining later was viewed under dissecting BX53 Microscope (Olympus, Tokyo, Japan) with built-in light source and camera attachment linked to LCD for the visualization of H&E staining.

2.15. Statistical Analysis. All data were expressed as mean \pm standard deviation (SD); a p value of <0.05 was considered statistically significant. SPSS software version 25 was used to carry out the statistical analysis. Data acquired were analyzed by using one-way ANOVA followed by a post hoc Bonferroni test.

3. Results

3.1. Clinical Observations. No physical and behavioural changes were observed on all treated rats after oral administration of *Z. officinale* Roscoe for 14 and 21 consecutive days in both pilot and toxicity studies. No mortality was recorded in both studies.

3.2. Rats' Body Weight of Pilot and Toxicity Studies. No change was observed on the BW of rats in the pilot study from day 0 till day 21 (Figure 2(a)). For acute toxicity study, the BW of the rats was retained throughout the study from day 0 till day 14 of the study (Figures 2(b) and 2(c)).

3.3. Relative Organ Weight (ROW) of Pilot and Toxicity Studies. The ROW of pilot study, single unrepeated dose of acute toxicity study, and daily dose of acute toxicity study is shown in Figure 3. The ROW of the lung for daily dose of acute toxicity study was significantly decreased compared to ROW of lung for pilot study ($p < 0.05$). However, the ROW of the liver for daily dose of acute toxicity study was

significantly increased as compared to ROW of liver for pilot study ($p < 0.05$). The ROW of the brain for single unrepeated dose and daily dose of acute toxicity study was significantly decreased as compared to the ROW of the brain for pilot study ($p < 0.05$).

3.4. Liver Function Test. The liver function test for pilot and acute toxicity studies on various days is shown in Table 1. The levels of total protein, albumin, globulin, albumin/globulin ratio, total bilirubin, aspartate transaminase, alanine transaminase, alkaline phosphatase, and gamma-glutamyl transferase of rats in the pilot study and single unrepeated dose of toxicity study were not significantly different between the different days. However, the levels of total protein and globulin on days 7 and 14 of daily dose of toxicity study were significantly increased compared to day 0 and day 7, respectively ($p < 0.05$).

3.5. Body Weight and Relative Organ Weight of Main Study. The BW of young, adult, and old rats was significantly increased within and between the group of treatments (Figure 4(a)). BW data were analyzed using a one-way repeated measure ANOVA followed by Bonferroni corrected t -test with p value < 0.05 .

Measurement of the organ weight showed that the ROW of spleen and brain was significantly increased in young rats treated with ginger as compared to untreated control ($p < 0.05$) (Figure 4(b)). For old rats however, the ROW of right kidney was significantly decreased compared to untreated control ($p < 0.05$) (Figure 4(d)).

3.6. Measurement of Grip Strength. The grip strength of front paws was significantly decreased at 3 months in control adult rats as compared to control young rats ($p < 0.05$) (Figure 5(a)). Treatment with ginger significantly increased the grip strength at 1, 2, and 3 months of young rats as compared to untreated control ($p < 0.05$). Treatment with ginger significantly increased the grip strength at 3 months of adults rats as compared to untreated control adult rats ($p < 0.05$).

The grip strength of hind paws was significantly increased at 0 and 2 months in young rats treated with ginger as compared to untreated control young rats ($p < 0.05$) (Figure 5(b)). A similar increase was observed in the grip strength at 0 months in control adult rats while it decreased at 3 months as compared to control young rats ($p < 0.05$). Treatment with ginger significantly increased the hind paws grip strength at 0 and 3 months in adult rats as compared to untreated control adult rats ($p < 0.05$). The grip strength of hind paws was significantly decreased at 1 and 3 months in control old rats as compared to control young rats ($p < 0.05$).

3.7. Measurement of Muscle and Bone Integrity. Muscle and bone integrity were represented by bone mineral content, bone mineral density, lean bone mineral content, and percentage of fat free mass (Figure 6). Bone mineral content was significantly decreased at 3 months in young rats treated with ginger as compared to untreated control young

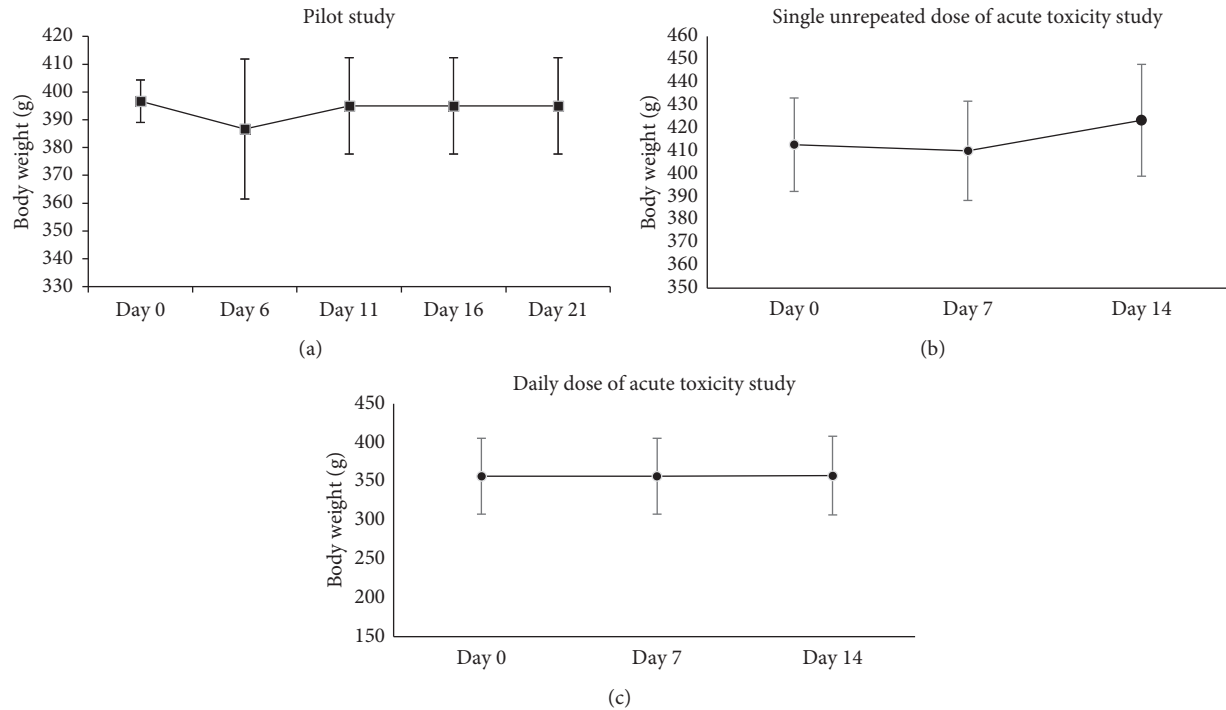


FIGURE 2: The body weight of (a) pilot study ($n = 3$), (b) single unrepeated dose of acute toxicity study ($n = 6$), and (c) daily dose of acute toxicity study ($n = 6$). The data are presented as mean \pm SD. No significant changes were found.

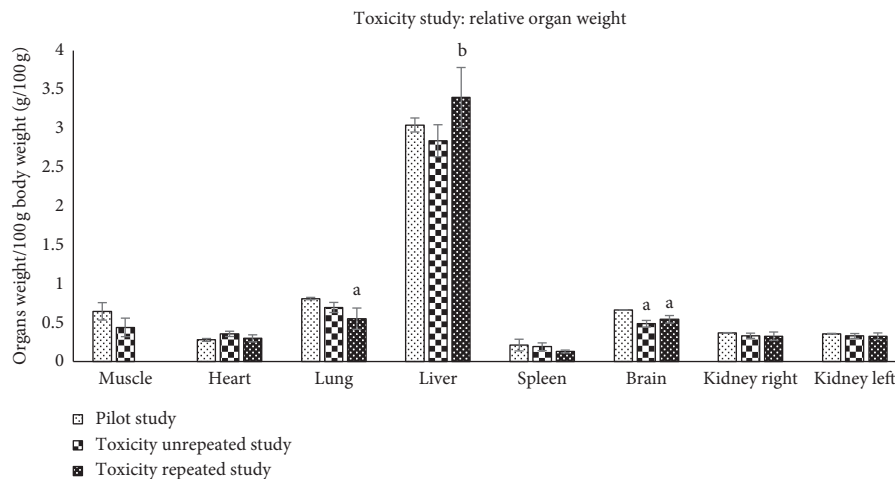


FIGURE 3: Relative organ weight of pilot study ($n = 3$), single unrepeated dose of acute toxicity study ($n = 6$), and daily dose of acute toxicity study ($n = 6$). The data are presented as mean \pm SD; ^a $p < 0.05$, significantly different compared to pilot study; ^b $p < 0.05$, significantly different compared to single unrepeated dose of acute toxicity study, with a post hoc Bonferroni test.

rats ($p < 0.05$) (Figure 6(a)). In control adult rats, bone mineral content was significantly increased at 2 and 3 months while in control old rats it was significantly increased at 1, 2, and 3 months as compared to control young rats ($p < 0.05$).

Bone mineral density was significantly decreased at 1 and 3 months in young rats treated with ginger as compared to untreated control young rats ($p < 0.05$) (Figure 6(b)). In control adult rats, bone mineral density was significantly increased at 0, 1, 2, and 3 months while

in control old rats, it was significantly increased at 0 and 1 month as compared to untreated control young rats ($p < 0.05$).

Lean bone mineral content was significantly decreased at 0, 1, and 3 months in young rats treated with ginger as compared to untreated control young rats ($p < 0.05$) (Figure 6(c)). In control adult rats, lean bone mineral content was significantly increased at 0, 1, and 3 months while in control old rats, it was significantly increased at 0, 1, and 3 months compared to untreated young control rats ($p < 0.05$).

TABLE 1: The liver function test results of pilot study, single unrepeated dose of acute toxicity study, and daily dose of acute toxicity study.

| | Total protein | Albumin | Globulin | A/G ratio | Total bilirubin | AST | ALT | Alkaline phosphatase | Gamma GT |
|---|---------------------------|--------------|---------------------------|-------------|-----------------|-----------------------------|----------------|----------------------|-------------|
| Pilot study, $n = 3$ | | | | | | | | | |
| Day 0 | 84.00 ± 1.00 | 28.00 ± 1.00 | 56.00 ± 1.00 | 0.50 ± 0.00 | 2.28 ± 0.99 | 248.00 ± 63.66 | 84.00 ± 17.44 | 251.67 ± 137.01 | 4.00 ± 0.00 |
| Day 6 | 74.00 ± 6.56 | 24.00 ± 2.65 | 50.00 ± 6.93 | 0.50 ± 0.10 | 1.71 ± 0.00 | 235.33 ± 125.13 | 94.00 ± 27.87 | 230.33 ± 117.17 | 4.00 ± 0.00 |
| Day 11 | 89.67 ± 8.62 | 28.00 ± 2.65 | 61.67 ± 6.03 | 0.47 ± 0.06 | 1.71 ± 0.00 | 244.67 ± 40.55 | 100.33 ± 26.56 | 230.33 ± 153.94 | 4.00 ± 0.00 |
| Day 16 | 88.67 ± 22.05 | 27.67 ± 3.79 | 61.00 ± 18.33 | 0.50 ± 0.10 | 2.85 ± 1.97 | 241.00 ± 59.40 | 111.33 ± 20.40 | 289.00 ± 145.66 | 4.00 ± 0.00 |
| Day 21 | 65.00 ± 0.00 | 25.00 ± 0.00 | 40.00 ± 0.00 | 0.60 ± 0.00 | 1.71 ± 0.00 | 118.00 ± 0.00 | 80.00 ± 0.00 | 162.00 ± 0.00 | 4.00 ± 0.00 |
| Single unrepeated dose of acute toxicity study, $n = 6$ | | | | | | | | | |
| Day 0 | 76.50 ± 3.94 | 26.83 ± 1.17 | 49.67 ± 4.18 | 0.55 ± 0.05 | 1.71 ± 0.00 | 305.17 ± 70.44 | 96.00 ± 15.56 | 285.00 ± 55.95 | 4.00 ± 0.00 |
| Day 8 | 78.83 ± 5.19 | 27.67 ± 1.86 | 51.17 ± 3.87 | 0.53 ± 0.05 | 1.71 ± 0.00 | 230.17 ± 22.13 | 98.00 ± 6.63 | 282.00 ± 71.56 | 4.00 ± 0.00 |
| Day 15 | 77.17 ± 2.32 | 25.83 ± 1.47 | 51.33 ± 2.16 | 0.48 ± 0.04 | 1.71 ± 0.00 | 319.67 ± 59.71 [#] | 110.83 ± 13.93 | 299.50 ± 68.95 | 4.00 ± 0.00 |
| Daily dose of acute toxicity study, $n = 6$ | | | | | | | | | |
| Day 0 | 71.33 ± 3.50 | 27.17 ± 1.17 | 44.17 ± 4.26 | 0.62 ± 0.08 | 1.71 ± 0.00 | 210.00 ± 47.72 | 79.00 ± 11.26 | 219.33 ± 43.02 | 4.00 ± 0.00 |
| Day 8 | 91.17 ± 14.50* | 30.67 ± 2.94 | 60.50 ± 11.91* | 0.52 ± 0.08 | 2.00 ± 0.07 | 241.67 ± 65.09 | 90.83 ± 25.88 | 215.33 ± 56.22 | 4.00 ± 0.00 |
| Day 15 | 73.67 ± 3.20 [#] | 28.00 ± 1.67 | 45.67 ± 3.83 [#] | 0.62 ± 0.08 | 1.71 ± 0.00 | 209.00 ± 43.72 | 88.00 ± 15.36 | 222.50 ± 43.26 | 4.00 ± 0.00 |

The data are presented as mean ± SD; * $p < 0.05$, significantly different compared to day 0; [#] $p < 0.05$, significantly different compared to day 8, with a post hoc Bonferroni test.

Percentage of fat free mass was significantly increased at 0, 1, and 2 months in control adult rats as compared to untreated young control rats (Figure 6(d)). No significant change in the percentage of fat mass was observed in other groups of rats.

3.8. Measurement of Muscle Function by Open Field Test. No significant change was observed in total path and speed of movement of young, adult, and old rats as measured by the open field test (Figure 7).

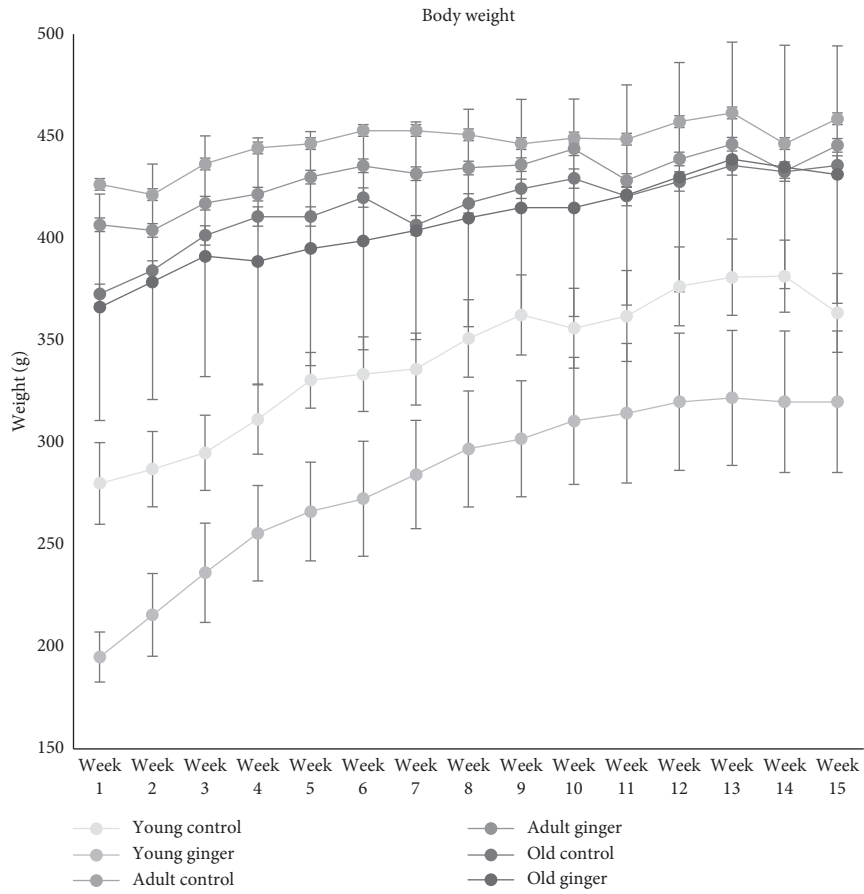
3.9. Measurement of Muscle Function by Rotarod Test. No significant change was observed in the time of fall of young, adult, and old rats as measured by the rotarod test (Figure 8)

3.10. Analysis of Damaged DNA. Damaged DNA was measured by comet assay in old rats which is represented by tail length, tail moment, tail DNA percentage, and olive moment. The tail length, tail moment, and olive moment were significantly increased at 1 month but decreased at 2 and 3 months in old rats treated with ginger ($p < 0.05$) (Figure 9(a)). A similar increase was observed in tail DNA percentage at 1 month in old rats treated with ginger but decreased at 3 months of ginger treatment ($p < 0.05$).

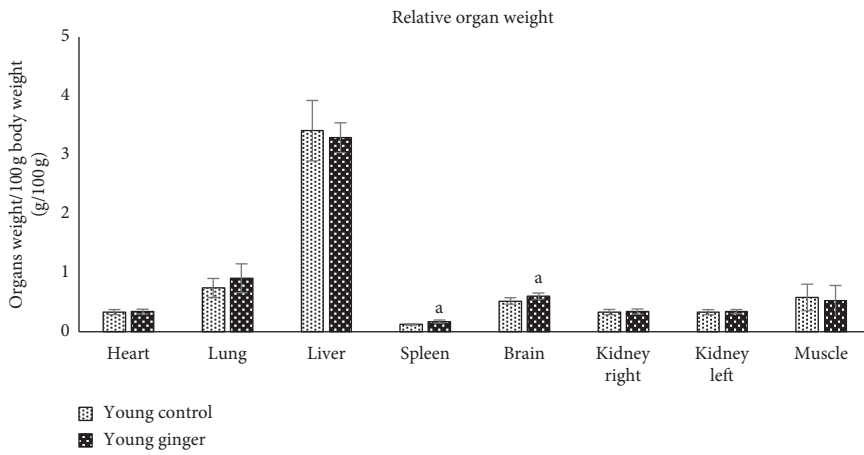
3.11. Histological Observation. Histological examination of H&E-stained cross sections of the quadriceps femoris muscle revealed polyhedral-shaped fibre with acidophilic sarcoplasm and peripherally located flat nuclei in both young and adult control groups and also in the ginger-treated groups (Figures 10(a), 10(b), 10(d), and 10(e)). Each muscle fibre was surrounded by thin connective tissue of perimysium (Figure 10, arrow).

There was an apparent decrease in the size and number of the muscle fibres and fascicles in the old control group (Figure 10(c)). The shape of the muscle fibres appeared angulated and separated by a wide connective tissue endomysium. Dilated blood vessel was also seen in between the muscle fibres (Figure 10(c)). The perimysium separating the muscle fascicles was wide.

Old rats treated with ginger showed heterogenous morphology of polyhedral and angulated muscle fibres of various sizes (Figure 10(f)). The connective tissue of endomysium and perimysium appeared narrower in most areas compared to that of the old control group. In longitudinal section, cellular infiltration was observed between the muscle fibres of the old control group (Figure 11(c)) but was not apparent in the old ginger-treated group (Figure 11(f)). Fat infiltration, disruption of muscle fibres, vacuole formation, and centrally located nuclei (evidence of regeneration) were not evident in all groups.



(a)



(b)

FIGURE 4: Continued.

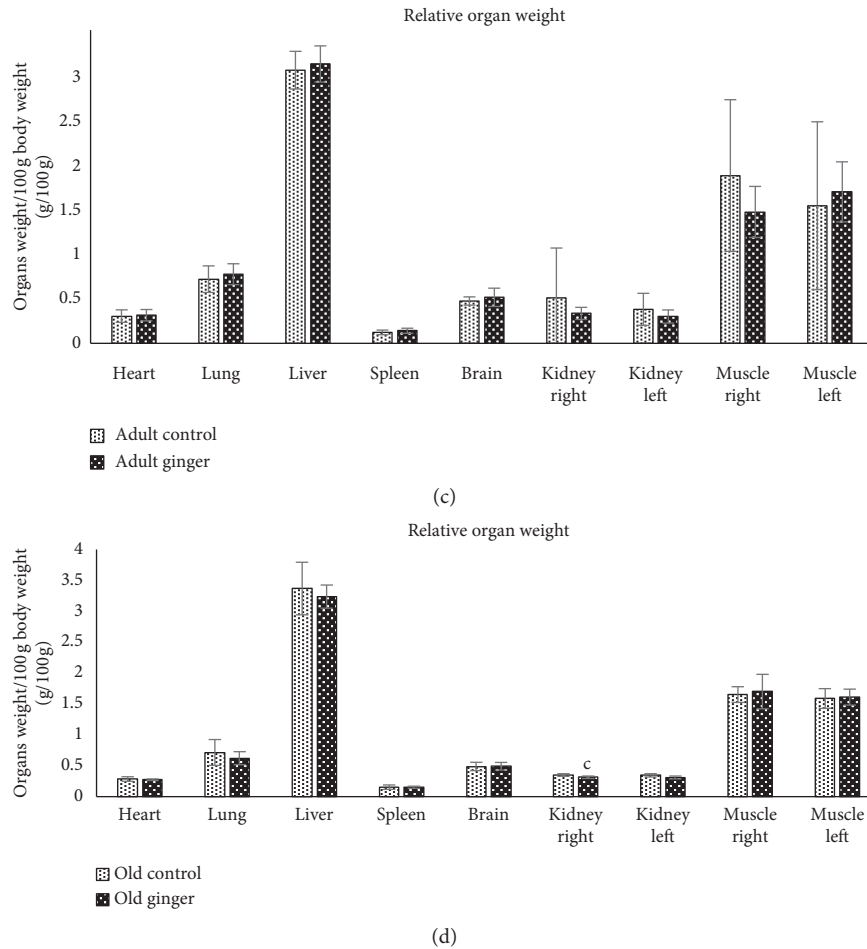


FIGURE 4: The (a) body weight and relative organ weight of (b) young, (c) adult, and (d) old rats. The data are presented as mean \pm SD ($n = 8$ (control rats); $n = 10$ (*Z. officinale*-treated rats)). ^a $p < 0.05$, significantly different compared to control young rats; ^c $p < 0.05$, significantly different compared to control old rats, with a post hoc Bonferroni test.

4. Discussion

Sarcopenia is a geriatric syndrome that involves decline of muscle mass and strength which increases the risk of disability, mobility loss, and mortality [27]. One of the causes that contribute to the pathogenesis of sarcopenia is the presence of high level of oxidative stress in the body [28]. Generally, oxidative stress occurs when the production of ROS is higher as compared to the production of antioxidant. The overproduction of ROS could result in DNA damage and cell dysfunction which later might contribute to the deterioration of muscle mass and strength. Thus, in this study, we elucidated the effect of ginger (*Z. officinale* Roscoe) in improving muscle performance in SD rats. Three groups of male SD rats were used in this study which were 3-, 9-, and 21-month-old rats. These three groups of rats were treated either with ginger extract or distilled water. Muscle performance of rats was evaluated by measuring muscle strength, muscle function, and muscle and bone integrity while DNA damage was measured via comet assay and histological analysis by H&E staining.

Ginger has been extensively studied as antioxidant and anti-inflammatory agent in various types of diseases including diabetes, cardiovascular disease, hypertension, and others. Ginger extract has been proven to improve the expression of antioxidant enzyme as well as restore the level of glutathione in Alzheimer's disease [29]. Besides, ginger extract also exhibits a positive effect in osteoarthritis disease by decreasing the level of TNF- α , IL-8, and hs-CRP [30, 31]. In type 2 diabetes, supplementation of powdered ginger capsule has attenuated the level of glucose, MDA, CRP, and insulin resistance together with the improvement of antioxidant capacity and serum paraoxonase-1 [32].

Our findings showed that the ginger extract used in this study did not cause any toxicity effect as no toxicity and mortality were observed in the pilot and toxicity studies. No change in BW was observed in this study. Gross pathological evaluations showed no signs of organs abnormalities on each organ of the pilot and toxicity studies. Generally, the ROW also showed no differences. The value of biochemical parameters of liver function test showed no differences in this study. This finding was in line with another study which reported that subchronic oral administration of ginger oil up

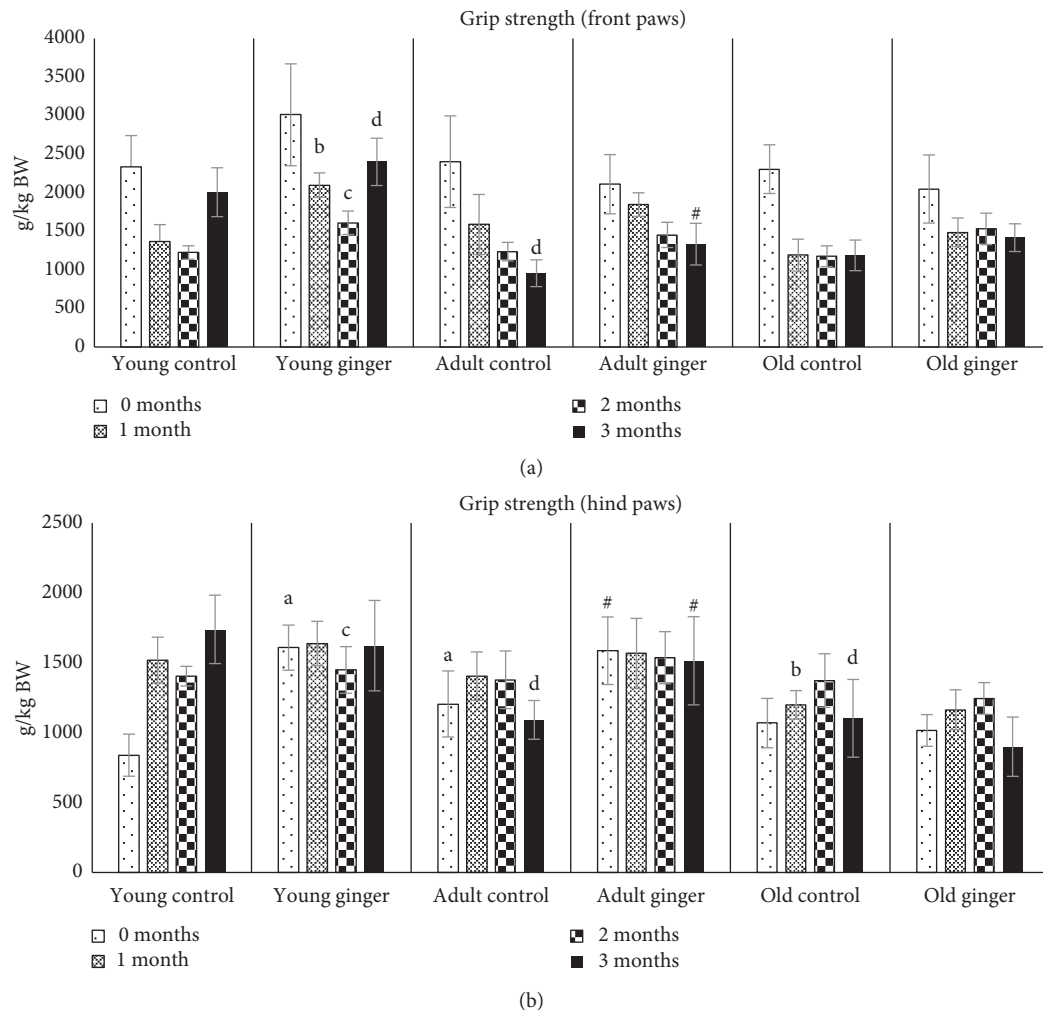


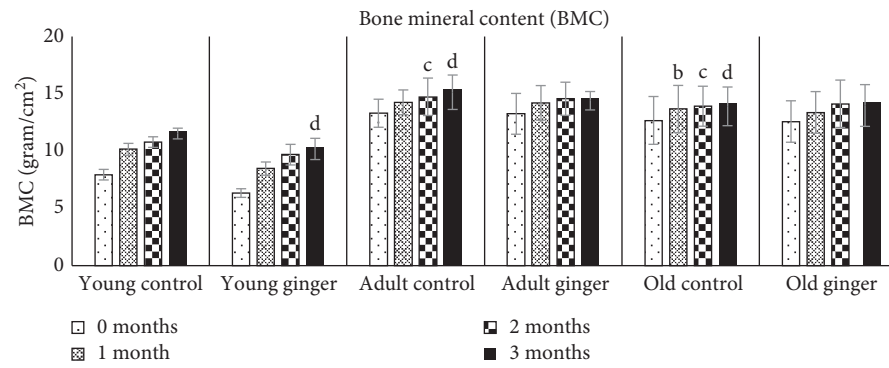
FIGURE 5: The grip strength of (a) front paws and (b) hind paws of young, adult, and old rats. The data are presented as mean \pm SD ($n = 8$ (control rats); $n = 10$ (*Z. officinale*-treated rats)). * $p < 0.05$, significantly different compared to control young rats on respective month; # $p < 0.05$ significantly different compared to control adult rats on respective month; ^a $p < 0.05$, significantly different compared to control young rats at 0 months; ^b $p < 0.05$, significantly different compared to control young rats at 1 month; ^c $p < 0.05$, significantly different compared to control young rats on at 2 months; ^d $p < 0.05$, significantly different compared to control young rats on at 3 months, with a post hoc Bonferroni test.

to 500 mg/kg per day did not show any toxic effect to Wistar rats in terms of hematological parameters, renal parameters, and histopathological parameters of kidney [33]. Conversely, another toxicity study of 60-day subchronic ginger supplementation reported that 10 mL/kg of ginger fixed oil induced oxidative stress, cellular toxicities, and organ toxicities in kidneys, liver, spleen, and lungs [34].

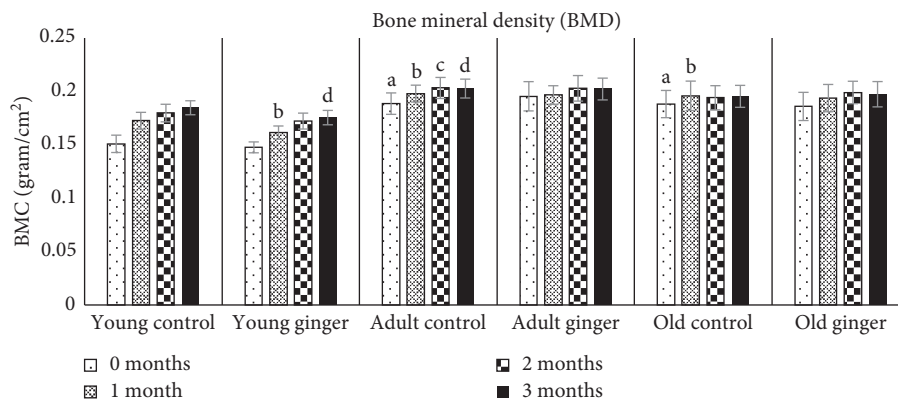
In this study, muscle strength was determined by the grip strength test while muscle function was assessed by the open field test and rotarod test. Our findings showed that muscle strength was decreased with increasing age of the rats. Treatment with ginger extract for 3 months was able to increase the grip strength of young rats as early as 1 month after treatment. However, no similar effect was observed in adult and old rats treated with ginger. This could be due to the higher muscle regenerative capacity of the young ginger-treated rats than adult or old ginger-treated rats. The muscle regenerative capacity totally depends on the regeneration of

satellite cells which slowly decreased with ageing [35]. It has been reported that the number of satellite cells decreased as ageing occurs [36]. A study conducted by Khor et al. [37] reported that senescent myoblast has low proliferative capacity, which showed downregulation of myogenic differentiation genes, but the expression of oxidative damage-associated gene was increased which may contribute to the decreased muscle regenerative capacity of adult and old ginger-treated rats observed in this study.

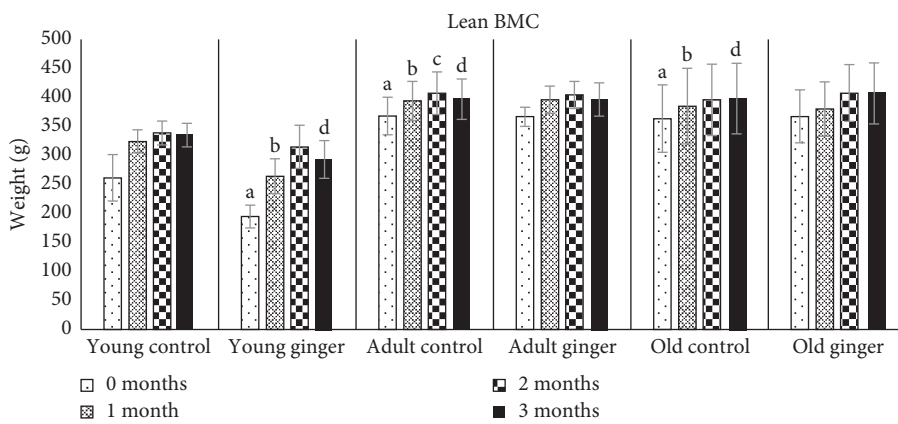
The findings on muscle strength in this study could also be due to the accumulation of ROS in adult and old ginger-treated rats which was higher than young ginger-treated rats. This is because with the advancing of age, there is overproduction of ROS in the body and the capacity to remove it from the body was decreased [38]. A previous study reported that the accumulation of ROS in senescent myoblast could contribute to the modifications in the cell membrane, extracellular matrix (ECM), and cytoskeleton by altering



(a)



(b)



(c)

FIGURE 6: Continued.

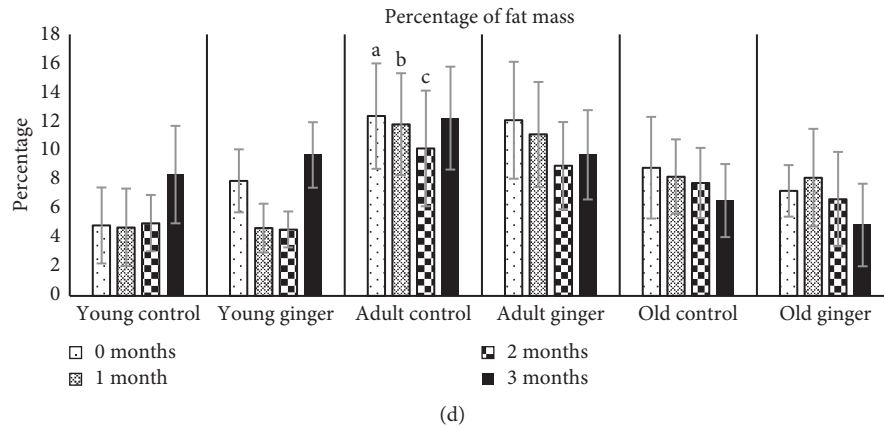


FIGURE 6: The (a) bone mineral content (BMC), (b) bone mineral density (BMD), (c) lean BMC, and (d) percentage of fat mass of young, adult, and old rats. Data are presented as mean \pm SD ($n = 8$ (control rats); $n = 10$ (*Z. officinale*-treated rats)). ^a $p < 0.05$, significantly different compared to control young rats at 0 months; ^b $p < 0.05$, significantly different compared to control young rats at 1 month; ^c $p < 0.05$, significantly different compared to control young rats at 2 months; ^d $p < 0.05$, significantly different compared to control young rats at 3 months, with a post hoc Bonferroni test.

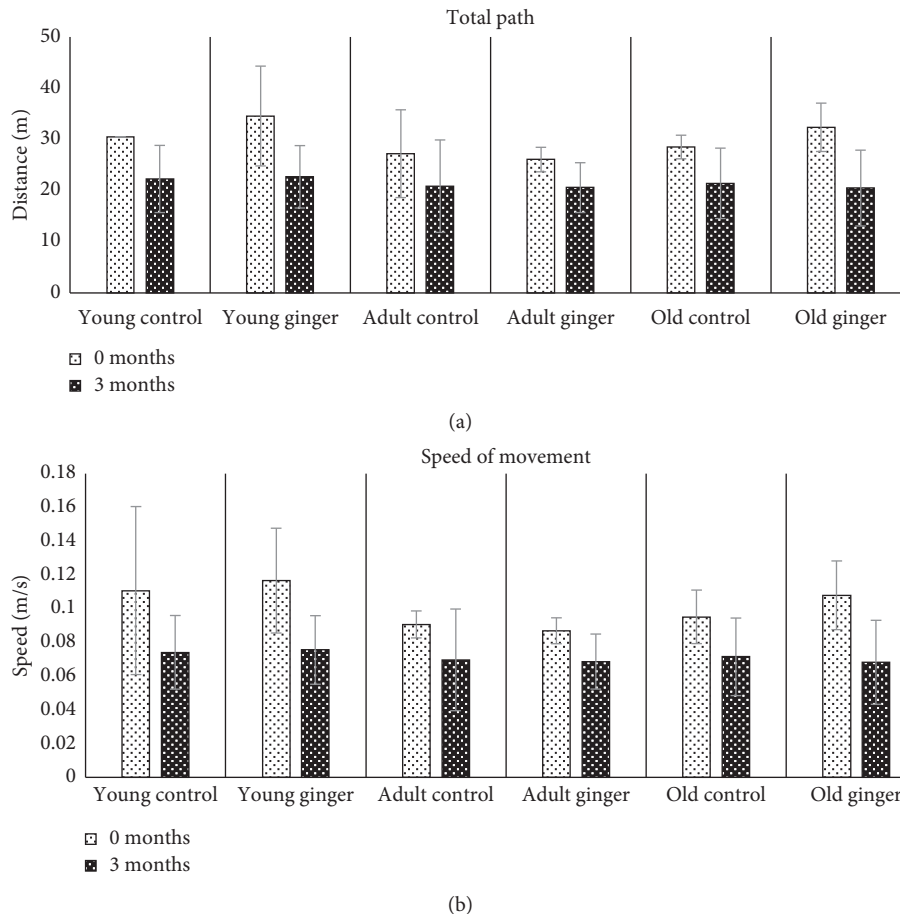


FIGURE 7: The (a) total path and (b) speed of movement of young, adult, and old rats. Data are presented as mean \pm SD ($n = 8$ (control rats); $n = 10$ (*Z. officinale*-treated rats)). No significant changes were found.

cellular metabolism and pathway [39]. These cell structures are essential in maintaining the integrity of myoblast cell structure.

Moreover, accumulation of ROS could lead to the content reduction of myosin protein as well as inhibit the occurrence of transcriptional process of myostatin gene

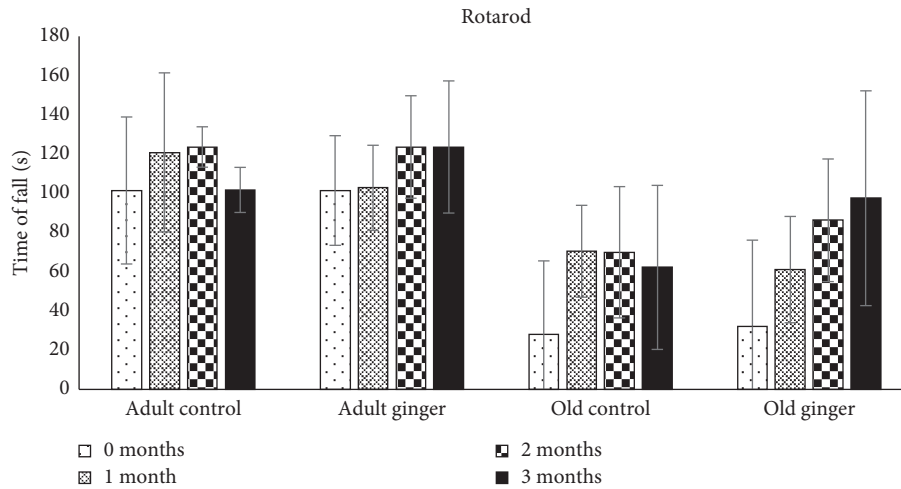


FIGURE 8: The rotarod performance test of young, adult, and old rats. Data are presented as mean \pm SD ($n = 8$ (control rats); $n = 10$ (*Z. officinale*-treated rats)). No significant change was observed.

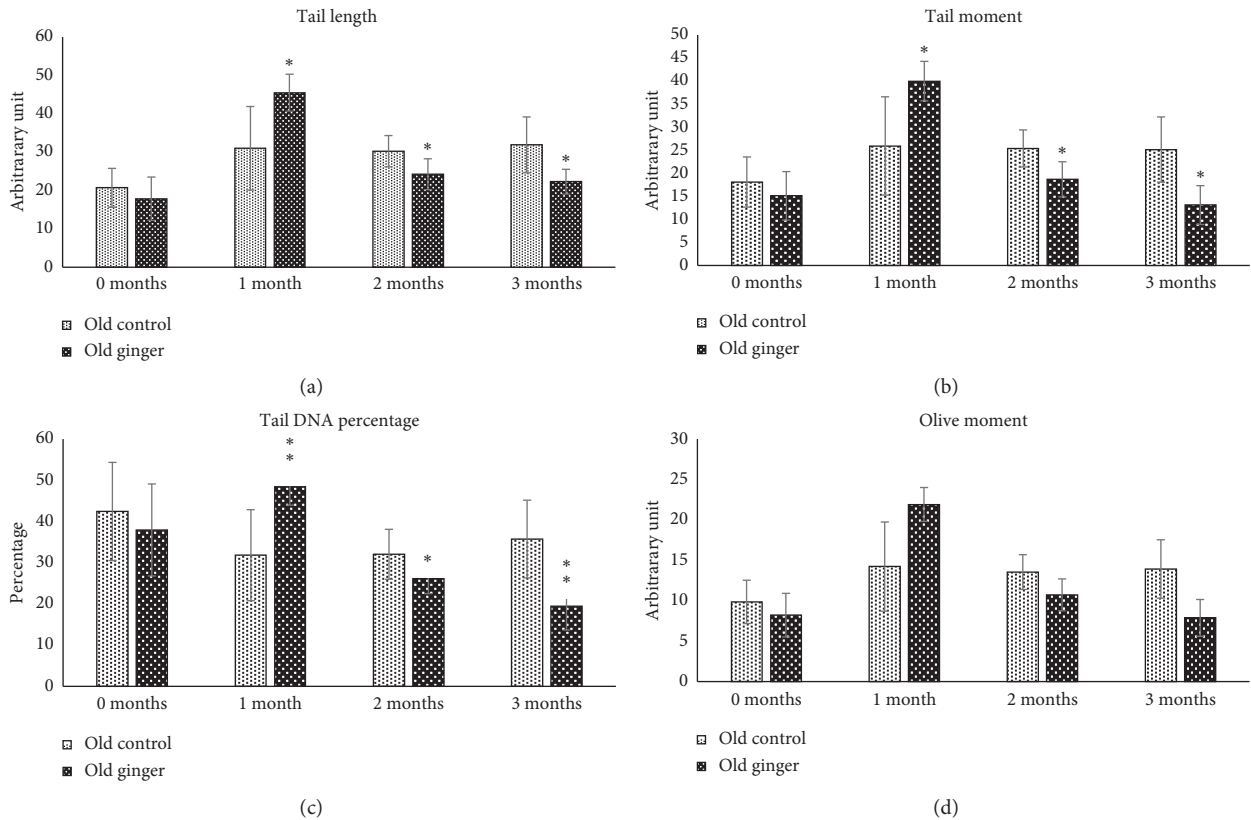


FIGURE 9: The level of damaged DNA of old rats was measured based on (a) tail length, (b) tail moment, (c) tail DNA percentage, and (d) olive moment using the comet assay method. Data are presented as mean \pm SD ($n = 8$ (control rats); $n = 10$ (*Z. officinale*-treated rats)). * $p < 0.05$, significantly different compared to control old rats with a post hoc Bonferroni test.

resulting in imbalanced protein synthesis and protein breakdown [40, 41]. The deterioration of myosin expression also caused dysfunction of myofilament which later can affect the muscle performance [41]. Besides, the presence of ROS in the body will result in decreased production of acetylcholine in synaptic cleft that contributes to the failure of action

potential production by sarcolemma as well as affects the neuromuscular junction which is essential in preserving muscle strength and quality [42, 43]. The continuous production of ROS also contributes to changing the morphology of neuromuscular junction and reducing the number of fibre and innervation [44].

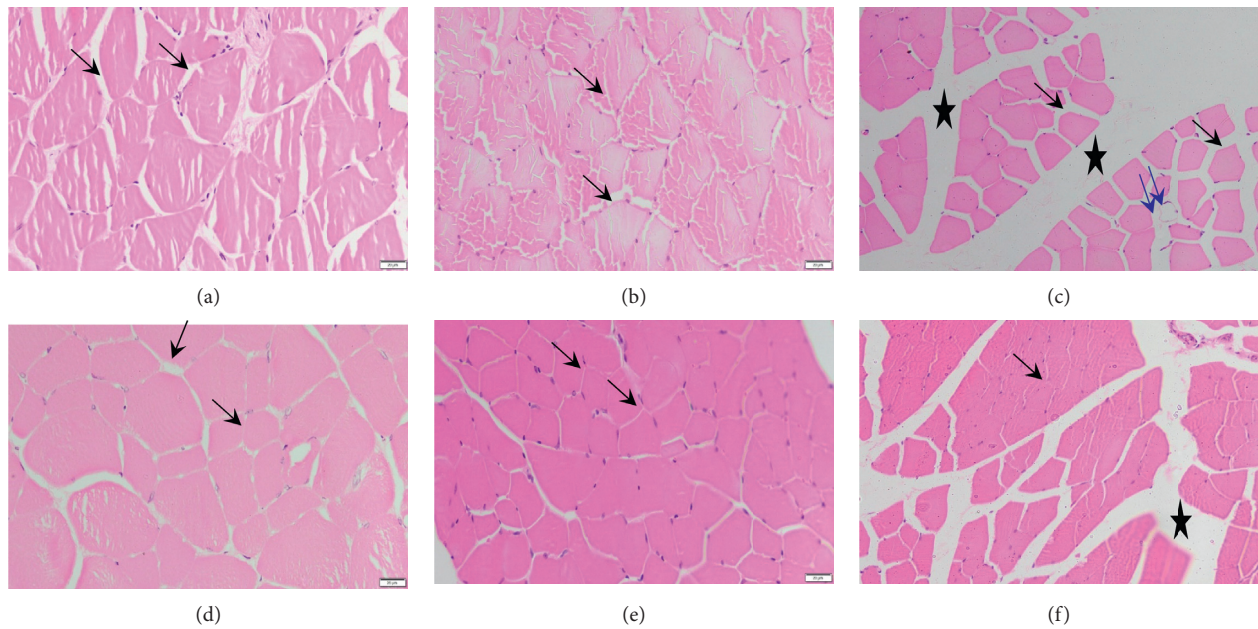


FIGURE 10: Cross section of H&E-stained rat muscle fibres and fascicles of the quadriceps femoris muscle. Rats treated with distilled water: (a) young, (b) adult, and (c) old control groups. Rats treated with *Z. officinale*: (d) young-, (e) adult-, and (f) old-treated groups. Each muscle fibre was surrounded by epimysium (black arrow), and the muscle fascicle was surrounded by abundant connective tissue (★). Dilated blood vessel is shown by blue double arrows. Images were photographed at 400x magnification.

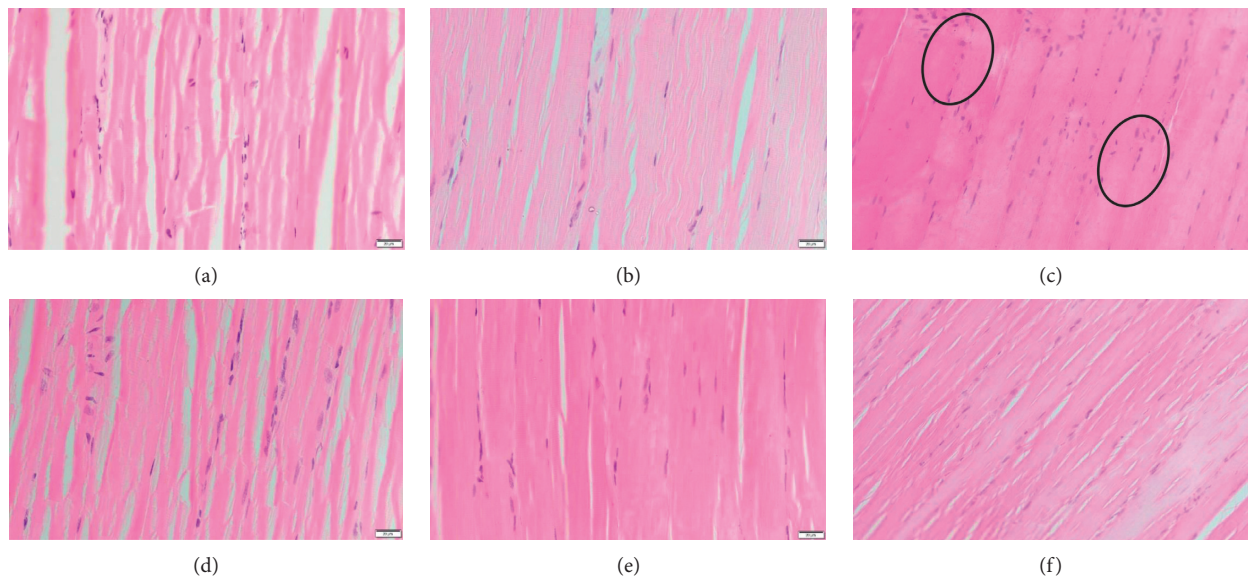


FIGURE 11: Longitudinal section of H&E-stained rat muscle fibres and fascicles of the quadriceps femoris muscle. Rats treated with distilled water: (a) young, (b) adult, and (c) old control groups. Rats treated with *Z. officinale*: (d) young-, (e) adult-, and (f) old-treated groups. Many nuclei are seen infiltrating the muscle fibres (oval area). Images were photographed at 400x magnification.

In this study, muscle and bone integrity were determined by measuring bone mineral density (BMD), bone mineral content (BMC), and fat free mass (FFM). The results of the present study showed that BMC, BMD, lean BMC, and FFM were increased with increasing age of the rats. Treatment with ginger for three months did not cause any significant effect to all parameters measured in all groups of rats. However, in young rats, ginger treatment caused a reduction

in BMC, BMD, and lean BMC. These observations could be due to short-term supplementation of ginger extract in the treated group of rats. BMD, BMC, and lean BMC are major determinants of bone strength since they are involved in bone structure process. As ageing occurs, there is abundant generation of ROS with insufficient support of antioxidant system which later gives a negative effect towards osteoblast and osteoclast regulation [45]. The accumulation of

oxidative stress during ageing could affect the bone turnover by triggering imbalance production of cells responsible for bone resorption and formation [46]. A previous study has proven that dietary compounds with enriched antioxidant and anti-inflammatory properties have promising bone protective effects. A study conducted by Varela-López et al. displayed that CoQ₁₀ supplementation could contribute to the lowest loss of BMD in aged rats by preventing DNA and lipid damage [47]. In another study, they found that intake of dried plum that consists of enriched antioxidant properties could improve alkaline phosphatase activity, insulin-like growth factor-1 (IGF-1), and BMD in postmenopausal women by suppressing the rate of bone turnover [48]. Moreover, blueberry supplementation in rats improved the bone formation rate, osteoblast number, and levels of trabecular bone volume together with inhibition of osteoblast senescence and bone loss [49]. Hence, long-term supplementation of ginger extract may exhibit a similar effect as other antioxidant dietary compounds in improving BMC, BMD, and lean BMC in aged rats.

The findings of this study also showed that treatment of ginger for 3 months to the old rats was able to decrease the level of damaged DNA. This indicates the potential of ginger in alleviating DNA damage caused by overproduction of ROS. This finding was in line with current result which found that treatment with ginger significantly increased the grip strength of front and hind paws of young and adult rats as compared to untreated control. The potential of ginger as antioxidant agent in decreasing the level of ROS has been reported in previous findings. A study conducted by Tung et al. found that ginger root extract has shown antioxidant and acetylcholinesterase inhibitory activity in Alzheimer's disease [50]. This was supported by another finding which reported that 6-gingerol in ginger extract has the ability to increase the expression of antioxidant enzyme as well as restore glutathione level [29]. The antioxidant properties of ginger have also been reported in a study carried out by Fahmi et al. [51] which found that ginger extract was able to lessen the severity of diethylnitrosamine (DEN) toxicity in rats by increasing the level of serum high-density lipoprotein (HDL) and plasma glutathione peroxidase (GSH-Px) activity, accompanied by decreased low-density lipoprotein (LDL), serum alanine aminotransferase (ALT), and alkaline phosphatase (ALP). In another study, ginger has been proven to attenuate lipid peroxidation with reduction of MDA level and increase glutathione S-transferase activity in the liver of Wistar rats [52]. There was also significant reduction in body weight and lipid droplet deposition in the rats' liver.

Histological analysis carried out in this study showed that sarcopenia is evident in the muscle of old rats but it is still in the early stage. Apparent reduction in the size of muscle fibre and fascicles with heterogenous morphology of the muscle fibres and mild sequestration of cellular infiltration were observed. However, the full-blown sarcopenic histological findings such as fat infiltration, mononuclear infiltration, disruption of muscle fibre arrangement, and vacuole formation were absent. These sarcopenic changes, however, were lesser in old rats treated with ginger extract

even though there was evidence of cellular infiltration (mild inflammation) and dilated blood vessels. The sarcopenic changes observed in old rats in this study were milder as compared to another study which showed that muscle fibres of diabetic rats treated with *Centella asiatica* have increased in size, appeared in closely space, and become more continuous as well as the muscle fibres have been restored in regular polygonal shape [53]. However, this result was similar with a previous study which found that treatment with mixed Japanese herbs known as "Dokhwalgisaeng-tang" on disuse muscle atrophy rats has decreased the myofibre size of the gastrocnemius muscle [54]. The accumulation of nuclei around the myofibres was also observed indicating the presence of inflammatory cells. The lesser sarcopenic changes in old rats treated with ginger observed in this study may indicate the ameliorative action of ginger as antioxidant agent by enhancing structural protein synthesis. This is because the production of excessive ROS in skeletal muscle could cause sarcopenia leading to deleterious structural changes by affecting the muscle fibres lipid membrane bilayer [55]. Furthermore, the presence of excess ROS will cause imbalance between protein synthesis and degradation which later contributes to the reduction in skeletal muscle fibres [56].

The molecular finding from this study was limited as it focused on the outcome of ginger supplementation on muscle performance. Therefore, further study is needed to elucidate the molecular mechanism of ginger in improving muscle performance. By performing a molecular study, the exact mechanism of ginger in reducing the level of oxidative stress in the muscle can be confirmed which can be used as a preventative measure for muscle disease, such as sarcopenia. However, the improvement of muscle performance in SD rats supported by the histological findings and the reduction of DNA damage observed in the present study strengthen the properties of ginger as an antioxidant agent, and thus it can be potentially used to alleviate oxidative stress and prevent age-related muscle disease.

5. Conclusions

In conclusion, ginger or *Zingiber officinale* Roscoe prevents DNA damage and improves muscle performance and bone integrity in Sprague Dawley rats indicating its potential in alleviating oxidative stress in ageing and thus delaying sarcopenia progression.

Abbreviations

| | |
|--------|---|
| SPSS: | Statistical Package for the Social Sciences |
| ANOVA: | Analysis of variance |
| SD: | Standard deviation |
| BW: | Body weight |
| ROW: | Relative organ weight |
| BBM: | Bold's basal media |
| DXA: | Dual energy X-ray absorptiometry |
| BMC: | Bone mineral content |
| BMD: | Bone mineral density |
| CKMM: | Creatine kinase-MM |

| | |
|------|-----------------------------------|
| MDA: | Malondialdehyde |
| HAE: | 4-Hydroxyalkenals |
| HRP: | Horseradish peroxidase |
| TMB: | 3, 3', 5, 5'-Tetramethylbenzidine |
| PBS: | Phosphate buffer saline |
| BHT: | Butylated hydroxytoluene |
| ROS: | Reactive oxygen species |
| RNS: | Reactive nitrogen species. |

Data Availability

The data supporting the conclusion of this article are included within the article.

Ethical Approval

The research has been approved by the Universiti Kebangsaan Malaysia Animal Ethics Committee (UKMAEC Approval Number: BOK/PP/2018/SUZANA/14-MAY/924-JUNE-2018-MAY-2020).

Disclosure

The funding bodies from this research did not have any role in the design of the study, collection, analysis, and interpretation of data, and in writing the manuscript.

Conflicts of Interest

The authors declare that they have no conflicts of interest.

Authors' Contributions

SM contributed to the experimental design, supervised the work, interpreted the data, and drafted, revised, and corrected the manuscript for publication. NFNMS drafted the manuscript and NFAS performed the experimentation, analyzed the data, and drafted the manuscript while NHH, NAR, SNAZ, and AFAR performed the experimentation. JKT, NAG, and MFMN were involved in data analysis and interpretation. All authors read and approved the final manuscript.

Acknowledgments

The authors are thankful for the contribution from all the researchers and staff of the Department of Biochemistry, Faculty of Medicine, Universiti Kebangsaan Malaysia Medical Centre. This research was supported by Universiti Kebangsaan Malaysia (UKM) Dana Cabaran Perdana Research Grant with project code: AP-2017-009/3.

References

- [1] J. D. Walston, "Sarcopenia in older adults," *Current Opinion in Rheumatology*, vol. 24, no. 6, pp. 623–627, 2012.
- [2] J. E. Morley, "Undernutrition in older adults," *Family Practice*, vol. 29, no. 1, pp. i89–i93, 2012.
- [3] M. Yamada, S. Nishiguchi, N. Fukutani et al., "Prevalence of sarcopenia in community-dwelling Japanese older adults," *Journal of the American Medical Directors Association*, vol. 14, no. 12, pp. 911–915, 2013.
- [4] A. J. Cruz-Jentoft, J. P. Baeyens, J. M. Bauer et al., "Sarcopenia: European consensus on definition and diagnosis: report of the European working group on sarcopenia in older people," *Age and Ageing*, vol. 39, no. 4, pp. 412–423, 2010.
- [5] O. Rom, S. Kaisari, D. Aizenbud, and A. Z. Reznick, "Lifestyle and sarcopenia—etiology, prevention, and treatment," *Rambam Maimonides Medical Journal*, vol. 3, no. 4, 2012.
- [6] S. Fulle, F. Protasi, G. Di Tano et al., "The contribution of reactive oxygen species to sarcopenia and muscle ageing," *Experimental Gerontology*, vol. 39, no. 1, pp. 17–24, 2004.
- [7] S. Palipoch and P. Koomhin, "Oxidative stress-associated pathology: a review," *Sains Malaysiana*, vol. 44, no. 10, pp. 1441–1451, 2015.
- [8] A. Phaniendra, D. B. Jestadi, and L. Periyasamy, "Free radicals: properties, sources, targets, and their implication in various diseases," *Indian Journal of Clinical Biochemistry*, vol. 30, no. 1, pp. 11–26, 2015.
- [9] S. Suzuki, N. Fujita, N. Hosogane et al., "Excessive reactive oxygen species are therapeutic targets for intervertebral disc degeneration," *Arthritis Research & Therapy*, vol. 17, no. 1, p. 316, 2015.
- [10] N. Khansari, Y. Shakiba, and M. Mahmoudi, "Chronic inflammation and oxidative stress as a major cause of age-related diseases and cancer," *Recent Patents on Inflammation & Allergy Drug Discovery*, vol. 3, no. 1, pp. 73–80, 2009.
- [11] A. Ayala, M. F. Muñoz, and S. Argüelles, "Lipid peroxidation: production, metabolism, and signaling mechanisms of malondialdehyde and 4-hydroxy-2-nonenal," *Oxidative Medicine and Cellular Longevity*, vol. 2014, Article ID 360438, 31 pages, 2014.
- [12] R. Koopman and L. J. C. van Loon, "Aging, exercise, and muscle protein metabolism," *Journal of Applied Physiology*, vol. 106, no. 6, pp. 2040–2048, 2009.
- [13] N. Noran, A. Bulgiba, T. Guat, and I. Mudl, "Sarcopenia in older people," *Geriatrics*, InTech, Shanghai, China, pp. 29–40, 2012.
- [14] C. D. McMahon, R. Chai, H. G. Radley-Crabb et al., "Lifelong exercise and locally produced insulin-like growth factor-1 (IGF-1) have a modest influence on reducing age-related muscle wasting in mice," *Scandinavian Journal of Medicine & Science in Sports*, vol. 24, no. 6, pp. e423–e435, 2014.
- [15] C. Vigorito and F. Giallauria, "Effects of exercise on cardiovascular performance in the elderly," *Frontiers in Physiology*, vol. 5, p. 51, 2014.
- [16] K. Tanaka, M. Arita, H. Sakurai, N. Ono, and Y. Tezuka, "Analysis of chemical properties of edible and medicinal ginger by metabolomics approach," *BioMed Research International*, vol. 2015, Article ID 671058, 7 pages, 2015.
- [17] M. Park, J. Bae, and D.-S. Lee, "Antibacterial activity of [10]-gingerol and [12]-gingerol isolated from ginger rhizome against periodontal bacteria," *Phytotherapy Research*, vol. 22, no. 11, pp. 1446–1449, 2008.
- [18] R. B. van Breemen, Y. Tao, and W. Li, "Cyclooxygenase-2 inhibitors in ginger (*Zingiber officinale*)," *Fitoterapia*, vol. 82, no. 1, pp. 38–43, 2011.
- [19] A. J. Akinyemi, A. O. Ademiluyi, and G. Oboh, "Inhibition of angiotensin-1-converting enzyme activity by two varieties of ginger (*Zingiber officinale*) in rats fed a high cholesterol diet," *Journal of Medicinal Food*, vol. 17, no. 3, pp. 317–323, 2014.
- [20] A. J. Akinyemi, G. Oboh, A. O. Ademiluyi, A. A. Boligon, and M. L. Athayde, "Effect of two ginger varieties on arginase activity in hypercholesterolemic rats," *Journal of Acupuncture and Meridian Studies*, vol. 9, no. 2, pp. 80–87, 2016.

- [21] S. Wang, M. Tian, R. Yang et al., "6-gingerol ameliorates behavioral changes and atherosclerotic lesions in ApoE^{-/-} mice exposed to chronic mild stress," *Cardiovascular Toxicology*, vol. 18, no. 5, pp. 420–430, 2018.
- [22] G. Park, H. G. Kim, M. S. Ju et al., "6-shogaol, an active compound of ginger, protects dopaminergic neurons in Parkinson's disease models via anti-neuroinflammation," *Acta Pharmacologica Sinica*, vol. 34, no. 9, pp. 1131–1139, 2013.
- [23] S. K. Ha, E. Moon, M. S. Ju et al., "6-shogaol, a ginger product, modulates neuroinflammation: a new approach to neuroprotection," *Neuropharmacology*, vol. 63, no. 2, pp. 211–223, 2012.
- [24] M. Sarip, *Subcritical Water Extraction of 6-gingerol and 6-shogaol from Zingiber Officinale*, Universiti Teknologi Malaysia, Skudai, Malaysia, 2012.
- [25] N. F. Sani, L. K. Belani, C. P. Sin et al., "Effect of the combination of gelam honey and ginger on oxidative stress and metabolic profile in streptozotocin-induced diabetic Sprague-Dawley rats," *BioMed Research International*, vol. 2014, Article ID 160695, 9 pages, 2014.
- [26] N. P. Singh, M. T. McCoy, R. R. Tice, and E. L. Schneider, "A simple technique for quantitation of low levels of DNA damage in individual cells," *Experimental Cell Research*, vol. 175, no. 1, pp. 184–191, 1988.
- [27] T. Lang, T. Streeper, P. Cawthon, K. Baldwin, D. R. Taaffe, and T. B. Harris, "Sarcopenia: etiology, clinical consequences, intervention, and assessment," *Osteoporosis International*, vol. 21, no. 4, pp. 543–559, 2010.
- [28] T. Brioché and S. Lemoine-Morel, "Oxidative stress, sarcopenia, antioxidant strategies and exercise: molecular aspects," *Current Pharmaceutical Design*, vol. 22, no. 18, pp. 2664–2678, 2016.
- [29] C. Lee, G. H. Park, C.-Y. Kim, and J.-H. Jang, "[6]-gingerol attenuates β -amyloid-induced oxidative cell death via fortifying cellular antioxidant defense system," *Food and Chemical Toxicology*, vol. 49, no. 6, pp. 1261–1269, 2011.
- [30] H. Mozaffari-Khosravi, Z. Naderi, A. Dehghan, A. Nadjarzadeh, and H. Fallah Huseini, "Effect of ginger supplementation on proinflammatory cytokines in older patients with osteoarthritis: outcomes of a randomized controlled clinical trial," *Journal of Nutrition in Gerontology and Geriatrics*, vol. 35, no. 3, pp. 209–218, 2016.
- [31] Z. Naderi, H. Mozaffari-Khosravi, A. Dehghan, A. Nadjarzadeh, and H. F. Huseini, "Effect of ginger powder supplementation on nitric oxide and C-reactive protein in elderly knee osteoarthritis patients: a 12-week double-blind randomized placebo-controlled clinical trial," *Journal of Traditional and Complementary Medicine*, vol. 6, no. 3, pp. 199–203, 2016.
- [32] F. Shidfar, A. Rajab, T. Rahideh, N. Khandouzi, S. Hosseini, and S. Shidfar, "The effect of ginger (*Zingiber officinale*) on glycemic markers in patients with type 2 diabetes," *Journal of Complementary and Integrative Medicine*, vol. 12, no. 2, pp. 165–170, 2015.
- [33] K. Jeena, V. B. Liju, and R. Kuttan, "A preliminary 13-week oral toxicity study of ginger oil in male and female Wistar rats," *International Journal of Toxicology*, vol. 30, no. 6, pp. 662–670, 2011.
- [34] E. O. Idang, O. K. Yemitan, H. O. Mbagwu, G. J. Udom, E. O. Ogbuagu, and J. A. Udobang, "Toxicological assessment of *Zingiber officinale Roscoe* (Ginger) root oil extracts in Albino rats," *Toxicology Digest*, vol. 4, no. 1, pp. 108–119, 2019.
- [35] N. A. Dumont, "Satellite cells and skeletal muscle regeneration," *Comprehensive Physiology*, vol. 5, no. 3, pp. 1027–1059, 2011.
- [36] N. Miljkovic, J.-Y. Lim, I. Miljkovic, and W. R. Frontera, "Aging of skeletal muscle fibers," *Annals of Rehabilitation Medicine*, vol. 39, no. 2, p. 155, 2015.
- [37] S. C. Khor, A. M. Razak, W. Z. W. Ngah, Y. A. M. Yusof, N. A. Karim, and S. Makpol, "The tocotrienol-rich fraction is superior to tocopherol in promoting myogenic differentiation in the prevention of replicative senescence of myoblasts," *PLoS One*, vol. 11, no. 2, 2016.
- [38] I. Liguori, G. Russo, F. Curcio et al., "Oxidative stress, aging, and diseases," *Clinical Interventions in Aging*, vol. 13, pp. 757–772, 2018.
- [39] X. Huang, L. Chen, W. Liu et al., "Involvement of oxidative stress and cytoskeletal disruption in microcystin-induced apoptosis in CIK cells," *Aquatic Toxicology*, vol. 165, pp. 41–50, 2015.
- [40] G. Musumeci, R. Imbesi, M. A. Szychlinska, and P. Castrogiovanni, "Apoptosis and skeletal muscle in aging," *Open Journal of Apoptosis*, vol. 4, no. 2, pp. 41–46, 2015.
- [41] W. R. Frontera and J. Ochala, "Skeletal muscle: a brief review of structure and function," *Calcified Tissue International*, vol. 96, no. 3, pp. 183–195, 2015.
- [42] C. W. Baumann, D. Kwak, H. M. Liu, and L. V. Thompson, "Age-induced oxidative stress: how does it influence skeletal muscle quantity and quality?" *Journal of Applied Physiology*, vol. 121, no. 5, pp. 1047–1052, 2016.
- [43] M. Gonzalez-Freire, R. de Cabo, S. A. Studenski, and L. Ferrucci, "The neuromuscular junction: aging at the crossroad between nerves and muscle," *Frontiers in Aging Neuroscience*, vol. 6, p. 208, 2014.
- [44] N. Pollock, C. A. Staunton, A. Vasilaki, A. McArdle, and M. J. Jackson, "Denervated muscle fibers induce mitochondrial peroxide generation in neighboring innervated fibers: role in muscle aging," *Free Radical Biology and Medicine*, vol. 112, pp. 84–92, 2017.
- [45] M. Almeida, "Aging mechanisms in bone," *BoneKEY Reports*, vol. 1, 2012.
- [46] P. Hubert, S. Lee, S.-K. Lee, and O. Chun, "Dietary polyphenols, berries, and age-related bone loss: a review based on human, animal, and cell studies," *Antioxidants*, vol. 3, no. 1, pp. 144–158, 2014.
- [47] A. Varela-López, J. Ochoa, J. Llamas-Elvira et al., "Age-related loss in bone mineral density of rats fed lifelong on a fish oil-based diet is avoided by coenzyme Q10 addition," *Nutrients*, vol. 9, no. 2, p. 176, 2017.
- [48] S. Hooshmand, S. C. Chai, R. L. Saadat, M. E. Payton, K. Brummel-Smith, and B. H. Arjmandi, "Comparative effects of dried plum and dried apple on bone in postmenopausal women," *British Journal of Nutrition*, vol. 106, no. 6, pp. 923–930, 2011.
- [49] J. Zhang, O. P. Lazarenko, M. L. Blackburn et al., "Feeding blueberry diets in early life prevent senescence of osteoblasts and bone loss in ovariectomized adult female rats," *PLoS One*, vol. 6, no. 9, 2011.
- [50] B. T. Tung, "Antioxidant and acetylcholinesterase inhibitory activities of ginger root (*Zingiber officinale Roscoe*) extract," *Journal of Complementary and Integrative Medicine*, vol. 14, no. 4, 2017.
- [51] A. Fahmi, N. Hassanen, M. Abdur-Rahman, and E. Shams-Eldin, "Phytochemicals, antioxidant activity and hepatoprotective effect of ginger (*Zingiber officinale*) on

- diethylnitrosamine toxicity in rats,” *Biomarkers*, vol. 24, no. 5, pp. 436–447, 2019.
- [52] D. T. Leal, G. G. Fontes, J. K. D. Villa et al., “Zingiber officinale formulation reduces hepatic injury and weight gain in rats fed an unhealthy diet,” *Anais da Academia Brasileira de Ciências*, vol. 91, no. 4, 2019.
- [53] A. B. Oyenihi, S. O. P. Langa, S. Mukaratirwa, and B. Masola, “Effects of *Centella asiatica* on skeletal muscle structure and key enzymes of glucose and glycogen metabolism in type 2 diabetic rats,” *Biomedicine & Pharmacotherapy*, vol. 112, p. 108715, 2019.
- [54] H. M. Gong, Y. K. Lee, B. H. Lee, J. S. Kim, and H.-J. Lee, “The effects of dokhwalgisaeng-tang against disuse muscle atrophy in gastrocnemius of rats,” *Journal of Acupuncture Research*, vol. 35, no. 4, pp. 207–213, 2018.
- [55] Y. Ding, X. Dai, Y. Jiang et al., “Grape seed proanthocyanidin extracts alleviate oxidative stress and ER stress in skeletal muscle of low-dose streptozotocin- and high-carbohydrate/high-fat diet-induced diabetic rats,” *Molecular Nutrition & Food Research*, vol. 57, no. 2, pp. 365–369, 2013.
- [56] S. S. Reddy, K. Shruthi, Y. K. Prabhakar, G. Sailaja, and G. B. Reddy, “Implication of altered ubiquitin-proteasome system and ER stress in the muscle atrophy of diabetic rats,” *Archives of Biochemistry and Biophysics*, vol. 639, pp. 16–25, 2018.